VERNALIZATION AND FLOWERING TIME: CELEBRATING 20 YEARS OF FLC

EDITED BY: Richard Amasino, Elizabeth Dennis, Caroline Dean, Joanna Putterill and Christian Jung

PUBLISHED IN: Frontiers in Plant Science

frontiers Research Topics

Frontiers eBook Copyright Statement

The copyright in the text of individual articles in this eBook is the property of their respective authors or their respective institutions or funders. The copyright in graphics and images within each article may be subject to copyright of other parties. In both cases this is subject to a license granted to Frontiers.

The compilation of articles constituting this eBook is the property of Frontiers.

Each article within this eBook, and the eBook itself, are published under the most recent version of the Creative Commons CC-BY licence. The version current at the date of publication of this eBook is CC-BY 4.0. If the CC-BY licence is updated, the licence granted by Frontiers is automatically updated to the new version.

When exercising any right under the CC-BY licence, Frontiers must be attributed as the original publisher of the article or eBook, as applicable.

Authors have the responsibility of ensuring that any graphics or other materials which are the property of others may be included in the CC-BY licence, but this should be checked before relying on the CC-BY licence to reproduce those materials. Any copyright notices relating to those materials must be complied with.

Copyright and source acknowledgement notices may not be removed and must be displayed in any copy, derivative work or partial copy which includes the elements in question.

All copyright, and all rights therein, are protected by national and international copyright laws. The above represents a summary only. For further information please read Frontiers' Conditions for Website Use and Copyright Statement, and the applicable CC-BY licence.

ISSN 1664-8714
ISBN 978-2-88971-739-2
DOI 10.3389/978-2-88971-739-2

About Frontiers

Frontiers is more than just an open-access publisher of scholarly articles: it is a pioneering approach to the world of academia, radically improving the way scholarly research is managed. The grand vision of Frontiers is a world where all people have an equal opportunity to seek, share and generate knowledge. Frontiers provides immediate and permanent online open access to all its publications, but this alone is not enough to realize our grand goals.

Frontiers Journal Series

The Frontiers Journal Series is a multi-tier and interdisciplinary set of open-access, online journals, promising a paradigm shift from the current review, selection and dissemination processes in academic publishing. All Frontiers journals are driven by researchers for researchers; therefore, they constitute a service to the scholarly community. At the same time, the Frontiers Journal Series operates on a revolutionary invention, the tiered publishing system, initially addressing specific communities of scholars, and gradually climbing up to broader public understanding, thus serving the interests of the lay society, too.

Dedication to Quality

Each Frontiers article is a landmark of the highest quality, thanks to genuinely collaborative interactions between authors and review editors, who include some of the world's best academicians. Research must be certified by peers before entering a stream of knowledge that may eventually reach the public - and shape society; therefore, Frontiers only applies the most rigorous and unbiased reviews.
Frontiers revolutionizes research publishing by freely delivering the most outstanding research, evaluated with no bias from both the academic and social point of view. By applying the most advanced information technologies, Frontiers is catapulting scholarly publishing into a new generation.

What are Frontiers Research Topics?

Frontiers Research Topics are very popular trademarks of the Frontiers Journals Series: they are collections of at least ten articles, all centered on a particular subject. With their unique mix of varied contributions from Original Research to Review Articles, Frontiers Research Topics unify the most influential researchers, the latest key findings and historical advances in a hot research area! Find out more on how to host your own Frontiers Research Topic or contribute to one as an author by contacting the Frontiers Editorial Office: frontiersin.org/about/contact

VERNALIZATION AND FLOWERING TIME: CELEBRATING 20 YEARS OF FLC

Topic Editors:
Richard Amasino, University of Wisconsin-Madison, United States
Elizabeth Dennis, Commonwealth Scientific and Industrial Research Organisation (CSIRO), Australia
Caroline Dean, John Innes Centre, United Kingdom
Joanna Putterill, The University of Auckland, New Zealand
Christian Jung, University of Kiel, Germany

Citation: Amasino, R., Dennis, E., Dean, C., Putterill, J., Jung, C., eds. (2021). Vernalization and Flowering Time: Celebrating 20 Years of FLC. Lausanne: Frontiers Media SA. doi: 10.3389/978-2-88971-739-2

Table of Contents

frontiers in Plant Science

ORIGINAL RESEARCH
published: 26 October 2020
doi: 10.3389/fpls.2020.572135

Photoperiod and Vernalization Control of Flowering-Related Genes: A Case Study of the Narrow-Leafed Lupin (*Lupinus angustifolius* L.)

*Sandra Rychel-Bielska[1,2], Piotr Plewiński[2], Bartosz Kozak[1], Renata Galek[1] and Michał Książkiewicz[2]**

[1] Department of Genetics, Plant Breeding and Seed Production, Wrocław University of Environmental and Life Sciences, Wrocław, Poland, [2] Department of Genomics, Institute of Plant Genetics, Polish Academy of Sciences, Poznań, Poland

Narrow-leafed lupin (*Lupinus angustifolius* L.) is a moderate-yielding legume crop known for its high grain protein content and contribution to soil improvement. It is cultivated under photoperiods ranging from 9 to 17 h, as a spring-sown (in colder locations) or as an autumn-sown crop (in warmer regions). Wild populations require a prolonged cold period, called vernalization, to induce flowering. The key achievement of *L. angustifolius* domestication was the discovery of two natural mutations (named *Ku* and *Jul*) conferring vernalization independence. These mutations are overlapping deletion variants in the promoter of *LanFTc1*, a homolog of the *Arabidopsis thaliana FLOWERING LOCUS T* (*FT*) gene. The third deletion, named here as *Pal*, was recently found in primitive germplasm. In this study, we genotyped *L. angustifolius* germplasm that differs in domestication status and geographical origin for *LanFTc1* alleles, which we then phenotyped to establish flowering time and vernalization responsiveness. The *Ku* and *Jul* lines were vernalization-independent and early flowering, wild (*ku*) lines were vernalization-dependent and late flowering, whereas *the Pal* line conferred intermediate phenotype. Three lines representing *Ku*, *Pal,* and *ku* alleles were subjected to gene expression surveys under 8- and 16-h photoperiods. *FT* homologs (*LanFTa1*, *LanFTa2*, *LanFTc1,* and *LanFTc2*) and some genes selected by recent expression quantitative trait loci mapping were analyzed. Expression profiles of *LanFTc1* and *LanAGL8* (*AGAMOUS-like 8*) matched observed differences in flowering time between genotypes, highlighted by high induction after vernalization in the *ku* line. Moreover, these genes revealed altered circadian clock control in *Pal* line under short days. *LanFD* (*FD*) and *LanCRLK1* (*CALCIUM/CALMODULIN-REGULATED RECEPTOR-LIKE KINASE 1*) were negatively responsive to vernalization in *Ku* and *Pal* lines but positively responsive or variable in *ku*, whereas *LanUGT85A2* (*UDP-GLUCOSYL TRANSFERASE 85A2*) was significantly suppressed by vernalization in all lines. Such a pattern suggests the opposite regulation of these gene pairs in the vernalization pathway. *LanCRLK1* and *LanUGT85A2* are homologs of *A. thaliana* genes involved in the *FLOWERING LOCUS C* (*FLC*) vernalization

OPEN ACCESS

Edited by:
Christian Jung,
University of Kiel, Germany

Reviewed by:
Dong-Hwan Kim,
Chung-Ang University, South Korea
Youbong Hyun,
Seoul National University, South Korea

***Correspondence:**
Michał Książkiewicz
mksi@igr.poznan.pl

Specialty section:
This article was submitted to Plant Development and EvoDevo, a section of the journal Frontiers in Plant Science

Received: *12 June 2020*
Accepted: *24 September 2020*
Published: *26 October 2020*

Citation:
Rychel-Bielska S, Plewiński P, Kozak B, Galek R and Książkiewicz M (2020) Photoperiod and Vernalization Control of Flowering-Related Genes: A Case Study of the Narrow-Leafed Lupin (Lupinus angustifolius L.). Front. Plant Sci. 11:572135. doi: 10.3389/fpls.2020.572135

pathway. Lupins, like many other legumes, do not have any *FLC* homologs. Therefore, candidate genes surveyed in this study, namely *LanFTc1*, *LanAGL8, LanCRLK1,* and *LanUGT85A2*, may constitute anchors for further elucidation of molecular components contributing to vernalization response in legumes.

Keywords: vernalization, photoperiod, flowering, expression, *FLOWERING LOCUS T*, duplication, deletion

INTRODUCTION

Narrow-leafed lupin (*Lupinus angustifolius* L.) is a legume plant that is cultivated as "green" manure or as a grain crop for animal feed or human consumption (Kurlovich, 2002). The exploitation of *L. angustifolius* as a crop is advantageous in many respects. First, *L. angustifolius* cultivation has a positive influence on soil fertility due to the mobilization of soil-bound phosphorus and diazotrophic nitrogen fixation (Evans et al., 1987; Lambers et al., 2013). Moreover, *L. angustifolius* grains are characterized by high protein content and the use of them in livestock farming systems has many benefits in terms of the economic and environmental impact (Abraham et al., 2019). As seed alkaloid content was reduced by breeding below 0.01% of seed dry weight, a bitter taste, a typical feature of lupins, was fully eliminated from modern cultivars (Kamel et al., 2016). Additionally, the postharvest stubble can be now safety grazed by livestock, because the risk of lupinosis disease was diminished by the introduction of Phomospis stem blight resistance genes (Mulholland et al., 1976; Jago et al., 1982; Cowling et al., 1987; Williamson et al., 1994; Shankar et al., 2002; Książkiewicz et al., 2020). Furthermore, *L. angustifolius* is currently being promoted in human food markets as a result of its nutritional, metabolomic, and other health benefits (Foyer et al., 2016; Kouris-Blazos and Belski, 2016).

Cultivated *L. angustifolius* germplasm primarily originated from the western Mediterranean basin (Mousavi-Derazmahalleh et al., 2018b). Natural adaptation of wild *L. angustifolius* populations to the Mediterranean climate is the requirement of the prolonged cold period (i.e., vernalization) during germination or juvenile phase to induce flowering (Gladstones and Hill, 1969; Rahman and Gladstones, 1972; Landers, 1995; Adhikari et al., 2012). The selection of early phenology was based on the removal of the vernalization requirement, a major achievement in the domestication of *L. angustifolius*, enabling temperature-independent sowing (French and Buirchell, 2005). *L. angustifolius* is grown in various environments ranging from the subtropics (Australia) and Mediterranean regions (including Morocco, Spain, southern France, and Italy), through temperate oceanic climates (such as the United Kingdom, northern France, and Benelux), humid continental climates (for example in Germany, the Baltic countries, and Ukraine), though to the subarctic zone, localized as far north as 60° latitude (Russia). In warmer regions it is usually autumn-sown, whereas in colder regions it is exclusively spring-sown (Annicchiarico and Carroni, 2009).

Lupin crops are cultivated in various photoperiod conditions, ranging from about 9 h (autumn sowing in Australia) to 16–17 h (spring sowing in Baltic countries and Russia) (Książkiewicz et al., 2017). The vernalization requirements of wild populations are so demanding that they can only be completely fulfilled by spring sowing in northern locations (Adhikari et al., 2012). Worldwide, *L. angustifolius* cultivation is based on vernalization independence selected from only two natural mutations (named *Ku* and *Jul*) that were discovered in domesticated germplasm just a little over half a century ago (Mikołajczyk, 1966; Gladstones and Hill, 1969). The use of only two donors of early flowering in *L. angustifolius* breeding, followed by a strong selection of key agronomic traits, have resulted in a lack of phenological diversity in domesticated germplasm (Stefanova and Buirchell, 2010; Berger et al., 2012; Cowling, 2020). Therefore, further adaptation of this crop to new agronomic conditions resulting from a rapidly changing climate, may only be possible with the incorporation of novel genetic resources of intermediate phenology.

During recent years *L. angustifolius* was supplemented with numerous molecular resources, including bacterial artificial chromosome libraries carrying nuclear DNA inserts, consecutively improved linkage maps with sequence-defined markers, transcriptome assemblies, and a progressively updated genome sequence of the reference cultivar Tanjil (Kasprzak et al., 2006; Nelson et al., 2006; Gao et al., 2011; Yang et al., 2013; Kamphuis et al., 2015; Wyrwa et al., 2016; Hane et al., 2017; Zhou et al., 2018; Kozak et al., 2019). These resources were harnessed to reveal the genetic identity of *Ku*, which was found to be a homolog of a *FLOWERING LOCUS T* (*FT*) gene, named *LanFTc1* (Książkiewicz et al., 2016; Nelson et al., 2017). *FT* gene is a well-recognized floral integrator gene, promoting flowering in response to environmental conditions signaled by photoperiod, vernalization, and circadian clock pathways (Turck et al., 2008). The functional mutation underlying the domesticated *Ku* allele in *L. angustifolius* was assigned to the 1423 bp deletion in the promoter region of *LanFTc1*, carrying potential binding sites for several transcription factors acting as *FT* gene repressors in *Arabidopsis thaliana* (Nelson et al., 2017). Interestingly, the second *L. angustifolius* early phenology mutation, *Jul*, was recently revealed to be the third *LanFTc1* allele, in the form of a 5162 bp deletion in the promoter region, fully encompassing that 1423 bp *Ku* deletion (Taylor et al., 2019). Screening of germplasm resources with the *LanFTc1* markers resulted in the identification of a fourth *LanFTc1* allele in wild population line originating from Palestine (a country annotated as Israel in Australian collection or Egypt in Polish gene bank), carrying 1208 bp deletion partially overlapping with domesticated *Ku* deletion (Rychel, 2018; Taylor et al., 2019). This Palestinian allele was named here as *Pal*.

Some genes involved in flowering time regulation are under strict circadian clock control and their expression levels fluctuate during a day (Shim et al., 2017). One such example in *Arabidopsis* is the *FT* gene, which expression is correlated

with the stability of CONSTANS (CO) protein and shows two peaks, the first in the morning (lower) and the second in the evening (higher) (Turck et al., 2008). This CO-dependent regulation is facilitated by enhancer protein binding to specific sites in the promoter sequence, located approximately 5 kbp upstream of the first codon, which results in forming a DNA loop bringing all the components together (Cao et al., 2014). Interestingly, *L. angustifolius* allelic variants of the *LanFTc1* promoter have the distal binding sequences (CCAAT-boxes) preserved (Książkiewicz et al., 2016; Nelson et al., 2017; Taylor et al., 2019). This study sought to explore whether the altered length of the *LanFTc1* promoter is associated with the altered circadian clock control of *LanFTc1* and other related genes.

Taking into consideration the (i) role of *FT* genes in integrating key environmentally responsive pathways, (ii) demonstrated allelic variability of *LanFTc1* gene associated with flowering time, and (iii) wide range of environmental variables occurring at lupin cultivation sites, we decided to explore the photoperiod and vernalization responsiveness in *L. angustifolius*. Here, the *L. angustifolius* germplasm differing in domestication status and geographical origin was genotyped for *LanFTc1* alleles and phenotyped for flowering time and vernalization responsiveness. Then, the transcriptomic response of candidate genes from the vernalization pathway in early (*Ku*), intermediate (*Pal*), and late flowering (*ku*) *L. angustifolius* germplasm was assayed under contrasting photoperiod and vernalization conditions, accounting the influence of circadian rhythm control. This study discusses the hypothetical function of these genes in terms of flowering time regulation and response to vernalization.

MATERIALS AND METHODS

Plant Material

Ninety-two *L. angustifolius* lines were subjected to genotyping and phenotyping. Lines were derived from the European Lupin Gene Resources Database maintained by the Poznań Plant Breeding Ltd. station located in Wiatrowo. The lines originated from 13 countries, including Spain (32 lines), Poland (15), Australia (11), Russia (11), Germany (7), Italy (4), Belarus (3), Israel (2), Algeria, Morocco, Palestine, Portugal and Republic of South Africa (1). Accession numbers and information on the domestication status and country of origin are provided in **Supplementary Table 1**.

Identification of *LanFTc1* Alleles

Young leaf tissue from three biological replicates per plant was sampled. Frozen (−80°C) plant tissue (50 mg) was homogenized using TissueLyser II (Qiagen, Hilden, Germany) and two stainless steel beads (ø 5 mm) in 2 ml tubes (Eppendorf, Hamburg, Germany). DNA was isolated using DNeasy Plant Mini Kit (Qiagen). PCR was performed using GoTaq Long PCR Master Mix (Promega, Mannheim, Germany) and published LanFTc1_INDEL2 primers (Taylor et al., 2019), provided here for reference in **Supplementary Table 2**. PCR conditions were as follows: initial denaturation (94°C for 2 min), then 35 cycles composed of denaturation (94°C for 30 s), annealing (62°C for 30 s), and elongation (72°C for 5 min), followed by the final extension (72°C for 10 min). Products were resolved by agarose gel electrophoresis and SYBR Safe DNA staining (Invitrogen, Carlsbad, CA, United States) and visualized on UV-transilluminator (Uvitec, Thermo Fisher Scientific, Waltham, MA, United States). Wild P27255 allele (*ku*, without deletion) was encoded as "A," Palestinian allele (*Pal*, 1208 bp deletion) as "B," 83A:476 allele (*Ku*, 1423 bp deletion) as "C," and Krasnolistny allele (*Jul*, 5162 bp deletion) as "D."

Evaluation of Vernalization Responsiveness in Greenhouse

Vernalization was carried out by placing imbibed seeds for 21 days at 5°C in darkness on moist filter paper in Petri dishes. Non-vernalized control plants were sown five days before the end of the vernalization procedure and kept at ∼21°C to maintain a similar thermal time (Huyghe, 1991). Plants were cultivated in a greenhouse maintained by the Institute of Plant Genetics, the Polish Academy of Sciences, Poznań, Poland (52°26′N 16°54′E) during growing seasons of 2014 (sowing of vernalized plants on 14.05) and 2015 (sowing of vernalized plants on 25.03) under ambient long day photoperiod (12–17 h). The greenhouse was equipped with automatic heating to keep the minimum air temperature above 18°C. Passive cooling was maintained by a temperature-dependent ventilation system (activated at 22°C). Air temperature (daily mean and maximum) and daily sunshine hours recorded by the nearby localized meteorological station (Poznań-Ławica, 5.1 km) as well as the theoretical photoperiod hours calculated for this latitude (covering 120 days from sowing date for both years) were provided for reference in **Supplementary Tables 3, 4**. Flowering time was recorded as the number of days from sowing date of vernalized plants until the first fully colored petal was observed. The average number of plants sampled in 2014 was 5.6 for the non-vernalized variant (min. 3, max. 6) and 6.9 for the vernalized variant (min. 4, max. 7), whereas in 2015 it was 4.7 for the non-vernalized variant (min. 4, max. 5) and 5.0 for the vernalized variant.

Controlled Environment Experiment for Gene Expression Profiling

Based on the results of *LanFTc1* allele genotyping and vernalization responsiveness phenotyping, three accessions were selected for gene expression profiling: P27255 from Morocco (96,234, carrying wild allele *ku*), 83A:476 from Australia (96,233, carrying domesticated allele *Ku*), and Palestyna from Palestine (95,799, carrying intermediate allele *Pal*). The vernalization of lines was performed as described above. Non-vernalized control plants were sown five days before the end of the vernalization procedure. Plants from both variants were cultivated in climatic chambers with controlled humidity (40–50% day, 70–80% night) and temperature (22°C day, 18°C night). Two types of photoperiods were studied, short day (SD, 8 h, from 8 AM to 4 PM) and long day (LD, 16 h, from 4 AM to 8 PM). Young leaves from five biological replicates were sampled every week at two times of day to follow a circadian rhythm, at 9 AM, and

3 PM under SD or at 7 AM and 6 PM under LD. Plant material was immediately frozen in liquid nitrogen and stored at −80°C. Three replicates with similar plant phenology (growth rate and time to flowering) were subjected to gene expression profiling. Taking into consideration observed flowering time, from 2 to 4 terms were selected for gene expression, representing the period from about 2 weeks before flowering to the flowering date and/or few days after flowering (**Supplementary Table 5**).

RNA Isolation and cDNA Synthesis

Frozen young leaf tissue (50 mg) was homogenized using TissueLyser II (Qiagen) and two stainless steel beads (ø 5 mm) in 2 ml tubes (Eppendorf). RNA isolation was performed using the SV Total RNA Isolation System (Promega) without any alterations to the protocol. RNA concentration and purity were measured using NanoDrop 2000 (Thermo Fisher Scientific) and A260/A280 ratio. RNA integrity was visualized by 1% agarose gel electrophoresis of denatured samples in 1 × TAE buffer. RNA concentration was equalized to 1000 ng/μl in nuclease-free water. First-strand cDNA synthesis was performed using GoScript (TM) Reverse Transcription System (Promega) and 5 μg of total RNA per sample.

Selection of Genes for Quantitative PCR

The set of genes selected for quantitative PCR included, among others, four *L. angustifolius* representatives of *FT* clade, namely *LanFTa1* (Lup021189, XM_019571501.1), *LanFTa2* (XM_019596455.1), *LanFTc1* (Lup015264, XM_019601808.1), and *LanFTc2* (Lup005674, XM_019565316.1) (Książkiewicz et al., 2016; Nelson et al., 2017). First names in parentheses correspond to gene names provided in the *L. angustifolius* pseudochromosome assembly paper (Hane et al., 2017), whereas the second names address *L. angustifolius* NCBI Reference Sequences LupAngTanjil_v1.0. Moreover, our assay endeavored also some candidate genes revealed by recent *L. angustifolius* (eQTL mapping) study (Plewiński et al., 2019) to be associated with the vernalization response, as follows: *LanUGT85A2* (Lup002110, XM_019574900.1), *LanCRLK1* (Lup011808, XM_019603391.1), *LanAGL8* (Lup018485, XM_019583439.1), and *LanFD* (Lup018024, XM_019567853.1). Alignment of coding sequences to the *L. angustifolius* genome assembly provided evidence that *LanAGL8* and *LanFD* are present in single copies.

Moreover, some major *A. thaliana* components of the flowering induction pathway were considered, as follows: *LEAFY* (*LFY*, AT5G61850), *APETALA1* (*AP1*, AT1G69120), *VERNALIZATION INSENSITIVE 3* (*VIN3*, AT5G57380), and *VERNALIZATION 5* (*VRN5*, AT3G24440). Multiple sequence alignment revealed that all these genes have putatively three copies in the *L. angustifolius* genome, namely Lup006312 (XM_019602464.1), Lup012189 (XM_019558971.1) and Lup027481 (XM_019607325.1) for *LFY*; Lup021855 (XM_019605469.1), Lup024348 (XM_019588203.1) and Lup006876 (XM_019572960.1) for *AP1*; Lup009440 (XM_019586787.1), Lup013437 (XM_019598860.1) and Lup026125 (XM_019608083.1) for *VIN3*; and Lup009144 (XM_019591910.1), Lup018692 (XM_019567058.1) and Lup032778 (XM_019590742.1) for *VRN5*. Analysis of leaf transcriptome data obtained for the *L. angustifolius* linkage mapping population, covering developmental phases from juvenile to generative growth after partial vernalization (Plewiński et al., 2019), revealed negligible expression of all *LFY* and *AP1* homologs (∼0.07 reads per kilobase million, RPKM), very low expression of *VRN5* (∼0.56 RPKM) and high expression of VIN3 copies (∼25.07 RPKM) (**Supplementary Table 6**). Therefore, *VRN5* and *VIN3* homologs were selected for the expression assay, whereas *LFY* and *AP1* homologs were discarded. Reference genes validated in previous *L. angustifolius* quantitative gene expression studies were selected for this assay, namely *LanDExH7* (Lup023733, XM_019579367.1), and *LanTUB6* (Lup032899, XM_019581544.1) (Taylor et al., 2016, 2019; Nelson et al., 2017). Primers were designed in Geneious Prime (Auckland, New Zealand) using Primer3 (Kearse et al., 2012; Untergasser et al., 2012). Due to the high similarity between particular copies, all three *VRN5* homologs were analyzed together using one primer pair. The remaining genes were profiled on one by one basis. Designed primers and expected product sizes are provided in **Supplementary Table 2**.

Quantitative Gene Expression Analysis

In prior experiments, a CFX Connect Real-Time PCR Detection System (Bio-Rad Polska, Warsaw, Poland) was calibrated using Melt Calibration Kit (Bio-Rad Polska) according to the manufacturer's protocol. A standard curve was developed to assess the performance of the quantitative PCR assay and its dynamic range following recent recommendations (Svec et al., 2015). Analyzed genes were amplified using GoTaq G2 Flexi DNA Polymerase (Promega) and subjected to 1% agarose gel electrophoresis. Amplicons were excised from a gel, extracted with the aid of QIAquick Gel Extraction Kit (Qiagen), quantified using NanoDrop 2000 (Thermo Fisher Scientific), and outsourced (Genomed Ltd., Warsaw, Poland) for direct Sanger sequencing on ABI PRISM 3130 Genetic Analyzer XL (Applied Biosystems, Hitachi). A series of dilutions in concentrations ranging from 1 to 10^{-10} of the original templates were prepared for every gene using an initial volume of 20 μl to reduce the sampling error. 6 replicates per each concentration were performed using the iTaq Universal SYBR Green Supermix (Bio-Rad Polska). A two-step PCR protocol was exploited according to the protocol. A calculation of R^2 and PCR efficiency values was done in Bio-Rad CFX Manager 3.1. The values obtained are provided in **Supplementary Table 7**.

The quantitative PCR analysis of gene expression was performed using 96-well PCR plates and two reference genes (*LanDExH7* and *LanTUB6*). Inter-run calibration sample (*LanTUB6*) and no template control were used on all plates. Three biological replicates were analyzed for each time point, and all samples were run in 3 technical repeats. High-resolution PCR product melting in the range of temperature from 65 to 85°C was performed after PCR to control the specificity of amplification. Melt profiles were inspected for the amplification of unspecific products, highlighted by the presence of melting peaks at different temperatures than those obtained during standard curve

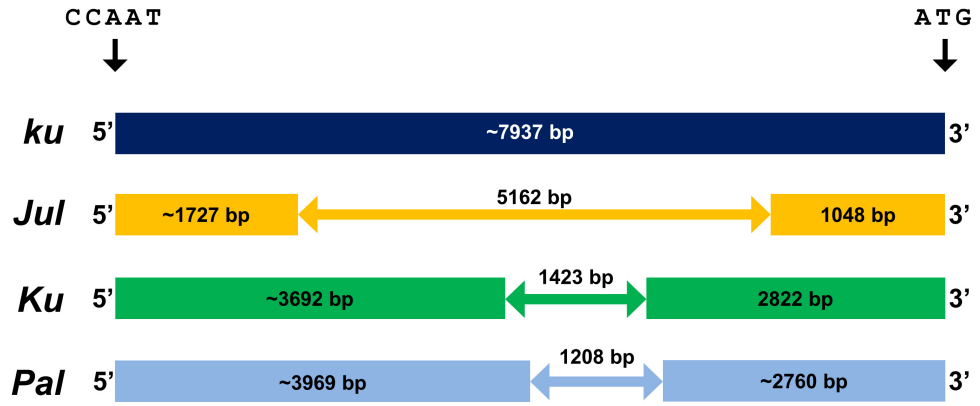

FIGURE 1 | Indel variation in the promoter sequence of *LanFTc1* gene controlling flowering induction in *L. angustifolius*. Allele *ku* is typical for wild populations, alleles *Jul* and *Ku* are present only in domesticated germplasm, whereas allele *Pal* was found only in wild germplasm from Palestine. The position is given in relation to the first nucleotide of CCAAT-box (Książkiewicz et al., 2016; Nelson et al., 2017; Taylor et al., 2019).

preparation. Calculations of ΔΔCq were performed in Bio-Rad CFX Manager 3.1 taking into consideration PCR efficiency values and results obtained for both reference genes. The final computations (mean value and standard deviation) and visualization (graphs) were performed in Microsoft Excel 2010.

Statistical Analysis

Calculations were performed to check the influence of circadian clock (expression in the evening divided by expression in the morning), growth phase (maximum expression at analyzed date divided by maximum expression at the first date), vernalization (fold change of expression after vernalization), and genotype (comparison of expression levels observed in studied lines, including *Ku*/*Pal*, *Ku*/*ku*, and *Pal*/*Ku*, performed for all data points). The values obtained are provided in **Supplementary Data Sheet 1**. The statistical significance of these quotients was tested using a t test for the mean ratio as proposed by Hauschke et al. (1999), Tamhane and Logan (2004)). Calculations were made in R (R Core Team, 2013) with custom script using "t.test.ratio" function from the ratios package. In the first step, the equal variance was tested. If this condition was satisficed classical t-test formula was used, otherwise, Welch's *t*-test formula was used (Welch, 1947). *P*-values were rounded up to four decimal places and are provided in the **Supplementary Data Sheet 1**.

RESULTS

European Lupin Gene Bank Preserves the *L. angustifolius* Donors of Four Alleles of LanFTc1 Promoter

Indel variation in the promoter region of the major flowering time gene *LanFTc1* (**Figure 1**) was recently revealed to be associated with flowering time and vernalization responsiveness in *L. angustifolius* (Nelson et al., 2017; Taylor et al., 2019). To evaluate allelic composition in germplasm exploited by European lupin breeders, ninety-two *L. angustifolius* accessions, encompassing 43 primitive populations or landraces, 23 cross derivatives or breeding lines, 25 cultivars, and one mutant, derived from the European Lupin Gene Resources Database, were screened with primers flanking polymorphic *LanFTc1* promoter region (**Table 1**). As expected, wild *LanFTc1* allele (*ku*) was found mainly in primitive accessions collected in the Mediterranean Basin as well as in a few old domesticated materials originating from Russia, Poland, Germany, and the Republic of South Africa. One wild population line, Palestyna originating from Palestine, was found to carry the shortest variant of deletion (1208 bp), named here as *Pal*. Alleles *Ku* (1423 bp deletion) and *Jul* (5162 bp deletion) were found only in domesticated germplasm – the first one was present mostly in released cultivars, whereas the second one was typically in breeding materials at a different stage of improvement. Accessions carrying *Ku* originated primarily from Australia, Germany, and Poland, whereas those carrying *Jul* from Poland and Russia. Results of marker screening are provided in **Supplementary Table 8**.

Palestinian *LanFTc1* Allele Confers Intermediate Flowering Time Moderately Responsive to Vernalization

Ninety-two *L. angustifolius* accessions with known *LanFTc1* promoter allele composition were evaluated for phenotypic response to vernalization in two consecutive years, 2014 and

TABLE 1 | Distribution of *LanFTc1* alleles across wild and domesticated *L. angustifolius* germplasm.

LanFTc1 allele	Lines	XC	CV	MU	WP
ku, without deletion	48	3	3	–	42
Pal, 1208 bp deletion	1	–	–	–	1
Ku, 1423 bp deletion	24	7	17	–	–
Jul, 5162 bp deletion	19	13	5	1	–

XC, cross derivative or breeding line; CV, cultivar; MU, mutant; WP, wild population or primitive landrace.

TABLE 2 | Comparison of flowering time and vernalization responsiveness of *L. angustifolius* germplasm carrying *Jul*, *Ku*, *Pal,* and *ku LanFTc1* alleles, cultivated in a greenhouse under natural long days (LD).

LanFTc1 allele	Days to flowering '2014	Vernalization response '2014	Days to flowering '2015	Vernalization response '2015
ku, without deletion	88.8 ± 15.6[a]	−41.1 ± 13.8	88.0 ± 5.9	−21.8 ± 6.0
Pal, 1208 bp deletion	53.5 ± 1.9	−14.5 ± 2.7	68.2 ± 5.6	−14.8 ± 3.4
Ku, 1423 bp deletion	40.5 ± 2.6	−3.3 ± 2.6	56.7 ± 2.1	−3.0 ± 2.5
Jul, 5162 bp deletion	38.8 ± 1.1	−0.2 ± 2.2	55.6 ± 1.9	−2.2 ± 2.2

[a]*Standard deviation.*

2015 (**Table 2**). Lines carrying wild *ku* allele revealed the longest vegetative phase, ranging from 61.2 ± 0.9 to 116.2 ± 3.0 days in '2014 and from 79.0 ± 5.8 to 101.5 ± 3.9 days in '2015. These lines demonstrated also high vernalization responsiveness, highlighted by the acceleration of flowering after vernalization by 13.9 to 66.4 days in 2014, and by 11.6 to 35.6 days in 2015. The line carrying *Pal* allele showed intermediate phenology and flowered about 20-35 days quicker than the average *ku* genotype, namely after ∼53 days from sowing in '2014 and ∼68 days in '2015. The vernalization procedure advanced flowering induction in this line by about two weeks. Accessions carrying domesticated *Ku* allele were very early and started flowering after 37.2 ± 0.4 to 46.2 ± 8.9 days in 2014, and after 54.0 ± 0.0 to 59.6 ± 2.6 days in 2015. This set contained germplasm low-responsive to vernalization, which accelerated flowering time by up to ∼8.6 days, as well as some truly thermoneutral accessions, which flowered at the same time regardless of the vernalization procedure. Lines carrying domesticated European *Jul* allele also revealed very early phenology, manifested by the onset of flowering after 37.0 ± 1.3 to 41.0 ± 5.9 days in 2014, and after 52.2 ± 1.5 to 60.8 ± 1.8 days in 2015. Most *Jul* lines were fully thermoneutral. On average, *Jul* lines flowered earlier than *Ku* lines in both years, however taking into consideration standard errors resulting from variability between biological replicates, differences between mean values were not statistically significant. Results of time to flowering and vernalization responsiveness in relation to LanFTc1_INDEL2 marker polymorphism are provided in **Supplementary Table 8** (2014) and **Supplementary Table 9** (2015).

Based on the results of LanFTc1_INDEL2 marker screening and vernalization responsiveness, three lines were selected for vernalization response phenotyping under 8-h (SD) and 16-h (LD) photoperiods: 84A:476 carrying domesticated *Ku* allele (early flowering, thermoneutral), Palestyna carrying wild *Pal* allele (moderately flowering and responsive to vernalization), and P27255 carrying wild *ku* allele (late flowering and highly responsive to vernalization). 83A:476 was revealed to be the earliest line in both photoperiods, followed by Palestyna (**Table 3**). Under SD, 83A:476 accelerated transition between phases in response to vernalization by about 5 days, whereas under LD by about 3 days. These responses were higher in Palestyna, amounting to about 12-19 days and 3-5 days, respectively. P27255 did not flower during the experiment (90 days) in all variants except vernalized plants under LD.

TABLE 3 | Number of days to first bud, flower, and pod in *L. angustifolius* germplasm carrying *Ku*, *Pal,* and *ku LanFTc1* alleles, cultivated under 8- and 16-h photoperiods.

LanFTc1 allele	Vernalization variant	Days to first bud	Days to first flower	Days to first pod
8-h photoperiod				
Ku	-	51.3 ± 1.6[a]	57.2 ± 4.3	63.3 ± 9.8
	+	45.7 ± 2.9	52.0 ± 4.2	58.1 ± 2.5
Pal	-	65.3 ± 3.7	71.2 ± 3.8	83.5 ± 2.7
	+	52.9 ± 3.0	55.9 ± 2.6	64.7 ± 4.6
ku	-	–	–	–
	+	–	–	–
16-h photoperiod				
Ku	-	33.6 ± 1.1	38.7 ± 1.3	44.1 ± 1.4
	+	29.8 ± 2.7	35.3 ± 1.0	41.2 ± 1.0
Pal	-	36.7 ± 0.5	43.8 ± 0.4	49.0 ± 0.5
	+	40.0 ± 0.0	48.4 ± 1.4	52.0 ± 0.8
ku	-	–	–	–
	+	55.1 ± 1.3	59.0 ± 1.2	69.0 ± 2.4

[a]*Standard deviation.*

LanFTc1 Expression Was High and Thermoneutral in *Ku*, High and Partially Vernalization-Independent in *Pal*, Whereas Low and Positively Responsive to Vernalization in *ku*

83A:476 (*Ku*), Palestyna (*Pal*), and P27255 (*ku*) grown under SD and LD conditions were used for gene expression profiling (**Supplementary Data Sheet 1**). The vernalization responsiveness of analyzed genes was calculated as a mean fold change of expression in vernalized plants compared to non-vernalized control (averaged across all day terms and dates measured for a particular line), as summarized in **Table 4**. The circadian clock responsiveness were calculated as a mean fold change of expression occurring between the morning and the evening terms (averaged across all dates measured for a particular line) and are provided in **Table 5**. The trend in expression level during plant growth was calculated as a fold change of expression occurring between the first and the last term (based on maximum daily values) and is provided in **Table 6**.

First, we analyzed the expression of the *LanFTc1* gene, which is considered as the major controller of vernalization responsiveness and early flowering in *L. angustifolius* (Nelson et al., 2017; Taylor et al., 2019). The studied genotypes showed different patterns of *LanFTc1* expression in response to photoperiod, vernalization, and circadian rhythm.

Under SD, *LanFTc1* expression in non-vernalized plants was the highest in 83A:476 and the lowest in P27255 (**Figure 2A**). Indeed, *LanFTc1* expression in 83A:476 was up to 2.4 times higher than in Palestyna (P = 0.0016) and 460-2213 times higher than in P27255 (P = 0.0000). After vernalization, *LanFTc1* expression in 83A:476 was up to 4.5 times higher than in Palestyna (P = 0.0064) and up to 686 times higher than in P27255 (P = 0.0029). The difference of *LanFTc1* expression between

83A:476 and P27255 increased during plant development in both vernalization variants, whereas for the pair 83A:476 and Palestyna it was decreasing. Under LD, *LanFTc1* expression was the highest in Palestyna and the lowest in P27255 (**Figure 2B**). Namely, in non-vernalized plants, expression in Palestyna was 1.8-5.4 times higher than in 83A:476 (P = 0.0125) and 121-2642 times higher than in P27255 (P = 0.0085), whereas in vernalized plants it was 1.5-13.8 times higher in Palestyna than in 83A:476 (not significant, NS) and 24-276 times higher than in P27255 (P = 0.0094). The difference to Palestyna was increasing during plant growth for 83A:476 in both vernalization variants and P27255 in the absence of vernalization.

Vernalization influence on *LanFTc1* expression in P27255 was manifested by up to a 7.2-fold increase under SD (NS) (**Figure 2C**) and up to 427-fold increase under LD (P = 0.0125) (**Figure 2D**). The vernalization effect under SD was changing in 83A:476 from a 0.5-fold decrease (P = 0.0115) to a 3.2-fold increase (P = 0.0094) and similarly in Palestyna from a 0.5-fold decrease (P = 0.0291) to 1.6-fold increase (NS). This effect under LD was neutral in 83A:476 and positive in Palestyna, up to 5.1-fold increase (P = 0.0351).

The circadian clock regulation differed between genotypes and partially between environments. In 83A:476, *LanFTc1* expression was generally higher in the evening than in the morning in all combinations of the photoperiod and vernalization (up to 18.4-fold increase, P = 0.0008). In Palestyna, *LanFTc1* expression under SD was usually higher in the morning (up to 2.9-fold increase, P = 0.0172), whereas under LD this effect was variable. In P27255, *LanFTc1* expression was higher in the evening, especially under LD after vernalization (P = 0.0046).

TABLE 4 | Vernalization responsiveness of analyzed genes in *L. angustifolius* germplasm carrying *Ku*, *Pal,* and *ku* alleles, cultivated under 8-h (SD) and 16-h (LD) photoperiods.

Gene name	Mean change of expression after vernalization under SD			Mean change of expression after vernalization under LD		
	Ku	***Pal***	***ku***	***Ku***	***Pal***	***ku***
LanAGL8	1.6[a]	2.2	13.0	1.8	6.1	138.6
LanCRLK1	0.7	0.6	2.6	0.6	1.3	1.0
LanFD	0.5	0.5	3.6	0.3	0.7	1.0
LanFTa1	9.9	1.3	0.9	1.8	2.1	14.7
LanFTa2	1.1	0.3	13.3	3.2	1.1	1.2
LanFTc1	1.3	0.9	4.3	1.3	3.6	144.4
LanFTc2	0.7	0.7	3.5	1.1	3.2	1.4
LanUGT85A2	0.3	0.2	0.4	0.2	0.2	0.4
LanVIN3-1	0.9	0.9	1.9	0.8	1.0	1.1
LanVIN3-2	0.7	1.1	2.3	0.7	1.3	1.6
LanVIN3-3	0.9	1.7	2.3	0.6	1.3	1.0
LanVRN5	0.8	1.0	2.3	0.9	1.0	0.8

[a]*Fold change of expression occurring in response to vernalization, averaged across all data points (day terms and dates).*

TABLE 5 | Circadian clock responsiveness of analyzed genes in *L. angustifolius* germplasm carrying *Ku*, *Pal,* and *ku* alleles, cultivated under 8-h (SD) and 16-h (LD) photoperiods without vernalization and with vernalization.

Gene name	Mean change of expression during light phase under SD			Mean change of expression during light phase under LD		
	Ku	***Pal***	***ku***	***Ku***	***Pal***	***ku***
LanAGL8	1.6 | 1.0[a]	0.3 | 0.7	0.8 | 0.7	2.6 | 1.6	1.3 | 3.6	2.0 | 0.5
LanCRLK1	0.9 | 1.0	0.7 | 1.0	0.8 | 0.7	0.8 | 0.5	0.8 | 1.3	1.0 | 1.0
LanFD	0.3 | 0.8	1.7 | 3.1	1.2 | 1.6	0.3 | 0.4	1.6 | 2.4	1.9 | 1.3
LanFTa1	1.0 | 1.7	0.6 | 0.6	0.7 | 0.8	0.8 | 2.7	0.8 | 4.5	0.8 | 0.7
LanFTa2	0.6 | 0.9	0.9 | 0.4	0.4 | 0.4	0.4 | 2.2	0.7 | 0.4	0.6 | 0.6
LanFTc1	4.8 | 3.1	0.5 | 0.8	1.2 | 2.4	1.8 | 2.9	1.2 | 1.1	2.7 | 4.3
LanFTc2	2.0 | 4.3	2.0 | 11.1	5.6 | 24.3	2.7 | 1.7	2.0 | 0.5	3.4 | 4.2
LanUGT85A2	5.0 | 3.4	2.6 | 2.1	2.4 | 2.4	3.2 | 4.6	3.8 | 2.2	3.3 | 2.9
LanVIN3-1	1.2 | 1.5	0.7 | 1.1	1.4 | 0.9	1.4 | 1.4	1.9 | 2.7	1.5 | 1.5
LanVIN3-2	1.9 | 1.2	1.0 | 1.2	1.3 | 0.9	1.7 | 1.4	1.5 | 2.4	1.4 | 1.4
LanVIN3-3	1.4 | 1.3	0.8 | 1.0	1.2 | 0.9	2.1 | 1.5	1.5 | 2.0	1.4 | 1.7
LanVRN5	0.7 | 0.8	0.7 | 0.7	0.7 | 0.7	1.3 | 0.9	1.1 | 0.9	1.0 | 0.9

[a]*Fold change of expression occurring between the morning and the evening terms, averaged across all dates; the first number corresponds to the experiment without vernalization, the second number to the experiment with vernalization.*

TABLE 6 | Change of expression level of analyzed genes in *L. angustifolius* germplasm carrying *Ku*, *Pal,* and *ku* alleles, during plant growth under 8-h (SD) and 16-h (LD) photoperiods.

Gene name	Change of expression during experiment under SD			Change of expression during experiment under LD		
	Ku	*Pal*	*ku*	*Ku*	*Pal*	*ku*
LanAGL8	1.5 | 2.3[a]	3.5 | 6.3	0.4 | 6.4	1.6 | 1.0	16.6 | 6.8	4.0 | 805.9
LanCRLK1	0.5 | 1.2	0.9 | 1.2	0.6 | 0.5	0.8 | 0.8	0.6 | 2.7	0.6 | 1.2
LanFD	0.2 | 0.6	0.7 | 1.2	0.4 | 1.9	0.4 | 0.2	0.3 | 0.4	1.7 | 4.7
LanFTa1	0.7 | 1.3	1.7 | 5.6	0.5 | 1.4	23.6 | 7.3	404.5 | 340.2	2.2 | 765.0
LanFTa2	0.2 | 0.4	7.6 | 1.6	0.09 | 9.2	0.05 | 0.5	0.4 | 1.9	0.2 | 2.6
LanFTc1	0.4 | 1.2	0.9 | 3.0	0.08 | 0.3	1.5 | 2.2	15.7 | 10.2	0.7 | 118.8
LanFTc2	0.4 | 1.5	1.2 | 2.5	0.5 | -	1.1 | 0.9	3.8 | 5.9	0.7 | 1.1
LanUGT85A2	0.1 | 0.1	0.3 | 0.3	0.4 | 1.2	0.3 | 0.1	0.02 | 0.02	0.5 | 0.08
LanVIN3-1	0.3 | 3.0	1.0 | 1.2	0.8 | 1.4	2.3 | 1.2	1.0 | 1.1	1.0 | 1.0
LanVIN3-2	0.4 | 2.6	1.3 | 1.3	0.9 | 1.9	3.3 | 1.1	1.0 | 1.8	0.9 | 1.9
LanVIN3-3	0.2 | 3.5	1.2 | 3.2	0.4 | 1.3	2.5 | 0.9	1.2 | 1.8	0.9 | 0.9
LanVRN5	0.3 | 1.5	1.4 | 1.1	0.3 | 0.9	3.7 | 2.2	1.1 | 1.0	1.0 | 0.8

[a]*Fold change in expression occurring between the first and the last term, based on the maximum daily values; the first number corresponds to the experiment without vernalization, the second number to the experiment with vernalization.*

LanFTa1 Expression Was Low and Uniform in All Lines Under SD, However, It Was Highly Induced Just Before Flowering, Especially in *Pal* and *ku* Genotypes Under LD

Besides *LanFTc1*, three other *FT* genes, namely *LanFTa1*, *LanFTa2,* and *LanFTc2*, were analyzed to complement our perspective on *FT* clade transcriptional activity in *L. angustifolius* response to major environmental cues. *LanFTa1* gene expression under SD did not reveal any significant trend during plant growth and differences between genotypes were also usually not significant (**Figure 3A**). The relative level of expression was rather low (mean 0.38). A different pattern was observed under LD, when the expression was highly induced before flowering compared to the first term, namely 24-fold ($P = 0.045$) in non-vernalized 83A:476 (7-fold in vernalized, NS), 405-fold ($P = 0.0051$) in non-vernalized Palestyna (340-fold in vernalized, $P = 0.0015$), and 765-fold in vernalized P27255 (**Figure 3B**). In non-vernalized P27255 *LanFTa1* expression remained at a low level but this genotype did not flower in such conditions.

The vernalization effect on *LanFTa1* expression under LD in 83A:476 and Palestyna was slightly positive, up to 2.5-fold (NS) and 2.8-fold ($P = 0.0011$) increase, respectively (**Figures 3C,D**). In P27255, the vernalization influence was initially moderately negative (0.14-fold and 0.35-fold decrease, $P = 0.0002$) but became highly positive just before flowering (43.6-fold increase). The circadian regulation was not stable across terms and genotypes, however, when *LanFTa1* was induced before flowering in Palestyna under LD, its expression was significantly higher in the evening than in the morning (up to 25.1-fold increase, $P = 0.0004$).

LanFTa2 and *LanFTc2* Expression Was Low in Both Photoperiods in All Lines

LanFTa2 gene expression was very low in both photoperiods, amounting to mean values of 0.095 under SD and 0.004 under LD (**Supplementary Figures 1A,B**). There was remarkable induction of expression in P27255 after vernalization under SD (up to 38-fold, $P = 0.0002$), however, the relative expression values achieved were much lower than those observed for *LanFTc1* and *LanFTa1* (**Supplementary Figures 1C,D**). This pattern was not recreated under LD.

LanFTc2 expression was on a low level in all lines under both photoperiods (**Supplementary Figures 2A,B**). A moderate induction by vernalization in P27255 under SD (up to 7.3-fold increase, $P = 0.0187$) and in Palestyna under LD (up to 4.7-fold increase, $P = 0.0023$) was observed but obtained levels were less than half of the mean expression obtained for control genes (**Supplementary Figures 2C,D**).

LanAGL8 Expression Profile Reflected Observed Differences in Plant Phenology and Was Similar to *LanFTc1*

Besides homologs constituting the *L. angustifolius FT* clade (Książkiewicz et al., 2016; Nelson et al., 2017), four novel candidate genes (*LanAGL8, LanFD, LanUGT85A2*, and *LanCRLK1*), recently considered to be putatively involved in *Ku*-based response (Plewiński et al., 2019), were profiled in this study. *LanAGL8* is an *L. angustifolius* homolog of the *A. thaliana FRUITFULL* gene participating in flowering time control, meristem identity, and fruit development (Mandel and Yanofsky, 1995; Gu et al., 1998). *LanAGL8* expression was consecutively increasing during plant growth for all studied combinations of lines, photoperiod, and vernalization variants except non-vernalized P27255 under SD. However, there were considerable differences in the observed expression levels between genotypes. Under SD without vernalization, expression of the *LanAGL8* gene in 83A:476 (*Ku*) was approximately 7-17 times higher ($P = 0.0028$) than in Palestyna (*Pal*) and 1420-6090 times higher ($P = 0.0035$) than in P27255 (*ku*) (**Figure 4A**). The influence of vernalization resulted in a reduction of differences in *LanAGL8* expression between 83A:476 and Palestyna by

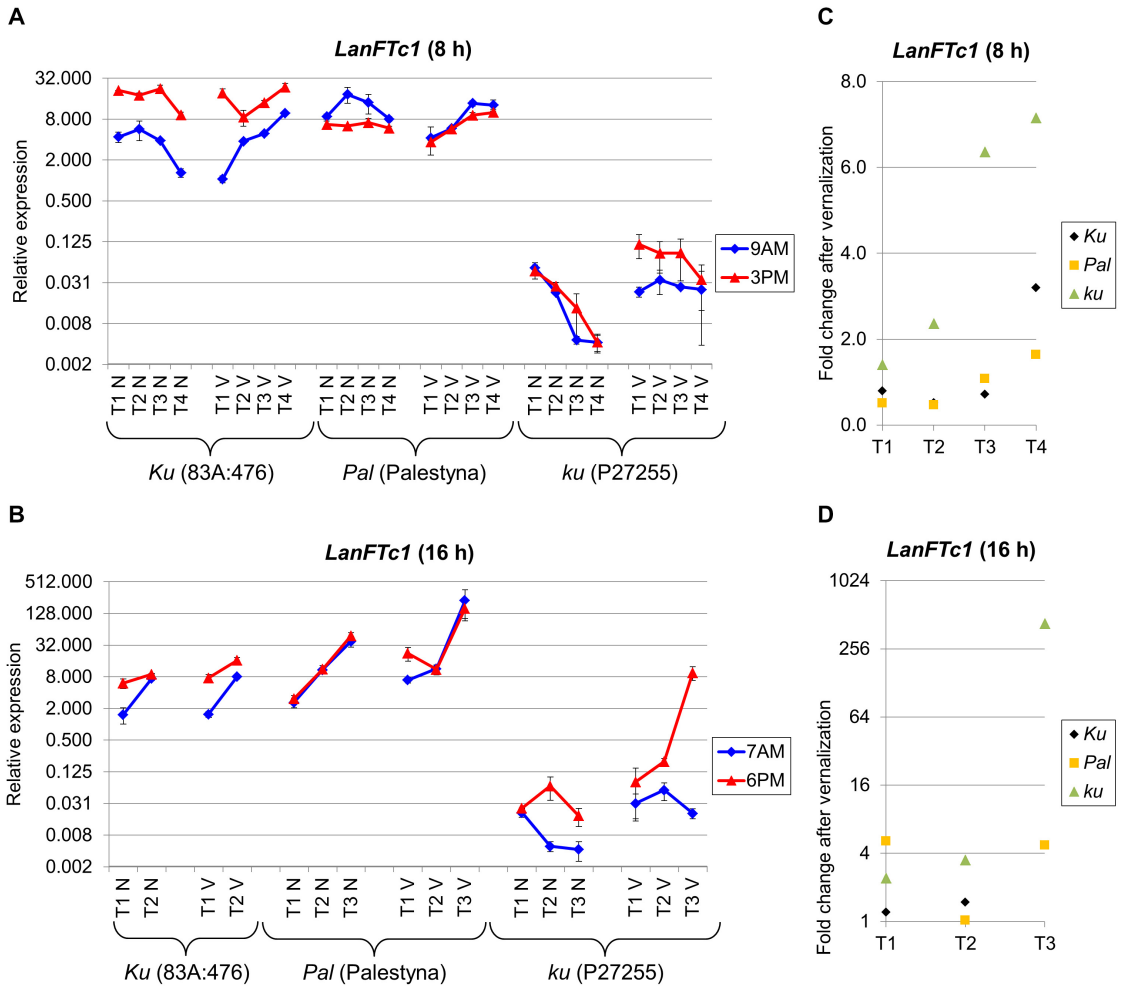

FIGURE 2 | Gene expression profile of the *LanFTc1* gene in response to photoperiod and vernalization in three lines (83A:476, Palestyna, and P27255) carrying different *LanFTc1* alleles (*Ku*, *Pal,* and *ku*). **(A)** expression under an 8-h photoperiod, **(B)** expression under 16-h photoperiod, **(C)** vernalization response under 8-h photoperiod, **(D)** vernalization response under 16-h photoperiod. T1-T4 stands for sampling terms (**Supplementary Table 5**), V for vernalized plants, and N for non-vernalized plants. Timespan of photoperiods: 8-h from 4 AM to 8 PM, 16-h from 4 AM to 8 PM. Two references were used for normalization (*LanDExH7* and *LanTUB6*) and one sample (*LanTUB6*) for inter-run calibration. Error bars indicate a standard deviation of 3 biological replicates, each representing a mean of 3 technical replicates. A logarithmic scale was used to accommodate observed large differences in gene expression values.

11–23%, and between 83A:476 and P27255 by 30–92%. Under LD without vernalization, *LanAGL8* expression in 83A:476 was higher up to 12-fold (P = 0.0086) than in Palestyna and up to 1805-fold (P = 0.0001) than in P27255 (**Figure 4B**). The application of vernalization reduced these differences considerably. To summarize, Palestyna revealed an intermediate *LanAGL8* expression profile, however, it was much more like 83A:476 than P27255.

The *LanAGL8* gene revealed high positive responsiveness to vernalization in P27255 in both photoperiods, and this effect was consecutively increasing during plant growth until flowering. Namely, the change of *LanAGL8* expression in P27255 after vernalization was raised from 2.1-fold (NS) to 29.8-fold (P = 0.0175) under SD (**Figure 4C**), and from 4.3-fold (P = 0.0121) to 398.2-fold (P = 0.0004) under LD (**Figure 4D**). Vernalization was also inductive in Palestyna, providing an up to 2.6-fold increase (P = 0.0329) of *LanAGL8* expression under SD (effect stable across sampling terms) and up to 11.8-fold increase (P = 0.0297) under LD (effect consecutively decreasing). In the 83A:476 line, the influence of vernalization was the lowest, yielding up to a 2.9-fold increase of *LanAGL8* expression under SD (P = 0.0066) and up to a 2.0-fold increase under LD (P = 0.0315).

The *LanAGL8* gene revealed diversified circadian clock regulation between genotypes and environments. Under SD, its expression was higher in the morning than in the evening in Palestyna and P27255, whereas in 83A:476 this relation was the opposite. Moreover, vernalization partially diminished these differences. Under LD, *LanAGL8* expression was usually higher in the evening terms for all lines, however, during the growth of vernalized P27255 this trend reversed.

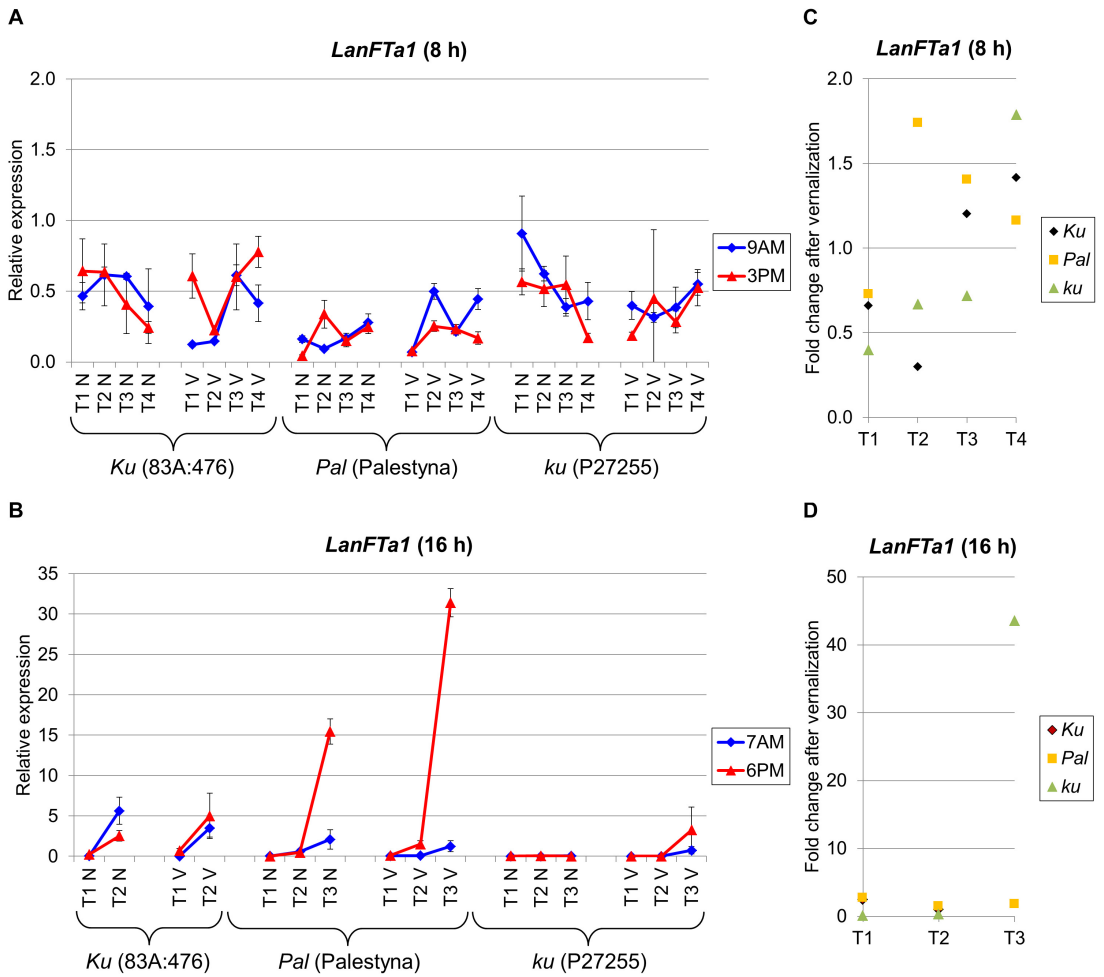

FIGURE 3 | Gene expression profile of the *LanFTa1* gene in response to photoperiod and vernalization in three lines (83A:476, Palestyna, and P27255) carrying different *LanFTc1* alleles (*Ku*, *Pal,* and *ku*). **(A)** expression under 8-h photoperiod, **(B)** expression under 16-h photoperiod, **(C)** vernalization response under 8-h photoperiod, **(D)** vernalization response under 16-h photoperiod. T1-T4 stands for sampling terms (**Supplementary Table 5**), V for vernalized plants, and N for non-vernalized plants. Timespan of photoperiods: 8-h from 4 AM to 8 PM, 16-h from 4 AM to 8 PM. Two references were used for normalization (*LanDExH7* and *LanTUB6*) and one sample (*LanTUB6*) for inter-run calibration. Error bars indicate a standard deviation of 3 biological replicates, each representing a mean of 3 technical replicates.

LanCRLK1 Expression Was Higher Under SD in All Lines and Negatively Responsive to Vernalization in Domesticated *Ku* Line

LanCRLK1 is an *L. angustifolius* homolog of the *A. thaliana CRLK1* gene which participates in response to low temperature in a calcium-dependent manner (Yang et al., 2010). Changes in *LanCRLK1* expression level were usually not related to the progress of plant growth, except P27255 cultivated under SD, which revealed a stable decrease of *LanCRLK1* both in non-vernalized and vernalized variants. The expression of *LanCRLK1* was higher under SD than under LD. Moreover, under SD without vernalization, *LanCRLK1* expression was the highest in Palestyna (up to 2.7-fold increase compared to 83A:476, P = 0.0002) and the lowest in P27255 (about 0.4-fold decrease, P = 0.0099). However, after vernalization, expression was highest in P27255 (up to a 3.5-fold increase compared to 83A:476, P = 0.0005) and lowest in 83A:476 (**Figure 5A**). The differences in the *LanCRLK1* expression between genotypes under LD were generally not significant (**Figure 5B**).

The effect of vernalization on *LanCRLK1* expression under SD was negative (from 0.4-fold to 0.7-fold decrease, P = 0.0009) or neutral in 83A:476, negative in Palestyna (from 0.6-fold to 0.8-fold decrease, P = 0.0000), and positive in P27255 (up to 3.0 fold increase, P = 0.0000) (**Figure 5C**). Under LD, the vernalization effect was also negative in 83A:476 (0.6-fold decrease, NS), however, in the remaining two lines, the effect changed during plant growth from negative to positive: from a 0.7-fold decrease to 1.9-fold increase in Palestyna (all NS) and from 0.6-fold decrease (P = 0.0001) to 1.4-fold increase in P27255

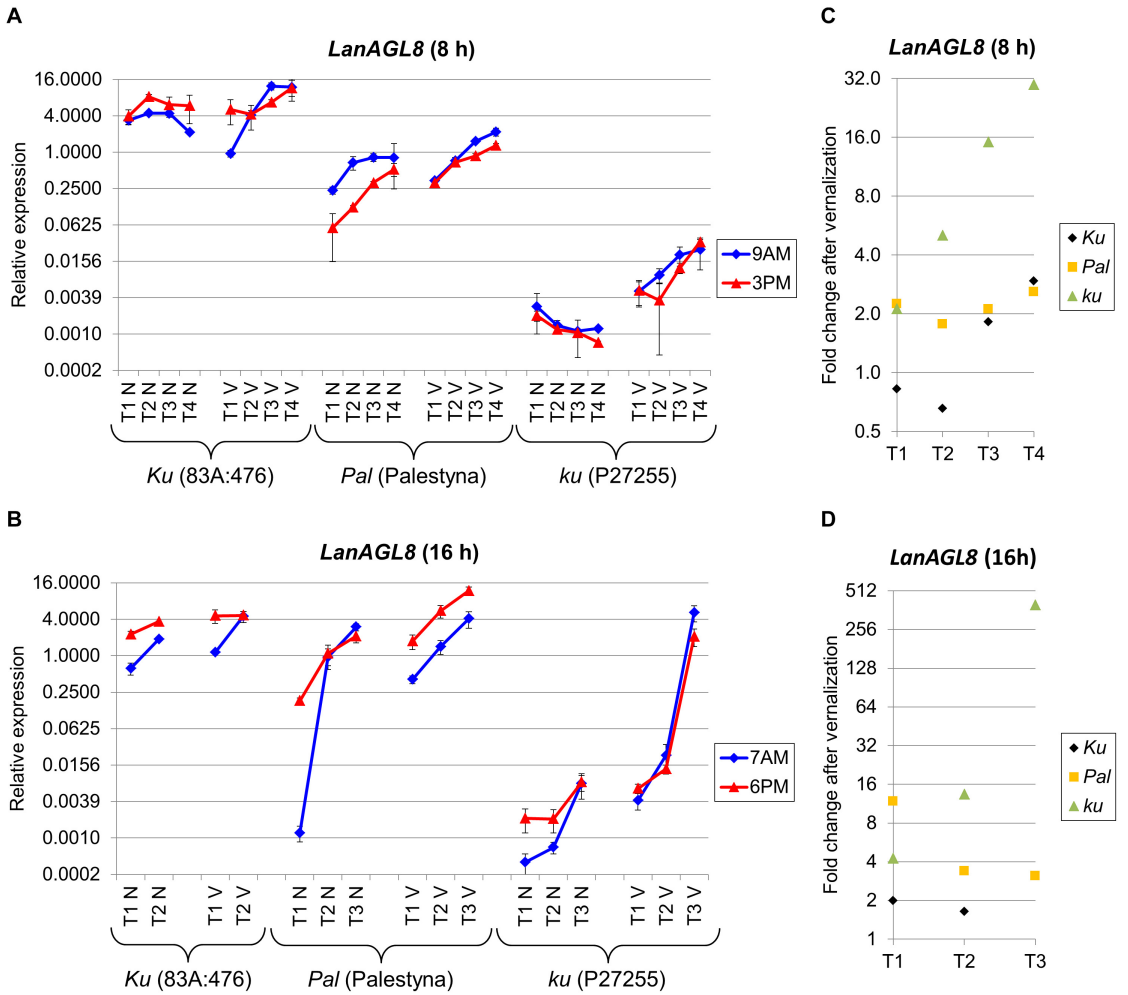

FIGURE 4 | Gene expression profile of the *LanAGL8* gene in response to photoperiod and vernalization in three lines (83A:476, Palestyna, and P27255) carrying different *LanFTc1* alleles (*Ku*, *Pal,* and *ku*). **(A)** expression under 8-h photoperiod, **(B)** expression under 16-h photoperiod, **(C)** vernalization response under 8-h photoperiod, **(D)** vernalization response under 16-h photoperiod. T1-T4 stands for sampling terms (**Supplementary Table 5**), V for vernalized plants, and N for non-vernalized plants. Timespan of photoperiods: 8-h from 4 AM to 8 PM, 16-h from 4 AM to 8 PM. Two references were used for normalization (*LanDExH7* and *LanTUB6*) and one sample (*LanTUB6*) for inter-run calibration. Error bars indicate a standard deviation of 3 biological replicates, each representing a mean of 3 technical replicates. A logarithmic scale was used to accommodate observed large differences in gene expression values.

(P = 0.0107) (**Figure 5D**). The influence of the circadian clock on *LanCRLK1* expression was variable in both photoperiods and usually not significant.

LanFD Expression Was Negatively Responsive to Vernalization in *Ku* and *Pal* Lines but Positively Responsive or Variable in *ku*

LanFD is an *L. angustifolius* homolog of the *A. thaliana FD* gene which triggers flowering based on FT-mediated signaling (Abe et al., 2005). *LanFD* expression in non-vernalized plants was usually the highest at the first sampling date and decreased during plant growth in both photoperiods, except in P27255 cultivated under LD. However, in vernalized plants, this decreasing trend was diminished or even reversed, as observed for P27255. Under SD, *LanFD* expression was the highest in Palestyna (1.1–5.6 times higher than in 83A:476, P = 0.0024) and the lowest in P27255 (0.3–0.9 times lower than in 83A:476, P = 0.0123) (**Figure 6A**). Interestingly, these relations were changed after vernalization as follows: *LanFD* expression in P27255 compared to 83A:476 was 3.2–12.2 times higher (P = 0.0011), whereas in Palestyna 2.1–7.4 times higher than in 83A:476 (P = 0.0001). Under LD without vernalization, differences in *LanFD* expression between genotypes were rather low, accounting for up to a 2.3-fold increase in Palestyna (P = 0.0205) and up to a 5.0-fold increase in P27255 (P = 0.0000) compared to 83A:476. However, vernalization exaggerated these contrasts and observed *LanFD* expression in P27255 was up to 25.7 times higher than in 83A:476 (P = 0.0078) and up to 5.5 times higher than in Palestyna (P = 0.0032) (**Figure 6B**).

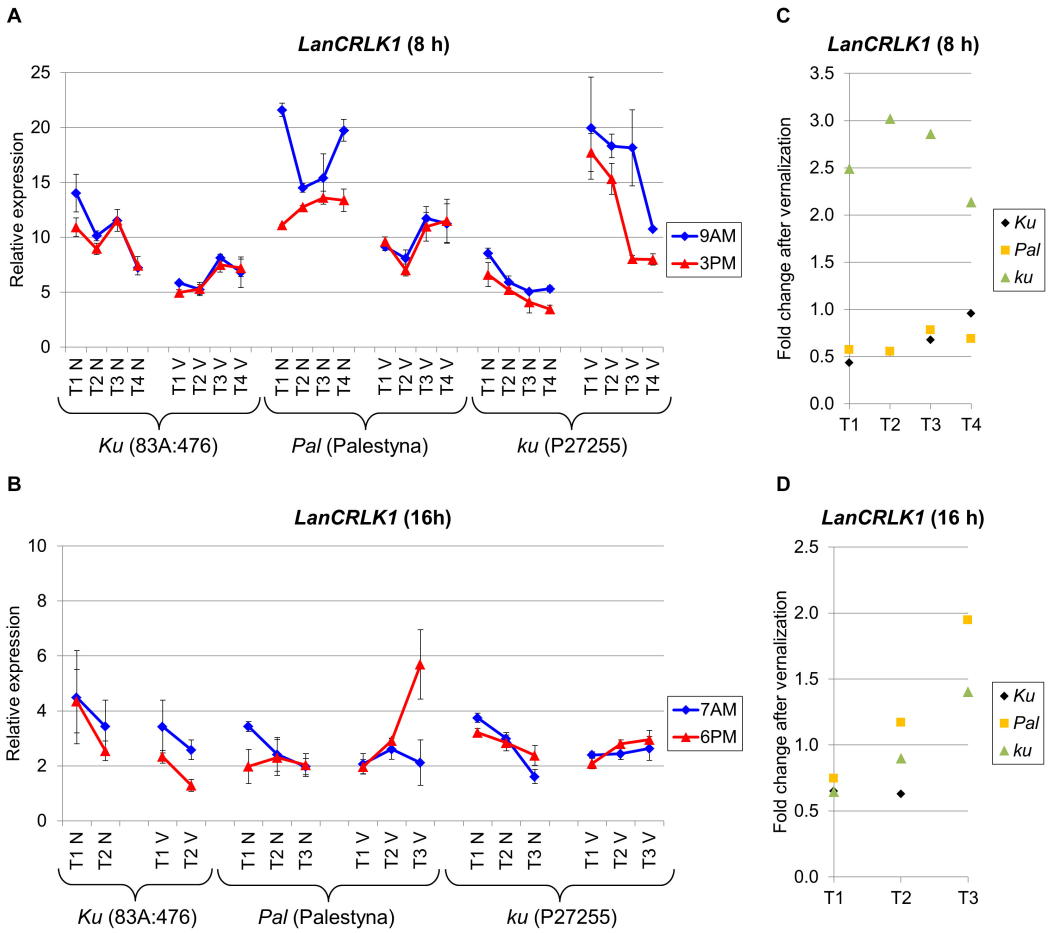

FIGURE 5 | Gene expression profile of the *LanCRLK1* gene in response to photoperiod and vernalization in three lines (83A:476, Palestyna, and P27255) carrying different *LanFTc1* alleles (*Ku*, *Pal,* and *ku*). **(A)** expression under 8-h photoperiod, **(B)** expression under 16-h photoperiod, **(C)** vernalization response under 8-h photoperiod, **(D)** vernalization response under 16-h photoperiod. T1-T4 stands for sampling terms (**Supplementary Table 5**), V for vernalized plants, and N for non-vernalized plants. Timespan of photoperiods: 8-h from 4 AM to 8 PM, 16-h from 4 AM to 8 PM. Two references were used for normalization (*LanDExH7* and *LanTUB6*) and one sample (*LanTUB6*) for inter-run calibration. Error bars indicate a standard deviation of 3 biological replicates, each representing a mean of 3 technical replicates.

The effect of vernalization on *LanFD* expression was negative in 83A:476 and Palestyna under both photoperiods (0.17-fold to 0.85-fold decrease), positive in P27255 under SD (up to 6.2-fold increase), and unstable in P27255 under LD (from 0.5-fold decrease to 1.4-fold increase) (**Figures 6C,D**). Genotypes differed in the circadian clock control of *LanFD* expression. Generally, in 83A:476 the levels were higher in the morning (up to 4.4 fold-increase), whereas in Palestine and P27255 in the evening (up to 4.5-fold and 3.1-fold increase, respectively).

LanUGT85A2 Expression Revealed a Growth-Dependent Decreasing Trend, Strong Circadian Clock Control, and Negative Response to Vernalization in All Lines Under Both Photoperiods

LanUGT85A2 is considered as an *L. angustifolius* homolog of the *A. thaliana UDP-glycosyltransferase 85A2* gene. The expression of this gene was the highest at the first sampling date in all lines and consecutively decreased during the experiment. Palestyna was revealed to have the biggest decrease of *LanUGT85A2* during the transition from juvenile to generative phase, whereas P27255 had the lowest. Indeed, this decrease of *LanUGT85A2* expression during plant growth under SD reached approximately 0.1-fold for 83A:476 ($P = 0.0114$), 0.3-fold for Palestyna ($P = 0.0033$) and 0.4-fold for P27255 ($P = 0.0003$), whereas under LD about 0.3-fold for 83A:476 ($P = 0.0501$), 0.02-fold for Palestyna ($P = 0.0182$) and 0.5-fold for P27255 ($P = 0.0196$).

Under SD, the highest first-term *LanUGT85A2* expression was observed in 83A:476, about 1.7-fold higher than in Palestyna ($P = 0.0448$) and P27255 (NS) (**Figure 7A**). These differences were doubled by vernalization. Contrary, under LD, the highest first-term expression was in P27255, 1.1-fold higher than in Palestyna (NS) and 3.7-fold higher than in 83A:476 ($P = 0.0006$), and these differences were tripled by vernalization (**Figure 7B**).

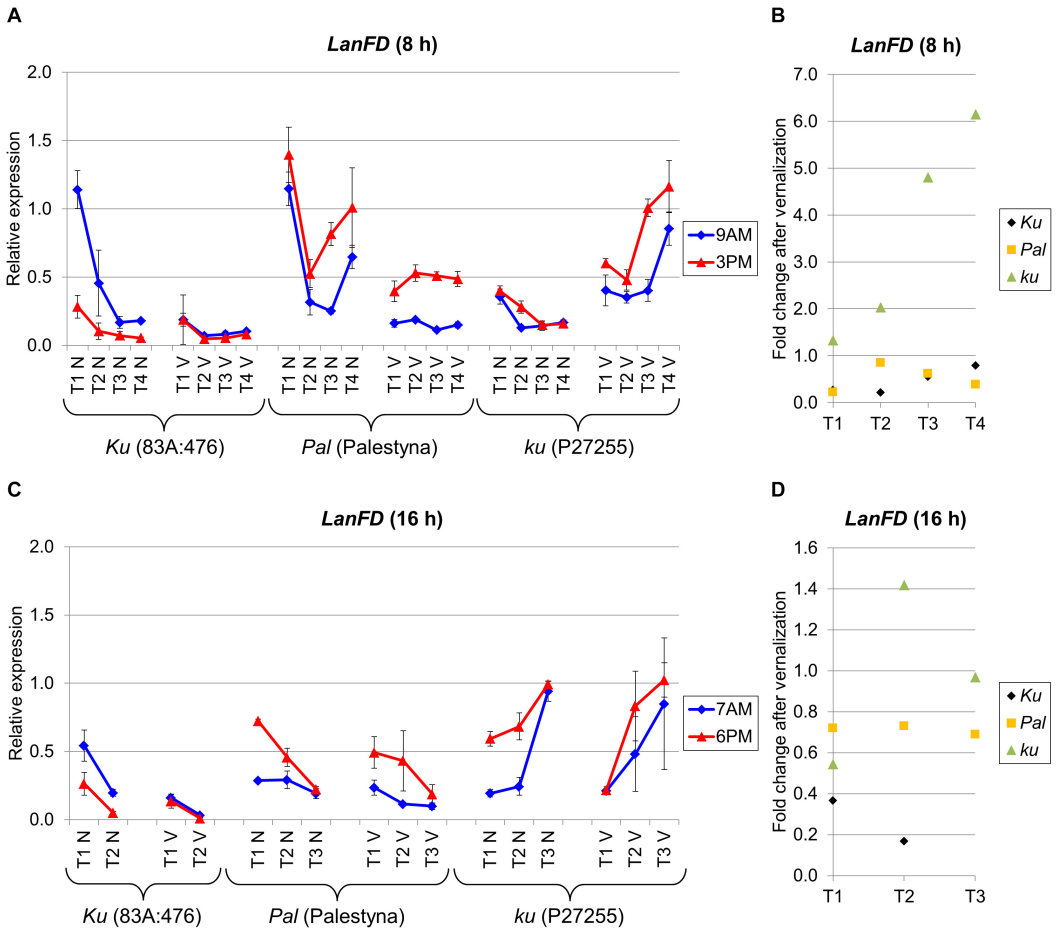

FIGURE 6 | Gene expression profile of the *LanFD* gene in response to photoperiod and vernalization in three lines (83A:476, Palestyna, and P27255) carrying different *LanFTc1* alleles (*Ku*, *Pal,* and *ku*). **(A)** expression under 8-h photoperiod, **(B)** expression under 16-h photoperiod, **(C)** vernalization response under 8-h photoperiod, **(D)** vernalization response under 16-h photoperiod. T1-T4 stands for sampling terms (**Supplementary Table 5**), V for vernalized plants, and N for non-vernalized plants. Timespan of photoperiods: 8-h from 4 AM to 8 PM, 16-h from 4 AM to 8 PM. Two references were used for normalization (*LanDExH7* and *LanTUB6*) and one sample (*LanTUB6*) for inter-run calibration. Error bars indicate a standard deviation of 3 biological replicates, each representing a mean of 3 technical replicates. A logarithmic scale was used to accommodate observed large differences in gene expression values.

Vernalization was observed to have a stable negative effect on *LanUGT85A2* gene expression, highlighted by an average 0.29-fold decrease under SD (**Figure 7C**) and a 0.28-fold decrease under LD (**Figure 7D**). Response to vernalization was the weakest in P27255 (0.38-fold) and the strongest in Palestyna (0.21-fold). Such a disproportion in vernalization response, combined with the observed difference in decreasing trend during plant growth, resulted in the highest *LanUGT85A2* expression in the P27255 line at the end of the experiment under both photoperiods (up to 31-fold increase compared to 83A:476 under LD, $P = 0.0233$).

The direction of circadian clock control was coherent across all genotypes and environments. *LanUGT85A2* expression was higher in the evening than in the morning for all terms, both with and without vernalization. Under SD, it increased during the day up to 13.9-fold in 83A:476 ($P = 0.0165$), 8.3-fold in Palestyna ($P = 0.0075$) and 28.2-fold in P27255 ($P = 0.0000$). Under LD, it increased up to 7.4-fold in 83A:476 ($P = 0.0326$), 12.8-fold in Palestyna ($P = 0.0005$) and 4.4-fold in P27255 ($P = 0.002$).

LanVIN3-1, *LanVIN3-2*, and *LanVIN3-3* Genes Revealed High Expression in *Ku* Without Vernalization

The *L. angustifolius* genome contains three homologs (named here as *LanVIN3-1*, *LanVIN3-2,* and *LanVIN3-3*) a *VIN3* gene that is involved in the vernalization response in *A. thaliana* (Sung and Amasino, 2004). Therefore, the transcriptional activity of these genes was also profiled. In general, *LanVIN3-1* revealed the highest expression, whereas *LanVIN3-3* the lowest (see **Supplementary Figures 3–5**).

All three copies revealed differences in expression levels between genotypes, usually in descending order, 83A:476 – Palestyna – P27255. Maximum differences between 83A:476

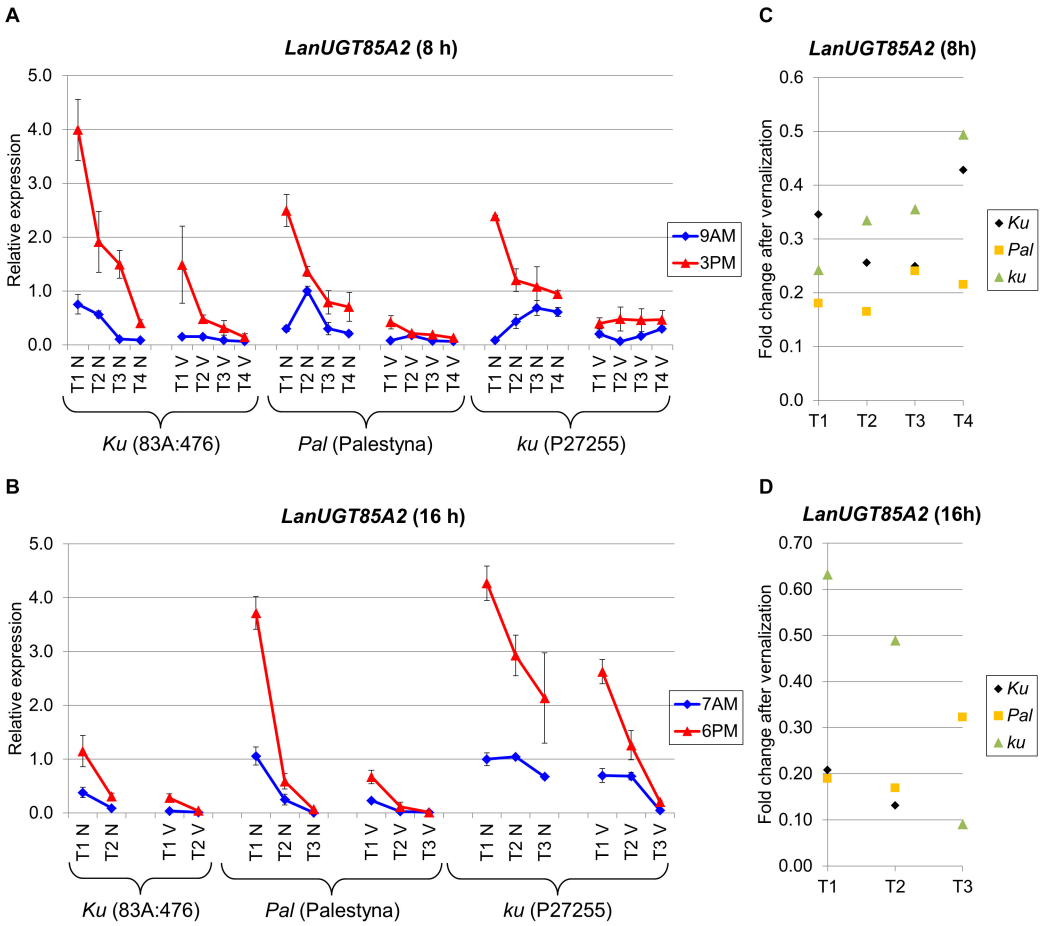

FIGURE 7 | Gene expression profile of the *LanUGT85A2* gene in response to photoperiod and vernalization in three lines (83A:476, Palestyna, and P27255) carrying different *LanFTc1* alleles (*Ku*, *Pal,* and *ku*). **(A)** expression under 8-hphotoperiod, **(B)** expression under 16-h photoperiod, **(C)** vernalization response under 8-h photoperiod, **(D)** vernalization response under 16-h photoperiod. T1-T4 stands for sampling terms (**Supplementary Table 5**), V for vernalized plants, and N for non-vernalized plants. Timespan of photoperiods: 8-h from 4 AM to 8 PM, 16-h from 4 AM to 8 PM. Two references were used for normalization (*LanDExH7* and *LanTUB6*) and one sample (*LanTUB6*) for inter-run calibration. Error bars indicate a standard deviation of 3 biological replicates, each representing a mean of 3 technical replicates.

and P27255 expression under LD reached 5.9-fold (*LanVIN3-1*, $P = 0.0016$), 25.6-fold (*LanVIN3-2*, $P = 0.0061$) and 8.4-fold (*LanVIN3-3*, $P = 0.0059$), whereas under SD these values were as follows: 4.8-fold (*LanVIN3-1*, $P = 0.0135$), 10.8-fold (*LanVIN3-2*, $P = 0.0036$) and 5.5-fold (*LanVIN3-3*, $P = 0.0072$). The expression levels of all three genes under LD were usually significantly higher in the evening than in the morning in all lines, whereas under SD, diurnal variations were frequently not significant or variable. Photoperiod conditions had a significant influence on expression changes during plant growth, especially for 83A:476. The expression levels of these genes in non-vernalized 83A:476 under LD increased by 2.3-fold (*LanVIN3-1*, $P = 0.0008$), 3.3-fold (*LanVIN3-2*, $P = 0.0048$) and 2.5-fold (*LanVIN3-3*, $P = 0.0036$) whereas under SD they decreased by up to 0.32-fold (*LanVIN3-1*, $P = 0.0000$), 0.37-fold (*LanVIN3-2*, $P = 0.0110$), and 0.24-fold (*LanVIN3-3*, $P = 0.0009$). The vernalization effect differed between genotypes and photoperiods. Under LD it was significant for 83A:476 (repression of all three genes, up to 0.43-fold) and Palestyna (induction of *LanVIN3-2* and *LanVIN3-3*, up to 2.0-fold), whereas under SD it was significant for 83A:476 (changing from repression, up to 0.18-fold, to induction, up to 2.3-fold) and P27255 (induction, up to 3.6-fold). To summarize, all *LanVIN3* homologs revealed different transcriptomic responses to vernalization than the *LanFTc1* and *LanAGL8* genes.

Besides VIN3, VRN5 protein is also considered to participate in the vernalization-induced epigenetic silencing in *A. thaliana* (Greb et al., 2007). Therefore, the expression of the latter gene was also profiled to supplement the analysis. All three *L. angustifolius* copies, *LanVRN5-1*, *LanVRN5-2,* and *LanVRN5-3*, were analyzed using one universal primer pair (**Supplementary Figure 6**). *LanVRN5* clade revealed an expression profile relatively similar to *LanVIN3*, especially to *LanVIN3-2*. Like *LanVIN3* genes, *LanVRN5* in 83A:476 revealed an increase of expression during plant growth under LD and decrease under SD. All lines showed a significant decrease of expression during the light phase under SD and usually not a significant diurnal trend under LD. In

both photoperiods without pre-sowing vernalization, 83A:476 revealed a significantly higher expression of *LanVRN5* than Palestyna and P27255. However, the vernalization responsiveness of *LanVRN5* considerably differed between photoperiods and genotypes. Under LD, only P27255 was responsive (showing repression), whereas under SD all lines responded but in different ways and with changing response during plant growth: namely from repression to induction in 83A:476, from induction to repression in Palestyna, and by continuously increasing induction in P27255. In vernalized plants under SD, *LanVRN5* expression was the highest in P27255.

DISCUSSION

INDEL Polymorphism in the *LanFTc1* Promoter as a Legume Model for Functional Studies Aiming Vernalization Responsiveness

FT is a major flowering time integrator gene, gathering signals from several pathways that detect environmental conditions (Turck et al., 2008). First studies on the conservation of *A. thaliana* genes in legumes have revealed the presence of the well-preserved homologs of many flowering time regulatory genes, including some representatives of *FT* clade found in *Pisum sativum* L., *Medicago truncatula* L., and *Glicyne max* (L.), Merrill (Hecht et al., 2005). When the first gene-based linkage map of *L. angustifolius* was published, it highlighted a conserved collinear block shared between the fragment of *M. truncatula* chromosome 7 and the so-called linkage group LG01 (currently NLL-10), carrying major early flowering locus *Ku* (Nelson et al., 2006). It was later revealed that the syntenic region in *M. truncatula* contained several *FT* homologs (Young et al., 2011). The development of a bacterial artificial chromosome library for the *L. angustifolius* nuclear genome opened a possibility of gene cloning by DNA hybridization and the sequencing of selected clones (Kasprzak et al., 2006). Such an approach, combined with novel high-throughput sequencing techniques and gene expression profiling, resulted in the identification of a candidate gene for *Ku* and enabled the formulation of the hypothesis that a 1423 bp deletion in the promoter region of this gene is a causal mutation conferring early flowering phenotype (Nelson et al., 2017). Then, two other overlapping deletion variants, covering 1208 bp (*Pal*) and 5162 bp (*Jul*) were identified (Taylor et al., 2019). In the *A. thaliana*, a variation in promoter length was found to modulate the photoperiodic response of *FT*, and some important regulatory blocks contributing to this response were identified (Adrian et al., 2010; Liu et al., 2014). However, comparative mapping revealed a low sequence similarity between *LanFTc1* and *A. thaliana FT* promoters, except RE-alpha and CCAAT boxes which were found at expected positions and indicated that *FT* promoter length in *L. angustifolius* may be at least as big as in *A. thaliana* (up to 7 kb) (Książkiewicz et al., 2016). All recognized *LanFTc1* deletions conferring *Ku*, *Pal,* and *Jul* alleles are located downstream of the pair of CCAAT boxes marking a putative beginning of the functional promoter (Książkiewicz et al., 2016; Nelson et al., 2017; Taylor et al., 2019). Thus, *L. angustifolius Ku*, *Pal,* and *Jul* alleles have both distal and proximal regions preserved (Taylor et al., 2019). However, deletion sequences encompassed candidate binding sites for many transcription factors, including those already evidenced to be involved in *FT* regulation in model plants (Nelson et al., 2017; Taylor et al., 2019). In *A. thaliana*, similarly to *L. angustifolius*, the functional *FT* promoter indels also retained distal and proximal regions (Adrian et al., 2010; Liu et al., 2014). On the contrary, the study involving the *FT* promoter from cotton provided evidence that the proximal region might play an important role in this species (Sang et al., 2019). To our knowledge, a model revealed for *L. angustifolius* is the only known legume example of *FT* promoter indel variation. However, in many legumes, *FT* genes were found to be associated with flowering traits. In the economically most important legume crop worldwide, a soybean, *Glycine max*, mutations in *FT* genes are responsible for at least three loci conferring early/late flowering, namely *E9* (*GmFT2a*), *E10* (*GmFT4*), and *qDTF-J1* (*GmFT5a*) (Takeshima et al., 2016; Zhao et al., 2016; Samanfar et al., 2017). Moreover, natural variations of the *GmFT2b* sequence are associated with soybean adaption to high−latitude regions (Chen et al., 2020). In *M. truncatula*, vernalization responsiveness and early flowering are conferred by the *FTa1* gene, whereas photoperiod response by the *FTb* gene (Laurie et al., 2011; Putterill et al., 2013). In pea (*Pisum sativum*), the *FTa1* gene corresponds to the pea *GIGAS* locus, which is essential for flowering under LD and promoting flowering under SD (Hecht et al., 2011). In chickpea, a major quantitative trait locus (QTL) for the flowering time under SD conditions was mapped in the region containing a cluster of three *FT* genes (*FTa1-FTa2-FTc*), which collectively showed upregulated expression in domesticated germplasm (Ortega et al., 2019). In the sister lupin crop species, white lupin (*L. albus* L.), one of the four major QTLs conferring early flowering and partial vernalization independence was found associated with the *FTa1* gene (Rychel et al., 2019). *L. angustifolius* genome contains two *FTa* and two *FTc* genes, which putatively arose from single copies by lineage-specific duplication, whereas the whole *FTb* subclade is absent (Książkiewicz et al., 2016). Indeed, *L. angustifolius* was recently used as a reference species in several phylogenetic studies addressing the influence of whole-genome and local duplications on the evolutionary fate of selected legume-specific and plant-wide gene clades (Przysiecka et al., 2015; Narożna et al., 2017; Szczepaniak et al., 2018; Czyż et al., 2020). The differences in the expression profiles for *FTa* and *FTc* genes, as established in the present study, provided novel evidence supporting the hypothesis on a functional divergence of particular duplicates.

Pal Allele Carrying Intermediate Phenology and Light Vernalization Responsiveness Provides Worldwide Opportunities for *L. angustifolius* Breeding

In the present study, based on experiments performed in a greenhouse under natural LD (12–17 h photoperiod), *Ku* and *Jul* alleles were found to be associated with early

flowering and vernalization independence, *Pal* with slightly delayed flowering and partial vernalization responsiveness, and *ku* with late flowering and high vernalization dependence. The same phenomenon was reported for the recent study performed in phytotron under natural 10–12 h photoperiod (intermediate between SD and LD) in Australia (Taylor et al., 2019). However, we observed relatively high differences in flowering time for early lines (*Ku*, *Pal,* and *Jul*) in a greenhouse between 2014 and 2015 repeats, accounting for about two weeks on average (earlier in 2014). These differences can be attributed to the variation in temperature which occurred during these experiments. During the first 70 days of the 2014 experiment, we observed 31 days with maximum temperature ≥25°C and 9 days with ≥30°C, whereas in '2015 these numbers were much lower, 3 and 0 days, respectively. The higher temperature could advance flowering because it is shown to strongly accelerate flowering in model plants as well as in many other plant species (Parmesan and Yohe, 2003; Thines et al., 2014). Moreover, the average photoperiod in 2014 was about 2 h longer than in 2015 due to differences in sowing terms. Indeed, our subsequent controlled-environment study revealed that even early *L. angustifolius* germplasm is responsive to LD conditions and accelerated transition between particular developmental phases by about 18–25 days compared to SD. The observed phenology of the *Pal* allele can be very beneficial for *L. angustifolius* cultivation in the era of changing climate, especially in Europe and Australia where the majority of worldwide lupin production occurs. Thus, the European land climate experienced rapid warming in recent decades, resulting in the mean year temperature surge to approximately 2°C above the 1910–1960 average (NOAA, 2020). Climate warming raised multiple challenging issues for grain legume breeders, including higher water deficits and severe drought periods, propagation of pests and diseases as well as de-regulation of temperature-based control of growth and development processes (Vadez et al., 2012; Scheelbeek et al., 2018; Lippmann et al., 2019). Affected regulatory pathways include, among others, the flowering time control (Nelson et al., 2010). The rapid flowering of domesticated germplasm may favor drought escape and adaptation for spring sowing in higher latitudes (Annicchiarico et al., 2010, 2018; Berger et al., 2017). However, the observed extension of the vegetation period has raised the demand for germplasm with intermediate phenology and cross-environment adaptation. Such research was recently initiated in *L. albus* in three European locations contrasting sowing time (autumn or spring) and climate type (Annicchiarico et al., 2019). Climatic variables were also addressed in an *L. angustifolius* genome-wide association study, providing some candidate polymorphisms that await further exploitation (Mousavi-Derazmahalleh et al., 2018a). *L. angustifolius Pal* allele confers flowering time and vernalization responsiveness phenotype intermediating between domesticated and wild lines. As this phenotype is consistent within the large range of photoperiod conditions (8, 10–12, and 16–17 h), it may be found applicable for all regions where lupins are currently cultivated.

LanFTc1, *LanAGL8*, *LanCRLK1*, and *LanUGT85A2* Are Candidate Genes Involved in the Vernalization Responsiveness of *L. angustifolius*

Previous studies have highlighted the negative association of *LanFTc1* and *LanAGL8* gene expression with the number of days to flowering in *L. angustifolius*, mapping population and the positive direction of such association for *LanFD*, *LanCRLK1,* and *LanUGT85A2* genes (Nelson et al., 2017; Plewiński et al., 2019). The present study revealed that these genes differ in vernalization responsiveness between genotypes and photoperiods. *LanFTc1* and *LanAGL8* genes were found to be highly induced by vernalization in wild germplasm, whereas *LanUGT85A2* was found to be significantly suppressed (**Table 4**). *LanAGL8* protein sequence revealed the highest similarity to *A. thaliana FRUITFULL* (*FUL*, *AGAMOUS-LIKE 8*, AT5G60910) and *APETALA1* (*AP1*, *AGAMOUS-LIKE 7*, AT1G69120) genes. Both *AP1* and *FUL* play a role in floral meristem identity but have different functions. *AP1* controls the formation of sepals and petals whereas *FUL* is involved in cauline leaf and fruit development (Irish and Sussex, 1990; Gu et al., 1998). These genes revealed tissue-specific expression during generative organ development (Irish and Sussex, 1990; Mandel and Yanofsky, 1995; Klepikova et al., 2016). In the present study, high levels of *LanAGL8* expression were revealed in leaf tissue. Moreover, the expression profiles and vernalization responsiveness of *LanAGL8* and *LanFTc1* were very similar. Both genes revealed comparable circadian clock control, i.e., morning induction in *Pal* line under short days. Confronting these observations with the information on a 100% association between the *LanFTc1* genotype and flowering time phenotype in a large germplasm collection (Nelson et al., 2017; Taylor et al., 2019), the conclusion can be raised that *LanAGL8* acts putatively downstream of *LanFTc1* in *L. angustifolius*, in which *LanAGL8* may perform a similar function, like its homolog in cereals, an *AP1*-like gene called *VRN1*, which regulates the transition from vegetative to generative phase in response to vernalization and is expressed in many organs, including leaves (Trevaskis et al., 2003; Yan et al., 2003). Indeed, the wheat homolog of *FT*, (*VRN3*), activates expression of *VRN1* in leaves and shoot apical meristem, promoting flowering under inductive long days (Li et al., 2015). As a MADS box transcription factor, VRN1 binds to many targets in the genome and may regulate many genes, linking vernalization and photoperiod pathways (Deng et al., 2015). Moreover, the allelic diversity of *VRN1* copies provides wide plasticity of temperature-based responses in winter wheat (Dixon et al., 2019).

In this study, we also revealed differences in the vernalization responsiveness of a *LanFD* gene between early and late flowering germplasm. In wheat, FD−like, VRN3, and 14−3−3 proteins form together a florigen activation complex which can bind the *VRN1* promoter, therefore a variation in *FD* expression may modulate the effect of mobile florigen signal (Li et al., 2015). Results obtained in this study, are supported by a significant correlation between the *LanFD* gene expression profile and vernalization responsiveness in the *L. angustifolius* mapping

population (Plewiński et al., 2019), which indicates that *LanFD* may contribute to *FT* regulatory function, especially in the wild, vernalization-responsive germplasm.

Our recent expression quantitative trait loci (eQTL) mapping study provided transcriptomic evidence for the contribution of several genes acting in C-repeat binding factor (CBF) cold responsiveness (*LanCRLK1),* and in UDP-glycosyltransferases (*LanUGT85A2)* pathways in the vernalization response via *LanFTc1* in *L. angustifolius* (Plewiński et al., 2019). *LanCRLK1* is a homolog of *A. thaliana CALCIUM/CALMODULIN-REGULATED RECEPTOR-LIKE KINASE 1*, which is the first component in the cold responsiveness pathway (Yang et al., 2010). Downstream genes in this pathway, the C-repeat binding factors (*CBF*) and *INDUCER OF CBF EXPRESSION 1* (*ICE1*), provide regulatory links to *FLOWERING LOCUS C* (*FLC*) (Kim et al., 2004; Lee et al., 2015). The present study has highlighted the positive vernalization responsiveness of the *LanCRLK1* gene but only in wild germplasm under SD. In other genotype x environment combinations, the response was *quasi* thermoneutral. This finding is coherent with the general observation that CBF cold responsiveness pathway is downregulated and less effective under LD conditions than under SD (Lee and Thomashow, 2012). The expression profile of *LanCRLK1* did not provide convincing evidence on the contribution of this gene in the vernalization responsiveness of *L. angustifolius*. Nevertheless, the reduction of *LanCRLK1* expression in the evening, combined with the decreasing trend during development that was revealed in this study for vernalized *ku* line under LD, may explain the direction of the association between the *LanCRLK1* expression pattern and the vernalization responsiveness observed in the *L. angustifolius* mapping population e-QTL study, which was also performed under LD with partial vernalization (Plewiński et al., 2019). The question arises as to whether these differences in the *LanCRLK1* gene expression profile between the *Ku*/*Pal* and the *ku* lines, may have consequences in terms of cold acclimation and freezing tolerance of early flowering lines. A negative correlation between early phenology and cold acclimation could be a very undesirable trait hampering the autumn sowing of *L. angustifolius* in many regions of Southern Europe.

This study evidenced the negative response of *LanUGT85A2* to vernalization in all genotypes under both photoperiods. The genotypes explored in this study revealed different responses to photoperiod, and under SD, the *LanUGT85A2* expression was highest in the early flowering line, whereas under LD, it was in late flowering. Indeed, during the *L. angustifolius* mapping population e-QTL assay, which was performed under LD with mild vernalization, *LanUGT85A2* expression revealed a significant positive correlation with the late-flowering phenotype (Plewiński et al., 2019). *LanUGT85A2* is a representative of the UDP-glycosyltransferases protein family. In *A. thaliana*, a relatively close homolog of this gene, *UGT87A2*, promotes flowering in the vernalization and gibberellin pathways by repression of *FLC* (Wang B. et al., 2012). Similarly, ectopic over-expression in tobacco of a putative glycosyltransferase gene 1, *PtGT1*, derived from poplar (*Populus tomentosa* Carr.), resulted in an early flowering phenotype (Wang Y.-W. et al., 2012). Contrary, another *A. thaliana* homolog, *UGT84A2*, delays flowering by activation of the indole-3-butyric acid (IBA) pathway, leading to down-regulation of *AUXIN RESPONSE FACTOR 6* (*ARF6*) and *ARF8* genes, and, consequently *FT* (Zhang et al., 2017). Taking into consideration the direction of the association between *LanUGT85A2* expression and time to flowering, the latter mechanism seems to be more probable in *L. angustifolius* than those of *UGT87A2* and *PtGT1*.

This research highlighted the hypothetical involvement of *FLC*-related genes in *L. angustifolius* vernalization-dependent flowering time regulation. However, legume genomes, except for soybean, generally do not have *FLC* homologs (Hecht et al., 2005; Lyu et al., 2020). Nevertheless, other genes from the vernalization pathway, including some potential activators and repressors of *FLC*, are present (Hane et al., 2017). Interestingly, soybean has retained one *FLC* copy within its genome and does not require vernalization to initiate flowering. *FLC* in this species is involved in long-term low temperature-triggered late flowering by inhibiting *FT* gene expression (Lyu et al., 2020).

In *Arabidopsis*, vernalization-dependent silencing of the *FLC* gene is performed by *VIN3* and *VRN5* proteins which contribute to H3K27me3 and H3K9me2 enrichments during cold periods (Sung and Amasino, 2004; Greb et al., 2007; Kim and Sung, 2013). Despite their similar function in *A. thaliana*, *VIN3* and *VRN5* genes differ in expression profiles and vernalization responsiveness. Namely, *VIN3* expression in *A. thaliana* is very low and highly induced during vernalization, but soon after the end of the cold period, it decreases again to pre-vernalization level; whereas the *VRN5* gene is constitutively expressed at much higher levels than *VIN3* with additional high upregulation after the end of vernalization (Kim and Sung, 2013). In our study, *LanVIN3* genes revealed significantly higher relative expression than *LanVRN5*. Apart from this difference, expression profiles of *LanVRN5* and *LanVIN3* homologs were similar to each other. Moreover, this research provided lines of evidence for the high expression of three *LanVIN3* homologs in early flowering 83A:476 lines without vernalization, highlighting the opposite effects of vernalization for particular genotypes. The observed differences in vernalization responses and expression profiles of *LanVIN3* and *LanVRN5* genes did not match observed differences in phenotypes (time to flowering). This may indicate that *LanVIN3* and *LanVRN5* genes are not involved in the vernalization response in *L. angustifolius*.

DATA AVAILABILITY STATEMENT

All datasets presented in this study are included in the article/**Supplementary Material**.

AUTHOR CONTRIBUTIONS

SR-B designed experiments and performed plant phenotyping for time to flowering and vernalization responsiveness, plant genotyping with molecular markers, and gene expression profiling by quantitative PCR. PP performed RNA isolation

and quantification. RG participated in the concept of the study and the interpretation of the results. BK contributed to data analysis and statistics. MK analyzed the data, interpreted the results, prepared the figures, and drafted the manuscript. All authors approved the final manuscript.

FUNDING

This study was supported by the Polish National Science Centre Project No. 2014/15/N/NZ9/03919.

ACKNOWLEDGMENTS

The authors would like to thank Magdalena Tomaszewska from the Department of Genomics of the Institute of Plant Genetics, Polish Academy of Sciences for help in performing plant experiments. The authors also thank Bogdan Wolko from the same department for mentoring during the project implementation.

SUPPLEMENTARY MATERIAL

The Supplementary Material for this article can be found online at: https://www.frontiersin.org/articles/10.3389/fpls.2020.572135/full#supplementary-material

Supplementary Table 1 | Accession numbers and information on domestication status and country of origin of *L. angustifolius* lines used in the study.

Supplementary Table 2 | Primers used in the study.

Supplementary Table 3 | Air temperature (daily mean and maximum) and daily sunshine hours recorded by the local/nearest meteorological station (Poznań-Ławica, 5.1 km) and theoretical photoperiod hours calculated for this location during the 2014 experiment.

Supplementary Table 4 | Air temperature (daily mean and maximum) and daily sunshine hours recorded by the local/nearest meteorological station (Poznań-Ławica, 5.1 km) and theoretical photoperiod hours calculated for this location during the 2015 experiment.

Supplementary Table 5 | Sampling terms selected for gene expression profiling.

Supplementary Table 6 | Leaf expression of selected flowering-related genes (reads per kilobase million, RPKM) derived from the transcriptome sequencing of *L. angustifolius* mapping population and correlation with vernalization responsiveness (*ku*).

Supplementary Table 7 | R2 and PCR efficiency values obtained for standard curves.

Supplementary Table 8 | Comparison of LanFTc1_INDEL2 marker scores and time to flowering in response to vernalization observed during '2014 experiment.

Supplementary Table 9 | Comparison of LanFTc1_INDEL2 marker scores and time to flowering in response to vernalization observed during '2015 experiment.

Supplementary Figure 1 | Gene expression profile of the *LanFTa2* gene in response to photoperiod and vernalization in three lines (83A:476, Palestyna, and P27255) carrying different *LanFTc1* alleles (*Ku*, *Pal,* and *ku*).

Supplementary Figure 2 | Gene expression profile of the *LanFTc2* gene in response to photoperiod and vernalization in three lines (83A:476, Palestyna, and P27255) carrying different *LanFTc1* alleles (*Ku*, *Pal,* and *ku*).

Supplementary Figure 3 | Gene expression profile of the *LanVIN3-1* gene in response to photoperiod and vernalization in three lines (83A:476, Palestyna, and P27255) carrying different *LanFTc1* alleles (*Ku*, *Pal,* and *ku*).

Supplementary Figure 4 | Gene expression profile of the *LanVIN3-2* gene in response to photoperiod and vernalization in three lines (83A:476, Palestyna, and P27255) carrying different *LanFTc1* alleles (*Ku*, *Pal,* and *ku*).

Supplementary Figure 5 | Gene expression profile of the *LanVIN3-3* gene in response to photoperiod and vernalization in three lines (83A:476, Palestyna, and P27255) carrying different *LanFTc1* alleles (*Ku*, *Pal,* and *ku*).

Supplementary Figure 6 | Gene expression profile of *LanVRN5* genes in response to photoperiod and vernalization in three lines (83A:476, Palestyna, and P27255) carrying different *LanFTc1* alleles (*Ku*, *Pal,* and *ku*).

Supplementary Data Sheet 1 | Gene expression data and calculations for *LanAGL8*, *LanCRLK1*, *LanFD*, *LanFTa1*, *LanFTa2*, *LanFTc1*, *LanFTc2,* and *LanUGT85A2* genes, obtained for two photoperiod variants (8- and 16-h) in response to vernalization in three lines (83A:476, Palestyna, and P27255) carrying different *LanFTc1* alleles (*Ku*, *Pal,* and *ku*).

REFERENCES

Abe, M., Kobayashi, Y., Yamamoto, S., Daimon, Y., Yamaguchi, A., Ikeda, Y., et al. (2005). *FD*, a bZIP protein mediating signals from the floral pathway integrator *FT* at the shoot apex. *Science* 309, 1052–1056. doi: 10.1126/science.1115983

Abraham, E. M., Ganopoulos, I., Madesis, P., Mavromatis, A., Mylona, P., Nianiou-Obeidat, I., et al. (2019). The use of lupin as a source of protein in animal feeding: genomic tools and breeding approaches. *Int. J. Mol. Sci.* 20:851. doi: 10.3390/ijms20040851

Adhikari, K. N., Buirchell, B. J., and Sweetingham, M. W. (2012). Length of vernalization period affects flowering time in three lupin species. *Plant Breed.* 131, 631–636. doi: 10.1111/j.1439-0523.2012.01996.x

Adrian, J., Farrona, S., Reimer, J. J., Albani, M. C., Coupland, G., and Turck, F. (2010). cis-Regulatory elements and chromatin state coordinately control temporal and spatial expression of *FLOWERING LOCUS T* in *Arabidopsis*. *Plant Cell* 22, 1425–1440. doi: 10.1105/tpc.110.074682

Annicchiarico, P., and Carroni, A. M. (2009). Diversity of white and narrow-leafed lupin genotype adaptive response across climatically-contrasting Italian environments and implications for selection. *Euphytica* 166, 71–81. doi: 10.1007/s10681-008-9836-9

Annicchiarico, P., Harzic, N., and Carroni, A. M. (2010). Adaptation, diversity, and exploitation of global white lupin (*Lupinus albus* L.) landrace genetic resources. *Field Crops Res.* 119, 114–124. doi: 10.1016/j.fcr.2010.06.022

Annicchiarico, P., Nazzicari, N., Ferrari, B., Harzic, N., Carroni, A. M., Romani, M., et al. (2019). Genomic prediction of grain yield in contrasting environments for white lupin genetic resources. *Mol. Breed.* 39:142.

Annicchiarico, P., Romani, M., and Pecetti, L. (2018). White lupin (*Lupinus albus*) variation for adaptation to severe drought stress. *Plant Breed.* 137, 782–789. doi: 10.1111/pbr.12642

Berger, J. D., Buirchell, B. J., Luckett, D. J., and Nelson, M. N. (2012). Domestication bottlenecks limit genetic diversity and constrain adaptation in narrow-leafed lupin (*Lupinus angustifolius* L.). *Theor. Appl. Genet.* 124, 637–652. doi: 10.1007/s00122-011-1736-z

Berger, J. D., Shrestha, D., and Ludwig, C. (2017). Reproductive strategies in mediterranean legumes: trade-offs between phenology, seed size and vigor within and between wild and domesticated *Lupinus* species collected along aridity gradients. *Front. Plant Sci.* 8:548. doi: 10.3389/fpls.2017.00548

Cao, S., Kumimoto, R. W., Gnesutta, N., Calogero, A. M., Mantovani, R., and Holt, B. F. III (2014). A distal *CCAAT/NUCLEAR FACTOR Y* complex promotes chromatin looping at the *FLOWERING LOCUS T* promoter and regulates the timing of flowering in *Arabidopsis*. *Plant Cell* 26, 1009–1017. doi: 10.1105/tpc.113.120352

Chen, L., Cai, Y., Qu, M., Wang, L., Sun, H., Jiang, B., et al. (2020). Soybean adaption to high-latitude regions is associated with natural variations of *GmFT2b*, an ortholog of *FLOWERING LOCUS T*. *Plant Cell Environ.* 43, 934–944. doi: 10.1111/pce.13695

Cowling, W. A. (2020). "Genetic diversity in narrow-leafed lupin breeding after the domestication bottleneck," in *The Lupin Genome*, eds K. B. Singh, L. G. Kamphuis, and M. N. Nelson, (Cham: Springer International Publishing), 1–17. doi: 10.1007/978-3-030-21270-4_1

Cowling, W. A., Hamblin, J., Wood, P. M., and Gladstones, J. S. (1987). Resistance to Phomopsis stem blight in *Lupinus angustifolius* L. *Crop Sci.* 27, 648–652. doi: 10.2135/cropsci1987.0011183x002700040007x

Czyż, K. B., Książkiewicz, M., Koczyk, G., Szczepaniak, A., Podkowiński, J., and Naganowska, B. (2020). A tale of two families: whole genome and segmental duplications underlie glutamine synthetase and phosphoenolpyruvate carboxylase diversity in narrow-leafed lupin (*Lupinus angustifolius* L.). *Int. J. Mol. Sci.* 21:2580. doi: 10.3390/ijms21072580

Deng, W., Casao, M. C., Wang, P., Sato, K., Hayes, P. M., Finnegan, E. J., et al. (2015). Direct links between the vernalization response and other key traits of cereal crops. *Nat. Commun.* 6:5882.

Dixon, L. E., Karsai, I., Kiss, T., Adamski, N. M., Liu, Z., Ding, Y., et al. (2019). *VERNALIZATION1* controls developmental responses of winter wheat under high ambient temperatures. *Development* 146:dev172684. doi: 10.1242/dev.172684

Evans, J., Turner, G. L., O'connor, G. E., and Bergersen, F. J. (1987). Nitrogen fixation and accretion of soil nitrogen by field-grown lupins (*Lupinus angustifolius*). *Field Crops Res.* 16, 309–322. doi: 10.1016/0378-4290(87)90069-4

Foyer, C. H., Lam, H. M., Nguyen, H. T., Siddique, K. H., Varshney, R. K., Colmer, T. D., et al. (2016). Neglecting legumes has compromised human health and sustainable food production. *Nat. Plants* 2:16112.

French, R. J., and Buirchell, B. (2005). Lupin: the largest grain legume crop in Western Australia, its adaptation and improvement through plant breeding. *Austr. J. Agric. Res.* 56, 1169–1180. doi: 10.1071/ar05088

Gao, L.-L., Hane, J. K., Kamphuis, L. G., Foley, R., Shi, B.-J., Atkins, C. A., et al. (2011). Development of genomic resources for the narrow-leafed lupin (*Lupinus angustifolius*): construction of a bacterial artificial chromosome (BAC) library and BAC-end sequencing. *BMC Genomics* 12:521. doi: 10.1186/1471-2164-12-521

Gladstones, J., and Hill, G. (1969). Selection for economic characters in *Lupinus angustifolius* and *L. digitatus*. 2. Time of flowering. *Austr. J. Exp. Agric.* 9, 213–220. doi: 10.1071/ea9690213

Greb, T., Mylne, J. S., Crevillen, P., Geraldo, N., An, H., Gendall, A. R., et al. (2007). The PHD finger protein VRN5 functions in the epigenetic silencing of *Arabidopsis FLC*. *Curr. Biol.* 17, 73–78. doi: 10.1016/j.cub.2006.11.052

Gu, Q., Ferrandiz, C., Yanofsky, M. F., and Martienssen, R. (1998). The *FRUITFULL* MADS-box gene mediates cell differentiation during *Arabidopsis* fruit development. *Development* 125, 1509–1517.

Hane, J. K., Ming, Y., Kamphuis, L. G., Nelson, M. N., Garg, G., Atkins, C. A., et al. (2017). A comprehensive draft genome sequence for lupin (*Lupinus angustifolius*), an emerging health food: insights into plant-microbe interactions and legume evolution. *Plant Biotechnol. J.* 15, 318–330. doi: 10.1111/pbi.12615

Hauschke, D., Kieser, M., and Hothorn, L. A. (1999). Proof of safety in toxicology based on the ratio of two means for normally distributed data. *Biometric. J. J. Math. Methods Biosci.* 41, 295–304. doi: 10.1002/(sici)1521-4036(199906)41:3<295::aid-bimj295>3.0.co;2-2

Hecht, V., Foucher, F., Ferrandiz, C., Macknight, R., Navarro, C., Morin, J., et al. (2005). Conservation of *Arabidopsis* flowering genes in model legumes. *Plant Physiol.* 137, 1420–1434. doi: 10.1104/pp.104.057018

Hecht, V., Laurie, R. E., Vander Schoor, J. K., Ridge, S., Knowles, C. L., Liew, L. C., et al. (2011). The pea *GIGAS* gene is a *FLOWERING LOCUS T* homolog necessary for graft-transmissible specification of flowering but not for responsiveness to photoperiod. *Plant Cell* 23, 147–161. doi: 10.1105/tpc.110.081042

Huyghe, C. (1991). Winter growth of autumn-sown white lupin (*Lupinus albus* L.) *main apex growth model*. *Ann. Bot.* 67, 429–434. doi: 10.1093/oxfordjournals.aob.a088160

Irish, V. F., and Sussex, I. M. (1990). Function of the apetala-1 gene during *Arabidopsis* floral development. *Plant Cell* 2, 741–753. doi: 10.2307/3869173

Jago, M. V., Peterson, J. E., Payne, A. L., and Campbell, D. G. (1982). Lupinosis: response of sheep to different doses of phomopsin. *Austr. J. Exp. Biol. Med. Sci.* 60, 239–251. doi: 10.1038/icb.1982.29

Kamel, K. A., Święcicki, W., Kaczmarek, Z., and Barzyk, P. (2016). Quantitative and qualitative content of alkaloids in seeds of a narrow-leafed lupin (*Lupinus angustifolius* L.) collection. *Genet. Resourc. Crop Evol.* 63, 711–719. doi: 10.1007/s10722-015-0278-7

Kamphuis, L. G., Hane, J. K., Nelson, M. N., Gao, L., Atkins, C. A., and Singh, K. B. (2015). Transcriptome sequencing of different narrow-leafed lupin tissue types provides a comprehensive uni-gene assembly and extensive gene-based molecular markers. *Plant Biotechnol. J.* 13, 14–25. doi: 10.1111/pbi.12229

Kasprzak, A., Safár, J., Janda, J., Dolezel, J., Wolko, B., and Naganowska, B. (2006). The bacterial artificial chromosome (BAC) library of the narrow-leafed lupin (*Lupinus angustifolius* L.). *Cell. Mol. Biol. Lett.* 11, 396–407.

Kearse, M., Moir, R., Wilson, A., Stones-Havas, S., Cheung, M., Sturrock, S., et al. (2012). Geneious basic: an integrated and extendable desktop software platform for the organization and analysis of sequence data. *Bioinformatics* 28, 1647–1649. doi: 10.1093/bioinformatics/bts199

Kim, D.-H., and Sung, S. (2013). Coordination of the vernalization response through a *VIN3* and *FLC* gene family regulatory network in *Arabidopsis*. *Plant Cell* 25, 454–469. doi: 10.1105/tpc.112.104760

Kim, H.-J., Hyun, Y., Park, J.-Y., Park, M.-J., Park, M.-K., Kim, M. D., et al. (2004). A genetic link between cold responses and flowering time through *FVE* in *Arabidopsis thaliana*. *Nat. Genet.* 36, 167–171. doi: 10.1038/ng1298

Klepikova, A. V., Kasianov, A. S., Gerasimov, E. S., Logacheva, M. D., and Penin, A. A. (2016). A high resolution map of the *Arabidopsis thaliana* developmental transcriptome based on RNA-seq profiling. *Plant J.* 88, 1058–1070. doi: 10.1111/tpj.13312

Kouris-Blazos, A., and Belski, R. (2016). Health benefits of legumes and pulses with a focus on Australian sweet lupins. *Asia Pac. J. Clin. Nutr.* 25, 1–17. doi: 10.1039/9781788015721-00001

Kozak, B., Galek, R., Zalewski, D., and Sawicka-Sienkiewicz, E. (2019). Preliminary genetic map of a new recombinant inbred line population for narrow-leafed lupin (*Lupinus angustifolius* L.). *Agronomy* 9:653. doi: 10.3390/agronomy9100653

Książkiewicz, M., Nazzicari, N., Yang, H., Nelson, M. N., Renshaw, D., Rychel, S., et al. (2017). A high-density consensus linkage map of white lupin highlights synteny with narrow-leafed lupin and provides markers tagging key agronomic traits. *Sci. Rep.* 7:15335.

Książkiewicz, M., Rychel, S., Nelson, M. N., Wyrwa, K., Naganowska, B., and Wolko, B. (2016). Expansion of the phosphatidylethanolamine binding protein family in legumes: a case study of *Lupinus angustifolius* L. *FLOWERING LOCUS T homologs, LanFTc1* and *LanFTc2*. *BMC Genomics* 17:820. doi: 10.1186/s12864-016-3150-z

Książkiewicz, M., Wójcik, K., Irzykowski, W., Bielski, W., Rychel, S., Kaczmarek, J., et al. (2020). Validation of *Diaporthe toxica* resistance markers in European *Lupinus angustifolius* germplasm and identification of novel resistance donors for marker-assisted selection. *J. Appl. Genet.* 61, 1–12. doi: 10.1007/s13353-019-00521-y

Kurlovich, B. S. (2002). *Lupins: Geography, Classification, Genetic Resources and Breeding*. St. Petersburg: Bogouslav Kourlovitch.

Lambers, H., Clements, J. C., and Nelson, M. N. (2013). How a phosphorus-acquisition strategy based on carboxylate exudation powers the success and agronomic potential of lupines (*Lupinus*, Fabaceae). *Am. J. Bot.* 100, 263–288. doi: 10.3732/ajb.1200474

Landers, K. F. (1995). Vernalization responses in narrow-leafed lupin (*Lupinus angustifolius*) genotypes. *Austr. J. Agric. Res.* 46, 1011–1025. doi: 10.1071/ar9951011

Laurie, R. E., Diwadkar, P., Jaudal, M., Zhang, L., Hecht, V., Wen, J., et al. (2011). The *Medicago FLOWERING LOCUS T* homolog, *MtFTa1*, is a key regulator of flowering time. *Plant Physiol.* 156, 2207–2224. doi: 10.1104/pp.111.180182

Lee, C.-M., and Thomashow, M. F. (2012). Photoperiodic regulation of the C-repeat binding factor (CBF) cold acclimation pathway and freezing tolerance in *Arabidopsis thaliana*. *Proc. Natl. Acad. Sci. U.S.A.* 109, 15054–15059. doi: 10.1073/pnas.1211295109

Lee, J.-H., Jung, J.-H., and Park, C.-M. (2015). INDUCER OF CBF EXPRESSION 1 integrates cold signals into *FLOWERING LOCUS* C-mediated flowering pathways in *Arabidopsis*. *Plant J.* 84, 29–40. doi: 10.1111/tpj.12956

Li, C., Lin, H., and Dubcovsky, J. (2015). Factorial combinations of protein interactions generate a multiplicity of florigen activation complexes in wheat and barley. *Plant J.* 84, 70–82. doi: 10.1111/tpj.12960

Lippmann, R., Babben, S., Menger, A., Delker, C., and Quint, M. (2019). Development of wild and cultivated plants under global warming conditions. *Curr. Biol.* 29, R1326–R1338.

Liu, L., Adrian, J., Pankin, A., Hu, J., Dong, X., Von Korff, M., et al. (2014). Induced and natural variation of promoter length modulates the photoperiodic response of *FLOWERING LOCUS T*. *Nat. Commun.* 5:4558.

Lyu, J., Cai, Z., Li, Y., Suo, H., Yi, R., Zhang, S., et al. (2020). The floral repressor *GmFLC*-like is involved in regulating flowering time mediated by low temperature in soybean. *Int. J. Mol. Sci.* 21:1322. doi: 10.3390/ijms2104 1322

Mandel, M. A., and Yanofsky, M. F. (1995). The *Arabidopsis AGL8* MADS box gene is expressed in inflorescence meristems and is negatively regulated by *APETALA1*. *Plant Cell* 7, 1763–1771. doi: 10.1105/tpc.7.11.1763

Mikołajczyk, J. (1966). Genetic studies in *Lupinus angustifolius*. Part. III. Inheritance of the alkaloid content, seed hardness and length of the growing season in blue lupin. *Genet. Polon.* 7, 181–196.

Mousavi-Derazmahalleh, M., Bayer, P. E., Nevado, B., Hurgobin, B., Filatov, D., Kilian, A., et al. (2018a). Exploring the genetic and adaptive diversity of a pan-mediterranean crop wild relative: narrow-leafed lupin. *Theor. Appl. Genet.* 131, 887–901. doi: 10.1007/s00122-017-3045-7

Mousavi-Derazmahalleh, M., Nevado, B., Bayer, P. E., Filatov, D. A., Hane, J. K., Edwards, D., et al. (2018b). The western mediterranean region provided the founder population of domesticated narrow-leafed lupin. *Theor. Appl. Genet.* 131, 2543–2554. doi: 10.1007/s00122-018-3171-x

Mulholland, J., Coombe, J., and Dann, P. (1976). Use of oat, lupin and field pea stubbles by grazing sheep. *Austr. J. Exp. Agric.* 16, 467–471. doi: 10.1071/ea9760467

Narożna, D., Książkiewicz, M., Przysiecka, Ł, Króliczak, J., Wolko, B., Naganowska, B., et al. (2017). Legume isoflavone synthase genes have evolved by whole-genome and local duplications yielding transcriptionally active paralogs. *Plant Sci.* 264, 149–167. doi: 10.1016/j.plantsci.2017.09.007

Nelson, M. N., Berger, J. D., and Erskine, W. (2010). Flowering time control in annual legumes: prospects in a changing global climate. *CAB Rev.* 5, 1–14.

Nelson, M. N., Książkiewicz, M., Rychel, S., Besharat, N., Taylor, C. M., Wyrwa, K., et al. (2017). The loss of vernalization requirement in narrow-leafed lupin is associated with a deletion in the promoter and de-repressed expression of a *Flowering Locus T* (*FT*) homologue. *New Phytol.* 213, 220–232. doi: 10.1111/nph.14094

Nelson, M. N., Phan, H. T. T., Ellwood, S. R., Moolhuijzen, P. M., Hane, J., Williams, A., et al. (2006). The first gene-based map of *Lupinus angustifolius* L.-location of domestication genes and conserved synteny with Medicago truncatula. *Theor. Appl. Genet.* 113, 225–238. doi: 10.1007/s00122-006-0288-0

NOAA, (2020). *National Centers for Environmental Information, Climate at a Glance: Global Time Series*. Washington, DC: NOAA.

Ortega, R., Hecht, V. F. G., Freeman, J. S., Rubio, J., Carrasquilla-Garcia, N., Mir, R. R., et al. (2019). Altered expression of an *FT* cluster underlies a major locus controlling domestication-related changes to chickpea phenology and growth habit. *Front. Plant Sci.* 10:824. doi: 10.3389/fpls.2019.00824

Parmesan, C., and Yohe, G. (2003). A globally coherent fingerprint of climate change impacts across natural systems. *Nature* 421, 37–42. doi: 10.1038/nature01286

Plewiński, P., Książkiewicz, M., Rychel-Bielska, S., Rudy, E., and Wolko, B. (2019). Candidate domestication-related genes revealed by expression quantitative trait loci mapping of narrow-leafed lupin (*Lupinus angustifolius* L.). *Int. J. Mol. Sci.* 20:5670. doi: 10.3390/ijms20225670

Przysiecka, Ł, Książkiewicz, M., Wolko, B., and Naganowska, B. (2015). Structure, expression profile and phylogenetic inference of chalcone isomerase-like genes from the narrow-leafed lupin (*Lupinus angustifolius* L.) *genome*. *Front. Plant Sci.* 6:268. doi: 10.3389/fpls.2015.00268

Putterill, J., Zhang, L., Yeoh, C. C., Balcerowicz, M., Jaudal, M., and Gasic, E. V. (2013). FT genes and regulation of flowering in the legume *Medicago truncatula*. *Funct. Plant Biol.* 40, 1199–1207. doi: 10.1071/fp13087

R Core Team, (2013). *R: A Language and Environment for Statistical Computing*. Vienna: R Foundation for Statistical Computing.

Rahman, M., and Gladstones, J. (1972). Control of lupin flower initiation by vernalization, photoperiod and temperature under controlled environment. *Austr. J. Exp. Agric.* 12, 638–645. doi: 10.1071/ea9720638

Rychel, S. (2018). *Charakterystyka Genów Uczestniczących w Procesie Indukcji Kwitnienia u Łubinu Wąskolistnego (Lupinus angustifolius L.) i Łubinu Białego (L. albus L.)*. PhD Thesis. Warsaw: Polish Academy of Sciences.

Rychel, S., Książkiewicz, M., Tomaszewska, M., Bielski, W., and Wolko, B. (2019). *FLOWERING LOCUS T*, *GIGANTEA*, *SEPALLATA* and *FRIGIDA* homologs are candidate genes involved in white lupin (*Lupinus albus* L.) early flowering. *Mol. Breed.* 39:43.

Samanfar, B., Molnar, S. J., Charette, M., Schoenrock, A., Dehne, F., Golshani, A., et al. (2017). Mapping and identification of a potential candidate gene for a novel maturity locus, E10, in soybean. *Theor. Appl. Genet.* 130, 377–390. doi: 10.1007/s00122-016-2819-7

Sang, N., Cai, D., Li, C., Sun, Y., and Huang, X. (2019). Characterization and activity analyses of the *FLOWERING LOCUS T* promoter in *Gossypium Hirsutum*. *Int. J. Mol. Sci.* 20, 4769. doi: 10.3390/ijms20194769

Scheelbeek, P. F. D., Bird, F. A., Tuomisto, H. L., Green, R., Harris, F. B., Joy, E. J. M., et al. (2018). Effect of environmental changes on vegetable and legume yields and nutritional quality. *Proc. Natl. Acad. Sci. U.S.A.* 115, 6804–6809. doi: 10.1073/pnas.1800442115

Shankar, M., Sweetingham, M. W., and Cowling, W. A. (2002). Identification of alleles at two loci controlling resistance to Phomopsis stem blight in narrow-leafed lupin (*Lupinus angustifolius* L.). *Euphytica* 125, 35–44.

Shim, J. S., Kubota, A., and Imaizumi, T. (2017). Circadian clock and photoperiodic flowering in *Arabidopsis*: *CONSTANS* is a hub for signal integration. *Plant Physiol.* 173, 5–15. doi: 10.1104/pp.16.01327

Stefanova, K. T., and Buirchell, B. (2010). Multiplicative mixed models for genetic gain assessment in lupin breeding. *Crop Sci.* 50, 880–891. doi: 10.2135/cropsci2009.07.0402

Sung, S., and Amasino, R. M. (2004). Vernalization in *Arabidopsis thaliana* is mediated by the PHD finger protein *VIN3*. *Nature* 427, 159–164. doi: 10.1038/nature02195

Svec, D., Tichopad, A., Novosadova, V., Pfaffl, M. W., and Kubista, M. (2015). How good is a PCR efficiency estimate: recommendations for precise and robust qPCR efficiency assessments. *Biomol. Detect. Quantific.* 3, 9–16. doi: 10.1016/j.bdq.2015.01.005

Szczepaniak, A., Książkiewicz, M., Podkowiński, J., Czyż, K. B., Figlerowicz, M., and Naganowska, B. (2018). Legume cytosolic and plastid acetyl-coenzyme-A carboxylase genes differ by evolutionary patterns and selection pressure schemes acting before and after whole-genome duplications. *Genes* 9:563. doi: 10.3390/genes9110563

Takeshima, R., Hayashi, T., Zhu, J., Zhao, C., Xu, M., Yamaguchi, N., et al. (2016). A soybean quantitative trait locus that promotes flowering under long days is identified as *FT5a*, a *FLOWERING LOCUS T* ortholog. *J. Exp. Bot.* 67, 5247–5258. doi: 10.1093/jxb/erw283

Tamhane, A. C., and Logan, B. R. (2004). Finding the maximum safe dose level for heteroscedastic data. *J. Biopharmac. Stat.* 14, 843–856. doi: 10.1081/bip-200035413

Taylor, C. M., Jost, R., Erskine, W., and Nelson, M. N. (2016). Identifying stable reference genes for qRT-PCR normalisation in gene expression studies of narrow-leafed lupin (*Lupinus angustifolius* L.). *PLoS One* 11:e0148300. doi: 10.1371/journal.pone.0148300

Taylor, C. M., Kamphuis, L. G., Zhang, W., Garg, G., Berger, J. D., Mousavi-Derazmahalleh, M., et al. (2019). INDEL variation in the regulatory region of the major flowering time gene *LanFTc1* is associated with vernalization response and flowering time in narrow-leafed lupin (*Lupinus angustifolius* L.). *Plant, Cell Environ.* 42, 174–187. doi: 10.1111/pce.13320

Thines, B. C., Youn, Y., Duarte, M. I., and Harmon, F. G. (2014). The time of day effects of warm temperature on flowering time involve *PIF4* and *PIF5*. *J. Exp. Bot.* 65, 1141–1151. doi: 10.1093/jxb/ert487

Trevaskis, B., Bagnall, D. J., Ellis, M. H., Peacock, W. J., and Dennis, E. S. (2003). MADS box genes control vernalization-induced flowering in cereals. *Proc. Natl. Acad. Sci. U.S.A.* 100, 13099–13104. doi: 10.1073/pnas.1635053100

Turck, F., Fornara, F., and Coupland, G. (2008). Regulation and identity of florigen: *FLOWERING LOCUS T* moves center stage. *Annu. Rev. Plant Biol.* 59, 573–594. doi: 10.1146/annurev.arplant.59.032607.092755

Untergasser, A., Cutcutache, I., Koressaar, T., Ye, J., Faircloth, B. C., Remm, M., et al. (2012). Primer3–new capabilities and interfaces. *Nucleic Acids Res.* 40:e115. doi: 10.1093/nar/gks596

Vadez, V., Berger, J. D., Warkentin, T., Asseng, S., Ratnakumar, P., Rao, K. P. C., et al. (2012). Adaptation of grain legumes to climate change: a review. *Agron. Sustain. Dev.* 32, 31–44.

Wang, B., Jin, S.-H., Hu, H.-Q., Sun, Y.-G., Wang, Y.-W., Han, P., et al. (2012). UGT87A2, an *Arabidopsis* glycosyltransferase, regulates flowering time via *FLOWERING LOCUS C*. *New Phytol.* 194, 666–675. doi: 10.1111/j.1469-8137.2012.04107.x

Wang, Y.-W., Wang, W.-C., Jin, S.-H., Wang, J., Wang, B., and Hou, B.-K. (2012). Over-expression of a putative poplar glycosyltransferase gene, *PtGT1*, in tobacco increases lignin content and causes early flowering. *J. Exp. Bot.* 63, 2799–2808. doi: 10.1093/jxb/ers001

Welch, B. L. (1947). The generalization ofstudent's' problem when several different population variances are involved. *Biometrika* 34, 28–35. doi: 10.2307/2332510

Williamson, P. M., Highet, A. S., Gams, W., Sivasithamparam, K., and Cowling, W. A. (1994). *Diaporthe toxica* sp. nov., the cause of lupinosis in sheep. *Mycol. Res.* 98, 1364–1368. doi: 10.1016/s0953-7562(09)81064-2

Wyrwa, K., Książkiewicz, M., Szczepaniak, A., Susek, K., Podkowiński, J., and Naganowska, B. (2016). Integration of *Lupinus angustifolius* L. (narrow-leafed lupin) genome maps and comparative mapping within legumes. *Chromosome Res.* 24, 355–378. doi: 10.1007/s10577-016-9526-8

Yan, L., Loukoianov, A., Tranquilli, G., Helguera, M., Fahima, T., and Dubcovsky, J. (2003). Positional cloning of the wheat vernalization gene *VRN1*. *Proc. Natl. Acad. Sci. U.S.A.* 100, 6263–6268. doi: 10.1073/pnas.0937399100

Yang, H., Tao, Y., Zheng, Z., Zhang, Q., Zhou, G., Sweetingham, M. W., et al. (2013). Draft genome sequence, and a sequence-defined genetic linkage map of the legume crop species *Lupinus angustifolius* L. *PLoS One* 8:e64799. doi: 10.1371/journal.pone.0064799.t002

Yang, T., Chaudhuri, S., Yang, L., Du, L., and Poovaiah, B. W. (2010). A calcium/calmodulin-regulated member of the receptor-like kinase family confers cold tolerance in plants. *J. Biol. Chem.* 285, 7119–7126. doi: 10.1074/jbc.m109.035659

Young, N. D., Debellé, F., Oldroyd, G. E. D., Geurts, R., Cannon, S. B., Udvardi, M. K., et al. (2011). The *Medicago* genome provides insight into the evolution of rhizobial symbioses. *Nature* 480, 520–524.

Zhang, G.-Z., Jin, S.-H., Li, P., Jiang, X.-Y., Li, Y.-J., and Hou, B.-K. (2017). Ectopic expression of *UGT84A2* delayed flowering by indole-3-butyric acid-mediated transcriptional repression of *ARF6* and *ARF8* genes in *Arabidopsis*. *Plant Cell Rep.* 36, 1995–2006. doi: 10.1007/s00299-017-2225-x

Zhao, C., Takeshima, R., Zhu, J., Xu, M., Sato, M., Watanabe, S., et al. (2016). A recessive allele for delayed flowering at the soybean maturity locus E9 is a leaky allele of *FT2a*, a *FLOWERING LOCUS T* ortholog. *BMC Plant Biol.* 16:20.

Zhou, G., Jian, J., Wang, P., Li, C., Tao, Y., Li, X., et al. (2018). Construction of an ultra-high density consensus genetic map, and enhancement of the physical map from genome sequencing in *Lupinus angustifolius*. *Theor. Appl. Genet.* 131, 209–223. doi: 10.1007/s00122-017-2997-y

Conflict of Interest: The authors declare that the research was conducted in the absence of any commercial or financial relationships that could be construed as a potential conflict of interest.

Copyright © 2020 Rychel-Bielska, Plewiński, Kozak, Galek and Książkiewicz. This is an open-access article distributed under the terms of the Creative Commons Attribution License (CC BY). The use, distribution or reproduction in other forums is permitted, provided the original author(s) and the copyright owner(s) are credited and that the original publication in this journal is cited, in accordance with accepted academic practice. No use, distribution or reproduction is permitted which does not comply with these terms.

frontiers in Plant Science

ORIGINAL RESEARCH
published: 09 November 2020
doi: 10.3389/fpls.2020.570915

Expression of *LhFT1*, the Flowering Inducer of Asiatic Hybrid Lily, in the Bulb Scales

Kana Kurokawa[1], Junya Kobayashi[1], Keiichirou Nemoto[2], Akira Nozawa[3], Tatsuya Sawasaki[3], Takashi Nakatsuka[1,4,5] and Masumi Yamagishi[6]*

[1] Graduate School of Integrated Science and Technology, Shizuoka University, Shizuoka, Japan, [2] Iwate Biotechnology Research Center, Kitakami, Japan, [3] Proteo-Science Center, Ehime University, Matsuyama, Japan, [4] Faculty of Agriculture, Shizuoka University, Shizuoka, Japan, [5] College of Agriculture, Academic Institute, Shizuoka University, Shizuoka, Japan, [6] Research Faculty of Agriculture, Hokkaido University, Sapporo, Japan

OPEN ACCESS

Edited by:
Joanna Putterill, The University of Auckland, New Zealand

Reviewed by:
Seonghoe Jang, World Vegetable Center Korea, South Korea
Antonio Chalfun-Junior, Universidade Federal de Lavras, Brazil
Erika Varkonyi-Gasic, The New Zealand Institute for Plant and Food Research Limited, New Zealand

***Correspondence:**
Takashi Nakatsuka
nakatsuka.takashi@shizuoka.ac.jp

Specialty section:
This article was submitted to Plant Development and EvoDevo, a section of the journal Frontiers in Plant Science

Received: *09 June 2020*
Accepted: *19 October 2020*
Published: *09 November 2020*

Citation:
Kurokawa K, Kobayashi J, Nemoto K, Nozawa A, Sawasaki T, Nakatsuka T and Yamagishi M (2020) Expression of LhFT1, the Flowering Inducer of Asiatic Hybrid Lily, in the Bulb Scales. Front. Plant Sci. 11:570915. doi: 10.3389/fpls.2020.570915

Asiatic hybrid lily leaves emerge from their bulbs in spring, after cold exposure in winter, and the plant then blooms in early summer. We identified four *FLOWERING LOCUS T* (*FT*)-like genes, *LhFT1*, *LhFT4*, *LhFT6*, and *LhFT8*, from an Asiatic hybrid lily. Floral bud differentiation initiated within bulbs before the emergence of leaves. *LhFT* genes were mainly expressed in bulb scales, and hardly in leaves, in which the *FT-like* genes of many plants are expressed in response to environmental signals. *LhFT1* was expressed in bulb scales after vernalization and was correlated to flower bud initiation in two cultivars with different flowering behaviors. *LhFT8* was upregulated in bulb scales after cold exposure and three alternative splicing variants with a nonsense codon were simultaneously expressed. *LhFT6* was upregulated in bulb scales after flower initiation, whereas *LhFT4* was expressed constantly in all organs. *LhFT1* overexpression complemented the late-flowering phenotype of *Arabidopsis ft-10*, whereas that of *LhFT8* did so partly. *LhFT4* and *LhFT6* overexpression could not complement. Yeast two-hybrid and *in vitro* analyses showed that the LhFT1 protein interacted with the LhFD protein. LhFT6 and LhFT8 proteins also interacted with LhFD, as observed in AlphaScreen assay. Based on these results, we revealed that *LhFT1* acts as a floral activator during floral bud initiation in Asiatic hybrid lilies. However, the biological functions of *LhFT4*, *LhFT6*, and *LhFT8* remain unclear.

Keywords: alternative splicing, cold exposure, flower initiation, *FLOWERING LOCUS T* like genes, geophytes, *Lilium* sp., ornamental plants

INTRODUCTION

The genus *Lilium* consists of approximately 100 species that are distributed throughout the cold and temperate regions of the Northern Hemisphere and are classified into seven sections (van Tuyl et al., 2018). Lilies are important ornamental plants that include three main distinctive hybrid groups, i.e., Easter lilies, Asiatic hybrid lilies, and Oriental hybrid lilies (Dole and Wilkins, 2005). Asiatic hybrid lilies are derived from interspecific hybridization among *L. dauricum*, *L. maculatum*, *L. lacifolium*, etc., which are species that belong to the sections Sinomartagon and Daurolirion (Marasek-Ciolakowska et al., 2018). Moreover, these plants are characterized by an upward-facing flower and

little or no fragrance (Dole and Wilkins, 2005). The color of their flowers is often uniform or with a contrasting perianth segment tips and/or throat, and they exhibit a wide variety of flower colors in different shades, from white to red and yellow (Yamagishi, 2013). Commercial Asiatic hybrid lily cultivars are usually propagated by bulbs, rather than seeds (Beattie and White, 1993).

The typical life cycle of Asiatic hybrid lilies starts with bulb planting in the autumn (October–November), followed by the exposure of bulbs to the low temperatures of winter, which in necessary for flower initiation. Most Asiatic hybrid lilies are vernalized at 1°C–2°C for at least 6 weeks (Nau, 2011). The bulbs sprout in spring and flower in late spring to early summer (Okubo and Sochacki, 2012). Based on the timing of flower bud initiation, 85 Asiatic hybrid cultivars were classified into two types (Ohkawa et al., 1990). In the majority of cultivars (69%), flower bud differentiation starts and is completed after shoot emergence. Conversely, in the remaining cultivars (31%), flower bud initiation commences inside the bulb. With a few exceptions, the former type of Asiatic hybrid lily cultivars flower later than do the latter (Ohkawa et al., 1990). Moreover, no relationship has been identified between shoot growth and flower bud initiation. In *L. longiflorum*, cold exposure is not an obligatory prerequisite for flowering, as an alternative flowering pathway can bypass vernalization in small bulbs (Lazare and Zaccai, 2016). Recently, the levels of glycerol in *L. longiflorum* bulbs was found to be associated with a delay in sprouting and flowering time and a reduction in abortion rate (Lazare et al., 2019).

The floral integrator *FLOWERING LOCUS T* (*FT*) is a key regulator of flowering time in *Arabidopsis* (Corbesier et al., 2007). The FT protein is induced under the flowering-inducive long-day photoperiod in leaves, and is then transported via the phloem to the shoot apical meristem (SAM), where it interacts with the bZIP transcription factor FD (Abe et al., 2005; Corbesier et al., 2007; Tamaki et al., 2007). This protein complex is assumed to comprise two FT monomers and two FD bZIP transcription factors, as well as a dimeric 14–3–3 protein, which acts to bridge the FT–FD interaction (Taoka et al., 2011). The florigen activation complex leads to the direct activation of the floral meristem identity genes, such as *APETALA1* (*AP1*) and *FRUITFULL* (*FUL*) (Taoka et al., 2011). *FT* is a member of the phosphatidyl ethanolamine-binding protein (*PEBP*) gene family (Danilevskaya et al., 2008). *Arabidopsis* carries another *PEBP* gene, *TERMINAL FLOWER 1* (*TFL1*), which determines inflorescence development and suppresses flowering (Bradley et al., 1997). Several amino acids are important for the specific and unique function of FT and TFL1 in *Arabidopsis* (Hanzawa et al., 2005; Ahn et al., 2006). Floral activators such as FT contain a tyrosine (Y) at position 85, whereas floral repressors contain a histidine (H) at the analogous position 88 (Hanzawa et al., 2005). The amino acid residues at position 140 can also affect the function of the protein. In the FT activator, a glutamic acid (Q) is present at position 140, whereas an aspartate (D) is positioned at the same analogous position in the repressors (Ahn et al., 2006). In sugar beets (*Beta vulgaris*), *BvFT2* is the functional *FT* ortholog, while *BvFT1* is a flowering suppressor, despite being in the FT subfamily (Pin et al., 2010). Chrysanthemums (*Chrysanthemum morifolium*) are categorized as absolute short-day plants. In addition, *CsFTL3* encodes a florigen that is induced under short photoperiod conditions in chrysanthemum plants, whereas *CsAFT* encodes an anti-florigen that acts systemically to inhibit flowering under long-day photoperiod conditions and plays a predominant role in the obligate photoperiodic response (Oda et al., 2012; Higuchi et al., 2013; Nakano et al., 2019).

In addition to functioning as activators or repressors of flowering, members of the PEBP family are also involved in a variety of other processes (Wickland and Hanzawa, 2015), such as tuberization (Navarro et al., 2011), bulb formation (Lee et al., 2013), stomatal opening (Kinoshita et al., 2011), and photoperiodic control of seasonal growth in trees (Bohlenius et al., 2006; Hsu et al., 2006, 2011). In *Arabidopsis*, *FT* genes are involved in the regulation of H^{++}-ATPase by blue light in stomatal guard cells, resulting in the regulation of stomatal opening by *FT* (Kinoshita et al., 2011). The tuberization of potatoes (*Solanum tuberosum*) under a short-day photoperiod is controlled by a homolog of *FT*, *StSP6A* (Navarro et al., 2011). Interestingly, an *StSP6A*-specific small RNA is induced by elevated temperatures and suppresses the tuberization of potatoes (Lehretz et al., 2019). Four *FT*-like genes (*AcFT1*, *AcFT2*, *AcFT4*, and *AcFT6*) have been identified in onions (*Allium cepa*) (Lee et al., 2013). *AcFT2* is expressed during vegetative growth and likely regulates growth cessation and bud set, which promotes flowering. *AcFT4* functions as an inhibitor of bulbing, whereas *AcFT1* as a promotor of bulbing. Moreover, *AcTFL1* is highly expressed during bulbing and inflorescence development in onions (Dalvi et al., 2019). The expression levels of *AcTFL1* within the bulb are lowest in the outmost layers and highest in the innermost layers.

Some species of the genus *Lilium* have been studied regarding the genes that control flowering and vernalization. An RNA-seq analysis of molecules involved in the vernalization response in the Oriental hybrid lily "Sorbonne" identified two vernalization genes, *SHORT VEGETATIVE PHASE* (*LoSVP*) and *VERNALIZATION 1* (*LoVRN1*), as well as the floral transition key gene *SUPPRESSOR OF OVEREXPRESSION OF CONSTANS 1* (*LoSOC1*) (Liu et al., 2014; Li et al., 2016). Similarly, *L. lancifolium* (which is a breeding material for Asiatic hybrid lilies), the Asiatic hybrid lily "Tiny ghost," and *L. longiflorum* "White Heaven" were also subjected to transcriptome profiling during the vernalization process by RNA-seq, which led to the identification of several cold signal transduction genes (Huang et al., 2014; Wang et al., 2014; Hamo et al., 2015; Villacorta-Martin et al., 2015). *L.* × *formolongi*, which is a lily hybrid between *L. formosanum* and *L. longiflorum*, flowers within 1 year of sowing. *CO-LIKE* (*COL*), *FT*, *TREHALOSE-6-PHOSPHATE SYNTHASE* (*TPS*), *SQUAMOSA PROMOTER-BINDING PROTEIN-LIKE* (*SPL*) homologs may play significant roles in the flowering-induction and transition process of *L.* × *formolongi* (Li et al., 2017). Thus, most flowering studies of the genus *Lilium* were based on integrated expression analyses and the detailed function of *FT*-like genes remains unclear. Conversely, the *LlFT* gene from *L. longiflorum* is upregulated by cold exposure, and the overexpression in *Arabidopsis* and lily plants leads to an early-flowering phenotype (Leeggangers et al., 2018). Therefore, *LlFT* may be involved

in the vernalization response of lily and may be able to replace cold exposure.

Several studies of *FT*-like genes have been reported in various monocot horticulture plants, with the exception of lily. Tulips (*Tulipa gesneriana*) carry three *FT*-like genes, *TgFT1*, *TgFT2*, and *TgFT3* (Leeggangers et al., 2017, 2018). *TgFT2* is considered to act as a flowering inducer, as it is involved in floral induction in tulips, whereas *TgFT3* is assumed to have a bulb-specific function. In Chinese narcissuses (*Narcissus tazetta*), which are plants that exhibit summer dormancy, high temperatures are necessary for release from dormancy (Li et al., 2013; Noy-Porat et al., 2013). Under high temperature conditions (25°C–30°C) in the dark, *NtFT* expression occurred simultaneously with floral induction in the bulb meristems of Chinese narcissus plants, indicating that floral induction is affected by high temperature, but not by photoperiod or vernalization (Li et al., 2013; Noy-Porat et al., 2013).

In this study, we attempted to isolate and characterize *FT*-like genes in ornamental Asiatic hybrid lily.

MATERIALS AND METHODS

Plant Materials

The bulbs (circumference, 16 cm) of the Asiatic hybrid lily 'Lollypop' [original name, 'Holebibi' (Matthews, 2007)] were purchased from the Niigata Flower Bulb Growers Cooperative Association (Niigata, Japan) in September 2016 and 2017 (**Figures 1A,B**). The bulbs of *L. leichtlinii* 'Hakugin' which is one of the breeding materials of this Asiatic hybrid lily, were also harvested in August 2015 from a field of Hokkaido University (Sapporo, Japan) and were stored at 20°C until use. Cold treatment of bulbs was performed in peat moss in the dark at 4°C for 4 months. In early March, all bulbs were planted at a density of 12 bulbs per 16 L planter, which was filled with a mix of akadama and leaf mold (2:1) containing 2.5 g·L^{-1} Magamp K (Hyponex Japan, Osaka, Japan). The plants were grown in a field of Shizuoka University (Shizuoka, Japan) under natural conditions.

During cold treatment and after planting, scales, SAMs, and leaves were sampled. The second and third outer scales and SAMs containing the basal plate were collected from bulbs, whereas SAMs with a height of approximately 1 cm were collected from sprouted plants. The mature leaves were also collected from sprouted plants.

Observation of Floral Development

Floral differentiation of SAM was observed in at least three independent samples for each point using a stereomicroscope. Floral developmental stage was defined as follows: (1) Vegetative (**Figure 1C**); (2) flower initiation (**Figure 1D**); (3) bract formation (**Figure 1E**); (4) outer perianth primordia (**Figure 1F**): (5) inner perianth primordia, (6) perianth development; (7) stamen differentiation; (8) pistil primordia (**Figure 1G**); (9) pistil differentiation; and (10) pistil development (**Figure 1H**; Fukai and Goi, 2001).

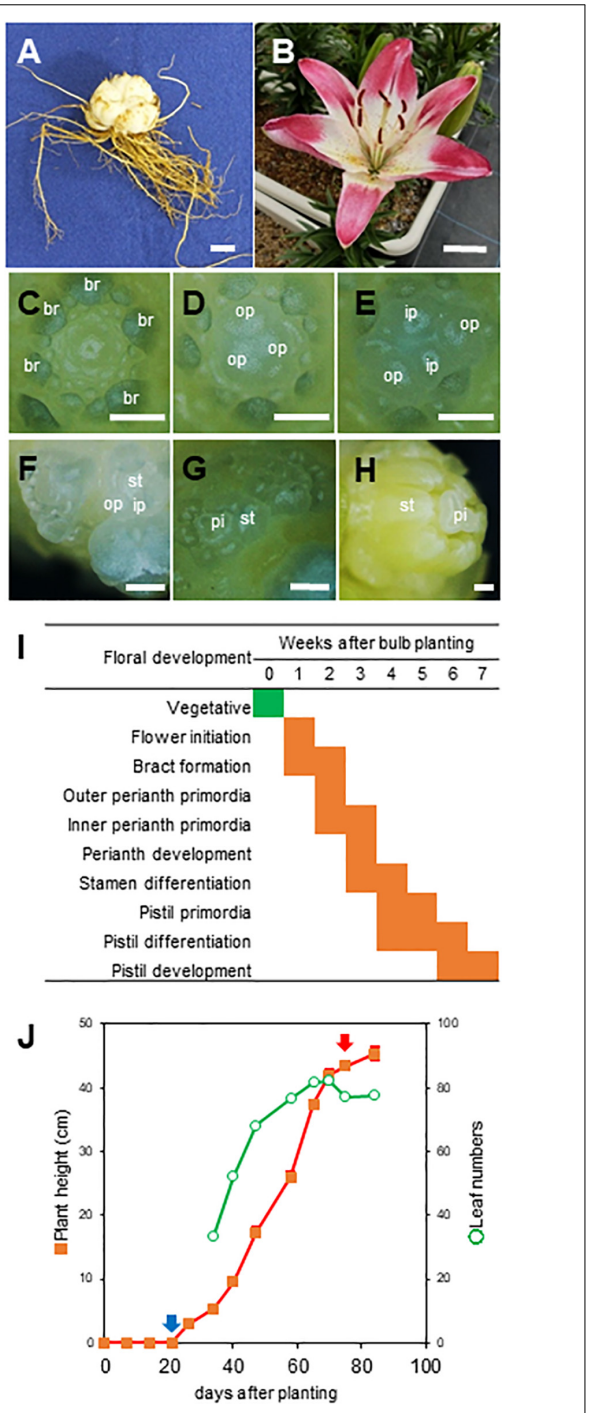

FIGURE 1 | Vegetative and reproductive development stages in the Asiatic hybrid lily 'Lollypop.' **(A)** Bulbs before chilling exposure. Bar, 2 cm. **(B)** Anthesis. Bar, 2 cm. **(C–H)** Definition of the floral development stages of the SAM. Bar, 500 μm. br, bract; op, outer perianth; ip, inner perianth; st, stamen; pi, pistil. **(C)** Vegetative SAM. **(D)** Flower initiation, rounded SAM. **(E)** Bract formation. **(F)** Formation of outer and inner perianthes primordia. **(G)** Formation of pistil primordia. **(H)** Pistil development. **(I)** Flower bud transition after planting. Flower developmental stages are defined in "Materials and Methods." We observed three independent SAMs each week. **(J)** Alteration of plant height and leaf number after planting. The blue arrow indicates leaves emerged from the soil at three weeks after planting. The red arrow indicates 'Lollypop' blooming at 75 days after planting.

Isolation of *FT* Orthologs From an Asiatic Hybrid Lily

The deposited transcriptome data (ERR578452 to ERR578471) of *L. longiflorum* were assembled using the trinity program of the DDBJ read annotation pipeline (Nagasaki et al., 2013); 300,375 contigs were obtained. *Lilium FT/TFL1* orthologs were identified in these contigs by the blast program using *FT*/*TFL1* orthologs from several plant species as queries. Several primers based on the nucleotide sequences of nine *FT*/*TFL1* candidate genes from *L. longiflorum* were designed to amplify *FT*/*TFL1* and flowering-related gene orthologs from an Asiatic hybrid lily, as shown in **Supplementary Table 1**.

Shoot apical meristems, scales, and leaves of *L. leichtlinii* 'Hakugin' were sampled at several developmental stages. Total RNA was isolated from each sample using the Fruit mate for RNA purification (Takara Bio, Shiga, Japan) and RNAiso Plus (Takara Bio). cDNAs were synthesized using a PrimeScript II 1st strand cDNA synthesis kit (Takara Bio). Using the primers that were designed as described above, we amplified putative *FT*/*TFL1* orthologs using the *L. leichtlinii* 'Hakugin' cDNA. The reaction mixture (25 μL) consisted of 1× *Ex Taq* buffer, 200 μM dNTPs, 0.2 μM each primer, 0.25 U of *Ex Taq* polymerase (Takara Bio) and 1 μL of template cDNA. The thermal cycler program was set as follows: 94°C for 2 min; followed by 35 cycles of 94°C for 20 s, 40°C–55°C for 40 s, and 72°C for 1 min; and a final step at 72°C for 10 min. The amplified fragments were subcloned into the pGEM-Teasy vector system (Promega, Madison, WI, United States). The sequences of all constructs were confirmed by DNA sequencing (Fasmac, Kanagawa, Japan).

Based on the partial sequences obtained for each *FT/TFL1* fragment, we used the rapid amplification of cDNA ends (RACE) technology to obtain full-length cDNA sequences with the SMARter RACE 5′/3′ kit (Takara Bio). The open reading frame (ORF) sequences were amplified using *Ex Taq* polymerase, and the primer sets are listed in **Supplementary Table 1**. The thermal cycler program was set as follows: 94°C for 2 min; followed by 35 cycles of 94°C for 20 s, 60°C for 40 s, and 72°C for 2 min; and a final step at 72°C for 10 min. The amplified fragments were cloned and sequenced as described above. A phylogenetic tree of FT-like protein was constructed using ClustalW with neighbor-joining algorithm and visualized using MEGA ver. 7 software (Kumar et al., 2016).

Expression Analysis

Total RNA was isolated from the SAMs, scales, and leaves of each treated plant. cDNA was synthesized from total RNAs, as described above. For the RT-PCR analyses, a reaction mixture (50 μL) consisted of 1 × *Ex Taq* buffer, 200 μM of dNTPs, 0.4 μM of each primer, 0.25 U of *Ex Taq* polymerase Hot Start version (Takara Bio), and 1 μL of template cDNA. The PCR cycling conditions were as follows: 2 min at 94°C; 26–34 cycles for 20 s at 95°C, 40 s at 55°C, and 1 min at 72°C; and final extension for 10 min at 72°C. The sequences of the primers are listed in **Supplementary Table 2**. The PCR products were separated on 1.5% agarose gels in TAE buffer and stained with ethidium bromide.

Reverse transcription-quantitative PCR (RT-qPCR) analyses used a Thermal Cycler Dice Real-Time System (TP850, Takara Bio), according to MIQE guidelines (Bustin et al., 2009). Briefly, the reaction mixture (10 μL) consisted of 1× KAPA SYBR Fast qPCR Master Mix (KAPA Biosystems, Wilmington, MA, United States), 0.2 μM of each primer, and 1 μL of template cDNA. Cycling conditions were as follows: 95°C for 20 s; followed by 40 cycles of 95°C for 1 s and 60°C for 20 s. The sequences of the primers used in this study are listed in **Supplementary Table 2**. The specificity of amplification was checked by the addition of a dissociation analysis step after the cycle reactions. Data were analyzed by second derivative maximum methods using Thermal Cycler Dice Real-Time System II software version 5.00 (Takara Bio). Transcript levels were calculated relative to the actin-encoding *LhACT* gene (AB438963) used as a reference (Yamagishi et al., 2014; Suzuki et al., 2016). In a preliminary experiment, similar amplification rates of *LhACT* were detected among scale, SAM, and leaf samples of 'Lollypop' at different developmental stages (**Supplementary Figure 1**). The RT-qPCR analyses used six biological replicates.

Yeast Two-Hybrid Analysis Between LhFT Proteins and LhFD

To investigate whether the LhFT proteins interact with the LhFD protein, we employed a yeast two-hybrid analysis using the Matchmaker Two-Hybrid System 3 (Clontech, Takara Bio, Shiga, Japan) as described previously (Nakatsuka et al., 2019). The coding regions of *LhFT1*, *LhFT4*, *LhFT6*, *LhFT8*, and *LhFD* were cloned into either pGAD-T7 (GAL4 activation domain) or pGBK-T7 (GAL4 DNA-binding domain) vectors. All the constructs were transformed into *Saccharomyces cerevisiae* AH109 (Clontech). Transformed yeast cells were grown on SD selective medium without leucine (−Leu) and tryptophan (−Trp) at 30°C for 3 days. A survival test was performed for each transformed yeast culture using selective quadruple-dropout medium (−Leu, −Trp, histidine [−His], and adenine [−Ade]) supplemented with 15 mM of 3-amino-1,2,4-triazole (3-AT) at 30°C for 3 days.

AlphaScreen-Based *in vitro* Protein–Protein Interaction Assay

The ORFs of *LhFTs*, *LhFD*, *AtFT*, and *AtFD* were modified with two-step PCR using gene-specific primer pairs with S1 or T1 linker sequences for the first step and primers attB1-S1 and attB2-T1 for the second step. The DNA fragments were cloned into pDONR221 vector using the gateway cloning system (Thermo Fisher Scientific). These expression vectors were generated using LR clonase recombination with pEU-E01-GW-AGIA (Yano et al., 2016) or pEU-E01-GW-bls (Iwasaki et al., 2016) vector for cell-free protein synthesis or transient expression vectors. All primer sequences are listed in **Supplementary Table 3**.

In vitro transcription and wheat cell-free protein synthesis were performed using the WEPRO1240 expression kit (Cell-Free Sciences, Matsuyama, Japan) according to the manufacturer's instructions. *In vitro* biotin labeling of recombinant protein was performed as previously described (Sawasaki et al., 2008).

AlphaScreen-based *in vitro* protein–protein interaction assay was performed as previously described with slight modifications (Nemoto et al., 2017). The assay was performed using a reaction mixture of 15 μL containing AlphaScreen buffer [100 mM Tris–HCl (pH 8.0), 0.1% Tween20, 1 mg·mL^{-1} BSA], 1 μL of C-terminal biotinylated LhFD, and 1 μL of C-terminal AGIA-tagged LhFTs in a 384-well Optiplate (PerkinElmer, Waltham, MA, United States). After incubation at 25°C for 1 h, 10 μL of detection mixture containing AlphaScreen buffer, 1 μg·mL^{-1} anti-AGIA antibody (Yano et al., 2016), 0.1 μL of streptavidin-coated donor beads (PerkinElmer), and 0.1 μL of protein A-coated acceptor beads (PerkinElmer) were added to each well of the 384-well Optiplate, followed by incubation at 25°C for 1 h. Luminescence was analyzed using the AlphaScreen detection program. All data represent the average of three independent experiments, and the background was controlled using a biotinylated dihydrofolate reductase (DHFR) from *E. coli*.

Complement Expression of *LhFT* Genes in the *Arabidopsis ft-10* Mutant

The ORFs of *LhFTs* were located between the cauliflower mosaic virus (CaMV*) 35S* promoter and the *Arabidopsis* heat-shock protein terminator (HT) of a binary vector, pShyg-35SproGUS-HT the hygromycin-resistance gene was modified from the pSMAB704 backbone vector (Igasaki et al., 2002). These constructs were then transformed into the *Agrobacterium tumefaciens* EHA101 strain. *Arabidopsis ft-10* mutant was transformed using the floral dip method, as described (Clough and Bent, 1998). Positive transformants were selected on germination medium supplemented with 30 mg·L^{-1} hygromycin, with T_2 seeds being obtained after self-pollination. Transgenic plants were grown at 22°C under 16-h day florescence light. Homozygotic T_2 lines of each transgenic plant were used to investigate flowering time.

The total RNA was isolated from the mature leaves of 3-week-old seedling in Col-1 and T_2 line, as described above. The expression levels of transgene *LhFTs* and *AtACT2* as internal standard were investigated by RT-PCR analysis, as described above.

Statistical Analysis

Data are presented as the mean ± SE. Statistical comparisons were carried out using Tukey–Kramer and Student's *t*-tests.

RESULTS

Growth Behavior of the Asiatic Hybrid Lily 'Lollypop' and *L. leichtlinii* 'Hakugin'

Before the investigation of the temporal and spatial expression of *LhFT* genes in pre-vernalization and during planting, we examined the floral development stages of the SAM of bulbs in each phase (**Figure 1I**). The SAM of bulbs that were pre-chilled over 4 months was kept in the vegetative phase. One week after planting on soil, the SAM of bulbs exhibited either a swollen round apex or produced a bract. Two weeks after planting, SAMs displayed perianth differentiation. Therefore, the SAM of bulbs of 'Lollypop' was assumed to engage in flower bud initiation at ∼2 weeks after planting. Three weeks after planting, leaves emerged from the soil, and flower buds were observed 8 weeks after planting (**Figure 1J**). The increase in the number of developed leaves stopped 82.3 ± 1.7 leaves at 10 weeks after planting, and flowers bloomed completely at 75 days after planting, resulting in a plant height of 45.3 ± 1.0 cm (**Figure 1J**).

Lilium lacifolium 'Hakugin' was observed to be swollen around the apex at 7 weeks after planting in the soil, and it bloomed at 16 weeks after planting. Both floral initiation and blooming of 'Hakugin' was 6 weeks later compared to those of Asiatic hybrid 'Lollypop.'

Isolation of *LhFT* Orthologs

We obtained four *FT*-like genes, which were termed *LhFT1* (accession number, LC544113), *LhFT4* (LC544114), *LhFT6* (LC544115), and *LhFT8* (LC544117), from *L. leichtlinii* 'Hakugin.' A phylogenetic analysis showed that they were classified into two subgroups (**Figure 2**). *LhFT1* and *LhFT8* were classified into the *FT*-like IA subgroup. The deduced amino acid sequence of *LhFT1*, which belonged to the FT-like IA subgroup, exhibited 96.6% and 94.9% identity with that of *LfFT1* from *L.* × *formolongi* (Li et al., 2017) and *TgFT2* from *T. gesneriana* (Leeggangers et al., 2018), respectively. The deduced amino acid sequence of *LhFT8* exhibited 96.6% and 77.5% identity with that of *LlFT* from *L. longiflorum* (Leeggangers et al., 2018) and *PaFT1* of *Phalaenopsis aphrodite* (Jang et al., 2015). *LhFT1* showed 72.2% identity with *LhFT8* based on amino acid sequences (**Supplementary Figure 2**). Conversely, *LhFT4* and *LhFT6* were classified into the *FT*-like IB subgroup (**Figure 2**). *LhFT4* exhibited 75.7% identity with *LhFT6* based on amino acid sequences. The deduced amino acid sequence of *LhFT6* showed 86.5% identity with that of *TgFT3* from *T. gesneriana* (Leeggangers et al., 2018) and *AcFT6* from *A. cepa* (Lee et al., 2013), respectively. The deduced amino acid sequence of *LhFT4* correlated well with that of *LiFTL3* (98.1% identity), as reported by Leeggangers et al. (2018). The *LhFT4* mRNA had a length of 1,164 bp, but its maximum ORF was 339 bp, from the 447th to 815th nucleotides, and encoded 112 amino acid residues. Thus, LhFT4 protein was shorter than LiFTL3 protein (181 residues), which resulted from the shortening of its N terminus (**Supplementary Figure 2**). After isolation of *LhFTs* from *L. leichtlinii* 'Hakugin,' we confirmed nucleotide sequences of the corresponding genes in the Asiatic hybrid 'Lollypop,' which showed 7 to 10 nucleotide substitutions compared with those of 'Hakugin.' Therefore, we designed primers for expression analysis based on the conserved sequences of *LhFTs* in 'Lollypop' and 'Hakugin.'

LhFT1, LhFT6, and LhFT8 proteins contain a tyrosine (Y, FT-type) at positions 87, 89, and 84, respectively, whereas LhFT4 protein contains a histidine (H, TFL1-type) residue at position 17 (**Supplementary Figure 2**). In segment B motif, LhFT1, LhFT4, and LhFT8 proteins contain a glutamine (Q, FT-type) at positions 139, 72, and 141, respectively, whereas the LhFT6 protein contains a proline (P) residue at position 136 (**Supplementary Figure 2**). Aspartic acid (D) at position 17 and

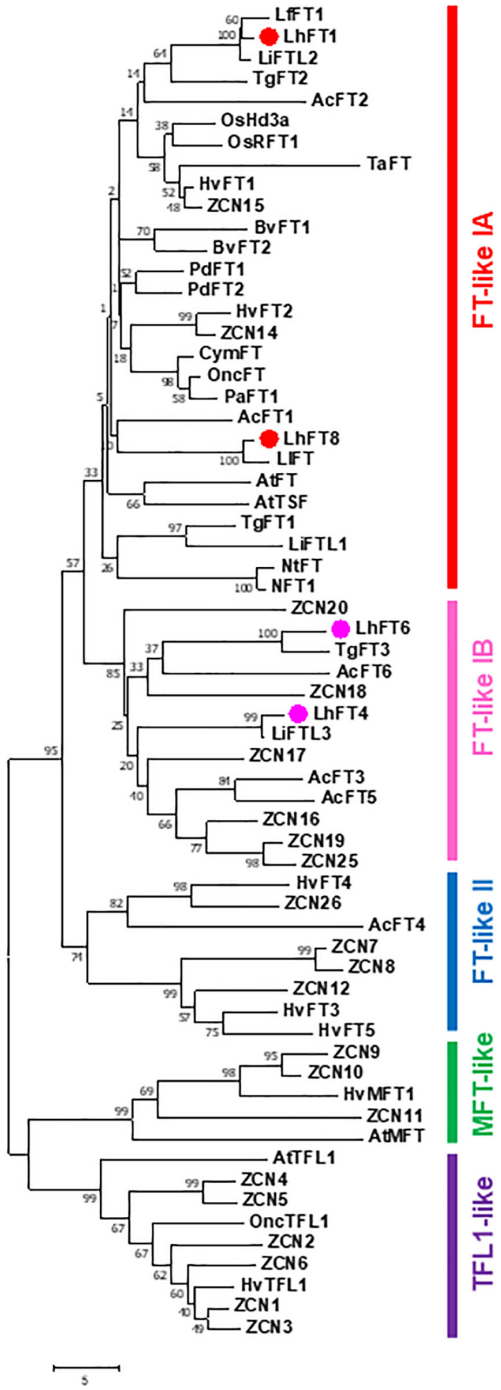

FIGURE 2 | Phylogenetic tree of FT-like protein sequences from different monocot plants. The phylogenetic tree was constructed using the neighbor-joining method. Bootstrap values from 1,000 replicates were used to assess the robustness of the tree. The scale indicates the average number of substitutions per site. The *FT*-like gene names and GenBank accession numbers were as follows: *Allium cepa AcFT1* (AG081838.1), *AcFT2* (AGZ20208.1), *AcFT3* (AGZ20209.1), *AcFT4* (AGZ20210.1), *AcFT5* (AGZ20211.1), and *AcFT6* (AGZ20212.1); *Arabidopsis thaliana AtFT* (NP_176726.1), *AtMFT* (NP_173250.1), *AtTFL1* (NP_196004.1), and *AtTSF* (NP_193770.1); *Cymbidium goeringii CymFT* (ADI58462.1); *Hordeum vulgare* *(Continued)*

FIGURE 2 | Continued
HvFT1 (AAZ38709.1), *HvFT2* (ABB99414.1), *HvFT3* (ABD75336.2), *HvFT4* (ABD75337.1), *HvFT5* (ABM26903.1), *HvMFT1* (BAH24198.1), and *HvTFL1* (ANO81637.1); *Lilium* hybrid *LfFT1* (AIF76295.1), *LhFT1*, *LhFT4*, *LhFT6*, and *LhFT8* (this study); *L. longiflorum FlFT* (ATU06687.1); *Lilium* sp. *LiFTL1* (ATU06689.1), *LiFTL2* (ATU06688.1), and *LiFTL3* (ATU06690.1); *Narcissus tazetta NtFT* (AFS50164.1); *Oncidium* hybrid *OncFT* (AIG6303.1) and *OncTFL1* (AIU44253.1); *Oryza sativa OsHd3a* (XP_01641951.1) and *OsRFT1* (XP_015642519.1); *Phalaenopsis aphrodite PaFT1* (AJF93423.1); *Triticum aestivum TaFT* (ACA25437.1); *Tulipa gesneriana TgFT1* (ATU06684.1), *TgFT2* (ATU006685.1), and *TgFT3* (ATU006686.1); *Zea mays ZCN1* (ONM42318.1), *ZCN2* (NP_00110624.1), *ZCN3* (NP_001106242.1), *ZCN4* (NP_001106243.1), *ZCN5* (NP001106244.1), *ZCN6* (NP_001106245.1), *ZCN7* (NP_001106246.1), *ZCN8* (NP_001106247.1), *ZCN9* (ABW96232.1), *ZCN10* (NP_00106249.1), *ZCN11* (AQK83984.1), *ZCN12* (NP_001106250.1), *ZCN14* (NP_001106251.1), *ZCN15* (NP_001106252.1), *ZCN16* (NP_001106253.1), *ZCN17* (NP_001106254.1), *ZCN18* (NP_001354358.1), *ZCN19* (NP_001106256.1), *ZCN20* (NP_001296779.1), *ZCN25* (NP_001106257.1), and *ZCN26* (NP_001106265.1).

valine (V) at position 18, which are important for the transport of FT, are conserved in the LhFT1, LhFT6, and LhFT8 proteins. Taken together, these results suggest that LhFT1 and LhFT8 are very similar to FT-like proteins, whereas LhFT4 is similar to TFL1-like proteins. Moreover, LhFT6 did not exhibit several characteristic features of the FT protein but was similar to the TgFT3 protein from tulips.

In addition to the four *FT*-like genes, we also identified one *FD* ortholog, *LhFD* (LC544121). The *LhFD* mRNA had a length of 816 bp and encoded a sequence of 221 amino acids. The phylogenetic tree showed that LhFD was classified into eudicots and non-Poacea monocots subgroup (**Supplementary Figure 3**). The deduced amino acid sequence of *LhFD* exhibited 34.6% and 41.0% identity with that of *AtFD* from *A. thaliana* (Abe et al., 2005) and *PaFD* from a *P. aphrodite* (Jang et al., 2015), respectively. The deduced amino acid sequences of *LhMADS5* exhibited 95.6% identity with *AP1* ortholog of *L. longiflorum* (ADT78582, Chen et al., 2008).

Spatial and Temporal Expression Profiles of *FT*-Like Genes in the Asiatic Hybrid Lily 'Lollypop' and *L. leichtlinii* 'Hakugin'

To investigate the expression profiles of *LhFT* genes in 'Lollypop' bulbs during the period from chilling exposure of bulbs to leaf emergence from the soil, we also performed a semiquantitative RT-PCR analysis using primer sets that amplified the ORF of each gene. The expression of *LhFT1* in bulb scales increased gradually as chilling exposure progressed and was further increased after planting (**Figure 3A**). Therefore, it was thought that the activation of *LhFT1* transcription occurred right after bulb planting. Similarly, the expression of *LhFT6* was activated in the scales after planting (**Figure 3A**). Two *LhFT6* mRNA variants were detected in the bulb scales (**Figure 3A**), whereas no amplified fragment of this gene was observed in SAMs throughout the chilling and planting periods (**Figure 3B**). The *LhFT6* genome was composed of four exons and three introns, and its full length (from the initial codon to the stop codon) was 1,152 bp (**Figure 4A**). The amplified fragment of 700 bp

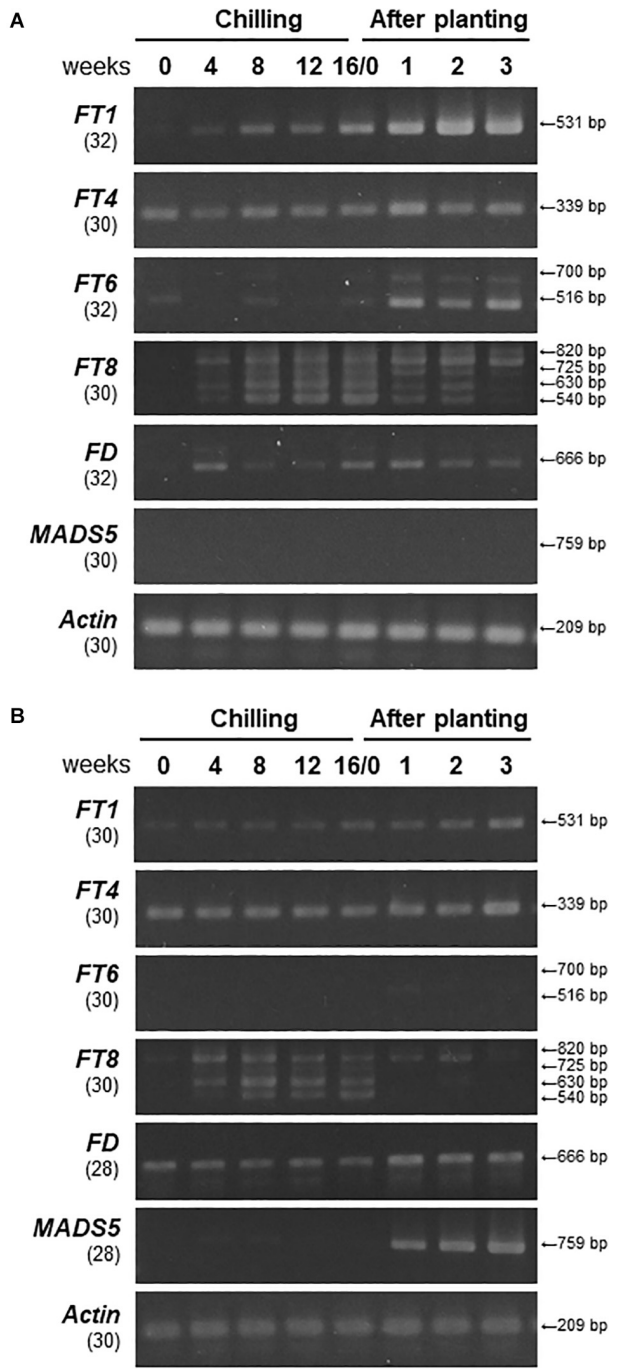

FIGURE 3 | Expression patterns of *LhFT* and flowering-related genes in 'Lollypop' bulbs during chilling and planting. **(A)** Semiquantitative RT-PCR analysis of *LhFT, LhFD*, *LhMADS5*, and *LhACT* genes using scales (**A**) and SAMs **(B)** of 'Lollypop' blubs. Scale and SAM samples were collected from bulbs exposed to chilling for 0, 4, 8, 12, and 16 weeks, and from bulbs grown for 1, 2, and 3 weeks after chilling for 16 weeks. The gene names and number of cycles are indicated to the left of the panel. The amplified fragment lengths are indicated to the right of the panels. The 516-bp fragment of *LhFT6* corresponds to the normal transcript, whereas the 700-bp fragment corresponds to the alternative transcript. The 540-bp fragment of *LhFT8* corresponds to normal transcript, whereas the 630-bp, 725-bp, and 820-bp fragments correspond to alternative transcripts.

corresponding to the alternative mRNA failed to splice out the third intron of *LhFT6* (**Figure 4A**). This alternative *LhFT6* variant included a nonsense codon at position 370 from the initial codon, leading to the lack of the C-terminal region containing segment B (**Supplementary Figure 2**). *LhFT6* was weakly amplified, whereas alternative *LhFT6* variant was strongly amplified (**Figure 3A**). The activation of the expression of *LhFT1* and *LhFT6* in the bulb scales was correlated with floral initiation from SAMs (**Figures 1**, **3A**). Four amplified fragments were detected in *LhFT8* in both scales and SAM of bulbs from 4 weeks after chilling to 2 weeks after planting (**Figures 3A,B**). The genome structure of *LhFT8* was composed of four exons and three introns, but its second intron could not be assessed completely using TAIL-PCR and inverted PCR because it was too long (>8 kb). Three longer *LhFT8* mRNA variants that were detected in scales at 12 weeks after chilling exposure were cloned and sequenced. The fragment of 820, 725, and 630 bp corresponding to alternative *LhFT8* variants included 280 bp or 90 bp *de novo* exons within the second intron (**Figure 4B**) and carried a nonsense codon at position 292 from the initial codon (**Supplementary Figure 2**). *LhFT8* was observed in both bulb scales and SAMs after 4 weeks of chilling exposure and decreased after planting (**Figures 3A,B**). An alternative *LhFT8* variant 1 increased in the bulb scales after

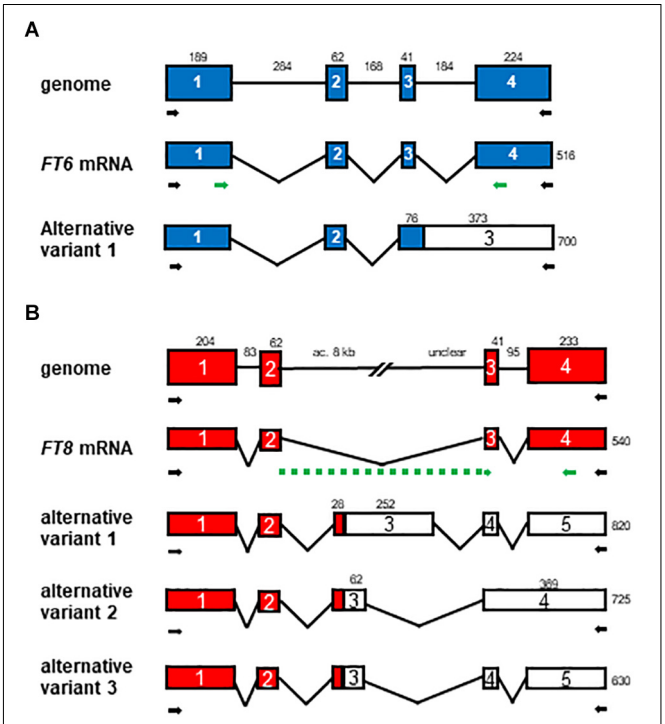

FIGURE 4 | Structure of the genome and mRNA variants of *LhFT6* **(A)** and *LhFT8* **(B)**. The boxes and lines indicate exons and intron, respectively. Filled and empty boxes indicate coding and non-coding regions, respectively. The numbers within the boxes correspond to the number of exons, whereas the numbers outside the boxes indicate the length (in base pairs). We were not able to obtain the complete sequences of the second intron of *LhFT8* because it was too long to allow amplification and sequence analysis. Black and green arrows indicate primer position in RT-PCR and RT-qPCR analyses.

planting and remained constant thereafter. *LhFT4* was expressed constantly in both scales and SAMs during chilling and planting (**Figures 3A,B**). Although the expression of *LhFD* was detected in both scales and SAMs, it was stronger in SAMs than it was in scales. The expression of *LhMADS5*, which is a floral identity gene, was detected exclusively in SAMs at planting and 1 week after planting, which implied that floral bud differentiation started in SAMs (**Figures 1**, **3B**).

We also investigated the expression levels of *LhFTs* and *LhMADS5* in bulb scales of *L. leichtlinii* 'Hakugin' (**Supplementary Figure 4**). The expression of *LhFT1* was detected 1 week after planting, which then increased markedly at 4 weeks after planting. The expression profiles of *LhFT6* were similar to those of *LhFT1*. *LhFT8* was detected in alternative splicing variants, and its expression decreased within two weeks of planting. No expression of *LhFT4* was detected in bulb scales. Increased expression of *LhFT1* and *LhFT6* at 4–6 weeks after planting was correlated with flower initiation, which occurred 7 weeks after planting.

Quantitative Expression Profiles of *FT*-Like Genes in the Asiatic Hybrid Lily 'Lollypop'

Using RT-qPCR, we investigated the expression profiles of *LhFT* and flowering-related genes using bulb scales, leaves, and SAMs of 'Lollypop' (**Figure 5**). The primer set used for *LhFT6* and *LhFT8* genes in the RT-qPCR analysis did not detect alternative variants (**Figure 4**). The expression of *LhFT1* was detected mainly in bulb scales, and not in SAMs. The expression levels of *LhFT1* were increased by 13.7-fold in bulb scales at 26 days compared with day 0 after planting, whereas the expression levels of *LhFT1* were weak in just-emerged leaves (**Figure 5**). The strong expression of *LhFT1* in bulb scales continued until 34 days after planting, after which the mother bulbs disappeared gradually. *LhFT4* was detected at weak but constant levels in bulb scales and leaves during plant development. In the SAM of non-vernalized bulbs and in differentiated floral meristem, the expression levels of *LhFT4* were about 2-fold those detected in other phases. The expression of *LhFT6* was detected exclusively in bulb scales, and was 59.8-fold higher at 34 days compared with day 0 after planting (**Figure 5**). This peak in *LhFT6* expression was observed 1 week later than that of *LhFT1*. The highest expression level of *LhFT8* was detected in bulb scales right after chilling exposure for 4 months, and was 75.6-fold higher than that of non-vernalized bulbs (**Figure 5**). Furthermore, the expression levels of *LhFT8* in bulb scales were reduced after planting. In leaves and SAMs, *LhFT8* transcripts were hardly detected throughout the investigation period. *LhFD* exhibited its highest expression levels in SAMs of non-vernalized bulbs. Subsequently, the expression levels of *LhFD* were reduced by 50% after chilling exposure and planting. Modest expression peaks of *LhFD* in bulb scales and leaves were detected right after chilling exposure and at 34 days after planting, respectively. The expression of *LhMADS5,* which is an *AP1* ortholog, was increased in SAMs after planting, and peaked at 34 days after planting. The expression levels of *LhMADS5* were 24.9-fold higher at 34 days compared with day 0 after planting. The expression of *LhMADS5* was also detected in leaves and was increased up to 40 days after planting.

Taken together, these results showed that enhanced expression of *LhFT1* and *LhFT6* was detected in bulb scales 1 week after planting and correlated well with the timing of floral initiation in SAMs. Conversely, *LhFD* was expressed constantly in SAMs throughout the chilling and planting periods, but was also expressed weakly in scales. Finally, *LhFT8* was expressed during chilling exposure.

Overexpression in the *Arabidopsis ft-10* Mutant

To evaluate the flowering-induction activity of *LhFT* genes, we produced transgenic plants using the late-flowering *Arabidopsis ft-10* mutant. We selected tree representable T_2 lines for each construct and investigated their gene expression patterns and phenotypes. In all selected transgenic T_2 lines, the expression of transgenes was detected (**Figure 6**). Any alternative splicing variants were not detected in *LhFT6*- and *LhFT8*-overexpressing plants. *LhFT1*-expressing plants nos. 2-1, 3-2, and 4-2 developed 8.1, 27.0, and 8.4 rosette leaves, respectively, during bolting, which was significantly lower compared with the 40.9 rosette leaves observed in *GFP*-expressing *ft-10* plants as a vector control (**Figure 6A**). The overexpression complemented the *ft-10* mutant, resulting in similar early-flowering time compared with the wild-type Col-1 plants (10.4 rosette leaves). Similarly, *LhFT8*-expressing plants nos. 2-7, 3-1, and 5-1 developed 15.8, 17.6, and 14.1 rosette leaves, respectively (**Figure 6B**), which was significantly lower than that observed in the *GFP*-expressing plant but higher than that in Col-1 and *LhFT1*-expressing plants nos. 2-4 and 4-2 (**Figures 6A,B**). Therefore, the overexpression also partially complemented the *ft-10* mutant phenotype. Conversely, *LhFT4* and *LhFT6* overexpression did not complement the *ft-10* mutant (**Figures 6C,D**). Taken together, these results suggest that *LhFT1* and *LhFT8* are potential inducers of the floral transition in Asiatic hybrid lilies.

Protein–Protein Interactions Between LhFT Proteins and LhFD

To confirm the presence of protein–protein interactions between LhFT proteins and LhFD, we employed the GAL4 yeast two-hybrid system (**Figure 7A**). Yeast harboring AD:LhFT1 and BK:LhFD grew on quadruple-dropout medium, which was indicative of protein–protein interactions (**Figure 7A**). However, yeast cells harboring the reversed vector combination, BK:LhFT1 and AD:LhFD, did not survive on quadruple-dropout medium. *In vitro* protein–protein interaction assay, AlphaScreen, also showed that LhFT1 protein interacted with LhFD (**Figure 7B**). This signal intensity emitted by LhFT1–LhFD is very similar to that by AtFT–AtFD (**Figure 7C**). In addition, LhFT6–LhFD and LhFT8–LhFD interactions were also detected with weaker signals than that of LhFT1-LhFD interaction, implying their weak but positive interactions with LhFD (**Figure 7B**). Taken together, these results suggest that

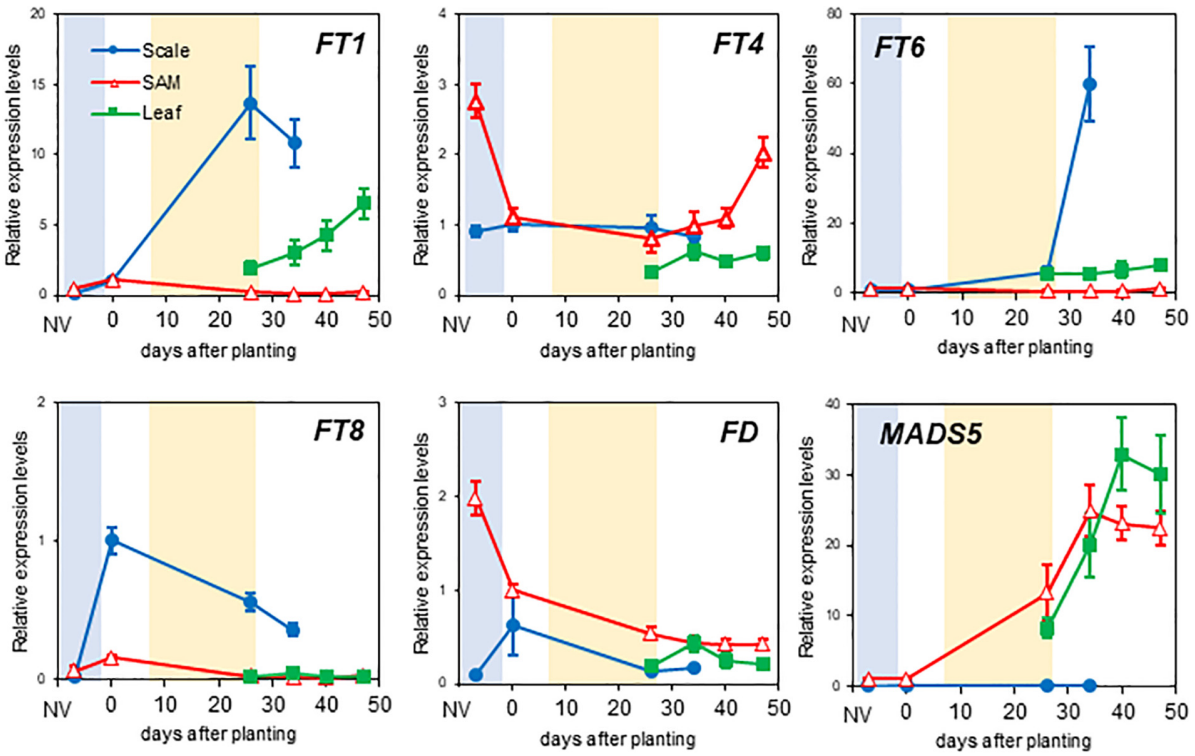

FIGURE 5 | Temporal expression patterns of *LhFT* and flowering-related genes in different organs of 'Lollypop.' The quantitative gene expression analysis of *LhFT1*, *LhFT4*, *LhFT6*, *LhFT8*, *LhFD*, and *LhMADS5* in SAM, scales, leaf samples of Asiatic hybrid 'Lollypop' was performed. Bulb scales samples were collected from bulbs under different development phase, including non-vernalization (NV) and vernalization (= 0 day after planting), 26, and 34 days after planting. Leaf samples were collected from 26, 34, 40, and 47 days after planting. SAM samples were collected from non-vernalized bulbs and vernalized bulb (0 day) and from shoots at 26, 34, 40, and 47 days after planting. Blue and orange fill boxes indicated chilling exposure period for 4 months and floral initiation period, respectively. The expression levels of *LhFT* and flowering-related genes were investigated by RT-qPCR and normalized using that of *LhACT*. Values are expressed as the mean ± SE (n = 6). Temporal expression pattern per each organ is shown in **Supplementary Figure 5**.

the LhFT1, LhFT6, and LhFT8 proteins form heterodimers with the LhFD protein.

DISCUSSION

To identify the molecular mechanisms underlying floral initiation in Asiatic hybrid lilies, we identified four *FT*-like genes, *LhFT1*, *LhFT4*, *LhFT6*, and *LhFT8*, in the Asiatic hybrid lily 'Lollypop' and characterized their functions.

Based on the deduced amino acid sequences of the *LhFT* genes, *LhFT1* and *LhFT8* were classified into the FT-like IA subgroup (**Figure 2**). *LhFT1* belonged to same clade as *LlFT* from *L. longiflorum* (Leeggangers et al., 2018), whereas *LhFT8* belonged to another clade containing *LfFT1* from *L.* × *formolongi* (Li et al., 2017) and *LiFTL2* from the Asiatic hybrid lily 'Connecticut King' (Leeggangers et al., 2018; **Figure 2**). A complementation experiment using the *Arabidopsis ft-10* mutant indicated that both *LhFT1* and *LhFT8* are potential inducers of the floral transition in Asiatic hybrid lilies (**Figures 6A,B**). The floral-inducer activity of *LhFT1* was stronger than that of *LhFT8*. The yeast two-hybrid and AlphaScreen analyses showed that LhFD protein interacted strongly with the LhFT1 protein; however, the interaction between LhFD and LhFT6/8 proteins was not detected (**Figures 7A,B**). The yeast two-hybrid assay can indirectly detect yeast survival and cannot control the expression levels of a transgene fused with the relative large GAL4 protein. We believe that AlphaScreen is more sensitive than the yeast two-hybrid assay because it detects the direct interaction between native proteins with short tag. Therefore, AlphaScreen would be useful to evaluate FT–FD interactions in plants.

The expression levels of *LhFT1* increased gradually in bulb scales during chill exposure, followed by a sharp increase at 1 week after planting (**Figure 3A**). This expression profile of *LhFT1* correlated well with that of a floral identity gene (*LhMADS5*) and with the initiation of floral differentiation (**Figures 1**, **3**). *L.* × *formolongi* is a lily that blooms within 1 year after sowing and expresses *LfFT* in its leaves (Li et al., 2017). *TgFT2* from *T. gesneriana* is expressed in the stem and leaves during rapid shoot elongation and in flowers in the blooming period (Leeggangers et al., 2018). However, previous studies did not investigate the expression of *FT*-like genes in bulb scales of these lilies. Perhaps *LhFTl* ortholog might be upregulated in the bulb scales of other species belonging to the family Liliaceae

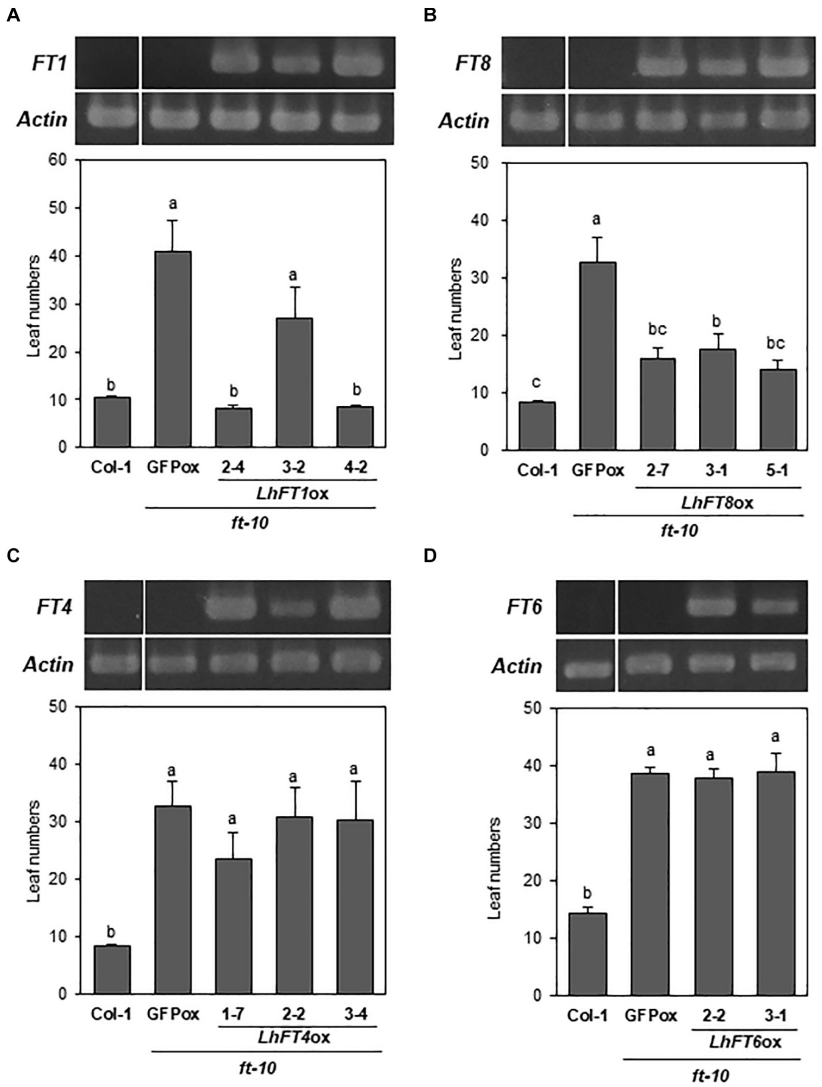

FIGURE 6 | Flowering time phenotypes of the lines overexpressing *LhFT* genes in the *Arabidopsis ft-10* mutant. **(A)** *LhFT1*-overexpressing transgenic plants. **(B)** *LhFT8*-overexpressing transgenic plants. **(C)** *LhFT4*-overexpressing transgenic plants. **(D)** *LhFT6*-overexpressing transgenic plants. All transgenic plants are T_2 homozygous specimens. Col-1 represents the wild-type. GFP indicates the vector control transgenic plants in the *Arabidopsis ft-10* background. RT-PCR analysis was performed to investigate the expression levels of transgenes and *AtACT2* (internal standard). The number of leaves in transgenic lines overexpressing each *LhFT* gene was investigated in 10 individuals of two or three independent lines during bolting. Values are expressed as the mean ± SE (n = 10). The different letters placed above columns are significantly different according to the Tukey–Kramer test ($P < 0.05$).

in response to environmental changes. In many plant species, *FT*-like genes are expressed in leaves under flowering-inducing conditions, followed by transportation via the phloem to the SAM (Abe et al., 2005; Corbesier et al., 2007; Tamaki et al., 2007). However, the four *LhFT* genes identified here in an Asiatic hybrid lily were expressed mainly in bulb scales, in which the expression levels were higher than those detected in leaves (**Figure 5**). *L. leichtlinii* 'Hakugin' also led to the detection of a strong expression of *LhFT1* in their bulb scales (**Supplementary Figure 4**). In 'Hakugin,' which underwent flower initiation 6 weeks later than 'Lollypop,' the expression of *LhFT1* also induced at 4 weeks after planting (**Supplementary Figure 4**). The later flowering of 'Hakugin' than 'Lollypop' correlated well with the delayed expression initiation of *LhFT1* in its scales (**Figure 3A** and **Supplementary Figure 4**). These results strongly suggest that *LhFT1* is a floral inducer in Asiatic hybrid lilies. Scales are leaf-like organs that make up the bulb, in addition to the true photosynthetic leaves and inflorescence base (Rees, 1972). The investigation of the levels of *NFT1* in Chinese narcissuses revealed its expression in apices of bulbs and leaves, but not in scales of bulbs (Li et al., 2013). Thus, this study provided new knowledge, in that the expression of *FT*-like transcripts was induced in bulb scales of an Asiatic hybrid lily.

The deduced amino acid sequence of *LhFT8* was highly similar to that of *LlFT* from *L. longiflorum* (Leeggangers et al., 2018) and orchid *FT* transcripts (Hou and Yang, 2009;

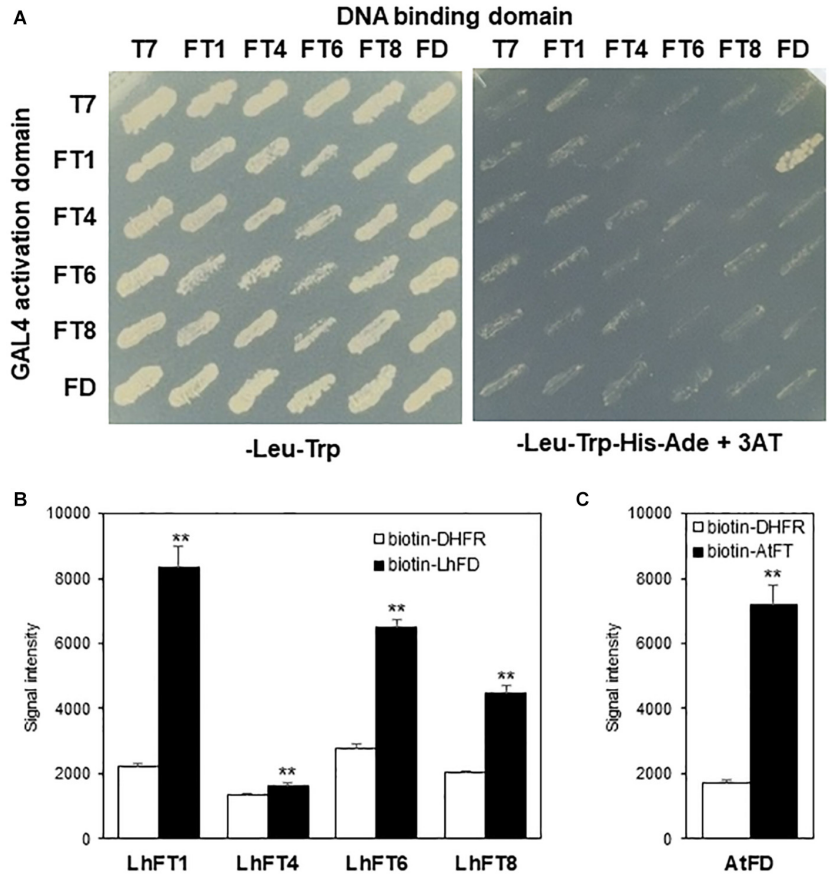

FIGURE 7 | Protein–protein interactions between the LhFT proteins and LhFD. **(A)** The LhFT1, LhFT4, LhFT6, LhFT8, and LhFD proteins were fused to the GAL4 DNA-binding domain (BK) or GAL4 activation domain (AD). pGBKT7 and pGADT7 were used as the negative controls, for bait and prey, respectively. Yeast cells were grown on double-selection medium (−Leu, and −Trp; left) and quadruple-dropout medium (−Leu, −Trp, −His, and −Ade) supplemented with 15 mM 3-AT (right) at 30°C for 3 days. **(B)** *in vitro* protein–protein interaction assay by AlphaScreen. AGIA-tagged LhFTs were incubated with biotinylated LhFD. The interaction intensity between LhFTs and LhFD was analyzed by AlphaScreen Biotinylated dihydrofolate reductase (DHFR), and *E. coli* was used as negative control. Data are mean ± SD. of three independent experiments ($n = 3$). **indicates the significant difference with student's *t*-test ($P < 0.01$). **(C)** AlphaScreen assay for *Arabidopsis* FT–FD interaction. AGIA-tagged AtFD was incubated with biotinylated AtFT. Data are represented as mean ± SD of three independent experiments ($n = 3$).

Jang et al., 2015). Since cold exposure for 9 weeks upregulates *LlFT* in the meristem of bulbs of *L. longiflorum*, *LlFT* has been proposed to be involved in the vernalization response of lilies. The overexpression of *LlFT* in wild-type *Arabidopsis* induces a mild early-flowering phenotype, and *LlFT*-overexpressing transgenic lilies exhibited flowering under non-inductive condition (Leeggangers et al., 2018). An *LhFT8*-overexpressing *Arabidopsis ft-10* mutant also exhibited a mild early-flowering phenotype (**Figure 6B**).

Interestingly, *LhFT8* expressed its four alternative mRNA variants in the bulbs of Asiatic hybrid lilies during chilling exposure (**Figures 3**, **4**). The expression of one functional and three alternative *LhFT8* variants was induced in both the scales and SAM of bulbs during the initial 8 weeks of chilling (**Figure 3**). The functional *LhFT8* mRNA detected in bulb scales and SAMs disappeared 3 weeks and 1 week after planting, respectively. The expression of the functional *LhFT8* gene was downregulated after the induction of floral meristems, unlike that observed for *LhFT1*. *LlFT* was considered to be involved in creating meristem competence to flowering cues in *L. longiflorum* (Leeggangers et al., 2018). Therefore, *LhFT8* is likely to be closely associated with the vernalization response of these plants, rather than act as a floral inducer. In perennial species, *FT*-like genes regulate growth cessation and dormancy (Bohlenius et al., 2006; Hsu et al., 2006, 2011; Ream et al., 2012). In perennial poplar, *PtFT1* expression in winter initiates the transition of vegetative meristems to the reproductive phase, whereas *PtFT2* controls vegetative growth by inducing growth cessation, bud set, and dormancy in the growing season (Hsu et al., 2006, 2011). In biennial sugar beets, the *FT* duplication products *BvFT1* and *BvFT2* have divergent functions (Pin et al., 2010). *BvFT2* is a flowering inducer, whereas *BvFT1*, resulting in part from a three-amino-acid change in segment B of BvFT2, is a flowering repressor, despite being in the FT-like IA subgroup (Pin et al., 2010, 2012). *BvFT1* is expressed at the juvenile stage, whereas *BvFT2* is expressed during the reproductive stage (Pin et al., 2012). The deduced amino acid sequence of *LhFT8* showed 72.2% identity with that of *LhFT1*, and a single residue of segment B of LhFT8 was replaced by

Glu (E) at position 132 (**Supplementary Figure 2**). Therefore, this single residue alteration of segment B between LhFT8 and LhFT1 might be responsible for their functional differentiation. Alternative splicing occurs in >61% of intron-containing genes in *Arabidopsis*, 60% in *Drosophila melanogaster*, and more than 95% in humans (Capovilla et al., 2015). However, the biological significance of most alternative splicing event in plants remains largely unknown. In *Brachypodium distachyon*, which is a model plant for major crop cereals, *BdFT2* undergoes age-dependent alternative splicing, resulting in two splicing variants, *BdFT2*α and *BdFT2*β (Qin et al., 2017). We were not able to clearly demonstrate the molecular mechanism underlying the *LhFT8* alternative splicing. Alternative variants of *LFT6* and *LhFT8* seem to lack segment B in their C-terminal ends (**Supplementary Figure 2**). Segment B is an important domain for binding to 14-3-3 proteins (Taoka et al., 2011). Because AlphaScreen showed that LhFT6 and LhFT8 also interacted with LhFD (**Figure 7**), C-terminal deficiency in LhFT6 and LhFT8 proteins might function as either the negative auto-regulators or antagonists of LhFT1 protein.

Upregulation of *LhFT6* in bulb scales after planting was detected prior to the timing of floral initiation (**Figures 3A**, **5**). The overexpression of *LhFT6* did not complement the delay in flowering in *Arabidopsis ft-10* (**Figure 6D**). The LhFT6 protein showed weaker interaction with LhFD protein than LhFT1 (**Figure 7B**). *LhFT6* was classified into the FT-like 1B subgroup (**Figure 2**), which includes *AcFT6* from *A. cepa* (Lee et al., 2013) and *TgFT3* from *T. gesneriana* (Leeggangers et al., 2018). *TgFT3* expression was initiated earlier and increased in the stem and leaves during rapid shoot elongation. *TgFT3* overexpression weakly repressed floral transition in *Arabidopsis*, and *TgFT3* might act as negative regulator of flowering in tulips (Leeggangers et al., 2018). Further studies are required to identify the function of *LhFT6*.

LhFT4 exhibited a length of 1,164 bp and encoded 112 amino acids, i.e., it was shorter than other FT/TFL proteins (**Supplementary Figure 2**). The deduced amino acid sequences of *LhFT4* were categorized into the FT-like IB clade (**Figure 2**), but contained a histidine (H) residue that is known to be important for the specific and unique TFL1 function in *Arabidopsis* (**Supplementary Figure 2**). The LhFT4 protein showed 98.1% identity with that encoded by *LiFTL3* from the *Lilium* spp. 'Connecticut King' (Leeggangers et al., 2018). However, the *LiFTL3* mRNA encoded sequences of 181 amino acids, suggesting the existence of an *LhFT4* allele encoding longer amino acid sequences in other cultivars of Asiatic hybrid lilies. The overexpression of *LhFT4* did not affect the flowering time in either *Arabidopsis ft-10* plants (**Figure 6C**). In addition, *LhFT4* expression was detected at constitutive levels in all samples (**Figures 3**, **5**). Therefore, we assumed that *LhFT4* does not function in flowering signaling in Asiatic hybrid lilies.

Asiatic hybrid lilies create meristem competence to flowering cues by exposing bulbs to low temperatures, and then the bulbs sprout in spring and flower in late spring to early summer (Okubo and Sochacki, 2012). In the most cultivars, including 'Lollypop,' flower bud differentiation starts and is completed after shoot emergence (Ohkawa et al., 1990). *LhFT8* was associated with the vernalization response in lily bulbs and was speculated to control the expression levels of *LhFT8* mRNA by occurring as splicing variants. When the bulb is released from cold exposure, *LhFT1* expression is induced in bulb scales, and floral transition occurs in SAM after shoot emergence. This study provides the first evidence that the expression of *LhFT1* in bulb scales is regulated by alterations of temperature in Asiatic hybrid lilies and contributes to flowering initiation. Furthermore, the generation of *LhFT8* splicing variants in lily bulbs during cold exposure might be involved in winter memory (Bouche et al., 2017). Further studies are required to reveal the function of *LhFT8* alternative variants and their generation mechanism. Our findings can help reveal the molecular mechanism of flowering and vernalization in geophytes.

DATA AVAILABILITY STATEMENT

The datasets presented in this study can be found in online repositories. The names of the repository/repositories and accession number(s) can be found below: https://www.ddbj.nig.ac.jp/, LC544113; https://www.ddbj.nig.ac.jp/, LC544114; https://www.ddbj.nig.ac.jp/, LC544115; https://www.ddbj.nig.ac.jp/, LC544116; https://www.ddbj.nig.ac.jp/, LC544117; https://www.ddbj.nig.ac.jp/, LC544118; https://www.ddbj.nig.ac.jp/, LC544119; https://www.ddbj.nig.ac.jp/, LC544120; https://www.ddbj.nig.ac.jp/, LC544121.

AUTHOR CONTRIBUTIONS

KK, TN, and MY conceived the experiments. KK and JK performed the gene expression analysis. KK and TN performed the yeast two-hybrid analysis and complement experiments of *ft-10*. KN, AN, and TS performed the AlphaScreen analysis. TN, KN, and MY wrote the manuscript. All authors approved the manuscript.

FUNDING

This work was supported by a Grant-In-Aid for Scientific Research (Nos. 15H04447 and 19H02945) from the Japan Society for the Promotion of Science.

ACKNOWLEDGMENTS

We thank Ms. Nobue Nakamura, Shizuoka University, for technical support.

SUPPLEMENTARY MATERIAL

The Supplementary Material for this article can be found online at: https://www.frontiersin.org/articles/10.3389/fpls.2020.570915/full#supplementary-material

REFERENCES

Abe, M., Kobayashi, Y., Yamamoto, S., Daimon, Y., Yamaguchi, A., Ikeda, Y., et al. (2005). FD, a bZIP protein mediating signals from the floral pathway integrator FT at the shoot apex. *Science* 309, 1052–1056. doi: 10.1126/science.1115983

Ahn, J. H., Miller, D., Winter, V. J., Banfield, M. J., Lee, J. H., Yoo, S. Y., et al. (2006). A divergent external loop confers antagonistic activity on floral regulators FT and TFL1. *EMBO J.* 25, 605–614. doi: 10.1038/sj.emboj.7600950

Beattie, D. J., and White, J. W. (1993). "Lilium – hybrids and species," in *The Physiology of Flower Bulbs*, eds A. de Hertogh and M. Le Nard (Amsterdam: Elsevier), 423–545.

Bohlenius, H., Huang, T., Charbonnel-Campaa, L., Brunner, A. M., Jansson, S., Strauss, S. H., et al. (2006). CO/FT regulatory module controls timing of flowering and seasonal growth cessation in trees. *Science* 312, 1040–1043. doi: 10.1126/science.1126038

Bouche, F., Woods, D. P., and Amasino, R. M. (2017). Winter memory throughout the plant kingdom: different paths to flowering. *Plant Physiol.* 173, 27–35. doi: 10.1104/pp.16.01322

Bradley, D., Ratcliffe, O., Vincent, C., Carpenter, R., and Coen, E. (1997). Inflorescence commitment and architecture in *Arabidopsis*. *Science* 275, 80–83. doi: 10.1126/science.275.5296.80

Bustin, S. A., Benes, V., Garson, J. A., Hellemans, J., Huggett, J., Kubista, M., et al. (2009). The MIQE guidelines: minimum information for publication of quantitative real-time PCR experiments. *Clin. Chem.* 55, 611–622. doi: 10.1373/clinchem.2008.112797

Capovilla, G., Pajoro, A., Immink, R. G., and Schmid, M. (2015). Role of alternative pre-mRNA splicing in temperature signaling. *Curr. Opin. Plant. Biol.* 27, 97–103. doi: 10.1016/j.pbi.2015.06.016

Chen, M. K., Lin, I. C., and Yang, C. H. (2008). Functional analysis of three lily (Lilium longiflorum) APETALA1-like MADS box genes in regulating floral transition and formation. *Plant Cell Physiol.* 49, 704–717. doi: 10.1093/pcp/pcn046

Clough, S. J., and Bent, A. F. (1998). Floral dip: a simplified method for Agrobacterium-mediated transformation of *Arabidopsis thaliana*. *Plant J.* 16, 735–743. doi: 10.1046/j.1365-313x.1998.00343.x

Corbesier, L., Vincent, C., Jang, S., Fornara, F., Fan, Q., Searle, I., et al. (2007). FT protein movement contributes to long-distance signaling in floral induction of *Arabidopsis*. *Science* 316, 1030–1033. doi: 10.1126/science.1141752

Dalvi, V. S., Patil, Y. A., Krishna, B., Sane, P. V., and Sane, A. P. (2019). Indeterminate growth of the umbel inflorescence and bulb is associated with increased expression of the TFL1 homologue. AcTFL1, in onion. *Plant Sci.* 287:110165. doi: 10.1016/j.plantsci.2019.110165

Danilevskaya, O. N., Meng, X., Hou, Z., Ananiev, E. V., and Simmons, C. R. (2008). A genomic and expression compendium of the expanded PEBP gene family from maize. *Plant Physiol.* 146, 250–264. doi: 10.1104/pp.107.109538

Dole, J. M., and Wilkins, H. F. (2005). "Lilium, asiatic and oriental," in *Floriculture Prinples and Species*, (Upper Saddle River, NJ: Pearson Prentice Hall), 645–656.

Fukai, S., and Goi, M. (2001). Floral initiation and development in Lilium longiflorum Thunb. *Tech. Vull. Fac. Agr. Kagawa Univ.* 53, 31–34.

Hamo, M. L. B., Martin, C. V., and Zaccai, M. (2015). Characterization of expressed sequence tags from Lilium longiflorum in vernalized and non-vernalized bulbs. *J. Plant Physiol.* 173, 72–81. doi: 10.1016/j.jplph.2014.09.015

Hanzawa, Y., Money, T., and Bradley, D. (2005). A single amino acid converts a repressor to an activator of flowering. *Proc. Natl. Acad. Sci. U.S.A.* 102, 7748–7753. doi: 10.1073/pnas.0500932102

Higuchi, Y., Narumi, T., Oda, A., Nakano, Y., Sumitomo, K., Fukai, S., et al. (2013). The gated induction system of a systemic floral inhibitor, antiflorigen, determines obligate short-day flowering in chrysanthemums. *Proc. Natl. Acad. Sci. U.S.A.* 110, 17137–17142. doi: 10.1073/pnas.1307617110

Hou, C. J., and Yang, C. H. (2009). Functional analysis of FT and TFL1 orthologs from orchid (Oncidium Gower Ramsey) that regulate the vegetative to reproductive transition. *Plant Cell Physiol.* 50, 1544–1557. doi: 10.1093/pcp/pcp099

Hsu, C. Y., Adams, J. P., Kim, H., No, K., Ma, C., Strauss, S. H., et al. (2011). FLOWERING LOCUS T duplication coordinates reproductive and vegetative growth in perennial poplar. *Proc. Natl. Acad. Sci. U.S.A.* 108, 10756–10761. doi: 10.1073/pnas.1104713108

Hsu, C. Y., Liu, Y., Luthe, D. S., and Yuceer, C. (2006). Poplar FT2 shortens the juvenile phase and promotes seasonal flowering. *Plant Cell* 18, 1846–1861. doi: 10.1105/tpc.106.041038

Huang, J., Liu, X., Wang, J., and Lu, Y. (2014). Transcriptomic analysis of Asiatic lily in the process of vernalization via RNA-seq. *Mol. Biol. Rep.* 41, 3839–3852. doi: 10.1007/s11033-014-3250-2

Igasaki, T., Ishida, Y., Mohri, T., Ichikawa, H., and Shinohara, K. (2002). Transformation of populus alba and direct selection of transformants with the herbicide bialaphos. *Bull. FFPRI* 1, 235–240.

Iwasaki, T., Kaneko, N., Ito, Y., Takeda, H., Sawasaki, T., Heike, T., et al. (2016). Nod2-nodosome in a cell-free system: implications in pathogenesis and drug discovery for blau syndrome and early-onset sarcoidosis. *ScientificWorldJournal* 2016:2597376. doi: 10.1155/2016/2597376

Jang, S., Choi, S. C., Li, H. Y., An, G., and Schmelzer, E. (2015). Functional characterization of Phalaenopsis aphrodite flowering genes PaFT1 and PaFD. *PLoS One* 10:e0134987. doi: 10.1371/journal.pone.0134987

Kinoshita, T., Ono, N., Hayashi, Y., Morimoto, S., Nakamura, S., Soda, M., et al. (2011). FLOWERING LOCUS T regulates stomatal opening. *Curr. Biol.* 21, 1232–1238. doi: 10.1016/j.cub.2011.06.025

Kumar, S., Stecher, G., and Tamura, K. (2016). MEGA7: molecular evolutionary genetics analysis version 7.0 for bigger datasets. *Mol. Biol. Evol.* 33, 1870–1874. doi: 10.1093/molbev/msw054

Lazare, S., Bechar, D., Fernie, A. R., Brotman, Y., and Zaccai, M. (2019). The proof is in the bulb: glycerol influences key stages of lily development. *Plant J.* 97, 321–340. doi: 10.1111/tpj.14122

Lazare, S., and Zaccai, M. (2016). Flowering pathway is regulated by bulb size in Lilium longiflorum (Easter lily). *Plant Biol.* 18, 577–584. doi: 10.1111/plb.12440

Lee, R., Baldwin, S., Kenel, F., McCallum, J., and Macknight, R. (2013). FLOWERING LOCUS T genes control onion bulb formation and flowering. *Nat. Commun.* 4:2884. doi: 10.1038/ncomms3884

Leeggangers, H., Rosilio-Brami, T., Bigas-Nadal, J., Rubin, N., van Dijk, A. D. J., Nunez de Caceres Gonzalez, F. F., et al. (2018). Tulipa gesneriana and Lilium longiflorum PEBP genes and their putative roles in flowering time control. *Plant Cell Physiol.* 59, 90–106. doi: 10.1093/pcp/pcx164

Leeggangers, H. A., Nijveen, H., Bigas, J. N., Hilhorst, H. W., and Immink, R. G. (2017). Molecular regulation of temperature-dependent floral induction in Tulipa gesneriana. *Plant Physiol.* 173, 1904–1919. doi: 10.1104/pp.16.01758

Lehretz, G. G., Sonnewald, S., Hornyik, C., Corral, J. M., and Sonnewald, U. (2019). Post-transcriptional regulation of FLOWERING LOCUS T modulates heat-dependent source-sink development in potato. *Curr. Biol.* 29, 1614–1624.e3. doi: 10.1016/j.cub.2019.04.027

Li, W., Liu, X., and Lu, Y. (2016). Transcriptome comparison reveals key candidate genes in response to vernalization of Oriental lily. *BMC Genomics* 17:664. doi: 10.1186/s12864-016-2955-0

Li, X. F., Jia, L. Y., Xu, J., Deng, X. J., Wang, Y., Zhang, W., et al. (2013). FT-like NFT1 gene may play a role in flower transition induced by heat accumulation in Narcissus tazetta var. chinensis. *Plant Cell Physiol.* 54, 270–281. doi: 10.1093/pcp/pcs181

Li, Y. F., Zhang, M. F., Zhang, M., and Jia, G. X. (2017). Analysis of global gene expression profiles during the flowering initiation process of Lilium x formolongi. *Plant Mol. Biol.* 94, 361–379. doi: 10.1007/s11103-017-0612-x

Liu, X., Wang, Q., Gu, J., and Lu, Y. (2014). Vernalization of oriental hybrid lily 'Sorbonne': changes in physiology metabolic activity and molecular mechanism. *Mol. Biol. Rep.* 41, 6619–6634. doi: 10.1007/s11033-014-3545-3

Marasek-Ciolakowska, A., Nishikawa, T., Shea, D. J., and Okazaki, K. (2018). Breeding of lilies and tulips-Interspecific hybridization and genetic background. *Breed. Sci.* 68, 35–52. doi: 10.1270/jsbbs.17097

Matthews, V. (2007). *The International Lily Register and Checklist 2007 Fourth Edition*. London: The Royal Horticultural Society.

Nagasaki, H., Mochizuki, T., Kodama, Y., Saruhashi, S., Morizaki, S., Sugawara, H., et al. (2013). DDBJ read annotation pipeline: a cloud computing-based pipeline for high-throughput analysis of next-generation sequencing data. *DNA Res.* 20, 383–390. doi: 10.1093/dnares/dst017

Nakano, Y., Takase, T., Takahashi, S., Sumitomo, K., Higuchi, Y., and Hisamatsu, T. (2019). Chrysanthemum requires short-day repeats for anthesis: gradual CsFTL3 induction through a feedback loop under short-day conditions. *Plant Sci.* 283, 247–255. doi: 10.1016/j.plantsci.2019.01.023

Nakatsuka, T., Suzuki, T., Harada, K., Kobayashi, Y., Dohra, H., and Ohno, H. (2019). Floral organ- and temperature-dependent regulation of anthocyanin biosynthesis in Cymbidium hybrid flowers. *Plant Sci.* 287:110173. doi: 10.1016/j.plantsci.2019.110173

Nau, J. (2011). *Ball Redbook 18th Edition Volume 2*. West Chicago, IL: Ball publishing.

Navarro, C., Abelenda, J. A., Cruz-Oro, E., Cuellar, C. A., Tamaki, S., Silva, J., et al. (2011). Control of flowering and storage organ formation in potato by FLOWERING LOCUS T. *Nature* 478, 119–122. doi: 10.1038/nature10431

Nemoto, K., Ramadan, A., Arimura, G. I., Imai, K., Tomii, K., Shinozaki, K., et al. (2017). Tyrosine phosphorylation of the GARU E3 ubiquitin ligase promotes gibberellin signalling by preventing GID1 degradation. *Nat. Commun.* 8:1004. doi: 10.1038/s41467-017-01005-5

Noy-Porat, T., Cohen, D., Mathew, D., Eshel, A., Kamenetsky, R., and Flaishman, M. A. (2013). Turned on by heat: differential expression of FT and LFY-like genes in Narcissus tazetta during floral transition. *J. Exp. Bot.* 64, 3273–3284. doi: 10.1093/jxb/ert165

Oda, A., Narumi, T., Li, T., Kando, T., Higuchi, Y., Sumitomo, K., et al. (2012). CsFTL3, a chrysanthemum FLOWERING LOCUS T-like gene, is a key regulator of photoperiodic flowering in chrysanthemums. *J. Exp. Bot.* 63, 1461–1477. doi: 10.1093/jxb/err387

Ohkawa, K., Kano, A., and Nukaya, A. (1990). Time of flower bud developmentiation in Asiatic hybrid lilies. *Acta Hort.* 266, 211–220. doi: 10.17660/actahortic.1990.266.27

Okubo, H., and Sochacki, D. (2012). "Botanical and horticultural aspects of major ornamental geophytes," in *Ornamental Geophytes*, eds R. Kamenetsky and H. Okubo (Boca Raton, FL: CRC press), 77–121. doi: 10.1201/b12881-5

Pin, P. A., Benlloch, R., Bonnet, D., Wremerth-Weich, E., Kraft, T., Gielen, J. J., et al. (2010). An antagonistic pair of FT homologs mediates the control of flowering time in sugar beet. *Science* 330, 1397–1400. doi: 10.1126/science.1197004

Pin, P. A., Zhang, W., Vogt, S. H., Dally, N., Buttner, B., Schulze-Buxloh, G., et al. (2012). The role of a pseudo-response regulator gene in life cycle adaptation and domestication of beet. *Curr. Biol.* 22, 1095–1101. doi: 10.1016/j.cub.2012.04.007

Qin, Z., Wu, J., Geng, S., Feng, N., Chen, F., Kong, X., et al. (2017). Regulation of FT splicing by an endogenous cue in temperate grasses. *Nat. Commun.* 8:14320. doi: 10.1038/ncomms14320

Ream, T. S., Woods, D. P., and Amasino, R. M. (2012). The molecular basis of vernalization in different plant groups. *Cold Spring Harb. Symp. Quant. Biol.* 77, 105–115. doi: 10.1101/sqb.2013.77.014449

Rees, A. R. (1972). *The growth of bulbs*. New York, NY: Academic press.

Sawasaki, T., Kamura, N., Matsunaga, S., Saeki, M., Tsuchimochi, M., Morishita, R., et al. (2008). *Arabidopsis* HY5 protein functions as a DNA-binding tag for purification and functional immobilization of proteins on agarose/DNA microplate. *FEBS Lett.* 582, 221–228. doi: 10.1016/j.febslet.2007.12.004

Suzuki, K., Suzuki, T., Nakatsuka, T., Dohra, H., Yamagishi, M., Matsuyama, K., et al. (2016). RNA-seq-based evaluation of bicolor tepal pigmentation in Asiatic hybrid lilies (Lilium spp.). *BMC Genomics* 17:611. doi: 10.1186/s12864-016-2995-5

Tamaki, S., Matsuo, S., Wong, H. L., Yokoi, S., and Shimamoto, K. (2007). Hd3a protein is a mobile flowering signal in rice. *Science* 316, 1033–1036. doi: 10.1126/science.1141753

Taoka, K., Ohki, I., Tsuji, H., Furuita, K., Hayashi, K., Yanase, T., et al. (2011). 14-3-3 proteins act as intracellular receptors for rice Hd3a florigen. *Nature* 476, 332–335. doi: 10.1038/nature10272

van Tuyl, J. M., Arens, P., Shahin, A., Marasek-Ciolakowska, A., Barba-Gonzalez, R., Kim, H. T., et al. (2018). "Lilium," in *Ornamental Crops*, ed. J. van Huylenbroeck (Berlin: Springer), 481–512.

Villacorta-Martin, C., Nunez de Caceres Gonzalez, F. F., de Haan, J., Huijben, K., Passarinho, P., Lugassi-Ben Hamo, M., et al. (2015). Whole transcriptome profiling of the vernalization process in Lilium longiflorum (cultivar White Heaven) bulbs. *BMC Genomics* 16:550. doi: 10.1186/s12864-015-1675-1

Wang, J., Yang, Y., Liu, X., Huang, J., Wang, Q., Gu, J., et al. (2014). Transcriptome profiling of the cold response and signaling pathways in Lilium lancifolium. *BMC Genomics* 15:203. doi: 10.1186/1471-2164-15-203

Wickland, D. P., and Hanzawa, Y. (2015). The FLOWERING LOCUS T/TERMINAL FLOWER 1 gene family: functional evolution and molecular mechanisms. *Mol. Plant* 8, 983–997. doi: 10.1016/j.molp.2015.01.007

Yamagishi, M. (2013). How genes paint lily flowers: regulation of colouration and pigmentation patterning. *Sci. Hort.* 163, 27–36. doi: 10.1016/j.scienta.2013.07.024

Yamagishi, M., Toda, S., and Tasaki, K. (2014). The novel allele of the LhMYB12 gene is involved in splatter-type spot formation on the flower tepals of Asiatic hybrid lilies (*Lilium* spp.). *New Phytol.* 201, 1009–1020. doi: 10.1111/nph.12572

Yano, T., Takeda, H., Uematsu, A., Yamanaka, S., Nomura, S., Nemoto, K., et al. (2016). AGIA tag system based on a high affinity rabbit monoclonal antibody against human dopamine receptor D1 for protein analysis. *PLoS One* 11:e0156716. doi: 10.1371/journal.pone.0156716

Conflict of Interest: The authors declare that the research was conducted in the absence of any commercial or financial relationships that could be construed as a potential conflict of interest.

Copyright © 2020 Kurokawa, Kobayashi, Nemoto, Nozawa, Sawasaki, Nakatsuka and Yamagishi. This is an open-access article distributed under the terms of the Creative Commons Attribution License (CC BY). The use, distribution or reproduction in other forums is permitted, provided the original author(s) and the copyright owner(s) are credited and that the original publication in this journal is cited, in accordance with accepted academic practice. No use, distribution or reproduction is permitted which does not comply with these terms.

frontiers in Plant Science

ORIGINAL RESEARCH
published: 09 November 2020
doi: 10.3389/fpls.2020.585927

Perspectives on Low Temperature Tolerance and Vernalization Sensitivity in Barley: Prospects for Facultative Growth Habit

María Muñoz-Amatriaín[1†], Javier Hernandez[2*†], Dustin Herb[2†], P. Stephen Baenziger[3], Anne Marie Bochard[4], Flavio Capettini[5], Ana Casas[6], Alfonso Cuesta-Marcos[7], Claus Einfeldt[8], Scott Fisk[2], Amelie Genty[9], Laura Helgerson[2], Markus Herz[10], Gongshe Hu[11], Ernesto Igartua[6], Ildiko Karsai[12], Toshiki Nakamura[13], Kazuhiro Sato[14], Kevin Smith[15], Eric Stockinger[16], William Thomas[17] and Patrick Hayes[2]*

[1] Department of Soil and Crop Sciences, Colorado State University, Fort Collins, CO, United States, [2] Department of Crop and Soil Science, Oregon State University, Corvallis, OR, United States, [3] Department of Agronomy and Horticulture, University of Nebraska-Lincoln, Lincoln, NE, United States, [4] Limagrain Europe, Clermont-Ferrand, France, [5] Field Crop Development Centre, Alberta Agriculture and Forestry, Lacombe, AB, Canada, [6] Consejo Superior de Investigaciones Científicas (CSIC), Aula Dei Experimental Station, Zaragoza, Spain, [7] Bayer – Crop Science, Woodland, CA, United States, [8] Saatzucht Ackermann GmbH & Co. KG, Irlbach, Germany, [9] Secobra Recherches, Centre de Bois Henry, Maule, France, [10] Bavarian State Research Center for Agriculture, Institute for Crop Science, Freising, Germany, [11] United States Department of Agriculture-Agricultural Research Service (USDA-ARS), Aberdeen, ID, United States, [12] Department of Molecular Breeding, Center for Agricultural Research, Martonvásár, Hungary, [13] Division of Field Crops and Horticulture Research Tohoku Agricultural Research Center National Agriculture and Food Research Organization (NARO), Morioka, Japan, [14] Institute of Plant Science and Resources, Okayama University, Kurashiki, Japan, [15] Department of Agronomy and Plant Genetics, University of Minnesota, St. Paul, MN, United States, [16] Department of Horticulture and Crop Science, The Ohio State University/Ohio Agricultural Research and Development Center (OARDC), Wooster, OH, United States, [17] The James Hutton Institute (JHI), Invergowrie, United Kingdom

One option to achieving greater resiliency for barley production in the face of climate change is to explore the potential of winter and facultative growth habits: for both types, low temperature tolerance (LTT) and vernalization sensitivity are key traits. Sensitivity to short-day photoperiod is a desirable attribute for facultative types. In order to broaden our understanding of the genetics of these phenotypes, we mapped quantitative trait loci (QTLs) and identified candidate genes using a genome-wide association studies (GWAS) panel composed of 882 barley accessions that was genotyped with the Illumina 9K single-nucleotide polymorphism (SNP) chip. Fifteen loci including 5 known and 10 novel QTL/genes were identified for LTT—assessed as winter survival in 10 field tests and mapped using a GWAS meta-analysis. *FR-H1*, *FR-H2*, and *FR-H3* were major drivers of LTT, and candidate genes were identified for *FR-H3*. The principal determinants of vernalization sensitivity were *VRN-H1*, *VRN-H2*, and *PPD-H1*. *VRN-H2* deletions conferred insensitive or intermediate sensitivity to vernalization. A subset of accessions with maximum LTT were identified as a resource for allele mining and further characterization. Facultative types comprised a small portion of the GWAS panel but may be useful for developing germplasm with this growth habit.

Keywords: barley, low temperature tolerance, GWAS, meta-analysis, facultative, multi-environments

OPEN ACCESS

Edited by:
Elizabeth Dennis, Commonwealth Scientific and Industrial Research Organisation (CSIRO), Australia

Reviewed by:
Ben Trevaskis, Commonwealth Scientific and Industrial Research Organisation (CSIRO), Australia
Martin Mascher, Leibniz Institute of Plant Genetics and Crop Plant Research (IPK), Germany

***Correspondence:**
María Muñoz-Amatriaín
maria.munoz_amatriain@colostate.edu
Javier Hernandez
hernanfr@oregonstate.edu

† These authors have contributed equally to this work

Specialty section:
This article was submitted to Plant Development and EvoDevo, a section of the journal Frontiers in Plant Science

Received: *24 August 2020*
Accepted: *01 October 2020*
Published: *09 November 2020*

Citation:
Muñoz-Amatriaín M, Hernandez J, Herb D, Baenziger PS, Bochard AM, Capettini F, Casas A, Cuesta-Marcos A, Einfeldt C, Fisk S, Genty A, Helgerson L, Herz M, Hu G, Igartua E, Karsai I, Nakamura T, Sato K, Smith K, Stockinger E, Thomas W and Hayes P (2020) Perspectives on Low Temperature Tolerance and Vernalization Sensitivity in Barley: Prospects for Facultative Growth Habit. Front. Plant Sci. 11:585927. doi: 10.3389/fpls.2020.585927

INTRODUCTION

To meet the challenges of climate change, there has been increasing interest in the agronomic potential of fall-sown barley in northern latitudes (Fisk et al., 2013; Cuesta-Marcos et al., 2015). Although fall-sown barley in regions with winter precipitation patterns can have significant yield advantages compared with spring-sown barley, there is a heightened risk of low temperature-induced crop injury. This risk is problematic at two stages of development: at the vegetative stage, which is the focus of this research, and at flowering. For recent research on low temperature injury at flowering in cereals, please see Trevaskis et al. (2007); Chen et al. (2009), and Powell et al. (2012). Low temperature tolerance (LTT) at the vegetative stage is an inducible trait that involves a complex gene regulon (reviewed by Cuesta-Marcos et al., 2015), and it is a key component of the mega-phenotype known as "winter-hardiness." Recognizing that a range of factors can determine winter-hardiness, in this report, we will focus on LTT, as measured by winter survival (WS). In this report, we will use LTT and WS synonymously. Additional traits that may contribute to winter-hardiness are sensitivity to vernalization (VRN) (Hayes et al., 1993) and sensitivity to short-day photoperiod (sd-PPD) (Fowler et al., 2001). The sd-PPD phenotype is defined as the case where the recessive "sensitive" (null) allele confers slow or no growth under short-day conditions and the "insensitive" (dominant) allele confers normal, or near-normal, growth rates under short-day conditions. It is difficult to measure VRN sensitivity under field conditions. This trait can be approximated by measuring the days to flowering (DTF) of unvernalized plants under controlled environment conditions and is the approach we follow in this report. Although barley and other cereals are considered long-day plants, there is phenotypic variation in barley for flowering time under short-day conditions; this variation is due to allelic variation at *PPD-H2* (Karsai et al., 2008; Kikuchi et al., 2012). The functional allele allows for flowering under sd-PPD; the non-functional allele delays flowering under sd-PPD. We use "sensitivity" in this context to refer to the non-functional allele. Sensitivity to sd-PPD is a challenge to measure as a phenotype. Under field conditions, the flowering time of fall-planted cereals is determined by multiple genes responding to a range of environmental signals. Sensitivity to sd-PPD can be measured under controlled environment conditions, but the requirement that experimental materials be exposed only to short photoperiod for an extended time makes it challenging to assess the phenotypic responses of larger germplasm arrays. Therefore, potential sensitivity to sd-PPD is most easily assessed based on the allele-specific genotyping of *PPD-H2* (Kikuchi et al., 2012). Understanding the genetics and physiology of LTT, VRN, and sd-PPD will, therefore, lead to more efficient breeding of fall-planted barley and utilization of the growth habit type "facultative."

Facultative growth habit, as defined by von Zitzewitz et al. (2011), is defined as maximum LTT, sd-PPD sensitivity, and no VRN sensitivity. The theoretical advantage of facultative growth habit in the context of climate change and climate volatility is that it could give growers and processors maximum flexibility because the same variety could be planted in the fall or in the spring. If planted in the fall, the variety would be capable of achieving maximum LTT, and sd-PPD would ensure a timely vegetative to reproductive transition once day length reached a critical threshold. If planted in the spring, the inducible LTT regulon would not be triggered, and thus there would be no cost in reproductive fitness to the variety. Likewise, day length would be sufficiently long that sd-PPD would not be a factor. Genetic keys to the facultative growth habit scenario are the loss-of-function deletion of the *VRN-H2* complex locus, or at least critical elements of it, and the presence of the winter allele in *VRN-H1* with the intact, full intron 1 region (Karsai et al., 2005; von Zitzewitz et al., 2005; Rizza et al., 2016).

There is an extensive literature on the association of VRN sensitivity with LTT (reviewed by Cuesta-Marcos et al., 2015). VRN sensitivity will delay the vegetative to reproductive transition and is therefore a potential mechanism for ensuring maximum LTT. However, a problem with VRN sensitivity in the context of climate change is that it cannot be relied upon to delay the vegetative to reproductive transition: the VRN requirement can be met–and the vegetative to reproductive transition initiated–long before the risk of low temperature injury is past. In contrast, sd-PPD sensitivity should be a much better "insurance" against precocious transition to reproductive growth because climate change is not altering day length. There is no known cost to VRN sensitivity under fall-sown conditions, and there are reported yield advantages whose physiological basis is not clear (Casao et al., 2011a). However, if it can be demonstrated that there is no intrinsic penalty in terms of reproductive fitness, elimination of VRN sensitivity within an overall genome architecture of maximum LTT and sd-PPD sensitivity could be beneficial. Variety development could be streamlined, and commercial production simplified. The breeder could reduce breeding cycle time by bypassing the need for vernalization; the grower could plant the same variety whenever field and/or market conditions were optimum; seed companies could potentially reduce the number of cultivars they need to have available; and the end-user would have the assurance of similar quality/processing attributes, regardless of production season.

There is accumulating evidence that facultative growth habit, as defined, is feasible and viable. Bi-parental quantitative trait locus (QTL) mapping (Fisk et al., 2013) and genome-wide association studies (GWAS) (von Zitzewitz et al., 2011) confirm that maximum LTT is possible with the deletion of *VRN-H2*. Cuesta-Marcos et al. (2015) used near-isogenic lines and a suite of genomics tools to make the same point. A brief review of the key genes discovered in these studies provides essential perspective and framework for the research described in this report. The QTLs and genes (when known) related to LTT are: *FR-H1* (*HvBM5a*) (Fu et al., 2005; von Zitzewitz et al., 2005; Dhillon et al., 2010), *FR-H2* (a cluster of CBF transcription factors) (Skinner et al., 2005, 2006), and *FR-H3* (Fisk et al., 2013). The VRN genes are *VRN-H1* (*HvBM5a*) (Danyluk et al., 2003; Trevaskis et al., 2003; Yan et al., 2003; von Zitzewitz et al., 2005; Cockram et al., 2007; Dhillon et al., 2010), *VRN-H2* (*ZCCT-Ha,b,c*) (Yan et al., 2004), and *VRN-H3* (*HvFT1*) (Yan et al., 2006; Faure et al., 2007; Kikuchi et al., 2009). Sd-PPD is determined by *PPD-H2* (Pan et al., 1994; Fowler et al., 2001; Faure et al., 2007;

Cuesta-Marcos et al., 2008; Kikuchi et al., 2009; Casao et al., 2011b; Kikuchi et al., 2012). *PPD-H1* (Karsai et al., 1999; Turner et al., 2005) determines flowering time under long-day conditions and is therefore not directly relevant to facultative growth habit but could be important for facultative varieties under spring-sown conditions. The cited studies were based on a relatively narrow sample of barley germplasm.

To further our understanding of LTT, VRN sensitivity, and facultative growth habit, we assembled a large (n = 882) panel of diverse barley germplasm and assessed it for WS under field conditions in a large number of field tests (24 locations over a 2-year period). The panel was also characterized for VRN sensitivity, measured as DTF, under controlled environment conditions. We conducted a GWAS meta-analysis based on Fisher's test of combined probabilities to integrate WS data from multiple environments. This approach increases the power of detection and reduces false-positive associations (Evangelou and Ioannidis, 2013). A subset of lines were then re-genotyped for targeted alleles at known LTT, VRN, and PPD loci in order to test the predictive utility of the genetic model for facultative growth habit.

MATERIALS AND METHODS

Plant Materials

An array of 882 barley accessions composed of cultivars, landraces, and advanced generation experimental lines contributed by 21 barley breeding and/or genetics programs from around the world was used to evaluate LTT (as WS) and VRN sensitivity (as DTF). Information on the accessions and programs contributing to germplasm is listed in **Supplementary Table S1**. With the goal of excluding spring accessions that would serve only to confirm the value of alleles at the known major LTT QTLs, a criterion for inclusion in the array was the expectation of some degree of LTT. The largest contributors to the panel were: (1) Oregon State University (OSU) and the University of Minnesota (UM), both United States via the Facwin-6 (Belcher et al., 2015), and (2) the James Hutton Institute (JHI) and the University of Dundee (Scotland, United Kingdom) via the Association Genetics of UK Elite Barley (AGOUEB) (Cockram et al., 2010) and Genomics-Assisted Exploration of Barley Diversity (ExBarDiv) projects (Tondelli et al., 2013).

Phenotyping

The array (or subsets thereof) was phenotyped for WS under field conditions at 13 locations in 2013–2014 [Canada, France, Germany (two sites), Hungary, Japan, Scotland, Spain, and the United States (five sites)] and 11 locations in 2014–2015 [Canada, France, Germany, Hungary, Scotland, Spain, and the United States (five sites)]. Details on the specific test sites are provided in **Supplementary Table S2**. Data from the locations that grew the full array were used for this report; data from the locations that grew the subsets of the array were not used. A Type II modified augmented design (Lin and Poushinsky, 1983, 1985) was used at each location. In this design, a single replicate of the accessions was distributed among blocks, each containing three replicated checks. The primary check was "Alba" (winter growth habit), and the secondary checks were "Maja" (facultative growth habit) and "Full Pint" (spring growth habit). Each entry was grown in a single row, 1-m long plot, and WS was assessed visually as the percentage of plants that survived the winter. This design allows entry values to be adjusted based on the primary and secondary checks. Based on the relative efficiency, there was no advantage to either primary or secondary adjustments: therefore, un-adjusted WS values were used for all subsequent analyses.

The array was phenotyped for VRN sensitivity, by measuring DTF, under greenhouse conditions in 2015 at OSU, Corvallis, Oregon (United States). A single unvernalized plant of each accession was grown in a six cell-pack, where each plant had a total soil volume of 85 cm^3. The Alba, Maja, and Full Pint checks were each replicated 10 times. The greenhouse was maintained at $18 \pm 2°C$. Natural daylight was supplemented with high intensity lighting to ensure a photoperiod regime of 16 h light/24 h. DTF was recorded for each plant when the first inflorescence was 50% emerged from the boot. The experiment was terminated at 154 days after planting, and any accession that had not flowered was assigned a DTF value of 154. Twenty-one accessions were not included in the VRN phenotyping due to the lack of seed, and three accessions that were included did not germinate. These 24 accessions were not included in subsequent analyses of DTF data. Growth habit classification data (winter, facultative, spring), when available, were obtained for these accessions from USDA-GRIN[1]. Based on DTF, accessions were separated into three groups: those with vernalization sensitivity (DTF $\geq$ 130), those with vernalization insensitivity (DTF $\leq$ 73), and those with intermediate sensitivity (DTF $\geq$ 74 and $\leq$ 129). A DTF threshold value $\leq$ 73 for vernalization insensitive germplasm was based on "Dicktoo," a well-characterized facultative barley (Karsai et al., 2005) and accession 06OR-20, as described in the "Results" section. Inflorescence type (2-row, 6-row) was recorded for each accession. The WS and DTF phenotype data for each accession are provided in **Supplementary Table S1**.

Genotyping

The 882 accessions were genotyped with the barley 9K iSelect array (Comadran et al., 2012). Genotyping of the AGOUEB and ExBarDiv germplasm was conducted at TraitGenetics GmbH in Gatersleben, Germany, whereas the remaining germplasm was genotyped at the USDA-ARS Small Grains Genotyping Center in Fargo, ND, United States. After combining all available data and filtering for data quality (>20% missing data) and minor allele frequency (MAF) <0.05, there were 5,725 single-nucleotide polymorphism (SNP) loci assayed on each of 882 accessions. Physical coordinates of iSelect SNPs on the barley reference genome (Mascher et al., 2017) were retrieved from BARLEX[2] (Colmsee et al., 2015). Of the 5,275 SNPs, 4,875 have an assigned physical position on the reference genome. The complete genotype data are provided in **Supplementary Table S3**.

[1]https://www.ars-grin.gov/

[2]http://barlex.barleysequence.org/

A KASP genotyping assay (LGC Genomics, Teddington, United Kingdom) targeting specific loci involved in growth habit and vernalization was performed in a selected subset of 93 accessions based on the first year of field WS data. The targeted loci were *PPD-H1*, *PPD-H2*, *VRN-H1*, and *VRN-H2*. Data are provided in **Supplementary Table S4**. After a second year of WS data were obtained, 23 of the original 93 accessions chosen in Year 1 were in the overall top 5% based on the average of the 10 environments, across 2 years, where there was differential WS. In this report, we focus on these 23 accessions (**Table 3**).

Data Analysis

Principal component analysis (PCA) and linkage disequilibrium (LD) analyses were conducted in TASSEL v.5 (Bradbury et al., 2007) using SNPs with MAF >0.05. LD was estimated as the correlation coefficient r^2 between pairs of SNPs within each chromosome. The decay of LD over physical distance was investigated by plotting pair-wise r^2 values and generating a locally weighted scatterplot smoothing (LOESS) curve. LD decay distance was determined when r^2 fell to the critical threshold estimated from the 99th percentile r^2 distribution for unlinked markers. For GWAS, the mixed-linear model (Zhang et al., 2010) implemented in TASSEL v.5 was used, with a principal component analysis (3 PCs) accounting for population structure in the dataset. For WS, GWAS was first performed on each individual environment. In order to statistically pool GWAS results from the different environments and to detect gene by environment interactions, a meta-analysis was performed (Manning et al., 2011; Kang, 2015). We used Fisher's method (Fisher, 1925) for combining *p*-values across environments, as follows:

$$X^2 = -2\sum_{i=1}^{k} ln\,(pi)$$

where p_i is the *p*-value for the i^{th} environment. Then, the new Fisher's *p*-value was calculated using the formula

$$p_{Fisher} = 1 - Pr\left(X^2_{2k} \leq X^2\right)$$

where X^2_{2k} is a chi-square variable with $2k$ degrees of freedom, and k is the number of environments being combined. A false discovery rate (FDR; Benjamini and Hochberg, 1995) threshold of 0.01 was used to identify significant associations. Genes within significant regions were retrieved from the barley reference genome (Mascher et al., 2017) available in BARLEX (see footnote 2).

To assess two locus interactions for VRN sensitivity and WS, a likelihood ratio test (LRT) was performed using a model that includes the two markers tested, their interactions, and population structure based on PCs and a model including only PCs (Cuesta-Marcos et al., 2010). The LRT for VRN sensitivity was based on SNPs with a *q*-value ≤0.1, based on association analysis. The significant SNPs from this analysis were then used to identify the interactions between loci associated with WS. A phylogenetic tree of the 5% accessions with maximum WS (using the average of 10 environments) was generated using the neighbor-joining clustering method implemented in TASSEL v.5.

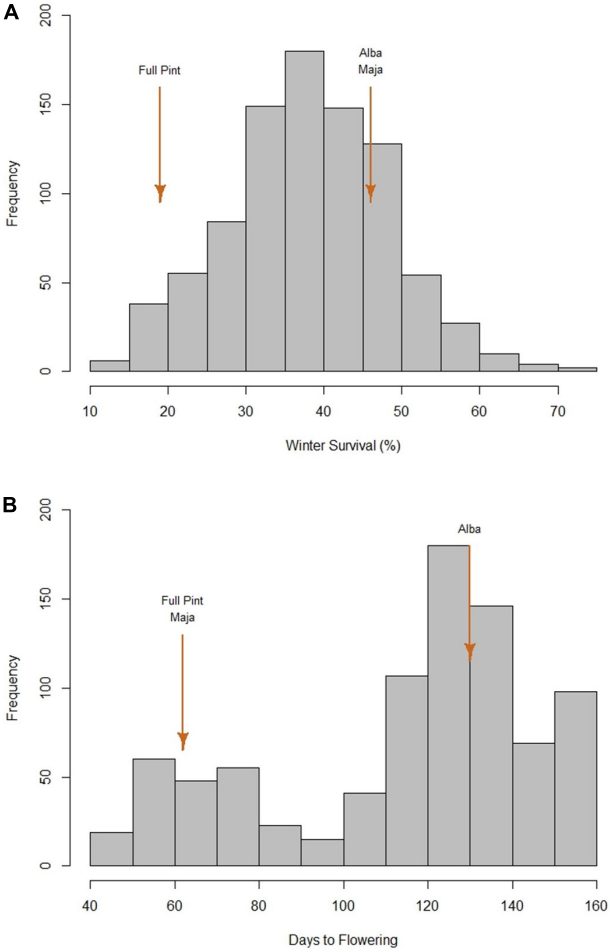

FIGURE 1 | Phenotypic frequency distributions for 882 barley accessions. **(A)** Average winter survival across 10 locations. **(B)** Days to flowering under greenhouse conditions without vernalization. Full Pint, Maja, and Alba are the spring, facultative, and winter checks, respectively.

RESULTS

LTT and VRN Sensitivity

We used data from the 10 of the 24 environments where there was differential WS: Minnesota (MN) and Ohio (OH) (United States) and Alberta (AB) (Canada) in 2014 and 2015; 2014 Germany (DE); and 2015 Idaho (ID), Scotland (United Kingdom), and Spain (ES). In 13 environments, there was either 100% WS, no detectable difference in WS, or the experiment was compromised in some fashion. In one environment (2014 Nebraska), no entries survived. The frequency distribution of average WS was normal (**Figure 1A**) and revealed substantial phenotypic variation, with a low of 11% (Mishima 41), a high of 74% (PI87835), and an average of 38%. Considering the checks, the winter (Alba) and facultative (Maja) checks had similar winter survival levels: 46 and 47%, respectively. The spring check (Full Pint) had a WS value of 19%.

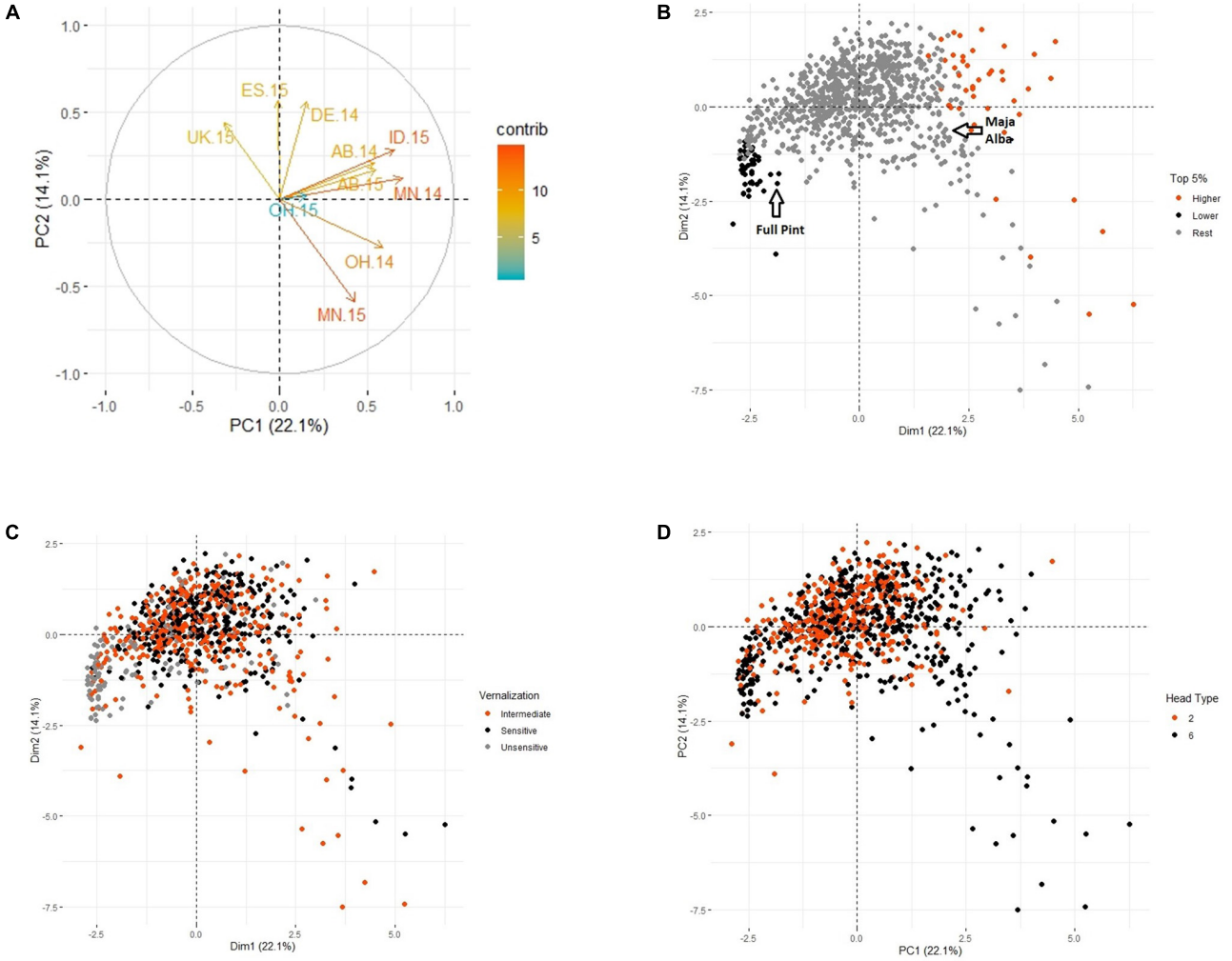

FIGURE 2 | Principal component analysis of average winter survival across 10 locations. **(A)** Contribution of each location to variation across all sites (locations are defined in the text). **(B)** Overlay of the top 5%, bottom 5%, and rest of the accessions for winter survival. **(C)** Overlay of vernalization sensitivity (see text for definitions). **(D)** Overlay of head type (2-row, 6-row).

The frequency distribution of DTF, without vernalization, clearly separates two groups of accessions, with the dividing point at 95 DTF (**Figure 1B**). A DTF of 95 under controlled environment conditions, however, is not necessarily predictive of agronomically relevant DTF under field conditions (data not shown). Both Full Pint (the spring check) and Maja (the facultative check) had DTF values of 62, as compared with Alba, the winter check, at 130. In this research, we defined the 139 vernalization-insensitive (spring or potentially facultative) accessions as those with DTF values $\leq$ 73 based on Dicktoo (DTF = 72) and one accession (O6OR-20) with a DTF of 73. There were 386 accessions with intermediate vernalization sensitivity ($\geq$ 74 and $\leq$ 129 DTF). The remaining 333 accessions where DTF data were obtained were classified as vernalization sensitive and are defined, for the purposes of this research, as having winter growth habit (**Supplementary Table S1**).

LTT and Its Relationship With Test Environments, VRN Sensitivity, and Inflorescence Type

The relationships between LTT, VRN sensitivity, and spike morphology were assessed using principal component analysis. The first four principal components accounted for 56.6% of the variation for WS. PC1 accounted for 22.1% of the variation, and PC2 accounted for 14.1% of the variation (**Figure 2A**). The 10 differential environments were clustered into three groups: 1) UK-15, ES-15, and DE-14, 2) OH-15, ID-15, AB-14, AB-15, and MN-14, and 3) OH-14 and MN-15, of which AB-14 and AB-15 were the most similar to each other, and UK-15 was the most unique. The overlay of WS values for the top and bottom 5% of accessions (**Figure 2B**) showed that accessions with the highest survival values (n = 44) were grouped with the Alba and Maja checks, whereas those with

TABLE 1 | Barley accessions in the top 5% for average winter survival.

Accession	Clade	Contributor	Source	Country of origin	Synonym	Type	Row type	DTF	Avg. WS	Avg. WS clade
06OR-20	1	OSU-OR	OSU-OR	United States		Breeding line	6	73	58	
MW09S4086-001	1	UMN	UMN	United States		Breeding line	6	69	59	
MW09S4076-002	1	UMN	UMN	United States		Breeding line	6	58	65	61
2011-F5-110-1	2	OSU-OR	OSU-OR	United States		Breeding line	6	139	59	
2011-F5-123-1	2	OSU-OR	OSU-OR	United States		Breeding line	6	146	59	
2011-F5-97-1	2	OSU-OR	OSU-OR	United States		Breeding line	6	130	57	
2011-F5-141-5	2	OSU-OR	OSU-OR	United States		Breeding line	6	127	62	
2011-F5-36-3	2	OSU-OR	OSU-OR	United States		Breeding line	6	154	69	
2011-F5-37-3	2	OSU-OR	OSU-OR	United States		Breeding line	6	126	55	
OBADV11-2	2	OSU-OR	OSU-OR	United States		Breeding line	6	89	58	
07OR-55	2	OSU-OR	OSU-OR	United States		Breeding line	6	82	56	59
29648/2329	3	Lfl	LfL	Germany		Breeding line	2	146	56	
Scala	3	OSU-OR	KWS	Germany		Cultivar	2	152	58	
85849_NH	3	OSU-OR	Secobra	France		Breeding line	2	118	58	
Diadem	3	JHI	AGOUEB	France		Cultivar	6	141	64	
JET	3	JHI	LS Plant Breeding	United Kingdom		Cultivar	2	131	55	
Ayana	3	JHI	AGOUEB	United Kingdom		Cultivar	6	116	58	58
Admire-1	4	OSU-OH	USDA-NSGC	United States	CIho 6377; CI 6377	Germplasm	6	102	65	
Admire-2	4	OSU-OH	USDA-NSGC	United States	CIho 6377; CI 6377	Germplasm	6	152	56	
MO_B475	4	OSU-OH	USDA-NSGC	United States	CIho 9168	Cultivar	6	116	73	
CIho6486	4	OSU-OR	USDA-NSGC	Germany	Berg	Cultivar	6	NA	56	
Friedrichswerther_Berg	4	OSU-OH	USDA-NSGC	Germany	PI174439	Landrace	6	138	56	
PI327603	4	OSU-OR	USDA-NSGC	Czech Republic	Stupicky Sestirady; WIR 18780	Landrace	6	NA	56	
Grete	4	JHI	AGOUEB	Germany		Cultivar	6	60	55	
Herefordia	4	JHI	AGOUEB	?		Cultivar	6	144	57	
Cetin	4	JHI	AGOUEB	Italy		Cultivar	6	118	62	60
NB09432	5	UNL	UNL	United States		Breeding line	6	133	65	
NB09433	5	UNL	UNL	United States		Breeding line	6	135	63	
NB07411	5	UNL	UNL	United States		Breeding line	6	139	56	
NB99875	5	UNL	UNL	United States		Breeding line	6	112	65	62
Leninakanskij	6	OSU-OH	USDA-NSGC	Armenia	PI327669; WIR 19018	Cultivar	6	143	60	
PI327764	6	OSU-OR	USDA-NSGC	Russia	WIR 13829	Landrace	6	NA	68	
PI327702	6	OSU-OR	USDA-NSGC	Russia	WIR 13906	Landrace	?	NA	67	
PI340977	6	OSU-OR	USDA-NSGC	Russia	Donskoj; WIR 19636	Cultivar	6	NA	67	
PI327709	6	OSU-OR	USDA-NSGC	Russia	WIR 14007	Landrace	6	NA	61	65
PI87835	7	OSU-OR	USDA-NSGC	North Korea	Omugi Kauru Pori	Landrace	?	NA	74	
P-721	7	UNL	UNL	United States		Breeding line	6	103	55	
NB10403	7	UNL	UNL	United States		Breeding line	6	137	56	
NB10444	7	UNL	UNL	United States		Breeding line	6	123	59	
NB09441	7	UNL	UNL	United States		Breeding line	6	126	56	
VA08B-85	7	VPI-SU	VPI-SU	United States	Secretariat; PI673931	Breeding line	6	124	55	
NB10406	7	UNL	UNL	United States		Breeding line	6	132	56	
NB10417	7	UNL	UNL	United States		Breeding line	6	128	57	
NB10419	7	UNL	UNL	United States		Breeding line	6	114	62	59

*Clade refers to **Figure 3**. Contributor codes are defined in the text. DTF, days to flowering without vernalization; Avg. WS, average winter survival for the accession across 10 locations; Avg. WS Clade, average winter survival of the accessions in the clade.*

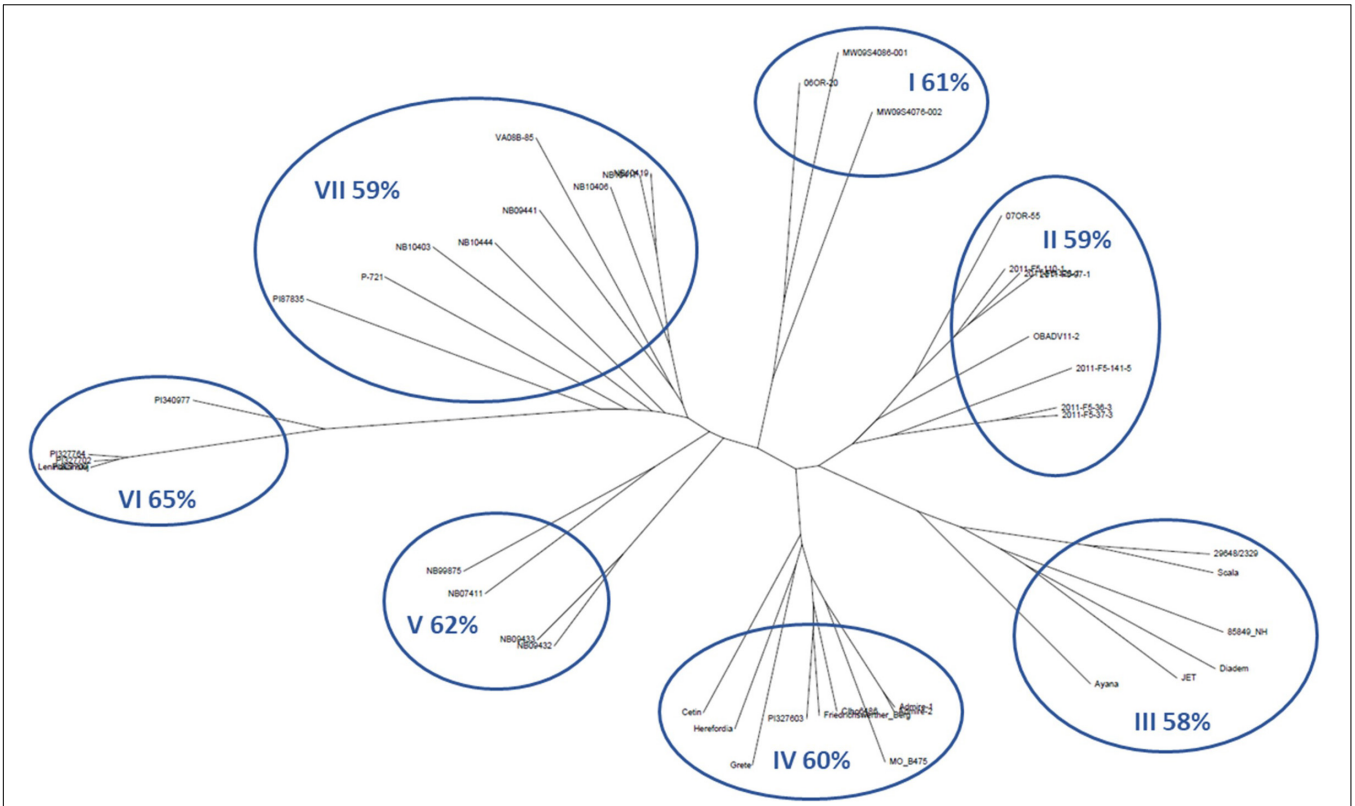

FIGURE 3 | Diversity dendrogram based on SNP genotype data for the top 5% lines of barley accessions for average winter survival across 10 locations. Clades are numbered clockwise, starting with I. The% values are average winter survival for the clade. See **Table 1** for more data on the accessions within each clade.

the lowest survival (n = 44) were grouped with the Full Pint check. The overlay of VRN sensitivity–classified as sensitive, intermediate, and insensitive–showed that most of the VRN-insensitive accessions grouped with Full Pint and the accessions with the lowest LTT, although some VRN-insensitive accessions grouped with the accessions with the highest winter survival. Accessions with intermediate VRN sensitivity, and VRN-sensitive accessions, are found throughput the PCA (**Figure 2C**). There was a relationship of spike morphology (2-row vs. 6-row) with LTT (**Figure 2D**): 84% of accessions within the top 5% for LTT were 6-rows. In the full array, there are 529 6-rows and 350 2-rows.

The relationships of LTT, VRN sensitivity, and spike morphology were explored in greater depth using the 5% of accessions with the highest WS across environments. The average WS for this group was 60% (**Table 1** and **Figure 3**). **Figure 3** shows an unrooted neighbor-joining dendrogram for these 44 accessions, based on 5,725 SNPs. Each of the seven clades is numbered from the top of the figure, proceeding clockwise, and the average survival of the accessions within each clade is given. The accessions in clade I are all VRN-insensitive 6-rows and trace to the UM or OSU programs. All entries in clade II are 6-rows from the OSU program and are VRN sensitive or are intermediate in their VRN sensitivity. Clade III is composed of 2-rows and 6-rows from European programs, all with winter habit. Clade IV is composed of 6-rows from the US GRIN germplasm collection, of European origin, and accessions contributed by the JHI. All are winters or have intermediate VRN sensitivity, except for Grete, which is VRN insensitive. No DTF data are available for two of the USDA accessions. Clade V is composed of 6-row winter types from the University of Nebraska, Lincoln (UNL) breeding program. Clade VI consists of 6-row germplasm accessions from the USDA collection, all tracing to Russia except for one accession from Armenia. The one accession for which DTF data are available is a winter. Clade VII consists of VRN-sensitive 6-rows from the UNL breeding program, a USDA accession tracing to North Korea, and one accession from the Virginia Polytechnical Institute and State University (VPI-SU) program.

GWAS of LTT and VRN Sensitivity

Prior to conducting GWAS, we assessed population structure and linkage disequilibrium in the LTT panel of 882 accessions. Structure was evaluated by performing PCA on 5,725 SNPs. As expected, there was strong population structure associated with spike morphology, with the first principal component of the PCA (PC1) mainly separating 2-row from 6-row barley accessions (**Figure 4A**). Accessions in the first two PCs were largely clustered based on their geographical origin, with PC1 mainly differentiating European from North American barleys, which largely correspond

to 2-row and 6-row accessions, respectively, and PC2 separating Asian accessions from the rest (**Figure 4B**). On a genome-wide level, LD decayed within 24,300 kb (**Supplementary Figure S1**), although LD varied significantly across the genome, with centromeric and pericentromeric regions generally having higher LD (**Supplementary Figure S2**). Considering only polymorphic SNPs with a MAF >0.05, there is, on average, one SNP every 793 kb. However, the SNP density is also much higher in more distal, low-LD regions (**Supplementary Figure S2**).

GWAS of WS was first performed using data from each of the 10 individual environments, and results were then combined via meta-analysis (see section "Materials and Methods" and **Supplementary Table S5**). A summary of QTL effects across individual environments is shown in **Supplementary Table S5**. The meta-analysis revealed 15 significant loci on all barley chromosomes except 3H (**Figure 5A** and **Table 2**). Five of these loci correspond to previously reported QTLs/genes (*FR-H3*, *PPD-H1*, *VRN-H2*, *FR-H2*, and *FR-H1/VRN-H1*), whereas the other 11 are novel (**Figure 5A** and **Table 2**). The major determinants of WS were *FR-H2* and *FR-H1/VRN-H1* (**Figure 5A** and **Table 2**), which were also the loci detected in the highest number of individual environments (6/10 environments). Both loci were detected at a very high resolution, with the peak SNP for *FR-H1/VRN-H1* (BOPA1_1501-353) located inside the causative MADS-box transcription factor gene (*HORVU5Hr1G095630*), and the highly significant SNPs on *FR-H2* BOPA2_12_30845 and BOPA2_12_30852 (**Supplementary Table S5**) contained inside the gene cluster of C-repeat-binding factors (CBFs). *VRN-H2* and the 2H locus with the highest significance level (BOPA2_12_21527; **Table 2**) were also identified in two individual environments (**Supplementary Table S5**), whereas another four loci (BOPA2_12_10938 on 1H, *PPD-H1* on 2H, BOPA2_12_10278 on 6H, and BOPA2_12_30645 on 7H; **Table 2**) were identified in one individual environment (**Supplementary Table S5**). Each of these eight loci showed gene by environment interactions (Manning et al., 2011; Kang, 2015). The remaining loci, including *FR-H3*, were only identified in the meta-analysis. Three candidate genes for *FR-H3* were identified: *HORVU1Hr1G012690*, which contains the peak SNP (SCRI_RS_114047) and encodes a tetraspanin family protein; *HORVU1Hr1G012680*, which encodes a protein belonging to UDP-glycosyltransferase superfamily; and *HORVU1Hr1G012710*, at 259 kb from the peak SNP, encoding the low temperature-induced protein lt101.2.

Three loci were significantly associated with DTF: *VRN-H2* on 4H, *VRN-H1* on 5H, and *PPD-H1* on 2H (**Figure 5B**, **Table 2**, and **Supplementary Table S5**). Peak SNPs on *PPD-H1* (BOPA2_12_30871) and *VRN-H1* (BOPA1_1501-353 and BOPA2_12_30930) are within the pseudo-response regulator encoded by *HORVU2Hr1G013400* and the MADS box transcription factor encoded by *HORVU5Hr1G095630*, respectively. As expected, the zinc-finger/CCT domain transcription factor encoded by *VRN-H2* could not be identified by significant SNPs on 4H since the reference genome "Morex" carries a *VRN-H2* deletion.

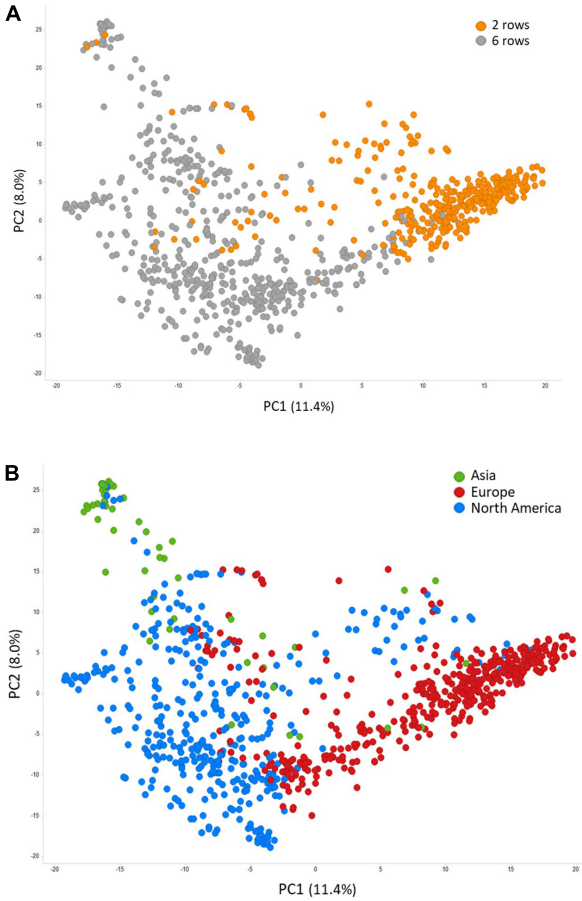

FIGURE 4 | Principal component analysis of 882 barley accessions colored by head type **(A)** and accession origin **(B)**.

Two Locus Interactions

For WS, interactions between VRN sensitivity and QTL/genes associated with LTT were assessed using data from the 6/10 environments where *FR-H2* had a significant effect in the GWAS. Different two-locus combinations were significant at each of the six locations including interactions between *VRN-H2/FR-H2*, *VRN-H1/FR-H2*, and *PPD-H1/FR-H2*. There was no significant *VRN-H1/VRN-H2* interaction in any environment. For VRN sensitivity, highly significant interactions were found between *VRN-H2*, *VRN-H1*, and *PPD-H1* (**Supplementary Table S6**). The most significant interaction was between *VRN-H1* and *VRN-H2*, and a large -log10 (*p*-value) was also found for the *VRN-H2/PPD-H1* interaction.

Allele-Specific Genotyping for Growth Habit-Related Genes

The results of the allele-specific genotyping of *PPD-H2*, *PPD-H1*, *VRN-H1*, and *VRN-H2* on accessions with the highest winter

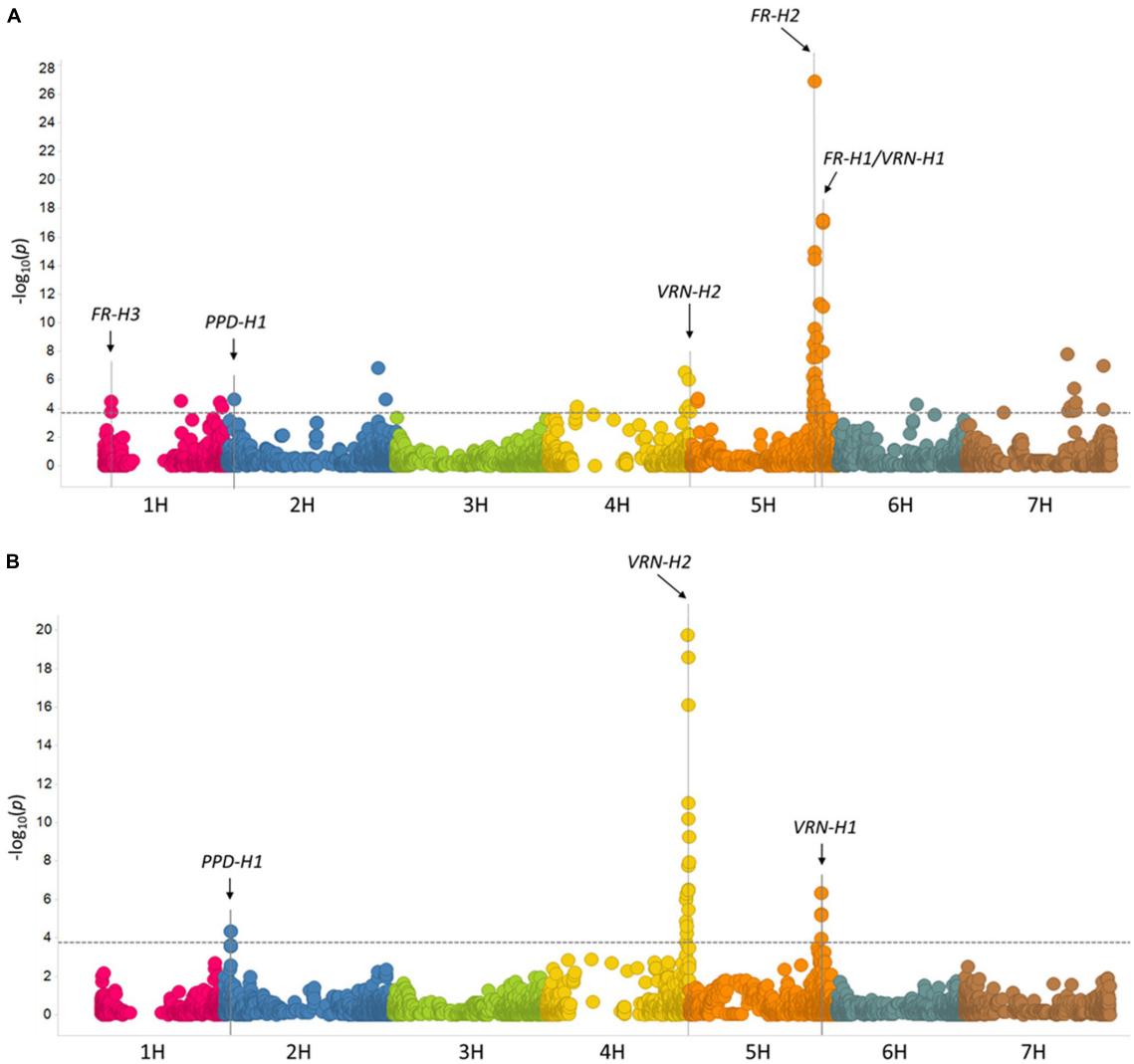

FIGURE 5 | Manhattan plots from the GWAS of 882 accessions. **(A)** Meta-analysis of winter survival. **(B)** Days to flowering without vernalization. -log10 (*p*-values) are shown for 4,875 SNPs with physical coordinates in the barley reference genome (Mascher et al., 2017). The dashed lines indicate the 0.01 FDR-corrected threshold [3.70 for **(A)** and 3.75 for **(B)**].

survival are shown in **Table 3**. At the *PPD-H2* locus, three of the VRN-insensitive accessions have the allele conferring sensitivity to sd-PPD, where the plant exhibits delayed flowering under short days. One accession (MW09S4086-001) has the sd-PPD insensitive (functional) allele, where flowering occurs under short-day conditions. Of the remaining VRN intermediate and VRN-sensitive accessions, 11 have the short-day sensitive allele, and 7 have the short-day insensitive allele. A novel deletion at this locus was found in one accession (Leninakanskij). At the *PPD-H1* locus, 22 accessions carry the dominant allele, which promotes flowering under long-day conditions (Turner et al., 2005); only Leninakanskij has the recessive allele, which delays flowering under long-day conditions. All 23 accessions have the "intact" *VRN-H1* winter allele, which is reported to be associated with LTT (Rizza et al., 2016). At *VRN-H2*, two of the four VRN-insensitive accessions have a deletion of all three *ZCCT-H* genes. Two accessions, tracing to the UMN program, have partial deletions at this locus. Complete deletions were observed in two of the accessions with intermediate VRN sensitivity, both from the OSU program. Partial deletions of *VRN-H2* were observed in four accessions, two in the intermediate group (MOB-475 and Cetin) and two in the winter growth habit group (Jet and Diadem).

DISCUSSION

The Challenges of Phenotyping LTT and VRN Sensitivity

There are advantages and disadvantages to assessing LTT and VRN sensitivity under field and/or controlled environment conditions. Assessment of a GWAS panel for LTT is feasible only

under field conditions, but naturally occurring low temperature events are rare, and variables besides low temperature can determine survival. In this study, fewer than half of the test sites provided useful data for GWAS of LTT, and yet every test site has, at some point in the past 30 years, generated useful data for mapping the genetic determinants of this phenotype. The implication is that a large number of test sites need to be sampled in order to ensure a reasonable chance of obtaining useful field data. Therefore, some future research could be directed at smaller subsets of informative germplasm, such as the top 5% identified in this panel. At each field site, perhaps selected based on the probability of generating representative differential survival (e.g., **Figure 2A**), assessment of WS using replicated large plots is recommended. For example, there was 100% mortality in the GWAS panel single rows at the Nebraska test site in 2014. The nine accessions that were also included in an adjacent replicated yield trial with four, 3 m row plots had WS values ranging from 40 to 81% (Baenziger, personal communication). Furthermore, we recommend that comprehensive weather data be obtained at each site. These multi-location data, coupled with genotype and phenotype data, will be useful in validating and enhancing climate models, such as the one recently reported by Byrns et al. (2020). Smaller subsets would also be amenable to controlled environment tests, where functional genomics approaches can complement GWAS (Fowler et al., 2001; Stockinger et al., 2007).

VRN sensitivity is straightforward to measure as DTF under controlled environment conditions, but the data are only an approximation of DTF under field conditions, where there are complex interactions involving changing photoperiod duration, diurnal fluctuations in temperature, and other environmental signals affecting plant growth and development. A deeper understanding of VRN sensitivity can be obtained under field conditions with repeated plantings from fall to spring (Igartua et al., 1999) and in controlled environment tests involving factorial combinations of time, temperature, and photoperiod duration (Casao et al., 2011a). These approaches are constrained by the number of genotypes that can be tested: therefore, as with LTT, we recommend that an informative subset of genotypes be used to empirically assess vernalization response within a framework of complete monitoring of environmental conditions.

Insights Into LTT and VRN Sensitivity From GWAS

The large panel of accessions used in this study (**Table 2** and **Figure 5A**) showed that the most significant determinants of WS were *FR-H1* and *FR-H2*, confirming previous work (reviewed by Cuesta-Marcos et al., 2015). Implications of this finding range from the trivial to the exciting. The large number of accessions with WS values within 20% of the spring check (**Figure 1A**) provides the trivial explanation: despite the stated criteria that all submissions to the panel have maximum LTT, additional phenotypic and genotypic pre-screening may have been advisable. For example, every accession in the top 5% for LTT has the complete intron in *VRN-H1* (**Table 3**), suggesting that this haplotype could have been a useful criterion for inclusion of accessions in the GWAS panel. The exciting implication of the finding that *FR-H1* and *FR-H2* are significant sources of variation is that there is much more to be learned about allelic variation at these loci, using locus in the broadest sense of the term. For example, *FR-H2* is a complex locus, where copy number variation (CNV) in CBF gene family members is a driver of differences in degree of LTT (Stockinger et al., 2007; Knox et al., 2010; Francia et al., 2016). The significant effect of this complex locus on LTT could, therefore, represent an example of the importance of CNV in barley, a topic addressed in general by Muñoz-Amatriaín et al. (2013), and with specific reference to *FR-H2* by Muñoz-Amatriaín and Mascher (2018). In the case of *FR-H1*, there are additional genes in physical proximity with *HvBM5A* whose annotation makes them intriguing possible determinants of LTT (Cuesta-Marcos et al., 2015). Allelic variation at this "super gene" complex could, therefore, account for the continued importance of this QTL.

The discovery of candidate genes for *FR-H3* in this GWAS panel is a key finding. While all three genes merit additional investigation, and two or more of them could be acting in concert as a complex locus, *HORVU1Hr1G012710* is the most obvious candidate, based on annotation. This gene encodes barley lipid transfer protein 101 (*blt101*), which is known to be induced by low temperatures (Brown et al., 2001) and may be involved in the differential WS of barley genotypes by slowing growth under low temperatures and

TABLE 2 | Significant peak SNPs associated with winter survival and days to flowering.

Trait	Peak SNP	Chr.	Pos (bp)	(-)Log10 (*p*)	Locus
Winter survival	SCRI_RS_114047	1H	31,685,164	4.48	*FR-H3*
	BOPA2_12_10938	1H	348,204,358	4.54	
	BOPA1_10360-563	1H	526,705,451	4.44	
	BOPA2_12_10880	2H	29,991,973	4.66	*PPD-H1*
	BOPA2_12_21527	2H	687,150,452	6.84	
	SCRI_RS_119513	2H	721,944,874	4.65	
	BOPA2_12_30503	4H	126,859,667	4.12	
	SCRI_RS_226787	4H	619,233,021	6.54	
	BOPA2_12_30873	4H	640,596,465	3.76	*VRN-H2*
	BOPA2_12_10864	5H	30,204,455	4.72	
	SCRI_RS_237352	5H	561,601,170	26.9	*FR-H2*
	BOPA1_1501-353	5H	599,123,281	17.21	*FR-H1/VRN-H1*
	BOPA2_12_10278	6H	356,677,926	4.31	
	BOPA1_8582-772	7H	167,862,263	3.74	
	BOPA2_12_30645	7H	460,352,694	7.79	
	SCRI_RS_233901	7H	624,138,380	7.01	
Days to flowering	BOPA2_12_30871	2H	29,127,021	4.33	*PPD-H1*
	SCRI_RS_142792	4H	639,214,876	19.75	*VRN-H2*
	BOPA1_1501-353	5H	599,123,281	6.33	*VRN-H1*
	BOPA2_12_30930	5H	599,128,110	6.33	*VRN-H1*

For winter survival, reported SNPs are the result of the GWAS meta-analysis.

TABLE 3 | Allele types at *PPD-H1*, *PPD-H2*, *VRN-H1*, and *VRN-H2* for 23 barley accessions in the top 5% for winter survival across 10 locations.

Genotype	WS	DTF	*PPD-H2* (1H)	*PPD-H1* (2H)	*VRN-H1* (5H)	*VRN-H2* (4H)
GRETE	55	60	Truncated *HvFT3*	*PPD-H1*	intact intron 1	Deletion *ZCCT_Ha ZCCT_Hb ZCCT_Hc*
MW09S4076-002	65	58	Truncated *HvFT3*	*PPD-H1*	intact intron 1	Deletion *ZCCT_Ha ZCCT_Hb*
06OR-20	58	73	Truncated *HvFT3*	*PPD-H1*	intact intron 1	Deletion *ZCCT_Ha ZCCT_Hb ZCCT_Hc*
07OR-55	56	82	Truncated *HvFT3*	*PPD-H1*	intact intron 1	Deletion *ZCCT_Ha ZCCT_Hb ZCCT_Hc*
OBADV11-2	58	89	Truncated *HvFT3*	*PPD-H1*	intact intron 1	Deletion *ZCCT_Ha ZCCT_Hb ZCCT_Hc*
MW09S4086-001	59	69	Intact *HvFT3*	*PPD-H1*	intact intron 1	Deletion *ZCCT_Ha ZCCT_Hb*
NB09433	63	135	Intact *HvFT3*	*PPD-H1*	intact intron 1	Intact *ZCCT_Ha ZCCT_Hb ZCCT_Hc*
NB10403	56	137	Intact *HvFT3*	*PPD-H1*	intact intron 1	Intact *ZCCT_Ha ZCCT_Hb ZCCT_Hc*
NB10417	57	128	Intact *HvFT3*	*PPD-H1*	intact intron 1	Intact *ZCCT_Ha ZCCT_Hb ZCCT_Hc*
CETIN	62	118	Truncated *HvFT3*	*PPD-H1*	intact intron 1	Partial deletion
DIADEM	64	141	Truncated *HvFT3*	*PPD-H1*	intact intron 1	Deletion *ZCCT_Hc*
JET	55	131	Truncated *HvFT3*	*PPD-H1*	intact intron 1	Partial deletion
NB09432	65	133	Intact *HvFT3*	*PPD-H1*	intact intron 1	Intact *ZCCT_Ha ZCCT_Hb ZCCT_Hc*
LENINAKANSKIJ	60	143	NA	*ppd-H1*	intact intron 1	Intact *ZCCT_Ha ZCCT_Hb ZCCT_Hc*
NB09441	57	126	Intact *HvFT3*	*PPD-H1*	intact intron 1	Intact *ZCCT_Ha ZCCT_Hb ZCCT_Hc*
NB10419	62	114	Intact *HvFT3*	*PPD-H1*	intact intron 1	Intact *ZCCT_Ha ZCCT_Hb ZCCT_Hc*
P-721	55	103	Intact *HvFT3*	*PPD-H1*	intact intron 1	Intact *ZCCT_Ha ZCCT_Hb ZCCT_Hc*
2011-F5-141-5	62	127	Truncated *HvFT3*	*PPD-H1*	intact intron 1	Intact *ZCCT_Ha ZCCT_Hb ZCCT_Hc*
2011-F5-36-3	69	154	Truncated *HvFT3*	*PPD-H1*	intact intron 1	Intact *ZCCT_Ha ZCCT_Hb ZCCT_Hc*
NB07411	56	139	Truncated *HvFT3*	*PPD-H1*	intact intron 1	Intact *ZCCT_Ha ZCCT_Hb ZCCT_Hc*
NB10444	59	123	Truncated *HvFT3*	*PPD-H1*	intact intron 1	Intact *ZCCT_Ha ZCCT_Hb ZCCT_Hc*
NB99875	65	112	Truncated *HvFT3*	*PPD-H1*	intact intron 1	Intact *ZCCT_Ha ZCCT_Hb ZCCT_Hc*
MO_B475	72	116	Truncated *HvFT3*	*PPD-H1*	intact intron 1	Partial deletion

WS, winter survival; DTF, days to flowering.

increasing tolerance to water stress (Choi and Hwang, 2015). Choi and Hwang (2015) also showed that transgenic wheat overexpressing *blt101* had greater LTT than the wild type. *HORVU1Hr1G012680* encodes a protein in the UDP-glycosyltransferase superfamily. Members of this family are reported to be involved in LTT via flavonoid glycosylation (Schulz et al., 2016; Zhao et al., 2019). *HORVU1Hr1G012690*, which contains the most significantly associated SNP (SCRI_RS_114047), encodes a tetraspanin family protein. Tetraspanins are small transmembrane proteins with important roles in plant development and responses to biotic and abiotic stresses, including low temperatures (reviewed by Reimann et al., 2017).

The significant effect of *VRN-H2* on LTT in this study is likely due to the prevalence of winter types with *VRN-H2* and high LTT and accessions lacking *VRN-H2* with low LTT (**Figure 2C**). This argument for non-causative correlation of *VRN-H2* with LTT is supported by the equal WS values for Alba (winter check) and Maja (facultative check) (**Figure 1A**) and the presence of the facultative accessions in the top 5% with *VRN-H2* deletions (**Table 3**). The significant main effect of *PPD-H1* on LTT requires additional research. Vegetative stage low temperature injury is expected under field conditions to occur during winter, when there are short photoperiod conditions. However, there are reports involving differential LTT in controlled environment studies using long photoperiods (Stockinger et al., 2007; Dhillon et al., 2010).

In addition to identifying *FR-H1*, *FR-H2*, *FR-H3*, *VRN-H2*, and *PPD-H1*, the GWAS meta-analysis of WS revealed additional novel loci that merit further investigation (**Table 2** and **Supplementary Table S5**). Most of these loci were not significant in any of the individual environments, supporting the power of the meta-analysis, which is used in human medicine for the identification of genetic risk factors for complex diseases (Evangelou and Ioannidis, 2013). By combining the results from different GWAS to increase sample size, this approach increases statistical power and reduces false positives (Wang and Xu, 2019). No WS QTLs were detected using the meta-analysis, or in the GWAS of individual environment data, in the vicinity of the *Vrs1* locus on chromosome 2H. This locus is the primary determinant of row type in barley (Komatsuda et al., 2007), and its lack of effect on LTT supports the hypothesis that the association of the 6-row phenotype and high LTT in this study (**Figures 2D**, **5A**) is due to unintentional bias in choosing accessions for inclusion. At the time the study was designed, the largest contributors of germplasm were breeding programs focusing on 6-rows. Given the current predominance of 2-row barley for malting and brewing, future LTT research should focus on this row type. Furthermore, our data suggest that the WS of 6-row barley can be transferred to 2-row barley.

With a complex trait, such as LTT, interactions will likely be the rule rather than the exception. We found significant two-locus interactions for *VRN-H1*, *VRN-H2*, and *PPD-H1* with *FR-H2* and novel QTLs. The lack of significant

interaction between *VRN-H1* and *VRN-H2* for WS at any test site is further evidence that specific combinations of alleles at these loci are not required for maximum LTT—an encouraging prospect for the potential of facultative growth habit. Understanding the interaction of *PPD-H1* with *FR-H2* will require further research. The results of these investigations could lead to the addition of *PPD-H1* as a criterion for facultative growth habit.

The GWAS of DTF under greenhouse conditions (**Figure 5B**) identified the principal determinants of vernalization response reported in the literature: *VRN-H1* and *VRN-H2* (reviewed by Cuesta-Marcos et al., 2015). Furthermore, these loci showed the largest two-locus interaction we detected in this study, as expected based on the model originally proposed by Takahashi and Yasuda (1971) and subsequently validated by Yan et al. (2003) and Szűcs et al. (2007). Interestingly, *VRN-H3* was not a determinant of DTF in this array: either because of monomorphism in the germplasm or the environmental conditions of the greenhouse assay. Loscos et al. (2014) characterized CNVs at this locus in barley germplasm and identified associations with DTF. Extending this research to the current germplasm, or subsets thereof, is warranted. The significance of *PPD-H1* in VRN sensitivity (**Figure 5B**) may be attributable to the long-day photoperiod (ld-PPD, 16 h light/8 h dark) used in the controlled environment assay. We also observed a significant interaction of *PPD-H1* and *VRN-H2*, as reported in other germplasm (Laurie et al., 1995; Karsai et al., 2005; Turner et al., 2013), providing additional evidence for the interconnectedness of the vernalization and photoperiod pathways under long-day conditions.

Additional Insights From the Top 5% for LTT

The top 5% (**Tables 1**, **3** and **Figure 3**) will be a resource for introgressing alleles contributing to maximum LTT into the current barley germplasm and for deeper analysis of the genetics and physiology of LTT. Most of these accessions are 6-rows, and most are feed barley cultivars or land race accessions. Therefore, targeted allele introgression into elite 2-row malting germplasm will be required. The prevalence of the sd-PPD sensitivity allele at *PPD-H2* in the top 5% is notable and suggests a fitness advantage to this phenotype, in the absence of direct selection. We hypothesize that significant QTL effects for this locus on LTT were not detected in the current data set because mid-winter warm temperature events did not occur in the test environments. The sd-PPD sensitivity phenotype, therefore, can be viewed as an insurance mechanism. Validation of its value will require controlled environment experiments and "fortuitous" field trials when winter warm temperature events occur. The presence of the sd-PPD insensitive allele in accessions with winter growth habit may be attributable to the historical dependency on VRN sensitivity to delay the vegetative to reproductive transition and/or to its importance in winter barleys from regions with mild winters (Casao et al., 2011b)

The prevalence of the ld-PPD sensitivity allele at *PPD-H1* in all of the top 5% could be due to selection for early maturity in fall-planted barley and not to a direct effect on LTT. The widespread occurrence of the ld-PPD insensitive allele in spring habit barley is credited with enhancing yield by extending the grain-filling period (Turner et al., 2005). Introgressing the ld-PPD insensitive into fall-planted germplasm could, therefore, be one path to increasing grain yield. There is evidence of selection for this allele in germplasm from Southern Europe (Casao et al., 2011b).

Prospects for Facultative Growth Habit

Climate change makes it imperative to ensure that crops are resilient in the face of volatility in temperature and precipitation. Facultative varieties offer one path forward for barley: the capacity to acclimate and achieve maximum LTT without vernalization sensitivity, coupled with the "insurance of sd-PPD sensitivity," will allow for flexibility in planting date. There is precedent in the literature that facultative growth habit types are capable of achieving the same LTT as winter growth habit types (Fowler et al., 2001; von Zitzewitz et al., 2011; Fisk et al., 2013; Rizza et al., 2016). In the current research, the facultative check Maja had a WS value comparable to the winter check Alba. The current GWAS panel was assembled to study LTT irrespective of growth habit. Therefore, it is encouraging that facultative types were among the top 5% for LTT. Marker assisted selection for loss-of-function alleles at *VRN-H2* at *PPD-H2* now provides an efficient path to target facultative growth habit. Rigorous assessment of the prospects for this growth habit type will (1) require extensive assessment of larger numbers of diverse facultative accessions, compared with winter checks, in multiple environments and (2) be facilitated by the development and deep characterization of isogenic lines developed through traditional introgression or, potentially, through genome editing.

DATA AVAILABILITY STATEMENT

The datasets generated for this study can be found in the online repositories. The names of the repository/repositories and accession number(s) can be found in the article/ **Supplementary Material**.

AUTHOR CONTRIBUTIONS

AC-M, PH, DH, SF, and LH designed the experiment, provided seed to the cooperators, curated the data, and conducted the preliminary analyses. MM-A and JH had primary responsibility for data analysis. JH, MM-A, and PH prepared the drafts, edited the drafts, and ensured co-author access to the evolving manuscript. Co-authors PH, FC, CE, AG, MH, GH, EI, IK, TN, KeS, ES, and WT grew the experiment and generated the WS data, they and all the other co-authors participated in reviewing and editing. All authors read and approved the manuscript.

FUNDING

Support was provided by the USDA-NIFA TCAP Project no. 2011-68002-30029.

ACKNOWLEDGMENTS

We thank Shiaoman Chao (retired) USDA-ARS Fargo, North Dakota for Illumina 9K genotyping and allele calling and Sassoum Lo (University of California Davis) for technical support in the GWAS meta-analysis. We are grateful for the contributions of germplasm by all co-authors and M. Gotz, V. Korzun, K. J. Muller, L. Cattivelli, I. Romagosa, and R. Sharma.

SUPPLEMENTARY MATERIAL

The Supplementary Material for this article can be found online at: https://www.frontiersin.org/articles/10.3389/fpls.2020.585927/full#supplementary-material

REFERENCES

Belcher, A. R., Graebner, R. C., Cuesta-Marcos, A., Fisk, S., Filichkin, T., Smith, K. P., et al. (2015). Registration of the TCAP FAC-WIN6 barley panel for genomewide association studies. *J. Plant Regist.* 9, 411–418. doi: 10.3198/jpr2014.12.0083crmp

Benjamini, Y., and Hochberg, Y. (1995). Controlling the false discovery rate: a practical and powerful approach to multiple testing. *J. R. Stat. Soc. Ser. B* 57, 289–300. doi: 10.1111/j.2517-6161.1995.tb02031.x

Bradbury, P. J., Zhang, Z., Kroon, D. E., Casstevens, T. M., Ramdoss, Y., and Buckler, E. S. (2007). TASSEL: software for association mapping of complex traits in diverse samples. *Bioinformatics* 23, 2633–2635. doi: 10.1093/bioinformatics/btm308

Brown, A. P., Dunn, M. A., Goddard, N. J., and Hughes, M. A. (2001). Identification of a novel low-temperature-response element in the promoter of the barley (*Hordeum vulgare* L) gene blt101.1. *Planta* 213, 770–780. doi: 10.1007/s004250100549

Byrns, B. M., Greer, K. J., and Fowler, D. B. (2020). Modelling winter survival in cereals: an interactive tool. *Crop. Sci.* 60, 2408–2419. doi: 10.1002/csc2.20246

Casao, M. C., Igartua, E., Karsai, I., Lasa, J. M., Gracia, M. P., and Casas, A. M. (2011a). Expression analysis of vernalization and day-length response genes in barley (*Hordeum vulgare* L.) indicates that VRNH2 is a repressor of PPDH2 (HvFT3) under long days. *J. Exp. Bot.* 62, 1939–1949. doi: 10.1093/jxb/erq382

Casao, M. C., Karsai, I., Igartua, E., Gracia, M. P., Veisz, O., and Casas, A. M. (2011b). Adaptation of barley to mild winters: a role for PPDH2. *BMC Plant Biol.* 11:164. doi: 10.1186/1471-2229-11-164

Chen, A., Gusta, L. V., Brûlé-Babel, A., Leach, R., Baumann, U., Fincher, G. B., et al. (2009). Varietal and chromosome 2H locus-specific frost tolerance in reproductive tissues of barley (*Hordeum vulgare* L.) detected using a frost simulation chamber. *Theor. Appl. Genet.* 119, 685–694. doi: 10.1007/s00122-009-1079-1

Choi, C., and Hwang, C. H. (2015). The barley lipid transfer protein, BLT101, enhances cold tolerance in wheat under cold stress. *Plant Biotechnol. Rep.* 9, 197–207. doi: 10.1007/s11816-015-0357-4

Cockram, J., Jones, H., Leigh, F. J., O'Sullivan, D., Powell, W., Laurie, D. A., et al. (2007). Control of flowering time in temperate cereals: genes, domestication, and sustainable productivity. *J. Exp. Bot.* 58, 1231–1244. doi: 10.1093/jxb/erm042

Cockram, J., White, J., Zuluaga, D. L., Smith, D., Comadran, J., Macaulay, M., et al. (2010). Genome-wide association mapping to candidate polymorphism resolution in the unsequenced barley genome. *Proc. Natl. Acad. Sci. U.S.A.* 107:21611. doi: 10.1073/pnas.1010179107

Colmsee, C., Beier, S., Himmelbach, A., Schmutzer, T., Stein, N., Scholz, U., et al. (2015). BARLEX - the barley draft genome explorer. *Mol. Plant* 8, 964–966. doi: 10.1016/j.molp.2015.03.009

Comadran, J., Kilian, B., Russell, J., Ramsay, L., Stein, N., Ganal, M., et al. (2012). Natural variation in a homolog of Antirrhinum centroradialis contributed to spring growth habit and environmental adaptation in cultivated barley. *Nat. Genet.* 44:1388. doi: 10.1038/ng.2447

Cuesta-Marcos, A., Casas, A. M., Yahiaoui, S., Gracia, M. P., Lasa, J. M., and Igartua, E. (2008). Joint analysis for heading date QTL in small interconnected barley populations. *Mol. Breed.* 21, 383–399. doi: 10.1007/s11032-007-9139-1

Cuesta-Marcos, A., Muñoz-Amatriaín, M., Filichkin, T., Karsai, I., Trevaskis, B., Yasuda, S., et al. (2015). The relationships between development and low temperature tolerance in barley near isogenic lines differing for flowering behavior. *Plant Cell Physiol.* 56, 2312–2324. doi: 10.1093/pcp/pcv147

Cuesta-Marcos, A., Szûcs, P., Close, T. J., Filichkin, T., Muehlbauer, G. J., Smith, K. P., et al. (2010). Genome-wide SNPs and re-sequencing of growth habit and inflorescence genes in barley: implications for association mapping in germplasm arrays varying in size and structure. *BMC Genomics* 11:707. doi: 10.1186/1471-2164-11-707

Danyluk, J., Kane, N. A., Breton, G., Limin, A. E., Fowler, D. B., and Sarhan, F. (2003). TaVRT-1, a putative transcription factor associated with vegetative to reproductive transition in cereals. *Plant Physiol.* 132, 1849–1860. doi: 10.1104/pp.103.023523

Dhillon, T., Pearce, S. P., Stockinger, E. J., Distelfeld, A., Li, C., Knox, A. K., et al. (2010). Regulation of freezing tolerance and flowering in temperate cereals: the VRN-1 connection. *Plant Physiol.* 153, 1846–1858. doi: 10.1104/pp.110.159079

Evangelou, E., and Ioannidis, J. P. A. (2013). Meta-analysis methods for genome-wide association studies and beyond. *Nat. Rev. Genet.* 14, 379–389. doi: 10.1038/nrg3472

Faure, S., Higgins, J., Turner, A., and Laurie, D. A. (2007). The flowering locus T-like gene family in barley (*Hordeum vulgare*). *Genetics* 176, 599–609. doi: 10.1534/genetics.106.069500

Fisher, R. (1925). *Statistical Methods for Research Workers*, 1st Edn. Edinburgh: Oliver & Boyd.

Fisk, S. P., Cuesta-Marcos, A., Cistué, L., Russell, J., Smith, K. P., Baenziger, S., et al. (2013). FR-H3: a new QTL to assist in the development of fall-sown barley with superior low temperature tolerance. *Theor. Appl. Genet.* 126, 335–347. doi: 10.1007/s00122-012-1982-8

Fowler, D. B., Breton, G., Limin, A. E., Mahfoozi, S., and Sarhan, F. (2001). Photoperiod and temperature interactions regulate low-temperature-induced gene expression in barley. *Plant Physiol.* 127, 1676–1681. doi: 10.1104/pp.010483

Francia, E., Morcia, C., Pasquariello, M., Mazzamurro, V., Milc, J. A., Rizza, F., et al. (2016). Copy number variation at the HvCBF4-HvCBF2 genomic segment is a major component of frost resistance in barley. *Plant Mol. Biol.* 92, 161–175. doi: 10.1007/s11103-016-0505-4

Fu, D., Szucs, P., Yan, L., Helguera, M., Skinner, J. S., von Zitzewitz, J., et al. (2005). Large deletions within the first intron in VRN-1 are associated with spring growth habit in barley and wheat. *Mol. Genet. Genomics* 273, 54–65. doi: 10.1007/s00438-004-1095-4

Hayes, P. M., Blake, T., Chen, T. H., Tragoonrung, S., Chen, F., Pan, A., et al. (1993). Quantitative trait loci on barley (*Hordeum vulgare* L.) chromosome 7 associated with components of winterhardiness. *Genome* 36, 66–71. doi: 10.1139/g93-009

Igartua, E., Casas, A. M., Ciudad, F., Montoya, J. L., and Romagosa, I. (1999). RFLP markers associated with major genes controlling heading date evaluated in a barley germ plasm pool. *Heredity* 83, 551–559. doi: 10.1046/j.1365-2540.1999.00589.x

Kang, H. (2015). Statistical considerations in meta-analysis. *Hanyang. Med. Rev.* 35, 23–32. doi: 10.7599/hmr.2015.35.1.23

Karsai, I., Mészáros, K., Szücs, P., Hayes, P. M., Láng, L., and Bedö, Z. (1999). Effects of loci determining photoperiod sensitivity (Ppd-H1) and vernalization response (Sh2) on agronomic traits in the 'Dicktoo'×'Morex' barley mapping population. *Plant Breed.* 118, 399–403. doi: 10.1046/j.1439-0523.1999.00408.x

Karsai, I., Szűcs, P., Köszegi, B., Hayes, P. M., Casas, A., Bedõ, Z., et al. (2008). Effects of photo and thermo cycles on flowering time in barley: a genetical phenomics approach. *J. Exp. Bot.* 59, 2707–2715. doi: 10.1093/jxb/ern131

Karsai, I., Szűcs, P., Mészáros, K., Filichkina, T., Hayes, P., Skinner, J., et al. (2005). The Vrn-H2 locus is a major determinant of flowering time in a facultative× winter growth habit barley (*Hordeum vulgare* L.) mapping population. *Theor. Appl. Genet.* 110, 1458–1466. doi: 10.1007/s00122-005-1979-7

Kikuchi, R., Kawahigashi, H., Ando, T., Tonooka, T., and Handa, H. (2009). Molecular and functional characterization of PEBP genes in barley reveal the diversification of their roles in flowering. *Plant Physiol.* 149:1341. doi: 10.1104/pp.108.132134

Kikuchi, R., Kawahigashi, H., Oshima, M., Ando, T., and Handa, H. (2012). The differential expression of HvCO9, a member of the CONSTANS-like gene family, contributes to the control of flowering under short-day conditions in barley. *J. Exp. Bot.* 63, 773–784. doi: 10.1093/jxb/err299

Knox, A. K., Dhillon, T., Cheng, H., Tondelli, A., Pecchioni, N., and Stockinger, E. J. (2010). CBF gene copy number variation at frost resistance-2 is associated with levels of freezing tolerance in temperate-climate cereals. *Theor. Appl. Genet.* 121, 21–35. doi: 10.1007/s00122-010-1288-7

Komatsuda, T., Pourkheirandish, M., He, C., Azhaguvel, P., Kanamori, H., Perovic, D., et al. (2007). Six-rowed barley originated from a mutation in a homeodomain-leucine zipper I-class homeobox gene. *Proc. Natl. Acad. Sci. U.S.A.* 104, 1424–1429. doi: 10.1073/pnas.0608580104

Laurie, D., Pratchett, N., Bezant, J., and Snape, J. (1995). RFLP mapping of five major genes and eight quantitative trait loci controlling flowering time in a winter x spring barley (*Hordeum vulgare* L.) cross. *Genome* 38, 575–585. doi: 10.1139/g95-074

Lin, C.-S., and Poushinsky, G. (1983). A modified augmented design for an early stage of plant selection involving a large number of test lines without replication. *Biometrics* 39, 553–561. doi: 10.2307/2531083

Lin, C.-S., and Poushinsky, G. (1985). A modified augmented design (type 2) for rectangular plots. *Can. J. Plant Sci.* 65, 743–749. doi: 10.4141/cjps85-094

Loscos, J., Igartua, E., Contreras-Moreira, B., Gracia, M. P., and Casas, A. M. (2014). HvFT1 polymorphism and effect-survey of barley germplasm and expression analysis. *Front. Plant Sci.* 5:251. doi: 10.3389/fpls.2014.00251

Manning, A. K., LaValley, M., Liu, C.-T., Rice, K., An, P., Liu, Y., et al. (2011). Meta-analysis of gene-environment interaction: joint estimation of SNP and SNP × environment regression coefficients. *Genet. Epidemiol.* 35, 11–18. doi: 10.1002/gepi.20546

Mascher, M., Gundlach, H., Himmelbach, A., Beier, S., Twardziok, S. O., Wicker, T., et al. (2017). A chromosome conformation capture ordered sequence of the barley genome. *Nature* 544, 427–433. doi: 10.1038/nature22043

Muñoz-Amatriaín, M., Eichten, S. R., Wicker, T., Richmond, T. A., Mascher, M., Steuernagel, B., et al. (2013). Distribution, functional impact, and origin mechanisms of copy number variation in the barley genome. *Genome Biol.* 14, R58. doi: 10.1186/gb-2013-14-6-r58

Muñoz-Amatriaín, M., and Mascher, M. (2018). "Sequence diversity and structural variation," in *The Barley Genome. Compendium of Plant Genomes*, eds N. Stein and G. Muehlbauer (Cham: Springer), 109–122. doi: 10.1007/978-3-319-92528-8_8

Pan, A., Hayes, P. M., Chen, F., Chen, T. H. H., Blake, T., Wright, S., et al. (1994). Genetic analysis of the components of winterhardiness in barley (s L.). *Theor. Appl. Genet.* 89, 900–910. doi: 10.1007/BF00224516

Powell, N., Ji, X., Ravash, R., Edlington, J., and Dolferus, R. (2012). Yield stability for cereals in a changing climate. *Funct. Plant Biol.* 39, 539–552. doi: 10.1071/fp12078

Reimann, R., Kost, B., and Dettmer, J. (2017). TETRASPANINs in plants. *Front. Plant Sci.* 8:545. doi: 10.3389/fpls.2017.00545

Rizza, F., Karsai, I., Morcia, C., Badeck, F.-W., Terzi, V., Pagani, D., et al. (2016). Association between the allele compositions of major plant developmental genes and frost tolerance in barley (*Hordeum vulgare* L.) germplasm of different origin. *Mol. Breed.* 36:156. doi: 10.1007/s11032-016-0571-y

Schulz, E., Tohge, T., Zuther, E., Fernie, A. R., and Hincha, D. K. (2016). Flavonoids are determinants of freezing tolerance and cold acclimation in *Arabidopsis thaliana*. *Sci. Rep.* 6:34027. doi: 10.1038/srep34027

Skinner, J. S., Szucs, P., von Zitzewitz, J., Marquez-Cedillo, L., Filichkin, T., Stockinger, E. J., et al. (2006). Mapping of barley homologs to genes that regulate low temperature tolerance in Arabidopsis. *Theor. Appl. Genet.* 112, 832–842. doi: 10.1007/s00122-005-0185-y

Skinner, J. S., von Zitzewitz, J., Szucs, P., Marquez-Cedillo, L., Filichkin, T., Amundsen, K., et al. (2005). Structural, functional, and phylogenetic characterization of a large CBF gene family in barley. *Plant Mol. Biol.* 59, 533–551. doi: 10.1007/s11103-005-2498-2

Stockinger, E. J., Skinner, J. S., Gardner, K. G., Francia, E., and Pecchioni, N. (2007). Expression levels of barley Cbf genes at the Frost resistance-H2 locus are dependent upon alleles at Fr-H1 and Fr-H2. *Plant J.* 51, 308–321. doi: 10.1111/j.1365-313X.2007.0141.x

Szűcs, P., Skinner, J. S., Karsai, I., Cuesta-Marcos, A., Haggard, K. G., Corey, A. E., et al. (2007). Validation of the VRN-H2/VRN-H1 epistatic model in barley reveals that intron length variation in VRN-H1 may account for a continuum of vernalization sensitivity. *Mol. Genet. Genomics* 277, 249–261. doi: 10.1007/s00438-006-0195-8

Takahashi, R., and Yasuda, S. (1971). "Genetics of earliness and growth habit in barley," in *Proceedings of the 2nd International Barley Genetics Symposium*, ed. R. Nilan (Washington, DC: Washington State University Press), 388–408.

Tondelli, A., Xu, X., Moragues, M., Sharma, R., Schnaithmann, F., Ingvardsen, C., et al. (2013). Structural and temporal variation in genetic diversity of european spring two-row barley cultivars and association mapping of quantitative traits. *Plant Genome* 6:Plantgenome2013.2003.0007. doi: 10.3835/plantgenome2013.03.0007

Trevaskis, B., Bagnall, D. J., Ellis, M. H., Peacock, W. J., and Dennis, E. S. (2003). MADS box genes control vernalization-induced flowering in cereals. *Proc. Natl. Acad. Sci. U.S.A.* 100:13099. doi: 10.1073/pnas.1635053100

Trevaskis, B., Tadege, M., Hemming, M. N., Peacock, W. J., Dennis, E. S., and Sheldon, C. (2007). Short vegetative phase-like MADS-box genes inhibit floral meristem identity in barley. *Plant Physiol.* 143, 225–235. doi: 10.1104/pp.106.090860

Turner, A., Beales, J., Faure, S., Dunford, R. P., and Laurie, D. A. (2005). The pseudo-response regulator Ppd-H1 provides adaptation to photoperiod in barley. *Science* 310, 1031–1034. doi: 10.1126/science.1117619

Turner, A. S., Faure, S., Zhang, Y., and Laurie, D. A. (2013). The effect of day-neutral mutations in barley and wheat on the interaction between photoperiod and vernalization. *Theor. Appl. Genet.* 126, 2267–2277. doi: 10.1007/s00122-013-2133-6

von Zitzewitz, J., Cuesta-Marcos, A., Condon, F., Castro, A. J., Chao, S., Corey, A., et al. (2011). The genetics of winterhardiness in barley: perspectives from genome-wide association mapping. *Plant Genome* 4, 76–91. doi: 10.3835/plantgenome2010.12.0030

von Zitzewitz, J., Szűcs, P., Dubcovsky, J., Yan, L., Francia, E., Pecchioni, N., et al. (2005). Molecular and structural characterization of barley vernalization genes. *Plant Mol. Biol.* 59, 449–467. doi: 10.1007/s11103-005-0351-2

Wang, M., and Xu, S. (2019). Statistical power in genome-wide association studies and quantitative trait locus mapping. *Heredity* 123, 287–306. doi: 10.1038/s41437-019-0205-3

Yan, L., Fu, D., Li, C., Blechl, A., Tranquilli, G., Bonafede, M., et al. (2006). The wheat and barley vernalization gene VRN3 is an orthologue of FT. *Proc. Natl. Acad. Sci. U.S.A.* 103:19581. doi: 10.1073/pnas.0607142103

Yan, L., Loukoianov, A., Blechl, A., Tranquilli, G., Ramakrishna, W., SanMiguel, P., et al. (2004). The wheat VRN2 gene is a flowering repressor down-regulated by vernalization. *Science* 303, 1640–1644. doi: 10.1126/science.1094305

Yan, L., Loukoianov, A., Tranquilli, G., Helguera, M., Fahima, T., and Dubcovsky, J. (2003). Positional cloning of the wheat vernalization gene VRN1. *Proc. Natl. Acad. Sci. U.S.A.* 100:6263. doi: 10.1073/pnas.0937399100

Zhang, Z., Ersoz, E., Lai, C.-Q., Todhunter, R. J., Tiwari, H. K., Gore, M. A., et al. (2010). Mixed linear model approach adapted for genome-wide association studies. *Nat. Genet.* 42, 355–360. doi: 10.1038/ng.546

Zhao, M., Jin, J., Gao, T., Zhang, N., Jing, T., Wang, J., et al. (2019). Glucosyltransferase CsUGT78A14 regulates flavonols accumulation and reactive oxygen species scavenging in response to cold stress in *Camellia sinensis*. *Front. Plant Sci.* 10:1675. doi: 10.3389/fpls.2019.01675

Conflict of Interest: AB was employed by the company Limagrain Europe, AC-M was employed by Bayer Crop Science, CE was employed by Saatzucht Ackermann GmbH & Co. KG, and AG was employed by the company Secobra Recherches.

The remaining authors declare that the research was conducted in the absence of any commercial or financial relationships that could be construed as a potential conflict of interest.

Copyright © 2020 Muñoz-Amatriaín, Hernandez, Herb, Baenziger, Bochard, Capettini, Casas, Cuesta-Marcos, Einfeldt, Fisk, Genty, Helgerson, Herz, Hu, Igartua, Karsai, Nakamura, Sato, Smith, Stockinger, Thomas and Hayes. This is an open-access article distributed under the terms of the Creative Commons Attribution License (CC BY). The use, distribution or reproduction in other forums is permitted, provided the original author(s) and the copyright owner(s) are credited and that the original publication in this journal is cited, in accordance with accepted academic practice. No use, distribution or reproduction is permitted which does not comply with these terms.

frontiers in Plant Science

ORIGINAL RESEARCH
published: 11 November 2020
doi: 10.3389/fpls.2020.582577

FLC and *SVP* Are Key Regulators of Flowering Time in the Biennial/Perennial Species *Noccaea caerulescens*

Yanli Wang[1,2], Edouard I. Severing[2†], Maarten Koornneef[2] and Mark G. M. Aarts[2]**

[1] State Key Laboratory of Protection and Utilization of Subtropical Agriculture Resource, College of Life Sciences, South China Agricultural University, Guangzhou, China, [2] Laboratory of Genetics, Wageningen University and Research, Wageningen, Netherlands

The appropriate timing of flowering is crucial for plant reproductive success. Studies of the molecular mechanism of flower induction in the model plant *Arabidopsis thaliana* showed long days and vernalization as major environmental promotive factors. *Noccaea caerulescens* has an obligate vernalization requirement that has not been studied at the molecular genetics level. Here, we characterize the vernalization requirement and response of four geographically diverse biennial/perennial *N. caerulescens* accessions: Ganges (GA), Lellingen (LE), La Calamine (LC), and St. Felix de Pallières (SF). Differences in vernalization responsiveness among accessions suggest that natural variation for this trait exists within *N. caerulescens*. Mutants which fully abolish the vernalization requirement were identified and were shown to contain mutations in the *FLOWERING LOCUS C* (*NcFLC)* and *SHORT VEGETATIVE PHASE* (*NcSVP)* genes, two key floral repressors in this species. At high temperatures, the non-vernalization requiring *flc-1* mutant reverts from flowering to vegetative growth, which is accompanied with a reduced expression of *LFY* and *AP1*. This suggested there is "crosstalk" between vernalization and ambient temperature, which might be a strategy to cope with fluctuations in temperature or adopt a more perennial flowering attitude and thus facilitate a flexible evolutionary response to the changing environment across the species range.

Keywords: flowering time, vernalization, Brassicaceae, perennial, regulation of flowering

OPEN ACCESS

Edited by:
Joanna Putterill, The University of Auckland, New Zealand

Reviewed by:
Richard Macknight, University of Otago, New Zealand
Timo Hytonen, University of Helsinki, Finland

****Correspondence:***
Yanli Wang
wylfriend@163.com
Mark G. M. Aarts
mark.aarts@wur.nl

†Present address:
Edouard I. Severing, Max-Planck-Institute for Plant Breeding Research, Cologne, Germany

Specialty section:
This article was submitted to Plant Development and EvoDevo, a section of the journal Frontiers in Plant Science

Received: *12 July 2020*
Accepted: *19 October 2020*
Published: *11 November 2020*

Citation:
Wang Y, Severing EI, Koornneef M and Aarts MGM (2020) FLC and SVP Are Key Regulators of Flowering Time in the Biennial/Perennial Species Noccaea caerulescens. Front. Plant Sci. 11:582577. doi: 10.3389/fpls.2020.582577

INTRODUCTION

The transition from vegetative to reproductive growth is an important event in the plant's life cycle and is determined by an interaction between developmental programs and pathways that respond to environmental cues such as day length and temperature (Andrés and Coupland, 2012). In many temperate plant species, including the model plant *Arabidopsis thaliana*, the transition to reproductive growth is accelerated by vernalization. The molecular genetics of the vernalization response has been well studied in *A. thaliana* (Andrés and Coupland, 2012) and many of its components are present in other, especially Brassicaceae, species (Leijten et al., 2018), suggesting that the pathway is conserved although minor differences between species cannot be excluded. In winter-annual *A. thaliana* accessions, the promotion of flowering by vernalization is controlled by the interaction of floral repressors such as FLOWERING LOCUS C (FLC), FRIGIDA (FRI), and

SHORT VEGETATIVE PHASE (SVP). FLC is a MADS domain protein that acts as a repressor of flowering (Michaels and Amasino, 1999; Sheldon et al., 1999). Its expression can be activated by FRI, which acts as part of a transcription complex that binds to the *FLC* promoter (Choi et al., 2011). *VERNALIZATION INSENSITIVE 3* (*VIN3*) (Bond et al., 2009; Kim et al., 2010) is the most upstream gene in the vernalization pathway (Kim et al., 2010). The VIN3 protein acts as a partner of a complexes such as LIKE -HETEROCHROMATIN PROTEIN 1 (LHP1) and POLYCOMB REPRESSION COMPLEX 2 (PRC2) to regulate histone methylation at the *FLC* locus, which represses *FLC* transcription (Sung and Amasino, 2004). The decline of *FLC* expression is maintained even when cold-treated plants are returned to warm conditions, thereby relieving the repression of *FT*, a potent activator of flowering and considered the main floral integrator in *A. thaliana* (Turck et al., 2008). In the perennial species *Arabis alpina*, the vernalization requirement and response are controlled by an *FLC* orthologue called *PEP1*. *PEP1* has a complex duplicated gene structure which differs from the simple structure of *PEP1* orthologues in related annual species such as *A. thaliana*. Furthermore, *PEP1* expression is upregulated again when the plants are transferred to warmer temperatures after the vernalization treatment, which implies that meristems that did not become induced, remain vegetative (Wang et al., 2009; Albani et al., 2012). SHORT VEGETATIVE PHASE (SVP) is another negative regulator of the floral transition (Hartmann et al., 2000). It is also a MADS box transcription factor, repressing flowering either in a transcriptional complex with FLC or independent from the latter (Mateos et al., 2015).

Noccaea caerulescens (formerly called *Thlaspi caerulescens*), is a diploid (2n = 14), biennial or facultative perennial plant from the *Brassicaceae* family. *N. caerulescens* is an extremophile, adapted to growth on soils with high concentration of Ni, Zn, Pb, or Cd. Next to displaying extreme heavy metal tolerance, it is also a heavy metal accumulator, with genotypes that are able to accumulate Ni, Zn, and Cd to over 1% of their dry weight in shoots (Assunção et al., 2003; Nascimento and Xing, 2006; Broadley et al., 2007; Krämer, 2010). Together with the Zn/Cd hyperaccumulator species *A. halleri*, *N. caerulescens* is among the most prominent plant model systems to study heavy metal hyperaccumulation and associated hypertolerance (Krämer, 2010; Hanikenne and Nouet, 2011; Pollard et al., 2014). *N. caerulescens* is a winter annual, biennial or facultative perennial species, depending on its location and especially water availability during summer. Seeds generally germinate in late summer, early autumn and overwinter as a rosette plant. Most plants will start to flower in early spring, provided rosettes are large enough. In a hot, dry summer, inflorescences will senesce and rosettes will wilt and die after flowering, however, if there is enough water available, either the rosettes remain and will overwinter to flower again next spring, or small secondary rosettes will form at the base of the senesced inflorescence, that will overwinter to flower the next spring. All known accessions will need a vernalization period of 2–3 months (Peer et al., 2003, 2006), which makes molecular genetic studies in this species challenging, as it limits the efficiency of genetic studies (Guan et al., 2008) and breeding efforts to enhance its application in metal phytoremediation. To overcome this disadvantage, two faster-cycling lines, which do not require vernalization, have been generated from the *N. caerulescens* "Ganges" background through fast neutron mutagenesis. The genetic basis of the early flowering phenotype of these lines, and the molecular nature of the mutations involved, is still unclear (Ó Lochlainn et al., 2011).

Associated with the genotypes and the local environments they adapt to, *A. thaliana* accessions show extensive natural variation in their vernalization requirement (Nordborg and Bergelson, 1999). The exact temperatures and length of cold exposure requires that the vernalization response varies among and within this plant species (Kim et al., 2010; Duncan et al., 2015). However, the role of these environmental and additional factors is only partly known in other temperate species. Recently, vernalization requirements and flowering time variations among *N. caerulescens* accessions were reported (Guimarães et al., 2013), but the genetic basis and molecular mechanisms of flowering time regulation has not been studied yet in this species.

A better understanding of the genetic control of flowering time in *N. caerulescens* will help us to understand its morphological and phenotypic behavior as an adaptation to climate conditions. Day lengths of 8 and 12 h did not influence the flowering time when a 4°C cold treatment was applied to induce flowering, indicating that only temperature seems important to induce flowering in *N. caerulescens* (Guimarães et al., 2013). In addition to the natural occurring variation, the identification of early flowering time mutations will also be important for uncovering the key genes involved in the flowering time regulation pathway. The present study investigates the variation of the vernalization requirement and response in four representative *N. caerulescens* accessions from diverse environments. We confirm the essential roles of *FLC* and *SVP* by the identification of mutations in these genes in early non-vernalization requiring plants obtained by forward screening of an EMS-mutagenesis-induced M2 population. Based on our findings, a flowering time regulation model in the biennial/perennial species *N. caerulescens* is proposed, including the effect of high ambient temperatures.

MATERIALS AND METHODS

Plant Materials and Growth Conditions

N. caerulescens accessions Lellingen (LE), La Calamine (LC), and Ganges (GA) are obtained by single seed descent propagation as described by Assunção et al. (2003). They originate respectively, from non-metallicolous soil in Wilwerwilz, close to Lellingen in Luxemburg (49°59′1.83″N, 5°59′39.0″ E); from calamine soil at the entry to a former Zn mine in La Calamine/Kelmis in Belgium (50°42′38.78″N, 6°0′37.39.4″ E); and, most likely, from calamine soil at a former Zn smelter in Les Avinières, close to St. Laurent le Minier in the south of France (43°56′11.2″N, 3°40′17.2″ E). The accession San Felix de Pallières (SF) has also been collected in the south of France from calamine soil at a former Zn mine (44°2′.40.03″ N, 3°56′18.05″ E) and was obtained from Dr. Henk Schat (Free University, Amsterdam, NL). Before this experiment, these accessions have been propagated by self-pollination for at least 4–5 generations (SF) or more than 8

generations (LE, LC, GA) since their collection in the field. Non-vernalization requiring early flowering mutants were identified in an EMS-mutagenized M2 population (approximately 8,000 plants) generated in the inbred SF accession background. Seeds of two early flowering lines (A2 and A7), probably originating from one mutation event, were obtained from Dr. Martin Broadley (University of Nottingham, United Kingdom). These mutants were selected from a fast-neutron mutagenized M2 population, for which the seeds used for mutagenesis were collected from plants growing in the wild in St. Laurent le Minier (Ganges) (Ó Lochlainn et al., 2011) and are further referred to as GA-A2 and GA-A7.

For all plants used in this experiment, the seeds were imbibed at 4°C for 4 days before sowing in pots with a mix of fertilized peat and sand under standard greenhouse conditions (16 h light/8 h dark cycle) set at 23°C and 65% relative humidity. For the flowering time variation study, the plants were vernalized in a cold growth room (at 4°C, 16 h light/8 h dark) for 4, 6, 8, 10, and 12 weeks, after 60 days of vegetative growth in the standard greenhouse conditions, and subsequently transferred back to the same greenhouse. To examine the temperature effect on flowering time, seeds were sown in a growth chamber (16 h light/8 h dark) set at 20°C or 30°C. The rosette leaves and inflorescences distal from open flowers were collected for RNA extraction when the first flower had opened. The inflorescence samples may have contained a few small bracts.

The effect of a cold period on inflorescence number was evaluated by counting the number of inflorescences 30 days after the transfer back to the warm greenhouse. The subsequent inflorescences on the side shoots were not included. Ten plants were scored per accession.

Gene Expression Analysis

RNA was extracted following a Trizol protocol (Oñate-Sánchez and Vicente-Carbajosa, 2008) and treated with DNA-free DNase (Promega)[1]. RNA quality and quantity were determined using agarose gel electrophoresis and a NanoDrop ND1000 spectrophotometer (NanoDrop Technologies, Wilmington, DE, United States). cDNA was synthesized from 1 μg of total RNA using a cDNA reverse transcription kit (iScript^{TM}cDNA Synthesis Kit) following the protocol recommended by the manufacturer.

Gene expression was determined upon quantitative reverse transcription-polymerase chain reaction (qRT-PCR). A 10-fold dilution of the cDNA was used for each reaction by mixing 4 μl cDNA, 1 μl forward and reverse primers (3 μM) and 5 μl SYBR Green quantitative PCR buffer (Bio-Rad, Cat. no.18080-044). The primer sequences of the different genes are presented in **Supplementary Table 1**. The following PCR protocol was used: denaturation at 95°C for 10 min to activate the DNA polymerase, followed by 45 cycles of denaturation at 95°C for 10 s, annealing at the primer-specific annealing temperature for 30 s and extension at 70°C for 30 s. Following the last cycle, the melting curve was determined in the temperature range 57–95°C. A last step of cooling was performed at 40°C for 10 s. The relative expressions were determined based on ΔCt values. The expression levels were normalized to the house keeping gene tubulin (see **Supplementary Table 1**). Three to five biological replicates for each treatment or accession were used for the analysis. Before performing the qRT-PCR, the appropriate primer efficiency for each gene was verified.

[1]www.promega.com

Analysis of Candidate Mutant Alleles and Amino Acid Sequences

The coding regions of *NcFLC*, *NcSVP, NcMAF-like-1,* and *NcMAF-like-2* were PCR-amplified from WT and mutant plants by using 2 μl 10 × diluted cDNA (as used for qRT-PCR) as template. PCR was performed using 35 cycles with regular Taq DNA polymerase. The PCR products were gel-purified using NucleoSpin Gel and PCR Clean-up kits[2] and the purified fragments were sent for DNA sequencing (Eurofins Genome Sequencing Company, Ebersberg, Germany). *NcFLC* and *NcSVP* genomic DNA (gDNA) fragments (∼600 bp) were also amplified and sequenced. The cDNA and gDNA sequences were aligned using Bioedit[3]. The primers were designed using Primer3Plus[4] based on a preliminary genome sequence of the GA accession (Severing et al., in preparation) or on published cDNA sequences (Lin et al., 2014). The primer sequences can be found in **Supplementary Table 1**. The amino-acid sequences of FLC from *A. thaliana, Brassica napus,* and *Arabis alpina* and the splice variants of NcFLC and NcSVP were aligned using the Bioedit program.

Genetic Complementation Analysis of *flc* and *svp* Mutants

The three mutants that carry *flc* mutant alleles were inter-crossed and crossed with putative *svp* mutants and WT. The early-flowering GA-A2 and GA-A7 lines, obtained from the Broadley lab, were also crossed to the *flc-1* and *svp-1* mutants and each other. The F1 plants were grown under control conditions. Flowering time of the F1 plants was determined as the number of days after sowing when the first flower opened. The flowering time of the F2 plants derived from the cross between the early flowering mutants and the SF WT was determined in the same way and the same conditions.

RESULTS

Different *N. caerulescens* Accessions Require Different Vernalization Times

Four *N. caerulescens* accessions, "Ganges" (GA), "St. Felix de Pallières" (SF), "Lellingen" (LE), and "La Calamine" (LC), originating from diverse environments, both in terms of local soil metal concentrations and climate conditions, were examined to determine their vernalization requirements. Sixty days after sowing, the plants were vernalized by keeping them for 4, 6, 8, 10,

[2]http://www.mn-net.com

[3]http://www.mbio.ncsu.edu/bioedit/bioedit.html

[4]http://www.bioinformatics.nl/cgi-bin/primer3plus/primer3plus.cgi/

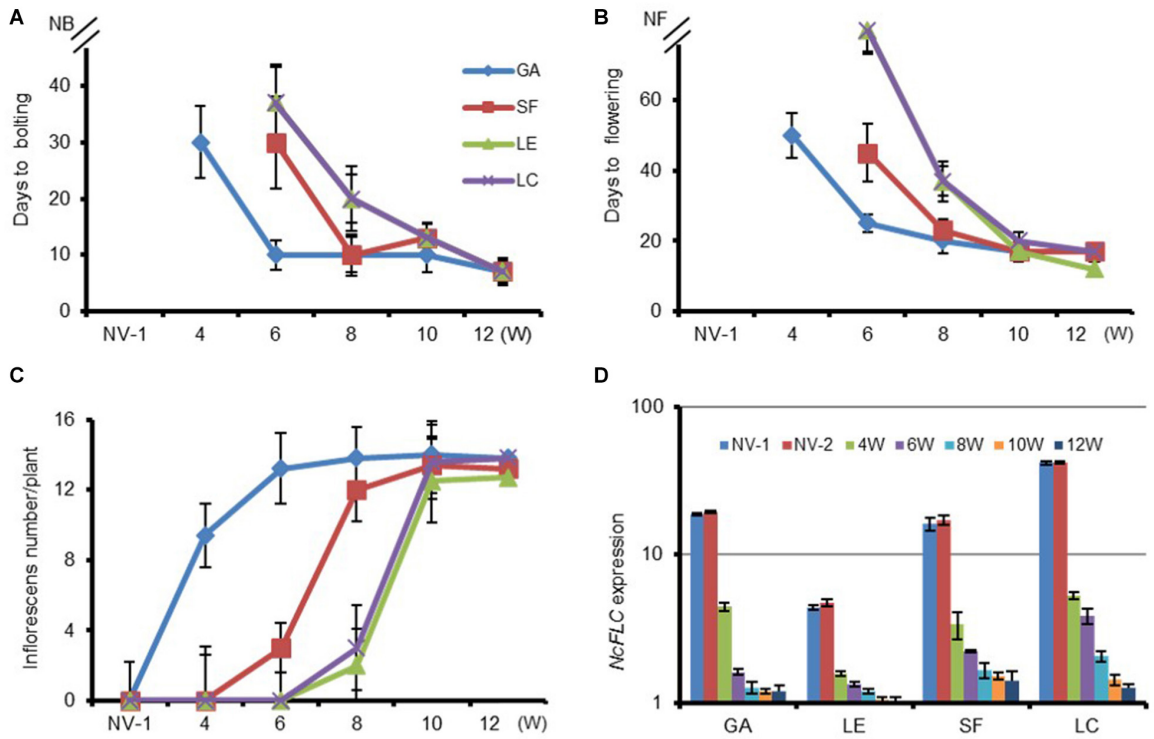

FIGURE 1 | Variation in vernalization response and *NcFLC* expression of *selected N. caerulescens* accessions. **(A)** The transition to flowering as determined by the time to bolting (first flower bud visible) for non-vernalized (NV) plants and for plants vernalized for the indicated number of weeks (W). **(B)** The time to flowering (first petal visible); and **(C)** the number of inflorescences per plant in the same treatments as **(A)**. **(D)** The relative expression of *NcFLC* in rosette leaves upon vernalization for the indicated number of weeks, relative to the expression of *NcFLC* in SF after 12 weeks of vernalization (=1). The expression of *NcTubulin* is used to normalize cDNA concentrations. Values are the mean of three to five plants. Bars show standard errors. NV-1: 2-month-old non-vernalized plants; NV-2: 5-month-old non-vernalized plants. NB, not bolting; NF, not flowering. Accessions are Ganges (GA), St. Felix de Pallières (SF), Lellingen (LE), and La Calamine (LC).

and 12 weeks in cold (4°C) conditions. The days to bolting (first flower buds visible) and the days to flowering (first petals visible) were determined for each accession (**Figures 1A,B**). As the length of the cold period increased, the response to the cold treatment varies greatly among the accessions. In general, the prolonged cold treatment accelerated the time to bolting and flowering in all accessions after returning them to warm greenhouse conditions. The largest difference in flowering time among accessions was observed after 4 weeks of cold treatment. Flowering of GA was induced completely with all plants flowering between 50 and 60 days after 4 weeks of vernalization, whereas in SF, LC and LE flowering did not occur until the end of the experiment (180 days after sowing). After a 6-week cold treatment, GA and SF flowered after, respectively, 25 and 45 days after vernalization, whereas LE and LC still did not flower during the whole 180-day period. The number of inflorescences was also higher with a longer cold period. Eight weeks of vernalization shortened the days to bolting in all accessions and increased the inflorescence numbers compared with 6 weeks of vernalization (**Figure 1C**). For the GA and SF accessions, more inflorescences developed after 8 (vs. 6) weeks of vernalization, whereas in LC and LE, only a few inflorescences developed after this cold treatment. However, the time to flowering was increased in LE and LC. In these accessions some parts of the inflorescences that had bolted did not start flowering at all, indicating that not in all meristems the transition to flowering was completed. After 10 weeks of cold treatment the number of days to bolting and to flowering was reduced to on average, respectively, 10 and 20 days for all accessions, indicating that the vernalization requirement was fully satisfied. After the 10- and 12-week treatments, and transfer to warm conditions, LE flowered the earliest amongst all accessions. It also had stopped flowering, with all siliques being well-developed at 30 days after 10 and 12 weeks of cold, while the other three accessions were still flowering.

Vernalization Represses *NcFLC* Expression in all Four Accessions

To explore the role of flowering repressors in *N. caerulescens*, we determined the *NcFLC* and *NcSVP* expression levels in the four examined accessions after different vernalization periods. Prolonged cold treatment of the four accessions resulted in a down-regulation of *NcFLC* transcript levels in all of them (**Figure 1D**), while *NcSVP* transcript levels were not changed with prolonged cold-treatment (data not shown). *NcFLC* expression is already down-regulated in all accessions after 4 weeks of cold treatment and continues decreasing the longer the cold period lasts (**Figure 1D**). However, the sensitivity to vernalization

among accessions does not correlate with the initial expression level of *NcFLC*. Accession LE, with the lowest initial *NcFLC* transcript level among all accessions, flowers only after 10 weeks of cold treatment, and not after 8 weeks, while only minor changes in *NcFLC* expression levels were observed between 8 and 10 weeks of cold treatment in this accession (**Figures 1A,B**). In the GA, SF and LC accessions, the *NcFLC* transcript threshold to repress flowering seems much higher than in LE, with GA only requiring 4 weeks of vernalization to induce flowering at a higher *NcFLC* expression level than LE.

One reason why the four accessions required different weeks of cold for the full acceleration of flowering could be that *NcFLC* expression recovers differently between accessions after the transfer to warmer conditions. Therefore, we also determined the maintenance of *NcFLC* gene expression in the four accessions at 10 and 30 days after the vernalization treatment (**Figure 2**). After 4–8 weeks of vernalization, the relative *NcFLC* expression indeed increased 10 days after returning to the warm greenhouse in LC, and only marginally in SF and LE, while in GA, *NcFLC* transcript levels stayed constantly low. In all accessions, *NcFLC* expression increased again after 30 days in the warm greenhouse, but the increase was less prominent in GA and LE compared to SF and LC. In general, the *NcFLC* expression remained more repressed the longer the cold period lasted. In GA and SF, however, *NcFLC* transcript levels are relatively more stably repressed than in LE and LC, when the cold treatment lasted up to 10 weeks, at which time flowering is induced in all accessions. This suggests that the recovery of *NcFLC* transcript levels immediately after the transfer to the warm greenhouse, correlates with the absence of flowering after a short period of vernalization.

Non-vernalization Requiring Early Flowering Mutants in *N. caerulescens*

To study the molecular mechanisms controlling flowering of *N. caerulescens*, mutants showing an impaired vernalization response were identified upon screening a total of 8,000 M2 seedlings (from 3,500 mutagenized SF plants). During the screen, the day temperature was kept at 20°C and long day conditions (16 h light/8 h dark) were applied. The latter did not induce flowering in the non-mutagenized control SF plants. The screen revealed five early flowering mutants that lacked the obligate vernalization requirement (**Figure 3A**). The T10-42 mutant is the most extreme early flowering mutant, flowering only 51 days after sowing without vernalization. The T10-58 and T27-2 mutants started flowering, respectively, at 66 and 78 days after sowing. No morphological differences in their inflorescences and flowers were observed between the mutants and their wild-type (WT). We hypothesized that most likely such early flowering mutants would have recessive mutations in floral repressor genes such as *NcFLC* and *NcSVP*. Therefore, we determined the expression of these genes in these early flowering mutants. Three mutants exhibited *NcFLC* transcript levels significantly lower than that of WT suggesting that flowering without vernalization correlated with reduced *NcFLC* transcript level (**Figure 3B**). Two other mutants exhibited *NcFLC* transcript levels at least as high as those found in the WT. In one of those, mutant T81-27, the *NcSVP* transcript level was significantly lower compared to that in the WT (**Figure 3C**). For mutant T64-35, as well as for the two lines of the previously published GA mutant (GA-A2 and -A7), the early flowering phenotypes did not relate with significantly reduced expression of *NcFLC* or *NcSVP* (**Figures 3B,C**).

Genetic Analysis

To test which mutations are allelic, the non-vernalization requiring mutants were inter-crossed. In addition, the mutants were also back-crossed (BC) to WT. Mutant T64-35 was sterile and no (hybrid) seeds could be obtained. The flowering time of all F1 plants were assessed as the days to bolting after sowing of plants grown in long days in the greenhouse (**Figure 3D**). All F1 plants derived from crosses between the mutants with low *NcFLC* transcript levels (T10-42, T10-58, and T27-2) flowered without vernalization, indicating that these mutants carry inactive, recessive alleles at the same locus, which means they cannot complement each other (**Figure 3D**). By contrast, all F1 plants derived from the back-cross with WT (T10-42, T10-58, T27-2, and T81-27) and the F1 hybrids between T81-27 and the three mutants of the first complementation group did not flower in these conditions indicating that T81-27 carries a mutation at a second locus. Analysis of the BC1S1 progeny of the mutant × WT crosses under non-vernalization conditions revealed that all the segregation ratios agreed with a Mendelian 3: 1 ratio of non-flowering: early flowering plants (data not shown), confirming the right crosses were made.

Splicing-Site Mutations in *NcFLC* and *NcSVP* Result in Early Flowering Mutants

Based on the hypothesis that recessive mutations in the floral repressors could result in early flowering, combined with the lower expression levels of *NcFLC* and *NcSVP* (**Figures 3B,C**) in the early flowering mutants, compared to WT, we cloned and sequenced the *NcFLC* and *NcSVP* cDNAs and genomic DNAs (gDNAs) from all mutants and WT (**Figure 4** and **Supplementary Figures S1**, **S2**). After alignment of the gDNA and cDNA sequences, G to A point mutations were found, of which two located at different splicing sites of *NcFLC*, one in mutants T10-48 (*flc-1*) and T10-52 (*flc-2*) and one in mutant T27-2 (*flc-3*), while another mutation was found in *NcSVP*, in mutant T81-27 (*svp-1*). Consistent with this, the cDNAs of the *flc* and *svp* variants were alternatively spliced resulting in shorter mRNAs in the mutants than in the WT (**Figure 4**). The T10-48 and T10-52 mutants (*flc-1* and *flc-2*), which carry the same mutation in the *NcFLC* gene, originated from the same tray of M2 plants (derived from one subset of M1 plants) suggesting that these two mutants are derived from the same mutation event. In the *flc-1* and *flc-2* mutants, the point mutation is located exactly at the exon-intron junction at the 3′ end of the third exon (**Figure 4A**). This disturbs proper splicing of *FLC* in these mutants substantially. Instead of splicing the 3′ end of exon 2 to the 5′ end of exon 3, the complete exon 3 is skipped, and exon 2 is combined with a new splice acceptor site in intron 3, which adds 38 bp of the end of intron 3 to exon 4. The open reading frame is maintained, but all of exon 3 is replaced with

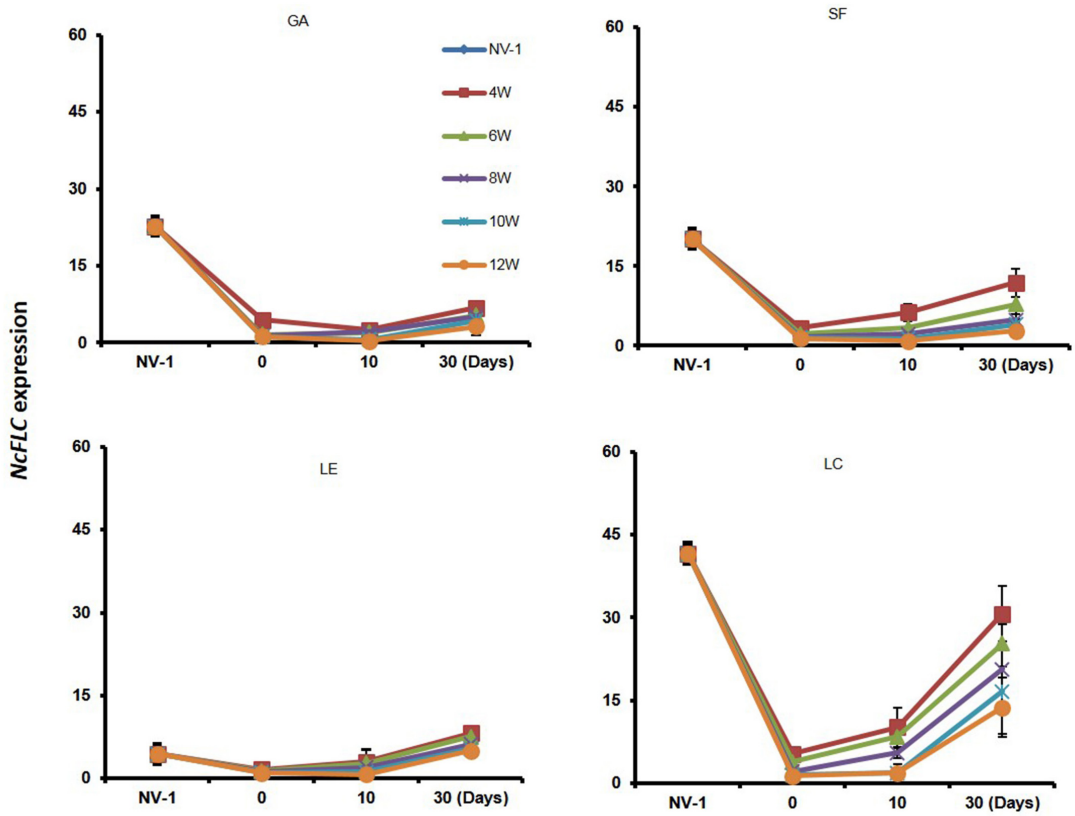

FIGURE 2 | Variation in maintaining repression of *NcFLC* expression upon vernalization. *NcFLC* expression in *N. caerulescens* rosette leaves of accessions Ganges (GA), St. Felix de Pallières (SF), Lellingen (LE), and La Calamine (LC) of plants either non-vernalized (NV-1; 6 months after sowing) or vernalized for 4, 6, 8, 10, or 12 weeks (W) at 4°C after 2 months of growth at 23°C, and subsequently returned to the warm greenhouse. Rosette leaves were collected at 0, 10, and 30 days (Days) following the vernalization treatment. Expression is expressed relative to the expression of *NcFLC* in SF after 12 weeks of vernalization in rosette leaves collected directly after vernalization (=1). The expression of *NcTubulin* is used to normalize cDNA concentrations. Each value represents the mean of three to five plants. Bars show standard errors.

a shorter part of intron 3 in the coding sequence, which has no homology with the original *NcFLC* coding sequence (**Figure 4B**). In the *flc-3* mutant, the point mutation is located at the intron-exon junction at the 5′ end of the third exon (**Figure 4A**), also causing aberrant splicing, which results in a 9 bp deletion in the cDNA at the very beginning of the third exon (**Figure 4B**). Both mutations are predicted to affect the K-domain of the FLC MADS-box protein (**Supplementary Figure S1**). For *svp-1*, a G to A point mutation was identified at the exon-intron boundary at the 3′ end of the fourth exon (**Figure 4C**), resulting in aberrant splicing and consequently a 26 bp deletion of the fourth exon in the cDNA (**Figure 4D**). This deletion causes a frame shift in the open reading frame and the introduction of a premature stop codon just N-terminal to the conserved MADS box domain in the SVP protein (**Supplementary Figure S2**). To explore whether the early-flowering phenotype in the GA mutant was also due to a mutation in the *NcFLC* or *NcSVP* gene, we sequenced the coding sequences of both genes in the GA mutant. No DNA sequence differences were found in the *NcFLC* and *NcSVP* genes when comparing the GA mutant and its WT type, while these genes are expressed (**Figure 3**), which shows that this mutant is affected in another gene.

The genetic complementation, together with the expression and sequence analyses, suggest that the identified point mutations explain the loss of *NcFLC* or *NcSVP*, functionality in the *flc-1, flc-2, flc-3,* and *svp-1* mutants, altering their flowering behavior. Sequencing of the *NcFLC* gene in the T64-35 mutant indicated no mutations, but sequencing of the *NcSVP* gene in this mutant revealed a C to T point mutation at position 103 of the cDNA, in the first exon (**Figure 4C**). This causes a non-synonymous amino acid substitution, altering Leu into Phe, in a conserved region of the predicted protein sequence (**Supplementary Figure S2**). As this is likely to alter the SVP function in this mutant, we designated this mutant as *svp-2*. Unfortunately, this could not be confirmed by allelism tests because of the complete sterility of this mutant, most likely due to another mutation.

The Effect of Ambient Temperature on Flowering Time in *N. caerulescens*

So far, the plants used in this study had been selected and grown during winter in a heated greenhouse. When growing the plants in late spring or summer, we noticed that these plants did not flower properly (**Supplementary Figure S3**). During these

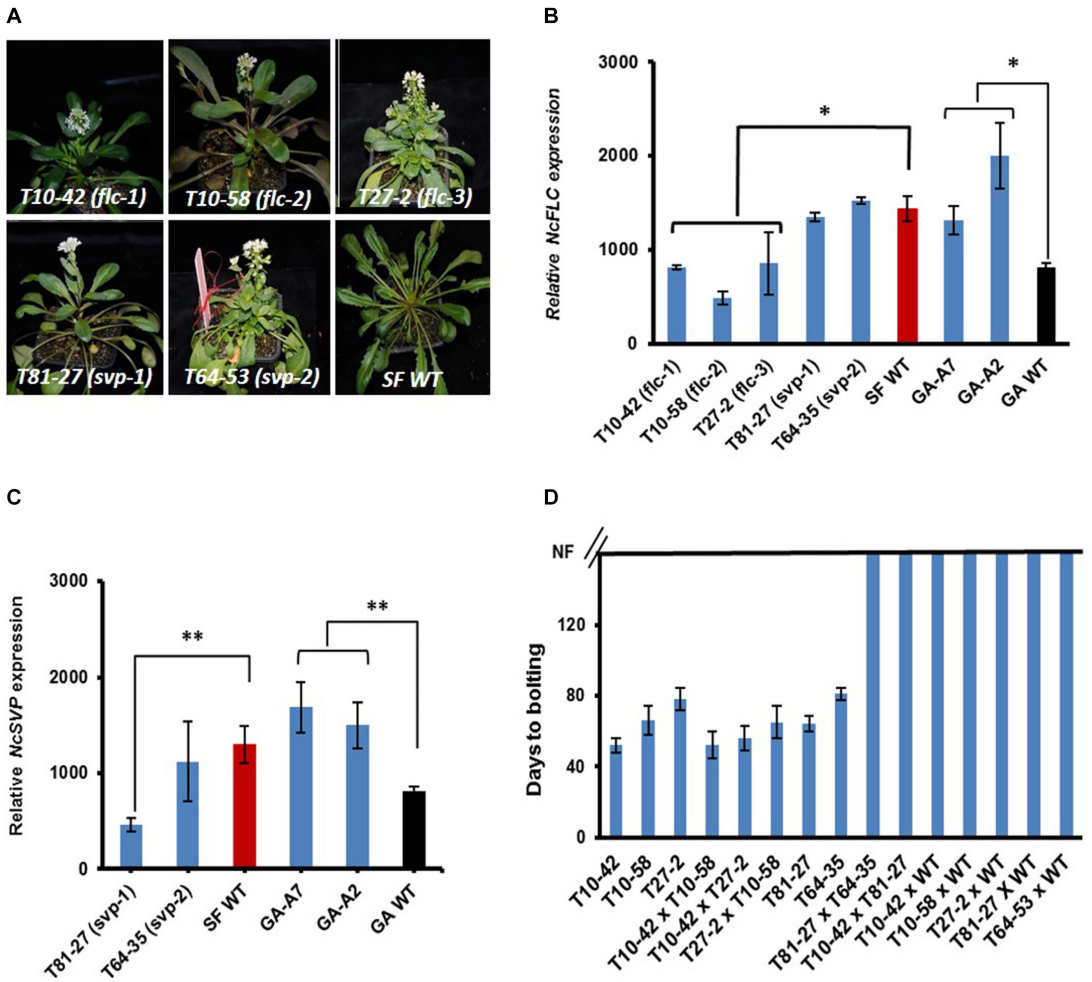

FIGURE 3 | Identification and analysis of early flowering *N. caerulescens* mutants. **(A)** Early flowering mutants (T10-42, T10-58, T81-27, T27-2, T64-35) and their St. Felix de Pallières (SF) wild type (WT) growing without vernalization. The photographs were taken 54, 69, 74, 81, 94, and 94 days after sowing for respectively, T10-42, T10-58, T81-27, T27-2, T64-35, and WT. **(B)** Relative expression of *NcFLC* in rosette leaves of early flowering mutants and WT plants. Both SF and GA WT plants are used. **(C)** Relative expression of *NcSVP* in rosette leaves of early flowering mutants and WT plants. Both SF and GA WT plants are used. **(D)** Days to bolting of self-fertilized and F1 progeny of the early flowering mutants and inter-mutant or mutant-WT crosses growing under non-vernalizing conditions. NF means not flowering. GA-A7 and GA-A2 are the early flowering mutants in Ganges (GA) background. Rosette leaves for expression analysis were collected when the first flower had opened. Expression levels were determined relative to the expression of *NcTubulin* (=1). Each value represents at least three plants ± SE. Asterisks indicate significant differences from WT, $*p < 0.05$, $**p < 0.01$, by Student's *t*-test. Red and black bars in **(B,C)** stand for, respectively, SF WT and GA WT.

periods the day temperature often exceeded 30°C, sometimes even 35°C. This prompted us to examine whether the higher ambient temperatures affect flowering in *N. caerulescens*. WT and *flc-1* mutant plants were grown in climate-controlled growth chamber under long day conditions (16/8 h day/night), with the day temperature set at either 20°C or 30°C and the night temperature at 18°C. The flowering time was determined as the number of days between sowing and bolting of each plant.

Various morphological differences were observed when comparing *flc-1* plants grown in these two temperatures (**Figure 5A**). Similar differences were observed for the *svp-1* and the GA-A7 and GA-A2 mutants, which were also grown (**Supplementary Figure S4**). The *flc-1* plants started bolting 50 days after sowing, in either temperature regime. However, the plants grown at 30°C took 1 week longer until the first flower opened, compared to the plants grown at 20°C. At 20°C, the primary and secondary inflorescences of *flc-1* flowered once 10-13 cauline leaves had developed (**Figures 5B,G**). At 30°C, at least 30 leaves were formed before the main inflorescence flowered (**Figure 5C**). Although secondary inflorescences were formed and started to elongate, most of these inflorescences developed more than 50 leaves without any visible flowers (**Figure 5D**). At 20°C, siliques developed well (**Figure 5E**) and more than 300 seeds/plant were formed (data not shown). Instead, the flowers that formed on the primary inflorescence at 30°C appeared not to be pollinated or fertilized, with the siliques remaining small and empty (**Figure 5F**), with no seeds to be obtained. This indicates that the reproductive fitness of the plants is fine at an ambient

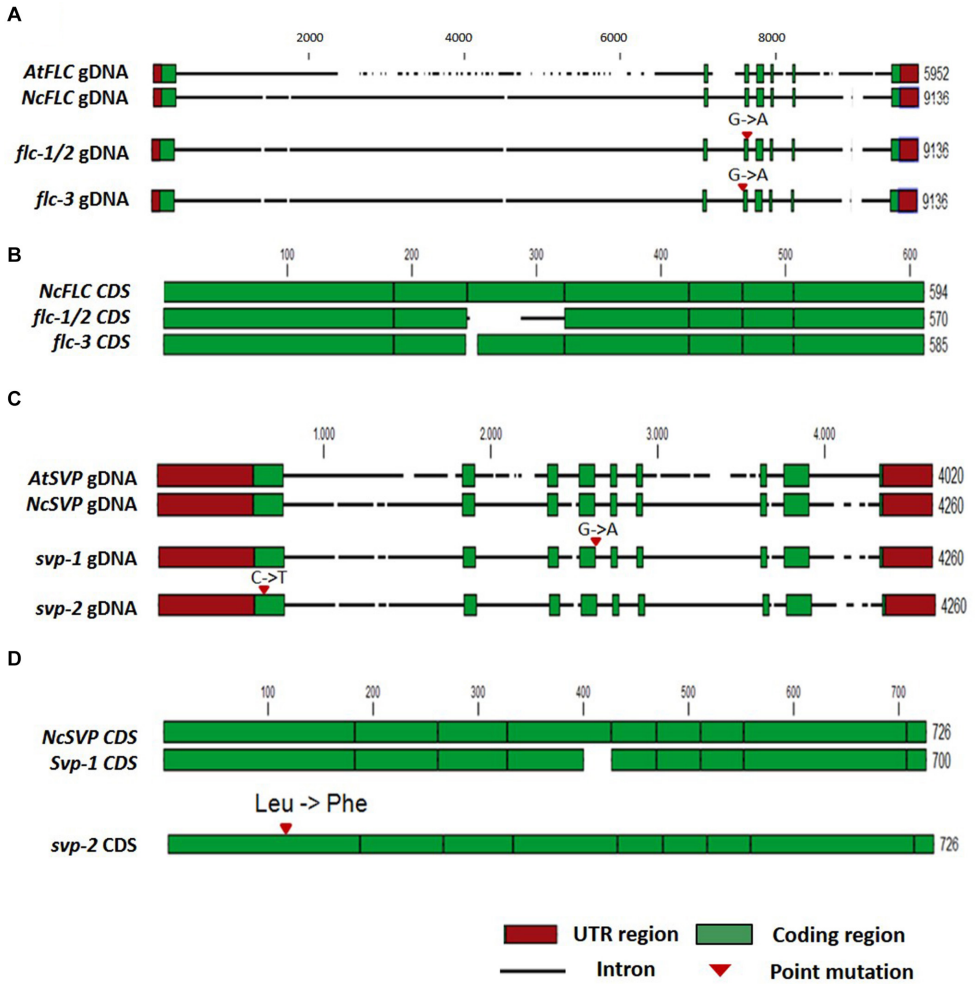

FIGURE 4 | Analysis of the *N. caerulescens FLC* and *SVP* DNA sequences in WT and the *flc* and *svp* mutants. **(A)** Schematic representation of the *Arabidopsis thaliana FLC* genomic DNA (gDNA) sequence (*AtFLC*) compared to the *NcFLC* genomic DNA sequence in *N. caerulescens* WT, *flc-1/flc-2,* and *flc-3* mutants. Numbers indicate total DNA sequence length in base pairs. Intron DNA sequences are indicated with a horizontal black line, with breaks to indicate InDels. 5′ and 3′ untranslated regions (UTR) are indicated with red boxes. Protein coding exons are indicated with green boxes. G to A single base pair mutations are found in all mutants. The mutations in *flc-1* and *flc-2* are identical, suggesting a common mutation event. The mutation in these mutants locates at the 3′ splice junction of exon 3, while the mutation in *flc-3* locates at the 5′ splice junction of exon 3. **(B)** Schematic representation of *NcFLC* coding sequences (CDS) of the *N. caerulescens* WT and *flc* mutants. The G to A mutation in *flc-1/flc-2* causes an in-frame substitution of exon 3 sequence, while the mutation in *flc-3* leads to a 9 bp deletion at the start of exon 3. Exons are indicated in green boxes, the alternative exon 3 in the *flc-1/flc-2* CDS is indicated with a horizontal black line. **(C)** The same as **(A)** for the *SVP* gene. In the *svp-1* mutant, a G to A mutation was found at the 3' splice junction of exon 4, in the *svp-2* mutant, a C to T mutation was found in exon 1. **(D)** The same as **(B)** for the *NcSVP* CDS. The mutation in *svp-1* causes an in-frame deletion of part of exon 4, while the mutation in *svp-2* leads to a single amino acid change of Leucine to Phenylalanine in exon 1. The numbers at the end of each line indicate the total number of nucleotides, the scale refers to the WT *N. caerulescens* sequence.

day temperature of 20°C, but strongly reduced at the higher temperature of 30°C.

The Effects of Ambient Temperature on Flowering Time and Flower Initiation Gene Expression

To further investigate the effects of the day temperature differences on flowering of *N. caerulescens*, the expression of flowering genes was determined in rosette leaves and the inflorescence heads (the top parts of an inflorescence, containing the flower buds and no open flowers) of *flc-1* and WT plants growing at 20°C and 30°C day temperatures (**Figure 6**). The analysis included the floral repressor genes *NcFLC* and *NcSVP*, the expression of floral integrators *FLOWERING LOCUS T* (*NcFT*) and *SUPPRESSOR OF OVEREXPRESSION OF CONSTANS* (*NcSOC1*) as well as the floral organ identify genes *LEAFY* (*NcLFY)* and *APETALA1 (NcAP1)*. Higher *NcFLC* transcript levels were detected in the rosette leaves of WT at 20°C than at 30°C indicating that the temperature influences the expression of *NcFLC*. *NcSVP* expression was up-regulated in rosette leaves at 30°C, compared to 20°C, in both the *flc-1* mutant

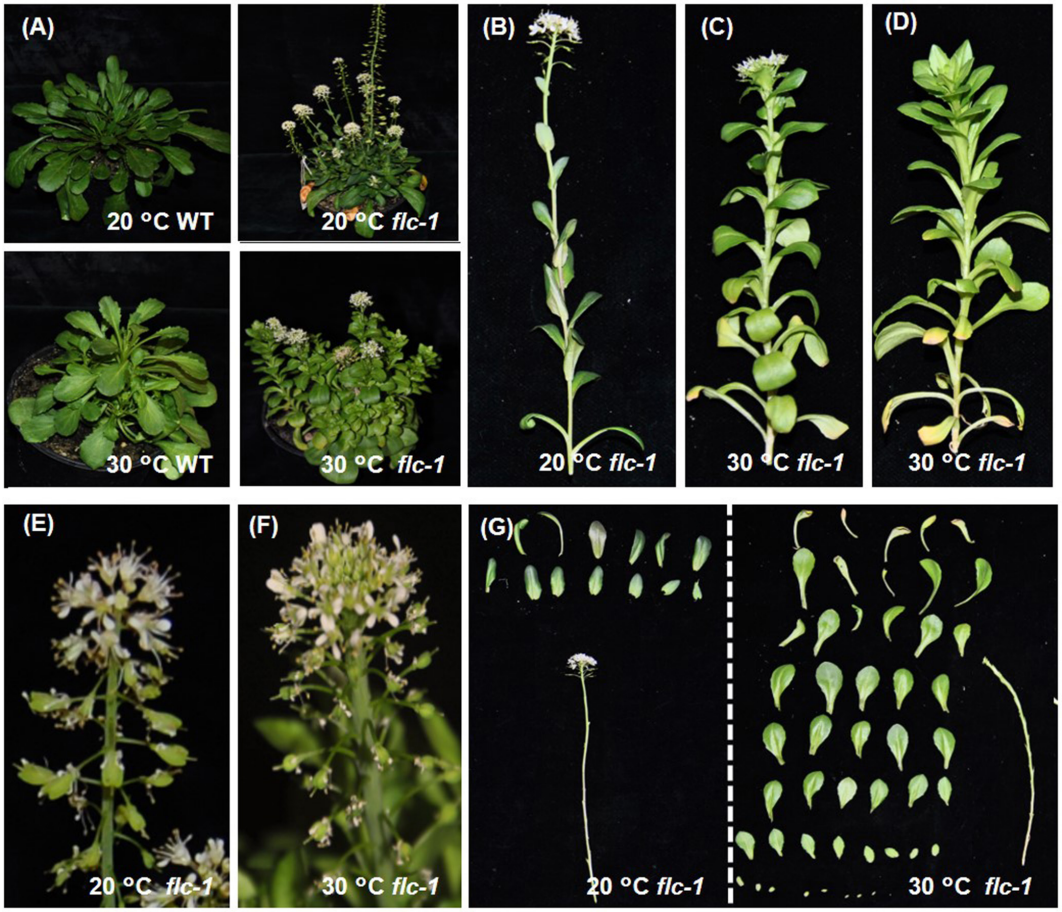

FIGURE 5 | The phenotype of WT and *flc-1* mutant plants at two different day temperatures. **(A)** Flowering plants of WT and the *flc-1* mutant grown for 2 months at either 20 or 30°C. **(B)** The primary inflorescence of the *flc-1* mutant grown at 20°C. **(C)** The primary inflorescence and **(D)** a secondary inflorescence of the *flc-1* mutant grown at 30°C. **(E)** The inflorescence top of the *flc-1* mutant at 20°C and at **(F)** 30°C. **(G)** The leaves on a primary inflorescence of the *flc-1* mutant when grown at 20°C (left) and 30°C (right).

and the WT, with slightly lower expression observed in the *flc-1* mutant. Both flower promotion genes, *NcFT* and *NcSOC1*, were up-regulated under high temperature, but more up-regulated in leaves of the *flc-1* mutant than in WT under both temperatures. In contrast, the expression levels of the floral organ identify genes *NcLFY* and *NcAP1* were considerably down-regulated in the inflorescence heads at 30°C compared to 20°C. Especially *NcAP1* expression was 14 times higher in the *flc-1* mutant at 20°C than at 30°C.

DISCUSSION

Natural Variation for Vernalization Requirement and Response Among *N. caerulescens* Accessions

Plants ensure their reproduction at the most appropriate time and correct stage of development by monitoring their environment and internal signals (Andrés and Coupland, 2012). The accurate regulation of the transition between vegetative and reproductive growth is therefore critical for propagation and survival. The promotion of flowering in response to prolonged exposure to cold temperatures (vernalization) is an adaptation to prevent plants from flowering in the fall, prior to winter, and to enable them to flower in spring. Natural genetic variation in vernalization requirement together with the temperature regimes define when the plant begins to flower and is critical for adaptation to different environments. However, the exact temperatures and length of cold exposure required for the optimal vernalization response vary among species (Kim et al., 2010).

To investigate natural variation for vernalization requirement in *N. caerulescens* we selected four accessions from different environments. Our results provide evidence that vernalization requirement and response among accessions vary within this species (**Figure 1**). The flowering time differs among *N. caerulescens* accessions depending on the length of the vernalization treatment. Both GA and SF are biennials from a

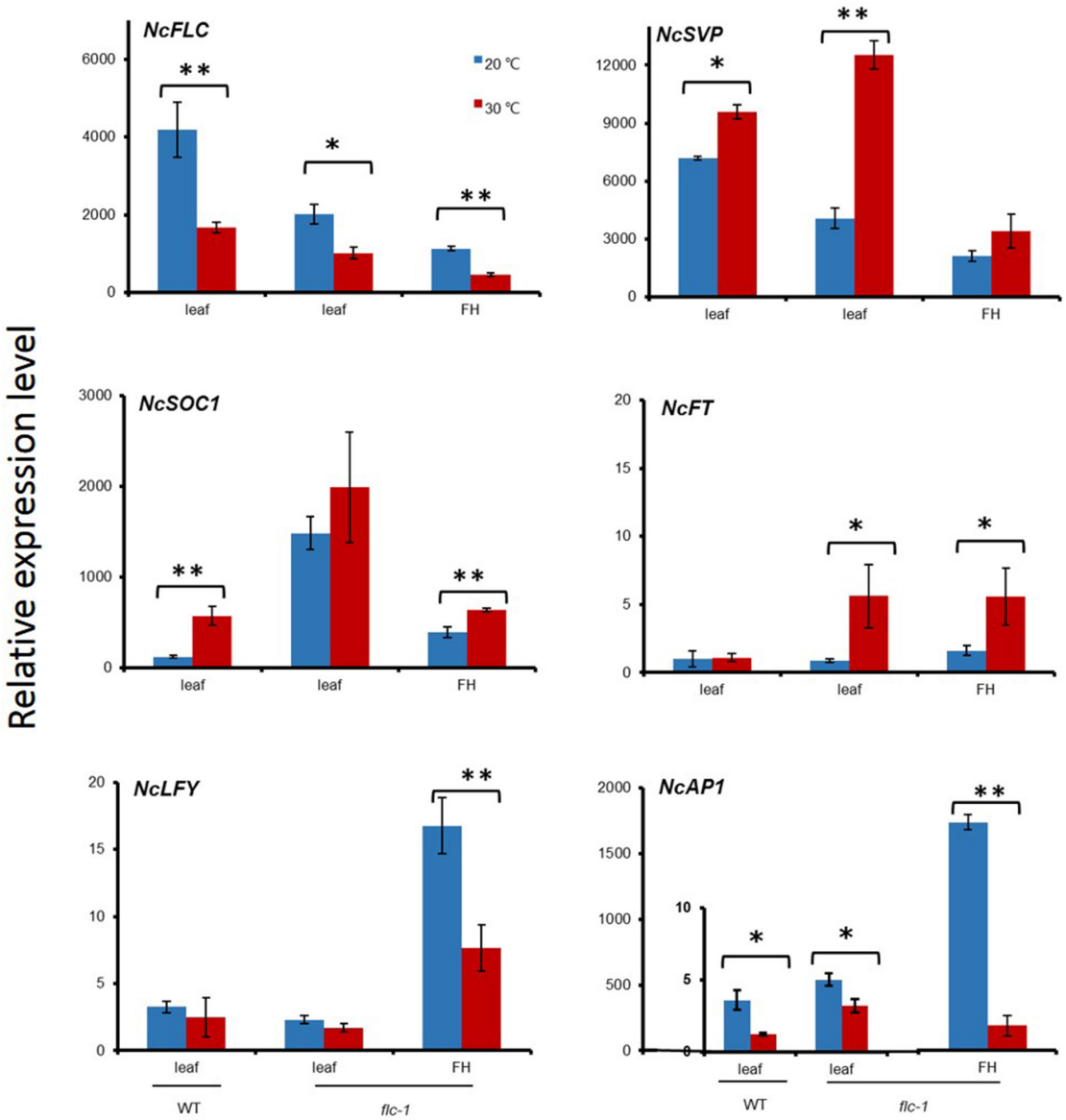

FIGURE 6 | Expression of flowering time regulating *N. caerulescens* genes in different organs and temperatures. The relative expression levels of *NcFLC*, *NcSVP*, *NcFT*, *NcSOC1*, *NcLFY* and *NcAP1* in rosette leaves (leaf) and flowering heads (FH) of St. Felix de Pallières wild-type (WT) and *flc-1* mutant plants grown at 20°C (blue bars) or 30°C (red bars). The expression of *NcTubulin* is used to normalize cDNA concentrations. Expression levels are expressed relative to the expression of *NcFT* in WT (=1). Values indicate the average of at least three plants ± SE. Asterisks indicate significant differences between 20°C and 30°C. $*p < 0.05$, $**p < 0.01$, by Student's *t*-test.

relatively dry region in the south of France, with a short winter (Dubois et al., 2003; Mousset et al., 2016). Consistent with this, a faster vernalization response is predicted to confer a selective advantage to plants that flower earlier thus to avoid early summer droughts and high temperatures that results in poor seed set. LE and LC originate from Luxembourg and Belgium, respectively, and are biennial or facultative perennial accessions, that will have to deal with more severe winters and cooler summers compared to the French accessions. This implies that these accessions should have more opportunities to satisfy the longer vernalization period they require and allowing them to flower later than the accessions from southern France when compared under the same conditions.

The Identification of Floral Repressors Affected by Vernalization in *N. caerulescens*

Plants that require vernalization to flower, encode repressors that block flowering during summer or autumn, and this block is relieved by reducing expression of the repressor when the plants are exposed to low temperatures (Andrés and Coupland, 2012).

The type of floral repressors and the regulatory framework for the vernalization response vary greatly among different species. In *A. thaliana*, expression of the repressor *FLC* drops during vernalization, upon which the transcription of *FT* is induced, which promotes floral initiation (Bastow et al., 2004; Helliwell et al., 2006; Kim et al., 2010). Similarly, SVP acts parallel to FLC to repress flowering in *A. thaliana* (Lee et al., 2007; Mateos et al., 2015). In the preliminary genome sequences of *N. caerulescens* (Severing et al., in prep.) we identified one *NcFLC* and one *NcSVP* orthologue, as well as at least two expressed orthologues of the *MAF* genes (Lin et al., 2014). However, no *NcFLM* and *NcFRI* orthologues were detected at the co-linear sites where they reside in *A. thaliana*. Our finding that early flowering loss-of-function mutants of *NcFLC* and *NcSVP* abolish the vernalization requirement, shows that *NcFLC* and *NcSVP* are the floral repressors in the control of flowering by the vernalization pathway in *N. caerulescens*. The allelic mutants in the GA background (Ó Lochlainn et al., 2011) were not affected in the expression of *NcFLC, NcSVP* or any of the *NcMAF* genes and did not show any mutations in the cDNA sequences of these genes (data not shown), which indicates that there is at least a third locus in *N. caerulescens* required for suppression of flowering in non-vernalizing conditions. Since none of the above-mentioned candidate genes are affected, map-based cloning and genome sequencing will be needed to identify the causal mutation. The observation that single mutants of all three genes result in early flowering indicates that they operate in mutual dependency.

In our analysis, expression of *NcSVP* is not affected by the vernalization treatment (data not shown), though expression is upregulated upon exposure to the higher temperature, while expression of *NcFLC* is downregulated (**Figure 6**). This suggests that the regulation of *NcSVP* is different from that of *NcFLC*. We did not pursue this any further though. The *svp* mutant flowered slightly later than the *flc* mutants. The Arabidopsis *svp* mutant flowers earlier under short day conditions than under long day conditions, suggesting a photoperiod response of *SVP*, that is not prominent for *FLC* (Albani and Coupland, 2010). Such may also be the case for the *N. caerulescens SVP* gene. Although *N.caerulescens* is typically a vernalization-obligate species, investigating the photoperiod response would enhance the understanding of *NcSVP* functionality.

FLC Expression in *N. caerulescens* Compared to *A. thaliana* and *A. alpina*

The expression pattern of *AtFLC*, and its *A. alpina* orthologue *AaPEP1*, differs between the two species. *AtFLC* remains stably repressed after the plants are transferred to warm temperatures in the winter annual *A. thaliana*, but in the perennial *A. alpina AtPEP1* expression rises again in these conditions, when flowering was induced in meristems present during the vernalization treatment (Wang et al., 2009). The latter has as a consequence that meristems that had not been converted to floral meristems remain vegetative, allowing them to be induced in a new vernalization round in the next season. Analysis of inter- and intraspecies variation demonstrated that the structure of *AaPEP1* is more complex than was found for *AtFLC* (Albani et al., 2012). *A. alpina* contains a tandem duplication of exon 1 of *AaPEP1* which results in two transcriptional start sites and two overlapping transcripts. The organization of *NcFLC* resembles the structure of *AaPEP1* (**Supplementary Figure S5**), however only one transcript has been detected in *N. caerulescens* (Lin et al., 2014), as in *NcFLC* the sequences of the exon 1 duplications are identical.

Expression analysis of plants after they returned from cold to warm conditions suggested that repression of *NcFLC* is partially stable, especially upon prolonged cold (**Figure 2**). However, its expression increased gradually upon transfer to the warm greenhouse after a short period of cold, especially in SF. Such increase indicates incomplete vernalization, reactivating *NcFLC* expression to perform the repression on flowering after transfer to a warm greenhouse. A similar phenomenon was also observed in *A. thaliana* accessions requiring very long vernalization periods (Shindo et al., 2006). With the increase of the cold treatment, the *NcFLC* expression is much more stably repressed. Up to 10 weeks of cold treatment, upon which flowering was completely induced in all accessions, the slight increase of *FLC* transcript that was detected was perhaps due to the increased turnover of the mRNA as plant growth accelerated (Shindo et al., 2006). The most likely role of the recovery of the expression level of *NcFLC* after flowering might be related to the maintenance of later formed meristems in a vegetative state, which is essential for perennial species such as *A. alpina* (Wang et al., 2009; Albani et al., 2012). Since both biennial and perennial plants were found in the field for the LE and LC accessions, the perpetual flowering habit might be part of the life style in some *N. caerulescens* accessions. It appears to be rarer for the SF and GA accessions, which may very well be related to the summer conditions at the locations where these accessions are found. These are much warmer and especially drier than those of the more northern accessions, and therefore much less likely to support proper perennial growth of *N. caerulescens*. The partially stable expression of *NcFLC* seems to be intermediate between *A. thaliana* and *A. alpina*, corresponding to the somewhat intermediate life style. Further research, including field observations, will be interesting to fully understand this complex trait.

The Higher Expression of *FT* and *SOC1* Did Not Promote *LFY* and *AP1* Expression Under High Temperature

During vernalization, leading to a decrease of *NcFLC* expression, *NcFT* and *NcSOC1* expression was upregulated, indicating the repression of *NcFLC* acts through these downstream genes. Both *NcFT* and *NcSOC1* were higher expressed in the non-functional *flc-1 N. caerulescens* mutant compared to its WT indicating that their suppression was eliminated. We observed that plants displayed a different flowering phenotype depending on the growth season (**Supplementary Figure S3**). When the temperature is higher than 30°C the inflorescences revert to

vegetative growth (**Figure 5G**) and the flowers become sterile. These observations prompted us to check the effect of day-time temperature on the flowering time control in the mutant under two different temperatures. The up-regulation of *NcFT* in the *flc-1* mutant compared to WT suggested that also in *N. caerulescens* the repression of flowering occurs via the repression of the *NcFT* gene (**Figure 6**). In the *flc-1* mutant, *NcFT* and *NcSOC1* are highly expressed at 30°C. However, the downstream genes *NcLFY* and *NcAP1* were notably lower expressed than at 20°C. We infer that the high expressions of *NcFT* and *NcSOC1* are the direct effect of the high temperature. In *A. thaliana*, alternative spliced isoforms of *AtFLM* and *AtMAF2* were up-regulated under high temperatures. These high-temperature isoforms lost the ability to combine with SVP to repress flowering (Posé et al., 2013; Airoldi et al., 2015). In *N. caerulescens* this scenario is unlikely given that flower initiation has not been observed at elevated temperatures. Alternatively, it was reported that in *A. thaliana* a repression complex formed by LIKE HETEROCHROMATIN 1 (LHP1) and the POLYCOMB REPRESSION COMPLEX 2 (PCR2) is required to maintain repression of *AtFT* (Dilkes et al., 2008). In *N. caerulescens*, the repression of *NcFT* was not maintained under high temperatures indicating that such a complex might also exist in this species. Future research could reveal if maintenance of a similar complex in *N. caerulescens* would be sensitive to high temperature and thus explain the loss of *NcFT* repression. In *A. thaliana*, SOC1, when expressed in the meristem, interacts with AGL24, another MADS box transcription factor, and together they promote the transcription of *LFY*, a meristem identity gene that is involved in the initiation of flower development (Lee et al., 2008). AP1 is also required to initiate and maintain flower meristem identity (Komeda, 2004). The high expression of *NcFT* and *NcSOC1* in the *flc-1* mutant, however, did not induce the expression of *NcLFY* and *NcAP1* at 30°C, suggesting that the promotion of *NcLFY* transcription by NcSOC1 is repressed directly, by the high temperature, or indirectly, by other components involved in this process. Consistent with the expression level of *NcLFY*, the expression level of *NcAP1* in inflorescences at 30°C was much lower than at 20°C. Thus, retarded inflorescence development or reversion from floral to vegetative meristems at 30°C (**Figure 5G**) is very likely due to the low *NcLFY* and *NcAP1* expression levels. Such reversion might be an advantage in dry and hot, summer, conditions, which would not be favorable for reproduction.

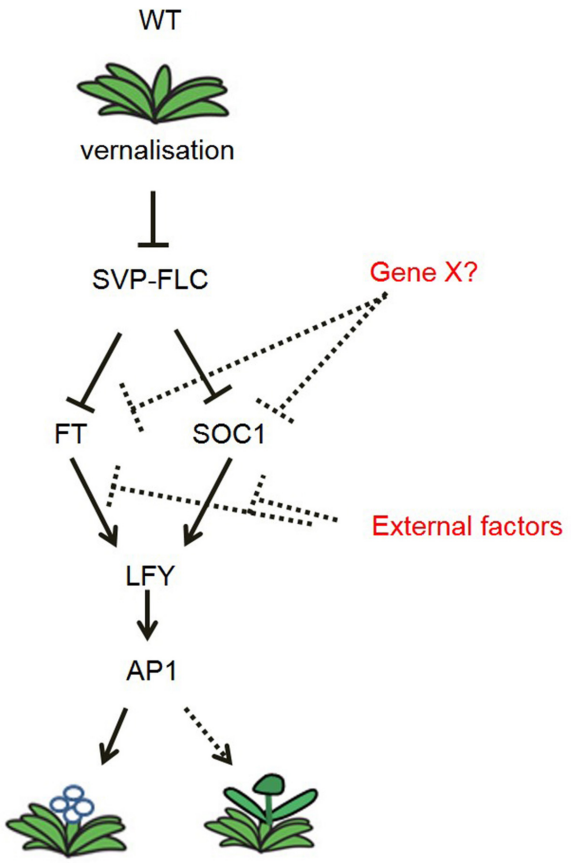

FIGURE 7 | Model of the flowering time regulation pathway in *N. caerulescens*. In general, the vernalization pathway resembles that of *A. thaliana*. In contrast to *A. thaliana*, under high temperature (30°C), *NcFT* and *NcSOC1* are highly expressed, but no longer able to induce the downstream floral identity genes *NcLFY* and *NcAP1*, which delays and disturbs floral initiation at this temperature. Gene X? stands for a third, yet unidentified, floral repressor, which functions parallel to *NcFLC* and *NcSVP*. External factors, e.g., elevated ambient temperature, may suppress the expression of *NcLFY* and *NcAP1* at 30°C. Arrows indicate induction of expression. Bar-ended lines indicate repression of expression. Solid lines indicate confirmed expression effects, while dotted lines indicate interactions still unconfirmed.

An Integrated Flowering Regulation Model in *N. caerulescens*

The identification of *N. caerulescens* genes that control flowering allows us to compare the molecular pathways controlling seasonal flowering in *N. caerulescens* with those in *A. thaliana*. Based on the transcriptional analysis of key genes in the vernalization pathway, in the non-vernalization requiring mutants, we propose a flowering time regulation model for *N. caerulescens* (**Figure 7**). In general, this model resembles that of *A. thaliana*. However, the vernalization pathway in *N. caerulescens* is further affected by down-regulation of the floral identity genes *NcLFY* and *NcAP1* under high temperatures, as we expect to happen late in spring or summer. This occurs despite the upregulated expression of floral integrators such as *NcFT* and *NcSOC1*. The temperature sensitivity of the regulating genes *LFY* and *AP1* will be an interesting topic for further study in other biennial or perennial species.

DATA AVAILABILITY STATEMENT

The datasets presented in this study can be found in online repositories. The names of the repository/repositories and accession number(s) can be found in the article/**Supplementary Material**.

AUTHOR CONTRIBUTIONS

YW, MK, and MA designed the experiments and wrote the manuscript. YW performed the experiments. ES provided the bioinformatic analysis. All authors contributed to the article and approved the submitted version.

ACKNOWLEDGMENTS

We thank Dr. Martin Broadley (University of Nottingham, United Kingdom) for providing the seeds of early flowering GA mutants and Corrie Hanhart (Laboratory of Genetics, Wageningen University) for her help with sowing M1 seeds and harvesting seeds from the M2 population.

FUNDING

This research was financially supported by the China Scholarship Council (CSC) and the Consortium for Improving Plant Yield (CIPY).

SUPPLEMENTARY MATERIAL

The Supplementary Material for this article can be found online at: https://www.frontiersin.org/articles/10.3389/fpls.2020.582577/full#supplementary-material

REFERENCES

Airoldi, C. A., McKay, M., and Davies, B. (2015). MAF2 is regulated by temperature-dependent splicing and represses flowering at low temperatures in parallel with FLM. *PLoS One* 10:e0126516. doi: 10.1371/journal.pone.0126516

Albani, M. C., Castaings, L., Wotzel, S., Mateos, J. L., Wunder, J., Wang, R., et al. (2012). PEP1 of *Arabis alpina* is encoded by two overlapping genes that contribute to natural genetic variation in perennial flowering. *PLoS Genet.* 8:e1003130. doi: 10.1371/journal.pgen.1003130

Albani, M. C., and Coupland, G. (2010). "Chapter eleven - comparative analysis of flowering in annual and perennial plants," in *Current Topics in Developmental Biology*, Vol. 91, ed. M. C. P. Timmermans (Cambridge, MA: Academic Press), 323–348. doi: 10.1016/S0070-2153(10)91011-9

Andrés, F., and Coupland, G. (2012). The genetic basis of flowering responses to seasonal cues. *Nat. Rev. Genet.* 13, 627–639. doi: 10.1038/nrg3291

Assunção, A. G. L., Bookum, W. M., Nelissen, H. J. M., Vooijs, R., Schat, H., and Ernst, W. H. O. (2003). Differential metal-specific tolerance and accumulation patterns among *Thlaspi caerulescens* populations originating from different soil types. *New Phytol* 159, 411–419. doi: 10.1046/j.1469-8137.2003.00819.x

Bastow, R., Mylne, J. S., Lister, C., Lippman, Z., Martienssen, A. R., and Dean, C. (2004). Vernalization requires epigenetic silencing of FLC by histone methylation. *Nature* 427, 164–167. doi: 10.1038/nature02269

Bond, D. M., Wilson, I. W., Dennis, E. S., Pogson, B. J., and Jean Finnegan, E. (2009). VERNALIZATION INSENSITIVE 3 (VIN3) is required for the response of *Arabidopsis* thaliana seedlings exposed to low oxygen conditions. *Plant J.* 59, 576–587. doi: 10.1111/j.1365-313x.2009.03891.x

Broadley, M. R., White, P. J., Hammond, J. P., Zelko, I., and Lux, A. (2007). Zinc in plants. *New Phytol.* 173, 677–702.

Choi, K., Kim, J., Hwang, H. J., Kim, S., Park, C., Kim, S. Y., et al. (2011). The FRIGIDA complex activates transcription of FLC, a strong flowering repressor in *Arabidopsis*, by recruiting chromatin modification factors. *Plant Cell* 23, 289–303. doi: 10.1105/tpc.110.075911

Dilkes, B. P., Jiang, D., Wang, Y., Wang, Y., and He, Y. (2008). Repression of FLOWERING LOCUS C and FLOWERING LOCUS T by the *Arabidopsis* polycomb repressive complex 2 components. *PLoS One* 3:e3404. doi: 10.1371/journal.pone.0003404

Dubois, S., Cheptou, P.-O., Petit, C., Meerts, P., Poncelet, M., Vekemans, X., et al. (2003). Genetic structure and mating systems of metallicolous and nonmetallicolous populations of *Thlaspi caerulescens*. *New Phytol.* 157, 633–641. doi: 10.1046/j.1469-8137.2003.00684.x

Duncan, S., Holm, S., Questa, J., Irwin, J., Grant, A., and Dean, C. (2015). Seasonal shift in timing of vernalization as an adaptation to extreme winter. *eLife* 4:e06620.

Guan, Z. Q., Chai, T. Y., Zhang, Y. X., Xu, J., Wei, W., Han, L., et al. (2008). Gene manipulation of a heavy metal hyperaccumulator species *Thlaspi caerulescens* L. via *Agrobacterium*-mediated transformation. *Mol. Biotechnol.* 40, 77–86. doi: 10.1007/s12033-008-9065-4

Guimarães, M. D., Loureiro, M. E., and Salt, D. E. (2013). Inducing flowering in *Noccaea caerulescens* (J. & C. Presl) F. K. Mey (*Brassicaceae*), a species having high heavy-metal accumulation. *Rev. Cienc. Agron.* 44, 834–841. doi: 10.1590/s1806-66902013000400021

Hanikenne, M., and Nouet, C. (2011). Metal hyperaccumulation and hypertolerance: a model for plant evolutionary genomics. *Curr. Opin. Plant Biol.* 14, 252–259. doi: 10.1016/j.pbi.2011.04.003

Hartmann, U., Susanne, H., Klaus, N., Ellen, W., Heinz, S., and Peter, H. (2000). Molecular cloning of SVP: a negative regulator of the floral transition in *Arabidopsis*. *Plant J.* 21, 351–360. doi: 10.1046/j.1365-313x.2000.00682.x

Helliwell, C. A., Wood, C. C., Robertson, M., James Peacock, W., and Dennis, E. S. (2006). The *Arabidopsis* FLC protein interacts directly in vivo with SOC1 and FT chromatin and is part of a high-molecular-weight protein complex. *Plant J.* 46, 183–192. doi: 10.1111/j.1365-313x.2006.02686.x

Kim, D. H., Zografos, B. R., and Sung, S. (2010). Mechanisms underlying vernalization-mediated VIN3 induction in *Arabidopsis*. *Plant Signal. Behav.* 5, 1457–1459. doi: 10.4161/psb.5.11.13465

Komeda, Y. (2004). Genetic regulation of time to flower in *Arabidopsis thaliana*. *Annu. Rev. Plant Biol.* 55, 521–535. doi: 10.1146/annurev.arplant.55.031903.141644

Krämer, U. (2010). Metal hyperaccumulation in plants. *Annu. Rev. Plant Biol.* 61, 517–534. doi: 10.1146/annurev-arplant-042809-112156

Lee, J., Oh, M., Park, H., and Lee, I. (2008). SOC1 translocated to the nucleus by interaction with AGL24 directly regulates leafy. *Plant J.* 55, 832–843. doi: 10.1111/j.1365-313x.2008.03552.x

Lee, J. H., Yoo, S. J., Park, S. H., Hwang, I., Lee, J. S., and Ahn, J. H. (2007). Role of SVP in the control of flowering time by ambient temperature in *Arabidopsis*. *Genes Dev.* 21, 397–402. doi: 10.1101/gad.1518407

Leijten, W., Koes, R., Roobeek, I., and Frugis, G. (2018). Translating flowering time from *Arabidopsis thaliana* to *Brassicaceae* and *Asteraceae crop* species. *Plants* 7:111. doi: 10.3390/plants7040111

Lin, Y. F., Severing, E. I., Hekkert, B. L., Schijlen, E., and Aarts, M. G. M. (2014). A comprehensive set of transcript sequences of the heavy metal hyperaccumulator *Noccaea caerulescens*. *Front. Plant Sci.* 5:261. doi: 10.3389/fpls.2014.00261

Mateos, J. L., Madrigal, P., Tsuda, K., Rawat, V., Richter, R., Romera-Branchat, M., et al. (2015). Combinatorial activities of SHORT VEGETATIVE PHASE and FLOWERING LOCUS C define distinct modes of flowering regulation in *Arabidopsis*. *Genome Biol.* 16:31.

Michaels, S. D., and Amasino, R. M. (1999). FLOWERING LOCUS C encodes a novel MADS domain protein that acts as a repressor of flowering. *Plant Cell* 11, 949–956. doi: 10.2307/3870827

Mousset, M., David, P., Petit, C., Pouzadoux, J., Hatt, C., Flaven, E., et al. (2016). Lower selfing rates in metallicolous populations than in non-metallicolous populations of the pseudometallophyte *Noccaea caerulescens* (*Brassicaceae*) in Southern France. *Ann. Bot.* 117, 507–519. doi: 10.1093/aob/mcv191

Nascimento, C. W. A., and Xing, B. S. (2006). Phytoextraction: a review on enhanced metal availability and plant accumulation. *Sci. Agr.* 63, 299–311. doi: 10.1590/s0103-90162006000300014

Nordborg, M., and Bergelson, J. (1999). The effect of seed and rosette cold treatment on germination and flowering time in some *Arabidopsis thaliana* (*Brassicaceae*) ecotypes. *Am. J. Bot.* 86, 470–475. doi: 10.2307/2656807

Ó Lochlainn, S., Fray, R. G., Hammond, J. P., King, G. J., White, P. J., Young, S. D., et al. (2011). Generation of nonvernal-obligate, faster-cycling *Noccaea caerulescens* lines through fast neutron mutagenesis. *New Phytol.* 189, 409–414. doi: 10.1111/j.1469-8137.2010.03554.x

Oñate-Sánchez, L., and Vicente-Carbajosa, J. (2008). DNA-free RNA isolation protocols for *Arabidopsis thaliana*, including seeds and siliques. *BMC Res. Notes* 1:93. doi: 10.1186/1756-0500-1-93

Peer, W. A., Mahmoudian, M., Freeman, J. L., Lahner, B., Richards, E. L., Reeves, R. D., et al. (2006). Assessment of plants from the *Brassicaceae* family as genetic models for the study of nickel and zinc hyperaccumulation. *New Phytol.* 172, 248–260. doi: 10.1111/j.1469-8137.2006.01820.x

Peer, W. A., Mamoudian, M., Lahner, B., Reeves, R. D., Murphy, A. S., and Salt, D. E. (2003). Identifying model metal hyperaccumulating plants: germplasm analysis of 20 *Brassicaceae* accessions from a wide geographical area. *New Phytol.* 159, 421–430. doi: 10.1046/j.1469-8137.2003.00822.x

Pollard, A. J., Reeves, R. D., and Baker, A. J. (2014). Facultative hyperaccumulation of heavy metals and metalloids. *Plant Sci.* 217-218, 8–17. doi: 10.1016/j.plantsci.2013.11.011

Posé, D., Verhage, L., Ott, F., Yant, L., Mathieu, J., Angenent, G. C., et al. (2013). Temperature-dependent regulation of flowering by antagonistic FLM variants. *Nature* 503, 414–417. doi: 10.1038/nature12633

Sheldon, C. C., Burn, J. E., Perez, P. P., Metzger, J., Edwards, J. A., James Peacock, W., et al. (1999). The FLF MADS Box Gene: a repressor of flowering in *Arabidopsis* regulated by vernalization and methylation. *Plant Cell* 11, 445–458. doi: 10.2307/3870872

Shindo, C., Lister, C., Crevillen, P., Nordborg, M., and Dean, C. (2006). Variation in the epigenetic silencing of FLC contributes to natural variation in *Arabidopsis* vernalization response. *Genes Dev.* 20, 3079–3083. doi: 10.1101/gad.405306

Sung, S. B., and Amasino, R. M. (2004). Vernalization in *Arabidopsis thaliana* is mediated by the PHD finger protein VIN3. *Nature* 427, 159–164. doi: 10.1038/nature02195

Turck, F., Fornara, F., and Coupland, G. (2008). Regulation and identity of florigen: FLOWERING LOCUS T moves center stage. *Annu. Rev. Plant Biol.* 59, 573–594. doi: 10.1146/annurev.arplant.59.032607.092755

Wang, R., Farrona, S., Vincent, C., Joecker, A., Schoof, H., Turck, F., et al. (2009). PEP1 regulates perennial flowering in *Arabis alpina*. *Nature* 459, 423–427. doi: 10.1038/nature07988

Conflict of Interest: The authors declare that the research was conducted in the absence of any commercial or financial relationships that could be construed as a potential conflict of interest.

Copyright © 2020 Wang, Severing, Koornneef and Aarts. This is an open-access article distributed under the terms of the Creative Commons Attribution License (CC BY). The use, distribution or reproduction in other forums is permitted, provided the original author(s) and the copyright owner(s) are credited and that the original publication in this journal is cited, in accordance with accepted academic practice. No use, distribution or reproduction is permitted which does not comply with these terms.

frontiers in Plant Science

REVIEW
published: 20 November 2020
doi: 10.3389/fpls.2020.605155

Regulation and Subfunctionalization of Flowering Time Genes in the Allotetraploid Oil Crop *Brassica napus*

Sarah Schiessl[1,2]*

[1] Department of Plant Breeding, IFZ Research Centre for Biosystems, Land Use and Nutrition, Justus Liebig University Giessen, Giessen, Germany, [2] Department of Botany and Molecular Evolution, Senckenberg Research Institute and Natural History Museum Frankfurt, Frankfurt, Germany

OPEN ACCESS

Edited by:
Elizabeth Dennis, Commonwealth Scientific and Industrial Research Organisation (CSIRO), Australia

Reviewed by:
Ryo Fujimoto, Kobe University, Japan
Chris Helliwell, Commonwealth Scientific and Industrial Research Organisation (CSIRO), Australia

***Correspondence:**
Sarah Schiessl
sarah-veronica.schiessl@agrar.uni-giessen.de

Specialty section:
This article was submitted to Plant Development and EvoDevo, a section of the journal Frontiers in Plant Science

Received: *11 September 2020*
Accepted: *29 October 2020*
Published: *20 November 2020*

Citation:
Schiessl S (2020) Regulation and Subfunctionalization of Flowering Time Genes in the Allotetraploid Oil Crop Brassica napus. Front. Plant Sci. 11:605155. doi: 10.3389/fpls.2020.605155

Flowering is a vulnerable, but crucial phase in building crop yield. Proper timing of this period is therefore decisive in obtaining optimal yields. However, genetic regulation of flowering integrates many different environmental signals and is therefore extremely complex. This complexity increases in polyploid crops which carry two or more chromosome sets, like wheat, potato or rapeseed. Here, I summarize the current state of knowledge about flowering time gene copies in rapeseed (*Brassica napus*), an important oil crop with a complex polyploid history and a close relationship to *Arabidopsis thaliana*. The current data show a high demand for more targeted studies on flowering time genes in crops rather than in models, allowing better breeding designs and a deeper understanding of evolutionary principles. Over evolutionary time, some copies of rapeseed flowering time genes changed or lost their original role, resulting in subfunctionalization of the respective homologs. For useful applications in breeding, such patterns of subfunctionalization need to be identified and better understood.

Keywords: polyploidy, gene evolution, subfunctionalization, flowering time, canola, oilseed rape

INTRODUCTION

Rapeseed for Future

In a future fossil-free mobility strategy, plant-based fuels cannot fully replace fossil fuels, as the production quantity of plant oils is by far too low (Carlsson et al., 2011), but they may be used in all cases where electricity-based machines cannot provide sufficient power, like tractors or harvesting machines (Bender, 1999). Plant-based fuels will therefore become an important building block in decarbonizing agriculture. The most popular plant-based fuel in temperate areas is biodiesel, which is mostly produced from rapeseed oil (Bušić et al., 2018). Although rapeseed oil is also a healthy edible oil, its use for fuel is dominating. Rapeseed is grown all across the globe in different climate zones from boreal to subtropical climates and constitutes the second most important oil crop of the world after soybean, comparable to oil palm (FAOSTAT, sourced July 2020). Breeding has formed three distinct oilseed rape growth types: spring rapeseed, which is grown as an annual,

mostly in Australia and Canada, semi-winter rapeseed, which gives better yield but has an increased vegetation period, and winter rapeseed, which is biennial and yields best of all three types. Growth type is largely determined by flowering behavior and winter hardiness. Winter types are winter-hardy and depend on a period of prolonged cold to attain the ability to flower (vernalization), while semi-winter types are less vernalization dependent and lack winter hardiness, and spring types lack both traits (Schiessl et al., 2017b). Besides those oilseed forms, a further subspecies, ssp. *napobrassica*, is cultivated as beets and known as swedes or rutabagas. Swedes are generally strongly vernalization-dependent, but lack strong winter hardiness. Due to the importance of those traits, each growth type usually constitutes its own breeding pool. However, breeding for other traits, mainly oil and seed quality, has strongly reduced genetic diversity within the breeding pools, and cross-breeding between pools might be one solution to increase genetic diversity and increase breeding gains (Snowdon and Iniguez Luy, 2012). Shifts in climate zones due to climate change may also demand growth type adaptation in future (IPCC, 2019).

Why Timing of Flowering Does Matter

In most plants and also in oilseed rape, flowering is the most sensitive phase for yield building due to various reasons: the increased energy demand due to flower formation (Borghi et al., 2019), but also due to shadowing of the leaves by the flowers, reducing photosynthesis (Diepenbrock, 2000). Flowering time is also critical in terms of nitrogen use efficiency, as N uptake after flowering is strongly correlated to yield (Berry et al., 2010). Moreover, drought stress during flowering was found to be much more devastating than during vegetative development (Hohmann, 2017). Many rapeseed growing areas face increased likelihoods of droughts during rapeseed flowering times due to climate change (Lu et al., 2019). If the drought period is short, drought avoidance including later flowering can be a successful strategy (Schiessl et al., 2020), but this is highly dependent on synchronization of drought period and flowering time. In winter oilseed rape, flowering time is also a general obstacle to breeding progress. Winter oilseed rape requires long periods of 6 to 10 weeks of vernalization to achieve flowering competence, leading to long generation times. In other crops and in spring rapeseed, attempts to shorten generation times in growth chambers were successful using special light regimes (Ghosh et al., 2018; Watson et al., 2018); however, this remains to be achieved for winter rapeseed. Finally, oilseed rape is a facultative outcrossing species and therefore not strictly dependent on pollinators, however, the presence of pollinators in the field normally increase seed yield and quality (Bommarco et al., 2012; Zou et al., 2017; Adamidis et al., 2019). It is thus helpful to synchronize flowering time with pollinators' activity. Flowering time has therefore an important influence on many agronomic traits and environment-specific flowering time adaptation needs to be carried out in individual breeding programs to maximize yield.

WHAT IS DIFFERENT TO *Arabidopsis thaliana*?

Brassica napus is a close relative to the model crucifer *Arabidopsis thaliana*. Most *A. thaliana* flowering time genes are conserved in the species (Osborn et al., 1997), indicating that flowering time regulation in oilseed rape is regulated in a similar way as in the model system. There are, however, species-specific drawbacks in this conclusion which are mainly due to the polyploid nature of the *B. napus* genome. *B. napus* is a recent allotetraploid carrying a subgenome A from the donor species *B. rapa* as well as a subgenome C from the donor species *B. oleracea* (Morinaga, 1934; Nagaharu, 1935). *B. rapa* and *B. oleracea* are two closely related species separated by around 4.5 Mio years of evolution, going back to a common hexaploid ancestor (Schiessl and Mason, 2020). This evolutionary history raises the theoretical number of homologs to six, although gene loss has reduced the average copy number to 4.4 (Parkin et al., 2010). For the main flowering time regulators, the average copy number was found to be 4.8, ranging from one to up to twelve copies (Schiessl et al., 2014). Moreover, the individual copy number in flowering time was found to be highly variable in a representative diversity set, although this did not affect all copies equally (Schiessl et al., 2017b). At the same time, several transcriptomic studies have shown that expression patterns vary a lot between copies of the same *Arabidopsis* homolog, with different expression maxima, different tissue or age specificity or different reactivity to stress (Zhou et al., 2007; Guo et al., 2014; Shah et al., 2018; Kittipol et al., 2019; Schiessl et al., 2019a). Together, this indicates that flowering time genes in *B. napus* underwent considerable subfunctionalization. To identify useful breeding targets, it is therefore crucial to identify the conserved or acquired role of each flowering time gene copy individually. In the next paragraphs, I will summarize the progress of such attempts for the different regulatory modules identified in *Arabidopsis*. A list of *B. napus* homologs detected within QTL, GWAS peaks or located in selective sweeps is given in **Table 1**. For general reviews about flowering time regulation in models and crops, please refer to the excellent works of others in this area (Jung and Muller, 2009; Srikanth and Schmid, 2011; Blümel et al., 2015).

The Central Hub: FT, FD, and SOC1

The major flowering regulator *FLOWERING LOCUS T (FT)* has six copies in *B. napus*, located on chromosomes A02, A07 (two copies), C02 and C06 (two copies) (Wang J. et al., 2009). BLAST positions in the first published reference genome, however, were partially different and assigned one copy to C04, which could be misassembly (Schiessl et al., 2017b). *Bna.FT.C02* was reported to be pseudogenized, obviously due to a transposon insertion into its promoter region (Wang et al., 2012). Non-expression of *Bna.FT.C02* was later confirmed in a winter type (Guo et al., 2014), while others found flowering time QTL (Rahman et al., 2018) and reported expression in spring type (Raman et al., 2019). The same study found a correlation between the expression of all copies with flowering time, at least in spring type *B. napus* (Raman et al., 2019). Several copies of *Bna.FT* (on A02 or

TABLE 1 | List of most important flowering time genes with respective QTL, GWAS peaks or within selective sweeps in *B. napus* with chromosomal locations and references.

Gene name in AT	Abbreviated as	Candidate in QTL study	Candidate in GWAS	Candidate in selective sweep analysis	References
FLOWERING LOCUS T	*FT*	A02, A07ab	A02	A02	Raman et al., 2013, 2019; Nelson et al., 2014; Wu et al., 2018
FLOWERING LOCUS D	*FD*			C01, C03	Schiessl et al., 2017b
FLOWERING LOCUS C	*FLC*	A02, A03ab, A10, C02, C03	A02, A10, C03	A10, C03	Quijada et al., 2006; Udall et al., 2006; Fletcher et al., 2014; Nelson et al., 2014; Raman et al., 2016; Schiessl et al., 2017b; Wu et al., 2018
FRIGIDA	*FRI*	A03	A03	A03	Wang et al., 2011; Raman et al., 2013, 2016; Schiessl et al., 2015, 2017b
VERNALIZATION INSENSITIVE 3	*VIN3*	A02, A03		A02	Shi et al., 2009; Nelson et al., 2014; Schiessl et al., 2017b; Shah et al., 2018
FY	*FY*	C02			Jian et al., 2019
CONSTANS (-like)	*CO (-like)*	A02, A10, C01, C03, C09	A02, A03, C09	A10, C09	Quijada et al., 2006; Nelson et al., 2014; Xu et al., 2016; Schiessl et al., 2017b; Li et al., 2018; Rahman et al., 2018
SENSITIVITY TO RED LIGHT REDUCED 1	*SRR1*			A02	Schiessl et al., 2017b
PHYTOCHROME A	*PHYA*	C05		A09, C08	Raman et al., 2014; Schiessl et al., 2017b
PHYTOCHROME B	*PHYB*	A05	A03, A05, C03, C05		Raman et al., 2013, 2016
CRYPTOCHROME 2	*CRY2*		A10	A10	Schiessl et al., 2017b; Raman et al., 2019
PHYTOCHROME INTERACTING FACTOR 4	*PIF4*		?		Raman et al., 2019
GIBBERELLIN 2-OXIDASE 1	*GA-2-ox-1*	A02			Raman et al., 2013; Jian et al., 2019
GIBBERELLIN 20-OXIDASE	*GA-20-ox*		C01		Schiessl et al., 2015
REPRESSOR OF GA1	*RGA1*	A02			Li et al., 2018
SQUAMOSA PROMOTER LIKE 3	*SPL3*		A03	A05	Raman et al., 2016; Schiessl et al., 2017b

?Location not reported.

A07) were found in major QTL intervals in different studies, all of them in populations derived from spring type rapeseed (Raman et al., 2013, 2019; Nelson et al., 2014). EMS mutants of *Bna.FT.C06b*, but not of *Bna.FT.C06a* changed flowering time in a winter type (Guo et al., 2014). The copies on A07 and C06 are located within inverted duplicated regions, indicating they arose from a tandem duplication before the speciation separating *B. rapa* and *B. oleracea* (Wang J. et al., 2009). Regulatory regions of *Bna.FT.A02* and *Bna.FT.C02* were lacking a binding site known to be important for binding of the vernalization regulator *FLC*, the so-called CArG box, but were containing a binding motif for the photoperiod regulator *CONSTANS (CO)* (Wang J. et al., 2009; Raman et al., 2019). The copies on A07 and C06 showed the opposite pattern (Wang J. et al., 2009; Raman et al., 2019). This indicates that regulation via vernalization and regulation via photoperiod might have been split between the A02/C02 copies and the A07/C06 copies, although this has not been demonstrated yet. An extensive study on natural variation in almost 1,000 *B. napus* accessions found that the second strongest selection signature between winter and spring type *B. napus* was located in a region harboring *Bna.FT.A02* (Wu et al., 2018). A region 3 kb upstream of this copy also showed the strongest GWAS peak for flowering time in the same study, indicating promoter variation accounts for the effect (Wu et al., 2018). Indeed *Bna.FT.A02* expression was different between winter, semi-winter and spring material (Wu et al., 2018). Another study found that *Bna.FT.A02* expression was not released directly after vernalization, but only later shortly before BBCH60, beginning of flowering (Guo et al., 2014). The A07/C06 copies, however, responded directly to vernalization (Guo et al., 2014). Together with the promoter motif analysis, this indicates that the A07/C06 copies may be majorly regulated by vernalization (*Bna.FLC*), while the A02 copy may be majorly regulated by day length (*Bna.CO*) (see **Figure 1** for a model). Interestingly, no functional variation for the coding regions of *Bna.FT.A02* and *Bna.FT.C02* was found across 280 accessions of *B. napus*, indicating expression variation was exclusively due to promoter variation (Schiessl et al., 2017b). The same study also found that *Bna.FT.A02* was never affected by a deletion event, supportive of this copy being essential (Schiessl et al., 2017b). *Bna.FT.A02* was also found to react to drought stress in winter type rapeseed (Schiessl et al., 2020), possibly via the age pathway. A recent study comparing *Bna.FT.A02* expression in early and late winter type rapeseed found that there may be genotypic variance in the responsiveness to vernalization, as the early flowering Cabriolet was able to upregulate *Bna.FT.A02* in response to vernalization, while the late flowering genotype Darmor was not or only slightly (Tudor et al., 2020).

The protein binding partner of *FT, FLOWERING LOCUS D (FD)* (note: there's also another gene named the same way, but abbreviated as FLD working in the autonomous pathway) has received much less attention than *FT*, and has also not be named as a candidate gene in any of the numerous QTL studies for flowering time up to date. Two copies, *Bna.FD.C01* and *Bna.FD.C03*, showed distinct patterns of allelic variation in swedes, indicating they would contribute to the differential flowering behavior of this subspecies (Schiessl et al., 2017b).

The second most important floral integrator, *SUPPRESSOR OF OVEREXPRESSION OF CONSTANS 1 (SOC1)* is also not well studied in *B. napus*. No data is available on *Bna.SOC1* expression patterns for its six copies. One of its copies, *Bna.SOC1.A05*, was found to be highly conserved across 280 diverse *B. napus* accessions, possibly indicating special functional importance (Schiessl et al., 2017b). Analysis of promoter sequences of different *Brassica SOC1* homologs point into the same direction (Sri et al., 2020). The authors found that all six *B. napus SOC1* promoter sequences show distinct patterns of transcription factor binding sites, similar to the diploid *Brassica* species and *B. juncea* (Sri et al., 2020). In *B. rapa* and *B. juncea*, the resulting expression patterns were markedly different, with differences in expression between tissues (for copies on A05 and A03) and in total expression level and response (for the A04 copy) (Sri et al., 2020). In *B. juncea*, the patterns of transcription factor binding sites were correlating with the respective expression patterns and with expression of putative regulators (Sri et al., 2020), showing elegantly how post-polyploidization diversification in promoter sequences can lead to subfunctionalization.

Vernalization: FLC, FRI, and VIN3

Most studies on *B. napus* flowering time genes have been performed on the main vernalization regulator *Bna.FLC*, mostly because it was recognized as a candidate gene for many flowering time QTL quite early on (Quijada et al., 2006; Udall et al., 2006; Fletcher et al., 2014; Nelson et al., 2014; Raman et al., 2016). *Bna.FLC* has nine annotated copies in the *B. napus* genome, located on chromosomes A02, A03 (two copies), A10, C02, and C03 (two copies), and C09 (two copies) (Zou et al., 2012). Moreover, an incomplete copy on A01 has also been reported, most likely a duplicate of the A02 copy (Schiessl et al., 2019a). Early transformation studies indicated not all of them have the same effect, with the copy on A10 having the strongest effect on vernalization (Tadege et al., 2001). Later on, it was found that this effect was due to a MITE transposon insertion into the promoter of *Bna.FLC* increasing *Bna.FLC* expression in winter type rapeseed (Hou et al., 2012). While semi-winter material originally showed a comparable *Bna.FLC.A10* expression, downregulation in response to cold happened much quicker than in a winter type, presumably because the transposon sequence interfered with the mechanism of downregulation (Hou et al., 2012). In spring type accessions, *Bna.FLC.A10* expression was found to be low even before vernalization (Wu et al., 2018; Schiessl et al., 2019a). Wu et al. (2018) subsequently also found that the strongest selection signal between winter and spring accessions was located close to the A10 copy, linked to differential expression between winter and spring material, a finding confirmed by others (Schiessl et al., 2017b, 2019a). At the same time, *Bna.FLC.C03b* was found to be a pseudogene (Zou et al., 2012; Schiessl et al., 2019a). Meanwhile, the role of the other seven copies remains unclear. Both copies on C09 and partly also *Bna.FLC.C03a* were found to have lost their cold responsiveness (Schiessl et al., 2019a). However, *Bna.FLC.A02*, *Bna.FLC.A03ab*, and *Bna.FLC.C02* as well as *Bna.FLC.A10* are downregulated by cold (Raman et al., 2016; Schiessl et al., 2019a). Raman et al.

claim that FLC2 (*Bna.FLC.A02/C02*) is responsible for 22% of the flowering time variation in non-vernalized conditions in a diverse population of spring type rapeseed (Raman et al., 2016). Only *Bna.FLC.A03a* and *Bna.FLC.C02* show some degree of differential expression between winter and spring, although this seems to be dependent on the age of the sampled leaf material (Schiessl et al., 2019a). Varying tissue-specific differences in *Bna.FLC* expression have been reported before (Zou et al., 2012). The data indicate that *Bna.FLC.A10* is not only responsible for the high vernalization dependency of winter types, but also for the moderate vernalization dependency of semi-winter types. A recent study identified additional transposon insertions influencing expression in the promoters of *Bna.FLC.A10* and *Bna.FLC.A02* and concluded that *Bna.FLC.A10* determines growth type in combination with *Bna.FLC.A02* (Yin et al., 2020). Interestingly, swedes (ssp. *napobrassica*), showing an extremely strong vernalization dependency, were reported to carry two copies of *Bna.FLC.A10*, possibly as a result of selection against bolting (Schiessl et al., 2017b). In case of monomorphic *Bna.FLC.A10*, other *Bna.FLC* copies (A02, A03, and C02) may still show up as modulating flowering time factors in non-vernalized conditions. Likewise, *Bna.FLC.A02*, *Bna.FLC.A03b,* and *Bna.FLC.C02* seem to be influential on flowering time in spring material, although they are only able to delay, but not to inhibit flowering. This was recently confirmed for *Bna.FLC.A02* (Tudor et al., 2020) (**Figure 2**).

In *A. thaliana*, vernalization requirement was attributed to variation in either *FLC* or *FRIGIDA (FRI)* (Jiang et al., 2009; Choi et al., 2011). *FRI* has four copies in the *B. napus* genome, of which one of them, *Bna.FRI.A03*, was associated to flowering variation quite early on (Wang et al., 2011). The same copy was later on found to be associated to the subspecies differentiation of swedes, but also for the winter-spring split (Schiessl et al., 2017b). All four copies are expressed (Wang et al., 2011; Schiessl et al., 2019a), and the expression level was found to be comparable between copies, growth types and seemed to be independent of vernalization, but the copies named *BnaA.FRI.a* (A03) and *BnaX.FRI.d* showed significant differences in tissue patterning, being expressed mostly in flowers, while showing very low expression in leaves (Wang et al., 2011). The copies on A03 and C03 were slightly upregulated upon cold, but returned to normal levels afterwards (Schiessl et al., 2019a). Four haplotypes which were associated to differential flowering behavior were detected, but not in spring types, loosely in semi-winter and strongly in winter type accessions (Wang et al., 2011). Those haplotypes contained several non-synonymous SNPs and InDels (Wang et al., 2011). A GWAS for flowering time in winter material in 12 different environments detected a respective peak in a Chinese environment with mild winters, indicating it might influence flowering under non-saturated vernalization conditions (Schiessl et al., 2015). A QTL study in spring material detected a QTL in the vicinity of *Bna.FRI.A03*, but no allelic effect of the copy itself (Raman et al., 2013) as well as a GWAS performed predominantly in semi-winter accessions (Raman et al., 2016). So while there is a clear consent that only *Bna.FRI.A03* is influential for flowering time, the reason for this is unclear. As two of the other copies were predicted to have altered protein structures as compared to *A. thaliana* (Wang et al., 2011), these copies might already have attained a different role.

Another vernalization gene which has been brought up as a candidate gene to influence flowering time in oilseed rape is *VERNALIZATION INSENSITIVE 3 (VIN3)* (Shi et al., 2009; Nelson et al., 2014; Schiessl et al., 2017b; Shah et al., 2018). It has four copies in *B. napus*, of which mostly the A02 copy was attributed to phenotypic effects (Shi et al., 2009; Nelson et al., 2014; Schiessl et al., 2017b; Shah et al., 2018). However, gene expression analysis in a spring accession (Westar) over time showed that all four copies get upregulated during cold in both leaf and apex, as expected from *A. thaliana*, and get downregulated upon return to warmer temperatures (Schiessl et al., 2019a). *Bna.VIN3.C03* had the lowest expression, while the others showed comparable expression levels. This would indicate a low level of subfunctionalization in terms of gene expression, and the reason why only *Bna.VIN3.A02* has been found as candidate might be attributed to existing variation in coding regions. Analysis of SNP distribution in *B. napus* populations of winter, spring and swede growth types found *Bna.VIN3.A02* as candidate for the winter-spring split, and *Bna.VIN3.A03* as a candidate for the swede split (Schiessl et al., 2017b). However, no non-synonymous SNP was found to associate with this pattern (Schiessl et al., 2017b), contradicting this hypothesis. Works in *B. oleracea* (cauliflower) have shown that the dynamics of upregulation in *Bol.VIN3* instead of absolute expression level are decisive for flowering time variation (Ridge et al., 2015). More precise time series of *Bna.VIN3* expression in cold are therefore needed to judge the degree of subfunctionalization between the *Bna.VIN3* copies.

Autonomous Pathway

The autonomous pathway in *A. thaliana* is regulating *FLC* mRNA concentration independently of cold (Cheng et al., 2017). The autonomous pathway gene *Bna.FY* was named particularly often in QTL studies before the publication of the *B. napus* reference genome, as many candidate regions showed a BLAST hit to "*a region at the top of chromosome 5 containing the flowering time genes FLC, FY, and CO*" (Raman et al., 2013; Fletcher et al., 2014; Luo et al., 2014); however, in most cases the major effects might rather have been due to *FLC* or *CO* than to *FY*. However, Jian et al. (2019) found seven members of the autonomous pathway were differentially expressed between parents of their RIL population and at the same time located in a respective flowering time QTL, also including *Bna.FY*, indicating it might still contribute to flowering time variation. Some other homologs of autonomous pathway genes have also been named as candidate genes for flowering time in *B. napus*, like *FLD* (Raman et al., 2016; Jian et al., 2019), *AGL18* (Raman et al., 2016), or two copies of *LD* (Schiessl et al., 2015). However, data allowing a deeper insight into copy-specific regulation or involvement is not available up to now,

and much is left to reveal for autonomous pathway genes in *B. napus*.

Photoperiod: CO, GI, SRR1, PHY, and CRY

In contrast to vernalization, the photoperiod behavior of rapeseed is not well studied. It is known that rapeseed does generally not flower at a day length of 8 h (most vernalization chambers run at this day length). However, in spring rapeseed, 24% of accessions were able to flower at 8 h day length (Raman et al., 2019), while in a different study, spring rapeseed was generally reported to flower at a day length of 10 h, although strongly delayed (Rahman et al., 2018). In the same study, flowering time was not different between 14 h day length and 18 h day length, so the critical day length at least for spring rapeseed lies between 10 and 14 h of light (Rahman et al., 2018). Others found that there

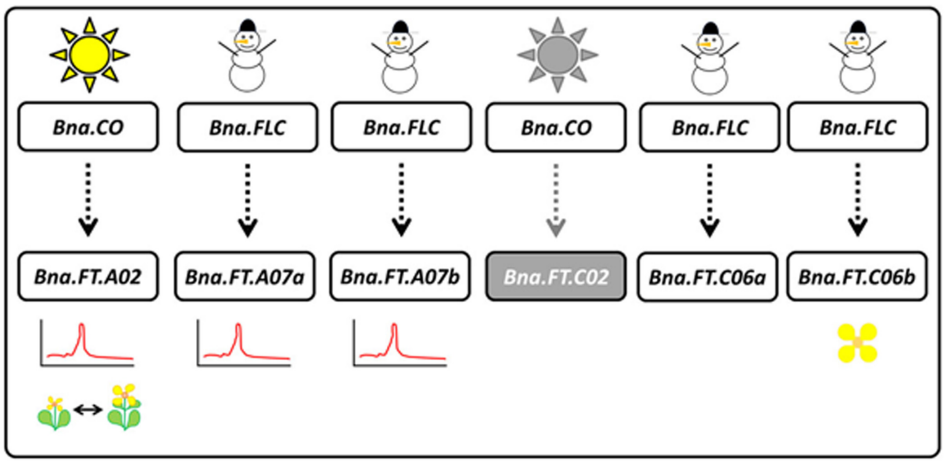

FIGURE 1 | Model of *Bna.FT* regulation based on available literature data (references see main text). *Bna.FT.C02* is most likely to be a pseudogene (gray). *Bna.FT.C06b* mutation was shown to influence flowering time (flower). *Bna.FT* copies on A02 and A07 were found in flowering time QTL (LOD plot). Promoter and gene expression analysis indicates that *Bna.FT.A02* (and unlikely *Bna.Ft.C02*, if expressed) responds to *Bna.CO* and day length regulation (sun), while copies on A07 and C06 respond to *Bna.FLC* and vernalization (snowman). *Bna.FT.A02* was also found to underlie a selective sweep between winter, semi-winter, and spring material (two contrasting rapeseed plants).

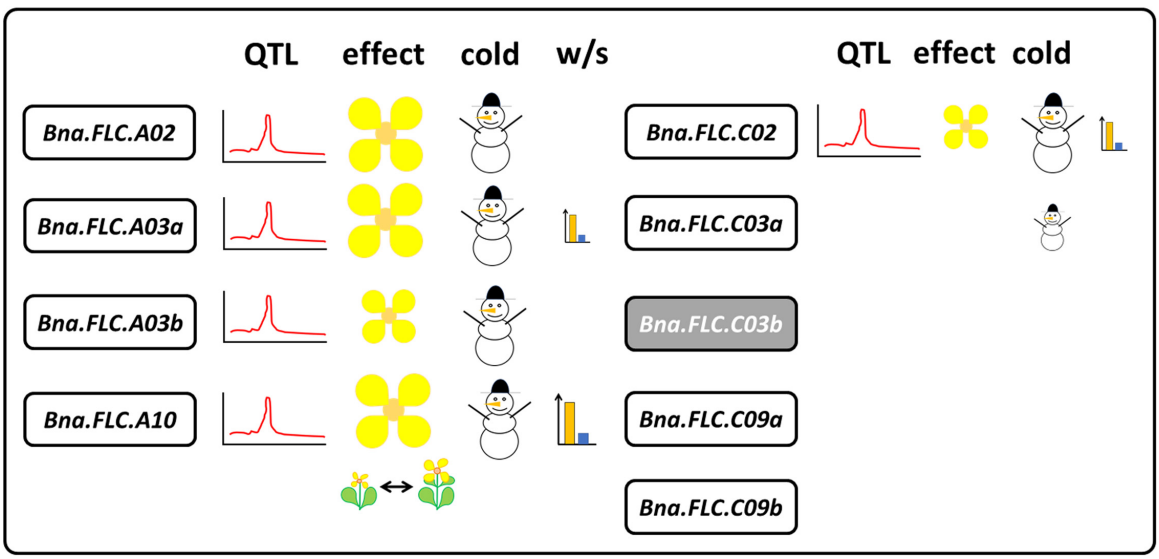

FIGURE 2 | Summary of *Bna.FLC* copy functionality based on literature data (references see main text). *Bna.FLC.C03b* is most likely a pseudogene (gray). Copies on A02, A03, A10, and C02 have been found in QTL for flowering time (LOD plot). The same copies were able to complement the *Arabidopsis* flc mutation (flower, size indicates effect). The same copies were also shown to be downregulated under cold (snowman), while *Bna.FLC.C03a* still showed partial downregulation. *Bna.FLC.A03b*, *Bna.FLC.A10*, and *Bna.FLC.C02* have been shown to be differentially expressed between winter and spring material (Barplot, size indicates degree), but only *Bna.FLC.A10* was located in a selective sweep between winter and spring (gene expression co-segregating) and between swede and non-swede (two contrasting rapeseed plants).

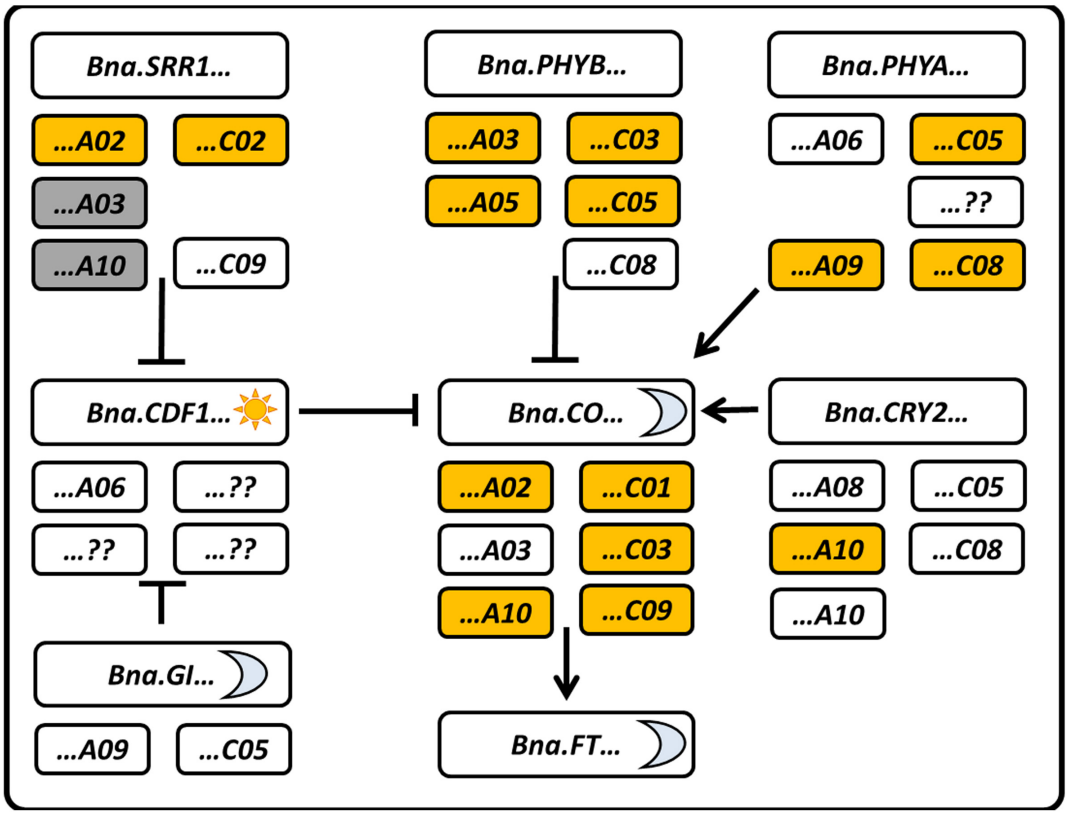

FIGURE 3 | Schematic representation of selected genes from the photoperiodic pathway with their locations in *B. napus*. Gray boxes indicate pseudogenes, yellow boxes indicate this copy has been named as a candidate in a GWAS, QTL, or selective sweep analysis. Thy sun symbol marks a gene which peaks in the morning, while the moon indicates it peaks in the evening as inferred from *A. thaliana*. Arrows and blunt end indicate activation and inhibition, respectively.

is genotypic variation for critical day length between accessions, ranging between 10 and 12 h (Luo et al., 2018). However, in field trials, photoperiod is often confounded with temperature, so the exact influence of photoperiod remains elusive to date.

At the same time, not a lot is known about the main photoperiod pathway gene *Bna.CO,* although it was one of the first *B. napus* flowering time genes to be investigated (Robert et al., 1998). This early study identified four copies which were all expressed (Robert et al., 1998). One of them was able to complement the *co-1* mutation in *A. thaliana* (Robert et al., 1998). When a reference genome for *B. napus* became available, six copies of *Bna.CO* were identified, along with four copies of *CO-like* genes, which complicate the analysis (Schiessl et al., 2014). Copies of *Bna.CO* or *Bna.CO-like* were named as candidate genes for flowering time QTL on A02 (Nelson et al., 2014) A10 (Quijada et al., 2006), C01 (Rahman et al., 2018), C03 (Li et al., 2018) and C09 (Xu et al., 2016). Copies of *Bna.CO* and *Bna.CO-like* on C09 with respective non-synonymous SNP variation were also found in regions separating swedes from non-swede material (Schiessl et al., 2017b). Although not every candidate gene might turn out as a true reason for phenotypic variance, the diversity of gene loci detected does not point to substantial subfunctionalization. This would in turn mean that gene dosage and therefore the number of loci able to produce functional protein could play a larger role here. *Bna.CO* copies on the C genome were found to be stable in copy number, while the other copies showed considerable variation (Schiessl et al., 2017b). When comparing gene expression between early and late flowering semi-winter accessions, no difference for any *Bna.CO* copy was found (Jian et al., 2019), however, the samples were taken at 10 am, where CO expression is normally still low. To our knowledge, more data on gene expression, subfunctionalization or protein stability have not been raised, and further conclusions on this important flowering time regulator are not possible to date.

In *A. thaliana*, *CO* transcription is repressed by CDF proteins, which in turn are negatively regulated by GIGANTEA (GI) and FKF1 (Johansson and Staiger, 2015). *Bna.CDF1* and *Bna.CDF2* were found to be down-regulated in early flowering semi-winter rapeseed relative to late flowering semi-winter in the morning, although single copies showed the opposite behavior (Jian et al., 2019). *Bna.CDF1* has four copies in the *B. napus* genome, of which two were found to vary strongly in copy number (Schiessl et al., 2017b).

CDF1 seems to be controlled by a novel protein called SENSITIVITY TO RED LIGHT REDUCED 1 (SRR1) (Johansson and Staiger, 2014). In *B. napus*, *Bna.SRR1* has five copies, of which two (on A03 and A10) were not expressed (Schiessl et al., 2019b). The remaining three showed differential expression

patterns between spring and winter type rapeseed (Schiessl et al., 2019b), in line with the finding that *Bna.SRR1.A02* was found to be a candidate for the winter-spring split earlier (Schiessl et al., 2017b). *Bna.SRR1.A02* and *Bna.SRR1.C02* were also able to complement the respective knockout mutant in *A. thaliana*, while *Bna.SRR1.C09* was not (Schiessl et al., 2019b). *Bna.SRR1.C09* carried a deletion of several amino acids in a putatively important region (Schiessl et al., 2019b). It is therefore highly likely that the gene copies underwent subfunctionalization, with *Bna.SRR1.A02* being the most functionally conserved copy, influencing flowering time via *CDF1* (Schiessl et al., 2019b).

In *Arabidopsis*, CO is further regulated post-translationally via the action of several ubiquitin-E3-ligases and photoreceptors like phytochromes and cryptochromes. Interestingly, *Bna.PHYA*, *Bna.PHYB,* and *Bna.CRY2* all retained the same copy number (five copies) in *B. napus* (Schiessl et al., 2017a). Both *Bna.PHYB*, a negative regulator of CO protein stability (Raman et al., 2013, 2016) as well as the positive regulators *Bna.PHYA* (Raman et al., 2014) and *Bna.CRY2* (Raman et al., 2019) were found to be candidates for flowering time in different QTL and GWAS studies. A structural rearrangement encompassing the A09 and C08 copies of *Bna.PHYA* was found to be associated to the swede morphotype, along with allelic variance in *Bna.CRY2.A10* (Schiessl et al., 2017b), likely to represent adaptation of swede flowering to longer days. Data on transcription or protein levels of those genes in *B. napus* are not available, so no conclusion on subfunctionalization or mode of action can be drawn so far (**Figure 3**).

Ambient Temperature: PIF4

In *Arabidopsis*, *FT* expression is further gated by binding of *PHYTOCHROME INTERACTING FACTOR 4 (PIF4)* to the *FT* promoter, which can only bind in warmer temperatures when the chromatin carries less H2A.Z histone (Wigge, 2013). *PIF4* itself is also under transcriptional control of the circadian clock (Wigge, 2013). A copy of *Bna.PIF4* was recently implicated in a photoperiod-sensitive flowering time QTL (Raman et al., 2019). In *B. rapa*, however, it was found that *Bra.FT.A02* expression was decreased at warmer temperatures (28°C) compared to normal (21°C), obviously via an increase in H2A.Z in *Bra.FT.A02* chromatin, resulting in later flowering (Del Olmo et al., 2019). Spring rapeseed growing at 18°C/8°C day/night cycles still flowered slightly later than plants at constant 20°C at the same photoperiod (16 h) (Rahman et al., 2018), so there seems to be an optimum temperature above 20°C and well below 28°C. Moreover, this indicates that temperature regulation in *Brassica* is different from what we observe in *A. thaliana*, and respective studies need to be carried out to dissect this trait in *B. napus*.

Gibberellins, Age, and Stress: SPL and DELLA

Two pathways regulate flowering time in absence of inductive conditions: the gibberellin (GA) pathway and the miR156/SPL module (Yu et al., 2012). GAs are negative regulators of DELLA proteins, which are interacting with SPLs, so there is interaction between both pathways (Yu et al., 2012). The miR156/SPL module is known as the age pathway, which is mediated via several highly conserved micro RNAs (miRNAs) like miR156 and miR172 (Wang J.-W. et al., 2009; Wang, 2014). miR156 is a negative post-transcriptional regulator of many different *SQUAMOSA PROMOTER LIKE (SPL)* genes (Wang J.-W. et al., 2009). In seedlings, miR156 levels are high, but steadily decrease with increasing plant age, and SPL repression is more and more released (Wang J.-W. et al., 2009; Wang, 2014). SPL9 induces expression of miR172, which in turn shuts off negative flowering regulators, while SPL3 directly activates downstream flowering time genes like *LFY* (Wang J.-W. et al., 2009; Yamaguchi et al., 2009).

In *B. napus*, two different GA synthesis enzymes have been found in QTL regions for flowering time: *GA-2-ox-1* (Raman et al., 2013; Jian et al., 2019) and *GA-20-ox* (Schiessl et al., 2015), along with the DELLA protein RGA1 (Li et al., 2018; Jian et al., 2019). While miRNAs were not considered or reported in any QTL region in *B. napus*, majorly due to the lack of suitable miRNA gene annotation, one study reports *Bna.SPL3.A03* to be located in a QTL region in spring material (Raman et al., 2016), while another claims the same copy to be a pseudogene (Schiessl et al., 2017b). Copies of DELLA proteins (A09, C09), *Bna.GA-3-ox.A06* and *Bna.SPL3.A05* were also found in selective sweeps between swede and non-swede material (Schiessl et al., 2017b). *Bna.SPL* has six copies in *B. napus*, of which one is a pseudogene, while all others carry some type of variation (Schiessl et al., 2017b). The relative lack of respective gene copies in QTLs might reflect the fact that most flowering time QTL studies take place under inductive conditions.

Interestingly, however, most flowering time genes affected under drought stress in *B. napus* were found to belong to the gibberellin and age pathway, which indicates that stress signaling might take this route to regulate flowering in response to abiotic stress (Schiessl et al., 2020). Candidates to mediate this response are, among others, miR156s, which were found to be differentially expressed under drought stress, possibly in reaction to altered sugar level under photosynthetic limitations (Schiessl et al., 2020). However, data from this study also confirmed the high complexity of those interactions in *B. napus*, as different copies of the same gene seemed to react differentially to the same miRNA level (Schiessl et al., 2020). This points to regulatory co-evolution of specific miRNA-gene pairs and stresses the strong need to perform studies on gene copy level in *B. napus* – inferring gene function from *A. thaliana* is a good start, but does not provide enough information on breeding targets.

DISCUSSION

Although much progress has been achieved to shed light on flowering time regulation in rapeseed, we still lack answers to important questions in regards to the specific situation in this polyploid oil crop. Major genetic effects on traits like vernalization dependency have been characterized down to gene copy level and revealed considerable subfunctionalization. Other pathways, however, like photoperiod and temperature signaling, still remain largely obscure in this respect. Moreover, the

few studies existing worked mainly with spring type rapeseed, and data on the same traits in semi-winter and winter rapeseed are scarce. More and more targeted studies will be necessary to provide reliable data for breeding programs, under consideration of cross-pathway effects, the influence of the circadian clock, the genetic background and epigenetic regulation. In the light of shifting climate zones, influences by day length, ambient temperature, and drought stress need more attention. While the close relationship to the model was and is very helpful for hypothesis development, the current review shows clearly that knowledge cannot be directly inferred from the model to the crop, making functional genetic studies in crops unreplaceable. On top of providing invaluable information for breeding programs, such data will also improve our understanding of post-polyploidization adaptation as an evolutionary principle.

AUTHOR CONTRIBUTIONS

SS conceptualized and wrote the manuscript.

FUNDING

SS is currently funded by the Deutsche Forschungsgemeinschaft (DFG), grant number SCHI 1296/2-1.

ACKNOWLEDGMENTS

The author like to thank Annaliese Mason for English language revisions.

REFERENCES

Adamidis, G. C., Cartar, R. V., Melathopoulos, A. P., Pernal, S. F., and Hoover, S. E. (2019). Pollinators enhance crop yield and shorten the growing season by modulating plant functional characteristics: a comparison of 23 canola varieties. *Sci. Rep.* 9:14208. doi: 10.1038/s41598-019-50811-y

Bender, M. (1999). Economic feasibility review for community-scale farmer cooperatives for biodiesel. *Bioresour. Technol.* 70, 81–87. doi: 10.1016/s0960-8524(99)00009-7

Berry, P. M., Spink, J., Foulkes, M. J., and White, P. J. (2010). The physiological basis of genotypic differences in nitrogen use efficiency in oilseed rape (*Brassica napus* L.). *Field Crops Res.* 119, 365–373. doi: 10.1016/j.fcr.2010.08.004

Blümel, M., Dally, N., and Jung, C. (2015). Flowering time regulation in crops-what did we learn from *Arabidopsis*? *Curr. Opin. Biotechnol.* 32, 121–129. doi: 10.1016/j.copbio.2014.11.023

Bommarco, R., Marini, L., and Vaissière, B. E. (2012). Insect pollination enhances seed yield, quality, and market value in oilseed rape. *Oecologia* 169, 1025–1032. doi: 10.1007/s00442-012-2271-6

Borghi, M., Perez de Souza, L., Yoshida, T., and Fernie, A. R. (2019). Flowers and climate change: a metabolic perspective. *New Phytol.* 224, 1425–1441. doi: 10.1111/nph.16031

Bušić, A., Kundas, S., Morzak, G., Belskaya, H., Marđetko, N., Ivančić Šantek, M., et al. (2018). Recent trends in biodiesel and biogas production. *Food Technol. Biotechnol.* 56, 152–173. doi: 10.17113/ftb.56.02.18.5547

Carlsson, A. S., Yilmaz, J. L., Green, A. G., Stymne, S., and Hofvander, P. (2011). Replacing fossil oil with fresh oil - with what and for what? *Eur. J. Lipid Sci. Technol.* 113, 812–831. doi: 10.1002/ejlt.201100032

Cheng, J.-Z., Zhou, Y.-P., Lv, T.-X., Xie, C.-P., and Tian, C.-E. (2017). Research progress on the autonomous flowering time pathway in *Arabidopsis*. *Physiol. Mol. Biol. Plants* 23, 477–485. doi: 10.1007/s12298-017-0458-3

Choi, K., Kim, J., Hwang, H.-J., Kim, S., Park, C., Kim, S. Y., et al. (2011). The FRIGIDA complex activates transcription of FLC, a strong flowering repressor in *Arabidopsis*, by recruiting chromatin modification factors. *Plant Cell* 23, 289–303. doi: 10.1105/tpc.110.075911

Del Olmo, I., Poza-Viejo, L., Piñeiro, M., Jarillo, J. A., and Crevillén, P. (2019). High ambient temperature leads to reduced FT expression and delayed flowering in *Brassica rapa* via a mechanism associated with H2A.Z dynamics. *Plant J.* 100, 343–356. doi: 10.1111/tpj.14446

Diepenbrock, W. (2000). Yield analysis of winter oilseed rape (*Brassica napus* L.): a review. *Field Crops Res.* 67, 35–49. doi: 10.1016/s0378-4290(00)00082-4

Fletcher, R. S., Mullen, J. L., Heiliger, A., and McKay, J. K. (2014). QTL analysis of root morphology, flowering time, and yield reveals trade-offs in response to drought in *Brassica napus*. *J. Exp. Bot.* 66, 245–256. doi: 10.1093/jxb/eru423

Ghosh, S., Watson, A., Gonzalez-Navarro, O. E., Ramirez-Gonzalez, R. H., Yanes, L., Mendoza-Suárez, M., et al. (2018). Speed breeding in growth chambers and glasshouses for crop breeding and model plant research. *Nat. Protoc.* 13, 2944–2963. doi: 10.1038/s41596-018-0072-z

Guo, Y., Hans, H., Christian, J., and Molina, C. (2014). Mutations in single FT- and TFL1-paralogs of rapeseed (*Brassica napus* L.) and their impact on flowering time and yield components. *Front. Plant Sci.* 5:282. doi: 10.3389/fpls.2014.00282

Hohmann, M. A. (2017). *Untersuchung von Anzuchtsystemen und Selektionstechniken zur Züchtung von Trockenstressresistenz in Winterraps (Brassica napus L.): Zur Erlangung des akademischen Grades Doctor agriculturae*. Ph.D. Dissertation, University of Giessen, Gießen.

Hou, J., Long, Y., Raman, H., Zou, X., Wang, J., Dai, S., et al. (2012). A tourist-like MITE insertion in the upstream region of the BnFLC.A10 gene is associated with vernalization requirement in rapeseed (*Brassica napus* L.). *BMC Plant Biol.* 12:238. doi: 10.1186/1471-2229-12-238

IPCC (2019). *Climate Change and Land: An IPCC Special Report on Climate Change, Desertification, Land Degradation, Sustainable Land Management, Food Security, and Greenhouse gas Fluxes in Terrestrial Ecosystems.* Technical Summary. Geneva: IPCC.

Jian, H., Zhang, A., Ma, J., Wang, T., Yang, B., Shuang, L. S., et al. (2019). Joint QTL mapping and transcriptome sequencing analysis reveal candidate flowering time genes in *Brassica napus* L. *BMC Genomics* 20:21. doi: 10.1186/s12864-018-5356-8

Jiang, D., Gu, X., and He, Y. (2009). Establishment of the winter-annual growth habit via FRIGIDA-mediated histone methylation at FLOWERING LOCUS C in *Arabidopsis*. *Plant Cell Online* 21, 1733–1746. doi: 10.1105/tpc.109.067967

Johansson, M., and Staiger, D. (2014). SRR1 is essential to repress flowering in non-inductive conditions in *Arabidopsis thaliana*. *J. Exp. Bot.* 65, 5811–5822. doi: 10.1093/jxb/eru317

Johansson, M., and Staiger, D. (2015). Time to flower: interplay between photoperiod and the circadian clock. *J. Exp. Bot.* 66, 719–730. doi: 10.1093/jxb/eru441

Jung, C., and Muller, A. E. (2009). Flowering time control and applications in plant breeding. *Trends Plant Sci.* 14, 563–573. doi: 10.1016/j.tplants.2009.07.005

Kittipol, V., He, Z., Wang, L., Doheny-Adams, T., Langer, S., and Bancroft, I. (2019). Genetic architecture of glucosinolate variation in *Brassica napus*. *J. Plant Physiol.* 240:152988. doi: 10.1016/j.jplph.2019.06.001

Li, B., Zhao, W., Li, D., Chao, H., Zhao, X., Ta, N., et al. (2018). Genetic dissection of the mechanism of flowering time based on an environmentally stable and specific QTL in *Brassica napus*. *Plant Sci.* 277, 296–310. doi: 10.1016/j.plantsci.2018.10.005

Lu, J., Carbone, G. J., and Grego, J. M. (2019). Uncertainty and hotspots in 21st century projections of agricultural drought from CMIP5 models. *Sci. Rep.* 9:157. doi: 10.1038/s41598-019-41196-z

Luo, T., Zhang, J., Khan, M. N., Liu, J., Xu, Z., and Hu, L. (2018). Temperature variation caused by sowing dates significantly affects floral initiation and floral bud differentiation processes in rapeseed (*Brassica napus* L.). *Plant Sci.* 271, 40–51. doi: 10.1016/j.plantsci.2018.03.004

Luo, Y. X., Luo, C. Y., Du, D. Z., Fu, Z., Yao, Y. M., Xu, C. C., et al. (2014). Quantitative trait analysis of flowering time in spring rapeseed (*B. napus* L.). *Euphytica* 200, 321–335. doi: 10.1007/s10681-014-1140-2

Morinaga, T. (1934). Interspecific hybridization in *Brassica*. *Cytologia* 6, 62–67. doi: 10.1508/cytologia.6.62

Nagaharu, U. (1935). Genome analysis in *Brassica* with special reference to the experimental formation of *B. napus* and peculiar mode of fertilisation. *Jpn. J. Bot.* 7, 389–452.

Nelson, M. N., Rajasekaran, R., Smith, A., Chen, S., Beeck, C. P., Siddique, K. H. M., et al. (2014). Quantitative trait loci for thermal time to flowering and photoperiod responsiveness discovered in summer annual-type *Brassica napus* L. *PLoS One* 9:e102611. doi: 10.1371/journal.pone.0102611

Osborn, T. C., Kole, C., Parkin, I. A. P., Sharpe, A. G., Kuiper, M., Lydiate, D. J., et al. (1997). Comparison of flowering time genes in *Brassica rapa*-*B. napus* and *Arabidopsis thaliana*. *Genetics* 146, 1123–1129.

Parkin, I. A. P., Clarke, W. E., Sidebottom, C., Zhang, W., Robinson, S. J., Links, M. G., et al. (2010). Towards unambiguous transcript mapping in the allotetraploid *Brassica napus*. *Genome* 25, 2013.

Quijada, P. A., Udall, J. A., Lambert, B., and Osborn, T. C. (2006). Quantitative trait analysis of seed yield and other complex traits in hybrid spring rapeseed (*Brassica napus* L.): 1. Identification of genomic regions from winter germplasm. *Theor. Appl. Genet.* 113, 549–561. doi: 10.1007/s00122-006-0323-1

Rahman, H., Bennett, R. A., and Kebede, B. (2018). Molecular mapping of QTL alleles of *Brassica oleracea* affecting days to flowering and photosensitivity in spring *Brassica napus*. *PLoS One* 13:e0189723. doi: 10.1371/journal.pone.0189723

Raman, H., Dalton-Morgan, J., Diffey, S., Raman, R., Alamery, S., Edwards, D., et al. (2014). SNP markers-based map construction and genome-wide linkage analysis in *Brassica napus*. *Plant Biotechnol. J.* 12, 851–860. doi: 10.1111/pbi.12186

Raman, H., Raman, R., Coombes, N., Song, J., Prangnell, R., Bandaranayake, C., et al. (2016). Genome-wide association analyses reveal complex genetic architecture underlying natural variation for flowering time in canola. *Plant Cell Environ.* 39, 1228–1239. doi: 10.1111/pce.12644

Raman, H., Raman, R., Eckermann, P., Coombes, N., Manoli, S., Zou, X., et al. (2013). Genetic and physical mapping of flowering time loci in canola (*Brassica napus* L.). *Theor. Appl. Genet.* 126, 119–132. doi: 10.1007/s00122-012-1966-8

Raman, H., Raman, R., Qiu, Y., Yadav, A. S., Sureshkumar, S., Borg, L., et al. (2019). GWAS hints at pleiotropic roles for FLOWERING LOCUS T in flowering time and yield-related traits in canola. *BMC Genomics* 20:636. doi: 10.1186/s12864-019-5964-y

Ridge, S., Brown, P. H., Hecht, V., Driessen, R. G., and Weller, J. L. (2015). The role of BoFLC2 in cauliflower (*Brassica oleracea* var. botrytis L.) reproductive development. *Exp. Bot. J.* 66, 125–135. doi: 10.1093/jxb/eru408

Robert, L. S., Robson, F., Sharpe, A., Lydiate, D., and Coupland, G. (1998). Conserved structure and function of the *Arabidopsis* flowering time gene CONSTANS in *Brassica napus*. *Plant Mol. Biol.* 37, 763–772.

Schiessl, S., Huettel, B., Kuehn, D., Reinhardt, R., and Snowdon, R. J. (2017a). Targeted deep sequencing of flowering regulators in *Brassica napus* reveals extensive copy number variation. *Sci. Data* 4:170013. doi: 10.1038/sdata.2017.13

Schiessl, S., Hüttel, B., Kuehn, D., Reinhardt, R., and Snowdon, R. J. (2017b). Post-polyploidisation morphotype diversification associates with gene copy number variation. *Sci. Rep.* 7:41845. doi: 10.1038/srep41845

Schiessl, S., Iniguez-Luy, F., Qian, W., and Snowdon, R. J. (2015). Diverse regulatory factors associate with flowering time and yield responses in winter-type *Brassica napus*. *BMC Genomics* 16:737. doi: 10.1186/s12864-015-1950-1

Schiessl, S., Quezada-Martinez, D., Tebartz, E., Snowdon, R. J., and Qian, L. (2019a). The vernalisation regulator FLOWERING LOCUS C is differentially expressed in biennial and annual *Brassica napus*. *Sci. Rep.* 9:14911. doi: 10.1038/s41598-019-51212-x

Schiessl, S., Samans, B., Hüttel, B., Reinhardt, R., and Snowdon, R. J. (2014). Capturing sequence variation among flowering-time regulatory gene homologs in the allopolyploid crop species *Brassica napus*. *Front. Plant Sci.* 5:404. doi: 10.3389/fpls.2014.00404

Schiessl, S., Williams, N., Specht, P., Staiger, D., and Johansson, M. (2019b). Different copies of sensitivity to red light reduced 1 show strong subfunctionalization in *Brassica napus*. *BMC Plant Biol.* 19:372. doi: 10.1186/s12870-019-1973-x

Schiessl, S. V., and Mason, A. S. (2020). "Ancient and recent polyploid evolution in *Brassica*," in *Brassica Improvement*, Vol. 120, eds S. Wani, A. Thakur, and K. Y. Jeshima (Cham: Springer), 49–66. doi: 10.1007/978-3-030-34694-2_3

Schiessl, S. V., Quezada-Martinez, D., Orantes-Bonilla, M., and Snowdon, R. J. (2020). Transcriptomics reveal high regulatory diversity of drought tolerance strategies in a biennial oil crop. *Plant Sci.* 297:110515. doi: 10.1016/j.plantsci.2020.110515

Shah, S., Weinholdt, C., Jedrusik, N., Molina, C., Zou, J., Große, I., et al. (2018). Whole-transcriptome analysis reveals genetic factors underlying flowering time regulation in rapeseed (*Brassica napus* L.). *Plant Cell Environ.* 41, 1935–1947. doi: 10.1111/pce.13353

Shi, J., Li, R., Qiu, D., Jiang, C., Long, Y., Morgan, C., et al. (2009). Unraveling the complex trait of crop yield with quantitative trait loci mapping in *Brassica napus*. *Genetics* 182, 851–861. doi: 10.1534/genetics.109.101642

Snowdon, R. J., and Iniguez Luy, F. L. (2012). Potential to improve oilseed rape and canola breeding in the genomics era. *Plant Breed.* 131, 351–360. doi: 10.1111/j.1439-0523.2012.01976.x

Sri, T., Gupta, B., Tyagi, S., and Singh, A. (2020). Homeologs of *Brassica* SOC1, a central regulator of flowering time, are differentially regulated due to partitioning of evolutionarily conserved transcription factor binding sites in promoters. *Mol. Phylogenet. Evol.* 147, 106777. doi: 10.1016/j.ympev.2020.106777

Srikanth, A., and Schmid, M. (2011). Regulation of flowering time: all roads lead to Rome. *Cell. Mol. Life Sci.* 68, 2013–2037. doi: 10.1007/s00018-011-0673-y

Tadege, M., Sheldon, C. C., Helliwell, C. A., Stoutjesdijk, P., Dennis, E. S., and Peacock, W. J. (2001). Control of flowering time by FLC orthologues in *Brassica napus*. *Plant J.* 28, 545–553. doi: 10.1046/j.1365-313x.2001.01182.x

Tudor, E. H., Jones, D. M., He, Z., Bancroft, I., Trick, M., Wells, R., et al. (2020). QTL-seq identifies BnaFT.A02 and BnaFLC.A02 as candidates for variation in vernalisation requirement and response in winter oilseed rape (*Brassica napus*). *Plant Biotechnol. J.* 1–16. doi: 10.1111/pbi.13421

Udall, J. A., Quijada, P. A., Lambert, B., and Osborn, T. C. (2006). Quantitative trait analysis of seed yield and other complex traits in hybrid spring rapeseed (*Brassica napus* L.): 2. Identification of alleles from unadapted germplasm. *Theor. Appl. Genet.* 113, 597–609. doi: 10.1007/s00122-006-0324-0

Wang, J., Hopkins, C. J., Hou, J., Zou, X., Wang, C., Long, Y., et al. (2012). Promoter variation and transcript divergence in brassicaceae lineages of FLOWERING LOCUS T. *PLoS One* 7:e47127. doi: 10.1371/journal.pone.0047127

Wang, J., Long, Y., Wu, B., Liu, J., Jiang, C., Shi, L., et al. (2009). The evolution of *Brassica napus* FLOWERING LOCUST paralogues in the context of inverted chromosomal duplication blocks. *BMC Evol. Biol.* 9:271. doi: 10.1186/1471-2148-9-271

Wang, J.-W. (2014). Regulation of flowering time by the miR156-mediated age pathway. *J. Exp. Bot.* 65, 4723–4730. doi: 10.1093/jxb/eru246

Wang, J.-W., Czech, B., and Weigel, D. (2009). miR156-regulated SPL transcription factors define an endogenous flowering pathway in *Arabidopsis thaliana*. *Cell* 138, 738–749. doi: 10.1016/j.cell.2009.06.014

Wang, N., Qian, W., Suppanz, I., Wei, L., Mao, B., Long, Y., et al. (2011). Flowering time variation in oilseed rape (*Brassica napus* L.) is associated with allelic variation in the FRIGIDA homologue BnaA.FRI.a. *J. Exp. Bot.* 62, 5641–5658. doi: 10.1093/jxb/err249

Watson, A., Ghosh, S., Williams, M. J., Cuddy, W. S., Simmonds, J., Rey, M.-D., et al. (2018). Speed breeding is a powerful tool to accelerate crop research and breeding. *Nat. Plants* 4, 23–29. doi: 10.1038/s41477-017-0083-8

Wigge, P. A. (2013). Ambient temperature signalling in plants. *Curr. Opin. Plant Biol.* 16, 661–666. doi: 10.1016/j.pbi.2013.08.004

Wu, D., Liang, Z., Yan, T., Xu, Y., Xuan, L., Tang, J., et al. (2018). Whole-genome resequencing of a world-wide collection of rapeseed accessions reveals genetic basis of their ecotype divergence. *Mol. Plant* 12, 30–43. doi: 10.1016/j.molp.2018.11.007

Xu, L., Hu, K., Zhang, Z., Guan, C., Chen, S., Hua, W., et al. (2016). Genome-wide association study reveals the genetic architecture of flowering time in rapeseed (*Brassica napus* L.). *DNA Res.* 23, 43–52. doi: 10.1093/dnares/dsv035

Yamaguchi, A., Wu, M. F., Yang, L., Wu, G., Poethig, R. S., and Wagner, D. (2009). The MicroRNA-regulated SBP-Box transcription factor SPL3 is a direct

upstream activator of leafy, fruitfull, and apetala1. *Dev. Cell* 17, 268–278. doi: 10.1016/j.devcel.2009.06.007

Yin, S., Wan, M., Guo, C., Wang, B., Li, H., Li, G., et al. (2020). Transposon Insertions within alleles of BnaFLC.A10 and BnaFLC.A2 are associated with rapeseed (*Brassica napus* L.) seasonal crop-type. *J. Exp. Bot.* 71, 4729–4741. doi: 10.1093/jxb/eraa237

Yu, S., Galvão, V. C., Zhang, Y.-C., Horrer, D., Zhang, T.-Q., Hao, Y.-H., et al. (2012). Gibberellin regulates the *Arabidopsis* floral transition through miR156-targeted SQUAMOSA promoter binding-like transcription factors. *Plant Cell* 24, 3320–3332. doi: 10.1105/tpc.112.101014

Zhou, Y. T., Wang, H. Y., Zhou, L., Wang, M. P., Li, H. P., Wang, M. L., et al. (2007). Analyses of the floral organ morphogenesis and the differentially expressed genes of an apetalous flower mutant in *Brassica napus*. *Plant Cell Rep.* 27, 9–20. doi: 10.1007/s00299-007-0426-4

Zou, X., Suppanz, I., Raman, H., Hou, J., Wang, J., Long, Y., et al. (2012). Comparative analysis of FLC homologues in brassicaceae provides insight into their role in the evolution of oilseed rape. *PLoS One* 7:e45751. doi: 10.1371/journal.pone.0045751

Zou, Y., Xiao, H., Bianchi, F. J. J. A., Jauker, F., Luo, S., and van der Werf, W. (2017). Wild pollinators enhance oilseed rape yield in small-holder farming systems in China. *BMC Ecol.* 17:6. doi: 10.1186/s12898-017-116-111

Conflict of Interest: The author declares that the research was conducted in the absence of any commercial or financial relationships that could be construed as a potential conflict of interest.

Copyright © 2020 Schiessl. This is an open-access article distributed under the terms of the Creative Commons Attribution License (CC BY). The use, distribution or reproduction in other forums is permitted, provided the original author(s) and the copyright owner(s) are credited and that the original publication in this journal is cited, in accordance with accepted academic practice. No use, distribution or reproduction is permitted which does not comply with these terms.

frontiers in Plant Science

REVIEW
published: 22 December 2020
doi: 10.3389/fpls.2020.617340

The Role of *FLOWERING LOCUS C* Relatives in Cereals

*Alice Kennedy and Koen Geuten**

Department of Biology, KU Leuven, Leuven, Belgium

FLOWERING LOCUS C (*FLC*) is one of the best characterized genes in plant research and is integral to vernalization-dependent flowering time regulation. Yet, despite the abundance of information on this gene and its relatives in *Arabidopsis thaliana*, the role *FLC* genes play in other species, in particular cereal crops and temperate grasses, remains elusive. This has been due in part to the comparative reduced availability of bioinformatic and mutant resources in cereals but also on the dominant effect in cereals of the *VERNALIZATION* (*VRN*) genes on the developmental process most associated with *FLC* in *Arabidopsis*. The strong effect of the *VRN* genes has led researchers to believe that the entire process of vernalization must have evolved separately in *Arabidopsis* and cereals. Yet, since the confirmation of the existence of *FLC*-like genes in monocots, new light has been shed on the roles these genes play in both vernalization and other mechanisms to fine tune development in response to specific environmental conditions. Comparisons of *FLC* gene function and their genetic and epigenetic regulation can now be made between *Arabidopsis* and cereals and how they overlap and diversify is coming into focus. With the advancement of genome editing techniques, further study on these genes is becoming increasingly easier, enabling us to investigate just how essential *FLC*-like genes are to modulating flowering time behavior in cereals.

Keywords: flowering time, cereals, *FLOWERING LOCUS C*, vernalisation, ambient temperature

OPEN ACCESS

Edited by:
Elizabeth Dennis, Commonwealth Scientific and Industrial Research Organisation (CSIRO), Australia

Reviewed by:
George Coupland, Max Planck Institute for Plant Breeding Research, Germany
Yuehui He, Chinese Academy of Sciences (CAS), China
Elizabeth Finnegan, Commonwealth Scientific and Industrial Research Organisation (CSIRO), Australia

***Correspondence:**
Koen Geuten
koen.geuten@kuleuven.be

Specialty section:
This article was submitted to Plant Development and EvoDevo, a section of the journal Frontiers in Plant Science

Received: *14 October 2020*
Accepted: *02 December 2020*
Published: *22 December 2020*

Citation:
Kennedy A and Geuten K (2020) The Role of FLOWERING LOCUS C Relatives in Cereals. Front. Plant Sci. 11:617340. doi: 10.3389/fpls.2020.617340

INTRODUCTION

FLOWERING LOCUS C (*FLC*) genes are a clade of MADS-box transcription factors in plants and are major regulators in many aspects of plant development. They are mostly associated with vernalization-regulated flowering but also have important roles in seed dormancy (Chen et al., 2014; Chen and Penfield, 2018), ambient temperature regulated development (Balasubramanian et al., 2006; Lee et al., 2013), germination (Chiang et al., 2009), as well as being associated with other processes like bud dormancy, circadian rhythm, water use efficiency, and indirect defense against herbivory (McKay et al., 2003; Edwards et al., 2006; Kumar et al., 2016; Mohammadin et al., 2017). In fact, there are over 500 FLC binding sites in the *Arabidopsis thaliana* (henceforth *Arabidopsis*) genome indicating that FLC is involved in much more than vernalization (Deng et al., 2011). In flowering time regulation, FLC acts as a repressor protein and acts mainly by repressing the activation of key floral promoting genes such as *FLOWERING LOCUS T* (*FT*) and *SUPPRESSOR OF OVEREXPRESSION OF CONSTANS 1* (*SOC1*; Searle et al., 2006; Deng et al., 2011).

The existence of *FLC*-like genes in cereals remained elusive for many years while the wealth of information on *Arabidopsis FLC* continued to accumulate. Many believed that *FLC* was restricted to eudicots and that monocot plants evolved separate mechanisms to regulate development and flowering time. However, a turning point came when it was concretely established through genome synteny analysis and phylogenetic reconstructions that *FLC* relatives did indeed exist in cereals (Ruelens et al., 2013). In this pivotal publication, it was shown that a clade of genes within monocots were phylogenetically related to the *FLC* genes of *Arabidopsis*. Within this monocot *FLC* clade, there are two subclades: the OsMADS51 and OsMADS37 subclades, so called after the representation of these rice genes within each clade. The OsMADS51 subclade is subsequently divided into two groups: the ODDSOC1-like and ODDSOC2-like groups. The name "ODDSOC" came from their weak similarity to the flowering time gene *SOC1* (Greenup et al., 2010). Members of the ODDSOC2 clade of genes are the most characterized out of all *FLC*-like genes in monocots thus far. The details of these relationships and their relationship to the *Arabidopsis FLC* genes can be seen in **Figure 1**. It must be noted that although the *Arabidopsis* and monocot *FLC* clades are related, it is likely that the ancestral gene function was partitioned differently within the groups. Therefore, direct comparisons of individual members across groups are not completely accurate.

Furthermore, *FLC*-like genes in cereals are Type II MADS-domain proteins despite having previously been annotated as Type I MADS-domain proteins, and have the typical MIKC protein structure (Zhao et al., 2006; Schilling et al., 2020).

Due to the advancement of genome sequencing technology, genetic mapping and genome editing methods, the nature of the function of *FLC*-like genes in cereals is coming into focus. Furthermore, avenues are now opening to further advance our knowledge on these genes which may reveal diversification of their function from their *Arabidopsis* homologs. This review aims to highlight the key findings over the last two decades of the role *FLC* relatives play in cereals and how progress made in biotechnology will further our understanding of the molecular control of plant development, perhaps leading us to utilize these genes as biotechnological tools for crop improvement.

EVIDENCE FOR CONSERVED FUNCTION: WHAT DO WE ALREADY KNOW?

FLCs Are Involved in Vernalization in Grasses

In cereals, the main determinants of vernalization-regulated flowering are the *VERNALIZATION* (*VRN*) genes *VRN1*, *VRN2*, and *VRN3* (Yan et al., 2003, 2004, 2006). Generally, vernalization results in the upregulation of the floral promoter *VRN1* which downregulates the floral repressor *VRN2*, alleviating its repressive effect on the flowering promoter *VRN3*, an orthologue of *FT* (reviewed in Trevaskis et al., 2007; Distelfeld et al., 2009; Ream et al., 2012). VRN3 then positively regulates *VRN1* expression resulting in a positive feedback loop which induces flowering. This feedback loop in general determines the flowering habit of cereals with mutations in any of these proteins leading to altered spring or winter growth habit (Yan et al., 2004, 2006; Fu et al., 2005). Yet, variation in vernalization response can still remain in cultivars which have shared alleles of these genes (Rizza et al., 2016), opening up the potential for other genes to have functional significance in this process. The identification of *FLC*-like genes in cereal research remained elusive for many years leading to the conclusion that the vernalization pathway of *Arabidopsis* and cereals evolved completely separately (Yan et al., 2004; Winfield et al., 2009; Greenup et al., 2010). Incorporating the finding that an FLC clade exists in monocots, it appears more likely that the ancestral species of dicots and monocots contained both *FLC* and *AP1*/*VRN1*-like genes, and each group was differentially recruited during the evolution of vernalization responsiveness. As *AP1* retains a role in regulating flowering in *Arabidopsis*, so too do *FLC* homologs play a role in similar processes in cereals. This section aims to highlight these roles *FLC*-like genes play in the vernalization process and flowering time regulation in crop species.

FLOWERING LOCUS C homologs were described as being involved in vernalization in cereals almost 20 years ago where Trevaskis et al. (2003) described *TaMX23*, a MADS-box gene repressed by vernalization in winter wheats. *TaMX23* increases in abundance in early vegetative development and the effect of vernalization on *TaMX23* expression depended on whether the cultivar was a spring or winter variety (Trevaskis et al., 2003). *TaMX23* shares homology with both *TaODDSOC2* (*TaOS2*; also known as *TaAGL33*) and *TaAGL42* (Winfield et al., 2009). Although it is more similar in sequence to *TaAGL42*, its reported expression pattern reflects that of *TaOS2*.

TaOS2 is the most described *FLC*-like gene in wheat so far. Like *FLC*, all three homeologs of *TaOS2* are downregulated by vernalization and repression is maintained 2 weeks post-vernalization (Winfield et al., 2009; Sharma et al., 2017; Appels et al., 2018). In winter varieties, *TaOS2* expression is initially high in leaf tissue and gradually declines throughout development as temperature decreases, yet its expression is constitutively low in spring lines, indicating that the function is cultivar-dependent and relevant to the flowering habit of these lines (Winfield et al., 2009; Sharma et al., 2017). Creating premature stop codons using CRISPR/Cas9 gene editing in the D-homeolog revealed an effect of this gene on flowering time, as mutants flower 3 days earlier than wild type (Appels et al., 2018). It is encouraging that a knockout of a single homeolog in hexaploid wheat reveals a phenotype. A 3-day alteration in flowering time is no mean feat in wheat breeding and can have great implications on yield in a region-specific manner. Validating this phenotype in the field will be enlightening to discover whether the phenotype is maintained and in which environments are the greatest effects found. It is also possible that functional redundancy is at play and multiple mutations in all homeologs of *TaOS2* might reveal more striking phenotypes to uncover the roles of these genes in flowering time regulation in wheat.

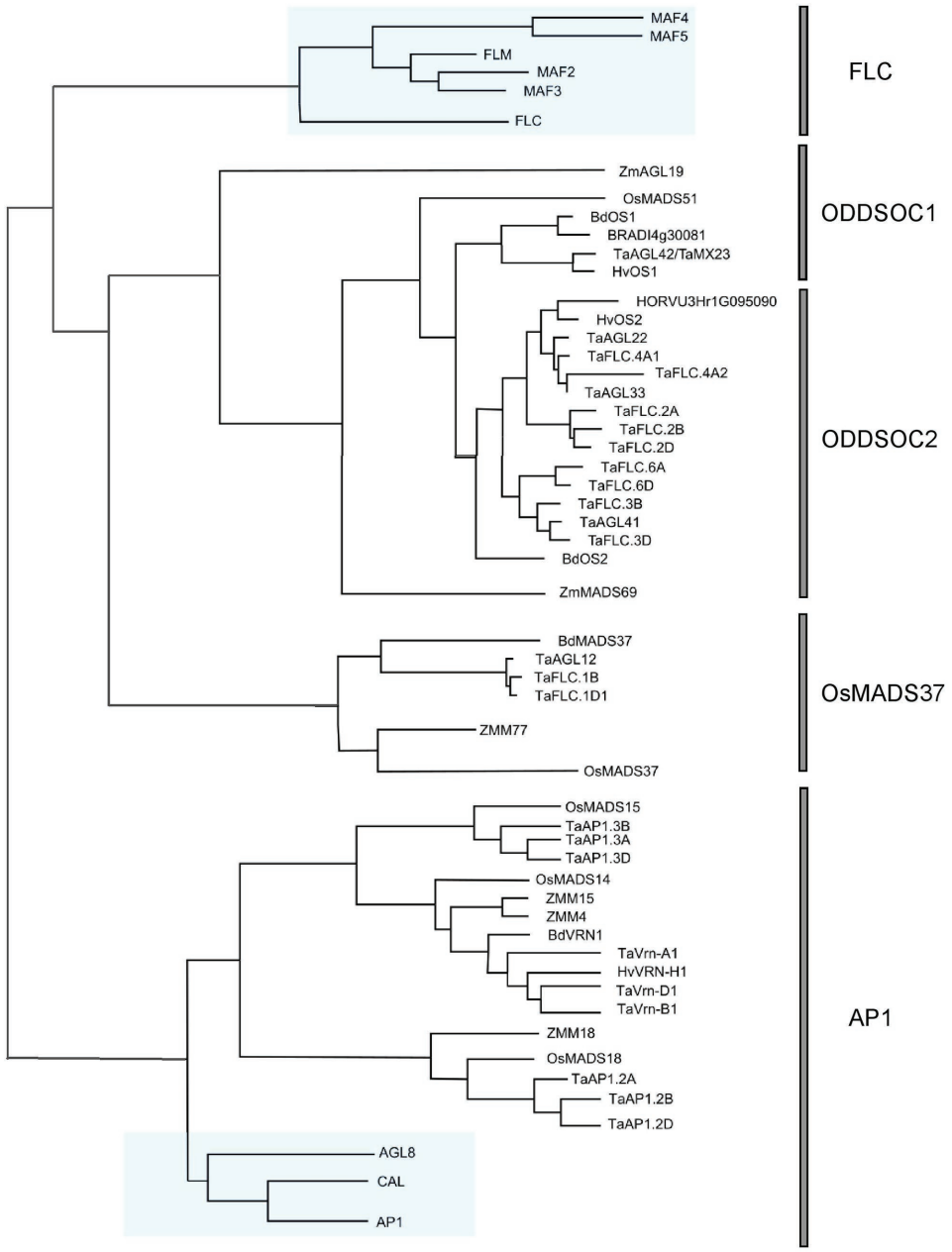

FIGURE 1 | Phylogenetic relationships of all *FLOWERING LOCUS C* (*FLC*) genes annotated in cereals. A maximum likelihood phylogeny was generated using Geneious Pro v5.5.4 using MADS-box genes from eudicots and monocots. A reconstructed phylogeny containing only *FLC* and *AP1* genes was drawn using InkScape. *AP1* genes were used as an outgroup. *Arabidopsis* genes are highlighted in blue. A full version of the tree including all accession numbers can be found in **Supplementary Figure S1**.

A second *FLC*-like gene, *TaAGL42* (or *TaODDSOC1*), has also been described as being regulated by vernalization in wheat (Winfield et al., 2009; Sharma et al., 2017); however, *TaAGL42* is upregulated in winter cultivars and is downregulated or stably expressed in spring varieties. Additionally, *TaAGL42* expression was shown to increase rapidly in response to a sudden drop in temperature in two winter varieties, suggesting that this gene could be involved in cold acclimation and tolerance in these lines (Winfield et al., 2009). In conclusion, although the gene is cold-regulated in a variety-specific manner, the function of *TaAGL42* remains unclear in wheat.

Relatives of these genes have also been described in barley, where their identification came about as a result of a desire to characterize new genes responsive to vernalization. Through the analysis of homologs of *TaMX23* (Trevaskis et al., 2003), two genes were identified: one sharing homology to *TaMX23*

and another sharing homology with *TaOS2* (Trevaskis et al., 2003; Winfield et al., 2009; Greenup et al., 2010). The two homologs were named *HvODDSOC1* (*HvOS1*) and *HvODDSOC2* (*HvOS2*), respectively, due to their weak sequence similarity to *SOC1* in *Arabidopsis*. *HvOS1* expression increased in response to vernalization, consistent with its homolog in wheat (Winfield et al., 2009). *HvOS2* expression was repressed in response to vernalization in both the leaves and apices, and this repression was maintained post-vernalization (Greenup et al., 2010). The expression of *HvOS2* was also strongest in winter barley varieties pre-vernalization and was dramatically reduced upon exposure to prolonged cold, while expression remained low and constant in spring varieties. This highlights the importance of choice of cultivar when studying *FLC* homologs in cereals. Overexpressing *HvOS2* in the spring barley resulted in delayed flowering in these lines, strongly suggesting that *HvOS2* acts as a repressor of the floral transition. In contrast, no phenotype was observed for *HvOS2* knockdown lines created using RNA interference (RNAi); however, this is to be expected in a spring line where *HvOS2* is low naturally and vernalization is not required. In a separate study, differences in the rate of reproductive development under insufficient vernalization conditions was also explained by a difference in *HvOS2* expression levels between two winter varieties (Monteagudo et al., 2019), further supporting the idea of *HvOS2* as a vernalization-dependent regulator of the floral transition.

Aside from the crops themselves, research has been conducted on *FLC*-like genes in the model temperate grass *Brachypodium distachyon* (henceforth *Brachypodium*). In fact, *Brachypodium* was the organism chosen to first analyze the response of monocot *FLC* homologs to vernalization after they were first reported by Ruelens et al. (2013). Three homologs were reported in *Brachypodium*: *BdODDSOC1* (*BdOS1*), *BdODDSOC2* (*BdOS2*), and *BdMADS37*. *BdOS1* was shown to be upregulated by vernalization, like its homologs *TaAGL42* and *HvOS1* in wheat and barley, respectively. *BdOS2* expression is also consistent with its homologs in these species, as it is downregulated by vernalization (Ruelens et al., 2013; Sharma et al., 2017). There is also evidence to suggest that *BdOS2* pre-vernalization expression levels determine the vernalization requirement of individual *Brachypodium* accessions, with winter accessions having higher pre-vernalization expression levels of *BdOS2* (Sharma et al., 2017). Overexpression of *BdOS2* led to a delay in flowering time under vernalized conditions in the facultative accession Bd21–3, with the delay comparative to wild type plants which were not vernalized. This suggests that overexpression of *BdOS2* keeps Bd21–3 in a non-vernalized state. It was also reported that *BdOS2* knockdown *via* RNAi influenced the flowering time of Bd21–3; however, we and others have been unable to replicate these findings, calling these results into question. Attempts are currently being made to vigorously test the effect of low *BdOS2* expression on flowering time regulation in *Brachypodium*, with most striking phenotypes expected in winter accessions, and not facultative lines like Bd21–3.

The third *FLC* homolog, *BdMADS37*, is also downregulated by vernalization and exists in a separate clade to the ODDSOC genes (**Figure 1**). No other reports about members of this gene group have been published since first described by Ruelens et al. (2013); however, *BdMADS37* appeared as a potential candidate for a QTL explaining the differences in flowering time and vernalization requirement between spring and winter accessions under specific environmental conditions (Bettgenhaeuser et al., 2017). We have identified a fourth *FLC* homolog in *Brachypodium*, BRADI4g30081 (**Figure 1**), a paralog of *BdOS1* which appears to be a truncated duplication of *BdOS1*, and expression has been detected in response to cold in the microarray dataset of Priest et al. (2014).

FLC and VRN1 Activities Are Entwined in Cereals

Much of what we have learned about *FLC*-like genes so far comes from basic research on flowering time regulation and vernalization in cereals. Therefore, many of these findings have been related to or are based on descriptions of the activities of VRN1. So far, a relationship between VRN1 and ODDSOC2 activity has been reported in wheat and its diploid relative *Triticum monococcum*, barley, and *Brachypodium*. In general, evidence exists to suggest that VRN1 is required to repress *ODDSOC2* post-vernalization to enable rapid flowering.

In *T. monococcum*, it was observed that *TmOS2* levels rose post-vernalization in mutant lines lacking functional *TmVRN1* while levels remained low in wild type lines. Analysis of *TmOS2* levels pre- and during vernalization showed that there was no difference in expression between wild type and mutant lines. It is only post-vernalization *TmOS2* levels that are affected by *TmVRN1* loss of function, suggesting that TmVRN1 is required to repress *TmOS2* post-vernalization but not to reduce its activity initially (Greenup et al., 2010).

Similar to *T. monococcum*, *HvOS2* expression is lowest in barley lines with dominant, active *VRN1* alleles, consistent with the hypothesis that VRN1 represses *OS2* in temperate cereals (Greenup et al., 2010). Supporting this hypothesis, it was subsequently reported that HvVRN1 binds to the *HvOS2* promoter in the spring variety Golden Promise (Deng et al., 2015). Several HvVRN1 binding sites have also been identified throughout the *HvOS2* locus (Monteagudo et al., 2019).

Likewise, there is an antagonistic relationship between *BdOS2* and *BdVRN1* expression patterns in *Brachypodium*. *BdOS2* expression is elevated in *BdVRN1* knockdown lines (Woods et al., 2016). As well as that, *BdOS2* expression is elevated in lines overexpressing *BdVRN2*, associated with low *BdVRN1* expression and delayed flowering (Woods et al., 2016). Interestingly, *BdOS2* expression patterns are not significantly influenced by overexpression of *BdVRN1* or knockdown of *BdVRN2*, indicating that the response of *BdOS2* to *BdVRN1* expression is qualitative and not dosage dependent.

This relationship between *VRN1* and *ODDSOC2* is conserved in hexaploid wheat, where *TaOS2* expression post-vernalization is linked to the nature of *VRN1* alleles found in a given

cultivar (Dixon et al., 2019). This relationship has implications for flowering time behavior which will be discussed in more detail in the next section.

ODDSOC2 and the Balancing Act of Vernalization and Ambient Temperature

Temperature is a key environmental signal which regulates many facets of plant development. Flowering time in both *Arabidopsis* and cereals is regulated by ambient temperature, with increasing temperatures generally resulting in earlier flowering times (McMaster and Wilhelm, 2003; Balasubramanian et al., 2006; Ejaz and von Korff, 2017; Dixon et al., 2018). Underlying this trait in *Arabidopsis* are the activities of FLC and its relative FLOWERING LOCUS M (FLM). FLM, like FLC, negatively regulates the floral transition, however, it is mostly involved in ambient temperature-dependent flowering (Balasubramanian et al., 2006; Lee et al., 2013; Posé et al., 2013). FLM functions as part of a repressor complex with another MADS-domain transcription factor, SHORT VEGETATIVE PHASE (SVP). This complex represses the activities of flowering promoters under cold temperatures to delay flowering and the stability of the complex and of the proteins themselves are affected by increasing temperature, reducing their repressive effects in warm conditions (Lee et al., 2013; Posé et al., 2013; Capovilla et al., 2017). Temperature-dependent alternative splicing of *FLM* is integral to this response, where the relative abundance of certain transcripts compared to others determines the flowering phenotype in response to temperature (Capovilla et al., 2017; Lutz et al., 2017).

High levels of *FLC* itself also results in thermal unresponsiveness, therefore, suggesting that FLC suppresses thermal induction of flowering (Balasubramanian et al., 2006). These findings could suggest that vernalization is the dominant process that must be realized to allow *Arabidopsis* to be receptive to temperature, likely to prevent precocious flowering in winter.

In cereals, the activities of *ODDSOC2* can also be linked to ambient-temperature regulated flowering. *ODDSOC2* has been shown to be responsive to ambient temperature in both wheat and barley, which both show earlier flowering phenotypes in response to increasing temperature (McMaster and Wilhelm, 2003; Ejaz and von Korff, 2017; Dixon et al., 2018). In wheat, however, it was shown that certain cultivars exhibited delayed flowering in response to increasing ambient temperature (Dixon et al., 2019). It was revealed that this trait arose from the incomplete vernalization of this cultivar, leading to the re-activation of floral repressors including *VRN2* and *TaOS2*. The increase in *TaOS2* expression was linked to the *VRN1* alleles found in this specific cultivar, which were unable to maintain repression of *TaOS2* after incomplete vernalization, explaining in part the delayed flowering phenotype (Dixon et al., 2019).

HvOS2 was also shown to be responsive to ambient temperature in barley. *HvOS2* expression increases under high temperature conditions, particularly under short day photoperiods – conditions which result in the slowest development of the shoot apex (Hemming et al., 2012; Ejaz and von Korff, 2017). Like *TaOS2* in wheat, the response of *HvOS2* is influenced by the *VRN1* allele present in the variety analyzed, with lines with the winter *Hvvrn1* allele having higher *HvOS2* expression levels in response to high ambient temperature (Ejaz and von Korff, 2017). *Hvvrn1* itself is downregulated under high temperature conditions, highlighting further the negative correlation between *VRN1* and *OS2* expression in cereals. Plants overexpressing *HvOS2* also exhibited delayed reproductive development under both cool and high temperatures while lines with a RNAi-mediated knockdown of *HvOS2* underwent more rapid reproductive growth at higher temperatures compared to wild type plants (Hemming et al., 2012). This is reflective of phenotypes obtained when *FLM* expression is modified in *Arabidopsis* (Posé et al., 2013).

Taken together, this evidence suggests that *ODDSOC2* functions in winter cereal varieties to repress the reproductive transition under warm temperatures until the vernalization requirement is completely saturated. It can be speculated that this is an adaptation to prevent precocious flowering during the winter should a brief period of warmth occur. Interestingly, this ecologically significant process is linked to *FLC* gene activity across both *Arabidopsis* and cereals; however, unlike FLM, the mode of action of ODDSOC2 remains unknown. There is no evidence so far to suggest that *ODDSOC2* is alternatively spliced to influence this process. It is also unknown whether this increase in *ODDSOC2* expression occurs in varieties which can be induced to flower using warm temperatures and short-day conditions (Evans, 1987). Regardless, parallels can be drawn on the roles these *FLC* genes play in fine-tuning flowering time in a temperature-specific manner in both *Arabidopsis* and cereals.

A summary of the roles *FLC* genes play in vernalization, ambient temperature, and their relationship to *VRN1* are outlined in **Figure 2** and **Table 1**.

FLC Is Relevant Outside of Temperate Cereals

Rice and maize diverged from the Pooideae roughly 64 million years ago and their flowering times are regulated in different ways to the temperate cereals (Wang et al., 2015). Reflective of the tropical regions in which they evolved, these species have no vernalization requirement and flowering is promoted by short day photoperiods. Nonetheless, both rice and maize contain *FLC* homologs which have been shown to regulate flowering time. *OsMADS51*, a homolog of *ODDSOC1*, acts as a flowering promoter under short days in rice (subsp. Japonica; Kim et al., 2007). Knockout of this protein correlates with the downregulation of *AP1* and *FT* homologs, which may explain the mode of action of this protein. In maize, *ZmMADS69* acts as a flowering promoter under both long and short days, and is thought to have been a target of selection to expand the cultivation zone of maize (Liang et al., 2019). Therefore, despite paucity of information on *FLC*-like genes in cereals, it is clear that flowering time regulation is a fundamental feature of these genes across the cereals.

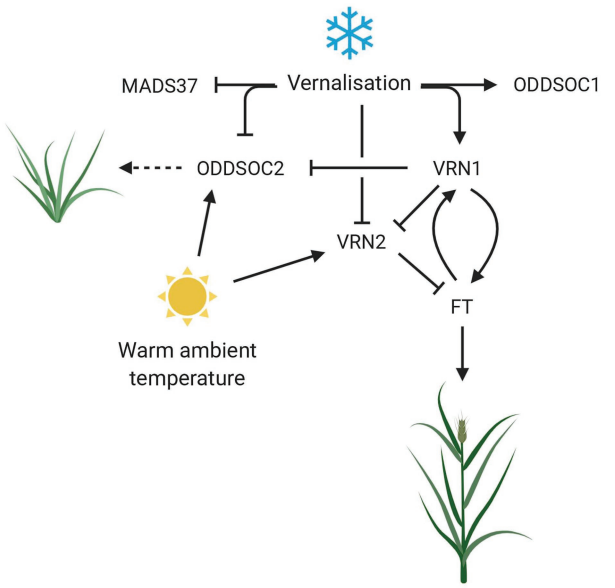

FIGURE 2 | The role of *FLC* genes in the response to temperature in temperate cereals with a vernalization requirement. Vernalization represses the activities of floral repressors ODDSOC2 and VRN2, while promoting the upregulation of *VRN1*. VRN1 is required to maintain the repression of *ODDSOC2* and *VRN2* while promoting the flowering time gene *FT*, creating a positive feedback loop to lock in the floral transition. Warm ambient temperature during the vernalization process results in the upregulation of floral repressors to coordinate reproductive development with the most optimal environmental conditions. Dashed arrow implies function not confirmed. MADS37 and ODDSOC1 are included but their function is still unknown. Created with www.BioRender.com.

Epigenetic Regulation of *FLC*-Like Genes in Cereals

The epigenetic regulation of *FLC* in *Arabidopsis* is well described and *FLC* can be considered a model gene for the study of epigenetics in general (Whittaker and Dean, 2017). *FLC* activity is regulated through the chromatin environment at the *FLC* locus and *via* RNA-mediated silencing mechanisms. Chromatin modification to promote *FLC* activity is regulated mainly through the actions of the FRIGIDA (FRI) complex (FRI-C). The FRI-C increases levels of active chromatin markers, such as H3K36me3 and H3K4me3, through the recruitment of chromatin modification proteins (Choi et al., 2011; Li et al., 2018). These markers are targeted during vernalization, where they are removed, and replaced with H3K9me3 and H3K27me3, resulting in a silenced chromatin state (Bastow et al., 2004; Finnegan and Dennis, 2007; Angel et al., 2011; Whittaker and Dean, 2017). The accumulation of chromatin silencing markers is mediated by the PHD-PRC2 complex (Plant Homeodomain-Polycomb Repression Complex 2; Wood et al., 2006; De Lucia et al., 2008).

Silencing of *FLC* is additionally associated with the action of long non-coding RNAs (lncRNAs) and components of the autonomous pathway (Sheldon et al., 2000; Ietswaart et al., 2012; Whittaker and Dean, 2017). RNA binding proteins of the autonomous pathway function to process *COOLAIR*, a set of lncRNAs transcribed antisense of *FLC* (Swiezewski et al., 2009; Hornyik et al., 2010; Whittaker and Dean, 2017). The significance of these lncRNAs in the regulation of vernalization remains controversial (Helliwell et al., 2011; Luo et al., 2019); however, much data have been gathered to indicate a functional if not essential role. The physical association of *COOLAIR* with *FLC* chromatin is associated with the reduction of H3K36me3 and H3K4me3, rendering the chromatin inactive (Csorba et al., 2014; Fang et al., 2020). *COOLAIR* is also induced by vernalization to assist with the inactivation of *FLC* (Swiezewski et al., 2009; Kim and Sung, 2017). The silencing of *FLC* is associated with two other lncRNAs, *COLDWRAP* and *COLDAIR*, which recruit the PHD-PRC2 complex to specific chromatin regions (Heo and Sung, 2011; Kim and Sung, 2017).

Due to the relatively recent discovery of *FLC*-like genes in cereals, no research has been done to test whether FRI or the FRI-C functions in cereal plants. Studies have shown that homologs of the various FRI-C components can be detected in monocots (Choi et al., 2011) and rice *FRI*-like genes form distinct clades with *Arabidopsis FRI*-like genes (Michaels et al., 2004). According to the plant genome database EnsemblPlants, 25 and 13 proteins have been annotated as FRI-like for *Triticum aestivum* (cv. Chinese Spring) and *Hordeum vulgare* (cv. Morex), respectively. Homologs can also be identified for *Brachypodium distachyon* (9), *Oryza sativa subsp. japonica* (12), *Sorghum bicolor* (10), *Triticum dicoccoides* (16), *Triticum turgidum* (15), and *Zea mays* (13). It is possible that these uncharacterized proteins may act as scaffold proteins similar to FRI but for other pathways and functions.

In *Arabidopsis*, *FLC* is silenced during vernalization *via* a series of histone modifications by the PHD-PRC2 complex (De Lucia et al., 2008). The utilization of this complex in plants as a method to regulate vernalization-dependent flowering is conserved across *Arabidopsis* and cereals. The major regulator of vernalization in cereals, *VRN1*, acts as a promoter of flowering, rather than a repressor like *FLC*. Before vernalization, H3K27me3 repressive marks are deposited at the *VRN1* locus in wheat and barley (Oliver et al., 2009; Diallo et al., 2012). During vernalization, H3K27me3 decreases while the active markers H3K4me3 and H3K36me3 increase (Oliver et al., 2009; Diallo et al., 2012). The same mode of epigenetic regulation of *VRN1* is conserved in *Brachypodium*, and is regulated by ENHANCER OF ZESTE-LIKE 1 (EZL1), a homolog of CURLY LEAF (CLF), and a methyltransferase in the PRC2 complex in *Arabidopsis* (Lomax et al., 2018). *VRN3/FT* is also regulated in the same way in wheat and *Brachypodium* (Oliver et al., 2009; Huan et al., 2018).

Recruitment of the PRC2 to epigenetically regulate the vernalization response evolved in both *Arabidopsis* and cereals. However, the nature of the chromatin modifiers deposited at *FLC* and *VRN1* is different due to their nature as a repressor and promoter, respectively. Therefore, this recruitment likely evolved after the independent evolution of the vernalization response pathway in monocots and dicots. Yet, some evidence exists to suggest that *FLC*-like genes are also regulated by

TABLE 1 | Overview of *FLC* gene function in cereals.

Species	Gene	Observation	Citation
Brachypodium distachyon	*BdOS1*	Upregulated by vernalization	Ruelens et al. (2013)
	BdOS2	Downregulated by vernalization	Ruelens et al. (2013); Sharma et al. (2017)
		Negatively regulated by VRN1	Woods et al. (2016)
	BdMADS37	Downregulated by vernalization	Ruelens et al. (2013)
Hordeum vulgare	*HvOS1*	Induced by ABA and JA	Kapazoglou et al. (2012)
		Role in seed development	
		Upregulated by vernalization	Greenup et al. (2010)
		Downregulated by high temperature	Hemming et al. (2012)
	HvOS2	Induced by JA	Kapazoglou et al. (2012)
		Role in seed development	
		Downregulated by vernalization	Greenup et al. (2010)
		Negatively regulated by VRN1	
		Regulates cell elongation	
		VRN1 binds to its promoter	Deng et al. (2015)
		Possible negative regulator of early reproductive development	Hemming et al. (2012); Monteagudo et al. (2019)
		Upregulated under high ambient temperature	Hemming et al. (2012); Ejaz and von Korff (2017)
Oryza sativa	*OsMADS51*	Short-day flowering promoter	Kim et al. (2007)
Triticum aestivum	*TaAGL33/TaOS2*	Downregulated by vernalization	Winfield et al. (2009); Sharma et al. (2017); Appels et al. (2018)
		Knockout of D-homeolog causes earlier flowering	Appels et al. (2018)
		Upregulated under high ambient temperature	Dixon et al. (2019)
	TaAGL42/TaMX23/TaOS1	Upregulated in response to cold	Winfield et al. (2009); Sharma et al. (2017)
		Gradual increase in expression throughout development	Trevaskis et al. (2003); Winfield et al. (2009)
Triticum monococcum	*TmODDSOC2*	Negatively regulated by VRN1	Greenup et al. (2010)
Zea mays	*ZmMADS69*	Flowering promoter	Liang et al. (2019)

the PRC2 in a similar manner to *FLC* in *Arabidopsis*. To analyze the effect of vernalization on histone modifications at *HvOS2* in barley, H3K27me3 marks were analyzed at the presumed transcriptional start site of *HvOS2* in plants with or without 7 weeks of vernalization (Greenup et al., 2010). There was no significant difference in H3K27 trimethylation at this region indicating that perhaps repression of *HvOS2* post-vernalization is regulated in a different way to *FLC*. The region tested by Greenup et al. begins ~100 bp upstream of the transcriptional start site (TSS). Although H3K27me3 deposits increase during vernalization at the TSS of *FLC* in *Arabidopsis*, the greatest increase is at the exon 1/intron 1 junction termed the "nucleation region" (Bastow et al., 2004; Finnegan and Dennis, 2007; Yuan et al., 2016). On return to warmth, H3K27me3 spreads from the nucleation region across the *FLC* locus. Future experiments targeting other regions within the *HvOS2* locus could reveal more similarities in the epigenetic regulation of both *FLC* and *HvOS2*. Regulation *via* other markers such as H3K9me3 or H3 acetylation levels could be investigated, as these markers are also involved in *FLC* regulation.

In contrast to barley, *BdOS2* in *Brachypodium* showed high levels of H3K27me3 after vernalization in both spring and winter accessions (Sharma et al., 2017). H3K27me3 was enriched at the *BdOS2* locus after vernalization for Bd21 and BdTR3C – spring and winter accessions, respectively, and the enrichment was maintained 1-week post-vernalization. For the winter allele of *BdOS2* in BdTR3C, H3K27me3 can be found spanning the entire locus post-vernalization. The extensive methylation marks of H3K27 in the locus of BdTR3C compared to Bd21 may explain the mechanism as to how *BdOS2* is stably repressed in the winter but not spring accession. It is possible that in strong winter varieties, *FLC* genes have evolved increasingly stringent or more complex methods of silencing to ensure flowering time is synchronized most optimally with the environment (Shindo et al., 2006; Hepworth et al., 2020). Analysis of winter varieties of *FLC* homologs in other cereal crops may reveal that the epigenetic regulation of *FLC*-like genes is more conserved than currently realized.

Brachypodium has also been shown to encode lncRNAs, similar to *COOLAIR*, which target *FLC*-like genes for downregulation during vernalization (Jiao et al., 2019). Two high confidence lncRNAs were detected for *BdOS2*, while one lncRNA could be detected for *BdOS1*. These lncRNAs were termed *BdCOOLAIR1* and *BdCOOLAIR2* for *BdOS1* and *BdOS2*, respectively, as although they are not homologous to the *AtCOOLAIR* sequence, their position relative to their sense counterparts is similar. Expression of these lncRNAs is induced by vernalization, and their induction is significantly higher in a winter accession compared to a facultative accession, while their expression is absent in a spring accession. Knockdown of *BdCOOLAIR2 via* RNAi also affects the rate of silencing of *BdOS2* in BdTR3C, though it is not essential for the complete silencing of *BdOS2* (Jiao et al., 2019). This information suggests that lncRNAs complement the mechanisms which silence *FLC*-like genes in grasses, in a similar fashion to *FLC* regulation in *Arabidopsis*, although this mode of regulation is accession dependent. In addition, lncRNAs have been annotated for *FLC*

genes in 6 other grass species, including wheat, although these still need to be experimentally verified.

DIVERSIFICATION OF FLC FUNCTION IN CROPS

Although thoroughly studied for its involvement in vernalization-dependent regulation of flowering time, FLC function is implicated in many other aspects of plant growth and development. Analysis of expression levels of *FLC*-like genes in cereals during development and under various experimental treatments also suggests that homologs of *FLC* play diverse roles in cereal physiology. For example, in the early gene expression experiments of Zhao et al. (2006), it was shown that at least one of the genes analyzed is expressed at, at least, one of the various life stages and in at least one of the various tissue types throughout wheat development. Expression can be detected from initial embryo imbibition to seed development post-anthesis while other genes are predominantly expressed in roots.

Curiously, in the dataset of both Zhao et al. (2006) and Schilling et al. (2020), *TaAGL41* could not be detected at significant levels but could be detected by Sharma et al. (2017) for several cultivars. Further analysis using the Wheat Expression Browser (Ramírez-González et al., 2018) indicates that *TaAGL41* is indeed expressed throughout development but the extent of its expression is cultivar-specific. This could suggest a role for this gene in fine tuning development in a cultivar-specific manner. The Wheat Expression Browser highlights that *TaAGL41* is downregulated by cold in the spring cultivar Manitou (Li et al., 2015), yet the main stimulus which affected *TaAGL41* across the dataset was infection by the wheat yellow rust pathogen *Puccinia striiformis f.* sp. *Tritici* (Dobon et al., 2016). Expression of two other high confidence *FLC* homologs in wheat, *TaFLC.4A1* and *TaFLC.4A2*, could not be detected at significant levels in the developmental time course analyzed by Schilling et al. (2020), and their expression does not change considerably across the different varieties available on the Wheat Expression Browser. Rather, these genes appear to be mainly influenced by drought stress (Liu et al., 2015; Ramírez-González et al., 2018). The relationship between flowering time and stress adaptation is complex and the molecular mechanisms determining this relationship are still not fully understood; however, a link between flowering time regulators and stress is found in plants (reviewed in Kazan and Lyons, 2016). It is possible that *FLC*-like genes not only play roles regulating development but also that their function has diversified to fine tune other developmental and growth processes. This reflects findings in the Brassicaceae that although the core function of *FLC* across species is the regulation of flowering time, different members of the *FLC* clade have been recruited for species-specific roles typically within stress response pathways (Mateos et al., 2017). Further investigation into these expression patterns as well as generation of knockout mutants may reveal a novel role for these genes in stress response pathways in cereals.

Additionally, *HvOS2* has been shown to negatively influence cell length and, therefore, leaf, internode, and spike length (Greenup et al., 2010). The data suggest that *HvOS2* downregulation by vernalization allows the process of stem elongation and bolting as secondary regulation of the reproductive process.

As well as being expressed during seed development stages in wheat, *FLC*-like genes have been implicated in seed development in barley. *HvOS1* and *HvOS2* are differentially expressed in cultivars of different seed size and at different stages of seed development (Kapazoglou et al., 2012). Analysis of their expression patterns revealed that *HvOS1* expression is induced more substantially in early seed development in cultivars with large seeds, while *HvOS2* levels are significantly higher in later developmental stages in cultivars with small seeds. This pattern could suggest an association between the expression of *FLC* genes and seed size in barley and that each gene is important for different stages of development – either endosperm cellularization or seed maturation. Additionally, both genes contained the endosperm-specific element GCN4 in their promoters, along with elements for responses to abscisic acid, an important phytohormone for seed maturation as well as abiotic stress (Takaiwa et al., 1996; Finkelstein et al., 2002; Kapazoglou et al., 2012). Taken together, these data implicate a role of *FLC* homologs in seed development and suggest that perhaps there is an association between them and seed size. An association study including more cultivars with a variety of seed sizes could be undertaken to fully determine whether *FLC*-like genes regulate this important agronomic trait.

Outside of the temperate cereals, *ZmAGL19*, an *FLC* homolog in maize, is targeted by OPAQUE11, a central regulator of endosperm development and nutrient metabolism (Feng et al., 2018). *OPAQUE11* is specifically expressed in the endosperm and positively regulates *ZmAGL19* expression, suggesting that *ZmAGL19* might be part of the seed development regulation process in maize.

FUTURE DIRECTIONS

Much has been learned about the roles *FLC* genes play in cereals, mostly indirectly through the study of flowering time in these species. The scientific community is now able to study *FLC* genes further due to the dramatically improved genetic resources available. Reference genome assemblies are now available for several hexaploid wheat cultivars, as well as tetraploid wheat, diploid progenitor species, and 2- and 6-row barley (Ling et al., 2013; Fox et al., 2014; Luo et al., 2017; Mascher et al., 2017; Appels et al., 2018; Maccaferri et al., 2019). Genes are also annotated to include SNP variations which can be easily identified using the online platform EnsemblPlants. Identifying homologs and SNP-variants across cultivars has never been easier for researchers without bioinformatics training. Access to tools such as these will increase the pace at which genes are identified and studied, increasing the potential to finally characterize the once enigmatic *FLC* gene family.

Additionally, populations of mutant plants have been created for widespread use in both hexaploid and tetraploid wheat and barley (Krasileva et al., 2017; Schreiber et al., 2019). TILLING lines containing homeolog-specific mutations in genes of interest

can be ordered and crossed, creating specific combinations to study gene function and redundancy. In a more targeted approach, protocols for wheat transformation and mutation *via* virus-induced gene silencing and CRISPR/Cas9 are available (see wheat-training.com for resources). In combination with speed breeding, it is possible to fully characterize the effect of mutations in both model and crop plants in considerably less time (Watson et al., 2018). At this moment in time, comparable resources to the model plant *Arabidopsis* from which most of our information on *FLC* genes comes from are available. This review also highlights how relevant *Brachypodium* is as a model for basic and translational research for temperate cereals and that research using this small grass will continue to be a valuable option to study *FLC* genes. It is possible within the next few years that we will see a greater increase in *FLC*-related knowledge outside of *Arabidopsis*. The availability of these resources provides hope that much more knowledge can be gained on *FLC* function in cereals in years to come.

AUTHOR CONTRIBUTIONS

AK prepared the outline and wrote the manuscript. KG contributed to discussions and critical revision of the manuscript. All authors contributed to the article and approved the submitted version.

FUNDING

AK and The Geuten Lab are supported by KU Leuven grant C24/17/037 and FWO grant G065713N.

ACKNOWLEDGMENTS

We thank Emma Doyle (University College Dublin), Sam Balzarini (KU Leuven), Philip Ruelens (WUR), and Daniel Woods (UC Davis) for their helpful comments, suggestions, and insights. We also thank three reviewers of this article for their valuable comments.

SUPPLEMENTARY MATERIAL

The Supplementary Material for this article can be found online at: https://www.frontiersin.org/articles/10.3389/fpls.2020.617340/full#supplementary-material

REFERENCES

Angel, A., Song, J., Dean, C., and Howard, M. (2011). A Polycomb-based switch underlying quantitative epigenetic memory. *Nature* 476, 105–109. doi: 10.1038/nature10241

Appels, R., Eversole, K., Feuillet, C., Keller, B., Rogers, J., Stein, N., et al. (2018). Shifting the limits in wheat research and breeding using a fully annotated reference genome. *Science* 361:eaar7191. doi: 10.1126/science.aar7191

Balasubramanian, S., Sureshkumar, S., Lempe, J., and Weigel, D. (2006). Potent induction of *Arabidopsis thaliana* flowering by elevated growth temperature. *PLoS Genet.* 2:e106. doi: 10.1371/journal.pgen.0020106

Bastow, R., Mylne, J. S., Lister, C., Lippman, Z., Martienssen, R. A., and Dean, C. (2004). Vernalization requires epigenetic silencing of FLC by histone methylation. *Nature* 427, 164–167. doi: 10.1038/nature02269

Bettgenhaeuser, J., Corke, F. M. K., Opanowicz, M., Green, P., Hernández-Pinzón, I., Doonan, J. H., et al. (2017). Natural variation in *Brachypodium* links vernalization and flowering time loci as major flowering determinants. *Plant Physiol.* 173, 256–268. doi: 10.1104/pp.16.00813

Capovilla, G., Symeonidi, E., Wu, R., and Schmid, M. (2017). Contribution of major FLM isoforms to temperature-dependent flowering in *Arabidopsis thaliana*. *J. Exp. Bot.* 68, 5117–5127. doi: 10.1093/jxb/erx328

Chen, M., Moore, K., Florance, H., MacGregor, D. R., Smirnoff, N., Paszkiewicz, K., et al. (2014). Maternal temperature history activates flowering locus T in fruits to control progeny dormancy according to time of year. *Proc. Natl. Acad. Sci.* 111, 18787–18792. doi: 10.1073/pnas.1412274111

Chen, M., and Penfield, S. (2018). Feedback regulation of COOLAIR expression controls seed dormancy and flowering time. *Science* 360, 1014–1017. doi: 10.1126/science.aar7361

Chiang, G. C. K., Barua, D., Kramer, E. M., Amasino, R. M., and Donohue, K. (2009). Major FLOWERING time gene, FLOWERING LOCUS C, regulates seed germination in *Arabidopsis thaliana*. *Proc. Natl. Acad. Sci.* 106, 11661–11666. doi: 10.1073/pnas.0901367106

Choi, K., Kim, J., Hwang, H. J., Kim, S., Park, C., Kim, S. Y., et al. (2011). The FRIGIDA complex activates transcription of FLC, a strong flowering repressor in *Arabidopsis*, by recruiting chromatin modification factors. *Plant Cell* 23, 289–303. doi: 10.1105/tpc.110.075911

Csorba, T., Questa, J. I., Sun, Q., and Dean, C. (2014). Antisense COOLAIR mediates the coordinated switching of chromatin states at FLC during vernalization. *Proc. Natl. Acad. Sci.* 111, 16160–16165. doi: 10.1073/pnas.1419030111

De Lucia, F., Crevillen, P., Jones, A. M. E., Greb, T., and Dean, C. (2008). A PHD-polycomb repressive complex 2 triggers the epigenetic silencing of FLC during vernalization. *Proc. Natl. Acad. Sci.* 105, 16831–16836. doi: 10.1073/pnas.0808687105

Deng, W., Casao, M. C., Wang, P., Sato, K., Hayes, P. M., Finnegan, E., et al. (2015). Direct links between the vernalization response and other key traits of cereal crops. *Nat. Commun.* 6:5882. doi: 10.1038/ncomms6882

Deng, W., Ying, H., Helliwell, C. A., Taylor, J. M., Peacock, W. J., and Dennis, E. S. (2011). FLOWERING LOCUS C (FLC) regulates development pathways throughout the life cycle of *Arabidopsis*. *Proc. Natl. Acad. Sci.* 108, 6680–6685. doi: 10.1073/pnas.1103175108

Diallo, A. O., Ali-Benali, M. A., Badawi, M., Houde, M., and Sarhan, F. (2012). Expression of vernalization responsive genes in wheat is associated with histone H3 trimethylation. *Mol. Ecol.* 287, 575–590. doi: 10.1007/s00438-012-0701-0

Distelfeld, A., Li, C., and Dubcovsky, J. (2009). Regulation of flowering in temperate cereals. *Curr. Opin. Plant Biol.* 12, 178–184. doi: 10.1016/j.pbi.2008.12.010

Dixon, L. E., Farré, A., Finnegan, E., Orford, S., Griffiths, S., and Boden, S. (2018). Developmental responses of bread wheat to changes in ambient temperature following deletion of a locus that includes FLOWERING LOCUS T1. *Plant Cell Environ.* 41, 1715–1725. doi: 10.1111/pce.13130

Dixon, L. E., Karsai, I., Kiss, T., Adamski, N. M., Liu, Z., Ding, Y., et al. (2019). VERNALIZATION1 controls developmental responses of winter wheat under high ambient temperatures. *Development* 146:dev172684. doi: 10.1242/DEV.172684

Dobon, A., Bunting, D. C. E., Cabrera-Quio, L. E., Uauy, C., and Saunders, D. G. O. (2016). The host-pathogen interaction between wheat and yellow rust induces temporally coordinated waves of gene expression. *BMC Genomics* 17:380. doi: 10.1186/s12864-016-2684-4

Edwards, K. D., Anderson, P. E., Hall, A., Salathia, N. S., Locke, J. C. W., Lynn, J. R., et al. (2006). FLOWERING LOCUS C mediates natural variation in the high-temperature response of the *Arabidopsis* circadian clock. *Plant Cell* 18, 639–650. doi: 10.1105/tpc.105.038315.1

Ejaz, M., and von Korff, M. (2017). The genetic control of reproductive development under high ambient temperature. *Plant Physiol.* 173, 294–306. doi: 10.1104/pp.16.01275

Evans, L. T. (1987). Short day induction of inflorescence initiation in some winter wheat varieties. *Funct. Plant Biol.* 14, 277–286.

Fang, X., Wu, Z., Raitskin, O., Webb, K., Voigt, P., Lu, T., et al. (2020). The 3' processing of antisense RNAs physically links to chromatin-based transcriptional control. *Proc. Natl. Acad. Sci.* 117, 15316–15321. doi: 10.1073/pnas.2007268117

Feng, F., Qi, W., Lv, Y., Yan, S., Xu, L., Yang, W., et al. (2018). OPAQUE11 is a central hub of the regulatory network for maize endosperm development and nutrient metabolism. *Plant Cell* 30, 375–396. doi: 10.1105/tpc.17.00616

Finkelstein, R. R., Gampala, S. S. L., and Rock, C. D. (2002). Abscisic acid signaling in seeds and seedlings. *Plant Cell* 14, 15–45. doi: 10.1105/tpc.010441

Finnegan, E., and Dennis, E. S. (2007). Vernalization-induced trimethylation of histone H3 lysine 27 at FLC is not maintained in mitotically quiescent cells. *Curr. Biol.* 17, 1978–1983. doi: 10.1016/j.cub.2007.10.026

Fox, S. E., Geniza, M., Hanumappa, M., Naithani, S., Sullivan, C., Preece, J., et al. (2014). De novo transcriptome assembly and analyses of gene expression during photomorphogenesis in diploid wheat *Triticum monococcum*. *PLoS One* 9:e96855. doi: 10.1371/journal.pone.0096855

Fu, D., Szűcs, P., Yan, L., Helguera, M., Skinner, J. S., Von Zitzewitz, J., et al. (2005). Large deletions within the first intron in VRN-1 are associated with spring growth habit in barley and wheat. *Mol. Gen. Genomics.* 273, 54–65. doi: 10.1007/s00438-004-1095-4

Greenup, A. G., Sasani, S., Oliver, S., Talbot, M. J., Dennis, E. S., Hemming, M. N., et al. (2010). ODDSOC2 is a MADS box floral repressor that is down-regulated by vernalization in temperate cereals. *Plant Physiol.* 153, 1062–1073. doi: 10.1104/pp.109.152488

Helliwell, C. A., Robertson, M., Finnegan, E., Buzas, D. M., and Dennis, E. S. (2011). Vernalization-repression of *Arabidopsis* FLC requires promoter sequences but not antisense transcripts. *PLoS One* 6:e21513. doi: 10.1371/journal.pone.0021513

Hemming, M. N., Walford, S. A., Fieg, S., Dennis, E. S., and Trevaskis, B. (2012). Identification of high-temperature-responsive genes in cereals. *Plant Physiol.* 158, 1439–1450. doi: 10.1104/pp.111.192013

Heo, J. B., and Sung, S. (2011). Vernalization-mediated epigenetic silencing by a long intronic noncoding RNA. *Science* 331, 76–79. doi: 10.1126/science.1197349

Hepworth, J., Antoniou-kourounioti, R. L., Berggren, K., Selga, C., Tudor, E. H., Yates, B., et al. (2020). Natural variation in autumn expression is the major adaptive determinant distinguishing *Arabidopsis* FLC haplotypes. *elife* 9:e57671. doi: 10.7554/eLife.57671

Hornyik, C., Terzi, L. C., and Simpson, G. G. (2010). The Spen family protein FPA controls alternative cleavage and polyadenylation of RNA. *Dev. Cell* 18, 203–213. doi: 10.1016/j.devcel.2009.12.009

Huan, Q., Mao, Z., Chong, K., and Zhang, J. (2018). Global analysis of H3K4me3/H3K27me3 in *Brachypodium distachyon* reveals VRN3 as critical epigenetic regulation point in vernalization and provides insights into epigenetic memory. *New Phytol.* 219, 1373–1387. doi: 10.1111/nph.15288

Ietswaart, R., Wu, Z., and Dean, C. (2012). Flowering time control: another window to the connection between antisense RNA and chromatin. *Trends Genet.* 28, 445–453. doi: 10.1016/j.tig.2012.06.002

Jiao, F., Pahwa, K., Dochy, N., Manning, M., and Geuten, K. (2019). Cold induced antisense transcription of FLOWERING LOCUS C in distant grasses. *Front. Plant Sci.* 10:72. doi: 10.3389/fpls.2019.00072

Kapazoglou, A., Engineer, C., Drosou, V., Kalloniati, C., Tani, E., Tsaballa, A., et al. (2012). The study of two barley type I-like MADS-box genes as potential targets of epigenetic regulation during seed development. *BMC Plant Biol.* 12:166. doi: 10.1186/1471-2229-12-166

Kazan, K., and Lyons, R. (2016). The link between flowering time and stress tolerance. *J. Exp. Bot.* 67, 47–60. doi: 10.1093/jxb/erv441

Kim, S. L., Lee, S., Kim, H. J., Nam, H. G., and An, G. (2007). OsMADS51 is a short-day flowering promoter that functions upstream of Ehd1, OsMADS14, and Hd3a. *Plant Physiol.* 145, 1484–1494. doi: 10.1104/pp.107.103291

Kim, D. H., and Sung, S. (2017). Vernalization-triggered intragenic chromatin loop formation by long noncoding RNAs. *Dev. Cell* 40, 302.e4–312.e4. doi: 10.1016/j.devcel.2016.12.021

Krasileva, K. V., Vasquez-Gross, H. A., Howell, T., Bailey, P., Paraiso, F., Clissold, L., et al. (2017). Uncovering hidden variation in polyploid wheat. *Proc. Natl. Acad. Sci.* 114, E913–E921. doi: 10.1073/pnas.1619268114

Kumar, G., Arya, P., Gupta, K., Randhawa, V., Acharya, V., and Singh, A. K. (2016). Comparative phylogenetic analysis and transcriptional profiling of MADS-box gene family identified DAM and FLC-like genes in apple (*Malusx domestica*). *Sci. Rep.* 6:20695. doi: 10.1038/srep20695

Lee, J. H., Ryu, H. -S., Chung, K. S., Posé, D., Kim, S., Schmid, M., et al. (2013). Regulation of temperature-responsive flowering by MADS-box transcription factor repressors. *Science* 342, 628–632. doi: 10.1126/science.1241097

Li, Z., Jiang, D., and He, Y. (2018). FRIGIDA establishes a local chromosomal environment for FLOWERING LOCUS C mRNA production. *Nat. Plants* 4, 836–846. doi: 10.1038/s41477-018-0250-6

Li, Q., Zheng, Q., Shen, W., Cram, D., Brian Fowler, D., Wei, Y., et al. (2015). Understanding the biochemical basis of temperature-induced lipid pathway adjustments in plants. *Plant Cell* 27, 86–103. doi: 10.1105/tpc.114.134338

Liang, Y., Liu, Q., Wang, X., Huang, C., Xu, G., Hey, S., et al. (2019). ZmMADS69 functions as a flowering activator through the ZmRap2.7-ZCN8 regulatory module and contributes to maize flowering time adaptation. *New Phytol.* 221, 2335–2347. doi: 10.1111/nph.15512

Ling, H. Q., Wang, J., Zhao, S., Liu, D., Wang, J., Sun, H., et al. (2013). Draft genome of the wheat A-genome progenitor *Triticum urartu*. *Nature* 496, 87–90. doi: 10.1038/nature11997

Liu, Z., Xin, M., Qin, J., Peng, H., Ni, Z., Yao, Y., et al. (2015). Temporal transcriptome profiling reveals expression partitioning of homeologous genes contributing to heat and drought acclimation in wheat (*Triticum aestivum* L.). *BMC Plant Biol.* 15:152. doi: 10.1186/s12870-015-0511-8

Lomax, A., Woods, D. P., Dong, Y., Bouché, F., Rong, Y., Mayer, K. S., et al. (2018). An ortholog of CURLY LEAF/ENHANCER OF ZESTE like-1 is required for proper flowering in *Brachypodium distachyon*. *Plant J.* 93, 871–882. doi: 10.1111/tpj.13815

Luo, X., Chen, T., Zeng, X., He, D., and He, Y. (2019). Feedback regulation of FLC by FLOWERING LOCUS T (FT) and FD through a 5' FLC promoter region in *Arabidopsis*. *Mol. Plant* 12, 285–288. doi: 10.1016/j.molp.2019.01.013

Luo, M. C., Gu, Y. Q., Puiu, D., Wang, H., Twardziok, S. O., Deal, K. R., et al. (2017). Genome sequence of the progenitor of the wheat D genome *Aegilops tauschii*. *Nature* 551, 498–502. doi: 10.1038/nature24486

Lutz, U., Nussbaumer, T., Spannagl, M., Diener, J., Mayer, K. F. X., and Schwechheimer, C. (2017). Natural haplotypes of FLM non-coding sequences fine-tune flowering time in ambient spring temperatures in *Arabidopsis*. *elife* 6:e22114. doi: 10.7554/eLife.22114

Maccaferri, M., Harris, N. S., Twardziok, S. O., Pasam, R. K., Gundlach, H., Spannagl, M., et al. (2019). Durum wheat genome highlights past domestication signatures and future improvement targets. *Nat. Genet.* 51, 885–895. doi: 10.1038/s41588-019-0381-3

Mascher, M., Gundlach, H., Himmelbach, A., Beier, S., Twardziok, S. O., Wicker, T., et al. (2017). A chromosome conformation capture ordered sequence of the barley genome. *Nature* 544, 427–433. doi: 10.1038/nature22043

Mateos, J. L., Tilmes, V., Madrigal, P., Severing, E., Richter, R., Rijkenberg, C. W. M., et al. (2017). Divergence of regulatory networks governed by the orthologous transcription factors FLC and PEP1 in Brassicaceae species. *Proc. Natl. Acad. Sci.* 114, E11037–E11046. doi: 10.1073/pnas.1618075114

McKay, J. K., Richards, J. H., and Mitchell-Olds, T. (2003). Genetics of drought adaptation in *Arabidopsis thaliana*: I. Pleiotropy contributes to genetic correlations among ecological traits. *Mol. Ecol.* 12, 1137–1151. doi: 10.1046/j.1365-294X.2003.01833.x

McMaster, G. S., and Wilhelm, W. W. (2003). Phenological responses of wheat and barley to water and temperature: improving simulation models. *J. Agric. Sci.* 141, 129–147. doi: 10.1017/S0021859603003460

Michaels, S. D., Bezerra, I. C., and Amasino, R. M. (2004). FRIGIDA-related genes are required for the winter-annual habit in *Arabidopsis*. *Proc. Natl. Acad. Sci.* 101, 3281–3285. doi: 10.1073/pnas.0306778101

Mohammadin, S., Nguyen, T. P., Van Weij, M. S., Reichelt, M., and Schranz, M. E. (2017). Flowering locus C (FLC) is a potential major regulator of glucosinolate content across developmental stages of *Aethionema arabicum* (Brassicaceae). *Front. Plant Sci.* 8:876. doi: 10.3389/fpls.2017.00876

Monteagudo, A., Igartua, E., Contreras-Moreira, B., Gracia, M. P., Ramos, J., Karsai, I., et al. (2019). Fine-tuning of the flowering time control in winter

barley: the importance of HvOS2 and HvVRN2 in non-inductive conditions. *BMC Plant Biol.* 19:113. doi: 10.1186/s12870-019-1727-9

Oliver, S., Finnegan, E., Dennis, E. S., Peacock, W. J., and Trevaskis, B. (2009). Vernalization-induced flowering in cereals is associated with changes in histone methylation at the VERNALIZATION1 gene. *Proc. Natl. Acad. Sci.* 106, 8386–8391. doi: 10.1073/pnas.0903566106

Posé, D., Verhage, L., Ott, F., Yant, L., Mathieu, J., Angenent, G. C., et al. (2013). Temperature-dependent regulation of flowering by antagonistic FLM variants. *Nature* 503, 414–417. doi: 10.1038/nature12633

Priest, H. D., Fox, S. E., Rowley, E. R., Murray, J. R., Michael, T. P., and Mockler, T. C. (2014). Analysis of global gene expression in *Brachypodium distachyon* reveals extensive network plasticity in response to abiotic stress. *PLoS One* 9:e87499. doi: 10.1371/journal.pone.0087499

Ramírez-González, R. H., Borrill, P., Lang, D., Harrington, S. A., Brinton, J., Venturini, L., et al. (2018). The transcriptional landscape of polyploid wheat. *Science* 361:eaar6089. doi: 10.1126/science.aar6089

Ream, T. S., Woods, D. P., and Amasino, R. M. (2012). The molecular basis of vernalization in different plant groups. *Cold Spring Harb. Symp. Quant. Biol.* 77, 105–115. doi: 10.1101/sqb.2013.77.014449

Rizza, F., Karsai, I., Morcia, C., Badeck, F. W., Terzi, V., Pagani, D., et al. (2016). Association between the allele compositions of major plant developmental genes and frost tolerance in barley (*Hordeum vulgare* L.) germplasm of different origin. *Mol. Breed.* 36:156. doi: 10.1007/s11032-016-0571-y

Ruelens, P., De Maagd, R. A., Proost, S., Theißen, G., Geuten, K., and Kaufmann, K. (2013). FLOWERING LOCUS C in monocots and the tandem origin of angiosperm-specific MADS-box genes. *Nat. Commun.* 4:2280. doi: 10.1038/ncomms3280

Schilling, S., Kennedy, A., Pan, S., Jermiin, L. S., and Melzer, R. (2020). Genome-wide analysis of MIKC-type MADS-box genes in wheat: pervasive duplications, functional conservation and putative neofunctionalization. *New Phytol.* 225, 511–529. doi: 10.1111/nph.16122

Schreiber, M., Barakate, A., Uzrek, N., Macaulay, M., Sourdille, A., Morris, J., et al. (2019). A highly mutagenised barley (cv. Golden promise) TILLING population coupled with strategies for screening-by-sequencing. *Plant Methods* 15:99. doi: 10.1186/s13007-019-0486-9

Searle, I., He, Y., Turck, F., Vincent, C., Fornara, F., Kröber, S., et al. (2006). The transcription factor FLC confers a flowering response to vernalization by repressing meristem competence and systemic signalling in *Arabidopsis*. *Genes Dev.* 20, 898–912. doi: 10.1101/gad.373506

Sharma, N., Ruelens, P., D'hauw, M., Maggen, T., Dochy, N., Torfs, S., et al. (2017). A flowering locus C homolog is a vernalization-regulated repressor in *Brachypodium* and is cold regulated in wheat. *Plant Physiol.* 173, 1301–1315. doi: 10.1104/pp.16.01161

Sheldon, C. C., Rouse, D. T., Finnegan, E., Peacock, W. J., and Dennis, E. S. (2000). The molecular basis of vernalization: the central role of FLOWERING LOCUS C (FLC). *Proc. Natl. Acad. Sci.* 97, 3753–3758. doi: 10.1073/pnas.060023597

Shindo, C., Lister, C., Crevillen, P., Nordborg, M., and Dean, C. (2006). Variation in the epigenetic silencing of FLC contributes to natural variation in *Arabidopsis* vernalization response. *Genes Dev.* 20, 3079–3083. doi: 10.1101/gad.405306

Swiezewski, S., Liu, F., Magusin, A., and Dean, C. (2009). Cold-induced silencing by long antisense transcripts of an *Arabidopsis* Polycomb target. *Nature* 462, 799–802. doi: 10.1038/nature08618

Takaiwa, F., Yamanouchi, U., Yoshihara, T., Washida, H., Tanabe, F., Kato, A., et al. (1996). Characterization of common cis-regulatory elements responsible for the endosperm-specific expression of members of the rice glutelin multigene family. *Plant Mol. Biol.* 30, 1207–1221. doi: 10.1007/BF00019553

Trevaskis, B., Bagnall, D. J., Ellis, M. H., Peacock, W. J., and Dennis, E. S. (2003). MADS box genes control vernalization-induced flowering in cereals. *Proc. Natl. Acad. Sci.* 100, 13099–13104. doi: 10.1073/pnas.1635053100

Trevaskis, B., Hemming, M. N., Dennis, E. S., and Peacock, W. J. (2007). The molecular basis of vernalization-induced flowering in cereals. *Trends Plant Sci.* 12, 352–357. doi: 10.1016/j.tplants.2007.06.010

Wang, X., Wang, J., Jin, D., Guo, H., Lee, T. H., Liu, T., et al. (2015). Genome alignment spanning major poaceae lineages reveals heterogeneous evolutionary rates and alters inferred dates for key evolutionary events. *Mol. Plant* 8, 885–898. doi: 10.1016/j.molp.2015.04.004

Watson, A., Ghosh, S., Williams, M. J., Cuddy, W. S., Simmonds, J., Rey, M. D., et al. (2018). Speed breeding is a powerful tool to accelerate crop research and breeding. *Nat. Plants* 4, 23–29. doi: 10.1038/s41477-017-0083-8

Whittaker, C., and Dean, C. (2017). The FLC locus: a platform for discoveries in epigenetics and adaptation. *Annu. Rev. Cell Dev. Biol.* 33, 555–575. doi: 10.1146/annurev-cellbio-100616-060546

Winfield, M. O., Lu, C., Wilson, I. D., Coghill, J. A., and Edwards, K. (2009). Cold- and light-induced changes in the transcriptome of wheat leading to phase transition from vegetative to reproductive growth. *BMC Plant Biol.* 9:55. doi: 10.1186/1471-2229-9-55

Wood, C. C., Robertson, M., Tanner, G., Peacock, W. J., Dennis, E. S., and Helliwell, C. A. (2006). The *Arabidopsis thaliana* vernalization response requires a polycomb-like protein complex that also includes VERNALIZATION INSENSITIVE 3. *Proc. Natl. Acad. Sci.* 103, 14631–14636. doi: 10.1073/pnas.0606385103

Woods, D. P., McKeown, M., Dong, Y., Preston, J. C., and Amasino, R. M. (2016). Evolution of *VRN2/Ghd7*-like genes in vernalization-mediated repression of grass flowering. *Plant Physiol.* 170, 2124–2135. doi: 10.1104/pp.15.01279

Yan, L., Fu, D., Li, C., Blechl, A., Tranquilli, G., Bonafede, M., et al. (2006). The wheat and barley vernalization gene VRN3 is an orthologue of FT. *Proc. Natl. Acad. Sci.* 103, 19581–19586. doi: 10.1073/pnas.0607142103

Yan, L., Loukoianov, A., Blechl, A., Tranquilli, G., Ramakrishna, W., SanMiguel, P., et al. (2004). The wheat VRN2 gene is a flowering repressor down-regulated by vernalization. *Science* 303, 1640–1644. doi: 10.1126/science.1094305

Yan, L., Loukoianov, A., Tranquilli, G., Helguera, M., Fahima, T., and Dubcovsky, J. (2003). Positional cloning of the wheat vernalization gene VRN1. *Proc. Natl. Acad. Sci.* 100, 6263–6268. doi: 10.1073/pnas.0937399100

Yuan, W., Luo, X., Li, Z., Yang, W., Wang, Y., Liu, R., et al. (2016). A cis cold memory element and a trans epigenome reader mediate Polycomb silencing of FLC by vernalization in *Arabidopsis*. *Nat. Genet.* 48, 1527–1534. doi: 10.1038/ng.3712

Zhao, T., Ni, Z., Dai, Y., Yao, Y., Nie, X., and Sun, Q. (2006). Characterization and expression of 42 MADS-box genes in wheat (*Triticum aestivum* L.). *Mol. Gen. Genomics.* 276, 334–350. doi: 10.1007/s00438-006-0147-3

Conflict of Interest: The authors declare that the research was conducted in the absence of any commercial or financial relationships that could be construed as a potential conflict of interest.

Copyright © 2020 Kennedy and Geuten. This is an open-access article distributed under the terms of the Creative Commons Attribution License (CC BY). The use, distribution or reproduction in other forums is permitted, provided the original author(s) and the copyright owner(s) are credited and that the original publication in this journal is cited, in accordance with accepted academic practice. No use, distribution or reproduction is permitted which does not comply with these terms.

frontiers in Plant Science

MINI REVIEW
published: 13 January 2021
doi: 10.3389/fpls.2020.620155

Resetting *FLOWERING LOCUS C* Expression After Vernalization Is Just Activation in the Early Embryo by a Different Name

E. Jean Finnegan, Masumi Robertson and Chris A. Helliwell*

Commonwealth Scientific and Industrial Research Organisation (CSIRO) Agriculture and Food, Canberra, ACT, Australia

The reproductive success of many plants depends on their capacity to respond appropriately to their environment. One environmental cue that triggers flowering is the extended cold of winter, which promotes the transition from vegetative to reproductive growth in a response known as vernalization. In annual plants of the *Brassicaceae*, the floral repressor, *FLOWERING LOCUS C* (*FLC*), is downregulated by exposure to low temperatures. Repression is initiated during winter cold and then maintained as the temperature rises, allowing plants to complete their life cycle during spring and summer. The two stages of *FLC* repression, initiation and maintenance, are distinguished by different chromatin states at the *FLC* locus. Initiation involves the removal of active chromatin marks and the deposition of the repressive mark H3K27me3 over a few nucleosomes in the initiation zone, also known as the nucleation region. H3K27me3 then spreads to cover the entire locus, in a replication dependent manner, to maintain *FLC* repression. *FLC* is released from repression in the next generation, allowing progeny of a vernalized plant to respond to winter. Activation of *FLC* in this generation has been termed resetting to denote the restoration of the pre-vernalized state in the progeny of a vernalized plant. It has been assumed that resetting must differ from the activation of *FLC* expression in progeny of plants that have not experienced winter cold. Considering that there is now strong evidence indicating that chromatin undergoes major modifications during both male and female gametogenesis, it is time to challenge this assumption.

Keywords: vernalized state, epigenetic memory, histone H3, chromatin, gametogenesis

OPEN ACCESS

Edited by:
Richard Amasino, University of Wisconsin-Madison, United States

Reviewed by:
Yuehui He, Chinese Academy of Sciences (CAS), China
Martin Howard, John Innes Centre, United Kingdom

****Correspondence:***
E. Jean Finnegan
jean.finnegan@csiro.au

Specialty section:
This article was submitted to Plant Development and EvoDevo, a section of the journal Frontiers in Plant Science

Received: *22 October 2020*
Accepted: *08 December 2020*
Published: *13 January 2021*

Citation:
Finnegan EJ, Robertson M and Helliwell CA (2021) Resetting FLOWERING LOCUS C Expression After Vernalization Is Just Activation in the Early Embryo by a Different Name. Front. Plant Sci. 11:620155. doi: 10.3389/fpls.2020.620155

INTRODUCTION

Plants must respond to environmental challenges to ensure their survival or reproductive success by changing patterns of gene expression. Gene expression is modulated not only by transcription factors but also by the associated chromatin environment, which can influence expression long after the event that triggered changes in local chromatin. Vernalization, the promotion of flowering in response to the prolonged cold of winter, is a well-studied example of the long-term memory provided by the epigenome (reviewed in Berry and Dean, 2015). In annual plants, the vernalized state is established during winter, maintained through the life

of the vernalized plant but is reset in the progeny so that each generation can respond appropriately to the seasonal cycles (Lang, 1965). The timing of resetting differs in perennials in which vegetative growth is restored in some shoots on return to warmer conditions (reviewed in Turck and Coupland, 2014).

In *Arabidopsis thaliana*, the key gene in the vernalization response is the repressor of flowering, *FLOWERING LOCUS C* (*FLC*), which is downregulated by low temperatures. Initially repression is transient, but *FLC* repression is stabilized as the duration of the exposure to low temperature increases (Angel et al., 2011). As ambient temperatures rise at the end of winter, *FLC* repression is maintained allowing the induction of two promoters of flowering, *FLOWERING LOCUS T* (*FT*) and *SUPPRESSOR OF CONSTANS 1* (*SOC1*), and the subsequent transition to flowering (Helliwell et al., 2006; Searle et al., 2006). *FLC* is released from repression in the next generation allowing the progeny of a vernalized plant to respond to winter (Sheldon et al., 2000). Activation of *FLC* in the next generation has been termed resetting to denote restoration of the non-vernalized state in the progeny of a vernalized plant. The process of resetting the vernalized state has long intrigued biologists because tissues giving rise to male and female gametes are not set aside early in embryo development as they are in mammals, but rather develop from somatic tissue that has accumulated changes to the epigenome during vegetative growth (reviewed in Gehring, 2019).

The molecular events associated with the long-term repression of *FLC* have been elucidated. In contrast to the gradual decline in the abundance of *FLC* mRNA that occurs during an extended period at low temperatures, the downregulation of transcription occurs more rapidly, and this may be initiated by a cold-induced physical change in *FLC* chromatin (Csorba et al., 2014; Finnegan, 2015; Helliwell et al., 2015; Rosa et al., 2016). Cold exposure also results in the induction of antisense transcripts, collectively known as *COOLAIR*, as well as *VERNALIZATION INSENSITIVE 3* (*VIN3*), a PHD domain protein that associates with a vernalization-specific polycomb repression complex, Polycomb Repressive Complex 2 (PRC2; Sung and Amasino, 2004; de Lucia et al., 2008; Swiezewski et al., 2009). Initially repression of *FLC* is transient but becomes stabilized in a time dependent manner that is cell (and locus) autonomous (Angel et al., 2011; Berry et al., 2015; Yang et al., 2017). This switch is associated with stabilization of the nucleosome in the +1 position relative to transcription, loss of active chromatin marks, and gain of H3K27me3 within the nucleation region of *FLC* chromatin that encompasses the +1 nucleosome (Finnegan and Dennis, 2007; Angel et al., 2011; Finnegan, 2015). After winter ends, H3K27me3 then spreads across the entire locus in a DNA replication-dependent process (Finnegan and Dennis, 2007; Angel et al., 2011; Hyun et al., 2013; Finnegan, 2015; Yang et al., 2017). PRC2 activity is essential for the switch between transient and stable repression, suggesting that H3K27me3 accumulation is important for stable repression (Gendall et al., 2001; Helliwell et al., 2011; Yang et al., 2017). Recruitment of PRC2 to *FLC* chromatin is facilitated by the binding of the B3 transcriptional repressors, VAL1 and/or VAL2, to RY-1 and RY-2 motifs (TGCATG; R, purine, Y, pyrimidine; Swaminathan et al., 2008) that constitute a cold memory element (CME) within the nucleation region of *FLC*, during cold exposure (Questa et al., 2016; Yuan et al., 2016). VAL1 interacts directly with components of PRC1 and PRC2 (AtBMI1 and LHP1, respectively), and SAP18, part of the SIN3-histone deactylase complex that in turn binds the histone deactylase HDA19, to shut down transcription and indirectly recruit PRC2 (Questa et al., 2016; Yuan et al., 2016). It has long been thought that resetting reverses these changes by the removal of H3K27me3 and activation of *FLC* transcription. This could occur prior to, or during, gamete formation in the vernalized plant or post-fertilization, in the developing embryo. To determine whether resetting is a process unique to vernalized plants, we must first consider the timing and genetic requirements for expression of *FLC* in each generation of non-vernalized plants.

FLC EXPRESSION MUST BE ACTIVATED IN THE EMBRYOS OF NON-VERNALIZED PLANTS

An *FLC::GUS* reporter construct, which mirrors the endogenous *FLC* gene, is expressed throughout the somatic tissues of non-vernalized plants and in both the carpel and stamens, but there is no expression in either the developing gametophytic embryo sac or in mature pollen (**Figure 1A**; Sheldon et al., 2008; Choi et al., 2009). Thus, even in the absence of vernalization, *FLC* is repressed during gametogenesis and must, therefore, be activated in the next generation. Activation of *FLC::GUS* is initiated at the earliest stage of embryo development although some β-glucuronidase (GUS) activity may result from maternal mRNA inherited *via* the egg cell (Sheldon et al., 2008; Tao et al., 2017; Luo et al., 2020). *FLC::GUS* expression continues to increase until early heart stage and is then maintained for the duration of embryo development (**Figure 1A**; Sheldon et al., 2008; Tao et al., 2017; Luo et al., 2020). In somatic tissue, a complex of proteins, the FRI complex (FRI^c), which includes FRI, FRL1, FES, FLX, and SUF4, is required for expression of *FLC* (Choi et al., 2011). However, *FLC::GUS* is activated in young embryos in both *fri* and *suf4* mutants, suggesting that FRI^c is not essential for activation of *FLC* in the early stages, although it promotes *FLC* expression in globular embryos and throughout the later stages of embryo development (Choi et al., 2009; Tao et al., 2019). This raises the question of what initiates *FLC* expression in the zygote.

As *FLC* expression is observed as early as 1 day after pollination (DAP), it was proposed that activation of *FLC* would most likely involve the action of an embryo transcription factor (Tao et al., 2017). *LEAFY COTYLEDON 1* (*LEC1*), which is expressed in the zygote and throughout embryogenesis, is a component of a seed specific NF-Y (nuclear factor of the Y box) transcription factor that is a master regulator of embryo development (Lotan et al., 1998; Le et al., 2010). NF-Y transcription factors are conserved across kingdoms and have been shown to act as pioneer transcription factors that can bind their target recognition site in the context of nonmodified chromatin or even closed chromatin marked with the repressive

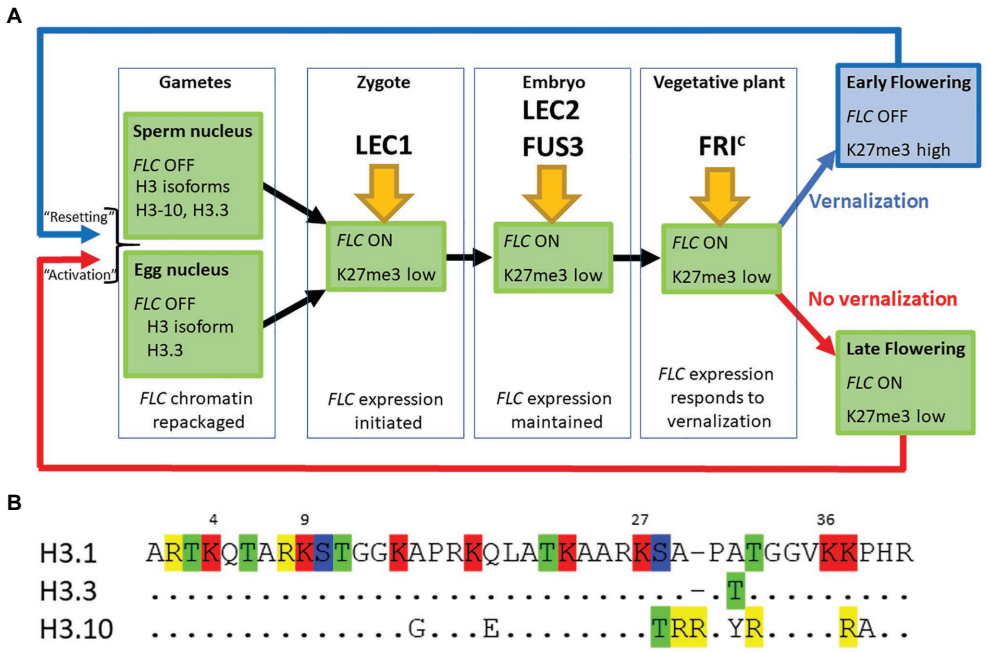

FIGURE 1 | (A) *FLOWERING LOCUS C* (*FLC*) expression is established in the zygote and maintained through the life of the plant unless the plant becomes vernalized by exposure to prolonged cold during winter. *FLC* is inactive in mature gametes of both vernalized and non-vernalized plants where the chromatin is repackaged and epigenetic marks are lost. The major transcription factors determining *FLC* expression at each developmental stage are indicated. **(B)** The first 40 amino acids of three different isoforms of Histone H3 are shown. Single letter nomenclature is used and the dots shown in H3.3 and H3.10 indicate that the sequence is conserved with H3.1. The commonly methylated lysines are numbered above the sequence. Amino acids that can be modified are highlighted; R, me; T, ph; K, ac/me; S, ph. H3.10 and H3.3 each have the potential for novel modifications not seen in H3.1 and the substitution S-T28 (H3.10) may disrupt the activity of the kinase that normally phosphorylates that position. The changes adjacent to K27 may also prevent methylation of that residue. H3.1 denoted the protein encoded by *HTR3*, H3.10 by *HTR10*, and H3.3 by *HTR5*.

modification, H3K27me3 (Fleming et al., 2013). They are comprised of three subunits, NF-YA, a site-specific DNA binding protein that targets CCAAT motifs and two proteins with a histone-domain fold, NF-YB and NF-YC that are structurally related to Histone H2B and H2A, respectively (reviewed in Mantovani, 1999).

To investigate the role of NF-Y on *FLC* activation, a null mutant of lec1, one of 10 NF-YB subunits encoded by the *Arabidopsis* genome, was introduced into Col^{FRISf2}. Loss of LEC1 activity partially suppresses the late flowering phenotype in non-vernalized plants, and the expression of both *FLC::GUS* and endogenous *FLC* is reduced throughout embryo development. Once established, the level of *FLC* expression appears to be fixed as the proportion of embryos showing weak, intermediate, or strong expression remains consistent across the first 3 DAP (**Table 1A**; Tao et al., 2017). *FLC* expression is even lower in embryos where there was decreased activity of all five members of the *LEC1* clade, indicating that NF-YB subunits from this clade act redundantly to activate the level of *FLC* in the zygote (Tao et al., 2017). Several lines of evidence indicate that LEC1 directly activates *FLC*. Mutation of the four putative NF-Y binding sites in the *FLC* promoter leads to early flowering; LEC1::FLAG is enriched at this region of the *FLC* promoter; *FLC* expression is induced in response to ectopic induction of a *LEC1* transgene and this is associated with the establishment of active chromatin at *FLC* (Tao et al., 2017).

TABLE 1 | GUS expression during embryo development is determined by the activity of LEC1 in the zygote **(A)** or FUS3 activity in the embryo (**B**; adapted from Tao et al., 2017, 2019).

(A)				
Genotype	**LEC1 FLC::GUS**	**lec1 FLC::GUS**		
Phenotype	Very strong	Weak	Intermediate	Strong – very strong
1 DAP	96%	28%	49%	23%
2 DAP	98%	29%	49%	22%
3 DAP	98%	29%	48%	23%
(B)				
Genotype	**FUS3 FLC::GUS**	**fus3 FLC::GUS**		
Phenotype	Very strong	Weak	Intermediate	Strong – very strong
3 DAP	97%	12%	55%	32%

While LEC1 is key to the activation of *FLC* in the zygote, two other embryo-specific transcription factors, LEC2 and FUSCA 3 (FUS3), are needed to maintain *FLC* expression from 2 DAP (**Figure 1A**; Tao et al., 2019). LEC2 and FUS3 are B3 domain transcription factors that are in the same subfamily as VAL1 and VAL2, proteins that recruit PRC2 to *FLC* chromatin during vernalization (Yuan et al., 2016). In *lec2* or *fus3* single mutants, *FLC::GUS* is re-activated in the

zygote, just as it is in wild type plants, but *FLC::GUS* expression in some embryos declined from 2 DAP (*lec*2) and 3 DAP (*fus*3; **Table 1B**). Binding of LEC2 and FUS3 to the CME within *FLC* chromatin is facilitated by LEC1. As enrichment of first LEC2 and then FUS3 increases from 2 to 6 DAP, there is a corresponding decrease in enrichment of VAL1 at the CME, suggesting that LEC2 and FUS3 antagonize VAL1 binding at the CME during embryogenesis to ensure that *FLC* transcription is maintained following activation by LEC1 (Tao et al., 2019). LEC2 and FUS3 interact with FRI and are required for the recruitment of FRI to the CME and adjacent regions of the *FLC* locus, consistent with the finding that FRI promotes *FLC* expression from 3 DAP. While LEC2 and FUS3 play an important role in maintaining *FLC* expression during early embryogenesis, these proteins are not expressed in post-embryonic stages of *Arabidopsis* allowing VAL1/2 to bind the CME and mediate *FLC* repression during vernalization.

WHAT DO WE KNOW ABOUT RESETTING OF THE VERNALIZED STATE?

The resetting of epigenetic regulation in plants varies with the epigenetic modifier involved (Gehring, 2019); for example, there is little evidence to support widespread erasure and replacement of DNA methylation in the developing plant embryo, as occurs in mammalian embryos, because epialleles can be stably inherited between plant generations (Becker et al., 2011; Schmitz et al., 2011). In contrast, the vernalized state, which is mediated by changes in histone modifications at *FLC* chromatin, is reset in each generation (Sheldon et al., 2000). Resetting of *FLC* expression in male and female gametes, the zygote, and developing embryo was examined using an *FLC::GUS* reporter construct (Sheldon et al., 2008; Choi et al., 2009).

Although some GUS activity can be detected in the developing anther, there is no GUS activity in mature pollen or the female gametophyte of vernalized plants (Sheldon et al., 2008; Choi et al., 2009). The timing of *FLC::GUS* reactivation differs between the paternally and maternally inherited transgene. The paternally derived *FLC::GUS* is expressed in up to 50% single-celled zygotes and expression continues throughout embryo development. When inherited from the vernalized maternal parent, expression of *FLC::GUS* is not detected until about 3 DAP (Sheldon et al., 2008). Neither maternally nor paternally inherited *FLC:GUS* are expressed in the fertilized central cell or the developing endosperm (Sheldon et al., 2008).

A mutagenesis screen for resetting mutants identified a hypomorphic mutation in *EARLY FLOWERING 6* (*ELF6*) that impairs resetting of the vernalized state and *FLC* expression in the progeny of vernalized *elf6-5* plants (Crevillen et al., 2014). ELF6 is a jumonji-domain-containing protein that demethylates di- and tri-methylated H3K27, and consistent with this, there is a small increase in H3K27me3 in some regions of *FLC* chromatin associated with somewhat lower *FLC* expression in non-vernalized *elf6-5* plants compared to wild type. Curiously, a null mutant, *elf6-3*, which also has reduced *FLC* expression prior to vernalization, shows no effect on resetting (Crevillen et al., 2014; Tao et al., 2017). A second weak mutant of ELF6, *elf6-4*, also has no effect on the resetting of *FLC* in progeny of a vernalized plant (Tao et al., 2017). Taken together, these observations suggest that ELF6 plays at most a minor role in reactivating *FLC* expression to pre-vernalized levels.

LEC1, LEC2, and FUS3 are essential for resetting expression of *FLC* in the progeny of vernalized plants just as they are for activation of *FLC* in the embryos of non-vernalized plants (**Figure 1A**; Tao et al., 2017, 2019). Consistent with this, the timing of *FLC::GUS* expression is similar in embryos of both vernalized and non-vernalized plants (Tao et al., 2017).

DISCUSSION

Our comparison of the genetic requirements for resetting of *FLC* in the progeny of a vernalized plant and those associated with the activation of *FLC* in the young embryo of non-vernalized parents indicates that there is essentially no difference between these processes (**Figure 1A**). This may seem surprising given that repression of *FLC* during vernalization causes the depletion of active chromatin marks followed by an enrichment with the repressive chromatin modification H3K27me3 across the entire *FLC* locus. We suggest that changes in the nucleosome composition of chromatin that occur during gametogenesis could account in part for these findings (**Figures 1A**,**B**).

Firstly, the chromatin of mature sperm cells differs from that in somatic tissue as sperm chromatin lacks histone H3.1, the H3 isoform associated with H3K27me3 (**Figure 1A**). Instead, sperm chromatin is enriched in H3.10, encoded by the sperm-specific gene *HTR10*, and an H3.3 isoform encoded by *HTR5* (Okada et al., 2005; Rotman et al., 2005; Brownfield et al., 2009; Ingouff et al., 2010; Borg et al., 2011). It has recently been shown that amino acid substitutions around the critical K27 residue in H3.10 (**Figure 1B**) prevent trimethylation of this residue by PRC2 (Borg et al., 2020). Indeed, H3K27me3 is barely detectable in sperm chromatin and, consistent with this, components of PRC2 are not expressed in *Arabidopsis* sperm cells (Borg et al., 2020). Similarly in monocots, H3K27me3 is observed only in the chromatin of the vegetative cell but not of sperm cells (Sano and Tanaka, 2010; Houben et al., 2011; Pandey et al., 2013). This suggests that the chromatin associated with *FLC* loci, inherited through the paternal gamete of a vernalized plant, would have been stripped of the repressive H3K27me3 mark prior to fertilization. It is hardly surprising then that an *ELF6* null mutant has little effect on resetting (Crevillen et al., 2014; Tao et al., 2017).

Secondly, chromatin dynamics during the development of the mature egg cell are extremely complex and include waves of depletion and presumptive restoration of H3K27m3 (as judged by chromatin localization of LHP1; Baroux and Autran, 2015). Like the sperm cell nuclei, the egg nucleus has a novel complement of histone variants, expressing only *HTR5*, an isoform of H3.3 (**Figures 1A**,**B**). Recent data suggest that the vernalized state is transmitted through egg cell chromatin and

that the vernalized state is not erased immediately following fertilization (Luo et al., 2020); this is consistent with the observation that *FLC::GUS* inherited from a vernalized maternal parent is not detected until about 3 DAP (Sheldon et al., 2008).

Finally, after fertilization, the paternally inherited H3.10 and the maternally inherited H3.3 are actively removed from chromatin in the zygote but the somatic complement of histone variants is not restored until after *de novo* synthesis of H3.1 and H3.3 during the first zygotic mitosis (Ingouff et al., 2007, 2010). It seems likely then that resetting is merely a consequence of the normal processes by which chromatin is remodeled during gametogenesis and following fertilization.

In conclusion, we suggest that the steps required to activate *FLC* expression in the young embryo are nearly identical regardless of whether the embryo is the progeny of a vernalized or non-vernalized plant. In each case, the chromatin associated with *FLC* loci undergoes major reprogramming during male and female gametogenesis. A shared route to *FLC* activation (**Figure 1A**) is supported by genetic data showing that the pioneer transcription factor NF-Y and the SWIR chromatin remodeling complex that deposits H2A.Z into chromatin are essential for activating *FLC* expression (Choi et al., 2011; Tao et al., 2017), with LEC2, FUS3, and FRI^c being required to fully activate *FLC* expression beyond the day after fertilization (Choi et al., 2009; Tao et al., 2019).

AUTHOR CONTRIBUTIONS

EF developed the concept and wrote the manuscript. MR and CH edited the manuscript and designed the figures. All authors contributed to the article and approved the submitted version.

REFERENCES

Angel, A., Song, J., Dean, C., and Howard, M. (2011). A Polycomb-based switch underlying quantitative epigenetic memory. *Nature* 476, 106–108. doi: 10.1038/nature10241

Baroux, C., and Autran, D. (2015). Chromatin dynamics during cellular differentiation in the female reproductive lineage of flowering plants. *Plant J.* 83, 160–176. doi: 10.1111/tpj.12890

Becker, C., Hagmann, J., Muller, J., Koenig, D., Stegle, O., Borgwardt, K., et al. (2011). Spontaneous epigenetic variation in the *Arabidopsis thaliana* methylome. *Nature* 480, 245–249. doi: 10.1038/nature10555

Berry, S., and Dean, C. (2015). Environmental perception and epigenetic memory: mechanistic insight through *FLC*. *Plant J.* 83, 133–148. doi: 10.1111/tpj.12869

Berry, S., Hartley, M., Olsson, T. S. G., Dean, C., and Howard, M. (2015). Local chromatin environment of a Polycomb target gene instructs its own epigenetic inheritance. *eLife* 4:e07205. doi: 10.7554/eLife.07205

Borg, M., Brownfield, L., Khatab, H., Sidorova, A., Lingaya, M., and Twell, D. (2011). The R2R3 MYB transcription factor DUO1 activates a male germline-specific regulon essential for sperm cell differentiation in *Arabidopsis*. *Plant Cell* 23, 534–549. doi: 10.1105/tpc.110.081059

Borg, M., Jacob, Y., Susaki, D., LeBlanc, C., Buendia, D., Axelsson, E., et al. (2020). Targeted reprogramming of H3K27me3 resets epigenetic memory in plant paternal chromatin. *Nat. Cell Biol.* 22, 621–629. doi: 10.1038/s41556-020-0515-y

Brownfield, L., Hafidh, S., Borg, M., Sidorova, A., and Twell, D. (2009). A plant germline-specific integrator of sperm specification and cell cycle progression. *PLoS Genet.* 5:e1000430. doi: 10.1371/journal.pgen.1000430

Choi, J., Hyun, Y., Kang, M. -J., Yun, H. I., Yun, J. -Y., Lister, C., et al. (2009). Resetting and regulation of *FLOWERING LOCUS C* expression during *Arabidopsis* reproductive development. *Plant J.* 57:918–931. doi: 10.1111/j.1365-313X.2008.03776.x

Choi, K., Kim, J., Hwang, H. -J., Kim, S., Park, C., Kim, S. Y., et al. (2011). The FRIGIDA complex activates transcription of *FLC*, a strong flowering repressor in *Arabidopsis*, by recruiting chromatin modification factors. *Plant Cell* 23, 289–303. doi: 10.1105/tpc.110.075911

Crevillen, P., Yang, H., Cui, X., Greeff, C., Trick, M., Qiu, Q., et al. (2014). Epigenetic reprogramming that prevents transgenerational inheritance of the vernalized state. *Nature* 515, 587–590. doi: 10.1038/nature13722

Csorba, T., Questa, J. I., Sun, Q., and Dean, C. (2014). Antisense *COOLAIR* mediates the coordinated switching of chromatin states at *FLC* during vernalization. *Proc. Natl. Acad. Sci. U. S. A.* 111, 16160–16165. doi: 10.1073/pnas.1419030111

de Lucia, F., Crevillen, P., Jones, A. M. E., Greb, T., and Dean, C. (2008). A PHD-polycomb repressive complex 2 triggers the epigenetic silencing of *FLC* during vernalization. *Proc. Natl. Acad. Sci. U. S. A.* 105, 16831–16836. doi: 10.1073/pnas.0808687105

Finnegan, E. J. (2015). Time-dependent stabilization of the +1 nucleosome is an early step in the transition to stable cold-induced repression of *FLC*. *Plant J.* 84, 875–885. doi: 10.1111/tpj.13044

Finnegan, E. J., and Dennis, E. S. (2007). Vernalization-induced trimethylation of histone H3 lysine 27 at *FLC* is not maintained in mitotically quiescent cells. *Curr. Biol.* 17, 1978–1983. doi: 10.1016/j.cub.2007.10.026

Fleming, J. D., Pavesi, G., Benatti, P., Imbriano, C., Mantovani, R., and Struhl, K. (2013). NF-Y coassociates with FOS at promoters, enhancers, repetitive elements, and inactive chromatin regions, and is stereo-positioned with growth-controlling transcription factors. *Genome Res.* 23, 1195–1209. doi: 10.1101/gr.148080.112

Gehring, M. (2019). Epigenetic dynamics during flowering plant reproduction: evidence for reprogramming? *New Phytol.* 224, 91–96. doi: 10.1111/nph.15856

Gendall, A. R., Levy, Y. Y., Wilson, A., and Dean, C. (2001). The *VERNALIZATION 2* gene mediates the epigenetic regulation of vernalization in *Arabidopsis*. *Cell* 107, 525–535. doi: 10.1016/s0092-8674(01)00573-6

Helliwell, C. A., Anderssen, R. A., Robertson, M., and Finnegan, E. J. (2015). How is *FLC* repressed by cold? *Trends Plant Sci.* 20, 76–82. doi: 10.1016/j.tplants.2014.12.004

Helliwell, C. A., Robertson, M., Finnegan, E. J., Buzas, D. M., and Dennis, E. S. (2011). Vernalization-repression of *Arabidopsis FLC* requires promoter sequences but not antisense transcripts. *PLoS One* 6:e21513. doi: 10.1371/journal.pone.0021513

Helliwell, C. A., Wood, C. C., Robertson, M., Peacock, W. J., and Dennis, E. S. (2006). The *Arabidopsis* FLC protein interacts directly *in vivo* with *SOC1* and *FT* chromatin and is part of a high-molecular-weight complex. *Plant J.* 46, 183–192. doi: 10.1111/j.1365-313X.2006.02686.x

Houben, A., Kumke, K., Nagaki, K., and Hause, G. (2011). CENH3 distribution and differential chromatin modifications during pollen development in rye (*Secale cereale* L.). *Chromosom. Res.* 19, 471–480. doi: 10.1007/s10577-011-9207-6

Hyun, Y., Yun, H., Park, K., Ohr, H., Lee, O., Kim, D. -H., et al. (2013). The catalytic subunit of *Arabidopsis* DNA polymerase α ensures stable maintenance of histone modification. *Development* 140, 156–166. doi: 10.1242/dev.084624

Ingouff, M., Hamamura, Y., Gourgues, M., Higashiyama, T., and Berger, F. (2007). Distinct dynamics of HISTONE3 variants between the two fertilization products in plants. *Curr. Biol.* 17, 1032–1037. doi: 10.1016/j.cub.2007.05.019

Ingouff, M., Rademacher, S., Holec, S., Soljic, L., Xin, N., Readshaw, A., et al. (2010). Zygotic resetting of the HISTONE 3 variant repertoire participates in epigenetic reprogramming in *Arabidopsis*. *Curr. Biol.* 20, 2137–2143. doi: 10.1016/j.cub.2010.11.012

Lang, A. (1965). "Physiology of flower initiation" in *Encyclopedia of plant physiology*. ed. W. Ruhland (Berlin: Springer Verlag), 1489–1536.

Le, B. H., Cheng, C., Bui, A. Q., Wagmaister, J. A., Henrya, K. F., Pelletier, J., et al. (2010). Global analysis of gene activity during *Arabidopsis* seed

development and identification of seed-specific transcription factors. *Proc. Natl. Acad. Sci. U. S. A.* 107, 8063–8070. doi: 10.1073/pnas.1003530107

Lotan, T., Ohto, M., Yee, K. M., West, M. A. L., Lo, R., Kwong, R. W., et al. (1998). *Arabidopsis* LEAFY COTYLEDON1 is sufficient to induce embryo development in vegetative cells. *Cell* 93, 1195–1205. doi: 10.1016/s0092-8674(00)81463-4

Luo, X., Ou, Y., Li, R., and He, Y. (2020). Maternal transmittion of the epigenetic 'memory of winter cold' in *Arabidopsis*. *Nat. Plants* 6, 1211–1218. doi: 10.1038/s41477-020-00774-0

Mantovani, R. (1999). The molecular biology of the CCAAT-binding factor NF-Y. *Gene* 239, 15–27. doi: 10.1016/s0378-1119(99)00368-6

Okada, T., Endo, M., Singh, M. B., and Bhalla, P. L. (2005). Analysis of the histone H3 gene family in *Arabidopsis* and identification of the male-gamete-specific variant *AtMGH3*. *Plant J.* 44, 557–568. doi: 10.1111/j.1365-313X.2005.02554.x

Pandey, P., Houben, A., Kumlehn, J., Melzer, M., and Rutten, T. (2013). Chromatin alterations during pollen development in *Hordeum vulgare*. *Genome Res.* 141, 50–57. doi: 10.1159/000351211

Questa, J. I., Song, J., Geraldo, N., An, A., and Dean, C. (2016). *Arabidopsis* transcriptional repressor VAL1 triggers Polycomb silencing at *FLC* during vernalization. *Science* 353, 485–488. doi: 10.1126/science.aaf7354

Rosa, S., Duncan, S., and Dean, C. (2016). Mutually exclusive sense–antisense transcription at *FLC* facilitates environmentally induced gene repression. *Nat. Commun.* 7:13031. doi: 10.1038/ncomms13031

Rotman, N., Durbarry, N., Wardle, A., Yang, W. C., Chabourd, A., Faure, J. E., et al. (2005). A novel class of MYB factors controls sperm-cell formation in plants. *Curr. Biol.* 15, 244–248. doi: 10.1016/j.cub.2005.01.013

Sano, Y., and Tanaka, I. (2010). Distinct localization of histone H3 methylation in the vegetative nucleus of lily pollen. *Cell Biol. Int.* 34, 253–259. doi: 10.1042/CBI20090124

Schmitz, R. J., Schultz, M. D., Lewsey, M. G., O'Malley, R. C., Urich, M. A., Libiger, O., et al. (2011). Transgenerational epigenetic instability is a source of novel methylation variants. *Science* 334, 369–373. doi: 10.1126/science.1212959

Searle, I., He, Y., Turck, F., Vincent, C., Fornara, F., Krober, S., et al. (2006). The transcription factor FLC confers a flowering response to vernalization by repressing meristem competence and systemic signaling in *Arabidopsis*. *Genes Dev.* 20, 898–912. doi: 10.1101/gad.373506

Sheldon, C. C., Hills, M. J., Lister, C., Dean, C., Dennis, E. S., and Peacock, W. J. (2008). Resetting of *FLOWERING LOCUS C* expression after epigenetic repression by vernalization. *Proc. Natl. Acad. Sci. U. S. A.* 105, 2214–2219. doi: 10.1073/pnas.0711453105

Sheldon, C. C., Rouse, D. T., Finnegan, E. J., Peacock, W. J., and Dennis, E. S. (2000). The molecular basis of vernalization: the central role of *FLOWERING LOCUS C* (*FLC*). *Proc. Natl. Acad. Sci. U. S. A.* 97, 3753–3758. doi: 10.1073/pnas.060023597

Sung, S., and Amasino, R. M. (2004). Vernalization in *Arabidopsis thaliana* is mediated by the PHD finger protein VIN3. *Nature* 427, 159–164. doi: 10.1038/nature02195

Swaminathan, K., Peterson, K., and Jack, T. (2008). The plant B3 superfamily. *Trends Plant Sci.* 13, 647–655. doi: 10.1016/j.tplants.2008.09.006

Swiezewski, S., Liu, F., Magusin, A., and Dean, C. (2009). Cold-induced silencing by long antisense transcripts of an *Arabidopsis* Polycomb target. *Nature* 462, 799–802. doi: 10.1038/nature08618

Tao, Z., Hu, H., Luo, X., Jia, B., Du, J., and He, Y. (2019). Embryonic resetting of the parental vernalized state by two B3 domain transcription factors in *Arabidopsis*. *Nat. Plants* 5, 424–435. doi: 10.1038/s41477-019-0402-3

Tao, Z., Shen, L., Gu, X., Wang, Y., Yu, H., and He, Y. (2017). Embryonic epigenetic reprogramming by a pioneer transcription factor in plants. *Nature* 551, 124–128. doi: 10.1038/nature24300

Turck, F., and Coupland, G. (2014). Natural variation in epigenetic gene regulation and its effects on plant developmental traits. *Evolution* 68, 620–631. doi: 10.1111/evo.12286

Yang, H., Berry, S., Olsson, T. S. G., Hartley, M., Howard, M., and Dean, C. (2017). Distinct phases of Polycomb silencing to hold epigenetic memory of cold in *Arabidopsis*. *Science* 357, 1142–1145. doi: 10.1126/science.aan1121

Yuan, W., Luo, X., Li, Z., Yang, W., Wang, Y., Liu, R., et al. (2016). A *cis* cold memory element and a *trans* epigenome reader mediate Polycomb silencing of *FLC* by vernalization in *Arabidopsis*. *Nat. Genet.* 48, 1528–1534. doi: 10.1038/ng.3712

Conflict of Interest: The authors declare that the research was conducted in the absence of any commercial or financial relationships that could be construed as a potential conflict of interest.

Copyright © 2021 Finnegan, Robertson and Helliwell. This is an open-access article distributed under the terms of the Creative Commons Attribution License (CC BY). The use, distribution or reproduction in other forums is permitted, provided the original author(s) and the copyright owner(s) are credited and that the original publication in this journal is cited, in accordance with accepted academic practice. No use, distribution or reproduction is permitted which does not comply with these terms.

frontiers in Plant Science

MINI REVIEW
published: 27 January 2021
doi: 10.3389/fpls.2021.628726

Feeling Every Bit of Winter – Distributed Temperature Sensitivity in Vernalization

Rea L. Antoniou-Kourounioti[1†], Yusheng Zhao[2†], Caroline Dean[2] and Martin Howard[1*]*

[1]*Computational and Systems Biology, John Innes Centre, Norwich Research Park, Norwich, United Kingdom,* [2]*Cell and Developmental Biology, John Innes Centre, Norwich Research Park, Norwich, United Kingdom*

Temperature intrinsically influences all aspects of biochemical and biophysical processes. Organisms have therefore evolved strategies to buffer themselves against thermal perturbations. Many organisms also use temperature signals as cues to align behavior and development with certain seasons. These developmentally important thermosensory mechanisms have generally been studied in constant temperature conditions. However, environmental temperature is an inherently noisy signal, and it has been unclear how organisms reliably extract specific temperature cues from fluctuating temperature profiles. In this context, we discuss plant thermosensory responses, focusing on temperature sensing throughout vernalization in Arabidopsis. We highlight many different timescales of sensing, which has led to the proposal of a distributed thermosensing paradigm. Within this paradigm, we suggest a classification system for thermosensors. Finally, we focus on the longest timescale, which is most important for sensing winter, and examine the different mechanisms in which memory of cold exposure can be achieved.

Keywords: vernalization, temperature-sensing, mathematical modeling, *FLC*, Arabidopsis, climate change, temperature fluctuations

OPEN ACCESS

Edited by:
Enamul Huq,
University of Texas at Austin, United States

Reviewed by:
Ana M. Casas,
Aula Dei Experimental Station (EEAD), Spain
Toshiro Ito,
Nara Institute of Science and Technology (NAIST), Japan

***Correspondence:**
Caroline Dean
caroline.dean@jic.ac.uk
Martin Howard
martin.howard@jic.ac.uk

[†]These authors have contributed equally to this work

Specialty section:
This article was submitted to Plant Development and EvoDevo, a section of the journal Frontiers in Plant Science

Received: *12 November 2020*
Accepted: *07 January 2021*
Published: *27 January 2021*

Citation:
Antoniou-Kourounioti RL, Zhao Y, Dean C and Howard M (2021) Feeling Every Bit of Winter – Distributed Temperature Sensitivity in Vernalization. Front. Plant Sci. 12:628726. doi: 10.3389/fpls.2021.628726

INTRODUCTION

Plants control their development in response to seasonal cues. A striking example of this is the floral bloom in spring. Monitoring seasons requires that plants read noisy signals over long time periods, as, for example, sampling temperature at a single time point cannot distinguish a cool period in autumn from the full length of winter. Different reproductive strategies differentially depend on seasonal monitoring. An overwintering, or winter annual habit, necessitates exposure to winter cold and restricts plants to one generation a year, but avoids summer mortality. In contrast, a rapid-cycling strategy without a cold requirement enables multiple generations each year if conditions allow (Satake, 2010). The overwintering requirement involves the process of vernalization, the acceleration of flowering by prolonged cold. The molecular basis of vernalization has been established in Arabidopsis, and is conserved throughout the Brassicaceae and in cereals (Dixon et al., 2019). In Arabidopsis, the central regulator is the flowering repressor *FLOWERING LOCUS C* (*FLC*), whose activity represses flowering in otherwise favorable conditions. *FLC* expression is repressed by cold and becomes epigenetically silenced (Michaels and Amasino, 1999; Sheldon et al., 1999). *FLC* is a repressor of the flowering

promoter *FT*, so after a sufficiently long period of cold, this repression is released. *FT* itself also responds to temperature and daylength, so that with the long, warm days of spring, flowering is promoted.

Plants in the field experience complex temperature fluctuations and even over a single day these fluctuations can be as large as the variation between seasons (**Figure 1A**). Furthermore, seasons are variable each year, and a recent study has found that plants need longer vernalization times in regions where temperature correlations persist for longer periods (Zhao et al., 2020a), as this can lead to extended durations of unseasonable temperature. A combination of long-term temperature and short-term daylength information was found to give the best seasonal predictor. Therefore, the question of how plants sense temperature in natural conditions is of central importance, especially in times of a changing climate. In this review, we discuss this question in the context of vernalization, with a focus on the role of fluctuations and on sensing at multiple timescales, including long-term cold sensing. We concentrate on the winter sensing of the *FLC* gene and its upstream regulators in *Arabidopsis thaliana*.

DISSECTING TEMPERATURE RESPONSE IN NATURAL ENVIRONMENTS

Most knowledge of temperature sensing in plants comes from studies of plants grown under constant laboratory conditions. However, vernalization and seed dormancy in *Arabidopsis thaliana* were shown to be different in fluctuating vs. constant temperature conditions (Burghardt et al., 2016; Topham et al., 2017). Molecular analysis of the floral repressor locus, *FLC* and its regulator *VERNALIZATION INSENSITIVE3 (VIN3)*, showed that expression of neither gene responds to the average temperature, with the response instead more closely matching the extreme temperatures (Hepworth et al., 2018). In particular, *VIN3* expression is more strongly affected by the highest daily temperatures, while, independent of *VIN3*, *FLC* responds to the low temperature fluctuations. Further work (Antoniou-Kourounioti et al., 2018) showed that the night-time temperature was most important for *FLC* shutdown independently of VIN3, while *VIN3* itself responds similarly to day-time and night-time temperatures, despite having a diurnal pattern of expression (Hepworth et al., 2018).

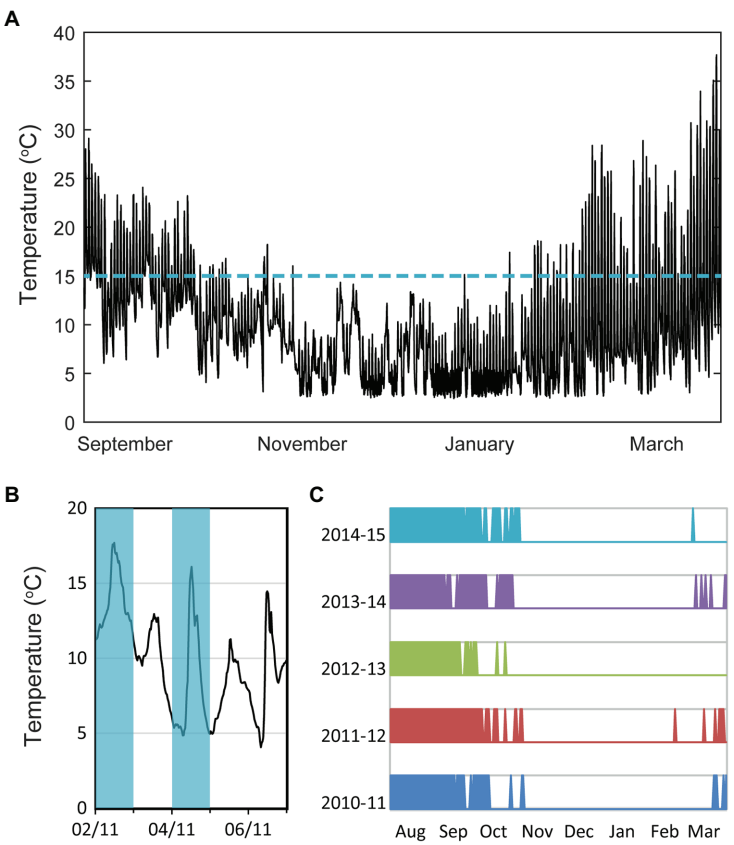

FIGURE 1 | Importance of temperature fluctuations in plant seasonal sensing. **(A)** Temperature profile at experimental site in Norwich, United Kingdom, measured over 200 days from September 29, 2014 (Hepworth et al., 2018). **(B)** Schematic of classification of days according to whether the temperature fluctuated to above 15°C or not, during the day. This classification is used in the next panel. **(C)** Data from Norwich Airport, United Kingdom for the indicated years. Information provided by the National Meteorological Library and Archive – Met Office, United Kingdom, under the Open Government License (The National Archives, n.d.). Schematic shows coloration for days where the temperature fluctuated above 15°C, and white for other days, as indicated in **(B)**. The continuous white period matches winter.

These studies demonstrate the importance of temperature fluctuations in seasonal registration, a feature which will become more pertinent as climate variability increases. Predictions of plant responses (particularly crop yield) to climate change are important for breeding and policy decisions, as there is an expectation of a decrease in yield with warming (Liu et al., 2016). To accurately predict how plants will respond to new climate conditions, we need to understand the temperature features that are being sensed by the plant directly and how these are integrated.

Recently, field studies combined with mathematical modeling have effectively revealed the properties of the temperature sensing networks, thus giving insight into the underlying mechanisms. The use of field studies enabled environmental fluctuations to be properly incorporated, while the modeling helped dissect mechanisms too complex to discern by intuition alone. This approach with *A. thaliana* at three field sites showed that the *FLC* levels in natural autumns decrease slowly while the temperature is fluctuating to above 15°C daily (Hepworth et al., 2018). The rate of decrease was faster once the daily fluctuations in temperature did not reach 15°C. This feature is a surprisingly simple and reliable signature for onset of winter in Norwich, United Kingdom (**Figures 1B,C**) but will not be reliable in other regions or under climate change. Instead, a mathematical model based on the epigenetic mechanism that controls *FLC*, and the multiple temperature features identified (described in the next section), was developed for the *A. thaliana* Col *FRI* genotype. The model was able to reproduce the *FLC* expression pattern over the three field experiments (Antoniou-Kourounioti et al., 2018). In building this model, we were able to find the minimal temperature sensing network that can mimic the properties of the true network. Such a model can also make useful predictions about gene expression and flowering time responses under any potential temperature profile. Accordingly, the model was used to predict *FLC* expression under simple climate change scenarios. In addition, earlier work with field experiments in Japan working on the perennial *A. halleri* and using mathematical modeling, showed that the average temperature of the last 6 weeks best correlates with the *FLC* expression at any time of year (Aikawa et al., 2010). By integrating field data, mathematical modeling, and transplantation experiments, Nishio et al. uncovered a comprehensive H3K27me3-mediated chromatin regulation system at *A. halleri FLC* that is required for robust gene regulation in a fluctuating natural environment (Nishio et al., 2020a,b). Overall, a field study/modeling approach can provide a route for predicting phenological shifts, and thereby helping to develop robust crops in a future changing climate.

TEMPERATURE SENSITIVITY AT DIFFERENT TIMESCALES IN A DISTRIBUTED THERMOSENSING PARADIGM

In sensing seasonal information for vernalization, plants were found to integrate temperature information over multiple timescales in the expression of the *VIN3* and *FLC* genes (Antoniou-Kourounioti et al., 2018). *VIN3* is controlled by at least three separate temperature sensing elements (Antoniou-Kourounioti et al., 2018), where temperature information at the three timescales is integrated into the regulation of *VIN3* expression (**Figure 2A**). At the longest timescale ("Long-term"), *VIN3* expression is slowly increased over weeks (Sung and Amasino, 2004; Antoniou-Kourounioti et al., 2018; Hepworth et al., 2018). A regulator controlling this increase must be slowly accumulating and so cannot also respond quickly. At the shortest timescale ("Current"), the response occurs within 1–2 h, and would override any slow response (Hepworth et al., 2018). Therefore, the same property of a regulator cannot hold both temperature inputs (of current and long-term temperature). However, parallel properties (e.g., concentration and molecular activity) could in theory each hold part of the temperature information. The third, intermediate temperature timescale ("Short-term") works over a night-and-day cycle, holding a short-term memory of recent temperature that is reset each evening, likely by the circadian clock (Antoniou-Kourounioti et al., 2018). Though the intuition described above can explain the fundamental timescale incompatibility, this issue was not obvious directly from experiments. Instead, mathematical models were developed with the aim to minimize the number of independent temperature inputs: this approach then demonstrated that multiple such inputs with different timescales were necessary.

FLC responds to temperature *via* the cold-induced VIN3, but also through a mechanism independent of VIN3, with a separate temperature input (Antoniou-Kourounioti et al., 2018). Similarly to *VIN3*, this mechanism is likely to involve multiple inputs, including through regulation of the *FLC* antisense transcript *COOLAIR* (**Figure 2A**). *COOLAIR* is cold-induced and antagonizes *FLC* expression (Swiezewski et al., 2009; Rosa et al., 2016). Furthermore, the VIN3-dependent epigenetic silencing of *FLC* has temperature sensitivity beyond the *VIN3* induction itself, as suggested by the absence of *FLC* silencing in lines expressing *VIN3* in the warm (Lee et al., 2015; Antoniou-Kourounioti et al., 2018). A candidate that could mediate this additional temperature sensitivity is VERNALIZATION2 (VRN2), a component of Polycomb Repressive Complex 2 (PRC2). VRN2 also accumulates in the cold (Wood et al., 2006) by a mechanism that involves inhibition of degradation through the Arg/N-end rule pathway (Gibbs et al., 2018). Overall, we can conclude that vernalization uses multiple temperature inputs to register the progression of winter, suggesting that multiple thermosensors are involved (**Figure 2A**).

This multiplicity of inputs required to control a single process suggested the principle of distributed thermosensing, by which the inherent temperature sensitivity of multiple molecules and reactions is combined, rather than only through specialized thermosensors (Antoniou-Kourounioti et al., 2018). The latter would require that multiple specialized sensors evolved to control each temperature responsive process, with temperature compensation used to ensure no response from many otherwise naturally temperature sensitive molecules

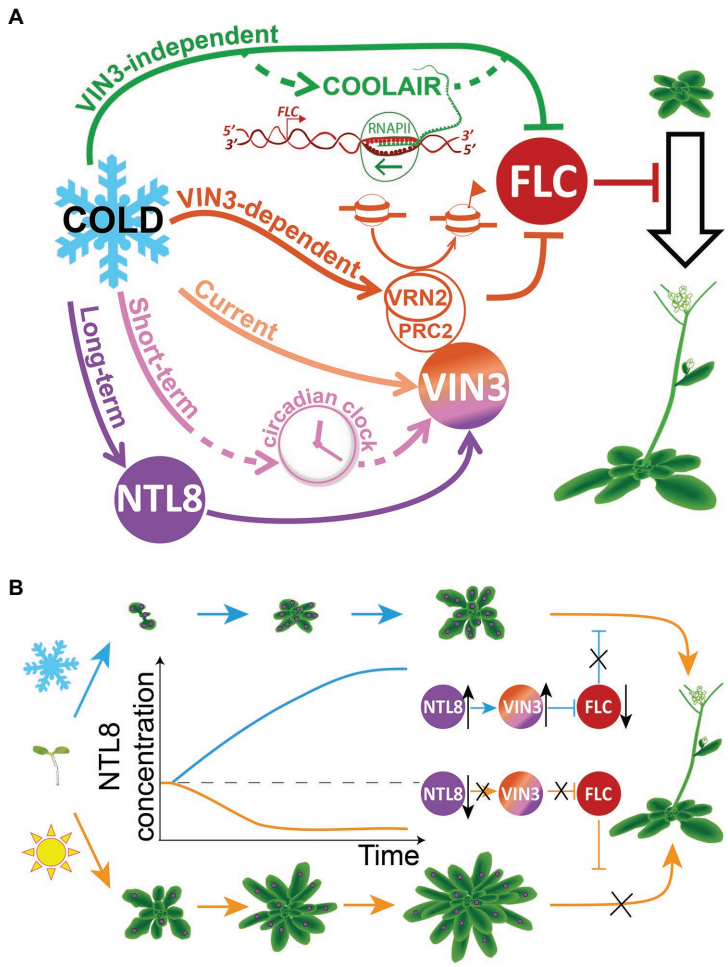

FIGURE 2 | Distributed temperature sensitivities in the regulation of *FLOWERING LOCUS C* (*FLC*) and *VERNALIZATION INSENSITIVE3* (*VIN3*), and indirect long-term temperature sensing through NTL8 during vernalization. **(A)** Temperature sensitivities are widely distributed in the regulation of *VIN3* and *FLC* during vernalization. Cold regulates *VIN3* and *FLC* through multiple pathways: at least five separate pathways have been shown to be needed. In some cases, such as the "Long-term" pathway, the mechanism and components are known (NTL8; Zhao et al., 2020b). Known and postulated components are illustrated schematically in the diagram. **(B)** Temperature-dependent growth is indirectly exploited by the NTL8 protein to sense long-term cold. NTL8 concentration decreases when the plant grows fast in the warm (bottom, orange arrows/curves), but slowly increases when the plant grows slowly in the cold (top, blue arrows/curves). The slow accumulation of NTL8 protein holds the memory of cold exposure in the cold, allowing a slow increase in VIN3 concentration, which promotes the epigenetic repression of *FLC* – a repressor of the floral transition. Purple circles on the plant indicate NTL8 protein. The total amount of protein shown is the same in warm and cold, but the concentration is different due to the difference in growth rate.

or reactions. Given that temperature compensation is probably a difficult response to generate, utilizing the widespread but weaker temperature sensitivity of many elements in distributed thermosensing is likely to be an easier strategy to evolve, as well as being highly redundant. By definition, distributed thermosensing allows a combination of many small responses to be integrated and so gives more room for a precise response to a large range of temperature stimuli. This flexibility may be needed for plants in the case of vernalization or that of thermomorphogenesis, the effect of ambient warm temperatures on plant morphogenesis, another process where multiple temperature sensors have been discovered (Jung et al., 2016; Legris et al., 2016; Chung et al., 2020; Jung et al., 2020).

CLASSIFICATION OF THERMOSENSORS

What kinds of thermosensor are possible in the distributed sensing paradigm? We suggest a classification into "direct" or "indirect" sensors, and within these two categories, a spectrum of sensitivity to temperature. In the "direct" case, there can be molecules with a strong, switch-like response to temperature changes, e.g., RNA thermoswitch (Chung et al., 2020) or the formation of speckles of ELF3 at 35°C due to its prion domain (Jung et al., 2020). These strong thermosensors are powerful, but not necessarily representative and it is important to realize that they are necessarily part of a larger network, which will itself also be thermosensitive. Molecules with weakly temperature sensitive properties are therefore likely to be pervasive within

a distributed thermosensing paradigm. These could be combined to give a synergistic response much stronger than the sum of its individual parts, giving a strongly temperature sensitive network.

In contrast, "indirect" sensors are qualitatively different: the temperature sensitivity is not in the "sensor" molecule, but instead non-temperature-sensitive properties of this molecule allow it to couple to the temperature sensitivity of a separate process. Rather than simply responding to this separate temperature input, indirect sensors can use it to measure a new feature of temperature, thus creating a temperature response that was not available in the input signal. Below, we will describe an example of this type of sensor involving NTL8, *VIN3*, and *FLC* (Zhao et al., 2020b). Stability and tissue localization allow NTL8 to use the temperature sensitivity of growth (which responds to recent temperature) to create a new temperature-sensing mechanism that measures temperature at a different timescale, in this case, long-term cold exposure duration.

Distributed sensing suggests that all of these sensor types can potentially be important for the plant to respond to temperature. Understanding how direct and indirect sensors, both strong and weak, are combined in the context of vernalization could therefore be valuable for a better understanding of temperature sensing in general.

INDIRECT LONG-TERM COLD SENSING THROUGH TEMPERATURE-DEPENDENT GROWTH

As described above, *VIN3* exhibits a long-term response to the duration of cold exposure (Antoniou-Kourounioti et al., 2018; Hepworth et al., 2018). This response was found to be graded at the single cell level, with *VIN3* expression increasing over time in each cell in the cold (Antoniou-Kourounioti et al., 2018). To understand the genetic basis of the temperature inputs of *VIN3* regulation during vernalization, a genetic screen was performed, and mutants with unusually high levels of *VIN3* expression in warm conditions were identified (Zhao et al., 2020b). These plants carry dominant mutations in the gene *NTL8* or its homolog *NTL14*, which encode proteins that directly regulate gene expression. In these mutants, NTL8 and NTL14 are more active than in the wildtype and so the mutant plants bypass the requirement of prolonged cold exposure to increase *VIN3* expression. Furthermore, in plants where both *NTL8* and *NTL14* are absent, *VIN3* expression in the cold is attenuated.

In the wildtype case, the transcript level of *NTL8* does not change over time in the cold. However, NTL8 protein concentration gradually increases. Normally, the timescale of any protein dynamics is dictated by its degradation rate. Indeed, NTL8 is quite stable, in keeping with its slow response. This protein stability is observed both in warm and cold conditions, arguing against a hypothesis whereby slow NTL8 accumulation is due to an enhanced stability of NTL8 in the cold. To help elucidate the underlying mechanism of accumulation, a computational simulation was generated to explore the effect of growth on the NTL8 protein dynamics. In warm conditions, fast growth led to the fast dilution of the NTL8 protein concentration, while slow growth in cold conditions led to slow dilution, and thus a slow, gradual increase of NTL8 protein concentration (**Figure 2B**). The mathematical model showed that slow growth alone is sufficient to drive an increase in NTL8 concentration in the cold. A clear prediction of this hypothesis was that inhibiting growth in the warm would also cause NTL8 accumulation, and this was subsequently observed experimentally. Overall, through a combination of experimental and theoretical approaches, it was demonstrated that NTL8 measures the duration of the cold at least in part through reduced dilution due to cold-inhibited growth.

We can now see why the NTL8 mechanism is an example of "indirect" sensing. Here, the long lifetime of NTL8, a property seemingly unrelated to thermosensing, is an essential requirement. This long lifetime allows NTL8 to couple to the temperature-dependent growth dynamics of the plant. Note that growth responds rapidly to temperature, yet NTL8 can respond at a much longer timescale due to its long lifetime. This allows its concentration to integrate over the plant's temperature-dependent growth history. NTL8 then transcriptionally activates *VIN3* which inputs long-term cold information into *FLC* epigenetic repression. Interestingly, the long-term cold information held *in trans* in the NTL8 cellular concentration is in a quantitative/graded form. This is in contrast to the cell-autonomous, ON/OFF digital epigenetic repression of *FLC*, mediated by histone modifications, which holds memory of the cold *in cis* after the cold has passed (Angel et al., 2011; Berry et al., 2015). These different memory systems reflect the different biophysical constraints faced by the system in the cold and warm. In the warm, growth would rapidly compromise any cold information held in a graded concentration, due to dilution. Hence, the cold duration information must be copied from the NTL8/VIN3 module to an alternative form, stable to growth, and also to DNA replication and division. This is achieved by conversion to an ON/OFF digital cis memory format encoded at *FLC* chromatin through histone modifications.

DISCUSSION

How plants integrate daily and seasonal fluctuating temperatures to maximize their fitness and survival has been a long-standing fundamental question. Recent advances in temperature sensing have revealed key features of how vernalization proceeds in the field, highlighting the importance of performing research in field conditions, or controlled fluctuating conditions in the laboratory. Such work, in combination with mathematical modeling, has uncovered a multiplicity of thermosensors and fostered the concept of distributed temperature sensing. Working within this paradigm, and our proposed thermosensor classification, will allow researchers to identify new types of sensing mechanisms with a focus on the overall thermosensory network.

Climate warming will massively affect the phenology of many plants, including major crops. Knowledge of thermosensing will be instrumental in breeding weather-proof crops in order to combat climate change. One interesting direction will be to see how the multiplicity of sensors due to the distributed thermosensing principle will be implemented in polyploid species, where multiplicity also comes from the many gene copies.

AUTHOR CONTRIBUTIONS

All authors listed have made a substantial, direct and intellectual contribution to the work, and approved it for publication.

FUNDING

This work was funded by the European Research Council grant "MEXTIM" and supported by the BBSRC Institute Strategic Programs GRO (BB/J004588/1) and GEN (BB/P013511/1).

ACKNOWLEDGMENTS

The authors would like to thank Dr. Jo Hepworth and the National Meteorological Library and Archive – Met Office, UK for providing the temperature data in **Figure 1**, and the Howard and Dean groups for useful discussions in developing these ideas.

REFERENCES

Aikawa, S., Kobayashi, M. J., Satake, A., Shimizu, K. K., and Kudoh, H. (2010). Robust control of the seasonal expression of the *Arabidopsis FLC* gene in a fluctuating environment. *Proc. Natl. Acad. Sci. U. S. A.* 107, 11632–11637. doi: 10.1073/pnas.0914293107

Angel, A., Song, J., Dean, C., and Howard, M. (2011). A Polycomb-based switch underlying quantitative epigenetic memory. *Nature* 476, 105–108. doi: 10.1038/nature10241

Antoniou-Kourounioti, R. L., Hepworth, J., Heckmann, A., Duncan, S., Questa, J., Rosa, S., et al. (2018). Temperature sensing is distributed throughout the regulatory network that controls *FLC* epigenetic silencing in vernalization. *Cell Syst.* 7, 643–655.e9. doi: 10.1016/j.cels.2018.10.011

Berry, S., Hartley, M., Olsson, T. S. G., Dean, C., and Howard, M. (2015). Local chromatin environment of a Polycomb target gene instructs its own epigenetic inheritance. *eLife* 4:e07205. doi: 10.7554/eLife.07205

Burghardt, L. T., Runcie, D. E., Wilczek, A. M., Cooper, M. D., Roe, J. L., Welch, S. M., et al. (2016). Fluctuating, warm temperatures decrease the effect of a key floral repressor on flowering time in *Arabidopsis thaliana*. *New Phytol.* 210, 564–576. doi: 10.1111/nph.13799

Chung, B. Y. W., Balcerowicz, M., Di Antonio, M., Jaeger, K. E., Geng, F., Franaszek, K., et al. (2020). An RNA thermoswitch regulates daytime growth in Arabidopsis. *Nat. Plants* 6, 522–532. doi: 10.1038/s41477-020-0633-3

Dixon, L. E., Hepworth, J., and Irwin, J. A. (2019). *Vernalisation. eLS*: John Wiley & Sons, Ltd.

Gibbs, D. J., Tedds, H. M., Labandera, A. -M., Bailey, M., White, M. D., Hartman, S., et al. (2018). Oxygen-dependent proteolysis regulates the stability of angiosperm polycomb repressive complex 2 subunit VERNALIZATION 2. *Nat. Commun.* 9:5438. doi: 10.1038/s41467-018-07875-7

Hepworth, J., Antoniou-Kourounioti, R. L., Bloomer, R. H., Selga, C., Berggren, K., Cox, D., et al. (2018). Absence of warmth permits epigenetic memory of winter in *Arabidopsis*. *Nat. Commun.* 9:639. doi: 10.1038/s41467-018-03065-7

Jung, J. -H., Barbosa, A. D., Hutin, S., Kumita, J. R., Gao, M., Derwort, D., et al. (2020). A prion-like domain in ELF3 functions as a thermosensor in Arabidopsis. *Nature* 585, 256–260. doi: 10.1038/s41586-020-2644-7

Jung, J. -H., Domijan, M., Klose, C., Biswas, S., Ezer, D., Gao, M., et al. (2016). Phytochromes function as thermosensors in *Arabidopsis*. *Science* 354, 886–889. doi: 10.1126/science.aaf6005

Lee, J., Yun, J. -Y., Zhao, W., Shen, W. -H., and Amasino, R. M. (2015). A methyltransferase required for proper timing of the vernalization response in Arabidopsis. *Proc. Natl. Acad. Sci. U. S. A.* 112, 2269–2274. doi: 10.1073/pnas.1423585112

Legris, M., Klose, C., Burgie, E. S., Rojas, C. C. R., Neme, M., Hiltbrunner, A., et al. (2016). Phytochrome B integrates light and temperature signals in *Arabidopsis*. *Science* 354, 897–900. doi: 10.1126/science.aaf5656

Liu, B., Asseng, S., Müller, C., Ewert, F., Elliott, J., Lobell, D. B., et al. (2016). Similar estimates of temperature impacts on global wheat yield by three independent methods. *Nat. Clim. Chang.* 6, 1130–1136. doi: 10.1038/nclimate3115

Michaels, S. D., and Amasino, R. M. (1999). *FLOWERING LOCUS C* encodes a novel MADS domain protein that acts as a repressor of flowering. *Plant Cell* 11, 949–956. doi: 10.1105/tpc.11.5.949

Nishio, H., Buzas, D. M., Nagano, A. J., Iwayama, K., Ushio, M., and Kudoh, H. (2020a). Repressive chromatin modification underpins the long-term expression trend of a perennial flowering gene in nature. *Nat. Commun.* 11:2065. doi: 10.1038/s41467-020-15896-4

Nishio, H., Nagano, A. J., Ito, T., Suzuki, Y., and Kudoh, H. (2020b). Seasonal plasticity and diel stability of H3K27me3 in natural fluctuating environments. *Nat. Plants* 6, 1091–1097. doi: 10.1038/s41477-020-00757-1

Rosa, S., Duncan, S., and Dean, C. (2016). Mutually exclusive sense-antisense transcription at *FLC* facilitates environmentally induced gene repression. *Nat. Commun.* 7:13031. doi: 10.1038/ncomms13031

Satake, A. (2010). Diversity of plant life cycles is generated by dynamic epigenetic regulation in response to vernalization. *J. Theor. Biol.* 266, 595–605. doi: 10.1016/j.jtbi.2010.07.019

Sheldon, C. C., Burn, J. E., Perez, P. P., Metzger, J., Edwards, J. A., Peacock, W. J., et al. (1999). The *FLF* MADS box gene: a repressor of flowering in *Arabidopsis* regulated by vernalization and methylation. *Plant Cell* 11, 445–458. doi: 10.1105/tpc.11.3.445

Sung, S., and Amasino, R. M. (2004). Vernalization in *Arabidopsis thaliana* is mediated by the PHD finger protein VIN3. *Nature* 427, 159–164. doi: 10.1038/nature02195

Swiezewski, S., Liu, F., Magusin, A., and Dean, C. (2009). Cold-induced silencing by long antisense transcripts of an *Arabidopsis* Polycomb target. *Nature* 462, 799–802. doi: 10.1038/nature08618

The National Archives (n.d.). *Open Government Licence* [Online]. Available at: http://www.nationalarchives.gov.uk/doc/open-government-licence/version/3/ (Accessed August 3, 2016).

Topham, A. T., Taylor, R. E., Yan, D., Nambara, E., Johnston, I. G., and Bassel, G. W. (2017). Temperature variability is integrated by a spatially embedded decision-making center to break dormancy in Arabidopsis seeds. *Proc. Natl. Acad. Sci.* 114, 6629–6634. doi: 10.1073/pnas.1704745114

Wood, C. C., Robertson, M., Tanner, G., Peacock, W. J., Dennis, E. S., and Helliwell, C. A. (2006). The *Arabidopsis thaliana* vernalization response requires a polycomb-like protein complex that also includes VERNALIZATION INSENSITIVE 3. *Proc. Natl. Acad. Sci. U. S. A.* 103, 14631–14636. doi: 10.1073/pnas.0606385103

Zhao, Y., Antoniou-Kourounioti, R. L., Calder, G., Dean, C., and Howard, M. (2020b). Temperature-dependent growth contributes to long-term cold sensing. *Nature* 583, 825–829. doi: 10.1038/s41586-020-2485-4

Zhao, L., Richards, S., Turck, F., and Kollmann, M. (2020a). Information integration and decision making in flowering time control. *PLoS One* 15:e0239417. doi: 10.1371/journal.pone.0239417

Conflict of Interest: The authors declare that the research was conducted in the absence of any commercial or financial relationships that could be construed as a potential conflict of interest.

Copyright © 2021 Antoniou-Kourounioti, Zhao, Dean and Howard. This is an open-access article distributed under the terms of the Creative Commons Attribution License (CC BY). The use, distribution or reproduction in other forums is permitted, provided the original author(s) and the copyright owner(s) are credited and that the original publication in this journal is cited, in accordance with accepted academic practice. No use, distribution or reproduction is permitted which does not comply with these terms.

frontiers in Plant Science

REVIEW
published: 09 February 2021
doi: 10.3389/fpls.2020.619417

Genome Triplication Leads to Transcriptional Divergence of *FLOWERING LOCUS C* Genes During Vernalization in the Genus *Brassica*

*Ayasha Akter[1,2], Etsuko Itabashi[3], Tomohiro Kakizaki[3], Keiichi Okazaki[4], Elizabeth S. Dennis[5,6] and Ryo Fujimoto[1]**

[1] Graduate School of Agricultural Science, Kobe University, Kobe, Japan, [2] Department of Horticulture, Faculty of Agriculture, Bangladesh Agricultural University, Mymensingh, Bangladesh, [3] Institute of Vegetable and Floriculture Science, National Agriculture and Food Research Organization (NARO), Tsu, Japan, [4] Graduate School of Science and Technology, Niigata University, Niigata, Japan, [5] CSIRO Agriculture and Food, Canberra, ACT, Australia, [6] School of Life Sciences, Faculty of Science, University of Technology, Sydney, Broadway, NSW, Australia

The genus *Brassica* includes oil crops, vegetables, condiments, fodder crops, and ornamental plants. *Brassica* species underwent a whole genome triplication event after speciation between ancestral species of *Brassica* and closely related genera including *Arabidopsis thaliana*. Diploid species such as *Brassica rapa* and *Brassica oleracea* have three copies of genes orthologous to each *A. thaliana* gene, although deletion in one or two of the three homologs has occurred in some genes. The floral transition is one of the crucial events in a plant's life history, and time of flowering is an important agricultural trait. There is a variation in flowering time within species of the genus *Brassica*, and this variation is largely dependent on a difference in vernalization requirements. In *Brassica*, like in *A. thaliana*, the key gene of vernalization is *FLOWERING LOCUS C* (*FLC*). In *Brassica* species, the vernalization response including the repression of *FLC* expression by cold treatment and the enrichment of the repressive histone modification tri-methylated histone H3 lysine 27 (H3K27me3) at the *FLC* locus is similar to *A. thaliana*. *B. rapa* and *B. oleracea* each have four paralogs of *FLC*, and the allotetraploid species, *Brassica napus*, has nine paralogs. The increased number of paralogs makes the role of *FLC* in vernalization more complicated; in a single plant, paralogs vary in the expression level of *FLC* before and after vernalization. There is also variation in *FLC* expression levels between accessions. In this review, we focus on the regulatory circuits of the vernalization response of *FLC* expression in the genus *Brassica*.

Keywords: *FLOWERING LOCUS C*, vernalization, epigenetics, non-coding RNA, *Brassica*

OPEN ACCESS

Edited by:
Amy Litt,
University of California, Riverside, United States

Reviewed by:
Francisco Madueño, Consejo Superior de Investigaciones Científicas (CSIC), Spain
Joseph Colasanti, University of Guelph, Canada

***Correspondence:**
Ryo Fujimoto
leo@people.kobe-u.ac.jp

Specialty section:
This article was submitted to Plant Development and EvoDevo, a section of the journal Frontiers in Plant Science

Received: *20 October 2020*
Accepted: *29 December 2020*
Published: *09 February 2021*

Citation:
Akter A, Itabashi E, Kakizaki T, Okazaki K, Dennis ES and Fujimoto R (2021) Genome Triplication Leads to Transcriptional Divergence of FLOWERING LOCUS C Genes During Vernalization in the Genus Brassica. Front. Plant Sci. 11:619417. doi: 10.3389/fpls.2020.619417

INTRODUCTION

Brassica is an economically important genus including many agricultural crops such as Chinese cabbage and turnip (*Brassica rapa* L.), cabbage, broccoli, cauliflower, kale, and kohlrabi (*Brassica oleracea* L.), and oilseed or rapeseed and rutabaga (*Brassica napus* L.). Three diploid species, *B. rapa*, *Brassica nigra* L., and *B. oleracea* are denoted as the A, B, and C genomes, respectively.

Allotetraploid species, *Brassica juncea* L. (AABB), *Brassica carinata* L. (BBCC), and *B. napus* (AACC) contain two diploid genomes, and this genomic relationship is known as the "Triangle of U" (Nagaharu, 1935). *Arabidopsis thaliana* L. is a close relative species to the genus *Brassica*, and both are contained in the Brassicaceae.

The genus *Brassica* needs vernalization for induction of flowering except for early flowering accessions, which have lost the genes responsible for a vernalization requirement. The length of cold treatment required for a vernalization response varies between accessions within a species; for example, the natural variation in flowering time in *B. napus* in response to vernalization is characterized into three groups: winter type (high vernalization requirement), semiwinter type (intermediate vernalization requirement), and spring type (low or no vernalization requirement) (Raman et al., 2016).

The molecular mechanism of vernalization is well studied in *A. thaliana*, and genes involved in vernalization networks have been characterized (Berry and Dean, 2015; Whittaker and Dean, 2017). No one doubts that *FLOWERING LOCUS C* (*FLC*) is a key gene in vernalization. *FLC* encodes a MADS-box transcription factor and acts as a floral repressor (Michaels and Amasino, 1999; Sheldon et al., 1999). *FLC* is expressed before cold exposure, and FRIGIDA (FRI) is involved in activation of *FLC* expression. *FLC* expression is repressed during cold exposure through epigenetic regulation (Groszmann et al., 2011; Berry and Dean, 2015; Whittaker and Dean, 2017). Upon return to warm conditions, silencing of *FLC* is maintained (Berry and Dean, 2015; Whittaker and Dean, 2017).

In the genus *Brassica*, *FLC* is also a key gene in the vernalization process, and the mechanism of vernalization in the genus *Brassica* has much in common with that in *A. thaliana* (Itabashi et al., 2018). However, molecular mechanisms specific to *Brassica* have also been identified. In this review, we describe the research findings on vernalization in the genus *Brassica*.

MULTIPLE COPIES OF *FLC* PARALOGS ARE GENERATED BY WHOLE GENOME TRIPLICATION OR ALLOTETRAPOLYPLOIDIZATION IN THE GENUS *BRASSICA*

The tribe Brassiceae has undergone a whole genome triplication after speciation, and the whole genome sequence of *B. rapa* confirmed the triplication of the *B. rapa* genome relative to *A. thaliana* (Wang et al., 2011). The total number of genes in *B. rapa* is much less than three times the gene number in *A. thaliana* due to gene loss after the whole genome triplication in *B. rapa* (Wang et al., 2011). In the genus *Brassica*, three subgenomes, the least fractioned subgenome (LF) and two more fractionated subgenomes (MF1 and MF2), are recognized. In *B. rapa*, the LF subgenome retains 70% of *A. thaliana* orthologs, while 46 and 36% of *A. thaliana* orthologs are retained in MF1 and MF2 subgenomes, respectively (Wang et al., 2011).

B. rapa has multiple copies of orthologs for each *A. thaliana* gene. For example, there are two *FRI* paralogs (*BrFRIa*, *BrFRIb*) and four *FLC* paralogs (*BrFLC1*, *BrFLC2*, *BrFLC3*, *BrFLC5*) (**Table 1**; Schranz et al., 2002; Wang et al., 2017; Shea et al., 2018). *BrFLC1*, *BrFLC2*, and *BrFLC3* are located on LF, MF2, and MF1 subgenomes, respectively, indicating that whole genome triplication state is preserved. However, it is not clear how *BrFLC5* was generated (Wang et al., 2011). In *B. oleracea*, there are two *FRI* and four *FLC* paralogs (**Table 1**), and *BoFLC5* is a pseudogene (Schranz et al., 2002; Irwin et al., 2012; Itabashi et al., 2019). The allotetraploid species, *B. napus*, has four *FRI* and nine *FLC* paralogs (**Table 1**; Chalhoub et al., 2014; Shea et al., 2018; Yi et al., 2018; Schiessl et al., 2019). The relationship of orthologs in *FRI* and *FLC* among three species is shown in **Table 1**.

Multiple copies of orthologs may lead to subfunctionalization in the genus *Brassica*. In *A. thaliana*, loss of function of the single-copy *AtFRI* is the main cause of natural variation in flowering time (Berry and Dean, 2015; Whittaker and Dean, 2017). However, there are few reports of *FRI* being a major contributor of flowering time variation in the genus *Brassica*. Since both FRIa and FRIb act as activators of *FLC* in the genus *Brassica* (Irwin et al., 2012; Takada et al., 2019), they complement each other so that there is little chance of simultaneous loss of FRI function in nature. In contrast, there are reports that loss of *FLC* function results in variation in flowering time in the genus *Brassica*.

QUANTITATIVE TRAIT LOCUS ANALYSIS SHOWS THAT FLC IS A FLOWERING TIME REGULATOR

To identify the key genes involved in vernalization, quantitative trait locus (QTL) analyses have been performed. QTLs affecting flowering time have been identified in different populations in *B. rapa*, *B. oleracea*, and *B. napus* (Shea et al., 2018). At the beginning of QTL analyses in the genus *Brassica*, a population derived from early and late flowering parental accessions was used. Some QTLs overlapped with the region covering the *FLC* gene, and some indicated that loss of FLC function results in early flowering (Kole et al., 2001; Schranz et al., 2002; Lou et al., 2007; Okazaki et al., 2007; Li et al., 2009; Zhao et al., 2010); loss of *FLC2* function has been detected in early flowering accessions of *B. rapa* and *B. oleracea* (**Table 2**; Okazaki et al., 2007; Li et al., 2009; Wu et al., 2012). In cauliflower (*B. oleracea*), there is an association between *BoFLC2* allelic variation and floral induction within populations of inbred lines (Ridge et al., 2015).

Loss of FLC function causes markedly early flowering and loss or reduction in the vernalization requirement. However, there is a variation in vernalization requirement among accessions not including early flowering accessions. QTL analysis using a population derived from parental accessions showing different vernalization requirements but both having a vernalization requirement also identified the colocalization of QTLs and the *FLC* gene. Using an F_2 population derived from a cross between two parental accessions of Chinese cabbage (*B. rapa*) both having a vernalization requirement, QTLs for flowering time colocalized

TABLE 1 | *FRI* and *FLC* paralogs in three species of the genus *Brassica*.

	***Brassica rapa* (AA)**	**var. *pekinensis* line Chiifu-401-42**		***Brassica oleracea* (CC)**	**var. *capitata* line 02-12**	***Brassica napus***	**European winter oilseed cultivar "Darmor-bzh"**
		ver. 1.5	**ver. 3.0**				
FLC1	*BrFLC1* (A10)	Bra009055	BraA10g027720.3C			*BnaFLC.A10*	BnaA10g22080D
				BoFLC1 (C09)	Bol043693	*BnaFLC.C09A*	BnaC09g46500D
						BnaFLC.C09B	BnaC09g46540D
FLC2	*BrFLC2* (A02)	Bra028599	BraA02g003340.3C			*BnaFLC.A02*	BnaA02g00370D
				BoFLC2 (C02)		*BnaFLC.C02*	BnaC02g00490D
FLC3	*BrFLC3* (A03)	Bra006051	BraA03g004170.3C			*BnaFLC.A03A*	BnaA03g02820D
				BoFLC3 (C03)	Bol008758	*BnaFLC.C03A*	BnaC03g04170D
FLC5	*BrFLC5* (A03)	Bra022771	BraA03g015950.3C			*BnaFLC.A03B*	BnaA03g13630D
				BoFLC5 (C03)		*BnaFLC.C03B*	BnaC03g16530D
FRIa	*BrFRIa* (A03)	Bra029192	BraA03g015670.3C			*BnaFRI.A03*	BnaA03g13320D
				BoFRIa (C03)	Bol028107	*Bna.FRI.C03*	BnaC03g16130D
FRIb	*BrFRIb* (A10)	Bra035723	BraA10g009310.3C			*BnaFRI.A10*	BnaA10g05850D
				BoFRIb (C09)	Bol004294	*Bna.FRI.C09*	BnaC09g27290D

TABLE 2 | Example of how variation in vernalization requirement arises.

Species	**Line**	**Vernalization requirement**	**Note**	**References**
B. rapa	Yellow Sarson (C634)	–	Low level of *BrFLC2* expression in pre-vernalized sample	Li et al., 2009
	Yellow Sarson (L147)	–	Deletion in exon 4 and intron 4 in *BrFLC2*	Wu et al., 2012
	Nou-6 (Chinese cabbage)	++	Low repression rate of *BrFLC1* and *BrFLC5* following vernalization	Kakizaki et al., 2011
	Tsukena No. 2 (Leafy Green/Tsukena)	+++	Low repression rate caused by TE insertion in *BrFLC2* and *BrFLC3*	Kitamoto et al., 2014
B. oleracea	Green Comet (broccoli)	–	Frameshift due to 1-bp deletion in exon 4 of *BoFLC2*	Okazaki et al., 2007
	Inbred lines (cauliflower)	–	Frameshift due to 1-bp deletion in exon 4 of *BoFLC2*	Ridge et al., 2015
	E9 (purple sprouting broccoli)	++	High reactivation rate of *BoFLC2* expression on return to warm condition	Irwin et al., 2016
B. napus	Westar etc. (spring type)	–	Loss of BnaFLC.A10 function by TE insertion in the first exon Loss of BnaFLC.A02 function by TE insertion in the exon 7	Yin et al., 2020
	NIL L06 (spring type)	–	Loss of BnaFLC.A02 function by 2,833 bp insertion in the intron 1	Chen et al., 2018
	Zhongshuang 11 etc. (semiwinter type)	+	*BnaFLC.A10* expression level before and following vernalization is lower than that in winter type, which may be due to TE insertion in the promoter region	Yin et al., 2020
	Darmor (European winter type)	++	Higher expression levels of *BnaFLC.A02* before vernalization, lower repression rate following vernalization, and higher reactivation rate on return to warm conditions of *BnaFLC.A02*	Tudor et al., 2020
	Tapidor etc. (European winter type)	++	Low rate of *BnaFLC.A10* repression following vernalization, which may be due to TE insertion in the promoter region	Hou et al., 2012; Yin et al., 2020

–, low or no vernalization requirement; +, vernalization requirement.

with *BrFLC1* and *BrFLC5* (Kakizaki et al., 2011). The repression rate of *BrFLC1* and *BrFLC5* following cold treatment in the later flowering time accession was lower than in the earlier flowering time accession (**Table 2**; Kakizaki et al., 2011), suggesting that this different rate of repression of *FLC* expression may be involved in the flowering time difference. It was considered that *BrFLC5* is a pseudogene because of a mutation in the splicing donor site (G to A). However, a functional *BrFLC5* allele has been identified in some accessions and shown to be a weak regulator of flowering time (Xi et al., 2018). We confirmed that the later flowering time accession used in Kakizaki et al. (2011) had a functional *FLC5* allele in spite of sequence basis (G allele), suggesting that colocalization of QTL and *BrFLC5* is due to the difference of BrFLC5 function between parental accessions. QTL analysis was also performed using 194 Chinese cabbage accessions including 40 spring, 37 summer, and 117 autumn types, of which 177 accessions showed a vernalization requirement. The order of increasing vernalization requirement is spring, autumn, and summer accessions. *B. rapa Vernalization Insensitive 3.1* (*BrVIN3.1*) and *BrFLC1* have been identified as sources of variation in bolting time (Su et al., 2018). In *A. thaliana*, *VIN3* is involved in *FLC* silencing during cold treatment and is induced by cold treatment (Kim and Sung, 2013). Five haplotypes of *BrVIN3.1* with sequence variation in the promoter regions have been identified. Three haplotypes of *BrFLC1* with two main groups and one minor group had sequence polymorphism in non-coding regions (Su et al., 2018). These sequence polymorphisms in non-coding regions in

BrVIN3.1 or *BrFLC1* may result in variation in the vernalization requirement in *B. rapa*. In case of the difference in vernalization requirement of *B. oleracea*, a QTL overlapping *BoFLC2* has been identified. There are *cis* polymorphisms in *BoFLC2* that influence the expression dynamics in response to cold treatment especially the reactivation rate on return to warm conditions in purple sprouting broccoli (**Table 2**; Irwin et al., 2016). In the European winter oilseed rape (*B. napus*), *BnaFLC.A02* (*BrFLC2* ortholog) has been detected as candidate gene giving rise to the QTL. Higher expression levels of *BnaFLC.A02* before cold treatment, lower repression rate following cold treatment, and higher reactivation rate on return to warm conditions of *BnaFLC.A02* were found in the later flowering time accession. The amino acid sequence of BnaFLC.A02 was identical between the earlier and later flowering time accessions. In contrast, there were sequence polymorphisms in non-coding intronic regions between them, which could result in a difference in *FLC* expression and modified vernalization requirement (**Table 2**; Tudor et al., 2020).

FLC1, FLC2, and FLC3 act as floral repressors in both *B. rapa* and *B. oleracea* (Kim et al., 2007; Itabashi et al., 2019; Takada et al., 2019). It has not been shown whether amino acid sequence differences among functional *FLC* paralogs could lead to differences in the function as floral repressor or variation in vernalization requirement. There is a variation in expression levels among *FLC* paralogs before and following vernalization, and this is also shown in the repression rate of their expression following vernalization (Itabashi et al., 2019; Schiessl et al., 2019; Takada et al., 2019). These results suggest that variation in vernalization requirement is due to the difference in transcriptional repression rate of *FLC* between accessions, and this may be due to sequence polymorphisms in the non-coding regions. Furthermore, the fact that a change in one *FLC* paralog affects vernalization requirement suggests that the *FLC* paralogs may be functioning additively.

TRANSPOSON INSERTION CAUSES VARIATION OF VERNALIZATION RESPONSE

Transposable elements (TEs) are DNA sequences that can change their location in the genome, and they can play a role in plant genome evolution (Fujimoto et al., 2012; Hosaka and Kakutani, 2018). In *B. rapa*, TE DNA is methylated, and TEs are epigenetically silenced (Fujimoto et al., 2008b; Sasaki et al., 2011; Takahashi et al., 2018a,b). The variation in the genome structure of orthologous loci between *B. rapa* and *B. oleracea* is due to TE insertions; the *B. oleracea* genome has more TE insertions than the *B. rapa* genome in orthologous genomic regions, which results in a larger genome size in *B. oleracea* than in *B. rapa* (Fujimoto et al., 2006a; Liu et al., 2014). TE insertions can cause loss of protein function or gene expression or generate a new expression pattern (Miura et al., 2001; Fujimoto et al., 2006b, 2008a, 2011; Saze and Kakutani, 2007; Naito et al., 2009; Hosaka and Kakutani, 2018).

A TE insertion has been identified in some alleles of *FLC* in the genus *Brassica*. Long TE insertions in the first intron of *BrFLC2* and *BrFLC3* were detected in the extremely late flowering time accession, Tsukena No. 2 (Kitamoto et al., 2014). In *A. thaliana*, the Landsberg *erecta* (L*er*) accession has a TE in the first intron, and this insertion results in a low level of *FLC* expression (Gazzani et al., 2003). In contrast, insertion of a TE in the first intron of *BrFLC2* or *BrFLC3* in Tsukena No. 2 does not affect the *FLC* expression *per se*. However, weak repression of *BrFLC2* and *BrFLC3* following cold exposure has been detected, suggesting that the TE insertion disrupts the vernalization response (**Table 2**; Kitamoto et al., 2014). A similar phenomenon has been observed in radish (*Raphanus sativus*); a 1,627-bp insertion in the first intron of *RsFLC2* did not affect the *RsFLC2* expression level before cold treatment but weakened its repression rate during vernalization, resulting in a late-bolting phenotype (Wang et al., 2018). These results suggest that a TE insertion might disrupt a *cis* element of the vernalization response in the first intron or inhibit the recruitment of the POLYCOMB REPRESSIVE COMPLEX 2 (PRC2), which plays a role in epigenetic silencing of *FLC* during vernalization, to the *FLC* locus. In addition to the TE insertion, an insertion/deletion in the second intron of *BoFLC1* may alter gene expression and is associated with variation in flowering time of cabbage varieties (Abuyusuf et al., 2019).

In *B. napus*, there was TE insertion in the promoter region of some *FLC* paralogs, and this insertion affects the vernalization requirement. A 621-bp TE insertion in the upstream region of *BnaFLC.A10* (*BrFLC1* ortholog) was associated with lower rate of *BnaFLC.A10* repression during cold treatment (**Table 2**; Hou et al., 2012). This 621-bp TE insertion is observed in 73% of winter-type accessions (449 of 619 accessions including Tapidor and Darmor-bzh) and associated with high vernalization requirement (Yin et al., 2020). A 4,422-bp TE insertion is observed in *BnaFLC.A10* of the semiwinter type (Zhongshuang 11, Ningyou 7), and its expression level before and following cold treatment in semiwinter type was lower than in winter types (**Table 2**). About 57% of semiwinter accessions have this 4,422-bp TE insertion (Yin et al., 2020). A TE insertion results in loss of FLC function in spring-type accessions; a 5,625-bp TE insertion in the first exon of *BnaFLC.A10* (in about 55% of spring-type accessions) and 810-bp TE insertion in the exon 7 of *BnaFLC.A02* (*BrFLC2* ortholog) (about 7%) cause loss of function as does a 2,833-bp insertion in the first intron of *BnaFLC.A02* (about 18%) (**Table 2**; Chen et al., 2018; Yin et al., 2020).

These data indicate that TE insertions play an important role in the determination of flowering time and vernalization requirement in the genus *Brassica*.

HISTONE MODIFICATION TRIGGERS EPIGENETIC SILENCING OF THE *FLC* FOLLOWING VERNALIZATION

Histone modification is an epigenetic modification that plays a role in the regulation of gene expression (Pfluger and Wagner, 2007; Richards, 2011; Fujimoto et al., 2012). Genome-wide histone modification states have been examined by chromatin

immunoprecipitation sequencing (ChIP-seq) in many plant species. In *B. rapa*, di-methylation of histone H3 lysine 9 (H3K9me2) and trimethylation of histone H3 lysine 27 (H3K27me3) have been mapped genome wide (Takahashi et al., 2018a; Akter et al., 2019; Payá-Milans et al., 2019). In *B. rapa*, H3K9me2 was overrepresented in TEs, and there were low number of genes having H3K9me2 marks (Takahashi et al., 2018a). About 30% of genes had H3K27me3 marks, and H3K27me3 marks were associated with low level of gene expression and high level of tissue-specific gene expression (Akter et al., 2019; Payá-Milans et al., 2019). H3K27me3 modification is catalyzed by the PRC2, and in *B. rapa*, a mutant of the *CURLY LEAF* (*CLF*) gene, which is the enzymatic core of PRC2, showed decreased H3K27me3 level (Payá-Milans et al., 2019), suggesting that PRC2 plays a role in H3K27me3 in *B. rapa* as in other plant species.

In *A. thaliana*, repression of *FLC* expression during vernalization is associated with switching of chromatin states from enrichment of active histone marks (H3K4me3, H3K36me3) to repressive histone marks (H3K27me3) at the *FLC* locus (Berry and Dean, 2015). During prolonged cold treatment, there is accumulation of H3K27me3 within the nucleation region, which consists of a DNA region associated with one or two nucleosomes and harboring the first exon and the start of first intron. H3K27me3 spreads over the entire region of *FLC* when temperatures are warm (Xi et al., 2020). A *cis* DNA element in the first intron of *FLC* [termed the RY element (CATGCA)] that is essential for *FLC* repression during vernalization and the maintenance of *FLC* silencing when temperatures are warm has been identified (Qüesta et al., 2016; Yuan et al., 2016). In *B. rapa*, H3K4me3 accumulation was found in the nucleation region of all four *BrFLC* paralogs before exposure to cold (Kawanabe et al., 2016). During vernalization, accumulation of H3K27me3 within the nucleation region of all four *BrFLC* paralogs with decreased expression was observed (Akter et al., 2020; **Figure 1**). After return to warm conditions, H3K27me3 accumulation spreads across the four *BrFLC* paralogs maintaining silencing (Kawanabe et al., 2016; Akter et al., 2019; **Figure 1**). The position of the nucleation region is conserved between *A. thaliana* and *B. rapa*, but there is less conservation of first intron sequences (**Figure 1**). Two RY elements are conserved in four *BrFLC* paralogs except in *BrFLC1* where there is a mutation in one of the two RY elements. Like in *A. thaliana*, PRC2 could be recruited to the nucleation regions of the four *BrFLC* paralogs (Akter et al., 2019).

The genome-wide level of H3K27me3 in *B. rapa* was compared between non-vernalized, 4 weeks vernalized, and sample upon return to warm temperature after 4 weeks vernalization. Between the non-vernalized and 4 weeks vernalized samples, 6,814 genes showed a difference in H3K27me3 level, and 99% of genes showed decreased H3K27me3 following vernalization. Between the non-vernalized and the sample upon return to warm temperature after 4 weeks vernalization, 189 genes showed a difference in H3K27me3 level, and 85% of genes showed increased H3K27me3 following vernalization. In *A. thaliana*, 380 genes showed a difference in H3K27me3 level between non-vernalized and sample upon return to warm temperature following 4 weeks vernalization, and only the *FLC* gene showed increased H3K27me3 levels following vernalization (Akter et al., 2019). A trend toward increased levels of H3K27me3 following vernalization in *A. thaliana* has been reported (Xi et al., 2020). A limited number of genes such as *B. rapa MADS AFFECTING FLOWERING* (*BrMAF*) genes, which are related to *FLC*, showed a similar H3K27me3 accumulation pattern; H3K27me3 accumulated in a specific region during vernalization and then spread upon returning to warm temperatures after vernalization (Akter et al., 2019). At the transcriptional level, some genes showed a similar expression pattern to *FLC* during cold treatment in *A. thaliana* (Xi et al., 2020). Some genes showed a change in H3K27me3 accumulation following vernalization, but only a limited number of genes showed an H3K27me3 modification pattern similar to that of *FLC*, where vernalization leads to H3K27me3 accumulation in the specific regions (nucleation region) and then spread throughout the gene when temperature is returned (Akter et al., 2019).

ARE LONG NON-CODING RNAs VERNALIZATION PLAYERS?

In *A. thaliana*, three cold-induced non-coding RNAs (COOLAIR, COLD ASSISTED INTRONIC NON-CODING

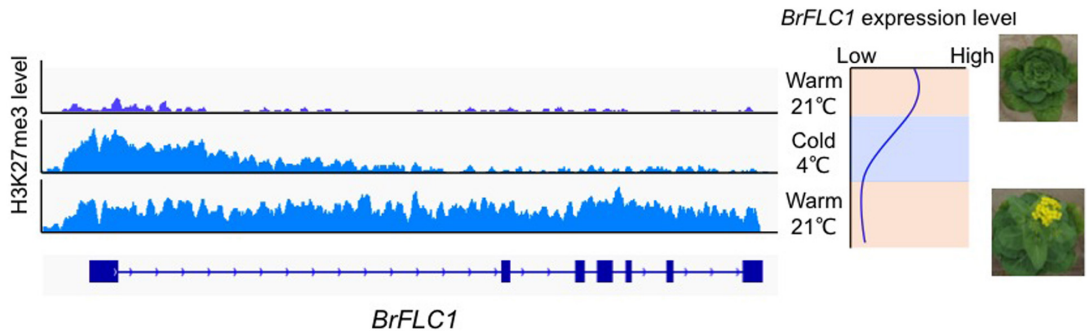

FIGURE 1 | H3K27me3 pattern during vernalization in *BrFLC1*. Left panel shows the pattern of accumulation of H3K27me3 marks during vernalization. Right panel shows the expression pattern of *BrFLC1* during vernalization. *BrFLC2*, *BrFLC3*, and *BrFLC5* showed similar H3K27me3 pattern to *BrFLC1* (Akter et al., 2019).

RNA (COLDAIR), and COLDWRAP) have been identified. COOLAIR is transcribed in the antisense direction, and COLDAIR and COLDWRAP are transcribed in the sense direction relative to *FLC* messenger RNA (mRNA) transcription. COOLAIR transcripts start from downstream of the poly-A site to the promoter region of *FLC* (**Figure 2**; Swiezewski et al., 2009). COLDAIR is derived from the first intron and COLDWRAP from the promoter region (starts at 225 bp upstream from transcription start site) of *FLC* (**Figure 2**; Heo and Sung, 2011; Kim and Sung, 2017). These non-coding RNAs are involved in *FLC* silencing and maintenance of the repressed condition (Swiezewski et al., 2009; Heo and Sung, 2011; Kim and Sung, 2017; Whittaker and Dean, 2017). COOLAIR-like transcripts have been identified in five species of Brassicaceae, *Arabidopsis lyrata*, *Arabis alpina*, *Capsella rubella*, *Eutrema salsugineum*, and *B. rapa*. Although there is low conservation of COOLAIR-like sequences between species, secondary structures show similarity, suggesting that the functional role, the regulation of *FLC* expression during vernalization, may be conserved in Brassicaceae species (Hawkes et al., 2016).

In *B. rapa*, COOLAIR-like transcripts have been identified only at the *BrFLC2* locus and are termed BrFLC2as, while no COOLAIR-like transcript was detected from the other three *BrFLC* loci (**Figure 2**; Li et al., 2016; Shea et al., 2019). COOLAIR has two transcripts, proximal site (class I, ∼400 nt) and distal site (class II, ∼750 nt), and BrFLC2as also has two different length transcripts, class I (short, 357, 425, and 510 nt) and class II (long, 665 and 767nt) (Li et al., 2016). BrFLC2as was highly induced by short-term cold treatment, and class II BrFLC2as was at a higher level than class I BrFLC2as (Li et al., 2016; Shea et al., 2019). Similarity of secondary structure and the characteristic of being induced by short-term cold treatment in both BrFLC2as and COOLAIR suggests a functional similarity (Li et al., 2016). However, the other three *BrFLC* paralogs also show decreased expression during vernalization in spite of no cold-induced COOLAIR-like transcripts being detected (Li et al., 2016; Shea et al., 2019). BrFLC2as may be involved in the silencing of the other three *BrFLC* paralogs. Overexpression of the BrFLC2as resulted in reduced *BrFLC1*, *BrFLC2*, and *BrFLC3* expression leading to an early flowering phenotype, suggesting that BrFLC2as may be involved not only in the repression of *BrFLC2* but also in the repression of the *BrFLC1* and *BrFLC3* genes (Li et al., 2016). However, this experiment does not rule out the possibility that repression of the three *BrFLC* genes is due to posttranscriptional gene silencing because the introduced BrFLC2as sequence includes the exon 1 region of *BrFLC2* and may silence all three genes (Li et al., 2016). Furthermore, there is a question whether BrFLC2as is able to function in *trans* because COOLAIR functions in *cis* (Csorba et al., 2014). Further study will be needed to elucidate the role of BrFLC2as in the vernalization mechanism in *B. rapa*.

In *A. thaliana*, COLDAIR and COLDWRAP play a role in recruitment of PRC2 to the *FLC* locus (Kim and Sung, 2017). However, neither COLDAIR nor COLDWRAP-like transcripts nor other cold-induced transcripts from the promoter or first intron have been identified in the four *FLC* paralogs of *B. rapa* (Li et al., 2016; Shea et al., 2019). However, accumulation of H3K27me3 was confirmed in all four *BrFLC* paralogs (Akter et al., 2019), leading to the question of how PRC2 is recruited to the *BrFLC* loci during vernalization.

Cold-induced natural antisense transcripts (NATs) were also identified in two *BrMAF* genes in *B. rapa*. In *B. rapa*, there are five *BrMAF* genes, and three of these five *BrMAF* genes were repressed following vernalization (Akter et al., 2019). Accumulation of H3K27me3 during vernalization also has been shown in these three *BrMAF* genes (Akter et al., 2019). In addition, MAF1 and MAF2 isolated from Pak-choi (*B. rapa* var. *chinensis*), termed BcMAF1 and BcMAF2, respectively, function as floral repressors (Huang et al., 2018, 2019). These cold-inducible NATs derived from *BrMAF* loci may have a similar function to COOLAIR. In *A. thaliana*, *MAF4* has an overlapped NAT termed MAS. *MAF4* is induced early in cold treatment, and MAS is coordinately expressed during the cold treatment (Zhao et al., 2018). Repression or silencing of *MAF4* expression did not affect MAS expression, while repression of MAS expression reduced *MAF4* induction. These results suggest that MAS plays a positive role in *MAF4* expression. In *B. rapa*, coordinate expression of mRNA and the NAT pair following vernalization was observed in some genes but not in *BrMAF* genes (Shea et al., 2019). This coordinate expression in mRNA and NAT pairs may have a role in vernalization or the cold response.

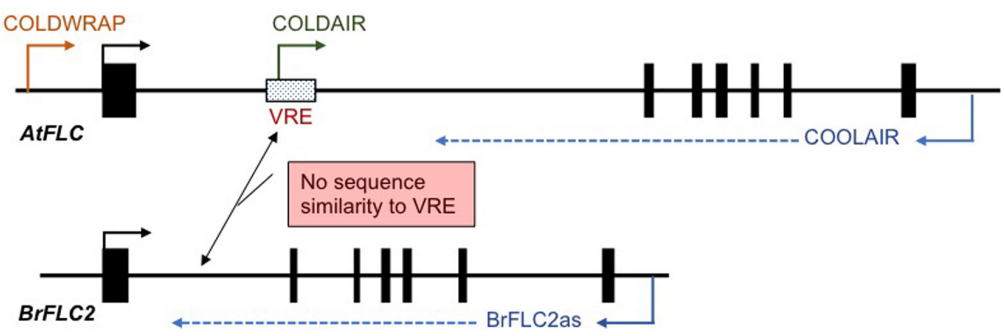

FIGURE 2 | Schematic view of the position of cold-induced non-coding RNAs in *A. thaliana* and *B. rapa*. There is no sequence similarity between the putative vernalization response element (VRE) in *A. thaliana* and the first intron of four *BrFLC* paralogs. Only *BrFLC2* has antisense transcripts, BrFLC2as.

PERSPECTIVE

Whole genome triplication results in multiple copies of *FLC* paralogs in the genus *Brassica*. FLC1, FLC2, and FLC3 act as floral repressors in both *B. rapa* and *B. oleracea* (Kim et al., 2007; Itabashi et al., 2019; Takada et al., 2019), suggesting that all three *FLC* paralogs need to be considered to understand the vernalization mechanism. There is a difference in transcriptional level before vernalization among three *FLC* paralogs in both *B. rapa* and *B. oleracea*, and between accessions within species, there are differences in which *FLC* paralog shows the highest expression (Itabashi et al., 2019; Takada et al., 2019). A similar situation is observed in *B. napus*, which has nine *FLC* paralogs (Schiessl et al., 2019). Different expression levels before vernalization between paralogs could be due to sequence polymorphisms in the promoter regions. In addition, sequence polymorphisms in the promoter region could also be involved in the difference in expression levels in each *FLC* between accessions. The correlation between the total level of *FLC* expression before vernalization and the vernalization requirement suggests that the level of *FLC* expression before vernalization is associated with the diversity of vernalization requirement in *B. rapa* (Takada et al., 2019). We need to identify the region or *cis*-element controlling *FLC* expression level to understand the variation in vernalization requirement between accessions.

There is also a variation in the rate of repression of *FLC* expression among paralogs during vernalization with a difference between accessions as to which *FLC* paralog shows a low repression rate. A low repression rate of *FLC* genes is an important factor in generating a vernalization requirement, and in this review, some examples are shown such as a TE insertion in the first intron or a TE insertion in the promoter region, which affect this requirement (Gazzani et al., 2003; Hou et al., 2012; Kitamoto et al., 2014; Yin et al., 2020). There is a need to clarify the complexity that arises from multiple *FLC* paralogs. Furthermore, non-coding RNAs, which can recruit PRC2 to *FLC* loci, have not been identified, and a vernalization responsive element (VRE) in the genus *Brassica* has not been identified. Identification of a VRE may clarify the association between VRE sequence polymorphism and variation in repression rate following vernalization between paralogs or between accessions within species.

AUTHOR CONTRIBUTIONS

TK, KO, ED, and RF conceptualized the manuscript. AA, EI, ED, and RF wrote the manuscript. TK, KO, ED, and RF edited the manuscript. All authors contributed to the article and approved the submitted version.

FUNDING

This work was supported by Grant-in-Aid for Scientific Research (B) (15H04433 and 18H02173) from the Japan Society for the Promotion of Science (JSPS) and Fund for the Promotion of International Joint Research (16KK0171) from JSPS.

REFERENCES

Abuyusuf, M., Nath, U. K., Kim, H. T., Islam, M. R., Park, J. I., and Nou, I. S. (2019). Molecular markers based on sequence variation in *BoFLC1.C9* for characterizing early-and late-flowering cabbage genotypes. *BMC Genet.* 20:42. doi: 10.1186/s12863-019-0740-1

Akter, A., Miyazaki, J., Shea, D. J., Nishida, N., Takada, S., Miyaji, N., et al. (2020). Gene expression analysis in response to vernalization in Chinese cabbage (*Brassica rapa* L). *Hort. J.* 89, 268–277. doi: 10.2503/hortj.UTD-150

Akter, A., Takahashi, S., Deng, W., Shea, D. J., Itabashi, E., Shimizu, M., et al. (2019). The histone modification H3 lysine 27 tri-methylation has conserved gene regulatory roles in the triplicated genome of *Brassica rapa* L. *DNA Res.* 26, 433–443. doi: 10.1093/dnares/dsz021

Berry, S., and Dean, C. (2015). Environmental perception and epigenetic memory: mechanistic insight through *FLC*. *Plant J.* 83, 133–148. doi: 10.1111/tpj.12869

Chalhoub, B., Denoeud, F., Liu, S., Parkin, I. A., Tang, H., Wang, X., et al. (2014). Early allopolyploid evolution in the post-neolithic *Brassica napus* oilseed genome. *Science* 345, 950–953. doi: 10.1126/science.1253435

Chen, L., Dong, F., Cai, J., Xin, Q., Fang, C., Liu, L., et al. (2018). A 2.833-kb insertion in *BnFLC.A2* and its homeologous exchange with *BnFLC.C2* during breeding selection generated early-flowering rapeseed. *Mol. Plant* 11, 222–225. doi: 10.1016/j.molp.2017.09.020

Csorba, T., Questa, J. I., Sun, Q., and Dean, C. (2014). Antisense COOLAIR mediates the coordinated switching of chromatin states at *FLC* during vernalization. *Proc. Natl. Acad. Sci. U.S.A.* 111, 16160–16165. doi: 10.1073/pnas.1419030111

Fujimoto, R., Kinoshita, Y., Kawabe, A., Kinoshita, T., Takashima, K., Nordborg, M., et al. (2008a). Evolution and control of imprinted *FWA* genes in the genus *Arabidopsis*. *PLoS Genet.* 4:e1000048. doi: 10.1371/journal.pgen.1000048

Fujimoto, R., Okazaki, K., Fukai, E., Kusaba, M., and Nishio, T. (2006a). Comparison of the genome structure of the self-incompatibility (*S*) locus in interspecific pairs of *S* haplotypes. *Genetics* 173, 1157–1167. doi: 10.1534/genetics.104.037267

Fujimoto, R., Sasaki, T., Inoue, H., and Nishio, T. (2008b). Hypomethylation and transcriptional reactivation of retrotransposon-like sequences in ddm1 transgenic plants of *Brassica rapa*. *Plant Mol. Biol.* 66, 463–473. doi: 10.1007/s11103-007-9285-1

Fujimoto, R., Sasaki, T., Ishikawa, R., Osabe, K., Kawanabe, T., and Dennis, E. S. (2012). Molecular mechanisms of epigenetic variation in plants. *Int. J. Mol. Sci.* 13, 9900–9922. doi: 10.3390/ijms13089900

Fujimoto, R., Sasaki, T., Kudoh, H., Taylor, J. M., Kakutani, T., and Dennis, E. S. (2011). Epigenetic variation in the *FWA* gene within the genus *Arabidopsis*. *Plant J.* 66, 831–843. doi: 10.1111/j.1365-313X.2011.04549.x

Fujimoto, R., Sugimura, T., Fukai, E., and Nishio, T. (2006b). Suppression of gene expression of a recessive *SP11/SCR* allele by an untranscribed *SP11/SCR* allele in *Brassica* self-incompatibility. *Plant Mol. Biol.* 61, 577–587. doi: 10.1007/s11103-006-0032-9

Gazzani, S., Gendall, A. R., Lister, C., and Dean, C. (2003). Analysis of the molecular basis of flowering time variation in *Arabidopsis* accessions. *Plant Physiol.* 132, 1107–1114. doi: 10.1104/pp.103.021212

Groszmann, M., Greaves, I. K., Albert, N., Fujimoto, R., Helliwell, C. A., Dennis, E. S., et al. (2011). Epigenetics in plants-vernalisation and hybrid vigour. *Biochim. Biophys. Acta* 1809, 427–437. doi: 10.1016/j.bbagrm.2011.03.006

Hawkes, E. J., Hennelly, S. P., Novikova, I. V., Irwin, J. A., Dean, C., and Sanbonmatsu, K. Y. (2016). COOLAIR antisense RNAs form evolutionarily conserved elaborate secondary structures. *Cell Rep.* 16, 3087–3096. doi: 10.1016/j.celrep.2016.08.045

Heo, J. B., and Sung, S. (2011). Vernalization-mediated epigenetic silencing by a long intronic noncoding RNA. *Science* 331, 76–79. doi: 10.1126/science.1197349

Hosaka, A., and Kakutani, T. (2018). Transposable elements, genome evolution and transgenerational epigenetic variation. *Curr. Opin. Genet. Dev.* 49, 43–48. doi: 10.1016/j.gde.2018.02.012

Hou, J., Long, Y., Raman, H., Zou, X., Wang, J., Dai, S., et al. (2012). A *Tourist*-like MITE insertion in the upstream region of the *BnFLC. A10* gene is associated with vernalization requirement in rapeseed (*Brassica napus L.*). *BMC Plant Biol.* 12:238. doi: 10.1186/1471-2229-12-238

Huang, F., Liu, T., and Hou, X. (2018). Isolation and functional characterization of a floral repressor, *BcMAF1*, from Pak-choi (*Brassica rapa* ssp. *chinensis*). *Front. Plant Sci.* 9:290. doi: 10.3389/fpls.2018.00290

Huang, F., Liu, T., Tang, J., Duan, W., and Hou, X. (2019). *BcMAF2* activates *BcTEM1* and represses flowering in Pak-choi (*Brassica rapa* ssp. *chinensis*). *Plant Mol. Biol.* 100, 19–32. doi: 10.1007/s11103-019-00867-1

Irwin, J. A., Lister, C., Soumpourou, E., Zhang, Y., Howell, E. C., Teakle, G., et al. (2012). Functional alleles of the flowering time regulator *FRIGIDA* in the *Brassica oleracea* genome. *BMC Plant Biol.* 12:21. doi: 10.1186/1471-2229-12-21

Irwin, J. A., Soumpourou, E., Lister, C., Ligthart, J. D., Kennedy, S., and Dean, C. (2016). Nucleotide polymorphism affecting *FLC* expression underpins heading date variation in horticultural brassicas. *Plant J.* 87, 597–605. doi: 10.1111/tpj.13221

Itabashi, E., Osabe, K., Fujimoto, R., and Kakizaki, T. (2018). Epigenetic regulation of agronomical traits in Brassicaceae. *Plant Cell Rep.* 37, 87–101. doi: 10.1007/s00299-017-2223-z

Itabashi, E., Shea, D. J., Fukino, N., Fujimoto, R., Okazaki, K., Kakizaki, T., et al. (2019). Comparison of cold responses for orthologs of cabbage vernalization-related genes. *Hort. J.* 4, 462–470. doi: 10.2503/hortj.UTD-059

Kakizaki, T., Kato, T., Fukino, N., Ishida, M., Hatakeyama, K., and Matsumoto, S. (2011). Identification of quantitative trait loci controlling late bolting in Chinese cabbage (*Brassica rapa* L.) parental line Nou 6 gou. *Breed. Sci.* 61, 151–159. doi: 10.1270/jsbbs.61.151

Kawanabe, T., Osabe, K., Itabashi, E., Okazaki, K., Dennis, E. S., and Fujimoto, R. (2016). Development of primer sets that can verify the enrichment of histone modifications, and their application to examining vernalization-mediated chromatin changes in *Brassica rapa* L. *Genes Genet. Syst.* 91, 1–10. doi: 10.1266/ggs.15-00058

Kim, D. H., and Sung, S. (2013). Coordination of the vernalization response through a *VIN3* and *FLC* gene family regulatory network in *Arabidopsis*. *Plant Cell* 25, 454–469. doi: 10.1105/tpc.112.104760

Kim, D. H., and Sung, S. (2017). Vernalization-triggered intragenic chromatin loop formation by long noncoding RNAs. *Dev. Cell* 40, 302–312. doi: 10.1016/j.devcel.2016.12.021

Kim, S. Y., Park, B. S., Kwon, S. J., Kim, J., Lim, M. H., Park, Y. D., et al. (2007). Delayed flowering time in *Arabidopsis* and *Brassica rapa* by the overexpression of *FLOWERING LOCUS C* (*FLC*) homologs isolated from Chinese cabbage (*Brassica rapa* L.: ssp. *pekinensis*). *Plant Cell Rep.* 26, 327–336. doi: 10.1007/s00299-006-0243-1

Kitamoto, N., Yui, S., Nishikawa, K., Takahata, Y., and Yokoi, S. (2014). A naturally occurring long insertion in the first intron in the *Brassica rapa FLC2* gene causes delayed bolting. *Euphytica* 196, 213–223. doi: 10.1007/s10681-013-1025-9

Kole, C., Quijada, P., Michaels, S. D., Amasino, R. M., and Osborn, T. C. (2001). Evidence for homology of flowering-time genes *VFR2* from *Brassica rapa* and *FLC* from *Arabidopsis thaliana*. *Theor. Appl. Genet.* 102, 425–430. doi: 10.1007/s001220051663

Li, F., Kitashiba, H., Inaba, K., and Nishio, T. (2009). A *Brassica rapa* linkage map of EST-based SNP markers for identification of candidate genes controlling flowering time and leaf morphological traits. *DNA Res.* 16, 311–323. doi: 10.1093/dnares/dsp020

Li, X., Zhang, S., Bai, J., and He, Y. (2016). Tuning growth cycles of *Brassica* crops via natural antisense transcripts of *BrFLC*. *Plant Biotechnol. J.* 14, 905–914. doi: 10.1111/pbi.12443

Liu, S., Liu, Y., Yang, X., Tong, C., Edwards, D., Parkin, I. A., et al. (2014). The *Brassica oleracea* genome reveals the asymmetrical evolution of polyploid genomes. *Nat. Commun.* 5:3930. doi: 10.1038/ncomms4930

Lou, P., Zhao, J., Kim, J. S., Shen, S., Del Carpio, D. P., Song, X., et al. (2007). Quantitative trait loci for flowering time and morphological traits in multiple populations of *Brassica rapa*. *J. Exp. Bot.* 58, 4005–4016. doi: 10.1093/jxb/erm255

Michaels, S. D., and Amasino, R. M. (1999). *FLOWERING LOCUS C* encodes a novel MADS domain protein that acts as a repressor of flowering. *Plant Cell* 11, 949–956. doi: 10.1105/tpc.11.5.949

Miura, A., Yonebayashi, S., Watanabe, K., Toyama, T., Shimada, H., and Kakutani, T. (2001). Mobilization of transposons by a mutation abolishing full DNA methylation in *Arabidopsis*. *Nature* 411, 212–214. doi: 10.1038/35075612

Nagaharu, U. (1935). Genome analysis in *Brassica* with special reference to the experimental formation of *B. napus* and peculiar mode of fertilization. *Jpn. J. Bot.* 7, 389–452.

Naito, K., Zhang, F., Tsukiyama, T., Saito, H., Hancock, C. N., Richardson, A. O., et al. (2009). Unexpected consequences of a sudden and massive transposon amplification on rice gene expression. *Nature* 461, 1130–1134. doi: 10.1038/nature08479

Okazaki, K., Sakamoto, K., Kikuchi, R., Saito, A., Togashi, E., Kuginuki, Y., et al. (2007). Mapping and characterization of *FLC* homologs and QTL analysis of flowering time in *Brassica oleracea*. *Theor. Appl. Genet.* 114, 595–608. doi: 10.1007/s00122-006-0460-6

Payá-Milans, M., Poza-Viejo, L., Martín-Uriz, P. S., Lara-Astiaso, D., Wilkinson, M. D., and Crevillén, P. (2019). Genome-wide analysis of the H3K27me3 epigenome and transcriptome in *Brassica rapa*. *GigaScience* 8:giz147. doi: 10.1093/gigascience/giz147

Pfluger, J., and Wagner, D. (2007). Histone modifications and dynamic regulation of genome accessibility in plants. *Curr. Opin. Plant Biol.* 10, 645–652. doi: 10.1016/j.pbi.2007.07.013

Qüesta, J., Song, J., Geraldo, N., An, H., and Dean, C. (2016). *Arabidopsis* transcriptional repressor VAL1 triggers Polycomb silencing at *FLC* during vernalization. *Science* 353, 485–488. doi: 10.1126/science.aaf7354

Raman, H., Raman, R., Coombes, N., Song, J., Prangnell, R., Bandaranayake, C., et al. (2016). Genome-wide association analyses reveal complex genetic architecture underlying natural variation for flowering time in canola. *Plant Cell Environ.* 39, 1228–1239. doi: 10.1111/pce.12644

Richards, E. J. (2011). Natural epigenetic variation in plant species: a view from the field. *Curr. Opin. Plant Biol.* 14, 204–209. doi: 10.1016/j.pbi.2011.03.009

Ridge, S., Brown, P. H., Hecht, V., Driessen, R. G., and Weller, J. L. (2015). The role of *BoFLC2* in cauliflower (*Brassica oleracea* var. *botrytis* L.) reproductive development. *J. Exp. Bot.* 66, 125–135. doi: 10.1093/jxb/eru408

Sasaki, T., Fujimoto, R., Kishitani, S., and Nishio, T. (2011). Analysis of target sequences of DDM1s in *Brassica rapa* by MSAP. *Plant Cell Rep.* 30, 81–88. doi: 10.1007/s00299-010-0946-1

Saze, H., and Kakutani, T. (2007). Heritable epigenetic mutation of a transposon-flanked *Arabidopsis* gene due to lack of the chromatin-remodeling factor DDM1. *EMBO J.* 26, 3641–3652. doi: 10.1038/sj.emboj.7601788

Schiessl, S. V., Quezada-Martinez, D., Tebartz, E., Snowdon, R. J., and Qian, L. (2019). The vernalisation regulator *FLOWERING LOCUS C* is differentially expressed in biennial and annual *Brassica napus*. *Sci. Rep.* 9:14911. doi: 10.1038/s41598-019-51212-x

Schranz, M. E., Quijada, P., Sung, S. B., Lukens, L., Amasino, R., and Osborn, T. C. (2002). Characterization and effects of the replicated flowering time gene *FLC* in *Brassica rapa*. *Genetics* 162, 1457–1468.

Shea, D. J., Itabashi, E., Takada, S., Fukai, E., Kakizaki, T., Fujimoto, R., et al. (2018). The role of *FLOWERING LOCUS C* in vernalisation of *Brassica*: the importance of vernalisation research in the face of climate change. *Crop Pasture Sci.* 69, 30–39. doi: 10.1071/CP16468

Shea, D. J., Nishida, N., Takada, S., Itabashi, E., Takahashi, S., and Akter, A. (2019). Long noncoding RNAs in *Brassica rapa* L. following vernalization. *Sci. Rep.* 9:9302. doi: 10.1038/s41598-019-45650-w

Sheldon, C. C., Burn, J. E., Perez, P. P., Metzger, J., Edwards, J. A., Peacock, W. J., et al. (1999). The *FLF* MADS box gene: a repressor of flowering in *Arabidopsis* regulated by vernalization and methylation. *Plant Cell* 11, 445–458. doi: 10.1105/tpc.11.3.445

Su, T., Wang, W., Li, P., Zhang, B., Li, P., Xin, X., et al. (2018). A genomic variation map provides insights into the genetic basis of spring Chinese cabbage (*Brassica rapa* ssp. *pekinensis*) selection. *Mol. Plant* 11, 1360–1376. doi: 10.1016/j.molp.2018.08.006

Swiezewski, S., Liu, F., Magusin, A., and Dean, C. (2009). Cold-induced silencing by long antisense transcripts of an *Arabidopsis* Polycomb target. *Nature* 462, 799–802. doi: 10.1038/nature08618

Takada, S., Akter, A., Itabashi, E., Nishida, N., Shea, D. J., Miyaji, N., et al. (2019). The role of *FRIGIDA* and *FLOWERING LOCUS C* genes in flowering time of *Brassica rapa* leafy vegetables. *Sci. Rep.* 9:13843. doi: 10.1038/s41598-019-50122-2

Takahashi, S., Fukushima, N., Osabe, K., Itabashi, E., Shimizu, M., Miyaji, N., et al. (2018b). Identification of DNA methylated regions by using methylated DNA immunoprecipitation sequencing in *Brassica rapa*. *Crop Pasture Sci.* 69, 107–120. doi: 10.1071/CP17394

Takahashi, S., Osabe, K., Fukushima, N., Takuno, S., Miyaji, N., Shimizu, M., et al. (2018a). Genome-wide characterization of DNA methylation, small RNA expression, and histone H3 lysine nine di-methylation in *Brassica rapa* L. *DNA Res.* 25, 511–520. doi: 10.1093/dnares/dsy021

Tudor, E. H., Jones, D. M., He, Z., Bancroft, I., Trick, M., Wells, R., et al. (2020). QTL-seq identifies *BnaFT.A02* and *BnaFLC.A02* as candidates for variation in vernalisation requirement and response in winter oilseed rape (*Brassica napus*). *Plant Biotechnol. J.* 18, 2466–2481. doi: 10.1111/pbi.13421

Wang, J., Qiu, Y., Cheng, F., Chen, X., Zhang, X., Wang, H., et al. (2017). Genome-wide identification, characterization, and evolutionary analysis of flowering genes in radish (*Raphanus sativus* L.). *BMC Genomics* 18:981. doi: 10.1186/s12864-017-4377-z

Wang, Q., Zhang, Y., and Zhang, L. (2018). A naturally occurring insertion in the *RsFLC2* gene associated with late-bolting trait in radish (*Raphanus sativus* L.). *Mol. Breed.* 38:137. doi: 10.1007/s11032-018-0897-8

Wang, X., Wang, H., Wang, J., Sun, R., Wu, J., Liu, S., et al. (2011). The genome of the mesopolyploid crop species *Brassica rapa*. *Nat. Genet.* 43, 1035–1039. doi: 10.1038/ng.919

Whittaker, C., and Dean, C. (2017). The *FLC* Locus: a platform for discoveries in epigenetics and adaptation. *Ann. Rev. Cell. Dev. Biol.* 33, 555–575. doi: 10.1146/annurev-cellbio-100616-060546

Wu, J., Wei, K., Cheng, F., Li, S., Wang, Q., Zhao, J., et al. (2012). A naturally occurring InDel variation in *BraA.FLC.b* (*BrFLC2*) associated with flowering time variation in *Brassica rapa*. *BMC Plant Biol.* 12:151. doi: 10.1186/1471-2229-12-151

Xi, X., Wei, K., Gao, B., Liu, J., Liang, J., Cheng, F., et al. (2018). BrFLC5: a weak regulator of flowering time in *Brassica rapa*. *Theor. Appl. Genet.* 131, 2107–2116. doi: 10.1007/s00122-018-3139-x

Xi, Y., Park, S. R., Kim, D. H., Kim, E. D., and Sung, S. (2020). Transcriptome and epigenome analyses of vernalization in *Arabidopsis thaliana*. *Plant J.* 103, 1490–1502. doi: 10.1111/tpj.14817

Yi, L., Chen, C., Yin, S., Li, H., Li, Z., Wang, B., et al. (2018). Sequence variation and functional analysis of a *FRIGIDA* orthologue (*BnaA3. FRI*) in *Brassica napus*. *BMC Plant Biol.* 18:32. doi: 10.1186/s12870-018-1253-1

Yin, S., Wan, M., Guo, C., Wang, B., Li, H., Li, G., et al. (2020). Transposon insertions within alleles of *BnaFLC. A10* and *BnaFLC. A2* are associated with seasonal crop type in rapeseed. *J. Exp. Bot.* 71, 4729–4741. doi: 10.1093/jxb/eraa237

Yuan, W., Luo, X., Li, Z., Yang, W., Wang, Y., Liu, R., et al. (2016). A *cis* cold memory element and a *trans* epigenome reader mediate Polycomb silencing of *FLC* by vernalization in *Arabidopsis*. *Nat. Genet.* 48, 1527–1534. doi: 10.1038/ng.3712

Zhao, J., Kulkarni, V., Liu, N., Del Carpio, D. P., and Bucher, J. (2010). BrFLC2 (*FLOWERINGLOCUS C*) as a candidate gene for a vernalization response QTL in *Brassica rapa*. *J. Exp. Bot.* 61, 1817–1825. doi: 10.1093/jxb/erq048

Zhao, X., Li, J., Lian, B., Gu, H., Li, Y., and Qi, Y. (2018). Global identification of *Arabidopsis* lncRNAs reveals the regulation of *MAF4* by a natural antisense RNA. *Nat. Commun.* 9:5056. doi: 10.1038/s41467-018-07500-7

Conflict of Interest: The authors declare that the research was conducted in the absence of any commercial or financial relationships that could be construed as a potential conflict of interest.

Copyright © 2021 Akter, Itabashi, Kakizaki, Okazaki, Dennis and Fujimoto. This is an open-access article distributed under the terms of the Creative Commons Attribution License (CC BY). The use, distribution or reproduction in other forums is permitted, provided the original author(s) and the copyright owner(s) are credited and that the original publication in this journal is cited, in accordance with accepted academic practice. No use, distribution or reproduction is permitted which does not comply with these terms.

frontiers in Plant Science

REVIEW
published: 15 February 2021
doi: 10.3389/fpls.2021.627258

The Diverse Roles of FLOWERING LOCUS C in Annual and Perennial Brassicaceae Species

*Wim J. J. Soppe[1], Natanael Viñegra de la Torre[2,3,4] and Maria C. Albani[2,3,4]**

[1] Rijk Zwaan, De Lier, Netherlands, [2] Institute for Plant Sciences, University of Cologne, Cologne, Germany, [3] Max Planck Institute for Plant Breeding Research, Cologne, Germany, [4] Cluster of Excellence on Plant Sciences, "SMART Plants for Tomorrow's Needs," Heinrich Heine University Düsseldorf, Düsseldorf, Germany

Most temperate species require prolonged exposure to winter chilling temperatures to flower in the spring. In the Brassicaceae, the MADS box transcription factor FLOWERING LOCUS C (FLC) is a major regulator of flowering in response to prolonged cold exposure, a process called vernalization. Winter annual *Arabidopsis thaliana* accessions initiate flowering in the spring due to the stable silencing of *FLC* by vernalization. The role of FLC has also been explored in perennials within the Brassicaceae family, such as *Arabis alpina.* The flowering pattern in *A. alpina* differs from the one in *A. thaliana*. *A. alpina* plants initiate flower buds during vernalization but only flower after subsequent exposure to growth-promoting conditions. Here we discuss the role of FLC in annual and perennial Brassicaceae species. We show that, besides its conserved role in flowering, FLC has acquired additional functions that contribute to vegetative and seed traits. *PERPETUAL FLOWERING 1* (*PEP1*), the *A. alpina FLC* ortholog, contributes to the perennial growth habit. We discuss that PEP1 directly and indirectly, regulates traits such as the duration of the flowering episode, polycarpic growth habit and shoot architecture. We suggest that these additional roles of *PEP1* are facilitated by (1) the ability of *A. alpina* plants to form flower buds during long-term cold exposure, (2) age-related differences between meristems, which enable that not all meristems initiate flowering during cold exposure, and (3) differences between meristems in stable silencing of *PEP1* after long-term cold, which ensure that *PEP1* expression levels will remain low after vernalization only in meristems that commit to flowering during cold exposure. These features result in spatiotemporal seasonal changes of *PEP1* expression during the *A. alpina* life cycle that contribute to the perennial growth habit. FLC and PEP1 have also been shown to influence the timing of another developmental transition in the plant, seed germination, by influencing seed dormancy and longevity. This suggests that during evolution, *FLC* and its orthologs adopted both similar and divergent roles to regulate life history traits. Spatiotemporal changes of *FLC* transcript accumulation drive developmental decisions and contribute to life history evolution.

Keywords: *Arabis alpina*, FLC, flowering, PEP1, perennial, perpetual flowering, polycarpic growth habit, vernalization

OPEN ACCESS

Edited by:
Caroline Dean,
John Innes Centre, United Kingdom

Reviewed by:
David Horvath,
Edward T. Schafer Agricultural Research Center (USDA-ARS), United States
Julia Qüesta,
Centre for Research in Agricultural Genomics (CRAG), Spain

***Correspondence:**
Maria C. Albani
malbani@uni-koeln.de;
albani@mpipz.mpg.de

Specialty section:
This article was submitted to Plant Development and EvoDevo, a section of the journal Frontiers in Plant Science

Received: *08 November 2020*
Accepted: *25 January 2021*
Published: *15 February 2021*

Citation:
Soppe WJJ, Viñegra de la Torre N and Albani MC (2021) The Diverse Roles of FLOWERING LOCUS C in Annual and Perennial Brassicaceae Species. Front. Plant Sci. 12:627258. doi: 10.3389/fpls.2021.627258

PLANTS HAVE DIFFERENT WAYS OF USING WINTER COLD TO SYNCHRONIZE FLOWERING IN THE SPRING

Winter annuals, biennials and perennial species overwinter as seedlings or plants and flower in the spring when favorable environmental conditions return. Annual and biennial species follow a monocarpic life strategy and die after setting seeds once, whereas the majority of perennials are polycarpic and are able to reproduce several times during their life time (Albani and Coupland, 2010; Bratzel and Turck, 2015). Low temperatures during the winter are important to enable synchronous flowering in the spring but generally regulate different stages of the flowering process in monocarpic compared to polycarpic species.

Winter annuals and biennials require prolonged exposure to cold to accelerate or to enable flowering, a process called vernalization. Prolonged cold exposure is effective when it is applied to imbibed seeds or young seedlings (of winter annual species), or to older plants (of winter annual and biennial species) (Lang, 1952; Chouard, 1960). The requirement of cold exposure for flowering is common in plants adapted to temperate climates and ensures that they will not flower before the winter (Chouard, 1960). Vernalization is considered as a preparatory process that has to take place before a plant can initiate flowering in response to increased daylength in the spring (Chouard, 1960). The effectiveness of vernalization is usually estimated by the reduction of days that plants take to flower after returning to growth-promoting conditions (Chouard, 1960). Thus, vernalization aligns with the life cycle of winter annual and biennial species that initiate flowering in the spring (**Figure 1A**; Chouard, 1960). In *A. thaliana*, vernalization has also a quantitative effect on flowering and the duration of cold that is required for the acceleration of flowering can vary between accessions (Shindo et al., 2006; Li et al., 2014). Plants can be vernalized at different temperatures ranging from 0 to 16°C (Wollenberg and Amasino, 2012; Duncan et al., 2015). In some habitats, this temperature range can be achieved during summer or autumn, suggesting that plants can be vernalized before the winter (Billings and Mooney, 1968; Duncan et al., 2015; O'Neill et al., 2019). In addition, older plants show a stronger response to vernalization than young seedlings, suggesting that the developmental stage/age of the plant influences its ability to respond to prolonged cold treatment (Chouard, 1960). The effect of cold exposure is also reversible and plants can devernalize when cold exposure is followed by high temperatures (Chouard, 1960; Périlleux et al., 2013). This suggests that the flower-promoting role of vernalization can be lost when plants are exposed to exceptionally high spring temperatures.

Polycarpic perennials do not commit all meristems to flowering and are able to maintain growth from one year to the next by keeping some meristems in a vegetative state (Albani and Coupland, 2010). Maintenance of vegetative growth after flowering is determined by the coordinated action of age-related factors, which determine whether individual meristems are sensitive to flower-inductive stimuli, and seasonal changes in expression patterns of environmentally-regulated flowering time genes (Wang et al., 2009; Bergonzi and Albani, 2011; Koskela et al., 2012; Hyun et al., 2017, 2019; Zhou et al., 2021). Perennials, however, still have to synchronize their annual cycle in order to flower and set fruits during favorable environmental conditions in spring and summer (Falavigna et al., 2019). The environmental conditions that induce flowering in temperate perennials vary greatly between species, although most of them concentrate their flowering season in the spring. For example, grapevine, sweet cherry and peach trees initiate flower buds during the summer (**Figure 1B**; Engin and Ünal, 2007; Carmona et al., 2008; Vimont et al., 2019). Therefore, spring flowering in these perennials occurs when the flower buds, which were initiated the previous year, grow out. Interestingly, the observed variation in spring flowering between cultivars is not associated with differences in flower bud initiation but rather with the requirement of prolonged cold exposure that is needed for plants to exit the endodormant state that they enter in autumn (Vimont et al., 2019). In general, bud dormancy can be divided into three phases: paradormancy, endodormancy and ecodormancy. Paradormancy (also referred as latency) is the stage during which the growth of a bud is inhibited by surrounding organs (Lang et al., 1987). The other stages of dormancy are environmentally regulated, with endodormancy being induced and ecodormancy being maintained by environmental cues (Lang et al., 1987). Buds enter endodormancy during the autumn and throughout this phase their growth is inhibited by internal signals (Lang et al., 1987). Prolonged exposure to low temperatures in the winter is required for endodormancy release, and once the chilling requirement is met the buds transition into ecodormancy (reviewed in Falavigna et al., 2019). Bud growth during ecodormancy is inhibited by unfavorable environmental conditions and can be reactivated again when plants experience growth-promoting conditions (Lang et al., 1987). Overall, prolonged cold exposure is important for bud dormancy release and synchronized resumption of growth the following spring (referred to as budbreak). Exposure to chilling temperatures for dormancy breaking is considered to be a distinct process from vernalization (Chouard, 1960). Specifically, because low temperatures during dormancy breaking do not induce a phase change that leads to the formation of new kinds of organs but cause the regrowth of already existing organs (Chouard, 1960). However, there are obvious similarities between both processes, which both require long-term cold to synchronize spring flowering (Or, 2009; Atkinson et al., 2013) and share a considerable overlap in their molecular pathways (reviewed in Horvath, 2009).

There is also a third variant by which low temperatures lead to flowering. This variant has been observed in several Brassicaceae species, including winter oil seed rape, *A. alpina*, *Arabidopsis lyrata,* pak choi, and Brussels sprouts (Chouard, 1960; Wang et al., 2009; Kemi et al., 2019; O'Neill et al., 2019). In these species, flower buds initiate and develop during cold exposure, suggesting that vernalization is not only a preparatory process for flowering but also directly regulates the initiation and formation of floral buds (**Figure 1C**; Chouard, 1960; Wang et al., 2009; Kemi et al., 2019; O'Neill et al., 2019). In the perennial

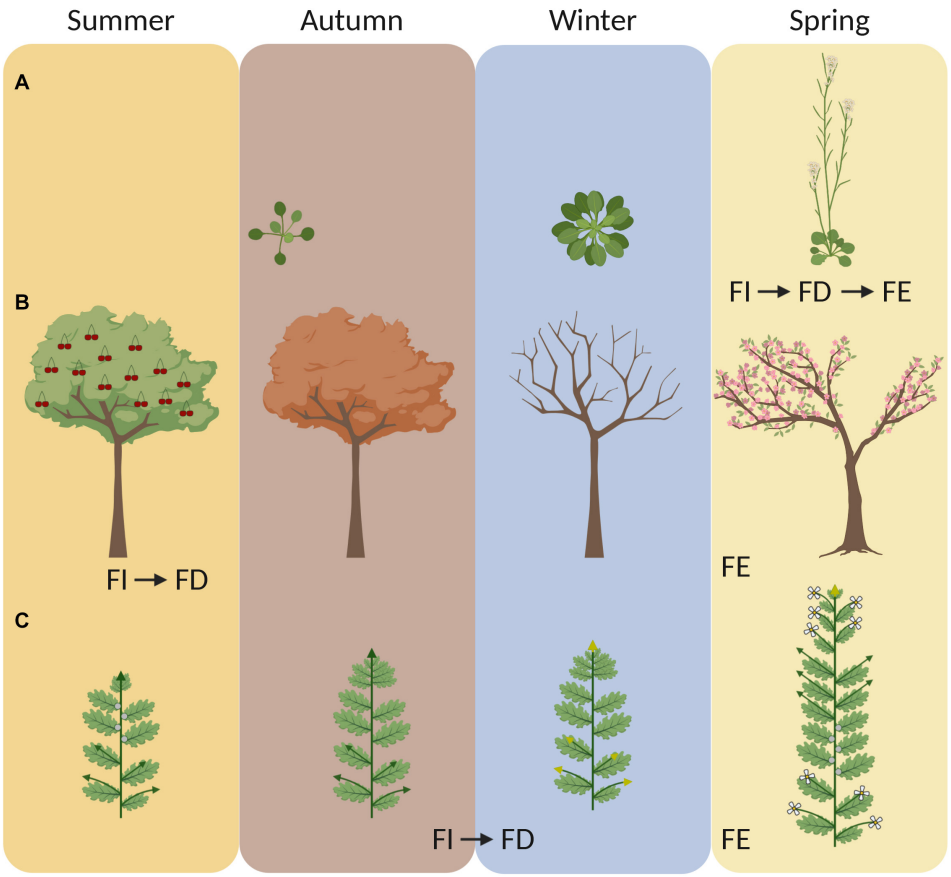

FIGURE 1 | Annuals and perennials initiate floral buds at different times during the year and use winter to synchronize flowering. Cartoons depict the yearly life cycle of **(A)** a winter annual (e.g., *A. thaliana*), **(B)** a woody perennial (e.g., cherry tree) and **(C)** an herbaceous alpine perennial (e.g., *A. alpina*). Winter annual *A. thaliana* accessions induce flowering in the spring. After floral induction (FI), flowering is initiated and floral buds develop (FD) and emerge (FE). In *A. thaliana*, all steps from floral induction to emergence are very rapid (FI, FD and FE). In perennials, the stages of floral induction (FI) and floral emergence (FE) are temporarily separated. Many woody perennials induce and initiate flowering during summer (FI and FD) but flower buds emerge (FE) in the spring of the next year. In *A. alpina*, flowering is induced and initiated (FI and FD) during cold exposure in the late autumn, but flowers emerge (FE) after plants return to warm temperatures. In panel **(C)**, *green arrows* represent vegetative branches and *yellow arrows* represent flowering branches. Image created with BioRender.com.

A. alpina, flowering is initiated during vernalization under short photoperiods (**Figures 1C**, **2**; Wang et al., 2009; Lazaro et al., 2018). Similarly, field studies in winter oil seed rape demonstrated that inflorescences are initiated during the autumn in response to low temperatures (O'Neill et al., 2019). In both species, the length of the cold exposure is also important for the outgrowth of flower buds after the return to warm temperatures (Lazaro et al., 2018; O'Neill et al., 2019). Flower buds may still enter dormancy during the winter or grow more slowly due to low temperatures. In field studies using oil seed rape plants, dissection of shoot apical meristems showed that inflorescence meristems gradually grow during the winter and thus may not be dormant (O'Neill et al., 2019). Although flower buds in such species develop during autumn, daylength is still important for flowering. As shown in *A. lyrata*, long photoperiods are important for inflorescence bolting in the spring (Kemi et al., 2019). Ecological studies in alpine species suggest that flower bud development during cold exposure can be an advantageous adaptive trait in harsh environments characterized by prolonged snow coverage and short growing seasons (Diggle, 1997; Meloche and Diggle, 2001). This modification of the role of vernalization on flowering does not seem to be related to the plant life strategy as both annual and perennial species have been reported to form flower buds during cold treatment (Chouard, 1960; Wang et al., 2009; Kemi et al., 2019; O'Neill et al., 2019).

THE ROLE AND REGULATION OF *FLOWERING LOCUS C* (*FLC*) IN *A. thaliana*

Several studies in *A. thaliana* demonstrated that the major regulator of flowering through the vernalization pathway is the MADS box transcription factor FLOWERING LOCUS C (FLC) (Michaels and Amasino, 1999; Sheldon et al., 2000). In temperate grasses, which also require prolonged cold exposure to flower, and also in biennials such as sugar beet, the regulation of vernalization is mediated by pathways independent of FLC

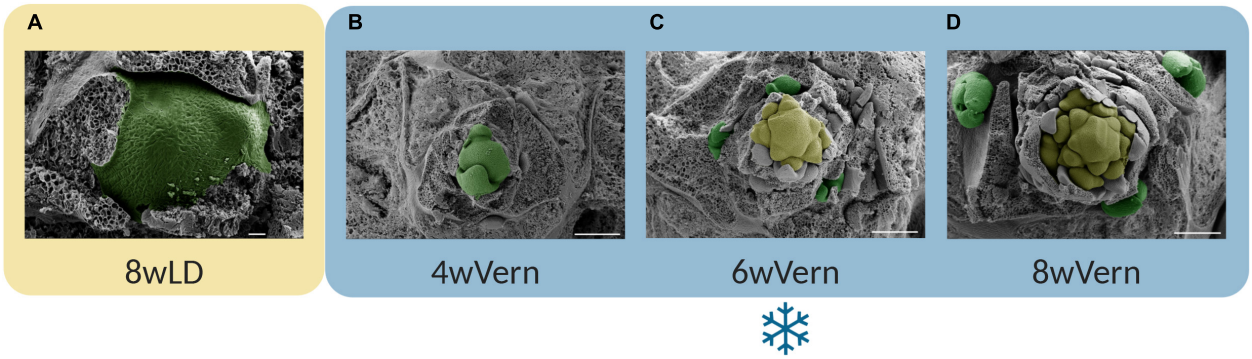

FIGURE 2 | Flower buds in *A. alpina* are initiated during vernalization. Progression of the shoot apical meristem of *A. alpina* accession Pajares imaged by *scanning electron microscopy* (*SEM*) in **(A)** plants were grown for 8 weeks in a long day greenhouse, and subsequently transferred to vernalization for **(B)** 4 weeks (4wVern), **(C)** 6 weeks (6wVern) or **(D)** 8 weeks (8wVern). The main shoot apex is vegetative in plants grown in greenhouse conditions or vernalized only for 4 weeks (4wVern) (**A,B**, highlighted in *green*). The main shoot apex initiates flowering after 6 weeks in vernalization (**C**, highlighted in *yellow*) and inflorescences develop during vernalization (**D**, highlighted in *yellow*). In the axils of leaf primordia close to the shoot apical meristem, new vegetative buds are also formed (**C,D**, highlighted in *green*). Scale bars correspond to 20 μm **(A)** or to 200 μm **(B–D)**. Colored boxes represent different growth conditions: the *yellow box* a long day greenhouse; and the *blue box* the vernalization at 4°C and short days (8 h light: 16 h dark). SEM pictures were modified from the Ph.D. dissertation of Zhou (2019). Image was composed using BioRender.com.

(reviewed in Bouché et al., 2017). FLC is a floral repressor that is highly expressed in *A. thaliana* accessions that require vernalization to accelerate flowering (Shindo et al., 2006; Li et al., 2014). Prolonged exposure to low temperatures regulates *FLC* in two ways: (1) by quantitatively repressing *FLC* transcript accumulation and (2) by ensuring that *FLC* will remain stably silenced after plants have returned to warm conditions. The major mechanism that drives *FLC* transcriptional regulation by long-term cold consists of chromatin modifications (reviewed in Berry and Dean, 2015). In *A. thaliana* accessions, non-coding *cis* polymorphisms at the *FLC* locus underlie variation in the length of cold required to achieve stable silencing of *FLC* (Coustham et al., 2012; Qüesta et al., 2020). *FLC* is transcriptionally repressed by long non-coding RNAs (lncRNAs), expressed at the locus in response to cold, which play an early role in the epigenetic silencing of *FLC* (Heo and Sung, 2011; Csorba et al., 2014). A parallel pathway that interprets long-term exposure to low temperatures involves the plant homeodomain (PHD) protein, VERNALIZATION INSENSITIVE 3 (VIN3) (Sung and Amasino, 2004; Wood et al., 2006; De Lucia et al., 2008; Swiezewski et al., 2009). *VIN3* expression increases gradually during cold by a mechanism that is mediated by the NAC transcription factor NTM1-LIKE 8 (NTL8) (Sung and Amasino, 2004; Bond et al., 2009; Zhao et al., 2020). NTL8 protein accumulates during cold exposure, due to growth retardation and reduced number of cell divisions that occur at low temperatures, and upregulates *VIN3* transcription (Zhao et al., 2020). Subsequently, VIN3 forms a complex with its homologous PHD protein VERNALIZATION5 (VIN5) and the Polycomb Repressive Complex 2 (PRC2) proteins VERNALIZATION2 (VRN2), MSI1, FIE/EED, and the E(z) homologs SWINGER (SWN) and CURLY LEAF (CLF) (reviewed in Berry and Dean, 2015). This PHD-PRC2 complex is recruited to the *FLC* locus at 3 nucleosomes, covering exon 1 and part of the first intron (which is called the nucleation region), and methylates H3 lysine 27 residues resulting in a gradual cell-autonomous *FLC* silencing (Angel et al., 2011). The B3-binding transcription factor VP1/ABI3-LIKE 1 (VAL1) is required for the PHD-PRC2 action at *FLC* (Qüesta et al., 2016; Yuan et al., 2016). After cold exposure, the H3K27me3 mark spreads over the entire *FLC* locus and ensures maintenance of long-term silencing of *FLC* (Finnegan and Dennis, 2007; De Lucia et al., 2008). This spreading of H3K27me3 is enabled by the PHD-PRC2 complex and requires the action of the Polycomb protein LIKE HETEROCHROMATIN PROTEIN1 (LHP1) that specifically binds to H3K27me3 marks (reviewed in Costa and Dean, 2019).

Similar to other MADS-domain proteins, FLC regulates its downstream genes by binding to conserved CArG-box motifs in their promoters or introns (Deng et al., 2011; Mateos et al., 2017). FLC target genes act in different pathways throughout development, of which several are implicated in flowering (Deng et al., 2011; Mateos et al., 2017). These include the floral promoter *FLOWERING LOCUS T* (*FT*), that regulates flowering through the photoperiod pathway; *SUPPRESSOR OF OVEREXPRESSION OF CONSTANS 1* (*SOC1*), that regulates several genes involved in floral transition at the shoot apex; the SQUAMOSA BINDING PROTEIN LIKE (SPL) family member SPL15, that contributes to reproductive competence and floral transition; and *SEPALLATA3* (*SEP3*), that regulates flower development (reviewed in Madrid et al., 2020). Stable *FLC* silencing after vernalization is, therefore, a key feature to explain the flowering pattern of winter annual *A. thaliana* accessions. This is because the reduced mRNA levels of *FLC* allow the activation of floral promoting pathways that ensure the initiation of flowering in the spring. For the life cycle of an annual plant it is important that *FLC* expression is restored in the next generation. In *A. thaliana* this occurs during embryo development and by the end of embryogenesis all H3K27me3 marks have been removed from the *FLC* locus so that the gene is fully reactivated (Tao et al., 2019; Luo et al., 2020).

Arabidopsis thaliana plants that carry weak *FLC* alleles can initiate flowering in the autumn due to low starting *FLC* mRNA levels (Hepworth et al., 2020). These genotypes bolt precociously and show higher mortality in the field, which emphasizes the importance of *FLC* in ensuring spring flowering in *A. thaliana* (Hepworth et al., 2020). In oil seed rape plants, which initiate flowering during cold exposure, the starting levels of *BnaFLC* also negatively correlate with the timing of flower bud initiation in the autumn (O'Neill et al., 2019). Cultivars with lower *BnaFLC* mRNA levels initiate flowering earlier compared to cultivars with higher starting *BnaFLC* mRNA levels (O'Neill et al., 2019). Interestingly, although oil seed rape plants do not bolt precociously, there is a penalty on plant yield if flowering is initiated earlier in the autumn (Brown et al., 2019).

THE ROLE OF FLC IN THE REGULATION OF FLOWERING IN PERENNIAL BRASSICACEAE SPECIES

The role of FLC has been explored in perennial Brassicaceae species such as *A. alpina* (Wang et al., 2009; Albani et al., 2012), *A. lyrata* (Kemi et al., 2013), *Arabidopsis halleri* (Aikawa et al., 2010), *Arabidopsis arenosa* (Baduel et al., 2016), and *Boechera stricta* (Lee et al., 2018). At regions, syntenic to the *FLC* locus in *A. thaliana*, some of these species contain tandem *FLC* copies derived from duplication events after their divergence from *A. thaliana* (Nah and Chen, 2010; Albani et al., 2012). *A. lyrata* has two tandemly duplicated *FLC* genes (*FLC1* and *FLC2*), whereas *A. arenosa* contains one partial and two complete *FLC* copies (Nah and Chen, 2010). In *A. alpina* a region of ∼2 kb at the *FLC* ortholog, *PERPETUAL FLOWERING 1* (*PEP1*), has been tandemly duplicated (Albani et al., 2012). This tandem duplication includes the first exon of *PEP1* (*AaFLC*) and parts of its promoter and first intron (Albani et al., 2012). Interestingly, this tandem duplication leads to the production of two overlapping *PEP1* transcripts (*PEP1a* and *PEP1b*) that have different transcriptional start sites, using the two tandemly duplicated first exons (Albani et al., 2012). This finding could suggest that duplication events in *FLC* orthologs may give rise to diverse functions or specialized forms of the protein. Nevertheless, tandem duplications in *FLC* do not contribute to the perennial life cycle. For example, several *FLC* orthologs in both annual and perennial Arabis species contain duplicated regions (Kiefer et al., 2017). In addition, even within *A. alpina* not all accessions contain the partial duplication at *PEP1* (*AaFLC*) (Albani et al., 2012).

The role of FLC in flowering in perennial Brassicaceae is similar to that reported in *A. thaliana* and other annual Brassicas. *FLC1* mRNA levels in *A. lyrata* are down regulated in response to vernalization and *FLC* genes are co-localized with QTLs determining flowering time differences between late and early flowering *A. lyrata* accessions (Kemi et al., 2013). Similarly, *A. alpina* accessions carrying lesions in *PEP1* (*AaFLC*) do not require vernalization to flower (Albani et al., 2012). The *A. alpina pep1* mutant also flowers without vernalization compared to its wild type accession Pajares, that has an obligate vernalization requirement to flower (Wang et al., 2009). An interesting feature in perennial Brassicaceae is that *FLC* is not stably silenced after vernalization, resembling *FLC* expression patterns of *A. thaliana* accessions that require extended vernalization to flower (Wang et al., 2009; Kemi et al., 2013; Baduel et al., 2016; Qüesta et al., 2020). Unstable silencing of *FLC* orthologs by vernalization has been observed in plants grown in controlled environmental conditions (Wang et al., 2009; Kemi et al., 2013; Lazaro et al., 2018) and also in plants experiencing winter chilling temperatures in the field (Aikawa et al., 2010; Nishio et al., 2020). For instance, transcript accumulation of the *A. halleri FLC* (*AhgFLC*) is reduced during winter and is upregulated again the following spring (Aikawa et al., 2010). Interestingly, the accumulation of the H3K27me3 mark mirrors the expression patterns of *AhgFLC* (Nishio et al., 2020). In *A. alpina* plants vernalized for 12 weeks, *PEP1* (*AaFLC*) is also temporarily silenced during cold exposure but it is transcriptionally activated again after plants return to growth-promoting conditions (Wang et al., 2009). On the contrary, *FLC* of the annual close relative *Arabis montbretiana* (*AmFLC*) is stably silenced by vernalization (Kiefer et al., 2017). Plants carrying introgressions of genomic segments containing the *AmFLC* into *A. alpina,* indicated that, in the same genetic background, *PEP1* and *AmFLC* are differentially silenced after vernalization (Kiefer et al., 2017; Hyun et al., 2019). The major difference between the *A. alpina* and *A. montbretiana FLC* orthologs lies in polymorphisms within non-coding regions suggesting that, similar to *A. thaliana FLC*, non-coding polymorphisms may confer differences between *PEP1* and *AmFLC* in stable silencing by vernalization (Coustham et al., 2012; Kiefer et al., 2017). Within the Arabideae, the annual life strategy arose several times during evolution (Kiefer et al., 2017). Phylogenetic studies in different taxa suggest that annuals were derived from perennial ancestors, although in some genera annuals seem to have switched back to the perennial growth habit (Friedman and Rubin, 2015). We can, therefore, hypothesize that Brassicaceae annual species may have gained independently *cis* polymorphisms at *FLC* non-coding regions to ensure stable silencing, which is important for the spring-flowering habit.

In addition to the seasonal cycling of *PEP1* mRNA levels, the perennial behavior in *A. alpina* is also characterized by a strong regulation of age-related factors that determine whether individual meristems will initiate flowering in response to vernalization or not (Wang et al., 2009; Bergonzi et al., 2013; Hyun et al., 2019; Lazaro et al., 2019; Zhou et al., 2021). Interestingly, the degree of *PEP1* (*AaFLC*) stable silencing by vernalization has been demonstrated to vary between meristems, depending on whether they initiated flowering during the cold exposure (Lazaro et al., 2018). In juvenile meristems that fail to initiate flowering during cold treatment, *PEP1* (*AaFLC*) mRNA levels are reduced during vernalization and upregulated again after plants return to warm temperatures (Wang et al., 2011; Lazaro et al., 2018). In this way, *PEP1* (*AaFLC*) ensures maintenance of vegetative growth after vernalization even when meristems develop further and acquire competence to flower. The underlying cause of the difference in *PEP1* (*AaFLC*) regulation by prolonged cold exposure between juvenile and adult meristems is not known. In *A. thaliana,* DNA replication

has been proposed to be essential for the maintenance of *FLC* silencing after vernalization (Finnegan and Dennis, 2007; Qüesta et al., 2020). On the same lines, differences in cell division and DNA replication between meristems may explain the variation observed in *PEP1* (*AaFLC*) stable silencing by cold. In *A. alpina*, *PEP1* (*AaFLC*) reactivation after vernalization has been shown to be facilitated by *PERPETUAL FLOWERING2* [*PEP2*, the *A. alpina* ortholog of *APETALA2* (*AP2*)], a role not previously reported for AP2 in *A. thaliana* (Bergonzi et al., 2013; Lazaro et al., 2019). The mechanism for this role of PEP2 (AaAP2) is not known. AP2 in *A. thaliana* interacts with chromatin remodeling factors such as HISTONE DEACETYLASE 19 (HDA19) (Krogan et al., 2012), but has never been associated with histone demethylases which could facilitate the upregulation of *PEP1* (*AaFLC*) mRNA levels after vernalization.

Flowering in adult/competent meristems is initiated at about 6 weeks after the start of vernalization (**Figure 2**; Wang et al., 2009; Lazaro et al., 2018). For plants to flower, however, exposure to a minimum of 12 weeks of vernalization is required as inflorescence meristems should develop further during vernalization (Wang et al., 2009; Lazaro et al., 2018). The molecular mechanisms enabling floral development during vernalization involve the floral integrator AaSPL15 and increased sensitivity to the growth regulator gibberellin (GA) (Hyun et al., 2019; Tilmes et al., 2019). *PEP1* expression is still not stably silenced after 12 weeks of vernalization, which leads to floral reversion phenotypes, such as the presence of bracts or flower to inflorescence reversion (Wang et al., 2009; Lazaro et al., 2018). Exposure to a minimum of 18 weeks of cold treatment is required to inhibit floral reversion and to stably silence *PEP1* (Lazaro et al., 2018). Floral reversion phenotypes are also observed in *A. halleri* plants, although in this species it has not been reported whether flower buds are formed the previous year (Aikawa et al., 2010; Nishio et al., 2020).

Interestingly, *A. alpina* genes that act in the age pathway to regulate the age-dependent response to vernalization also influence the duration of vernalization required for flowering. For example, PEP2, TARGET OF EAT2 (AaTOE2), TERMINAL FLOWER1 (AaTFL1), and AaSPL15 determine the age at which plants become competent to flower in response to cold treatment, but also control the duration of vernalization required for flowering (Wang et al., 2011; Lazaro et al., 2018; Hyun et al., 2019; Zhou et al., 2021). The *pep2* and *Aatoe2* mutants and transgenic lines with reduced function of AaTFL1 (DsRNAi *AaTFL1*) flower when vernalized at a young age (at 3 weeks old compared to 5 weeks for wild type plants) and require less than 8 weeks of vernalization to flower (compared to 12 weeks for wild type plants) (Wang et al., 2011; Lazaro et al., 2019; Zhou et al., 2021).

In woody perennials, bud dormancy is regulated by a cluster of tandemly duplicated genes, *DORMANCY ASSOCIATED MADS-BOX* 1-6 (*DAM1-6*) (reviewed in Falavigna et al., 2019). Similar to *FLC*, *DAM* genes encode MADS box transcription factors, but these are more closely related to *A. thaliana* SHORT VEGETATIVE PHASE (SVP) and AGAMOUS-like 24 (AGL24) (reviewed in Falavigna et al., 2019). The expression of *DAM* genes is upregulated during dormancy induction and downregulated during the transition from endo- to ecodormancy (Maurya and Bhalerao, 2017; Vimont et al., 2019). *DAM* genes are also regulated by epigenetic mechanisms such as histone modifications (Leida et al., 2012; de la Fuente et al., 2015; Saito et al., 2015) and DNA methylation (Rothkegel et al., 2017). In *A. thaliana*, SVP is a floral repressor that interacts with other transcription factors to regulate floral development and flowering time (De Folter et al., 2005; Gregis et al., 2006; Lee et al., 2007; Balanzà et al., 2014; Mateos et al., 2015). FLC is an interactor of SVP *in A. thaliana* and both proteins act together to regulate flowering time by repressing FT and SOC1 or GA-related genes (Lee et al., 2007; Andrés et al., 2014; Mateos et al., 2015). These data suggest that SVP or other MADS box genes might have taken the role of FLC in woody perennials to regulate developmental traits related to prolonged cold exposure.

PLEIOTROPIC ROLES OF FLC IN PERENNIAL BRASSICACEAE

In addition to the role of FLC in flowering, studies in *A. thaliana* and other Brassicaceae species demonstrated that FLC has pleiotropic effects on other developmental traits. Pleiotropic phenotypes may be an indirect effect caused by differences in flowering behavior adopted by different species and/or may be due to direct roles of FLC on other traits. Examples of direct and indirect pleiotropic effects of FLC are reported below.

Polycarpic Growth Habit and Shoot Architecture in the Perennial *A. alpina*

PERPETUAL FLOWERING 1 (AaFLC) contributes to the polycarpic growth habit and ensures that *A. alpina* plants maintain vegetative growth after flowering (Wang et al., 2009). In *pep1* mutants all axillary branches flower, suggesting that PEP1 (AaFLC) regulates the fate of axillary meristems (Wang et al., 2009; Vayssières et al., 2020). This role of PEP1 (AaFLC) is facilitated by the ability of *A. alpina* plants to initiate flowering during vernalization (**Figure 2**; Wang et al., 2009; Lazaro et al., 2018). Flower bud development during vernalization is also coupled with the formation of axillary meristems in the leaf axils close to the shoot apical meristem (Wang et al., 2009; Ponraj and Theres, 2020; Vayssières et al., 2020). These newly formed axillary meristems develop into buds in a basipetal sequence and do not commit to reproductive development during cold exposure (*green* in **Figures 2C,D**; Wang et al., 2009; Ponraj and Theres, 2020; Vayssières et al., 2020). *A. alpina* mutants that carry lesions in floral repressors in the age pathway (AaTOE2 and AaAP2/PEP2) but also transgenic lines with altered levels of SPLs (e.g., microRNA cleavage-resistant forms of SPL15, rSPL15) have axillary branches at these subapical nodes which develop and become reproductive (Hyun et al., 2019; Lazaro et al., 2019; Zhou et al., 2021). A closer look at the *A. alpina toe2* mutant demonstrated that these subapical buds initiate flowering already during vernalization (**Figure 3B**; Zhou et al., 2021). This result suggests that the fate of the subapical buds is determined during vernalization by the age pathway.

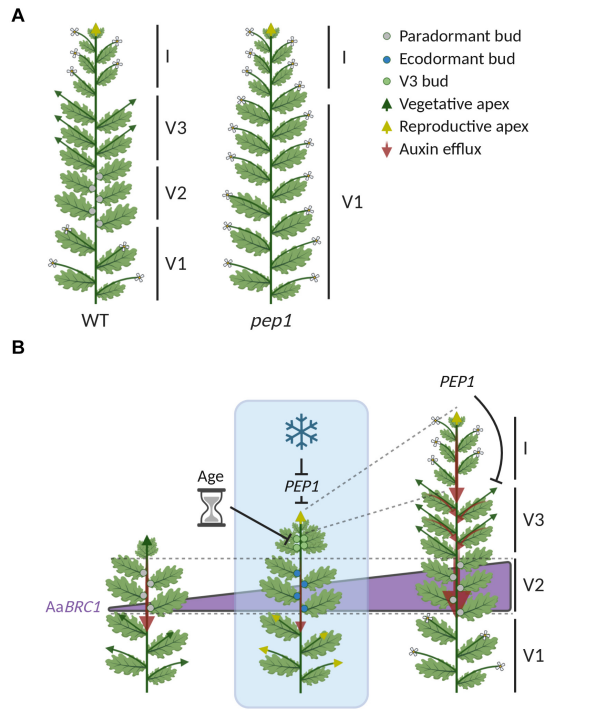

FIGURE 3 | Shoot architecture in *A. alpina* is shaped by vernalization and *PEP1*. **(A)** Representation of wild type *A. alpina* (WT) and *pep1* mutant plants after flowering. Wild type plants require exposure to long-term cold to flower, whereas *pep1* mutants do not and can flower directly in greenhouse conditions. Flowering wild type plants have a complex shoot architecture, which is organized in differentiated zones of basal flowering axillary branches (V1) that partially senesce; dormant buds (V2); vegetative axillary branches (V3); and the inflorescence (I). The *pep1* mutant lacks this zonation and has only V1 axillary branches and the inflorescence. **(B)** Representation of the shoot architecture of a wild type plant during its life cycle before, during and after vernalization. *Blue box* represents exposure to prolonged cold, whereas the time before and after cold exposure is not colored. During long-term cold, *PEP1* (*AaFLC*) transcript levels are reduced and both the main shoot apex and the apices of V1 axillary branches initiate flowering (*yellow arrowheads*). In addition, new buds (V3 buds, *green circles*) are formed in those leaf primordia close to the main shoot apex. These V3 buds (*green circles*) do not initiate flowering during cold exposure due to the repressive action of the age pathway. After cold exposure, V3 buds give rise to V3 axillary branches, which grow vegetatively because *PEP1* (*AaFLC*) transcript levels are upregulated and repress flowering. The outgrowth of V2 buds is inhibited by paradormancy (or apical dominance) before vernalization (*gray circles*), by ecodormancy during cold exposure (*blue circles*) and by paradormancy (or latency) after plants return to growth-promoting conditions (*gray circles*). The dormancy status of V2 buds increases during and after vernalization, and is regulated by a mechanism that is independent of PEP1 (AaFLC). Increased dormancy in V2 buds correlates with the upregulation of *BRANCHED 1* (*AaBRC1*), a repressor of bud outgrowth (*illustrated with the purple triangle*). After vernalization, increased dormancy in V2 buds is correlated with increased endogenous IAA levels in the stem and auxin transport (*red arrows*). Image created using BioRender.com.

Wild type *A. alpina* flowering plants exhibit a complex shoot architecture in which axillary meristems behave in different ways and are organized in different zones (**Figure 3A**; Lazaro et al., 2018; Ponraj and Theres, 2020; Vayssières et al., 2020). Zonation patterns of differential bud activity and fate have also been reported in other perennials (Costes et al., 2014). The main stem of *A. alpina* plants consist of zones of basal axillary flowering branches (V1), axillary vegetative branches (V3) and dormant buds (V2) (**Figure 3A**; Lazaro et al., 2018; Ponraj and Theres, 2020; Vayssières et al., 2020). PEP1 (AaFLC) contributes to this complex shoot architecture considering that the *pep1* mutant consists only of V1 axillary branches and lacks the V2 dormant buds and V3 vegetative branches (**Figure 3A**; Wang et al., 2009; Vayssières et al., 2020). In wild type plants, V1 axillary branches behave similarly to the main shoot apex and initiate flowering during vernalization, when *PEP1* mRNA levels are reduced (*yellow arrows* in **Figure 3B**; Wang et al., 2009; Vayssières et al., 2020). V3 axillary branches arise after vernalization from buds formed at the subapical nodes during cold (*green* in **Figures 2C,D**; *green circles* in **Figure 3B**; Wang et al., 2009; Lazaro et al., 2018; Ponraj and Theres, 2020; Vayssières et al., 2020; Zhou et al., 2021). PEP1 determines the fate of these buds after vernalization (Wang et al., 2009; Lazaro et al., 2018). Specifically, *PEP1* mRNA levels are upregulated after vernalization to repress flowering and ensure that these branches will maintain vegetative development (V3 *green arrows* in **Figure 3B**; Wang et al., 2009; Lazaro et al., 2018). V2 buds follow a different developmental path, in which their growth is repressed before and after vernalization by paradormancy (or latency) and their activity is influenced by their position on the shoot (*gray circles* in **Figure 3B**; Vayssières et al., 2020). During cold exposure, V2 buds become ecodormant (*blue circles* in **Figure 3B**; Vayssières et al., 2020). The activity of V2 buds is not directly regulated by PEP1 (AaFLC) but rather by the *A. alpina* ortholog of *BRANCHED 1* (*AaBRC1*), whose expression increases during and after vernalization (*Purple triangle* in **Figure 3B**; Vayssières et al., 2020). Flowering time genes such as FT in *A. thaliana* and SPL15 (OsSPL14) in rice have been reported to influence bud activity (Miura et al., 2010; Tsuji et al., 2015). PEP1 (AaFLC) might indirectly inhibit the outgrowth of buds in the nodes within the V2 zone. Specifically, PEP1 (AaFLC), by repressing flowering in V3 axillary branches, ensures the continuous formation of young leaves that may act as an auxin source to inhibit the outgrowth of V2 buds (*Red arrows* in **Figure 3B**; Vayssières et al., 2020). Many studies in *A. thaliana* support the theory that auxin saturation in the transport stream of the main stem can inhibit bud outgrowth by blocking auxin transport from lateral sources (Prusinkiewicz et al., 2009). Dormant buds are always located at the axils of leaves below the zone of V3 vegetative branches, supporting the hypothesis that V3 branches may become the new auxin source that represses the outgrowth of V2 buds (*Red arrows* in **Figure 3B**; Vayssières et al., 2020). Nevertheless, mutants in which V3 branches flower still have a dormant bud zone (Hyun et al., 2019; Zhou et al., 2021). This phenotype can be explained by the fact that flowering V3 branches still maintain vegetative development through secondary or tertiary branching and can still act as auxin sources (Zhou et al., 2021).

Overall, the complex architecture in *A. alpina* is a result of the effect of prolonged cold exposure on the regulation of flowering and on bud dormancy, which differs between meristems. These roles of cold are partially controlled by PEP1 (AaFLC).

Duration of the Flowering Season in the Perennial *A. alpina*

Many temperate perennials restrict the duration of the flowering season to spring and summer. In *A. alpina, pep1* mutants and accessions that carry inactive *PEP1* alleles flower perpetually (continuously) (Wang et al., 2009; Albani et al., 2012). In the field, perpetual flowering genotypes with non-functional *PEP1* alleles show extended and asynchronous flowering (Hughes et al., 2019). Interestingly, these genotypes also exhibit reduced survival in the field, suggesting that PEP1 contributes to plant fitness (Hughes et al., 2019). The role of PEP1 on the duration of the flowering season is a result of the upregulation of *PEP1* mRNA levels after vernalization. PEP1 restricts the duration of flowering season by ensuring that no further meristems will initiate flowering after the return to warm temperatures.

So far, there are only a few studies exploring the regulation of flowering duration in other perennials. In the Rosaceae, there is natural variation for this trait. Genotypes that follow either the seasonal flowering habit (and restrict the duration of the flowering episode) or the perpetual flowering habit (and flower continuously) can be found (Brown and Wareing, 1965; Crespel et al., 2002; Albani et al., 2004). In the wild strawberry *Fragaria vesca* and rose, the perpetual flowering habit arose from loss of function mutations in the floral repressor TERMINAL FLOWER1 (TFL1) (Iwata et al., 2012; Koskela et al., 2012). Interestingly, all perpetual flowering *F. vesca* accessions contain the same 2 bp deletion in *FvTFL1*, suggesting that in *F. vesca* (but not in *A. alpina* and rose) the perpetual flowering habit arose only once during evolution (Albani et al., 2012; Iwata et al., 2012; Koskela et al., 2012). It is also worth noting that the perpetual flowering habit in most genotypes is linked to a loss of environmental sensitivity for flowering-promoting conditions. *F. vesca* accessions that flower seasonally require exposure to short photoperiods to induce flowering, whereas perpetual flowering accessions are day neutral (Koskela et al., 2012). Similarly, seasonal flowering *A. alpina* accessions require vernalization to flower, whereas perpetual flowering accessions can flower without being exposed to vernalization (Wang et al., 2009; Albani et al., 2012).

Leaf Traits in the Annual *Cardamine hirsuta*

FLOWERING LOCUS C has been detected in QTL studies to underlie differences in leaf size and complexity in the annual Brassicaceae *Cardamine hirsuta* (Cartolano et al., 2015). Accessions with reduced expression of the *C. hirsuta FLC* ortholog (*ChFLC*) flower early and have leaves with more leaflets (Cartolano et al., 2015). Interestingly, *cis* polymorphisms in the nucleation region of *ChFLC* seem to be responsible for the differences in leaf complexity and flowering time (Cartolano et al., 2015). This effect of *ChFLC* on leaf shape cannot be uncoupled from flowering (Cartolano et al., 2015), suggesting that the leaf phenotype in *C. hirsuta* may be associated with flowering time.

Pleiotropic Roles of FLC in Seed Traits in *A. thaliana* and *A. alpina*

Plant fitness can be influenced by seed traits such as seed dormancy and longevity. Seed dormancy is defined as the incapacity of seeds to germinate under favorable conditions and enables seeds to prevent germination outside the favorable growth season. Seed longevity determines how long seeds remain viable in the seed bank. Monocarpic plants are usually characterized by seeds with higher seed longevity, as seeds constitute their only option to persist in a certain habitat (Thompson et al., 1998).

In *A. thaliana*, several studies using the (low dormant) accessions Landsberg *erecta* (L*er*) and Columbia (Col) provided evidence that *FLC* enhances germination (**Figure 4**; Chiang et al., 2009; Auge et al., 2017; Blair et al., 2017). However, this positive effect of *FLC* on germination has not always been observed. Other studies (also using the L*er* and Col accessions) indicated that *FLC* plays a negative role in germination by enhancing seed dormancy (**Figure 4**; Chen et al., 2014; Chen and Penfield, 2018) or that it does not influence dormancy (Liu et al., 2011). These different results suggest a role of *FLC* in germination and dormancy in *A. thaliana* that could depend on environmental conditions and genetic backgrounds. This is also suggested by the observation that the germination phenotype of FLC depends on the dormancy level of seeds (Blair et al., 2017). In addition, these different observations

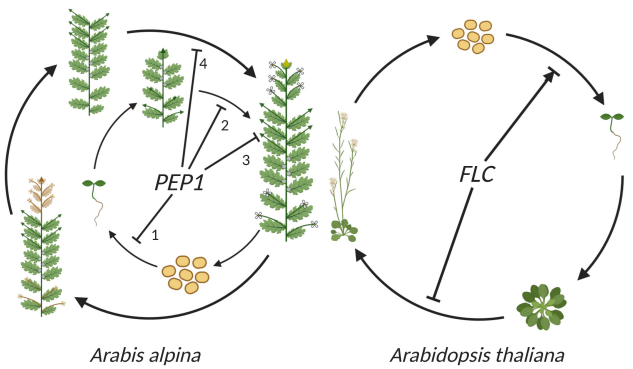

FIGURE 4 | The role of *FLC* in the life cycle of perennial *A. alpina* and annual *A. thaliana*. In *A. alpina*, *PEP1* (*AaFLC*) regulates flowering in response to vernalization and contributes to the perennial life cycle by acting at different developmental stages and tissues. Starting from seeds, *PEP1* acts as a negative regulator of germination and an enhancer of seed longevity (1). Later on, *PEP1* represses flowering and ensures that plants will synchronize anthesis with favorable environmental conditions in the spring (2). *PEP1* also ensures that V3 axillary branches will remain vegetative after flowering (3). The role of *PEP1* in flowering and maintenance of vegetative development are repeated every year (4). In Arabidopsis, *FLC* acts as a floral repressor in accessions that require vernalization to flower. *FLC* also influences germination in *A. thaliana*, either positively or negatively depending on the environmental conditions and genetic background. Lines with (→) indicate positive influence and lines with (⊥) indicate negative influence. As in **Figures 1**, **3**, *green arrows* represent vegetative branches, *yellow arrows* represent flowering branches and *gray circles* represent dormant V2 buds. Image created using BioRender.com.

could be explained by the function of other genes, such as *FT*, that control *FLC* expression during germination and independently affect seed germination (Auge et al., 2019). To further enhance the complexity by which these flowering time genes regulate seed traits, *FT* has also been shown to either enhance or reduce dormancy in different studies (Chiang et al., 2009; Chen et al., 2014; Chen and Penfield, 2018). Although complex, the observed phenotypes indicate a role for *FLC* and other flowering time genes in the control of germination. The exact role and mechanism of *FLC* in germination control is still unclear, but it seems likely to be influenced by environmental factors (in particular temperature) that vary between experiments. This is consistent with the observation that FLC is maternally controlled in its influence on dormancy (Chiang et al., 2009; Chen and Penfield, 2018). FLC is therefore likely to have a role in the translation of environmental conditions experienced by the mother plant into the dormancy level of its progeny seeds.

Although both flowering and germination should be properly timed to ensure reproductive success, the suppressive role of FLC on flowering seems to be more consistent among experiments and species, compared to its role in seed traits. An interesting difference between these two developmental transitions is that seed germination can be arrested and postponed for a year if conditions are unfavorable, which is not possible for flowering in monocarpic plants. Seed dormancy induction on the mother plant is also more sensitive to subtle differences in ambient temperature compared to flowering induction. Small differences in temperature before and during seed development can have a strong impact on seed dormancy (Springthorpe and Penfield, 2015). If FLC has a role in translating these subtle temperature differences to dormancy differences, it could explain the varying phenotypes between experiments. Another difference is that exposure to long-term low temperatures (below 10°C) downregulates *FLC* transcript accumulation and leads to flowering, whereas exposure of plants to mildly low temperatures (16 versus 22°C) before seeds are fully ripe can enhance *FLC* expression (Chen and Penfield, 2018). This suggests a different mechanism by which temperature regulates *FLC* expression, which could be related with its more flexible role in germination compared to flowering.

In annuals, FLC regulates both flowering time and germination traits and therefore constitutes a connecting factor between both traits. Different scenarios for this connection can be hypothesized which could be advantageous in different climates. The combination of late flowering and low dormancy could cause seeds to germinate in autumn and enable the plant to survive in a vegetative state during winter. Late flowering and high dormancy would delay germination till the next spring and enable plants to grow vegetatively during the year and flower the following spring. Early flowering and low dormancy would be advantageous in a climate with humid summers and enable two generations within one year. Early flowering and high dormancy would enable flowering and seed set in spring and delay germination until the next spring. In perennials, all these different scenarios are less relevant as plants can persist longer in their ecosystems.

In *A. alpina*, *PEP1* (*AaFLC*) also influences seed dormancy and seed longevity. The *pep1* mutant alleles have low dormancy and reduced longevity, suggesting that PEP1 positively regulates these traits (**Figure 4**; Hughes et al., 2019). The influence of *PEP1* on seed dormancy seems more consistent in *A. alpina* compared to that of *FLC* in *A. thaliana*. Although there has only been a single study of this trait in *A. alpina* until now, it showed a consistent role of PEP1 in greenhouse and garden experiments. The existence of many *A. alpina* accessions with non-functional *PEP1* alleles suggests an advantage of the combination of perpetual flowering and low dormancy in certain environments.

Overall, the role of FLC in the two major developmental transitions of plants and its adjustment to temperature give it an important regulatory role to determine the life cycle of Brassicaceae species. Additional functions of FLC as described in this review also suggest a link between the regulation of these developmental transitions and the architecture of the plant. This could have selective advantages in nature but also implies that breeding for altered flowering time in Brassicaceae species could have unexpected effects on seed traits and/or plant architecture or other still unknown trade-offs. Therefore, functional studies of this link can provide new insights in the relation between these traits and support breeding for crop adaptation to local and changing climates. Whereas *FLC* has been demonstrated to affect different traits in Brassicaceae, other genes are expected to fulfill its function in other plant families. For instance, in cereals the *VRN* genes have a similar role in the regulation of vernalization as *FLC* in the Brassicaceae. It would be of great interest to find out whether these genes also have similar roles in other traits that are regulated by FLC. Conservation of this link would indicate its general importance for survival and adaptation of plants to their environment.

AUTHOR CONTRIBUTIONS

All authors developed the concept and wrote the manuscript. NVdIT prepared the figures.

FUNDING

This work was supported by the Cluster of Excellence on Plant Sciences (CEPLAS) funded by the Deutsche Forschungsgemeinschaft (DFG, German Research Foundation) under Germany's Excellence Strategy – EXC 2048/1 – Project ID: 390686111.

ACKNOWLEDGMENTS

We thank Margaret Kox for critical reading of the manuscript and Alice Vayssières for contributing in the design of the *A. alpina* model.

REFERENCES

Aikawa, S., Kobayashi, M. J., Satake, A., Shimizu, K. K., and Kudoh, H. (2010). Robust control of the seasonal expression of the *Arabidopsis FLC* gene in a fluctuating environment. *Proc. Natl. Acad. Sci. U.S.A.* 107, 11632–11637. doi: 10.1073/pnas.0914293107

Albani, M. C., Battey, N. H., and Wilkinson, M. J. (2004). The development of ISSR-derived SCAR markers around the *SEASONAL FLOWERING LOCUS* (*SFL*) in *Fragaria vesca*. *Theor. Appl. Genet.* 109, 571–579. doi: 10.1007/s00122-004-1654-4

Albani, M. C., Castaings, L., Wötzel, S., Mateos, J. L., Wunder, J., Wang, R., et al. (2012). PEP1 of *Arabis alpina* is encoded by two overlapping genes that contribute to natural genetic variation in perennial flowering. *PLoS Genet.* 8:e1003130. doi: 10.1371/journal.pgen.1003130

Albani, M. C., and Coupland, G. (2010). Comparative analysis of flowering in annual and perennial plants. *Curr. Top. Dev. Biol.* 91, 323–348. doi: 10.1016/S0070-2153(10)91011-9

Andrés, F., Porri, A., Torti, S., Mateos, J., Romera-Branchat, M., García-Martínez, J. L., et al. (2014). SHORT VEGETATIVE PHASE reduces gibberellin biosynthesis at the *Arabidopsis* shoot apex to regulate the floral transition. *Proc. Natl. Acad. Sci. U.S.A.* 111, E2762–E2769. doi: 10.1073/pnas.1409567111

Angel, A., Song, J., Dean, C., and Howard, M. (2011). A Polycomb-based switch underlying quantitative epigenetic memory. *Nature* 476, 105–109. doi: 10.1038/nature10241

Atkinson, C. J., Brennan, R. M., and Jones, H. G. (2013). Declining chilling and its impact on temperate perennial crops. *Environ. Exp. Bot.* 91, 48–62. doi: 10.1016/j.envexpbot.2013.02.004

Auge, G. A., Blair, L. K., Neville, H., and Donohue, K. (2017). Maternal vernalization and vernalization-pathway genes influence progeny seed germination. *New Phytol.* 216, 388–400. doi: 10.1111/nph.14520

Auge, G. A., Penfield, S., and Donohue, K. (2019). Pleiotropy in developmental regulation by flowering-pathway genes: is it an evolutionary constraint? *New Phytol.* 224, 55–70. doi: 10.1111/nph.15901

Baduel, P., Arnold, B., Weisman, C. M., Hunter, B., and Bomblies, K. (2016). Habitat-Associated life history and stress-tolerance variation in *Arabidopsis arenosa*. *Plant Physiol.* 171, 437–451. doi: 10.1104/pp.15.01875

Balanzà, V., Martínez-Fernández, I., and Ferrándiz, C. (2014). Sequential action of *FRUITFULL* as a modulator of the activity of the floral regulators *SVP* and *SOC1*. *J. Exp. Bot.* 65, 1193–1203. doi: 10.1093/jxb/ert482

Bergonzi, S., and Albani, M. C. (2011). Reproductive competence from an annual and a perennial perspective. *J. Exp. Bot.* 62, 4415–4422. doi: 10.1093/jxb/err192

Bergonzi, S., Albani, M. C., Van Themaat, E. V. L., Nordström, K. J. V., Wang, R., Schneeberger, K., et al. (2013). Mechanisms of age-dependent response to winter temperature in perennial flowering of *Arabis alpina*. *Science* 340, 1094–1097. doi: 10.1126/science.1234116

Berry, S., and Dean, C. (2015). Environmental perception and epigenetic memory: mechanistic insight through *FLC*. *Plant J.* 83, 133–148. doi: 10.1111/tpj.12869

Billings, W. D., and Mooney, H. A. (1968). The ecology of arctic and Alpine plants. *Biol. Rev. Camb. Philos. Soc.* 43, 481–529.

Blair, L., Auge, G., and Donohue, K. (2017). Effect of *FLOWERING LOCUS C* on seed germination depends on dormancy. *Funct. Plant Biol.* 44, 493–506. doi: 10.1071/FP16368

Bond, D. M., Dennis, E. S., Pogson, B. J., and Finnegan, E. J. (2009). Histone acetylation, *VERNALIZATION INSENSITIVE 3*, *FLOWERING LOCUS C*, and the vernalization response. *Mol. Plant* 2, 724–737. doi: 10.1093/mp/ssp021

Bouché, F., Woods, D. P., and Amasino, R. M. (2017). Winter memory throughout the plant kingdom: different paths to flowering. *Plant Physiol.* 173, 27–35. doi: 10.1104/pp.16.01322

Bratzel, F., and Turck, F. (2015). Molecular memories in the regulation of seasonal flowering: from competence to cessation. *Genome Biol.* 16, 1–14. doi: 10.1186/s13059-015-0770-6

Brown, J. K. M., Beeby, R., and Penfield, S. (2019). Yield instability of winter oilseed rape modulated by early winter temperature. *Sci. Rep.* 9, 1–9. doi: 10.1038/s41598-019-43461-7

Brown, T., and Wareing, P. F. (1965). The genetical control of the everbearing habit and three other characters in varieties of *Fragaria vesca*. *Euphytica* 14, 97–112. doi: 10.1007/BF00032819

Carmona, M. J., Chaïb, J., Martínez-Zapater, J. M., and Thomas, M. R. (2008). A molecular genetic perspective of reproductive development in grapevine. *J. Exp. Bot.* 59, 2579–2596. doi: 10.1093/jxb/ern160

Cartolano, M., Pieper, B., Lempe, J., Tattersall, A., Huijser, P., Tresch, A., et al. (2015). Heterochrony underpins natural variation in *Cardamine hirsuta* leaf form. *Proc. Natl. Acad. Sci. U.S.A.* 112, 10539–10544. doi: 10.1073/pnas.1419791112

Chen, M., MacGregor, D. R., Dave, A., Florance, H., Moore, K., Paszkiewicz, K., et al. (2014). Maternal temperature history activates Flowering Locus T in fruits to control progeny dormancy according to time of year. *Proc. Natl. Acad. Sci. U.S.A.* 111, 18787–18792. doi: 10.1073/pnas.1412274111

Chen, M., and Penfield, S. (2018). Feedback regulation of COOLAIR expression controls seed dormancy and flowering time. *Science* 12, 1014–1017.

Chiang, G. C. K., Barua, D., Kramer, E. M., Amasino, R. M., and Donohue, K. (2009). Major flowering time gene, *FLOWERING LOCUS C*, regulates seed germination in *Arabidopsis thaliana*. *Proc. Natl. Acad. Sci. U.S.A.* 106, 11661–11666.

Chouard, P. (1960). Vernalization and its relations to dormancy. *Annu. Rev. Plant Physiol.* 11, 191–238. doi: 10.1146/annurev.pp.11.060160.001203

Costa, S., and Dean, C. (2019). Storing memories: the distinct phases of Polycomb-mediated silencing of *Arabidopsis* FLC. *Biochem. Soc. Trans.* 47, 1187–1196. doi: 10.1042/BST20190255

Costes, E., Crespel, L., Denoyes, B., Morel, P., Demene, M.-N., Lauri, P.-E., et al. (2014). Bud structure, position and fate generate various branching patterns along shoots of closely related *Rosaceae* species: a review. *Front. Plant Sci.* 5:666. doi: 10.3389/fpls.2014.00666

Coustham, V., Li, P., Strange, A., Lister, C., Song, J., and Dean, C. (2012). Quantitative modulation of polycomb silencing underlies natural variation in vernalization. *Science* 337, 584–587. doi: 10.1126/science.1221881

Crespel, L., Chirollet, M., Durel, C. E., Zhang, D., Meynet, J., and Gudin, S. (2002). Mapping of qualitative and quantitative phenotypic traits in *Rosa* using AFLP markers. *Theor. Appl. Genet.* 105, 1207–1214. doi: 10.1007/s00122-002-1102-2

Csorba, T., Questa, J. I., Sun, Q., and Dean, C. (2014). Antisense COOLAIR mediates the coordinated switching of chromatin states at FLC during vernalization. *Proc. Natl. Acad. Sci. U.S.A.* 111, 16160–16165. doi: 10.1073/pnas.1419030111

De Folter, S., Immink, R. G. H., Kieffer, M., Pařenicová, L., Henz, S. R., Weigel, D., et al. (2005). Comprehensive interaction map of the *Arabidopsis* MADS box transcription factors. *Plant Cell* 17, 1424–1433. doi: 10.1105/tpc.105.031831

de la Fuente, L., Conesa, A., Lloret, A., Badenes, M. L., and Ríos, G. (2015). Genome-wide changes in histone H3 lysine 27 trimethylation associated with bud dormancy release in peach. *Tree Genet. Genomes* 11:45. doi: 10.1007/s11295-015-0869-7

De Lucia, F., Crevillen, P., Jones, A. M. E., Greb, T., and Dean, C. (2008). A PHD-polycomb repressive complex 2 triggers the epigenetic silencing of *FLC* during vernalization. *Proc. Natl. Acad. Sci. U.S.A.* 105, 16831–16836. doi: 10.1073/pnas.0808687105

Deng, W., Ying, H., Helliwell, C. A., Taylor, J. M., Peacock, W. J., and Dennis, E. S. (2011). FLOWERING LOCUS C (FLC) regulates development pathways throughout the life cycle of *Arabidopsis*. *Proc. Natl. Acad. Sci. U.S.A.* 108, 6680–6685. doi: 10.1073/pnas.1103175108

Diggle, P. K. (1997). Extreme preformation in alpine *Polygonum viviparum*: an architectural and developmental analysis. *Am. J. Bot.* 84, 154–169. doi: 10.2307/2446077

Duncan, S., Holm, S., Questa, J., Irwin, J., Grant, A., and Dean, C. (2015). Seasonal shift in timing of vernalization as an adaptation to extreme winter. *eLife* 4:e06620. doi: 10.7554/elife.06620

Engin, H., and Ünal, A. (2007). Examination of flower bud initiation and differentiation in sweet cherry and peach by scanning electron microscope. *Turk. J. Agric. For.* 31, 373–379. doi: 10.3906/tar-0707-1

Falavigna, V. D. S., Guitton, B., Costes, E., and Andrés, F. (2019). I want to (Bud) break free: the potential role of *DAM* and *SVP*-Like genes in regulating dormancy cycle in temperate fruit trees. *Front. Plant Sci.* 9:1990. doi: 10.3389/fpls.2018.01990

Finnegan, E. J., and Dennis, E. S. (2007). Vernalization-induced Trimethylation of histone H3 Lysine 27 at *FLC* is not maintained in mitotically quiescent cells. *Curr. Biol.* 17, 1978–1983. doi: 10.1016/j.cub.2007.10.026

Friedman, J., and Rubin, M. J. (2015). All in good time: understanding annual and perennial strategies in plants. *Am. J. Bot.* 102, 497–499. doi: 10.3732/ajb.1500062

Gregis, V., Sessa, A., Colombo, L., and Kater, M. M. (2006). AGL24, *SHORT VEGETATIVE PHASE*, and *APETALA1* redundantly control *AGAMOUS* during early stages of flower development in *Arabidopsis*. *Plant Cell* 18, 1373–1382. doi: 10.1105/tpc.106.041798

Heo, J. B., and Sung, S. (2011). Vernalization-mediated epigenetic silencing by a long intronic noncoding RNA. *Science* 331, 76–79. doi: 10.1126/science.1197349

Hepworth, J., Antoniou-kourounioti, R. L., Berggren, K., Selga, C., and Tudor, E. H. (2020). Natural variation in autumn expression is the major adaptive determinant distinguishing *Arabidopsis FLC* haplotypes. *eLife* 9:e57671.

Horvath, D. (2009). Common mechanisms regulate flowering and dormancy. *Plant Sci.* 177, 523–531. doi: 10.1016/j.plantsci.2009.09.002

Hughes, P. W., Soppe, W. J. J., and Albani, M. C. (2019). Seed traits are pleiotropically regulated by the flowering time gene *PERPETUAL FLOWERING 1* (*PEP1*) in the perennial *Arabis alpina*. *Mol. Ecol.* 28, 1183–1201. doi: 10.1111/mec.15034

Hyun, Y., Richter, R., and Coupland, G. (2017). Competence to flower: age-controlled sensitivity to environmental cues. *Plant Physiol.* 173, 36–46. doi: 10.1104/pp.16.01523

Hyun, Y., Vincent, C., Tilmes, V., Bergonzi, S., Kiefer, C., Richter, R., et al. (2019). A regulatory circuit conferring varied flowering response to cold in annual and perennial plants. *Science* 363, 409–412. doi: 10.1126/science.aau8197

Iwata, H., Gaston, A., Remay, A., Thouroude, T., Jeauffre, J., Kawamura, K., et al. (2012). The *TFL1* homologue *KSN* is a regulator of continuous flowering in rose and strawberry. *Plant J.* 69, 116–125. doi: 10.1111/j.1365-313X.2011.04776.x

Kemi, U., Leinonen, P. H., Savolainen, O., and Kuittinen, H. (2019). Inflorescence shoot elongation, but not flower primordia formation, is photoperiodically regulated in *Arabidopsis lyrata*. *Ann. Bot.* 124, 91–102. doi: 10.1093/aob/mcz035

Kemi, U., Niittyvuopio, A., Toivainen, T., Pasanen, A., Quilot-Turion, B., Holm, K., et al. (2013). Role of vernalization and of duplicated *FLOWERING LOCUS C* in the perennial *Arabidopsis lyrata*. *New Phytol.* 197, 323–335. doi: 10.1111/j.1469-8137.2012.04378.x

Kiefer, C., Severing, E., Karl, R., Bergonzi, S., Koch, M., Tresch, A., et al. (2017). Divergence of annual and perennial species in the Brassicaceae and the contribution of cis-acting variation at *FLC* orthologues. *Mol. Ecol.* 26, 3437–3457. doi: 10.1111/mec.14084

Koskela, E. A., Mouhu, K., Albani, M. C., Kurokura, T., Rantanen, M., Sargent, D. J., et al. (2012). Mutation in *TERMINAL FLOWER1* reverses the photoperiodic requirement for flowering in the wild strawberry *Fragaria vesca*. *Plant Physiol.* 159, 1043–1054. doi: 10.1104/pp.112.196659

Krogan, N. T., Hogan, K., and Long, J. A. (2012). APETALA2 negatively regulates multiple floral organ identity genes in *Arabidopsis* by recruiting the co-repressor TOPLESS and the histone deacetylase HDA19. *Development* 139, 4180–4190. doi: 10.1242/dev.085407

Lang, A. (1952). Physiology of flowering. *Annu. Rev. Plant Physiol.* 3, 265–306.

Lang, G. A., Early, J. D., Martin, G. C., and Darnell, R. L. (1987). Endo-, para-, and ecodormancy: physiological terminology and classification for dormancy research. *Hortscience* 22, 371–377.

Lazaro, A., Obeng-Hinneh, E., and Albani, M. C. (2018). Extended vernalization regulates inflorescence fate in *Arabis alpina* by stably silencing *PERPETUAL FLOWERING1*. *Plant Physiol.* 176, 2819–2833. doi: 10.1104/pp.17.01754

Lazaro, A., Zhou, Y., Giesguth, M., Nawaz, K., Bergonzi, S., Pecinka, A., et al. (2019). PERPETUAL FLOWERING2 coordinates the vernalization response and perennial flowering in *Arabis alpina*. *J. Exp. Bot.* 70, 995–1004. doi: 10.1093/jxb/ery423

Lee, C. R., Hsieh, J. W., Schranz, M. E., and Mitchell-Olds, T. (2018). The functional change and deletion of *FLC* homologs contribute to the evolution of rapid flowering in *Boechera stricta*. *Front. Plant Sci.* 9:1078. doi: 10.3389/fpls.2018.01078

Lee, H. L., Seong, J. Y., Soo, H. P., Hwang, I., Jong, S. L., and Ji, H. A. (2007). Role of *SVP* in the control of flowering time by ambient temperature in *Arabidopsis*. *Genes Dev.* 21, 397–402. doi: 10.1101/gad.1518407

Leida, C., Conesa, A., Llácer, G., Badenes, M. L., and Ríos, G. (2012). Histone modifications and expression of *DAM6* gene in peach are modulated during bud dormancy release in a cultivar-dependent manner. *New Phytol.* 193, 67–80. doi: 10.1111/j.1469-8137.2011.03863.x

Li, P., Filiault, D., Box, M. S., Kerdaffrec, E., van Oosterhout, C., Wilczek, A. M., et al. (2014). Multiple *FLC* haplotypes defined by independent *cis*-regulatory variation underpin life history diversity in *Arabidopsis thaliana*. *Genes Dev.* 28, 1635–1640. doi: 10.1101/gad.245993.114

Liu, Y., Geyer, R., van Zanten, M., Carles, A., Li, Y., Hörold, A., et al. (2011). Identification of the *Arabidopsis REDUCED DORMANCY 2* gene uncovers a role for the polymerase associated factor 1 complex in seed dormancy. *PLoS One* 6:e0022241. doi: 10.1371/journal.pone.0022241

Luo, X., Ou, Y., Li, R., and He, Y. (2020). Maternal transmission of the epigenetic 'memory of winter cold' in *Arabidopsis*. *Nat. Plants* 6, 1211–1218. doi: 10.1038/s41477-020-00774-0

Madrid, E., Chandler, J. W., and Coupland, G. (2020). Gene regulatory networks controlled by FLOWERING LOCUS C that confer variation in seasonal flowering and life history. *J. Exp. Bot.* 72, 4–14. doi: 10.1093/jxb/eraa216

Mateos, J. L., Madrigal, P., Tsuda, K., Rawat, V., Richter, R., Romera-Branchat, M., et al. (2015). Combinatorial activities of SHORT VEGETATIVE PHASE and FLOWERING LOCUS C define distinct modes of flowering regulation in *Arabidopsis*. *Genome Biol.* 16, 1–23. doi: 10.1186/s13059-015-0597-1

Mateos, J. L., Tilmes, V., Madrigal, P., Severing, E., Richter, R., Rijkenberg, C. W. M., et al. (2017). Divergence of regulatory networks governed by the orthologous transcription factors FLC and PEP1 in Brassicaceae species. *Proc. Natl. Acad. Sci. U.S.A.* 114, E11037–E11046. doi: 10.1073/pnas.1618075114

Maurya, J. P., and Bhalerao, R. P. (2017). Photoperiod- and temperature-mediated control of growth cessation and dormancy in trees: a molecular perspective. *Ann. Bot.* 120, 351–360. doi: 10.1093/aob/mcx061

Meloche, C. G., and Diggle, P. K. (2001). Preformation, architectural complexity, and developmental flexibility in *Acomastylis rossii* (Rosaceae). *Am. J. Bot.* 88, 980–991. doi: 10.2307/2657079

Michaels, S. D., and Amasino, R. M. (1999). *FLOWERING LOCUS C* encodes a novel MADS domain protein that acts as a repressor of flowering. *Plant Cell* 11:949. doi: 10.2307/3870827

Miura, K., Ikeda, M., Matsubara, A., Song, X. J., Ito, M., Asano, K., et al. (2010). *OsSPL14* promotes panicle branching and higher grain productivity in rice. *Nat. Genet.* 42, 545–549. doi: 10.1038/ng.592

Nah, G., and Chen, Z. J. (2010). Tandem duplication of the *FLC* locus and the origin of a new gene in *Arabidopsis* related species and their functional implications in allopolyploids. *New Phytol.* 186, 228–238. doi: 10.1111/j.1469-8137.2009.03164.x

Nishio, H., Buzas, D. M., Nagano, A. J., Iwayama, K., Ushio, M., and Kudoh, H. (2020). Repressive chromatin modification underpins the long-term expression trend of a perennial flowering gene in nature. *Nat. Commun.* 11, 1–12. doi: 10.1038/s41467-020-15896-4

O'Neill, C. M., Lu, X., Calderwood, A., Tudor, E. H., Robinson, P., Wells, R., et al. (2019). Vernalization and floral transition in autumn drive winter annual life history in oilseed rape. *Curr. Biol.* 29, 4300–4306. doi: 10.1016/j.cub.2019.10.051

Or, E. (2009). "Grape bud dormancy release-the molecular aspect," in *Grapevine Molecular Physiology & Biotechnology*, ed. K. A. Roubelakis-Angelakis (Cham: Springer), 1–29. doi: 10.1007/978-90-481-2305-6

Périlleux, C., Pieltain, A., Jacquemin, G., Bouché, F., Detry, N., D'Aloia, M., et al. (2013). A root chicory MADS box sequence and the *Arabidopsis* flowering repressor *FLC* share common features that suggest conserved function in vernalization and de-vernalization responses. *Plant J.* 75, 390–402. doi: 10.1111/tpj.12208

Ponraj, U., and Theres, K. (2020). Keep a distance to be different: axillary buds initiating at a distance from the shoot apical meristem are crucial for the perennial lifestyle of *Arabis alpina*. *New Phytol.* 227, 116–131. doi: 10.1111/nph.16512

Prusinkiewicz, P., Crawford, S., Smith, R. S., Ljung, K., Bennett, T., Ongaro, V., et al. (2009). Control of bud activation by an auxin transport switch. *Proc. Natl. Acad. Sci. U.S.A.* 106, 17431–17436. doi: 10.1073/pnas.0906696106

Qüesta, J. I., Antoniou-Kourounioti, R. L., Rosa, S., Li, P., Duncan, S., Whittaker, C., et al. (2020). Noncoding SNPs influence a distinct phase of Polycomb silencing to destabilize long-term epigenetic memory at *Arabidopsis FLC*. *Genes Dev.* 34, 446–461. doi: 10.1101/gad.333245.119

Qüesta, J. I., Song, J., Geraldo, N., An, H., and Dean, C. (2016). *Arabidopsis* transcriptional repressor VAL1 triggers Polycomb silencing at FLC during vernalization. *Science* 353, 485–488. doi: 10.1126/science.aaf7354

Rothkegel, K., Sánchez, E., Montes, C., Greve, M., Tapia, S., Bravo, S., et al. (2017). DNA methylation and small interference RNAs participate in the regulation of MADS-box genes involved in dormancy in sweet cherry (*Prunus avium* L.). *Tree Physiol.* 37, 1739–1751. doi: 10.1093/treephys/tpx055

Saito, T., Bai, S., Imai, T., Ito, A., Nakajima, I., and Moriguchi, T. (2015). Histone modification and signalling cascade of the dormancy-associated *MADS-box gene*, *PpMADS13-1*, in Japanese pear (*Pyrus pyrifolia*) during endodormancy. *Plant Cell Environ.* 38, 1157–1166. doi: 10.1111/pce.12469

Sheldon, C. C., Rouse, D. T., Finnegan, E. J., Peacock, W. J., and Dennis, E. S. (2000). The molecular basis of vernalization: the central role of *FLOWERING LOCUS C* (*FLC*). *Proc. Natl. Acad. Sci. U.S.A.* 97, 3753–3758. doi: 10.1073/pnas.060023597

Shindo, C., Lister, C., Crevillen, P., Nordborg, M., and Dean, C. (2006). Variation in the epigenetic silencing of *FLC* contributes to natural variation in *Arabidopsis* vernalization response. *Genes Dev.* 20, 3079–3083. doi: 10.1101/gad.405306

Springthorpe, V., and Penfield, S. (2015). Flowering time and seed dormancy control use external coincidence to generate life history strategy. *eLife* 2015:e05557. doi: 10.7554/eLife.05557

Sung, S., and Amasino, R. M. (2004). Vernalization in *Arabidopsis thaliana* is mediated by the PHD finger protein VIN3. *Nature* 427, 159–164. doi: 10.1038/nature02195

Swiezewski, S., Liu, F., Magusin, A., and Dean, C. (2009). Cold-induced silencing by long antisense transcripts of an *Arabidopsis* Polycomb target. *Nature* 462, 799–802. doi: 10.1038/nature08618

Tao, Z., Hu, H., Luo, X., Jia, B., Du, J., and He, Y. (2019). Embryonic resetting of the parental vernalized state by two B3 domain transcription factors in *Arabidopsis*. *Nat. Plants* 5, 424–435. doi: 10.1038/s41477-019-0402-3

Thompson, K., Bakker, J. P., Bekker, R. M., and Hodgson, J. G. (1998). Ecological correlates of seed persistence in soil in the North-West European Flora. *J. Ecol.* 86, 163–169.

Tilmes, V., Mateos, J. L., Madrid, E., Vincent, C., Severing, E., Carrera, E., et al. (2019). Gibberellins act downstream of *Arabis* PERPETUAL FLOWERING1 to accelerate floral induction during vernalization. *Plant Physiol.* 180, 1549–1563. doi: 10.1104/pp.19.00021

Tsuji, H., Tachibana, C., Tamaki, S., Taoka, K. I., Kyozuka, J., and Shimamoto, K. (2015). Hd3a promotes lateral branching in rice. *Plant J.* 82, 256–266. doi: 10.1111/tpj.12811

Vayssières, A., Mishra, P., Roggen, A., Neumann, U., Ljung, K., and Albani, M. C. (2020). Vernalization shapes shoot architecture and ensures the maintenance of dormant buds in the perennial *Arabis alpina*. *New Phytol.* 227, 99–115. doi: 10.1111/nph.16470

Vimont, N., Fouché, M., Campoy, J. A., Tong, M., Arkoun, M., Yvin, J. C., et al. (2019). From bud formation to flowering: transcriptomic state defines the cherry developmental phases of sweet cherry bud dormancy. *BMC Genomics* 20:974. doi: 10.1186/s12864-019-6348-z

Wang, R., Albani, M. C., Vincent, C., Bergonzi, S., Luan, M., Bai, Y., et al. (2011). Aa *TFL1* confers an age-dependent response to vernalization in perennial *Arabis alpina*. *Plant Cell* 23, 1307–1321. doi: 10.1105/tpc.111.083451

Wang, R., Farrona, S., Vincent, C., Joecker, A., Schoof, H., Turck, F., et al. (2009). PEP1 regulates perennial flowering in *Arabis alpina*. *Nature* 459, 423–427. doi: 10.1038/nature07988

Wollenberg, A. C., and Amasino, R. M. (2012). Natural variation in the temperature range permissive for vernalization in accessions of *Arabidopsis thaliana*. *Plant Cell Environ.* 35, 2181–2191. doi: 10.1111/j.1365-3040.2012.02548.x

Wood, C. C., Robertson, M., Tanner, G., Peacock, W. J., Dennis, E. S., and Helliwell, C. A. (2006). The *Arabidopsis thaliana* vernalization response requires a polycomb-like protein complex that also includes VERNALIZATION INSENSITIVE 3. *Proc. Natl. Acad. Sci. U.S.A.* 103, 14631–14636. doi: 10.1073/pnas.0606385103

Yuan, W., Luo, X., Li, Z., Yang, W., Wang, Y., Liu, R., et al. (2016). A *cis* cold memory element and a trans epigenome reader mediate Polycomb silencing of *FLC* by vernalization in *Arabidopsis*. *Nat. Genet.* 48, 1527–1534. doi: 10.1038/ng.3712

Zhao, Y., Antoniou-kourounioti, R. L., Calder, G., Dean, C., and Howard, M. (2020). Temperature-dependent growth contributes to long-term cold sensing. *Nature* 583, 825–829. doi: 10.1038/s41586-020-2485-4

Zhou, Y. (2019). *Identification and Characterisation of Genes that Regulate Flowering and Perennial Traits in Arabis alpina*. Köln: Universität zu Köln.

Zhou, Y., Gan, X., Viñegra de la Torre, N., Neumann, U., and Albani, M. C. (2021). Beyond flowering time: diverse roles of an APETALA2-like transcription factor in shoot architecture and perennial traits. *New Phytol.* 229, 444–459. doi: 10.1111/nph.16839

Conflict of Interest: WJJS was employed by company Rijk Zwaan.

The remaining authors declare that the writing of this review was conducted in the absence of any commercial or financial relationships that could be construed as a potential conflict of interest.

Copyright © 2021 Soppe, Viñegra de la Torre and Albani. This is an open-access article distributed under the terms of the Creative Commons Attribution License (CC BY). The use, distribution or reproduction in other forums is permitted, provided the original author(s) and the copyright owner(s) are credited and that the original publication in this journal is cited, in accordance with accepted academic practice. No use, distribution or reproduction is permitted which does not comply with these terms.

frontiers in Plant Science

ORIGINAL RESEARCH
published: 05 March 2021
doi: 10.3389/fpls.2021.640324

Identification and Characterization of Perennial Ryegrass (*Lolium perenne*) Vernalization Genes

Rowan Herridge, Samarth, Lynette Brownfield and Richard Macknight*

Department of Biochemistry, University of Otago, Dunedin, New Zealand

Perennial ryegrass (*Lolium perenne*) is a temperate grass species commonly used as pasture for livestock. Flowering (heading) of ryegrass impacts metabolizable energy content and seed yield, therefore this trait is important for both farmers and seed producers. In related grass species, the *VRN* genes (*VRN1-3*) have been largely implicated in the determination of vernalization response and are responsible for much of the intra-species variation in this trait. Many other important flowering-time regulators have been cataloged in the model grass *Brachypodium distachyon;* however, in several cases, such as *VRN2*, their ryegrass homologs have not been well-characterized. Here, ryegrass homologs of important flowering time genes from *B. distachyon* were identified through available synteny data and sequence similarity. Phylogenetic analysis of *VRN3/FT-like* and *VRN2-like* genes was performed to elucidate these families further. The expression patterns of these genes were assessed during vernalization. This confirmed the key roles played by *LpVRN1* and *LpFT3* in the promotion of flowering. Furthermore, two orthologs of *VRN2* identified here, as well as an ortholog of *CO9,* were expressed prior to vernalization, and were repressed in flowering plants, suggesting a role in floral repression. Significant variability in expression of these flowering pathway genes in diverse genotypes was detected and may underlie variation in flowering time and vernalization response.

Keywords: flowering time, vernalization, grasses, forage, transcriptome

OPEN ACCESS

Edited by:
Richard Amasino, University of Wisconsin-Madison, United States

Reviewed by:
Jill Christine Preston, University of Vermont, United States
Ana M. Casas, Aula Dei Experimental Station (EEAD), Spain

****Correspondence:***
Rowan Herridge
Rowan.Herridge@otago.ac.nz

Specialty section:
This article was submitted to Plant Development and EvoDevo, a section of the journal Frontiers in Plant Science

Received: *11 December 2020*
Accepted: *15 February 2021*
Published: *05 March 2021*

Citation:
Herridge R, Samarth, Brownfield L and Macknight R (2021) Identification and Characterization of Perennial Ryegrass (Lolium perenne) Vernalization Genes. Front. Plant Sci. 12:640324. doi: 10.3389/fpls.2021.640324

INTRODUCTION

Perennial ryegrass (*Lolium perenne*) is a temperate grass, widely grown as pasture for livestock for its high levels of metabolizable energy. Ryegrass flowering (heading) occurs in the spring after a period of cold (i.e., winter) referred to as vernalization. As ryegrass is an obligate outcrosser, it is important that minimal variation in heading date occurs within a cultivar to ensure good seed production. Heading also impacts the availability of metabolizable energy, as plants switch from producing leaves toward less-nutritious stems and floral structures (Stockdale, 1999). Selection for different heading dates occurs during the breeding process, and many varieties with early and late heading dates are currently available. While some variation in heading date has been captured through introgression, a better understanding of the genetic mechanisms underlying heading date will enable breeders to develop cultivars with more specific and reliable heading dates.

The genetic mechanisms of flowering have been well studied in other model plants, such as *Arabidopsis thaliana* (Arabidopsis) and *Brachypodium distachyon*. In addition, a number of

important flowering time genes have been identified in related crops such as wheat (*Triticum* sp.), barley (*Hordeum vulgare*) and rice (*Oryza sativa*). This intensive study has led to the description of a number of important genes and pathways controlling flowering time in grasses. The genes controlling vernalization response have been particularly well studied, as natural variation in vernalization requirement is widespread amongst different cultivars of wheat and barley. VRN1 is a MADS-box transcription factor which is induced by low temperatures (Yan et al., 2003). Extended periods of low temperatures result in mitotically stable expression of *VRN1* through epigenetic marks (Oliver et al., 2009). Some varieties of spring wheat and barley have mutations at the *VRN1* locus which result in constitutive expression of *VRN1* and do not require vernalization in order to flower (Yan et al., 2003; Chu et al., 2011). Upon transition to long days, *VRN1* is capable of activating transcription of the *FLOWERING LOCUS T* (*FT*) gene, *VRN3*, in leaves (Shimada et al., 2009). The VRN3/FT protein is transported from the leaves to the apical meristem, where it acts as a transcriptional co-activator (Tamaki et al., 2007). *VRN1* is induced by FT in concert with a number of other proteins in the meristem, resulting in transcriptional activation of genes involved in floral meristem production (Li and Dubcovsky, 2008). In barley and *B. distachyon* natural variation exists in a relative of *FT*, *HvFT3*/*BdFTL9*, which acts during short days to promote flowering (Faure et al., 2007; Qin et al., 2019; Woods et al., 2019). In the case of *BdFTL9*, this is through a process called short day vernalization, and promotes floral competency upon return to long days (Woods et al., 2019).

Prior to vernalization, *VRN2* is expressed in leaves, which represses *VRN3* and possibly *VRN1* (Yan et al., 2004; Dubcovsky et al., 2006). VRN2 is a zinc-finger CCT-domain protein and is down-regulated by short days and cold through the activity of VRN1 at the promoter (Chen and Dubcovsky, 2012; Deng et al., 2015). The CCT-domain is named after a 43-amino acid C-terminal domain found in three Arabidopsis proteins, CONSTANS (CO), CO-LIKE, and TIMING OF CAB1 (TOC1). Variations in the CCT domain of VRN2 have a profound impact on vernalization response in wheat, with non-functional variants abolishing vernalization requirement in spring varieties (Distelfeld et al., 2009). In rice, the CCT-domain protein Ghd7 acts to repress flowering in long days and is the ortholog of *VRN2* from wheat (Griffiths et al., 2003; Xue et al., 2008; Woods et al., 2016). Other close homologs of *VRN2*/*Ghd7* include the *CO9-like* genes, although these are less well-studied (Woods et al., 2016). The *CO9-like* gene from barley is expressed in short-day conditions and acts to repress flowering, suggesting that *CO9-like* genes also act as floral repressors (Kikuchi et al., 2012).

Ryegrass has been the subject of many flowering time studies, primarily using quantitative trait analysis, and a number of important flowering time genes have been identified (reviewed by Wang and Forster, 2017). *VRN1* has been identified in ryegrass, and natural variation in the first intron affects vernalization response (Jensen et al., 2005; Andersen et al., 2006; Asp et al., 2011). A number of *FT-like* genes have also been described in ryegrass, with some of these homologs in close proximity to QTL affecting flowering time (Studer et al., 2009). Allelic variation at *FT* genes underlying these QTL has not yet been described. However, variation at the promoter of *LpFT3*, a putative ortholog of *FT*/*VRN3* genes from other grasses, has been proposed to impact flowering time in a panel of different ryegrass germplasms (Skøt et al., 2011; Wang and Forster, 2017). No ortholog of *VRN2* has been thoroughly described in ryegrass, although a locus on LG4 and a partial sequence have been reported (Paina et al., 2016; Woods et al., 2016). Two genes, named *vrn2_2* and *vrn2_3* were identified in a QTL analysis and corresponded to two CCT-domain proteins on LG7 (Andersen et al., 2006). *Vrn2_2* was reported to be similar to *VRN2* from wheat, while *Vrn2_3* was a *CO* homolog (*LpCO*), although neither gene appeared to be regulated by vernalization.

Recently, a number of genomic resources have been developed for ryegrass, including two draft genomes, transcriptomic data, synteny data, and high-density mapping data (Studer et al., 2012; Paina et al., 2014; Byrne et al., 2015; Velmurugan et al., 2016). In this study, we aimed to use these resources to identify orthologs of important flowering time genes from *B. distachyon*. We further investigated *FT-like* genes and CCT-domain genes in an effort to find orthologous genes to *BdFTL9*, *BdVRN3* and *BdVRN2*. We characterized homologs of *VRN2* in a commercial cultivar during vernalization, flowering, and post-flowering. Finally, we looked for variation in the expression of these genes in a variety of different genotypes, which may underlie differences in their flowering habit.

MATERIALS AND METHODS

Plant Materials and Growth Conditions

Lolium perenne plants were grown at 22°C 16 h light/8 h dark (Long Days; LD) or 8 h light/16 h dark (Short Days; SD) unless otherwise stated. A list of the ryegrass cultivars and accessions used in this study is provided in **Table 1**.

Flowering Time Gene Identification

tBLASTn was performed using *B. distachyon* peptides from *B. distachyon* predicted proteins (v1.2) against the *L. perenne* genome (The International Brachypodium Initiative, 2010; Byrne et al., 2015). For ease of identifying the matching annotations, predicted proteins from the ryegrass genome (Byrne et al., 2015) were also searched (BLASTp), and in cases where the top tBLASTn hit matched the top annotated protein hit, the annotation was noted and classified as the most-likely homolog. In cases where these did not match, the tBLASTn hit was examined on a genome browser (Integrative Genomics Viewer, IGV) to identify overlapping masked transcripts, or unannotated regions. The sequences of these genes/regions were aligned to their *B. distachyon* homologs to identify exons, and RNAseq reads (Paina et al., 2014) were simultaneously examined to determine splice sites where possible.

Phylogenetic Analysis of FT-Family and CCT-Domain Proteins

Homologous FT-family protein sequences in ryegrass were obtained from Veeckman et al. (2016). Homologous FT-like

TABLE 1 | Details of different genotypes used in this study.

Name/Origin/MFGC[a] ID	Heading date[b]
Nui (Grasslands, New Zealand)	Mid (+ 0)
"Cyprus" (A15336/PI206376)	Early[c]
"Turkey" (B5186/PI173724)	Early
Medea (Australia/Algeria)	Early
"Iran" (A15352/PI227020)	Early[c]
Barberia (Barenbrug, New Zealand)	Early[c] (−21)
Tyson (Barenbrug, New Zealand)	Early (−10)
Tabu (Barenbrug, New Zealand)	Late (+10)[c]
Alto (Barenbrug, New Zealand)	Late (+14)
Trojan (Barenbrug, New Zealand)	Late (+16)
Kleppe (Norway)	Late[d]
"Sweden" (A15365/PI265335)	Late[d]
"Japan" (A24819/PI420127)	Late[d]
"Norway" (A171783/PI577269)	Late[d]
ONE50 (PGG Wrightson, New Zealand)	Late (+20)

[a]Margot Forde Germplasm Centre. [b]Heading date relative to Nui in brackets (data from supplier). [c]No vernalization requirement. [d]Strong vernalization requirement.

genes from *B. distachyon*, *O. sativa* and *H. vulgare* were also identified from the literature (Griffiths et al., 2003; Higgins et al., 2010). CCT-protein sequences were extracted from the *L. perenne* draft genome by searching predicted proteins (BLASTp) and a translated nucleotide database (tBLASTn) with the CCT domain of *B. distachyon* VRN2 (Byrne et al., 2015). Annotated CCT-domain proteins were identified in *B. distachyon*, *O. sativa* and *H. vulgare* genomes by searching for PFAM domain 06203 on Phytozome (*B. distachyon* and *H. vulgare*)[1], or the rice genome[2]. All sequences were aligned using MUSCLE program followed by a gblock scan to identify conserved regions among the alignment which can later be used to infer phylogenetic relationship (Edgar, 2004). Phylogenetic trees were created using the CLC Genomics workbench (version 10) with the following settings: maximum likelihood method with JTT substitution matrix and 1000 bootstrap replication.

RNAseq Data Analysis

Previously published RNAseq data from two ecotypes (Falster and Veyo) was re-analzsed. Full details of the experimental conditions can be found in Paina et al. (2014). To summarize, leaf tissue from clonal Falster and Veyo plants was taken in short day conditions prior to vernalization in short days at 5°C. Leaf tissue was sampled after 2 days, 4 weeks, and 9 weeks of vernalization, and 7 days after returning to long days. Meristem tissue was taken after 9 weeks of vernalization, and 1 day, and 7 days after returning to long days. Raw data from Paina et al. (2014; EMBL-EBI ArrayExpress, accession no. E-MTAB-2623) was mapped to the *L. perenne* genome (Byrne et al., 2015) using STAR mapper (Dobin et al., 2013). Feature counts were extracted using HT-seq count (Anders et al., 2015) with the following settings: htseq-count -q -s no -f bam -t gene -i ID. A customized.gff file containing only the flowering genes of interest was used to avoid overlapping features preventing accurate quantification. Expression levels of each gene were normalized by the total number of mapped reads, and by the transcript length for plotting.

Sample Collection

For the 10 week vernalization time course, seeds of ONE50 were sterilized in a 1% bleach solution for 15 min and placed onto moist sterile filter paper in a petri dish and sealed with cling film. Seeds were chilled for 2 days in the dark at 4°C before transfer to LD conditions to germinate for 2 weeks, at which point seedlings are typically capable of responding to vernalization (Gangi et al., 1983). After 2 weeks in LD conditions, plates were transferred to 4°C in the dark for 10 weeks, and after 10 weeks of vernalization, seedlings were transferred to soil and grown in LD conditions at 22°C. Samples were collected prior to vernalization (0dV) and at 1 day, 1 week, 2 weeks, 4 weeks, 7 weeks, and 10 weeks vernalization (1dV, 1wV, 4wV, 7wV and 10wV), and at 7 days, 2 weeks and 4 weeks post-vernalization (7dLD, 2wLD, 4wLD). Each RNA sample from 0dV until 10wV was prepared by pooling tissue from the primary leaf of ∼10 seedlings. Samples after transfer to soil were prepared from a pool of single leaves from 3 plants. Samples were taken between 1–2 h after lights were turned on (ZT1-ZT2; 9am–10am), and at the same time each day in dark conditions. Leaf tissue was frozen in liquid nitrogen prior to RNA extraction.

For the comparison of flowering and non-flowering plants, each sample was prepared from leaves from several tillers from a single plant. Leaves were taken from three flowering and three non-flowering plants at ∼6 weeks after the transition to LD conditions when spikelets had clearly emerged in flowering plants. Further samples were taken from these plants 8 weeks later, and after 1 day or 1 week under vernalization conditions (SD + 5°C).

For comparison of gene expression between genotypes, seeds of the cultivars/accessions shown in **Table 1** were sterilized and germinated as above for ONE50. Samples were taken after 2–3 weeks growth in long days (0dV) and after 2 days of cold (4°C)/dark treatment (2dV). Each RNA sample was prepared by pooling tissue from the primary leaf of ∼10 seedlings. Samples were taken between 1–2 h after lights were turned on (ZT1- ZT2; 9am–10am), and at the same time each day in dark conditions.

For analysis of *LpFT08* expression in SD conditions, ONE50 plants were grown for 8 weeks in LD conditions (20 h light; 4 h dark). Leaf material from each plant was collected and pooled at T0 (prior to SD treatment), and 4 plants were moved to SD (8h light; 16 h dark) and 4 plants remained in LD (20 h light; 4 h dark). After 2.5 weeks in SD or LD, several leaves from each plant were pooled into a single sample (SD or LD) and frozen in liquid nitrogen prior to RNA extraction.

[1]https://phytozome.jgi.doe.gov/

[2]http://rice.plantbiology.msu.edu/

RNA Extraction, cDNA Synthesis and qPCR

Frozen leaf tissue (∼10 mg) was thawed in 300 μL Trizol (Invitrogen) prior to transfer to a ziplock bag. A dowel was rolled over the bag to homogenize the leaf tissue. Debris was removed by centrifugation at 16,000 × *g* for 5 min and discarding the pellet. RNA was extracted using Zymo Quickzol RNA microprep kit according to manufacturer's instructions, eluting in 15 μL of water. cDNA was synthesized with 1 μg of RNA using SuperScript III Reverse transcriptase (Invitrogen) and oligo dT primers according to manufacturer's instructions. qPCR was performed with SYBR 2x Mastermix (KAPA), using 0.2 μM each primer, in a final volume of 10 μL. Reactions were run in a Roche Lightcycler 480 with the following cycling conditions: a hold of 94 ℃ for 2 min followed by 50 cycles of 94 ℃ for 8 s, 58 ℃ for 10 s and 72 ℃ for 10 s. Tumor Homolog Protein (*THP*; Samarth and Jameson, 2019) and "expressed protein" (*ExP*; Narsai et al., 2010) were used as reference genes, and gene expression was calculated using the ΔCt method based on the geometric mean Ct of the two reference genes. Primers used for each gene are given in **Supplementary Table 1**. To compare variance of gene expression between different target genes in the array of genotypes, expression level of each sample was first normalized to the mean value, followed by pairwise F-tests to compare the variance of each target gene (*LpVRN1*, *LpVRN2a/b* and *LpCO9*). The $\log_2$ fold-change in expression level upon introduction to vernalization conditions was also calculated, and subsequent pairwise F-tests were performed on these values to determine significantly variable responses between target genes.

RESULTS

Identification of Flowering Time Gene Homologs Based on Synteny and Sequence Similarity

To investigate the roles of known flowering time genes in vernalization response, we firstly identified likely orthologs of important flowering time genes from related grass species. A list of important flowering time proteins in *B. distachyon* identified by Higgins et al. (2010) was used to search for ryegrass homologs by searching a translated nucleotide database (tBLASTn) and this analysis was supplemented by identifying putative genomic locations using the *L. perenne* GenomeZipper (Byrne et al., 2015). In most cases, regions/genes identified in the GenomeZipper as homologous to *B. distachyon* flowering genes also contained the top tBLASTn hit. In some cases, no syntenic regions were identified in the GenomeZipper, and in these cases, the top BLAST hit was chosen as the most likely ortholog. In cases where the top BLAST hit was already associated with another *B. distachyon* gene, preference was given to the gene that was predicted to be syntenic (i.e., present in the GenomeZipper), and the non-syntenic gene was left without a likely homolog. Overall, from 158 *B. distachyon* genes, 89 had ryegrass homologs present in the GenomeZipper, while 56 had likely homologs identified via BLAST search, and 13 had no confidently predicted homologs. Five tBLASTn hits occurred in regions without an annotated transcript, in which case a note of the location of the BLAST hit was recorded, and the predicted protein was identified for future use (**Supplementary Datasets 1, 2**). A number of annotated ryegrass genes were previously omitted from the transcriptome/proteome (Byrne et al., 2015); the protein sequences of these genes have also been predicted and included in **Supplementary Dataset 2**. We also identified a small number of genes with truncated sequences in the proteome, which we manually re-annotated using homology to *B. distachyon* and RNAseq data to predict intron/exon boundaries and identify likely start and stop codons (**Supplementary Dataset 2**; Paina et al., 2014).

To validate these genes as orthologs of their respective *B. distachyon* genes, we performed a reciprocal BLAST search using their protein sequences against the *B. distachyon* proteome. Of the 89 homologs identified in the GenomeZipper, 82 were also the top hit to their respective *B. distachyon* counterpart, suggesting they are orthologous (**Supplementary Dataset 1**). A number of these genes have been previously identified via QTL analyses or other means, such as *LpVRN1, LpCO* and *LpVRN3/FT3*. Of particular interest are orthologs of important flowering time genes that have not been previously described. We discovered likely orthologs of *B. distachyon VRN2* (discussed later), *LEAFY* (on scaffold_1714), and *BdSOC1* and *BdSOC1-like* (on scaffold_156 and scaffold_10825). The expression of all identified homologs/orthologs during vernalization was assessed using available RNAseq data from leaves and meristems (Paina et al., 2014; **Supplementary Dataset 3**). This data was generated by sampling two genotypes (Falster and Veyo) with differing vernalization requirements at several time points during and after vernalization. Combining the expression pattern data for each gene, alongside its homology to known *B. distachyon* genes, unique identifiers from the draft genome, and putative genomic location, allows researchers to rapidly access useful information about these genes without the need to re-analyze next generation sequencing data.

Phylogeny and Expression Patterns Indicate *LpFT3* and *LpFT08* Likely Play Key Roles in Regulation of Ryegrass Flowering

FT-like genes are responsible for many aspects of flowering, and duplications and neo-functionalization of genes often occur in this family (Pin and Nilsson, 2012). For this reason, it is possible that there are some duplications or deletions of *FT-like* genes in *L. perenn*e that confound the homology search performed above. For example, *BdFTL7a* and *BdFTL7b* both matched the same ryegrass gene using tBLASTn, which may indicate a duplication in *B. distachyon* or a deletion in *L. perenne,* and therefore requires further analysis. *FT-like* genes have been previously identified in ryegrass which we matched with annotated transcripts from the ryegrass proteome/transcriptome (Byrne et al., 2015; Veeckman et al., 2016; **Supplementary Dataset 4**). We constructed a phylogenetic tree of these *FT* genes, alongside those from *B. distachyon,* rice, and barley (**Figure 1A**). This analysis revealed

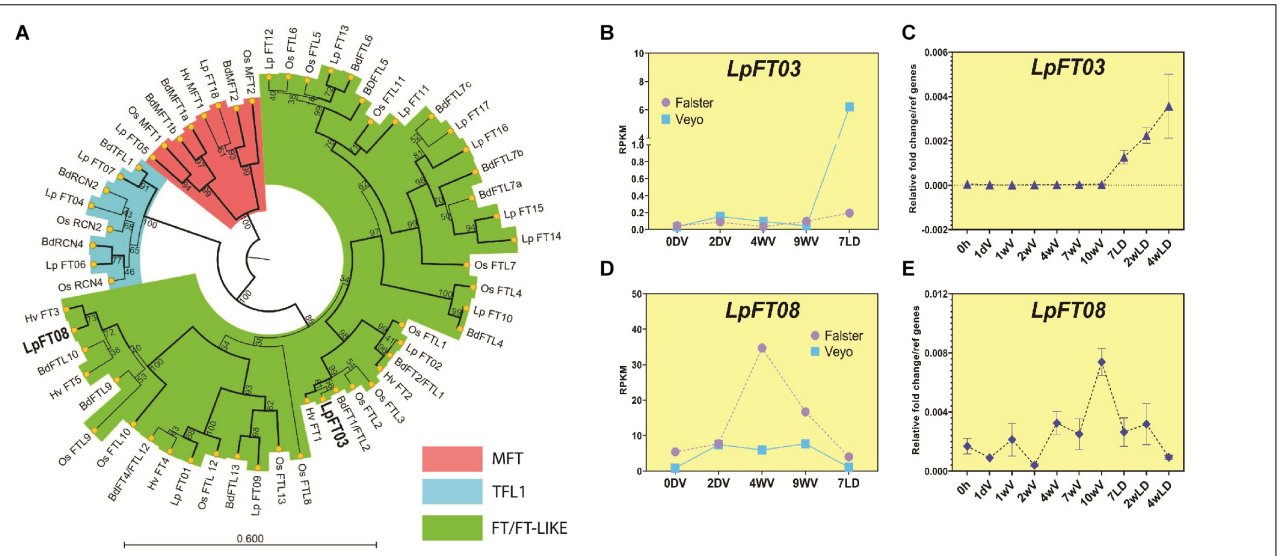

FIGURE 1 | Phylogenetic relationships and expression patterns of FT-like proteins/genes from *L. perenne*. **(A)** Phylogenetic tree of LpFT01-LpFT18 proteins and their homologs from *B. distachyon* (Bd), *H. vulgare* (Hv) and *O. sativa*. (Os). The evolutionary history was inferred by using the Maximum Likelihood method based on the JTT matrix-based model. The bootstrap consensus tree inferred from 1000 replicates is taken to represent the evolutionary history of the taxa analyzed (scores represent the bootstrap support as a percentage). Branches with bootstrap support >70 are shown in bold. Branches in red represent the MFT clade, blue represent the TFL1 clade and green represent the FT clade. Bold highlights genes analyzed further in this study. MFT is the ancestral clade to TFL and FT clades and acts as an outgroup to root the tree. **(B)** Expression pattern of *LpFT3* during and after vernalization in Falster and Veyo cultivars from RNAseq (data from Paina et al., 2014). **(C)** Expression pattern of *LpFT3* during and after vernalization using qPCR in seedlings of the ONE50 cultivar. Expression was normalized to the geometric mean of two reference genes (*ExP* and *THP*), and shows the mean and standard deviation of two biological replicates of leaf tissue from ∼10 pooled seedlings. **(D)** Expression of *LpFT08* during and after vernalization in Falster and Veyo from RNAseq (data from Paina et al., 2014). **(E)** Expression pattern of *LpFT08* during and after vernalization using qPCR in seedlings of the ONE50 cultivar. Expression was normalized to the geometric mean of two reference genes (*ExP* and *THP*) and shows the mean and standard deviation of two biological replicates of leaf tissue from ∼10 pooled seedlings. RPKM, Reads Per Kilobase of transcript per Million mapped reads.

that *LpFT3* was most likely to be the ortholog of floral-inducers (e.g., *BdFTL2*/*BdFT1* and *OsFTL2* aka *Hd3a*; bootstrap support, 99) as has been previously proposed, and this was consistent with the synteny analysis, where it was predicted as the most likely ortholog of *BdFTL2* (**Supplementary Dataset 1**). *B. distachyon FTL9* has been implicated in a process known as short day vernalization, and grouped with *LpFT08*, as well as *HvFT3* and *BdFTL10* (**Figure 1A**; bootstrap support, 100; Qin et al., 2019; Woods et al., 2019). A ryegrass ortholog of *TERMINAL FLOWER 1* (*TFL1*) has been previously identified, *LpTFL1*, which was closely grouped with *BdTFL1* (bootstrap support, 91; Jensen et al., 2001). *RCN2* and *RCN4* are also important members of the FT family, controlling grain production in rice, and orthologs of these were detected in ryegrass – *LpFT04* and *LpFT06*, respectively (bootstrap support, 68 and 46; Nakagawa et al., 2002; Ariyaratne et al., 2009). Despite the low bootstrap values of *LpFT04* and *LpFT06*, these were also reciprocal BLAST hits of their *B. distachyon* orthologs (*BdRCN2* and *BdRCN4*), although more comprehensive analysis may be required to fully elucidate the *RCN2*/*RCN4* clade (**Supplementary Dataset 1**). In *B. distachyon*, *FTL7* has three copies (*BdFTL7a, b* and *c*), while ryegrass has four copies (*LpFT14-17*; bootstrap support, 96), although these genes are yet to be characterized. Ryegrass also had two copies of *MFT*, one closer to *BdMFT1a/b* and one closer to *BdMFT2* (*LpFT05* and *LpFT18*, respectively; bootstrap support, 99 and 99).

To determine which of the *FT-like* genes from ryegrass were responding to vernalization, we examined levels of *FT-like* genes during vernalization using available RNA-seq data (Paina et al., 2014). As expected of a floral inducer, *LpFT3* expression occurred after vernalization when plants were returned to long days (**Figure 1B**). No other *FT-like* gene showed a similar expression pattern, suggesting that *LpFT3* is likely to be the predominant *FT-like* gene acting as a floral inducer in these conditions (**Supplementary Dataset 4**). We confirmed the expression pattern of *LpFT3* in a commercial cultivar (ONE50) during vernalization, which was similar to RNA seq data, despite differences in experimental approach (**Figure 1C**; see Methods). *LpFT3* was also more highly expressed in flowering plants than non-flowering plants resulting from this experiment (discussed later; **Supplementary Figure 1A**). RNAseq data showed that *LpFT08* was expressed during vernalization, and repressed upon introduction to long days, suggesting that it may act in a similar manner to *BdFTL9* which is activated during short days (**Figure 1D**). *LpFT08* expression in our vernalization conditions was not similar to the RNAseq data, as it initially decreased in expression, before increasing with prolonged vernalization (**Figure 1E**). This may be caused by differences in the genotype used for this study, or the difference in vernalization treatments. As the vernalization treatment in this experiment occurred under dark conditions, we tested *LpFT08* expression in short days, which are known to induce the expression of *BdFTL9* (Woods

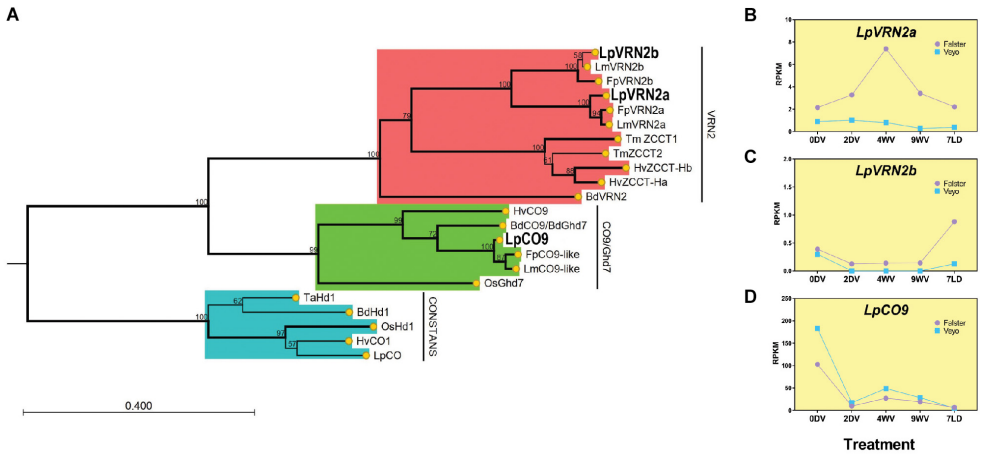

FIGURE 2 | Phylogenetic relationships and expression patterns of VRN2/CO9-like proteins/genes from *L. perenne*. **(A)** Phylogenetic tree containing VRN2-like and CO9-like proteins from *L. perenne* (Lp), *L. multiflorum* (Lm), *F. pratensis* (Fp), *B. distachyon* (Bd), *O. sativa* (Os), *T. monococcum* (Tm), and *H. vulgare* (Hv). The evolutionary history was inferred by using the Maximum Likelihood method based on the JTT + G matrix-based model. The bootstrap consensus tree inferred from 1000 replicates is taken to represent the evolutionary history of the taxa analyzed (scores represent the bootstrap support as a percentage). Branches with bootstrap support >70 are shown in bold. Branches in red represent the VRN2 clade, green represent the CO9/Ghd7 clade and blue represent the CONSTANS clade. CONSTANS acts as an outgroup to root the tree. **(B–D)** Expression patterns of *LpVRN2a*, *LpVRN2b* and *LpCO9* during and after vernalization in Falster and Veyo cultivars from RNAseq (data from Paina et al., 2014). Expression was normalized to total mapped reads and transcript length. RPKM, Reads Per Kilobase of transcript per Million mapped reads.

et al., 2019). *LpFT08* expression increased in short days in the ONE50 cultivar in the absence of cold treatment, similarly to *BdFTL9* (**Supplementary Figure 1B**). Initially we classified *LpFT08* as an ortholog of *BdFTL9* as these genes were linked in the GenomeZipper (**Supplementary Dataset 1**). However, *LpFT08* grouped with *BdFTL9* and *BdFTL10* in the phylogenetic tree (**Figure 1A**) and we observed that *BdFTL10* was absent from the GenomeZipper. To determine if *LpFT08* was syntenic to *BdFTL10* we examined the surrounding genes on scaffold_5827 and *B. distachyon* chromosome 2, revealing synteny between *LpFT08* and *BdFTL10* (**Supplementary Figure 1C**). *LpFT08* is likely to be present on LG1 between markers PTA.648.C1 and P5G13, as that is the putative location of other genes on scaffold_5827.

Overall, the phylogenetic analysis of ryegrass *FT-like* genes has confirmed the identification of *LpFT3* as a likely floral inducer, and *LpFT08* as a potential inducer of floral competency similar to *BdFTL9*. We also grouped other known *FT-like* genes (such as *LpTFL1*) with their appropriate *B. distachyon* orthologs, and this has matched with the synteny data above. This suggests that our approaches to finding important flowering-time genes are appropriate and may be applied to less-well-known gene families.

Phylogenetic Analysis of CCT-Domain Proteins Revealed Candidates for *VRN2* and *CO9* in Ryegrass

To characterize the CCT-domain encoding genes from ryegrass, we queried predicted peptides from a translated nucleotide database based on the draft genome of *L. perenne* using the 43 amino acid CCT domain from BdVRN2 (Bradi3g10010) with tBLASTn. Simultaneously, we queried predicted proteins from the ryegrass transcriptome, to account for some cases where an intron interrupts the CCT domain (Cockram et al., 2012; Byrne et al., 2015). We identified annotated transcripts for each hit from which we derived the protein sequences (**Supplementary Dataset 5**). We also included the "*vrn2_2*" gene (present on scaffold_1808) which has been previously described but was not detected in our tBLASTn search as the CCT domain spans an intron, and is absent from the transcriptome (Andersen et al., 2006). Thirty-six CCT-domain proteins from ryegrass were aligned with CCT-domain proteins from *B. distachyon*, rice, and barley to generate a phylogenetic tree (**Supplementary Figure 2**). The ryegrass genes fell broadly into clades including *PPD-like*, *CONSTANS-like*, *VRN2/Ghd7/CO9*. From this tree we identified two putative *VRN2-like* genes, as well as a *CO9-like* gene in ryegrass. The gene annotated as "*vrn2_2*" present on scaffold_1808 was more similar to *CO-like 14* from *B. distachyon* (**Supplementary Figure 2**; Andersen et al., 2006; Cockram et al., 2012). As no ryegrass homolog of *VRN2* has been fully described to-date, we examined the *VRN2/Ghd7/CO9-like* clade more closely to identify genes which may act as floral repressors in a manner similar to *VRN2* from wheat and barley (**Figure 2A**). From this tree, we could detect two possible homologs of *VRN2* in ryegrass, present on scaffold_936 (*LpVRN2a*) and scaffold_1700 (*LpVRN2b*). These two genes had homologs in the *L. multiflorum* and *F. pratensis* genomes, suggesting conservation in the *Lolium/Festuca* complex (bootstrap support, 100; Knorst et al., 2019; Samy et al., 2020). A single ortholog of *CO9/Ghd7* was also present on scaffold_10876 which was also present in the *L. multiflorum* and *F. pratensis* genomes (bootstrap support, 100).

Next, we aligned the CCT domains of *LpVRN2a*, *LpVRN2b*, and *LpCO9* alongside homologs from wheat, barley, *B. distachyon*, *L. multiflorum*, *F. pratensis* and rice to

determine whether any known functional residues were mutated in ryegrass species. Arginine residues 16, 35 and 39 have been reported to be mutated in non-functional versions of ZCCT in spring wheat, and these residues were unchanged in *L. perenne* or *L. multiflorum*, suggesting that the CCT domains of these proteins were likely to be functional (Distelfeld et al., 2009; **Supplementary Figure 3A**). In addition, residues conserved amongst a wide range of CCT-domain proteins, identified by Cockram et al. (2012), were unchanged in *L. perenne*, *L. multiflorum* and *F. pratensis* VRN2 and CO9-like proteins (**Supplementary Figure 3A**).

We also examined whether these three putative repressors were syntenic to known *VRN2* genes in other grasses. Only *LpVRN2a* was present on a scaffold with more than one annotated gene, allowing us to easily determine syntenic regions from *B. distachyon* and wheat. The genes surrounding *LpVRN2a* were present on chromosome 1 from *B. distachyon* and 4B from durum wheat (*Triticum turgidum*; **Supplementary Figure 3B**). *LpVRN2a* was downstream of a norcoclaurine synthase gene; however, it was absent from *B. distachyon* and wheat. This suggests that *LpVRN2a* likely results from a novel insertion of a *VRN2-like* gene during the divergence of the *Lolium* genus.

Expression Analysis Indicates *LpVRN2a, LpVRN2b* and *LpCO9* May Function as Floral Repressors

To gain a better understanding of the likely roles of *LpVRN2a, LpVRN2b* and *LpCO9*, we examined their expression pattern during vernalization in previously published RNAseq datasets from two ecotypes with differing vernalization requirements (Paina et al., 2014). *LpVRN2a* showed increased expression during vernalization in Falster compared to pre-vernalization levels, but was very lowly expressed in Veyo, while *LpVRN2b* showed very low expression in both varieties (**Figures 2B,C**). As the experiment had been conducted solely in short days, it is possible that both *VRN* homologs are repressed before cold treatment in these samples, as *VRN2-like* genes are repressed in short days in other species (Dubcovsky et al., 2006). *LpCO9* was repressed during vernalization and stayed repressed on introduction to LD, similar to *VRN2* from wheat as previously reported (**Figure 2D**; Paina et al., 2014).

We further characterized these expression patterns in the ONE50 cultivar, alongside the expression of *LpVRN1*, homologs of which act as repressors of *VRN2* (Chen and Dubcovsky, 2012; Deng et al., 2015; **Figure 3**). *LpVRN1* increased expression during vernalization, as previously demonstrated (Andersen et al., 2006; **Figure 3A**). *LpVRN2a* showed a similar expression pattern to the RNAseq data with a peak after several weeks of vernalization (**Figure 3B**). In contrast to the RNAseq data, *LpVRN2b* was expressed in ONE50 and showed a similar pattern to *LpVRN2a* (**Figure 3C**). *LpCO9-like* was also expressed; however, the pattern did not closely match that seen in the RNA seq data (**Figure 3D**). All three of these genes showed a reduction upon transfer from long days to vernalization conditions but unexpectedly increased later during vernalization, in contrast to similar experiments in wheat and barley (**Figures 3B–D**).

Samples used for qPCR time-course experiments were pooled from a number of related, but not identical ONE50 seedlings. Upon introduction to long days in our conditions, certain plants did not undergo flowering, suggesting that the pooled samples may contain induced and un-induced seedlings. We reasoned that the increase in expression of *LpVRN2a*, *LpVRN2b* and *LpCO9* seen after ∼4 weeks of vernalization was due to expression in seedlings that were not responding to the vernalization treatment. To test this, we performed qPCR on flowering and non-flowering plants derived from this experiment (**Figures 3E–H**). As expected, *VRN1* was highly expressed in flowering plants at heading (H), but not in non-flowering plants (**Figure 3E**). *LpVRN2a*, *LpVRN2b* and *LpCO9* expression was low in flowering plants and high in non-flowering plants at heading (H; **Figures 3F–H**), suggesting that non-flowering seedlings may be the source of the observed increase in gene expression of these genes after ∼4 weeks of vernalization (**Figures 3B–D**).

As ryegrass is perennial, the vernalization response must be reset after flowering. We hypothesized that this would entail reversion of *LpVRN1* and the floral repressors to their pre-vernalization levels, and that they would be able to respond to vernalization conditions again. We re-tested gene expression in the flowering and non-flowering plants from above 8 weeks after the completion of flowering (H + 8wLD), and also after 1 day (+ 1dV) and 1 week (+ 1wV) in vernalization conditions. Eight weeks after heading, *LpVRN1* expression had returned to low pre-vernalization levels (**Figure 3E**), while *LpVRN2a, LpVRN2b* and *LpCO9* had increased in plants that had previously flowered (**Figures 3F–H**). Upon re-introduction to vernalization conditions, *LpVRN1* and the floral repressors responded as expected, suggesting that the plants were competent to undergo vernalization again (**Figures 3E–H**). Surprisingly, plants that had not initially flowered showed lower expression of floral repressors 8 weeks after heading (H + 8wLD) than plants that had flowered (**Figures 3F–H**). However, *LpVRN2a, LpVRN2b* and *LpCO9* expression was still repressed upon introduction to vernalization conditions in these plants, suggesting that they were competent to respond to vernalization despite their already low levels of expression (**Figures 3F–H**). Interestingly, *LpVRN1* did not strongly respond to vernalization conditions in the non-flowering plants, perhaps indicating that some genetic differences underlay the initial non-flowering phenotype (**Figure 3E**). In parallel, we assayed clones of these plants under short days (without cold; **Supplementary Figure 4**). *LpVRN1* did not respond to short days, while the repressors responded in a similar manner in short days as they did to short days with cold (**Supplementary Figure 4**).

Variation in the Expression of Key Flowering-Time Genes Occurs in Ryegrass Genotypes With Different Vernalization Responses

Given the differences in *LpVRN1* response seen in ONE50 plants above, we next aimed to determine whether the expression levels of *LpVRN1*, *LpVRN2a*, *LpVRN2b* and *LpCO9* might contribute to the differences in vernalization response in

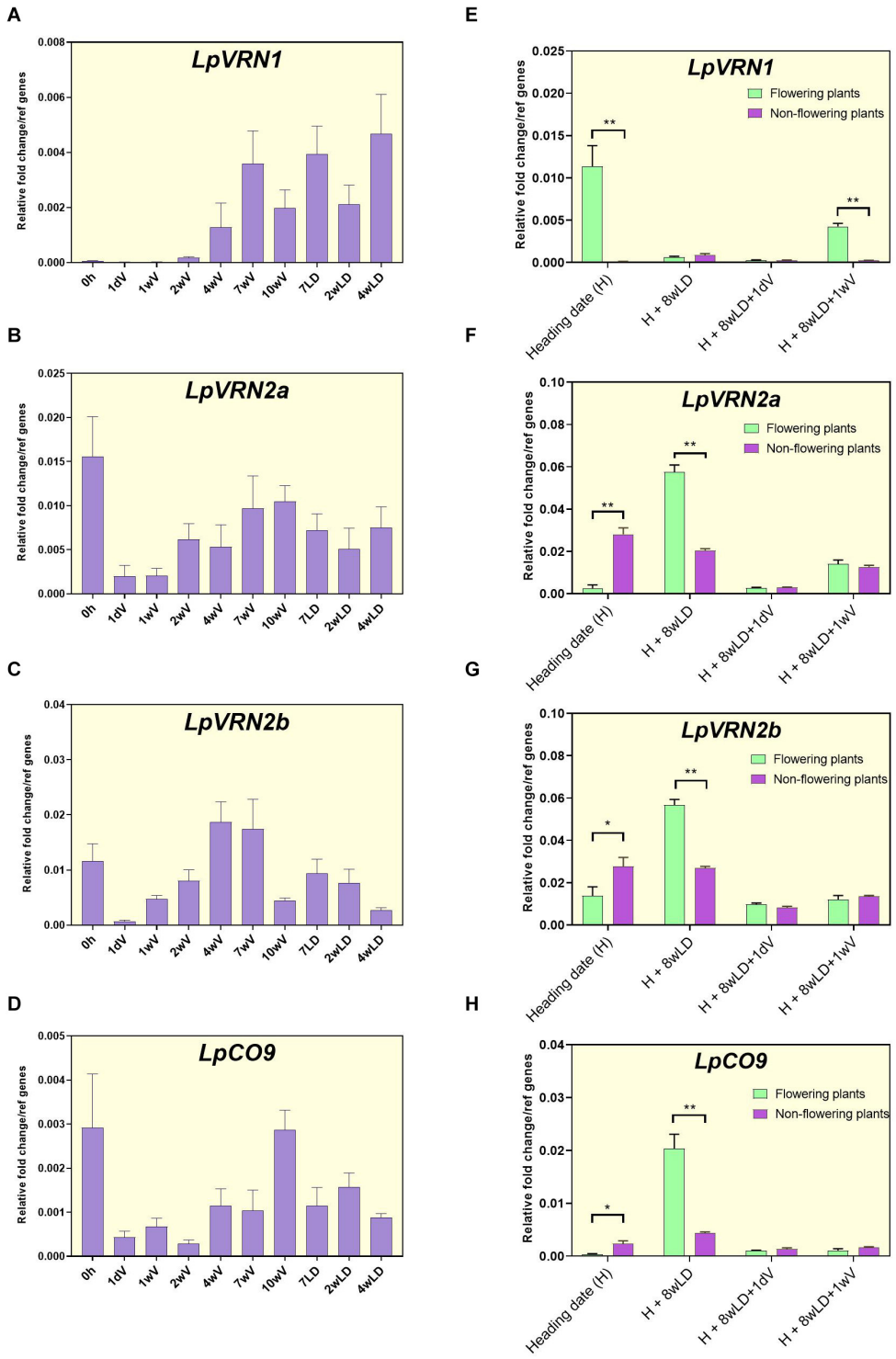

FIGURE 3 | Expression patterns of *VRN1* and *VRN2-like* genes from *L. perenne* during vernalization, heading, and re-vernalization. **(A–D)** Expression pattern of *LpVRN1*, *LpVRN2a*, *LpVRN2b*, and *LpCO9* during and after vernalization using qPCR in seedlings of the ONE50 cultivar. Expression was normalized to the geometric mean of two reference genes (*ExP* and *THP*) and shows the mean and standard deviation of two biological replicates of leaf tissue from ∼10 pooled seedlings. **(E–H)** Expression pattern of *LpVRN1*, *LpVRN2a*, *LpVRN2b*, and *LpCO9* at heading **(H)**, 8 weeks after heading (H + 8wLD), and during reintroduction to vernalization conditions (H + 8wLD + 1dSDV and H + 8wLD + 1wSDV). Data is shown for plants that flowered ($n = 3$) and plants that did not flower ($n = 3$). Expression was normalized to the geometric mean of two reference genes (*ExP* and *THP*), the mean and standard deviation of three biological replicates is shown. Each biological replicate is from several leaf samples from a single plant. Asterisks represent the results of Student's *t*-test between flowering and non-flowering results (*$p < 0.1$; **$p < 0.05$). LD, long days; SDV, short days with vernalization.

different ryegrass genotypes (**Table 1**). Ryegrass genotypes were selected from a range of geographic locations, as well as a number of commercially grown cultivars with different flowering habits, in an effort to capture a wide array of genetic variation (**Table 1**; Faville et al., 2020). In wheat and barley, vernalization induces changes in gene expression of *VRN1*, firstly transiently, and then through stable epigenetic marks (Yan et al., 2003; Oliver et al., 2009; Diallo et al., 2012). Many spring varieties of wheat, as well as some ryegrass genotypes have high levels of *VRN1* expression prior to vernalization which contributes to their lack of vernalization requirement (Andersen et al., 2006; Chu et al., 2011). We were interested in detecting variation in the level of *LpVRN1* prior to vernalization and the transient response which may be indicative of genetic variation underlying different flowering habits. Overexpression of *VRN2* and *CO9-like* genes also leads to delayed flowering, and may be another mechanism by which ryegrass can modulate its vernalization response (Kikuchi et al., 2012; Woods et al., 2016). As VRN1 regulates *VRN2* expression at the promoter in other species, the absence of *VRN2* repression upon transient VRN1 induction may indicate changes at the *VRN2* promoter which could also contribute to varying vernalization responses (Deng et al., 2015). We predicted that the expression levels of *LpVRN1* may be higher in earlier flowering varieties [similar to that seen in Veyo (early) compared to Falster (late); Andersen et al., 2006], and that the expression levels of the repressors may be lower. Alternatively, response to vernalization conditions may occur sooner in earlier flowering varieties, which would be illustrated by large changes in expression upon introduction to vernalization conditions. Genotypes with unusual expression levels or responses may contain useful genetic variation in the assayed genes that can be investigated further.

We examined the expression level of *LpVRN1*, *LpVRN2a*, *LpVRN2b* and *LpCO9* prior to introduction to vernalization conditions in pooled 3-week-old seedlings to determine the pre-vernalization level of each gene (**Supplementary Figure 5**). To determine whether there was variation in the initial/transient response of these genes to vernalization conditions we also tested the expression of these genes after 2 days in cold (4°C) and dark and compared the values (**Supplementary Figure 5**). Gene expression was detected for all genes in all genotypes, except for *LpCO9* in the Medea genotype (**Supplementary Figure 5**). In terms of their transient response to vernalization conditions, all plants had higher *LpVRN1* expression after 2 days of cold, exemplified most clearly in the Iranian ecotype (**Supplementary Figure 5E**). *LpVRN2a* and *LpVRN2b* were repressed in all genotypes except Medea and Barberia, while *LpCO9* varied greatly between genotypes upon transfer to vernalization conditions (**Supplementary Figure 5F–H**). Despite our earlier predictions, there was no association between early flowering and high *LpVRN1* or low levels of repressors, and the transient response also did not appear to be significantly associated with flowering habit (**Supplementary Figure 6**). However, *LpCO9* was more highly expressed in late-flowering genotypes prior to vernalization, which may implicate it in the late-flowering phenotype (**Supplementary Figure 6**).

Although we did not detect strong associations between flowering habit and gene expression in most cases, there was a high level of variation in expression and response between genotypes, particularly in *LpVRN1* and *LpCO9* which may indicate the presence of natural variation. We examined the variance between genotypes of *LpVRN1*, *LpVRN2a*/*b* and *LpCO9* expression before and after 2 days in vernalization conditions, and also the variance in response (expressed as $\log_2$ fold change between conditions) to determine which genes are most likely to have underlying genetic variation (**Figure 4**). *LpVRN1* and *LpCO9* were highly variable, both in terms of expression level, and in terms of response, while *LpVRN2a* and *LpVRN2b* were significantly less variable (**Figure 4**). Overall, these results suggest that *LpCO9* might hold more natural variation in expression than *LpVRN2a* and *LpVRN2b*. Natural variation in *LpVRN1* has already been demonstrated and may exist in the genotypes examined here as well (Andersen et al., 2006).

DISCUSSION

Ryegrass flowering impacts metabolizable energy and seed production, and is therefore an important trait for breeders to target. The advent of genomic selection now allows breeders to more accurately select for heading date (Hayes et al., 2013). However, understanding the genes and alleles responsible for variation in heading date is required to more easily identify useful germplasm, and for more targeted approaches, such as gene editing with CRISPR/Cas9. Translating knowledge from model species and well-studied crops is therefore an efficient way to further our understanding of heading date in ryegrass.

Here, we have used available genomic resources to compile a list of likely orthologs of important flowering-time genes from *B. distachyon* in *L. perenne*. We have further confirmed orthology for *FT-like* and *VRN2-like* genes using phylogeny (**Figures 1**, **2**). Further phylogenetic analyses may confirm the orthology between other genes identified here (e.g., MADS-box domain genes, such as *SOC1*), and additional genomic sequences may enable the identification of more genes/paralogs in ryegrass. It is hoped that this thorough analysis can be used as a reference, particularly for determining the functions of *FT-like* and *VRN2-like* genes in ryegrass. Our phylogenetic analysis of *FT-like* genes in *L. perenne* was more complete than previous analyses (Arojju et al., 2016), and incorporated expression data to strengthen hypotheses regarding the function of each *L. perenne FT-like* gene. For example, it has been suggested that the *FT-like* gene present on scaffold_13332 (*LpFT02*) corresponds to the *LpVRN3* marker (Arojju et al., 2016). However, the analysis by Arojju et al. (2016) did not include *LpFT3* (likely because it was not included in the transcriptome), which perfectly matches the entire sequence of the *LpVRN3* marker, and is supported to be the functional *FT* homolog in this (and other) studies (Skøt et al., 2011; Studer et al., 2012). Similarly, the gene associated with the vrn2_2 marker on scaffold_1808 matches more closely with *CO-like 14* from *B. distachyon* (Andersen et al., 2006; **Supplementary Figure 3**). The two *VRN2* homologs identified here are the closest match to *VRN2* from *B. distachyon* and also ZCCT1 and

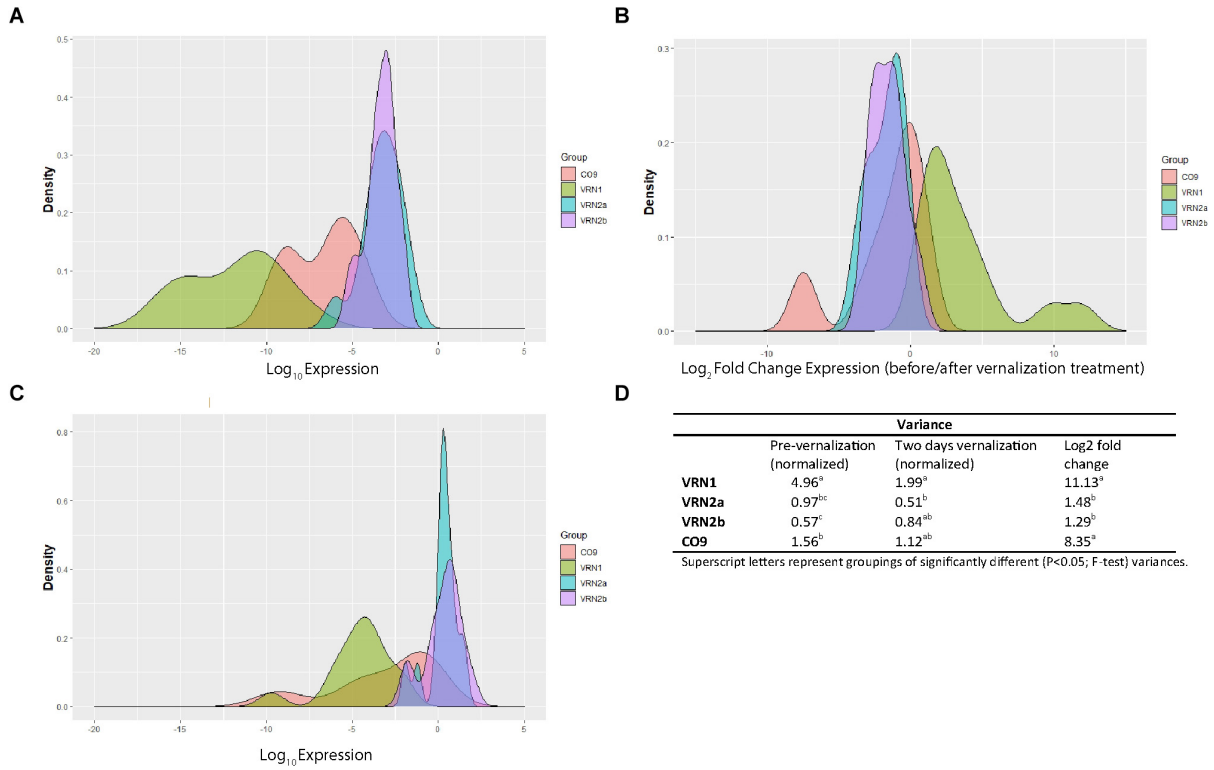

D

	Variance		
	Pre-vernalization (normalized)	Two days vernalization (normalized)	Log2 fold change
VRN1	4.96^{a}	1.99^{a}	11.13^{a}
VRN2a	0.97^{bc}	0.51^{b}	1.48^{b}
VRN2b	0.57^{c}	0.84^{ab}	1.29^{b}
CO9	1.56^{b}	1.12^{ab}	8.35^{a}

Superscript letters represent groupings of significantly different (P<0.05; F-test) variances.

FIGURE 4 | Analysis of the variability in expression and response to vernalization treatment of *LpVRN1, LpVRN2a, LpVRN2b* and *LpCO9* in a variety of different ryegrass genotypes. **(A)** Density plot of log-transformed gene expression before transfer to vernalization conditions. **(B)** Density plot of log-transformed gene expression after 2 days in vernalization conditions. **(C)** Density plot of $\log_2$ fold change in gene expression after transfer to vernalization conditions. **(D)** Table showing significant differences in variances ($p < 0.05$; F-test) between each gene. *LpVRN1* and *LpCO9* were more variable than *LpVRN2a* and *LpVRN2b*.

ZCCT2 from wheat (**Figure 3A**). In addition, no closer genes were identified in *F. pratensis* or *L. multiflorum*, suggesting that it is unlikely that more *VRN2-like* genes exist in *L. perenne* than the two identified here.

In wheat, *VRN2* is a key determinant of flowering habit between different cultivars. QTL analyses on ryegrass vernalization response identified *LpVRN1* and *LpCO* as important determinants of the different responses between Falster and Veyo cultivars (Jensen et al., 2005; Andersen et al., 2006). *LpVRN2a* and *LpVRN2b* were not identified in this screen, although the genes underlying all QTL from this experiment are yet to be identified. *LpVRN2a* has been assigned to linkage group 4 and is included in a QTL relating to winter survival (Paina et al., 2016). *LpVRN2b* and *LpCO9* have not been assigned to a linkage group in GenomeZipper or the recent high-density mapping population, making it difficult to determine whether these genes may correspond to a flowering QTL (Byrne et al., 2015; Velmurugan et al., 2016). Our data suggest that less variation in the expression levels (and response to vernalization conditions) of *LpVRN2a* and *LpVRN2b* exists in comparison to *LpVRN1* and *LpCO9* (**Figure 4**), which may explain why these genes have not been detected in previous QTL analyses; mutational studies or targeted F2 populations (e.g., utilizing Medea or Barberia individuals as parents, which lacked response in *VRN2a and VRN2b,* respectively) would be required to determine their function (**Supplementary Figure 5**). There may also be variation in *LpVRN2a* and *LpVRN2b* expression after long-term cold exposure/vernalization which was not represented in the initial response.

The high variability of *LpCO9* response (**Figure 4**), and high expression levels of *LpCO9* in late-flowering genotypes (**Supplementary Figure 6**), suggests that some genetic variation exists in the promoter of *LpCO9*, or in proteins that regulate its expression. How much variation in the expression levels of these genes exists between individuals of a cultivar/ecotype is also of interest – as we have pooled samples for our expression analysis (**Supplementary Figure 5**), it is possible that some individuals from each pool largely dictate the observed expression level of a gene. Whether the variability in *LpCO9* expression observed after 2 days in vernalization conditions translates to variability at later stages remains to be seen.

VRN2 was also reported to be absent from the *L. multiflorum* transcriptome prior to vernalization, however, we have detected *LpVRN2a* and *LpVRN2b* transcripts in annual ryegrasses (Tabu, Barberia, and the Cypriot and Iranian ecotypes; **Supplementary Figure 5**; Czaban et al., 2015). This discrepancy may be due to differences in genotype, or to plant age, as we have used 3-week-old seedlings, compared to mature plants, which may indicate a role for *LpVRN2a* and *LpVRN2b* in repressing flowering in young annual ryegrass plants. The alleles present in *L. multiflorum*

appear to have functional CCT domains (**Supplementary Figure 3A**), and the sequence of *L. multiflorum VRN2a* is present in the Falster transcriptome (data not shown; Paina et al., 2014). Alleles of *LpVRN2a* and *LpVRN2b* may play a more minor role in heading date and vernalization requirement compared to the large effect of different *LpVRN1* alleles. We did not detect an association between early flowering and high *LpVRN1* expression prior to vernalization (**Supplementary Figure 5A**), perhaps indicating that the early flowering (and annual) genotypes examined here contain novel variation affecting this trait, distinct from that which affects *LpVRN1* expression (as seen in Falster and Veyo; Andersen et al., 2006). Alternatively, *LpVRN1* expression may only be induced later in these genotypes, again suggesting that plant age plays a role in modulating expression of *VRN* genes in ryegrass.

How LpVRN1 impacts the expression level of *LpVRN2a, LpVRN2b* and *LpCO9* in ryegrass remains to be determined. In the non-flowering ryegrass plants, and in ryegrass exposed to short days in the absence of cold, *LpVRN1* was not induced, however, *LpVRN2a/b* and *LpCO9* expression was reduced in these conditions, suggesting that regulators other than LpVRN1 are able to repress these genes (**Figure 3** and **Supplementary Figure 3**). The alleles underlying *LpVRN1*, *LpVRN2a/b* and *LpCO9* expression differences in the various genotypes we assayed here may also be of interest (**Figure 4** and **Supplementary Figure 5**). Transgenic studies to test the function of *LpFT08*, *LpVRN2a/b* and *LpCO9* will be critical to further our understanding of these genes in *L. perenne*.

DATA AVAILABILITY STATEMENT

The datasets presented in this study can be found in online repositories. The names of the repository/repositories and accession number(s) can be found in the article/ **Supplementary Material**.

AUTHOR CONTRIBUTIONS

RH, S, LB, and RM designed the experiments and wrote and edited the manuscript. RH and S performed the experiments. All authors contributed to the article and approved the submitted version.

FUNDING

This work was supported by Ministry of Business Innovation and Employment (MBIE) funding grant number UOOX1911.

SUPPLEMENTARY MATERIAL

The Supplementary Material for this article can be found online at: https://www.frontiersin.org/articles/10.3389/fpls.2021.640324/full#supplementary-material

REFERENCES

Anders, S., Pyl, P. T., and Huber, W. (2015). HTSeq—a Python framework to work with high-throughput sequencing data. *Bioinformatics* 31, 166–169.

Andersen, J. R., Jensen, L. B., Asp, T., and Lubberstedt, T. (2006). Vernalization response in perennial ryegrass (*Lolium perenne* L.) involves orthologues of diploid wheat (*Triticum monococcum*) VRN1 and rice (*Oryza sativa*) Hd1. *Plant Mol. Biol.* 60, 481–494. doi: 10.1007/s11103-005-4815-1

Ariyaratne, M., Takamure, I., and Kato, K. (2009). Shoot branching control by reduced culm number 4 in rice (*Oryza sativa* L.). *Plant Sci.* 176, 744–748.

Arojju, S. K., Barth, S., Milbourne, D., Conaghan, P., Velmurugan, J., Hodkinson, T. R., et al. (2016). Markers associated with heading and aftermath heading in perennial ryegrass full-sib families. *BMC Plant Biol.* 16:160. doi: 10.1186/s12870-016-0844-y

Asp, T., Byrne, S., Gundlach, H., Bruggmann, R., Mayer, K. F., Andersen, J. R., et al. (2011). Comparative sequence analysis of VRN1 alleles of *Lolium perenne* with the co-linear regions in barley, wheat, and rice. *Mol. Genet. Genomics* 286, 433–447. doi: 10.1007/s00438-011-0654-8

Byrne, S. L., Nagy, I., Pfeifer, M., Armstead, I., Swain, S., Studer, B., et al. (2015). A synteny-based draft genome sequence of the forage grass *Lolium perenne*. *Plant J.* 84, 816–826. doi: 10.1111/tpj.13037

Chen, A., and Dubcovsky, J. (2012). Wheat TILLING mutants show that the vernalization gene VRN1 down-regulates the flowering repressor VRN2 in leaves but is not essential for flowering. *PLoS Genet.* 8:e1003134. doi: 10.1371/journal.pgen.1003134

Chu, C.-G., Tan, C., Yu, G.-T., Zhong, S., Xu, S., and Yan, L. (2011). A novel retrotransposon inserted in the dominant Vrn-B1 allele confers spring growth habit in tetraploid wheat (*Triticum turgidum* L.). *G3 Genes Genomes Genet.* 1, 637–645.

Cockram, J., Thiel, T., Steuernagel, B., Stein, N., Taudien, S., Bailey, P. C., et al. (2012). Genome dynamics explain the evolution of flowering time CCT domain gene families in the Poaceae. *PLoS One* 7:e45307. doi: 10.1371/journal.pone.0045307

Czaban, A., Sharma, S., Byrne, S. L., Spannagl, M., Mayer, K. F., and Asp, T. (2015). Comparative transcriptome analysis within the *Lolium*/*Festuca* species complex reveals high sequence conservation. *BMC Genomics* 16:249. doi: 10.1186/s12864-015-1447-y

Deng, W., Casao, M. C., Wang, P., Sato, K., Hayes, P. M., Finnegan, E. J., et al. (2015). Direct links between the vernalization response and other key traits of cereal crops. *Nat. Commun.* 6:5882. doi: 10.1038/ncomms6882

Diallo, A. O., Ali-Benali, M. A., Badawi, M., Houde, M., and Sarhan, F. (2012). Expression of vernalization responsive genes in wheat is associated with histone H3 trimethylation. *Mol. Genet. Genomics* 287, 575–590.

Distelfeld, A., Tranquilli, G., Li, C., Yan, L., and Dubcovsky, J. (2009). Genetic and molecular characterization of the VRN2 loci in tetraploid wheat. *Plant Physiol.* 149, 245–257. doi: 10.1104/pp.108.129353

Dobin, A., Davis, C. A., Schlesinger, F., Drenkow, J., Zaleski, C., Jha, S., et al. (2013). STAR: ultrafast universal RNA-seq aligner. *Bioinformatics* 29, 15–21. doi: 10.1093/bioinformatics/bts635

Dubcovsky, J., Loukoianov, A., Fu, D., Valarik, M., Sanchez, A., and Yan, L. (2006). Effect of photoperiod on the regulation of wheat vernalization genes VRN1 and VRN2. *Plant Mol. Biol.* 60, 469–480. doi: 10.1007/s11103-005-4814-2

Edgar, R. C. (2004). MUSCLE: multiple sequence alignment with high accuracy and high throughput. *Nucleic Acids Res.* 32, 1792–1797.

Faure, S., Higgins, J., Turner, A., and Laurie, D. A. (2007). The FLOWERING LOCUS T-like gene family in barley (*Hordeum vulgare*). *Genetics* 176, 599–609. doi: 10.1534/genetics.106.069500

Faville, M. J., Griffiths, A. G., Baten, A., Cao, M., Ashby, R., Ghamkhar, K., et al. (2020). Genomic assessment of white clover and perennial ryegrass genetic resources. *J. N. Z. Grassl.* 82, 27–34.

Gangi, A. S., Chilcote, D. O., and Frakes, R. V. (1983). Growth, floral induction and reproductive development in selected perennial ryegrass *Lolium perenne* L. Cultivars. *Appl. Seed Prod.* 1, 34–38.

Griffiths, S., Dunford, R. P., Coupland, G., and Laurie, D. A. (2003). The evolution of CONSTANS-like gene families in barley, rice, and *Arabidopsis*. *Plant Physiol.* 131, 1855–1867. doi: 10.1104/pp.102.016188

Hayes, B. J., Cogan, N. O., Pembleton, L. W., Goddard, M. E., Wang, J., Spangenberg, G. C., et al. (2013). Prospects for genomic selection in forage plant species. *Plant Breed.* 132, 133–143.

Higgins, J. A., Bailey, P. C., and Laurie, D. A. (2010). Comparative genomics of flowering time pathways using *Brachypodium distachyon* as a model for the temperate grasses. *PLoS One* 5:e10065. doi: 10.1371/journal.pone.0010065

Jensen, C. S., Salchert, K., and Nielsen, K. K. (2001). A TERMINAL FLOWER1-like gene from perennial ryegrass involved in floral transition and axillary meristem identity. *Plant Physiol.* 125, 1517–1528. doi: 10.1104/pp.125.3.1517

Jensen, L. B., Andersen, J. R., Frei, U., Xing, Y., Taylor, C., Holm, P. B., et al. (2005). QTL mapping of vernalization response in perennial ryegrass (*Lolium perenne* L.) reveals co-location with an orthologue of wheat VRN1. *Theor. Appl. Genet.* 110, 527–536. doi: 10.1007/s00122-004-1865-8

Kikuchi, R., Kawahigashi, H., Oshima, M., Ando, T., and Handa, H. (2012). The differential expression of HvCO9, a member of the CONSTANS-like gene family, contributes to the control of flowering under short-day conditions in barley. *J. Exp. Bot.* 63, 773–784. doi: 10.1093/jxb/err299

Knorst, V., Yates, S., Byrne, S., Asp, T., Widmer, F., Studer, B., et al. (2019). First assembly of the gene−space of *Lolium multiflorum* and comparison to other Poaceae genomes. *Grassl. Sci.* 65, 125–134.

Li, C., and Dubcovsky, J. (2008). Wheat FT protein regulates VRN1 transcription through interactions with FDL2. *Plant J.* 55, 543–554. doi: 10.1111/j.1365-313X.2008.03526.x

Nakagawa, M., Shimamoto, K., and Kyozuka, J. (2002). Overexpression of RCN1 and RCN2, rice TERMINAL FLOWER 1/CENTRORADIALIS homologs, confers delay of phase transition and altered panicle morphology in rice. *Plant J.* 29, 743–750. doi: 10.1046/j.1365-313x.2002.01255.x

Narsai, R., Ivanova, A., Ng, S., and Whelan, J. (2010). Defining reference genes in *Oryza sativa* using organ, development, biotic and abiotic transcriptome datasets. *BMC Plant Biol.* 10:56. doi: 10.1186/1471-2229-10-56

Oliver, S. N., Finnegan, E. J., Dennis, E. S., Peacock, W. J., and Trevaskis, B. (2009). Vernalization-induced flowering in cereals is associated with changes in histone methylation at the VERNALIZATION1 gene. *Proc. Natl. Acad. Sci. U.S.A.* 106, 8386–8391. doi: 10.1073/pnas.0903566106

Paina, C., Byrne, S. L., Domnisoru, C., and Asp, T. (2014). Vernalization mediated changes in the *Lolium perenne* transcriptome. *PLoS One* 9:e107365. doi: 10.1371/journal.pone.0107365

Paina, C., Byrne, S. L., Studer, B., Rognli, O. A., and Asp, T. (2016). Using a candidate gene-based genetic linkage map to Identify QTL for winter survival in perennial ryegrass. *PLoS One* 11:e0152004. doi: 10.1371/journal.pone.0152004

Pin, P. A., and Nilsson, O. (2012). The multifaceted roles of FLOWERING LOCUS T in plant development. *Plant Cell Environ.* 35, 1742–1755.

Qin, Z., Bai, Y., Muhammad, S., Wu, X., Deng, P., Wu, J., et al. (2019). Divergent roles of FT-like 9 in flowering transition under different day lengths in *Brachypodium distachyon*. *Nat. Commun.* 10:812. doi: 10.1038/s41467-019-08785-y

Samarth and Jameson, P. E. (2019). Selection of reference genes for flowering pathway analysis in the masting plants, *Celmisia lyallii* and *Chionochloa pallens*, under variable environmental conditions. *Sci. Rep.* 9:9767.

Samy, J. K. A., Rognli, O. A., and Kovi, M. R. J. D. (2020). ForageGrassBase: molecular resource for the forage grass meadow fescue (*Festuca pratensis* Huds.). *Database* 2020:baaa046. doi: 10.1093/database/baaa046

Shimada, S., Ogawa, T., Kitagawa, S., Suzuki, T., Ikari, C., Shitsukawa, N., et al. (2009). A genetic network of flowering-time genes in wheat leaves, in which an APETALA1/FRUITFULL-like gene. VRN1, is upstream of FLOWERING LOCUS T. *Plant J.* 58, 668–681. doi: 10.1111/j.1365-313X.2009.03806.x

Skøt, L., Sanderson, R., Thomas, A., Skøt, K., Thorogood, D., Latypova, G., et al. (2011). Allelic variation in the perennial ryegrass FLOWERING LOCUS T gene is associated with changes in flowering time across a range of populations. *Plant Physiol.* 155, 1013–1022. doi: 10.1104/pp.110.169870

Stockdale, C. (1999). Effects of season and time since defoliation on the nutritive characteristics of three irrigated perennial pasture species in northern Victoria 1. Energy, protein and fibre. *Aust. J. Exp. Agric.* 39, 555–565.

Studer, B., Byrne, S., Nielsen, R. O., Panitz, F., Bendixen, C., Islam, M. S., et al. (2012). A transcriptome map of perennial ryegrass (*Lolium perenne* L.). *BMC Genomics* 13:140. doi: 10.1186/1471-2164-13-140

Studer, B., Jensen, L. B., Fiil, A., and Asp, T. (2009). "Blind" mapping of genic DNA sequence polymorphisms in *Lolium perenne* L. by high resolution melting curve analysis. *Mol. Breed.* 24, 191–199.

Tamaki, S., Matsuo, S., Wong, H. L., Yokoi, S., and Shimamoto, K. (2007). Hd3a protein is a mobile flowering signal in rice. *Science* 316, 1033–1036. doi: 10.1126/science.1141753

The International Brachypodium Initiative (2010). Genome sequencing and analysis of the model grass *Brachypodium distachyon*. *Nature* 463, 763–768. doi: 10.1038/nature08747

Veeckman, E., Vandepoele, K., Asp, T., Roldàn-Ruiz, I., and Ruttink, T. (2016). "Genomic variation in the FT gene family of perennial ryegrass (*Lolium perenne*)," in *Breeding in a World of Scarcity*, eds I. Roldán-Ruiz, J. Baert, and D. Reheul (Cham: Springer), 121–126.

Velmurugan, J., Mollison, E., Barth, S., Marshall, D., Milne, L., Creevey, C. J., et al. (2016). An ultra-high density genetic linkage map of perennial ryegrass (*Lolium perenne*) using genotyping by sequencing (GBS) based on a reference shotgun genome assembly. *Ann. Bot.* 118, 71–87. doi: 10.1093/aob/mcw081

Wang, J. P., and Forster, J. W. (2017). Flowering time regulation in perennial ryegrass. *Euphytica* 213:106.

Woods, D., Dong, Y., Bouche, F., Bednarek, R., Rowe, M., Ream, T., et al. (2019). A florigen paralog is required for short-day vernalization in a pooid grass. *eLife* 8:e42153. doi: 10.7554/eLife.42153

Woods, D. P., McKeown, M. A., Dong, Y., Preston, J. C., and Amasino, R. M. (2016). Evolution of VRN2/Ghd7-like genes in vernalization-mediated repression of grass flowering. *Plant Physiol.* 170, 2124–2135. doi: 10.1104/pp.15.01279

Xue, W., Xing, Y., Weng, X., Zhao, Y., Tang, W., Wang, L., et al. (2008). Natural variation in Ghd7 is an important regulator of heading date and yield potential in rice. *Nat. Genet.* 40, 761–767. doi: 10.1038/ng.143

Yan, L., Loukoianov, A., Blechl, A., Tranquilli, G., Ramakrishna, W., SanMiguel, P., et al. (2004). The wheat VRN2 gene is a flowering repressor down-regulated by vernalization. *Science* 303, 1640–1644. doi: 10.1126/science.1094305

Yan, L., Loukoianov, A., Tranquilli, G., Helguera, M., Fahima, T., and Dubcovsky, J. (2003). Positional cloning of the wheat vernalization gene VRN1. *Proc. Natl. Acad. Sci. U.S.A.* 100, 6263–6268. doi: 10.1073/pnas.0937399100

Conflict of Interest: The authors declare that the research was conducted in the absence of any commercial or financial relationships that could be construed as a potential conflict of interest.

Copyright © 2021 Herridge, Samarth, Brownfield and Macknight. This is an open-access article distributed under the terms of the Creative Commons Attribution License (CC BY). The use, distribution or reproduction in other forums is permitted, provided the original author(s) and the copyright owner(s) are credited and that the original publication in this journal is cited, in accordance with accepted academic practice. No use, distribution or reproduction is permitted which does not comply with these terms.

frontiers in Plant Science

MINI REVIEW
published: 11 March 2021
doi: 10.3389/fpls.2021.640442

The Flowering Season-Meter at FLOWERING LOCUS C Across Life Histories in Crucifers

Diana Mihaela Buzas[1], Haruki Nishio[2] and Hiroshi Kudoh[2]*

[1] Faculty of Life and Environmental Sciences, Tsukuba-Plant Innovation Research Center, University of Tsukuba, Tsukuba, Japan, [2] Center for Ecological Research, Kyoto University, Otsu, Japan

Many plant species overwinter before they flower. Transition to flowering is aligned to the seasonal transition as a response to the prolonged cold in winter by a process called vernalization. Multiple well-documented vernalization properties in crucifer species with diverse life histories are derived from environmental regulation of a central inhibitor of the flowering gene, *Flowering Locus C* (*FLC*). Episode(s) of flowering are prevented during high *FLC* expression and enabled during low *FLC* expression. *FLC* repression outlasts the winter to coincide with spring; this heterochronic aspect is termed "winter memory." In the annual *Arabidopsis thaliana*, winter memory has long been associated with the highly conserved histone modifiers Polycomb and Trithorax, which have antagonistic roles in transcription. However, there are experimental limitations in determining how dynamic, heterogenous histone modifications within the *FLC* locus generate the final transcriptional output. Recent theoretical considerations on cell-to-cell variability in gene expression and histone modifications generating bistable states brought support to the hypothesis of chromatin-encoded memory, as with other experimental systems in eukaryotes. Furthermore, these advances unify multiple properties of vernalization, not only the winter memory. Similarly, in the perennial *Arabidopsis halleri* ssp. *gemmifera*, recent integration of molecular with mathematical and ecological approaches unifies *FLC* chromatin features with the all-year-round memory of seasonal temperature. We develop the concept of FLC season-meter to combine existing information from the contrasting annual/perennial and experimental/theoretical sectors into a transitional framework. We highlight simplicity, high conservation, and discrete differences across extreme life histories in crucifers.

Keywords: Flowering Locus C, polycomb and trithorax chromatin regulators, bistable states, annual and perennial life history, convergent cross mapping

OPEN ACCESS

Edited by:
Elizabeth Dennis, Commonwealth Scientific and Industrial Research Organization (CSIRO), Australia

Reviewed by:
Ryo Fujimoto, Kobe University, Japan
Chris Helliwell, Commonwealth Scientific and Industrial Research Organization (CSIRO), Australia
Martin Howard, John Innes Centre, United Kingdom
Pedro Crevillén, National Institute of Agricultural and Food Research and Technology, Spain

****Correspondence:***
Diana Mihaela Buzas
buzas.mihaela.ka@u.tsukuba.ac.jp

Specialty section:
This article was submitted to Plant Development and EvoDevo, a section of the journal Frontiers in Plant Science

Received: *11 December 2020*
Accepted: *04 February 2021*
Published: *11 March 2021*

Citation:
Buzas DM, Nishio H and Kudoh H (2021) The Flowering Season-Meter at FLOWERING LOCUS C Across Life Histories in Crucifers. Front. Plant Sci. 12:640442. doi: 10.3389/fpls.2021.640442

INTRODUCTION

As a standing proof of a sharp divide between winter and spring, some plant species burst into flower at this precise time to secure reproductive success in this vacant niche. The process of vernalization, enabling precision in timing of the floral transition after the prolonged cold of winter, is versatile in nature and agriculture. Species with single and multiple reproductive episodes (herein annual and perennial), ecotypes adapted to local climates, including those of the model plant species *Arabidopsis thaliana* (*A. thaliana*) from the representative crucifer family, and crop varieties with distinct timing for harvesting, all overwinter before they flower. How can reproductive transition be so precisely timed to occur in spring in a variety of biological systems?

In crucifers, central to vernalization is a gene that blocks flowering termed *Flowering Locus C* (*FLC*) (Michaels and Amasino, 2000). Across life histories, abundant *FLC* expression facilitates vegetative growth until, under the influence of low temperatures, *FLC* expression gradually becomes negligible by the end of winter. Also, as *FLC* repression outlasts the winter, plants become competent to flower in spring—this is often referred to as "winter memory." The length of winter memory, i.e., the length of time the low FLC expression is maintained, varies especially across extreme life histories: in the annual *A. thaliana*, the *FLC* minimum is prolonged into the final senescence stage; ancestral perennial forms have short winter memory, allowing only a narrow window of flowering before reverting to vegetative growth based on high *FLC* levels (Wang et al., 2009; Aikawa et al., 2010).

Intensive genetic screens dissecting winter memory in *A. thaliana* frequently recover core and accessory proteins of the Polycomb group (PcG) and Trithorax group (TrxG) complexes (reviewed in Buzas et al., 2012; Berry and Dean, 2015a; Luo and He, 2020), highly conserved in eukaryotes (Steffen and Ringrose, 2014). PcG/TrxG catalyze mainly trimethylation of lysine 27 and four of histone 3 (H3K27me3, H3K4me3), while other associated activities, including, for example, H3K36me3, also mediate PcG/TrxG regulated processes (Steffen and Ringrose, 2014). There are two main long-standing conundrums in this area. One is whether (PcG/TrxG induced) chromatin modifications produce memory (Moazed, 2011). The other is how to unify the well-known role of PcG/TrxG in stably maintaining expression states independent of the inducing signals at a gene, with highly dynamic regulation at other PcG/TrxG target genes (Steffen et al., 2012; Steffen and Ringrose, 2014; Reinig et al., 2020). From theoretical consideration on how cell-to-cell variability in gene expression and histone modifications influence the vernalization process, recent advances support the hypothesis of chromatin coding of memory (Angel et al., 2011; Berry et al., 2015b; Yang et al., 2017; Nishio et al., 2020a) as we outline in the section "*Insights From Annual Vernalization: Experiments and Theory*" and in the section "*Initial Insights From Perennial Vernalization*". By comparing winter memory mechanisms in annuals and perennials, we formulate a model of how stable and flexible gene expression states residing together at *FLC* may account for precise detection of seasons in diverse life histories (see section "*The Flowering Locus C Season-Meter for Flowering Across Life Histories*"). As such, findings from the vernalization example are more generally relevant to chromatin regulation.

INSIGHTS FROM ANNUAL VERNALIZATION: EXPERIMENTS AND THEORY

Models for *Arabidopsis thaliana*

Establishing a gene expression state at the chromatin level involving PcG/TrxG was initially determined experimentally with the Hox genes in *Drosophila* as a two-step process: initiation and maintenance. Initiation commonly requires DNA-based mechanisms, mediated by transcription factor binding. Maintenance over cell generations is under the influence of histone modifications, recruited locally by *cis*-acting elements termed Polycomb/ TrxG recruiting elements (PRE/TRE) (Steffen and Ringrose, 2014; Buzas, 2017). Essentially memory elements PRE/TREs can maintain a high degree of stability of gene expression across cell divisions that outlast the initiating signals. The states maintained as development proceeds are either ON or OFF; this can be visualized in reporter assays as variegation (Chan et al., 1994; Steffen et al., 2012).

Theoretical approaches also bridge PcG/TrxG-related phenomena across eukaryotes and are deemed suitable to tackle the complex dynamics, especially in quantitative terms (Steffen et al., 2012). How an array of nucleosomes can remain stable over many cell divisions even when individual nucleosomes change modification states randomly has been predicted from a purely theoretical study (Dodd et al., 2007). In this model, various histone-modifying biochemical activities result in nucleosome states, distilled down to three categories: "active," "unmodified," and "repressed." The transitions between these states can be *via* either feedback (a nucleosome state generates the same state in neighboring nucleosomes) or noise (random addition or removal of modifications). The model asks what conditions generate bistability, a state where the whole array of nucleosomes is either ON or OFF, giving rise to variegation (Chan et al., 1994; Steffen et al., 2012). Feedback is required for system stability, while noise generates switching. How the Dodd model is applicable to vernalization (Angel et al., 2011; Satake and Iwasa, 2012) is outlined in the section "*Cell-to-Cell Variation Underlies Measuring of Cold Duration, Robust Response to Noisy Temperatures, and Memory of Winter.*"

The Repertoire of Stable *AtFLC* Expression States

Both active and repressed states of *AtFLC* are biologically relevant: active *AtFLC* reliably prevents flowering until plants have experienced winter/saturating cold treatment, while repressed *AtFLC* ensures that flowering takes place in spring/after cold treatment. How each of the active and the repressed *AtFLC* states are established has been investigated as two-step processes, as in *Drosophila*, especially as *AtFLC* regulatory regions satisfying both PRE and TRE requirements have been found (reviewed in Buzas et al., 2012).

When considering how active *AtFLC* is established, the two steps can be delineated: a transcription factor transiently expressed in embryos initiates *AtFLC* activation; then, this memory of the embryonic state is maintained *via* TrxG-like activity during the vegetative phase (Tao et al., 2017). However, the process of *AtFLC* repression does not entirely fit the paradigm. A transcription factor transiently induced in the early stages of cold that would initiate *AtFLC* repression has not been identified (Helliwell et al., 2015). Nevertheless, an early cold event leads to rapid reduction in *AtFLC* transcription rate (Finnegan, 2015). Then, a dynamic cascade of chromatin

events during early stages of cold leads to stabilization of *AtFLC* repression over time (Berry et al., 2015b; Finnegan, 2015; Qüesta et al., 2016; Yuan et al., 2016; Yang et al., 2017) (also see section The cell autonomous chromatin switch), before *AtFLC* repression is maintained in a PcG-dependent manner (Buzas et al., 2012; Berry and Dean, 2015a).

Adding support to the PcG/TrxG control *via* bistable states, *AtFLC* ON and OFF states have been evidenced experimentally (Angel et al., 2011; Berry and Dean, 2015a; Yang et al., 2017; Qüesta et al., 2020). However, surprisingly, *AtFLC* ON/OFF states are not exclusively found in developmental windows of active/repressed *AtFLC*. Instead, mixed ON/OFF states are present during the transition from active to repressed *FLC* (Angel et al., 2011; Berry et al., 2015b; Yang et al., 2017) as well as possibly during the reverse transition (Qüesta et al., 2020). In fact, the transition intervals support further *AtFLC* biological functions: an accelerated increase (*FLC* dial-up) of *AtFLC* levels in the seed both resets the vernalization requirement in the next generation (Sheldon et al., 2008; Choi et al., 2009; Crevillén et al., 2014), and ensures that flowering is prevented (Sheldon et al., 2008); gradually decreasing *AtFLC* (*FLC* dial-down) levels results in corresponding degrees of earliness in flowering (Michaels and Amasino, 2000; Sheldon et al., 2006).

In conclusion, current data prompts a view of the *AtFLC* locus as a dynamic PcG/TrxG target where switching between ON and OFF states generates a cyclic response with four types of *AtFLC* quantities, tightly regulated over time: minimum, dial-up, maximum, and dial-down.

AtFLC Chromatin: Three Domains

It is of great interest to understand how the PcG/TrxG-induced chromatin modifications control *FLC* expression. The whole tissue level dynamics of H3K27me3/H3K4me3 has been quantified at the di-tri nucleosome level resolution along the FLC chromatin during vernalization treatments in many *A. thaliana* studies (Finnegan and Dennis, 2007; Angel et al., 2011; Buzas et al., 2011; Yang et al., 2017). A group of over 30 nucleosomes of the *AtFLC* locus appears to be structured in three regions with distinct H3K4me3/H3K27me3 dynamics (Finnegan and Dennis, 2007; Yang et al., 2014). We note that all three domains can also be distinguished in *A. halleri* (Nishio et al., 2020a,b). The few nucleosomes spanning the short first exon and part of the first intron form a chromatin domain termed the nucleation region, NR. The greater bulk of nucleosomes along the coding region, including the long first intron, which is generally termed the gene body (GB). Finally, the distal end of *FLC*, encompassing the promoter and the 5′ end of the antisense non-coding RNA *COOLAIR* (Swiezewski et al., 2009), marks the third domain, later termed distal Nucleation Region (dNR) (Nishio et al., 2020a,b).

In **Table 1**, we summarize H3K27me3/H3K4me3 dynamics during *A. thaliana* vernalization treatments for NR, GB, and dNR at the whole tissue level. Intuitive deductions on how distinct dynamics at each/all three chromatin domains input into an overall *AtFLC* transcriptional outcome under different temperature regimes are difficult to make, even when further genetic and biochemical experimental evidence is considered.

TABLE 1 | The whole tissue level quantities of gene expression and histone modifications from *At* vernalization treatments and yearly *Ahg* in the natural environment.

	***FLC* minimum**		***FLC* dial-up**		***FLC* maximum**		***FLC* dial-down**		
NR		m	–	⇑		M		⇓	H3K4me3
		M	–	M		m		⇑	H3K27me3
GB	M	⇑	–	M		m	m	⇑	H3K27me3
dNR	⇑	m	–	m	⇑	m	M	⇑⇓	H3K4me3
	M	m	–	⇑⇓		m	⇑	m	H3K27me3
	At	*Ahg*	*At*	*Ahg*	*At*	*Ahg*	*At*	*Ahg*	

Flowering locus C (FLC) expression is divided into minimum, dial-up, maximum, and dial-down. H3K4me3 and H3K27me3 levels are indicated, as follows: m, minimum; M, maximum; ⇑, increasing; ⇓, decreasing. Data are from Yang et al. (2014) for Arabidopsis thaliana (At) and Nishio et al. (2020a, b) for Arabidopsis halleri (Ahg). Quantifications of histone modification data during AtFLC dial-up in young embryo are not available, which is denoted as "–." NR, Nucleation Region; dNR, distal Nucleation Region; GB, gene body.

Cell-to-Cell Variation Underlies Measuring of Cold Duration, Robust Response to Noisy Temperatures and Memory of Winter

One way to advance the chromatin profiles outlined in **Table 1** to the next level for understanding vernalization characteristics is to move to single nucleosome and single cell level experiments. The immediate alternative is to advance from tissue to cell level based on theoretical predictions and then devise suitable tests with currently available techniques. Two studies have adapted the Dodd model to stochastically implement the chromatin dynamics described in **Table 1** for NR and GB in *A. thaliana* by including additional parameters specific to vernalization (temperature-dependent replication rates, etc.) and have simulated these numerically to reproduce the chromatin dynamics observed (Angel et al., 2011; Satake and Iwasa, 2012). Outcomes have been reviewed in more detail (Berry and Dean, 2015a), as well as in more general terms on how epigenetics contributes to quantitative biology (Steffen et al., 2012).

One merit of these models is that they reveal the simplest way to unify the multiple characteristics of the vernalization system, previously dissected molecularly on a one-by-one basis. When the underlying assumption is that the chromatin status links with transcriptional outcome to give memory (H3K27me3 correlates with repression), at least three characteristics of the vernalization system are generated. First, when each cell is in either ON or OFF FLC state and the timing of transition between states is not synchronized in all cells, the length of cold can be measured at the population level as the proportion of cells in the OFF state. For this, strong cooperativity of histone modifications is required. Second, as a warm-to-cold temperature shift triggers de-synchronized switching in individual cells, a robust response to noise is realized at the cell population

level (Satake and Iwasa, 2012). Third, to understand how full *FLC* repression can outlast the cold interval Satake and Iwasa (2012) explicitly addressed the duration of winter memory. They found that the speed of deposition of repressive histone modifications after vernalization is critical. The prediction is that the length of winter memory in annuals is large, essentially irreversible, based on high deposition speed, while in perennials, comparatively slower deposition creates shorter winter memory. This also implies that a plant can respond to diverse intervals of cold by adjusting the speed of deposition of repressive marks (Satake and Iwasa, 2012).

The first critical experimental support for these characteristics came from assays in vernalized root cells. Plants expressing a translational *FLC:GUS* fusion exposed to non-saturating vernalization treatment, then transferred to warm, displayed variegated, all-or-nothing *FLC:GUS* expression sectors reflecting the stochastic nature of silencing and re-activation (Angel et al., 2011).

The Cell-Autonomous Chromatin Switch

A frequent hypothesis is that histone modifications maintain transcription states, i.e., they encode memory. However, a reciprocal relationship between transcription and H3K27me3 accumulation was demonstrated at *AtFLC* (Buzas et al., 2011). Recent studies have shown that *AtFLC* alleles in ON and OFF states co-exist within the same cell in plants that had been vernalized (Berry et al., 2015b; Yang et al., 2017; Qüesta et al., 2020). This indicates a cell autonomous chromatin switch functions during the quantitative stage in the cold (Berry et al., 2015b). There is also additional evidence from the *Lov-1* ecotype of *A. thaliana* where *AtFLC* re-activation occurs, that re-activation is also a cell-autonomous process (Qüesta et al., 2020).

INITIAL INSIGHTS FROM PERENNIAL VERNALIZATION

Perennial Life Cycle

Perennial crucifers cycle through episodes of vegetative and reproductive growth (Wang et al., 2009; Aikawa et al., 2010; Kemi et al., 2013). Genetic studies in the *Arabis alpina* perennial support the role of the FLC ortholog *PERPETUAL FLOWERING 1* in preventing flowering before vernalization based on high *PEP1* expression and restricting flowering to a short episode, before PEP1 reverts to high levels in some meristems (Wang et al., 2009). The perennial life cycle in *Arabidopsis halleri* ssp. *gemmifera* (*A. halleri*) is unique in that all developing meristems first become reproductive, then revert to the vegetative phase by developing aerial rosettes, which then propagate clonally (Aikawa et al., 2010; Satake et al., 2013; Nishio et al., 2016, 2020a,b; Honjo and Kudoh, 2019). These characteristics confer experimental advantages, especially in studies in the natural environment. As *AhgFLC* expression is monitored over an entire year, chromatin events are less rapid than in vernalization treatments and can be captured in slow motion (Nishio et al., 2020a). Particularly, the *FLC* dial-up, restricted to embryonic cells concealed in tiny seeds in *A. thaliana* and to some meristems in *A. alpina*, is represented in readily accessible *A. halleri* tissues.

Theoretical and Experimental Approaches in *Arabidopsis halleri*

Frequent, long-term time series of gene expression and histone modifications, combined with environmental data in a natural *A. halleri* population (Nishio et al., 2020a) enabled application of two main types of parameter estimations and mathematical models. First, linear regressions were applied assuming the *AhgFLC* expression follows the amount of chilling accumulation below a certain threshold temperature for a set period (Aikawa et al., 2010; Nishio et al., 2020a). This approach allowed us to estimate the length of past exposure to low temperature affecting the current gene expression (L). Second, an empirical dynamic modeling test called convergent cross-mapping (CCM) was used. This test can be applied on multiple data series, when each has more than 30–40 time points (Sugihara et al., 2012; Ye et al., 2015). CCM examines causality between variables by testing whether the information of a casual variable is encoded in the time series of an affected variable. For example, when a variable X affects another variable Y, the signature of X can be found in the time-series of Y. Thus, it is possible to predict the dynamics of X using those of Y, which is called cross-mapping. This is applicable even when there are two-way causal relationships between the elements. CCM was used to infer the causal relationships between H3K4me3 and H3K27me3 at different locations along the *AhgFLC* locus and between mRNA and H3K4me3/H3K27me3 (Nishio et al., 2020a).

All-Year-Round Memory: Seasonal Temperature and Repertoire of Stable *AhgFLC* States

Yearly dynamics of *AhgFLC* expression revealed a cyclic pattern with maximum, dial-down, minimum, and dial-up quadrants (Aikawa et al., 2010; Nishio et al., 2020a). The transitions between quadrants were delayed relative to the break of seasons (Kudoh, 2016). Indeed, maximum likelihood analysis in simple chilling unit models between temperature and *AhgFLC* expression in a natural habitat revealed that the expression level is determined by temperature during the past period of 42 days, i.e., $L = 42$ days (Aikawa et al., 2010). Furthermore, past temperature also determined the accumulation of histone modifications: H3K27me3 appeared to index the long-term seasonal trend along the *AhgFLC* locus (Nishio et al., 2020a). These results indicate that *AhgFLC* serves as a memory of seasonal temperature throughout the year, not just during the cold season and that all four *AhgFLC* quadrants manifest stability characteristic of PcG/TrxG states. Notably, stability of *AhgFLC* dial-up and dial-down states was supported further: intermediate *AhgFLC* dial-up levels are maintained when plants were transplanted to cold (Nishio et al., 2020a), and the *AhgFLC* dial-down levels are proportional with the length of cold treatments (Nishio et al., 2020b), as known from *A. thaliana* (Sheldon et al., 2006) and *Arabis alpina* (Wang et al., 2009).

Causal Relationships Between H3K27me3 and Transcription in *Arabidopsis halleri*

The seasonal dynamics of H3K4me3 and H3K27me3 in the natural environment at the three *AhgFLC* chromatin domains is outlined in **Table 1**. Remarkably similar with the data from *A. thaliana* vernalization treatments are dynamics at the NR region. As this region plays a critical role in the cell autonomous chromatin switch in *A. thaliana* (Angel et al., 2011; Berry et al., 2015b; Yang et al., 2017), it was of interest to interrogate the causal relationship between H3K27me3/H3K4me3 and transcription at the NR in *A. halleri*. The CCM analysis indicated bidirectional causalities at NR between all three pairs: between mRNA and H3K4me3, between mRNA and H3K27me3, and between H3K4me3 and H3K27me3 (Nishio et al., 2020a). Therefore, a causal relationship between transcription and H3K27me3 at NR in *A. halerii* is consistent with the cell autonomous chromatin switch from *A. thaliana* operating in *A. halleri* as well (Nishio et al., 2020a).

THE FLOWERING LOCUS C SEASON-METER FOR FLOWERING ACROSS LIFE HISTORIES

The current state of knowledge on how Pcg/TxG contributes to precision in determining seasonal transition in a variety of crucifers will undoubtedly advance in the future to better bridge across the life histories and between experiment and theory. Today's exercise is to create a transitional framework to identify conserved mechanisms across annual and perennial life histories in crucifers.

Simplicity in composition and precision of measurements combine in the operating principles of a mechanical watch, which, once set, can run indefinitely with exquisite precision. Similarly, we envisage that an "FLC season-meter" might precisely detect seasons in the natural environment based on the simple yet versatile properties conferred by bistable states supporting the repertoire of stable *FLC* states. Considering that perennial life history is the ancestral form (Kiefer et al., 2017), it is difficult to imagine that bistable states arose in the derivative annual forms.

Based on arguments outlined in the section "*Insights From Annual Vernalization: Experiments and Theory*" for the annual *A. thaliana* and in the section "*Initial Insights From Perennial Vernalization*" mainly for the perennial *A. halleri*, we propose that the FLC season-meter may have three core principles (**Figure 1**):

i) It is anchored, i.e., vernalization requirement aligns the dial-down–minimum transition to the winter–spring transition.
ii) It has a cyclic response with four quadrants of *FLC* expression.
iii) It is hybrid, i.e., two types of inputs trigger changes in *FLC* expression: signals generated by external/developmental triggers (transcription factor based) and cell autonomous switches (chromatin based).

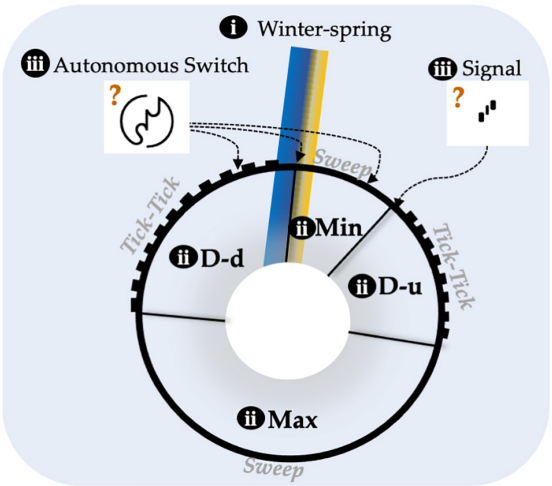

FIGURE 1 | Putative conserved features of the Flowering Locus C (*FLC*) season-meter across annual and perennial crucifers. The cyclic pattern of *FLC* expression is represented as a black circle divided into four quadrants: Max, FLC maximum; Min, FLC minimum; D-d, FLC dial-down; D-u, *FLC* dial-up (ii). The transition D-d-Min is anchored onto the Winter-Spring transition, represented by the blue/yellow (for cold-warm temperatures) gradient rectangular (i). There are two types of inputs into the cyclic response, i.e., the *FLC* season-meter is "hybrid": autonomous chromatin switch and transcription-factor based signal (iii). The autonomous Chromatin switch generates graded response (tick-tick) quadrants when switching is still taking place and ON/OFF states are mixed and smooth response (sweep) when switching had resolved into full either ON or OFF states. The three arrows from the autonomous switch and one arrow from the signal indicate control points based on Angel et al. (2011); Berry et al. (2015b), Yang et al. (2017), and Tao et al. (2017). The length of each quadrant in the image is approximated from Nishio et al. (2020a) (Max, 50%; D-d 25%, Min 10%, and D-u 15%). Brown question marks indicate that the inputs could be located elsewhere.

In this view, *FLC* is neither a repressed/active PcG/TrxG target gene nor one that simply switches dynamically, but both. Stability and flexibility induced by PcG/TrxG is manifested during all four *FLC* quadrants, although to different extents within and across life histories.

FINAL REMARKS

The season-meter concept can generate a list of new questions. How does an autonomous switch influence the length of the consecutive sweep quadrant? Do autonomous switches and signal-triggered transitions alternate? Does a season-meter need to contain more than the minimum number of autonomous switches and signal triggers to maintain the noise buffering function? The list goes on. It is difficult to imagine how to engineer a live-cell measurement system that can track *FLC* switching during an entire cycle in a crucifer growing in the natural environment, but experimentalists and theoretical biologists working together can make the task of deciphering the *FLC* season-meter less insurmountable in the near future.

AUTHOR CONTRIBUTIONS

DB conceptualized and wrote the manuscript. HN and HK contributed to the drafting of the paragraphs.

FUNDING

This research was supported by JSPS KAKENHI (20K06699) to DB, JST CREST (JPMJCR15O1) and JSPS KAKENHI (JP19H01001) to HK, and by a Cooperative Research Grant from Plant Transgenic Design Initiative, University of Tsukuba.

ACKNOWLEDGMENTS

We apologize for possible important omissions from research literature due to space limitation. We would like to thank Liz Dennis and DeMar Taylor for editing the manuscript.

REFERENCES

Aikawa, S., Kobayashi, M. J., Satake, A., Shimizu, K. K., and Kudoh, H. (2010). Robust control of the seasonal expression of the *Arabidopsis* FLC gene in a fluctuating environment. *Proc. Natl. Acad. Sci. U.S.A.* 107, 11632–11637. doi: 10.1073/pnas.0914293107

Angel, A., Song, J., Dean, C., and Howard, M. (2011). A Polycomb-based switch underlying quantitative epigenetic memory. *Nature* 476, 105–109. doi: 10.1038/nature10241

Berry, S., and Dean, C. (2015a). Environmental perception and epigenetic memory: mechanistic insight through FLC. *Plant J.* 83, 133–148. doi: 10.1111/tpj.12869

Berry, S., Hartley, M., Olsson, T. S. G., Dean, C., and Howard, M. (2015b). Local chromatin environment of a Polycomb target gene instructs its own epigenetic inheritance. *Elife* 4:e07205. doi: 10.7554/eLife.07205

Buzas, D. M. (2017). Capturing environmental plant memories in DNA, with a little help from chromatin. *Plant Cell Physiol.* 58, 1302–1312. doi: 10.1093/pcp/pcx092

Buzas, D. M., Robertson, M., Finnegan, E. J., and Helliwell, C. A. (2011). Transcription-dependence of histone H3 lysine 27 trimethylation at the *Arabidopsis* polycomb target gene FLC. *Plant J.* 65, 872–881. doi: 10.1111/j.1365-313X.2010.04471.x

Buzas, D. M., Tamada, Y., and Kurata, T. (2012). FLC: a hidden polycomb response element shows up in silence. *Plant Cell Physiol.* 53, 785–793. doi: 10.1093/pcp/pcr163

Chan, C. S., Rastelli, L., and Pirrotia, V. (1994). A Polycomb response element in the Ubx gene that determines an epigenetically inherited state of repression. *EMBO J.* 13, 2553–2564. doi: 10.1002/j.1460-2075.1994.tb06545.x

Choi, J., Hyun, Y., Kang, M. J., In Yun, H., Yun, J. Y., Lister, C., et al. (2009). Resetting and regulation of FLOWERING LOCUS C expression during *Arabidopsis* reproductive development. *Plant J.* 57, 918–931. doi: 10.1111/j.1365-313X.2008.03776.x

Crevillén, P., Yang, H., Cui, X., Greeff, C., Trick, M., Qiu, Q., et al. (2014). Epigenetic reprogramming that prevents transgenerational inheritance of the vernalized state. *Nature* 515, 587–590. doi: 10.1038/nature13722

Dodd, I. B., Micheelsen, M. A., Sneppen, K., and Thon, G. (2007). Theoretical analysis of epigenetic cell memory by nucleosome modification. *Cell* 129, 813–822. doi: 10.1016/j.cell.2007.02.053

Finnegan, E. J. (2015). Time-dependent stabilization of the +1 nucleosome is an early step in the transition to stable cold-induced repression of FLC. *Plant J.* 84, 875–885. doi: 10.1111/tpj.13044

Finnegan, E. J., and Dennis, E. S. (2007). Vernalization-induced trimethylation of histone H3 lysine 27 at FLC is not maintained in mitotically quiescent cells. *Curr. Biol.* 17, 1978–1983. doi: 10.1016/j.cub.2007.10.026

Helliwell, C. A., Anderssen, R. S., Robertson, M., and Finnegan, E. J. (2015). How is FLC repression initiated by cold? *Trends Plant Sci.* 20, 76–82. doi: 10.1016/j.tplants.2014.12.004

Honjo, M. N., and Kudoh, H. (2019). *Arabidopsis halleri*: a perennial model system for studying population differentiation and local adaptation. *AoB Plants* 11:plz076. doi: 10.1093/aobpla/plz076

Kemi, U., Niittyvuopio, A., Toivainen, T., Pasanen, A., Quilot-Turion, B., Holm, K., et al. (2013). Role of vernalization and of duplicated FLOWERING LOCUS C in the perennial arabidopsis lyrata. *New Phytol.* 197, 323–335. doi: 10.1111/j.1469-8137.2012.04378.x

Kiefer, C., Severing, E., Karl, R., Bergonzi, S., Koch, M., Tresch, A., et al. (2017). Divergence of annual and perennial species in the Brassicaceae and the contribution of cis-acting variation at FLC orthologues. *Mol. Ecol.* 26, 3437–3457. doi: 10.1111/mec.14084

Kudoh, H. (2016). Molecular phenology in plants: in natura systems biology for the comprehensive understanding of seasonal responses under natural environments. *New Phytol.* 210, 399–412. doi: 10.1111/nph.13733

Luo, X., and He, Y. (2020). Experiencing winter for spring flowering: a molecular epigenetic perspective on vernalization. *J. Integr. Plant Biol.* 62, 104–117. doi: 10.1111/jipb.12896

Michaels, S. D., and Amasino, R. M. (2000). Memories of winter: vernalization and the competence to flower. *Plant Cell Environ.* 23, 1145–1153. doi: 10.1046/j.1365-3040.2000.00643.x

Moazed, D. (2011). Mechanisms for the inheritance of chromatin states. *Cell* 146, 510–518. doi: 10.1016/j.cell.2011.07.013

Nishio, H., Buzas, D. M., Nagano, A. J., Iwayama, K., Ushio, M., and Kudoh, H. (2020a). Repressive chromatin modification underpins the long-term expression trend of a perennial flowering gene in nature. *Nat. Commun.* 11:2065. doi: 10.1038/s41467-020-15896-4

Nishio, H., Buzas, D. M., Nagano, A. J., Suzuki, Y., Sugano, S., Ito, M., et al. (2016). From the laboratory to the field: assaying histone methylation at FLOWERING LOCUS C in naturally growing *Arabidopsis halleri*. *Genes Genet. Syst.* 91, 15–26. doi: 10.1266/ggs.15-00071 article **

Nishio, H., Iwayama, K., and Kudoh, H. (2020b). Duration of cold exposure defines the rate of reactivation of a perennial FLC orthologue via H3K27me3 accumulation. *Sci. Rep.* 10:16056. doi: 10.1038/s41598-020-72566-7

Qüesta, J. I., Antoniou-Kourounioti, R. L., Rosa, S., Li, P., Duncan, S., Whittaker, C., et al. (2020). Noncoding SNPs influence a distinct phase of Polycomb silencing to destabilize long-term epigenetic memory at *Arabidopsis* FLC. *Genes Dev.* 34, 446–461. doi: 10.1101/gad.333245.119

Qüesta, J. I., Song, J., Geraldo, N., An, H., and Dean, C. (2016). *Arabidopsis* transcriptional repressor VAL1 triggers Polycomb silencing at FLC during vernalization. *Science* 353, 485–488. doi: 10.1126/science.aaf7354

Reinig, J., Ruge, F., Howard, M., and Ringrose, L. (2020). A theoretical model of Polycomb/Trithorax action unites stable epigenetic memory and dynamic regulation. *Nat. Commun.* 11:4782 . doi: 10.1038/s41467-020-18507-4

Satake, A., and Iwasa, Y. (2012). A stochastic model of chromatin modification: cell population coding of winter memory in plants. *J. Theor. Biol.* 302, 6–17. doi: 10.1016/j.jtbi.2012.02.009

Satake, A., Kawagoe, T., Saburi, Y., Chiba, Y., Sakurai, G., and Kudoh, H. (2013). Forecasting flowering phenology under climate warming by modelling the regulatory dynamics of flowering-time genes. *Nat. Commun.* 4:2303. doi: 10.1038/ncomms3303

Sheldon, C. C., Hills, M. J., Lister, C., Dean, C., Dennis, E. S., and Peacock, W. J. (2008). Resetting of FLOWERING LOCUS C expression after epigenetic repression by vernalization. *Proc. Natl. Acad. Sci. U.S.A.* 105, 2214–2219. doi: 10.1073/pnas.0711453105

Sheldon, C. C., Finnegan, E., Dennis, E. S., and James Peacock, W. (2006). Quantitative effects of vernalization on FLC and SOC1 expression. *Plant J.* 45, 871–883. doi: 10.1111/j.1365-313X.2006.02652.x

Steffen, P. A., Fonseca, J. P., and Ringrose, L. (2012). Epigenetics meets mathematics: towards a quantitative understanding of chromatin biology. *BioEssays* 34, 901–913. doi: 10.1002/bies.201200076

Steffen, P. A., and Ringrose, L. (2014). What are memories made of? How polycomb and trithorax proteins mediate epigenetic memory. *Nat. Rev. Mol. Cell Biol.* 15, 340–356. doi: 10.1038/nrm3789

Sugihara, G., May, R., Ye, H., Hsieh, C. H., Deyle, E., Fogarty, M., et al. (2012). Detecting causality in complex ecosystems. *Science* 338, 496–500. doi: 10.1126/science.1227079

Swiezewski, S., Liu, F., Magusin, A., and Dean, C. (2009). Cold-induced silencing by long antisense transcripts of an *Arabidopsis* Polycomb target. *Nature* 462, 799–802. doi: 10.1038/nature08618

Tao, Z., Shen, L., Gu, X., Wang, Y., Yu, H., and He, Y. (2017). Embryonic epigenetic reprogramming by a pioneer transcription factor in plants. *Nature* 551, 124–128. doi: 10.1038/nature24300

Wang, R., Farrona, S., Vincent, C., Joecker, A., Schoof, H., Turck, F., et al. (2009). PEP1 regulates perennial flowering in *Arabis alpina*. *Nature* 459, 423–427. doi: 10.1038/nature07988

Yang, H., Berry, S., Olsson, T. S. G., Hartley, M., Howard, M., and Dean, C. (2017). Distinct phases of Polycomb silencing to hold epigenetic memory of cold in *Arabidopsis*. *Science* 357, 1142–1145. doi: 10.1126/science.aan1121

Yang, H., Howard, M., and Dean, C. (2014). Antagonistic roles for H3K36me3 and H3K27me3 in the cold-induced epigenetic switch at *Arabidopsis* FLC. *Curr. Biol.* 24, 1793–1797. doi: 10.1016/j.cub.2014.06.047

Ye, H., Deyle, E. R., Gilarranz, L. J., and Sugihara, G. (2015). Distinguishing time-delayed causal interactions using convergent cross mapping. *Sci. Rep.* 5:14750. doi: 10.1038/srep14750

Yuan, W., Luo, X., Li, Z., Yang, W., Wang, Y., Liu, R., et al. (2016). A cis cold memory element and a trans epigenome reader mediate Polycomb silencing of FLC by vernalization in *Arabidopsis*. *Nat. Genet.* 48, 1527–1534. doi: 10.1038/ng.3712

Conflict of Interest: The authors declare that the research was conducted in the absence of any commercial or financial relationships that could be construed as a potential conflict of interest.

Copyright © 2021 Buzas, Nishio and Kudoh. This is an open-access article distributed under the terms of the Creative Commons Attribution License (CC BY). The use, distribution or reproduction in other forums is permitted, provided the original author(s) and the copyright owner(s) are credited and that the original publication in this journal is cited, in accordance with accepted academic practice. No use, distribution or reproduction is permitted which does not comply with these terms.

frontiers in Plant Science

ORIGINAL RESEARCH
published: 30 March 2021
doi: 10.3389/fpls.2021.639014

A Vernalization Response in a Winter Safflower (*Carthamus tinctorius*) Involves the Upregulation of Homologs of *FT*, *FUL*, and *MAF*

Darren P. Cullerne[1†], Siri Fjellheim[2], Andrew Spriggs[1], Andrew L. Eamens[3], Ben Trevaskis[1] and Craig C. Wood[1]*

[1] Agriculture and Food, Commonwealth Scientific and Industrial Research Organisation, Canberra, ACT, Australia, [2] Department of Plant Sciences, Norwegian University of Life Sciences, Ås, Norway, [3] School of Environmental and Life Sciences, The University of Newcastle, Callaghan, NSW, Australia

OPEN ACCESS

Edited by:
Joanna Putterill,
The University of Auckland,
New Zealand

Reviewed by:
Philip Ruelens,
Wageningen University and Research,
Netherlands
Frédéric Bouché,
University of Liège, Belgium

***Correspondence:**
Craig C. Wood
craig.wood@csiro.au

†Present address:
Darren P. Cullerne,
Murdoch Childrens Research Institute, Royal Children's Hospital,
Melbourne, VIC, Australia

Specialty section:
This article was submitted to Plant Development and EvoDevo, a section of the journal Frontiers in Plant Science

Received: 08 December 2020
Accepted: 24 February 2021
Published: 30 March 2021

Citation:
Cullerne DP, Fjellheim S, Spriggs A, Eamens AL, Trevaskis B and Wood CC (2021) A Vernalization Response in a Winter Safflower (Carthamus tinctorius) Involves the Upregulation of Homologs of FT, FUL, and MAF. Front. Plant Sci. 12:639014. doi: 10.3389/fpls.2021.639014

Safflower (*Carthamus tinctorius*) is a member of the Asteraceae family that is grown in temperate climates as an oil seed crop. Most commercially grown safflower varieties can be sown in late winter or early spring and flower rapidly in the absence of overwintering. There are winter-hardy safflower accessions that can be sown in autumn and survive over-wintering. Here, we show that a winter-hardy safflower possesses a vernalization response, whereby flowering is accelerated by exposing germinating seeds to prolonged cold. The impact of vernalization was quantitative, such that increasing the duration of cold treatment accelerated flowering to a greater extent, until the response was saturated after 2 weeks exposure to low-temperatures. To investigate the molecular-basis of the vernalization-response in safflower, transcriptome activity was compared and contrasted between vernalized versus non-vernalized plants, in both 'winter hardy' and 'spring' cultivars. These genome-wide expression analyses identified a small set of transcripts that are both differentially expressed following vernalization and that also have different expression levels in the spring versus winter safflowers. Four of these transcripts were quantitatively induced by vernalization in a winter hardy safflower but show high basal levels in spring safflower. Phylogenetic analyses confidently assigned that the nucleotide sequences of the four differentially expressed transcripts are related to *FLOWERING LOCUS T (FT)*, *FRUITFUL (FUL)*, and two genes within the *MADS-like* clade genes. Gene models were built for each of these sequences by assembling an improved safflower reference genome using PacBio-based long-read sequencing, covering 85% of the genome, with N50 at 594,000 bp in 3000 contigs. Possible evolutionary relationships between the vernalization response of safflower and those of other plants are discussed.

Keywords: safflower, vernalization, genome, PacBio, flowering time

INTRODUCTION

Vernalization is the acceleration of flowering by exposure to the prolonged cold of winter (Chouard, 1960). In temperate regions, vernalization coordinates the plant life cycle with the changing seasons by delaying flowering before winter, thereby avoiding freezing/chilling damage to reproductive organs. By promoting rapid flowering in spring, vernalization also allows some plants to flower before the onset of heat and dry conditions in summer. Vernalization is widespread in flowering plants, occurring in both dicots and monocots. Many crops cultivated in temperate regions exhibit vernalization-induced flowering, including wheat (*Triticum aestivum*), oilseed rape (*Brassica napus*), pea (*Pisum sativum*), and sugar beet (*Beta vulgaris*) (Chouard, 1960).

The molecular basis of vernalization-induced flowering was first resolved in the model plant Arabidopsis (*Arabidopsis thaliana*). The vernalization response of Arabidopsis is mediated by the *FLOWERING LOCUS C (FLC)* gene, which encodes a MADS (MCM1/AGAMOUS/DEFICIENS/SRF) box transcription factor protein (Michaels and Amasino, 1999; Sheldon et al., 1999). *FLC* delays flowering before winter by repressing transcription of genes that would otherwise promote flowering, including *FLOWERING LOCUS T (FT)*, which accelerates flowering in long days (Michaels et al., 2005; Helliwell et al., 2006). Transcription of *FLC* is repressed by vernalization (Michaels and Amasino, 1999; Sheldon et al., 1999). This repression is retained post-vernalization through the action of protein complexes that change the state of chromatin at the *FLC* locus (Bastow et al., 2004; Schubert et al., 2006; Wood et al., 2006; Finnegan and Dennis, 2007). Thus, plants retain a molecular memory of winter and flower rapidly when exposed to normal growth temperatures and long days after vernalization. *FRIGIDA (FRI)* is required for high levels of *FLC* expression prior to vernalization and loss of *FRI* gene function leads to early flowering without the normal requirement for vernalization (Johanson et al., 2000). *FLC*-like genes mediate vernalization-induced flowering in other *Brassicaceae*, including oilseed rape (Tadege et al., 2001; Irwin et al., 2016; O'Neill et al., 2019; Tudor et al., 2020; Yin et al., 2020). As outlined below, the molecular basis of vernalization has been resolved to varying extents in plants outside the *Brassicaceae*.

In wheat, *VERNALIZATION 2 (VRN2)* encodes a zinc-finger CCT (CONTANS, CONSTANS-LIKE, TOC1) domain protein that blocks long-day induction of *FT* (*FT1* in wheat) and thereby delays flowering before winter (Yan et al., 2004). Vernalization activates transcription of *VRN1*, a promoter of flowering related to the *APETALA1* (*AP1*) and *FRUITFUL* (*FUL*) MADS box genes of Arabidopsis (Danyluk et al., 2003; Trevaskis et al., 2003; Yan et al., 2003). Activation of *VRN1* is maintained post-vernalization and this is associated with changes in the state of chromatin at the *VRN1* locus (Oliver et al., 2009). Elevated expression of *VRN1* then down-regulates *VRN2* and a second repressor of flowering, *ODDSOC2 (OS2)*, a MADS box gene that appears to have evolved from the *FLC*-clade of MADS box gene family (Greenup et al., 2011; Ruelens et al., 2013). The VRN1 protein binds directly to sites in the *VRN2*, *OS2*, and *FT1* genes, suggesting that the VRN1 protein triggers vernalization-induced flowering by directly regulating both repressors and activators of flowering (Deng et al., 2015). Naturally occurring mutations in the *VRN1* gene that activate expression of this gene without prolonged exposure to cold are the main driver of the reduced vernalization requirement in cultivated "spring" wheats (Fu et al., 2005). In barley (*Hordeum vulgare*), loss-of-function mutations in *VRN2* are another driver of reduced vernalization requirement, in addition to active alleles of *VRN1* (Yan et al., 2004). There are also examples of mutations that activate *FT1* expression and thereby bypass the normal need for vernalization-induced flowering of wheat and barley (Yan et al., 2006).

There are several examples of vernalization-responsive species amongst the temperate legumes, including chickpea, pea, narrow leaf lupin (*Lupinus angustifolius*), and *Medicago* species. In the model legume *Medicago truncatula*, the *FT*-like gene *FTa1* is upregulated by vernalization and by long days. Mutations that disrupt *FTa1* function delay flowering of vernalized plants (Laurie et al., 2011). Conversely, genetic activation of *FTa1* in transgenic plants or by retroelement insertion leads to early flowering without vernalization (Laurie et al., 2011; Jaudal et al., 2013; Yeoh et al., 2013). Taken together these findings suggest that *FTa1* plays a key role in mediating vernalization-induced flowering of legumes. The *FTa1* gene is not transcriptionally activated by vernalization *per se*, suggesting that a different mechanism mediates the actual response to prolonged cold in legumes (Laurie et al., 2011).

The Asteraceae family is the largest amongst the flowering plants, comprising 25000–35000 species that represent approximately 10% of all angiosperm species (Mandel et al., 2019). The Asteraceae contain several economically important species, examples being crops like lettuce (*Lactuca sativa*) and sunflower (*Helianthus annuus*). Many Asteraceae are adapted to temperate climates and vernalization-induced flowering has been described in several species (Harwood and Markaria, 1968; Baskin and Baskin, 1989; Prins et al., 1990; Bender et al., 2002; Niu et al., 2002; Ha and Johnston, 2013; Perilleux et al., 2013) (see **Figure 1**). The molecular basis for vernalization-induced flowering in these plants is not well understood.

Safflower (*Carthamus tinctorius* L.) is a member of the Asteraceae family that is cultivated to produce seed oils, traditional medicines and dyes (Zohary et al., 2012). Genetically modified safflower has also been used to produce oils with distinct properties not normally found or easily produced in nature (Nykiforuk et al., 2012; Wood et al., 2018). The commercial safflower cultivars grown in Australia, North America and Mexico are sown in late winter or early spring and flower rapidly without over-wintering. Safflower is considered a long-day plant (Dole, 2015) and although "spring" cultivars dominate global safflower production there are reports that some accessions can be sown in autumn and survive winter conditions that are too extreme for spring safflower (Ghanavati and Knowles, 1977; Yazdisamadi and Zali, 1979). These same winter hardy cultivars have delayed flowering and reduced seed set when sown in spring. This was attributed to a lack of cold stimulation during the growth period (Yazdisamadi and Zali, 1979), but a vernalization response has not yet been demonstrated.

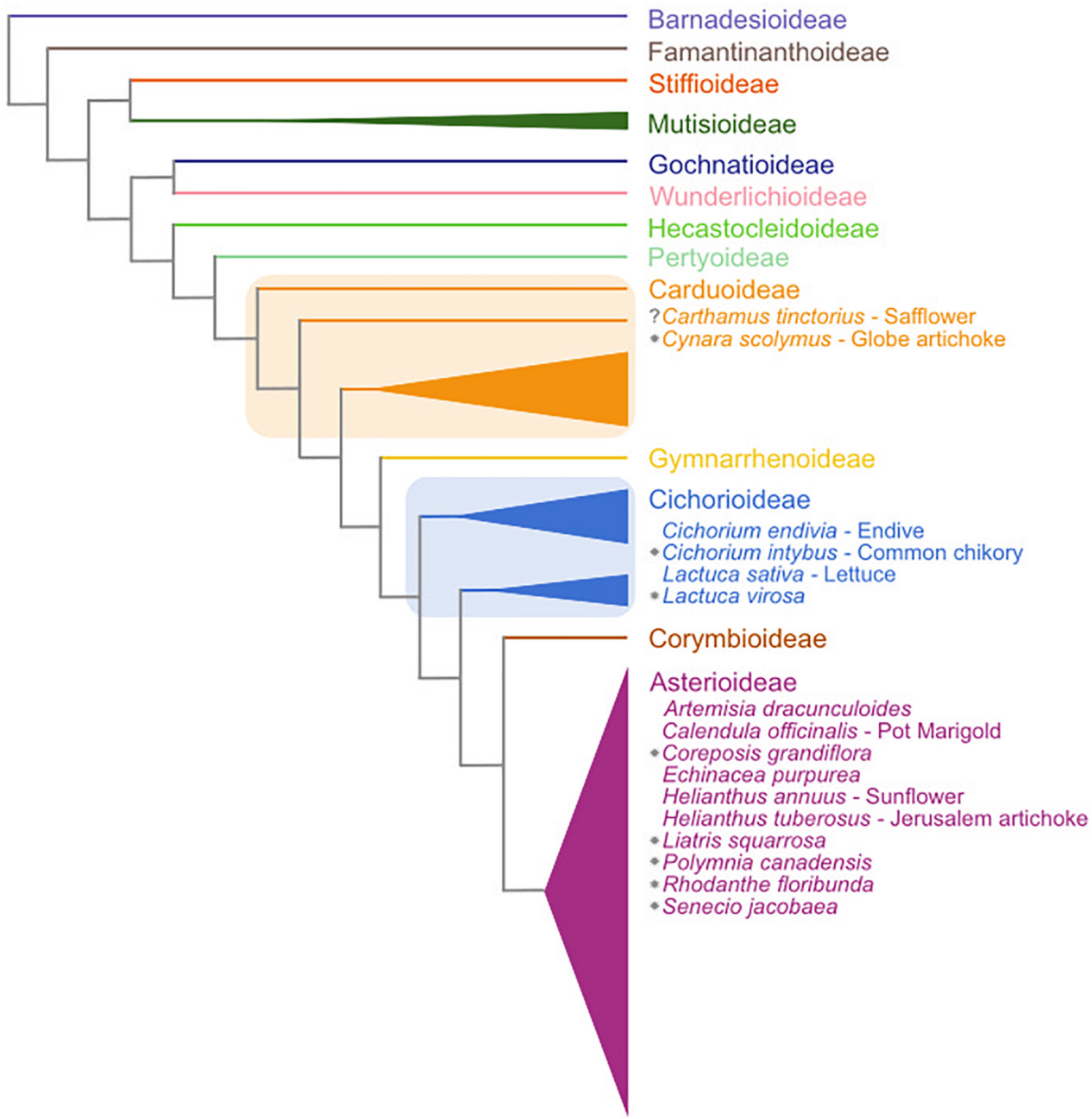

FIGURE 1 | Schematic overview of the subfamilies of the Asteraceae family based on Mandel et al. (2019). Central Asteraceae crop species are listed in their respective subfamilies. Gray stars indicate species that have a documented vernalization response in flowering. Subfamily assignments are based on Fu et al. (2016) and Mandel et al. (2019). Note that two of the subfamilies (Carduoideae and Cichorioideae) are paraphyletic and are thus marked with boxes.

High-quality genomes are increasingly important resources for plant breeders, with accurate DNA sequencing and long contigs being noteworthy features. Safflower has a 1.35 Gb genome distributed on 12 chromosomes. While there are existing genomic resources available for safflower (Bowers et al., 2016), these have been generated with so called 'short read' technologies (100 bp reads; Bentley et al., 2008). To date, the most current safflower assembly is fragmented (57,000 contigs with an average contig length ∼2000 bp) and is estimated to cover less than 70% of the genome. The development of 'long read' technologies (>10,000 bp reads, Eid et al., 2009) addresses these shortcomings by enabling the construction of assemblies with far longer contigs, and potentially a significantly improved physical assembly.

Here, using controlled condition experiments, we show that a winter hardy safflower accession is vernalization responsive.

Using transcriptome sequencing to compare gene-expression patterns in "spring" versus "winter" safflower varieties we then identify a small set of genes that potentially mediate vernalization-induced flowering in safflower. Gene models of these transcripts, including their long intronic sequences, were generated using a significantly improved genome assembly based on PacBio technologies. The evolutionary implications of these findings are discussed.

MATERIALS AND METHODS

Plant Materials and Growth Conditions

Two safflower varieties were used in this study: 'winter hardy' C311, known to survive extended cold periods (including overwintering under snow) and 'spring' S317, which is a widely grown commercial cultivar (Wood et al., 2018). C311 was sourced from US Department of Agriculture Genetic Resources Information Network (PlantID WSRC03, Johnson and Dajue, 2008). Prior to more detailed analysis of flowering time in growth cabinets, S317 and C311 were cultivated in parallel in a small experimental plot at CSIRO Black Mountain site (alluvial soil) in late spring. This plot demonstrated that C311 was significantly later to flower than S317 in the absence of a defined cold period (see **Supplementary Figure 1**).

For detailed vernalization experiments safflower seeds were treated as described below. Specifically, seeds were imbibed overnight by hydrating in aerated distilled water at room temperature. After 24 h, seeds were visually inspected for a cracking of the seed coat, and any seed not cracked was discarded. Imbibed seeds were placed onto moistened filter paper disks within plastic petri dishes, covered in foil and the temperature maintained at 4°C for varying durations (vernalization). Similarly, vernalization at different temperatures was performed by placing imbibed seeds into 15 mL falcon tubes and incubating in Echotherm programmable temperature blocks (Torrey Pines Scientific Instruments, CA, United States), set to desired temperatures and each experiment used a 20-day vernalization period that had been found to be saturating in preliminary tests. Following all vernalization treatments, germinated seeds were transferred to 20 cm pots with soil and buried at 2 cm depth. Soil comprised of 70:30% soil perlite mixture, with a small quantity of slow release fertilizer (Osmocote) and liquid fertilizer (Aquasol) applied occasionally throughout growth. In all controlled growth chambers plants were grown in simulated long-day conditions (26°C, 16 h light at approximately 450 $\mu M.m^{-2}s^{-1}$; Conviron, Canada) for recording of flowering time. Flowering time was recorded as the time when the floret on the main stem had emerged. Vernalization days were calculated, using a method outlined previously (Baloch et al., 2003) and the days to heading were adjusted accordingly. The relationship between length of vernalization exposure at 4°C and heading date for each of the two cultivars were tested with regressions. Differences in heading date between plants treated with different vernalization temperatures over a 28-day duration were tested with an ANOVA, followed by a Tukey Honestly Significant Difference (HSD) test performed in the R stats package (R Core Team, 2016).

Genetic Analysis of Growth Habit

Crossing was performed as outlined previously (Mundel and Bergman, 2009). Then, the progeny were grown in warm, long-day conditions (see above for conditions) and the timing of bolting (when stem elongation begins) was used to differentiate between winter and spring growth habit; bolting before 4 weeks indicated spring growth habit, whereas bolting taking longer than 4 weeks indicated a winter growth habit. All F_1 seeds were grown to maturity, then the F_2 progeny were grown and scored in a similar manner.

Assembling an Improved Safflower Reference Genome

Nuclear genomic DNA from S317 was isolated in a method as previously described (Naim et al., 2012). Genomic DNA was sequenced using both Illumina (Bentley et al., 2008) and PacBio (Eid et al., 2009) chemistries. Illumina-based methods used the HiSeq2000 instrument at the Australian Genome Research Facility, Melbourne, and generated Paired End (PE) reads (100 bp with an insert length of 180 bp) and Mate Pair (MP) reads (36 bp read length with an insert length of 10 Kbp). PE reads were first processed for quality by visual examination with FastQC (Andrews et al., 2012) then using BioKanga "filter" (v3.1.1) to remove any reads that: were duplicates; that did not overlap by at least 50% with another read; or contained more than a single ambiguous base. A *de novo* assembly was constructed with the PE reads using BioKanga "assemb" protocol, then repeated combining the *de novo* PE assembly and MP reads. The second *de novo* assembly was scaffolded twice with BioKanga "scaffold," first using a fragment size of 180 bp, then again with 10 Kbp. The second scaffolded *de novo* assembly was further scaffolded with SCUBAT (Elsworth and Weitemier, 2013) using a *de novo* reference transcriptome for S317, as constructed previously (Wood et al., 2018). PacBio-based reads were acquired from a RSII sequencer (Version 6 chemistry) at the Queensland University of Technology Diamantina Institute, Brisbane. A completely independent genome assembly using the PacBio reads was constructed using Canu software (v1.5, Koren et al., 2017), requiring a minimum read length of 10 Kbp and an estimated genome size of 1.4 Gbp. The overall quality and coverage of the *de novo* assemblies was assessed using BUSCO (v3.0.2) (Simao et al., 2015) using the core gene set downloaded from the "embryophyta_odb9" reference database.

Transcriptome Analysis

Seeds were germinated and vernalized in the dark for 5, 10, 15, or 20 days at 4°C as described above, then sown in pots in long day conditions (as described above) for 1 week before RNA extraction. By this stage plants had emerged from the soil, cotyledons were fully expanded and two true leaves were present. Non-vernalized controls were germinated in a similar manner but shifted directly to long-day growth conditions and grown in for a week. At approximately 3 h after dawn the collar (transition between root and stem) of each plant was located and a location 2 mm below the collar was cut and all tissue above that location was harvested for further analysis. Tissue samples were then frozen in liquid nitrogen and kept at −80°C until further

processing. Total RNA was extracted using PureLink reagent (cat#: 12322-012, Life Technologies) following the manufacturer's instructions. RNA, enriched in poly-adenylated RNA (Epicenter Technologies, United States), was sequenced at the Australian Genome Research Facility (AGRF) using an Illumina HiSeq2000 sequencer, using 100 bp paired-end reads. Reads were adapter filtered and aligned against a *de novo* reference transcriptome for S317 as constructed previously (Wood et al., 2018) using BioKanga 'Align' (v3.8.1)[1] with default settings.

Aligned read counts were normalized and analyzed using DESeq2 (v1.6.3) (Love et al., 2014), using a model that identifies transcripts that are differentially expressed between spring and winter safflower cultivars (summarized as non-vernalized S317 vs. non-vernalized C311, or nvS317:nvC311) and as the duration of exposure to vernalization conditions increased (non-vernalized C311 vs. vernalized C311, or nvC311:vC311). Transcripts were identified that were significantly differentially expressed (adjusted p-value < 0.05) between winter and spring safflower and across all time points. Initial visualizations of the intersections between groups of differentially expressed genes we used the UpSetR plotting package in R.

Additionally, a *de novo* transcriptome assembly was created for the winter safflower accession, C311, using the BioKanga 'Assemb' and 'Scaffold' software (v3.5.3 – see text footnote 1) with the default parameters (hereby referred to as the "winter safflower transcriptome" and using the naming nomenclature "CarTin_tx_WSRC03_Scaff<#>_<#>"). This assembly of the C311 transcriptome was used primarily to examine variation in transcripts homologs between winter and spring safflower and to compare against genes from other plant species.

After the identification of transcripts that were differentially expressed in winter and spring varieties and during vernalization treatments, a simple BLAST search (NCBI default parameters, Altschul et al., 1997) was used to conduct an initial identification of genes putatively involved in vernalization in safflower.

Real-Time PCR Analysis of Candidate Genes

Primers were generated using Oligo Explorer[2] (v1.1.2) and with Netprimer[3] (v3). Primers were also developed for *CtActin* as a normalizing gene in the analysis (Czechowski et al., 2005). Primers were designed from the 3′ end of the transcript, with at least 18nt and a predicted melting temperature (T_m) above 62°C (Sigma-Aldrich Inc., Sydney, NSW, Australia; **Supplementary Table 1**) with a final amplicon length in the range of 100–200 bp. Amplicons were cloned and sequenced to confirm their target sequence.

Total RNA samples from each time point in the time course treated with RQ1 DNase (M6101, Promega) with Maxima Reverse Transcriptase (Thermo Fisher Scientific) for first strand cDNA synthesis. Four biological samples were used and each of these were split to generate four technical replicates for real-time PCR analysis. Each 20 μL reaction contained 2 μL reaction buffer, 1.4 μL of 50 mM $MgCl_2$, 1 μL Fast SYBR Green (Thermo Fisher Scientific), 0.5 μL of 10 μM forward and reverse primer, 0.8 μL of 10 mM dNTPs and 0.1 μL Platinum Taq Polymerase (Thermo Fisher Scientific) and 20 ng first strand cDNA template. PCR amplification was performed on a Rotor Gene Q (Qiagen). Thermal cycling conditions were 95°C for 5 min followed by forty-five cycles of 95°C for 20 s, 59°C for 20 s and 72°C for 20 s. This was followed by a melt curve analysis consisting of cooling samples to 50°C before increasing the temperature to 99°C in 1°C increments, and by holding for 5 s at each increment.

Phylogenetic Analysis of Candidate Transcripts

We used phylogenetics to conduct a more thorough characterization of transcripts, using well-characterized gene families from Arabidopsis as a reference. Genes putatively related to MADS-box transcription factors and FT-like were compared against the serum response factor (SFR)-type transcription factor gene family (pfam00319) and the phosphatidylethanolamine-binding protein (PBP) gene family (pfam01161), respectively, as downloaded from the pfam database (El-Gebali et al., 2019). Sequences from the sunflower (*Helianthus annuus)* genome were used as a reference for the Asteraceae family. Pfam reference numbers were matched to UniProt accessions [The UniProt Consortium 2019 (Morgat et al., 2020)] and duplicates were removed so that each unique genome locus was represented only by one sequence. The sequences from Arabidopsis, safflower and differentially expressed safflower transcripts were aligned using MUSCLE (Edgar, 2004) through the EMBL-EBI web service (Madeira et al., 2019). An initial 'maximum-likelihood' (ML) phylogenetic analysis of the SFR-type transcription factor gene family (MADS-box) using PHY-ML with default settings, including a LHRt support value assessment, revealed that the safflower transcripts belong to the MIKC-MADS box group of SFR-type genes (Parenicova et al., 2003). Thus, the analysis was repeated but only including the MIKC-MADS box genes and using PHY-ML with default values, except that a bootstrap evaluation with 250 replicates was performed. The ML trees were midpoint rooted. For the PBP (FT) gene family a ML phylogenetic analysis was performed in PHY-ML (Dereeper et al., 2008) using default values, except from validating the phylogeny with 250 replicates in a bootstrap analysis. Two sequences were removed as they did not align to the rest of the sequences and clustered outside the other sequences and were assumed to likely represent falsely annotated sequences (At5g01300 and HannXRQ_Chr10g0291491). Four sunflower sequences were removed from the analysis as they were shorter than 100 amino acids.

To investigate the presence of transcripts more closely related to the Arabidopsis *FLC* than the noteworthy candidate transcripts identified in our experiment, we did a BLAST search with Arabidopsis *FLC* against the transcriptomes of S317. The best hits were included in a phylogeny with sequences from the *MAF*- and *FUL*-clades from the larger MIKC MADS phylogeny following the same setup for analysis as described above. Similarly to investigate the presence of a safflower transcript being closely

[1]https://github.com/csiro-crop-informatics/biokanga

[2]www.genelink.com/tools/gl-oe.asp

[3]www.premierbiosoft.com/netprimer/

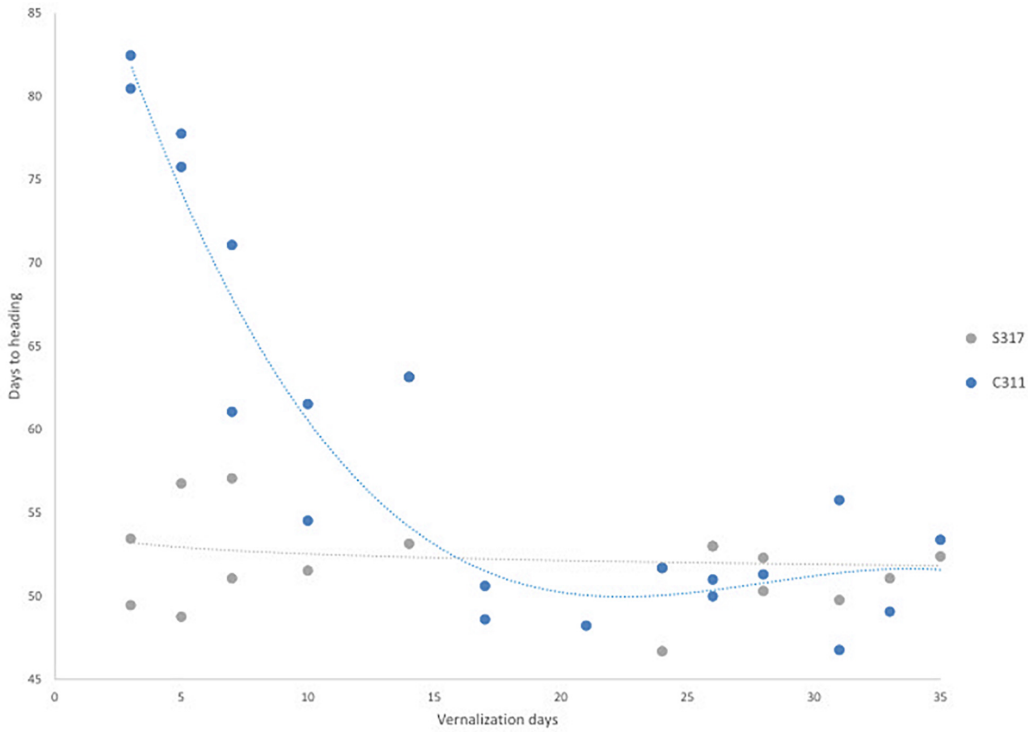

FIGURE 2 | The effect of vernalization on flowering time for S317 and C311. Germinated seeds were exposed to increasing longer durations of a vernalization (4°C) treatment. In C311, there is a steep decrease in the time to flowering as the length of vernalization increases and the relationship between duration of vernalization and days to heading was significant. This slope levels out at approximately 17 days and does not decrease the time to flowering after further exposure to vernalization conditions.

related to the *Cichorium intybus FLC-like* gene, *CiFL1*, we conducted a BLAST search of the safflower genome, and the closest hit was included in a further phylogenetic analysis as described above.

Gene Models

The noteworthy transcripts from the *de novo* transcriptome that were identified as candidates for control of vernalization response (see previous section) were aligned against the *de novo* genomic reference using BioKanga 'Blitz' to define the structure of the genes. The settings used were a minimum of 40% alignment, a mismatch penalty score of 2 and a maximum over-exploring seed depth of 10,000. Intron/exon boundaries were identified by large alignment gaps when mapping the transcriptomic contigs. Upstream and downstream untranslated regions were identified by transcriptomic alignments before start and after stop codons, respectively.

RESULTS

Vernalization-Responsive Flowering of a Winter-Hardy Safflower

The flowering behavior of a modern spring safflower cultivar (S317) and a winter hardy safflower (C311) were compared in different growth habitats, including growth chambers under long-day conditions, 26°C, 16 h of light at approximately 450 $\mu M.m^{-2}s^{-1}$) and in small field plots (**Supplementary Figure 1**). Preliminary experiments indicated that in the absence of exposure to cold the two varieties had visibly different growth habits, where C311 was always slower to bolt than S317. More detailed studies were conducted in growth chambers under long-day conditions and S317 bolted rapidly in these growth conditions and produced the first flower after approximately 50 days, whereas C311 was slower to bolt, formed a larger rosette and produced the first flower after 80 days (**Figure 2**). To test whether the delayed flowering of C311 was due to a vernalization requirement, imbibed seeds were exposed to cold (4°C) for different durations before being placed in long-day conditions, and then the days until the appearance of the first flower recorded. Exposing imbibed seeds of C311 to prolonged cold reduced the number of days required for the first flower to appear from ∼80 days to ∼45–50 days (**Figure 2**). Simple linear regression showed a significant relationship between the duration of cold exposure and the number of days until the first flower appearance for C311 ($p < 0.001$, slope coefficient −0.889, R^2 0.662). In contrast, there was no significant relationship between cold treatment and flowering time for the spring safflower S317 ($p = 0.229$, slope coefficient −0.070, R^2 0.095). The maximal acceleration of flowering of C311 was observed following 14 days of cold pre-treatment of imbibed seeds. In these experiments the seeds of cold treated plants were collected and these progeny seed were re-tested for their response to a cold-treatment and the hastening of flowering time in C311 was

confirmed. Overall, these observations are consistent with winter safflower possessing a vernalization requirement. Comparison of vernalization at different temperatures showed that there were significant differences in heading dates between the temperature applied (**Supplementary Figure 2**; $F = 14.11$, $p < 0.001$). Temperatures between 0°C and 12°C degrees were equally effective for vernalization of safflower, however treatment with 16°C was less effective for hastening heading date. We used a vernalization temperature of 4°C in subsequent experiments and a vernalization treatment of longer than 14 days was considered a saturating response in C311.

Transcriptome Analysis of Vernalization Response of Safflower

Transcriptome sequencing (RNASeq) was used to identify vernalization-responsive genes in winter safflower. Specifically, transcriptomes were generated from young seedlings of both the spring and winter safflower, grown in long-day conditions from non-vernalized seeds or from seeds exposed to cold for 5, 10, 15, or 20 days. We found that more than 4000 genes were differentially expressed across all of the treatments (**Supplementary Figure 3**), however, as a subset of these various classes of changes we were specifically interested in genes that were differentially expressed both between the different non-vernalized genotypes (S317 vs. C311) and in response to vernalization (C311 non-vernalized vs. C311 vernalized). This analysis identified 57 transcripts as being significantly differentially expressed according to these combined criteria (**Supplementary Figure 3** and **Table 1**). Of these 57 transcripts, only 14 unique sequences showed greater than two-fold change in expression (i.e., normalized read counts) both between genotypes and in response to vernalization (**Table 1**). As an additional round of assessment we also inspected the time course of transcript abundance for each of these transcripts to identify those genes that responded to vernalization in a dose-dependent manner, consistent with the response to extended cold treatment. This analysis pipeline found four transcripts (Tr32761.1, Tr26769.1, Tr33367.4, and Tr33519.70) that showed a quantitative response to vernalization, with increasing transcript abundance in seedlings exposed to progressively longer cold treatments, and these four transcripts all had higher expression in the S317 accession relative to C311 (**Figure 3**). Two other transcripts, Tr870612.1 and Tr636776.1, were induced by vernalization in the spring safflower (**Supplementary Figure 4**). Another transcript, Tr123834.1, had higher levels in non-vernalized seedlings of the winter safflower relative to the spring type (**Supplementary Figure 4**). Levels of Tr123834.1 were lower in winter safflower plants vernalized for more than 5 days but showed the opposite response to vernalization in the spring type (**Supplementary Figure 4**). Other differentially expressed transcripts included Tr69290.1, which was repressed by vernalization in the winter safflower, and Tr31946.1 that showed large differences in transcript levels between the spring and winter safflowers but no similarity to genes of known function (**Table 1** and **Supplementary Figure 4**). The remaining transcripts detected by the differential expression analysis showed no clear overall relationship between read counts, genotype or exposure to vernalization (**Supplementary Figure 4**).

TABLE 1 | List of 14 differentially expressed safflower transcripts identified during a vernalization treatment in a winter variety and in a comparison of transcripts differentially expressed in a non-vernalized treatment of the winter and spring variety.

Transcript	Top match putative annotation	Log_2FC C311V:CS311NV	Log_2FC S317NV:C311NV
Tr26769.1	MADS FUL-like	>10	>10
Tr33367.4	MADS FLC-like	>10	>10
Tr33519.70	MADS FLC-like	6	7.2
Tr32761.1	FT-like	3.8	4.8
Tr849506.1	Unknown	3.4	6
Tr4835.1	Proteinase inhibitor	1.1	2.4
Tr355653.1	HMG-CoA reductase	1	2.1
Tr32216.1	Zinc finger, RING/FYVE/PHD-type	−1	−1.4
Tr59634.1	Unknown	−1.1	−1.4
Tr18241.1	Unknown	−1.2	−1.3
Tr123834.1	RAN BP2 zinc finger	−1.3	−1.5
Tr69290.1	Methylene-furan-reductase-like	−2.6	−2.1
Tr31946.1	Unknown	−3.4	+5
Tr636776.1	Unknown	−3.4	+1.6

*Log_2FC_C311V:C311NV, refers to the log_2 fold-change between a vernalized (V) and a non-vernalized (NV) treatment on a winter variety (C311). Log_2FC_S317NV:C311NV, refer to the log_2 fold-change between a transcript in a non-vernalized spring variety (S317) and non-vernalized winter variety (C311). Transcripts were BLASTED to provide a putative annotation. The abundance of the transcripts during a time course of vernalization is graphed in **Figure 3** and **Supplementary Figure 2**.*

We used RT-qPCR to access the abundance levels of both Tr32761.1 and Tr33367.4 in S317 and C311 during a vernalization timecourse. Both transcripts were constitutively expressed in S317, but the abundance of both transcripts was below detection limits at both zero and 5 days vernalization in C311, yet both transcripts became detectable after 10, 15 and 20 days of cold treatment (**Supplementary Figure 5**). These results based on RT-qPCR are in agreement with conclusions from methods based on RNASeq.

Sequence Relationships Between Vernalization-Responsive Transcripts of Safflower and Genes From Other Plants

Comparisons with DNA databases showed the four transcripts that exhibited quantitative responses to vernalization in C311 (namely Tr32761.1, Tr26769.1, Tr33367.4, and Tr33519.70) are related to genes known to regulate flowering in other plants (**Table 1**). A simple BLAST search revealed that Tr32761.1 is similar to *FT-like* genes in other plants (**Table 1**). Phylogenetic analyses further showed that Tr32761.1 grouped with the Arabidopsis *FT* and *TWIN SISTER OF FT* genes in a monophyletic clade with high bootstrap support (bs = 1, **Figure 4**). Thus, hereafter we refer to Tr32761.1 as the safflower ortholog of the *FT* gene, namely *CtFT1*.

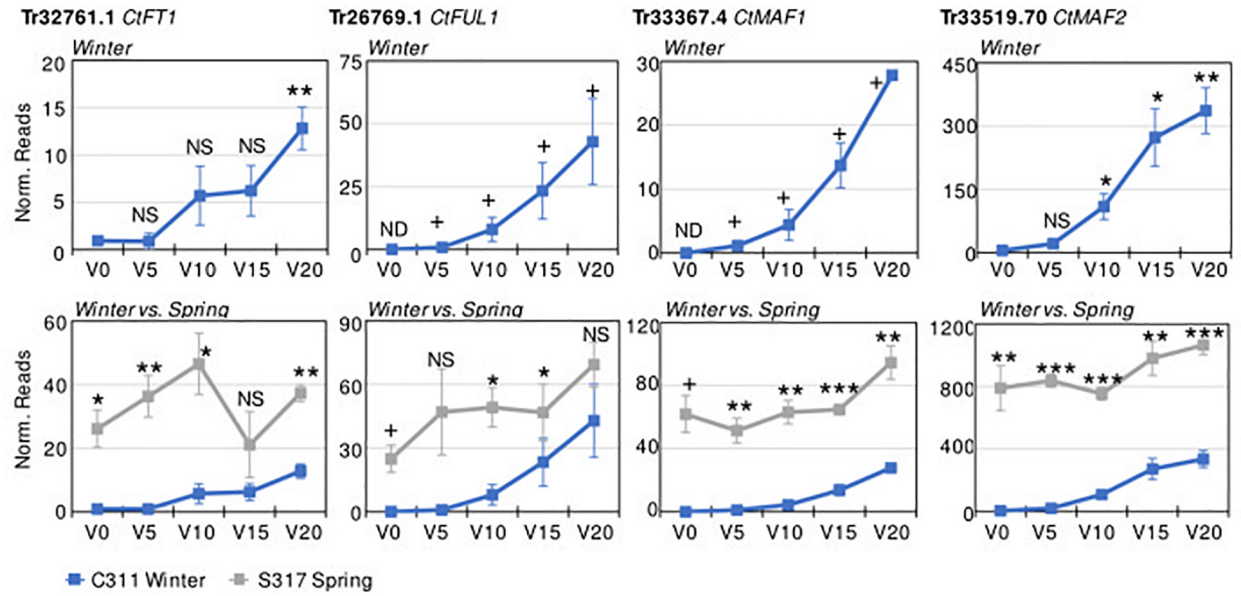

FIGURE 3 | Differential expression of key safflower transcripts with vernalization treatment and genotype. Plotted on the *y*-axes are the average normalized transcript read counts, from three biological replicates for key transcripts from transcriptomes of non-vernalized plants (V0) or plants that had been vernalized for 5, 10, 15, or 20 days. Data are presented for the winter safflower accession (C311, blue line), showing the impact of increasing durations or vernalization pre-treatment (top row). Then, gene expression in the winter type is contrasted with the spring cultivar (S317, gray line). Error bars show standard error. Statistical tests include Student's *t*-test comparison to the non-vernalized control for time course analysis of expression in the winter safflower (when plotted alone) or comparison between the spring versus winter safflower when genotypes are compared (NS, non-significant, $^{*}P < 0.05$, $^{**}P < 0.01$, $^{***}P < 0.001$). Expression not detected in some samples (ND), resulting in an absolute or presence/absence contrast (+).

A BLAST search revealed that the sequence Tr26769.1 sits in the large MADS box gene family, and more similar to *AP1/FUL*-like genes from other plants. More in-depth phylogenetic analyses placed Tr26769.1 in a monophyletic cluster with high bootstrap support (bs = 0.98), together with the Arabidopsis *AP1*, *CAL* and *FUL* genes (**Figure 5**). Precise relationships between the safflower sequence and the different Arabidopsis MADS box genes within the clade are uncertain because bootstrap support for a key branch node is weak. Nevertheless, the Tr26769.1 is unlikely to be a direct ortholog of the Arabidopsis *AP1* gene, as it was not placed within the well supported (bs = 0.95) clade with *AP1* and *CAL*. Therefore, we refer to Tr26769.1 as a safflower homolog of *FUL*, namely *CtFUL1*.

A BLAST search indicated that Tr33367.4 and Tr33519.70 also showed sequence similarity to *MADS*-box genes, with the strongest similarity to genes annotated as being '*FLC*-like.' Phylogenetic analysis placed the safflower sequences in a clade with the Arabidopsis *FLC* gene family, which includes *FLC* and the *MADS AFFECTING FLOWERING* genes and has strong bootstrap support (bs = 0.95) (**Figure 5**). Within this *FLC/MAF*-like group the safflower sequences grouped into a subclade with the sunflower *AGAMOUS*-like 31 MADS box gene. Hereafter we refer to Tr33367.4 and Tr33519.70 as safflower homologs of *MAF*-like genes, namely *CtMAF1* and *CtMAF2*, respectively.

We also used the *AtFLC* transcript as a search term using BLAST analysis within the safflower transcriptome and the closest hit was Tr32019, with two isoforms Tr32019.1 and Tr32019.2, but notably *AtFLC* did not hit upon any of the safflower candidate genes identified from the differential expression analysis. These Tr32019 isoforms were included in a new phylogenic analysis with members of the MAF- and FUL-clades (**Supplementary Figure 6**). Tr32019 groups with high confidence with sunflower *MAF1* and *MAF4*, which are themselves most closely related to *FLC* in Arabidopsis. Chicory, also a member of the Asteraceae with a vernalization response (**Figure 1**), has a functional homolog of *FLC*, namely *CiFL1* (Perilleux et al., 2013). We used *CiFL1* as a search term in a BLAST analysis of safflower transcripts and the closest hit was Tr32019, and not one of our candidate genes identified via differential gene expression analysis. We further examined the transcript abundance of Tr32019 in our RNASeq data and found there was no difference in expression in this transcript across a timecourse of vernalization nor between the two varieties S317 or C311 (**Supplementary Figure 7**). These analyses support the naming of Tr33367.4 and Tr33519.70 as *MAF* related genes and further work would be needed to see if either gene is a functional homolog of *AtFLC*.

An Improved Reference Genome for Safflower

As part of an ongoing effort to improve the genomic resources in safflower we constructed a genome assembly for S317 using either Illumina short read technologies (~100 bp reads) or PacBio long-read technologies (~20,000 bp reads). Although both approaches assembled similar overall sequence lengths

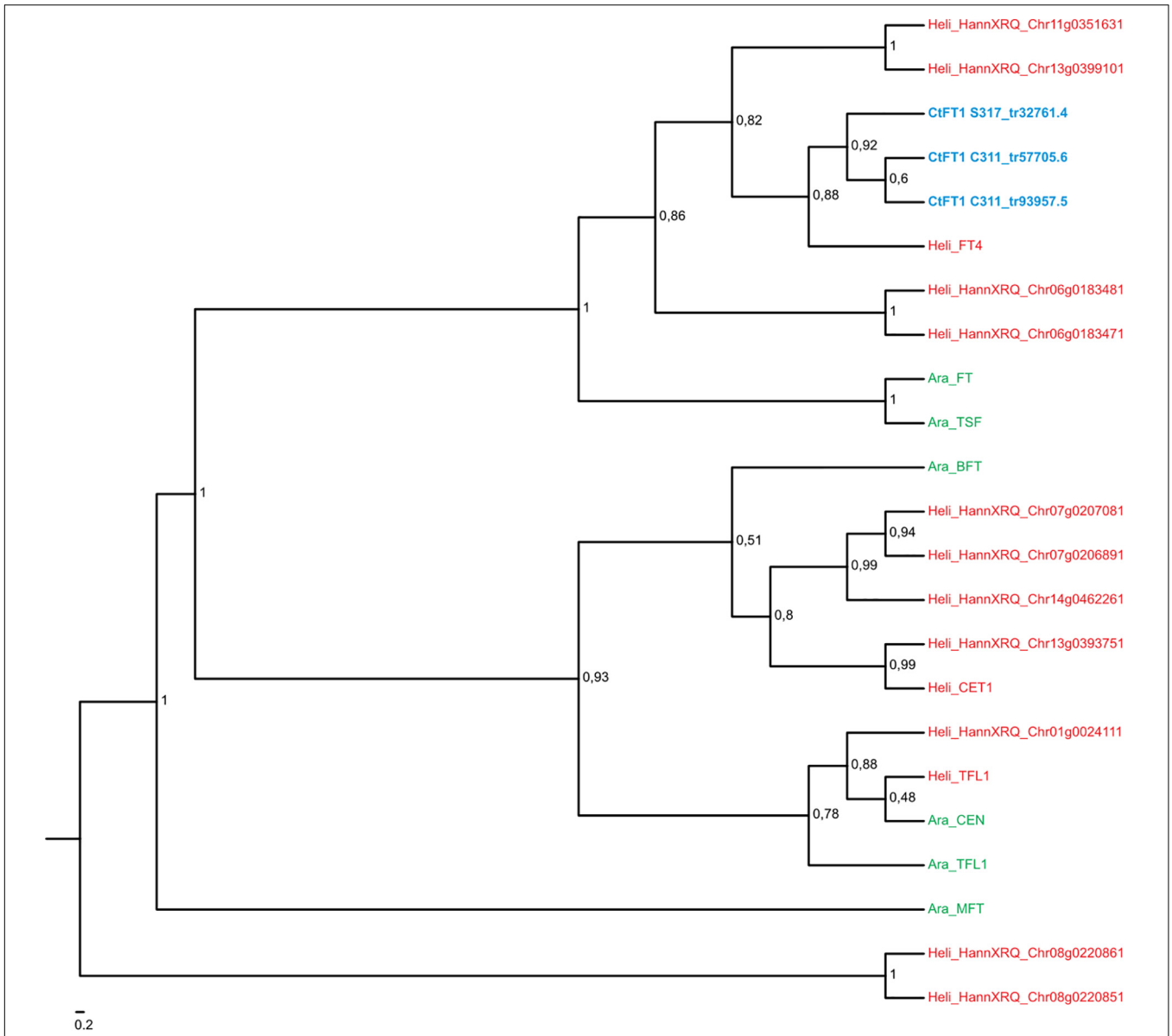

FIGURE 4 | Maximum likelihood phylogeny of the MIKC-MADS gene family in *Arabidopsis thaliana* (in green) and *Helianthus annum* (in red). Transcripts of *Carthamus tinctorius* (in blue) found to be differentially expressed in response to vernalization were included. Bootstrap support values are shown for nodes with higher than 50% support. *CtMAF1* sequences from spring safflower (S317_tr33367.4 and S317_tr33367.5) appear to be isoforms of the same transcript, with variations found in the 3′ end of S317_tr33367.4. Similarly, the *CtMAF1* sequences from the winter safflower transcriptome (C311_tr20021.6 and C311_tr23886.4) also appear to be isoforms of the same transcript, with a 5′ truncation and single codon gap in C311_tr23886.4. Information about the genes can be found in **Supplementary Table 2**.

∼1.1 Gb representing ∼80% of the predicted genome, summary data from PacBio-based compared to Illumina-based assembly showed significant improvements, including longer average length contigs (∼300,000 bp vs. 1,200 bp), reduced number of contigs (∼3,000 vs. 900,000) and a greatly improved N50 (∼600,000 bp vs. 2,000 bp) (**Table 2**). A generally accepted measure of genome completeness is provided by Benchmarking Universal Single-Copy Orthologs (BUSCO), where a core set of 1440 conserved genes across all known genomes is used to interrogate the completeness of an assembled genome (Simao et al., 2015). BUSCO metrics on the PacBio-based assembly indicate that the genome is at least 83% complete, with only 8% of the BUSCO core gene set missing (**Table 3**). The Illumina-based assembly was found to be at least 60% complete but has 22% of the BUSCO core gene set completely missing from the assembly. Overall, we found the PacBio-based assembly to be more complete, and less fragmented, relative to the Illumina-based analysis.

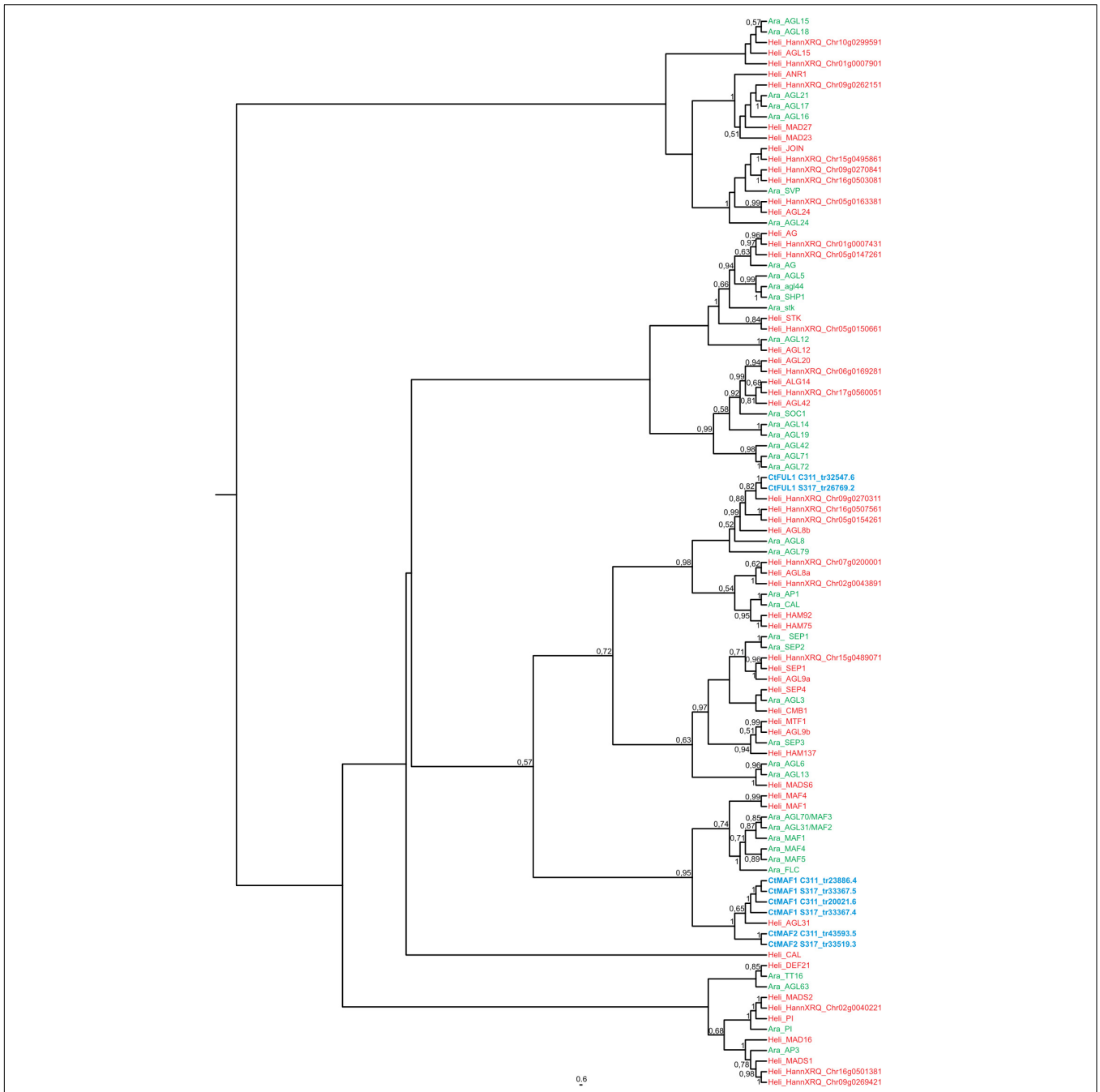

FIGURE 5 | Maximum likelihood phylogeny of the *FT* gene family in *Arabidopsis thaliana* (in green) and *Helianthus annum* (in red). Transcripts of *Carthamus tinctorius* (in green) found to be differentially expressed in response to vernalization were included. Bootstrap support values are shown for nodes with higher than 50% support. Regarding the two transcripts from the winter safflower transcriptomic assembly, namely C311_tr57705.6 and C311_tr93957.5. The former is a transcript containing a truncation at the 3′ end that closely resembles the CtFT1 from the spring safflower transcriptome (S317_tr32761.4). The latter closely resembles C311_tr57705.6 but also contains a 5′ truncation. Information about the genes can be found in **Supplementary Table 2**.

Construction of Gene Models for *CtFT1*, *CtFUL1*, *CtMAF1*, and *CtMAF2* Using a New Safflower Genome Assembly

Although there are many uses for a high-quality reference genome in safflower, in this report we limit ourselves to generating accurate gene models for four candidate genes identified from transcriptomic analysis, namely *CtFT1, CtFUL1, CtMAF1 and CtMAF2*. Each of the genes were confidently identified in the PacBio-based assembly. The structures of the four genes were assigned by aligning the transcripts of the genes against the DNA assembly, and therefore, the gene models are an accurate representation of exon-intron structures rather than predictions (**Figure 6**). *CtFT1* is found within a 107,218 bp

TABLE 2 | Summary statistics for the *de novo* assemblies of safflower S317 using two different sequencing and software combinations.

Platform/assembler	Illumina/BioKanga	PacBio/Canu
Total size assembled (bp)	1,163,499,791	1,085,248,405
Contigs	904,199	3,565
Minimum contig length (bp)	300	14,010
N50 (bp)	1,940	594,302
Mean contig length (bp)	1,286	304,417
Maximum contig length (bp)	32,974	1,828,491

See text for more details.

TABLE 3 | Assessment of Illumina- and PacBio-based assemblies using the BUSCO core gene set.

(a) *De novo* genome assembly using Illumina/BioKanga.

BUSCOs searched	1440	%
Complete single-copy	863	60.0
Complete duplicated	39	2.7
Fragmented	222	15.4
Missing	316	21.9

(b) *De novo* genome assembly using PacBio/Canu.

BUSCOs searched	1440	%
Complete single-copy	1206	83.8
Complete duplicated	88	6.1
Fragmented	35	2.4
Missing	111	7.7

The assemblies were measured for completeness using the 1440 genes curated in the BUSCO (v3.0.1) protocol.

contig and the gene contains two introns, the longest being 2,706 bp. *CtFUL1* is found within a contig that is 921,593 bp long and contains five introns, with the longest, intron 1, being over 10,000 bp in the first intron. *CtMAF1* is found on a contig being 1.2 Mbp long, contains five introns, including a 13,000 bp intron and an intron of undefined length, presumably due to the alignment needing to span two independent contigs. *CtMAF2* sits within a 1.6 Mb contig and contains three introns, the longest being 9,919 bp long.

Genetics of Growth Habit in Safflower

Reciprocal crosses were conducted between C311 and S317 to test the genetic basis of growth habit in safflower. In total, 58 F1 plants were produced (20 F1 from C311♂xS317♀ and 38 F1 seed from S317♂xC311♀), and all displayed a rapid flowering 'spring' growth habit, indicating that spring growth habit is dominant. One F1 plant was self-pollinated generating a family of 142 F2 plants. Within this F2 family, 10 plants displayed a late flowering phenotype while the remaining 132 plants were early flowering. The observed frequency of late versus early flowering plants is consistent with a two gene model, with two unlinked dominant genes for spring-growth habit (expect 9 late and 133 early, $\chi^2 = 0.73$).

DISCUSSION

Here, we have shown that exposing imbibed safflower seeds to cold accelerates flowering when plants are subsequently grown in glasshouse conditions. This satisfies the formal definition of vernalization, that plants retain a memory of prolonged exposure to cold that accelerates flowering (Chouard, 1960). Similar to other plants, the vernalization response of safflower is quantitative, with longer exposure to cold accelerating flowering to greater extents, and seeds harvested from vernalized C311 exhibiting the same vernalization requirement as the parent, showing that the memory of cold is reset between generations. Similar to other species like *Arabidopsis* (Sheldon et al., 2008) and barley (Trevaskis et al., 2007) the need for vernalization is reset in a new generation. The requirement for vernalization was saturated after 2-weeks at 4 degrees, with no additional acceleration of flowering occurring with longer cold treatments. This response is rapid relative to some plants. For example, seeds of some cereals require 9–11 weeks of vernalization to saturate the vernalization response (Sasani et al., 2009). Based on the data presented here, we conclude that winter accessions of safflower possess a facultative vernalization response, such that vernalization accelerates flowering but plants are able to flower without vernalization. It should be noted that only one winter safflower accession has been studied here and that there are likely numerous other accessions possessing a vernalization requirement (Ghanavati and Knowles, 1977). Thus, there is potential that some winter safflower accessions might need longer periods of cold to fulfill the vernalization requirement.

Having established that winter-hardy safflower C311 has a vernalization response, we utilized an unbiased transcriptomics approach to investigate the molecular basis of this epigenetic pathway. This approach was based on those used previously to explore the molecular basis of vernalization in other plants. For example, microarray comparisons of gene expression in vernalized versus non-vernalized barley plants identified key genes that mediate the memory of vernalization amongst a relatively limited number of differentially expressed genes (Greenup et al., 2011). Similarly, gene-expression comparisons have proven to be an effective way to identify genes associated with the differences between spring versus winter cultivars of barley (Cuesta-Marcos et al., 2015). A key component of the experimental design was the sampling of tissue for vernalization treatments after allowing an extra week of growth at warm conditions. This approach takes advantage of the observation that genes involved in vernalization, as an epigenetic response, show lasting responses to prolonged cold and may contribute to the memory of winter (see Greenup et al., 2011). Additionally, genes that show lasting responses to vernalization and that are also differentially expressed between plants with winter and spring growth habit are of particular interest, since such genes potentially mediate both the vernalization response and reflect differences in vernalization requirement; as shown for *FLC* in Arabidopsis and *VRN1* in cereals. Finally, based on the dose-dependent response of vernalization we also visually inspected transcripts that also responded in a dose-dependent manner in C311. This experimental design and multi-layered analysis

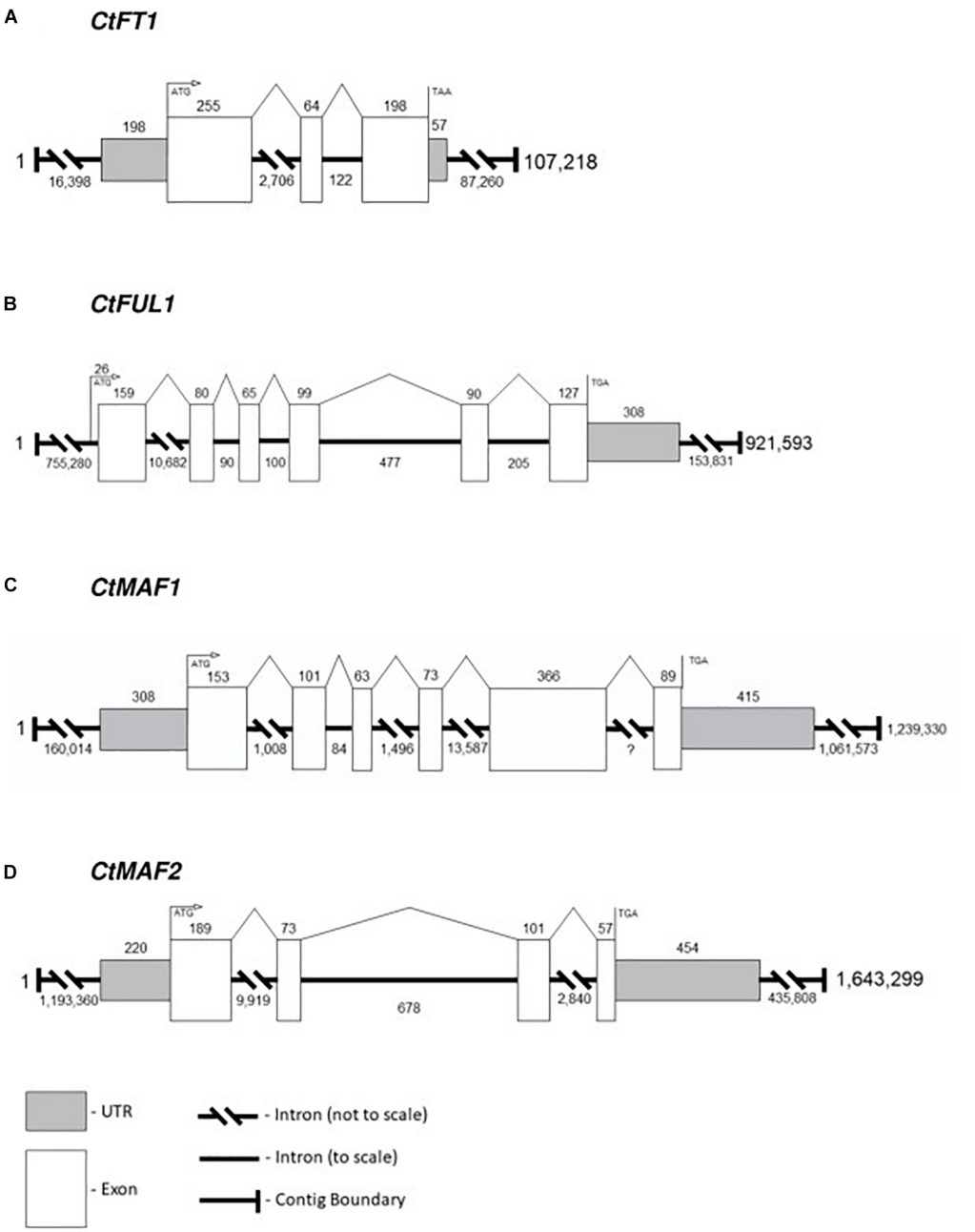

FIGURE 6 | Gene models for **(A)** *CtFT1*, **(B)** *CtFUL1*, **(C)** *CtMAF1*, and **(D)** *CtMAF2* based on alignments of transcript with the genome assembly of S317.

identified four transcripts, Tr32761.1, Tr26769.1, Tr33367.4 and Tr33519.70, that represent potential genes-of-interest with respect to the vernalization response of safflower. Through phylogenetic analyses we verified that Tr32761.1, Tr26769.1, Tr33367.4 and Tr33519.70 represent homologs of a *FT* gene, a *CUL*-like MADS-box gene and two closely related *FLC/MAF* MADS box genes. All of these safflower genes are quantitatively induced by vernalization, such that the increase in transcript levels in vernalized plants is proportional to the duration of the vernalization pre-treatment. Additionally, all these genes show elevated expression without vernalization in a spring versus winter safflower. Taken together, these findings strongly suggest that the expression of these genes is associated with the memory of vernalization in C311 and also the reduced vernalization requirement associated with spring growth habit in S317.

The data presented here, taken together with the findings of previous studies of vernalization-responsive genes, provides insights into the evolution of vernalization-induced flowering. Increased expression of *FT*-like genes in vernalized plants, relative to non-vernalized controls, has now been observed

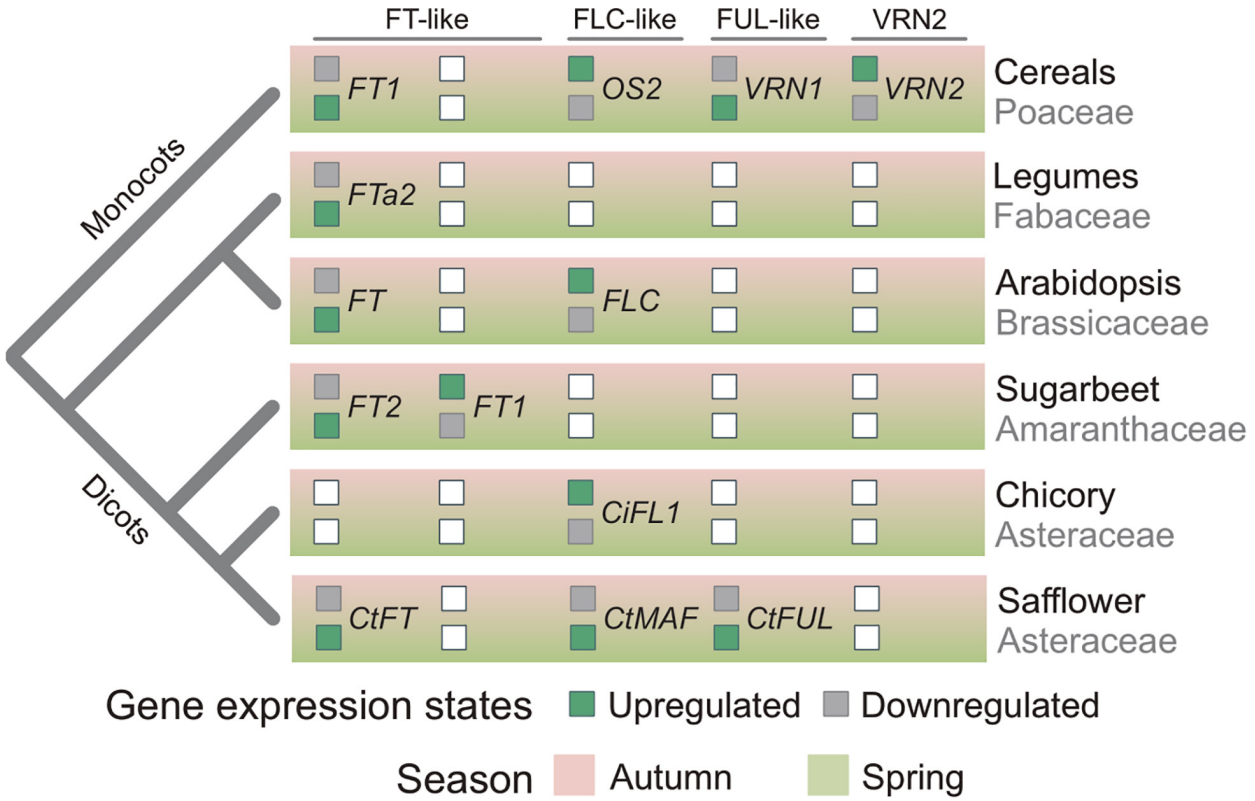

FIGURE 7 | Relationships between phylogeny and seasonal gene expression signatures. Inferred seasonal gene-expression states of flowering regulators in plants related to phylogenetic relationships. Boxes filled green indicates whether a gene is actively expressed in either autumn or spring. Gray filled boxes indicate a gene is repressed in autumn or spring. White box denotes that the gene has not been found in a plant lineage or that the expression state is unknown. *CtMAF* refers to both *CtMAF1* and *CtMAF2*, which show similar seasonal gene expression patterns.

in diverse species, including monocots and all the major dicot lineages (**Figure 7**) (Michaels et al., 2005; Helliwell et al., 2006; Yan et al., 2006; Hemming et al., 2008; Laurie et al., 2011). This common pattern of transcriptional regulation observed across these diverse plant lineages suggests that limiting daylength activation of *FT* in non-vernalized plants is a common mechanism that delays flowering before winter, giving rise to the winter growth habit (vernalization requirement). This mechanism has potentially evolved independently in at least some lineages. For example, in sugar beet it appears that mutations have occurred recently in genes that regulate daylength flowering-responses and that these are a pre-requisite for the vernalization-responsive biennial/winter growth habit (Dally et al., 2014).

Elevated expression of a *FUL*-like gene (*VRN1*) in vegetative tissues following prolonged cold treatment is a distinctive feature of the vernalization response of cereals and related temperate grasses (McKeown et al., 2016). The elevated expression of *CtFUL1* (Tr26769.1) in vernalized safflower plants is similar to that observed for *VRN1* in cereals. Furthermore, *CtFUL1* showed elevated expression without vernalization in a spring safflower, relative to a winter accession. This pattern is also similar to the gene expression observed for the *VRN1* gene in cereals. This suggests that *FUL*-like genes might play a role in vernalization-induced flowering of both monocots and dicots. It is important to note here however, that there is a positive feedback loop between *FT*-like and *FUL*-like genes, such that increasing transcriptional activity of one class of gene can upregulate the other (Teper-Bamnolker and Samach, 2005; Deng et al., 2015). Since safflower *FUL1* and *FT1* genes have such similar gene expression patterns in response to vernalization, there is potential that either of these genes plays an active role in vernalization-induced flowering and that the other is up-regulated as a secondary response. This occurs in legumes, where *FUL*-like genes also show elevated expression in the vegetative tissues of vernalized plants, but are up-regulated by expression an *FT*-like gene as part of the long-day flowering response, rather than be induced directly by low temperatures as is the case for the *VRN1* gene of cereals (Jaudal et al., 2015). Assaying gene expression during seed vernalization, in darkness, could resolve whether safflower *FUL*-like or *FT*-like genes are directly regulated by cold.

Repression of *FLC* by vernalization is the central feature of vernalization-induced flowering of Arabidopsis and related *Brassicaceae* (Sheldon et al., 2000; Tadege et al., 2001; Irwin et al., 2016; O'Neill et al., 2019; Tudor et al., 2020; Yin et al., 2020). Genes related to *FLC* are also down regulated by vernalization

in cereals and related grasses, likely downstream of the *VRN1* gene (Greenup et al., 2011; Ruelens et al., 2013; Deng et al., 2015). This study identified two safflower *MAF/FLC*-like genes, *CtMAF1* and *CtMAF2*, that are induced by vernalization. Induction of both genes was quantitative, with stronger induction occurring after longer vernalization pre-treatments, and both genes were expressed at elevated levels in spring versus winter safflower accessions. This is the inverse of the gene expression pattern observed for *FLC* in response to vernalization in Arabidopsis. Furthermore, it is unlike the pattern of *FLC* expression observed for winter versus spring ecotypes of Arabidopsis, with reduced expression of *MAF*-like genes in a winter safflower accession. The *MAF/FLC*-like group of MADS box genes appears to have expanded independently in *Asteraceae* and *Brassicaceae* (**Figure 5**). And so while the identified safflower genes are related to *FLC*, they are the most closely related orthologs and it is not possible to assume that these genes are direct functional equivalents. However, in the closely related Asteraceae species *Cichorium intybus*, a *FLC*-like gene, *CiFL1*, is the closest ortholog to the *A. thaliana FLC/MAF*-clade (Ruelens et al., 2013). *CiFL1* is induced by cold and represses flowering (Perilleux et al., 2013), suggesting functional conservation between *C. intybus* and *A. thaliana*. Interestingly, whereas *FLC* is repressed during longer cold treatments (>20 days) (Kim and Sung, 2013), *AtMAF4* and *AtMAF5* are induced by intermediate durations of cold (10–20 days), a result similar to the time course of *CtMAF1* and *CtMAF2* genes during the vernalization conditions examined here for safflower. Thus, it is possible that transcriptional activation by cold is a conserved feature of some *MAF/FLC*-like genes. Induction of *AtMAF4* and *AtMAF5* seems to mediate repression of flowering after short durations of vernalization, whereas induction of safflower *CtMAF/FLC*-like genes is associated with earlier flowering. As both safflower *MAF-like* genes identified here are also transcriptionally activated by low-temperature treatment, so this too appears to be a shared feature that is possibly conserved amongst some members of the *MAF/FLC-like* clade. Alternatively, low-temperature regulation of *MAF/FLC*-like genes might have evolved rapidly. Irrespective of evolutionary history, gene expression behavior of the Arabidopsis *FLC* gene cannot be assumed to be indicative of the broader *MAF/FLC*-like gene family.

Based on the data presented here, together with knowledge from other vernalization responsive plants, we suggest that vernalization-induced flowering has evolved on more than one occasion through the recruitment of common genes that are predisposed to function in seasonal flowering. These include the *FT*-like gene family, which are recruited to vernalization pathways when a requirement for cold evolves to override the daylength flowering response. Similarly, the conserved feedback loop between *FUL*-like and *FT*-like genes could lead to recruitment of *FUL*-like genes into vernalization pathways, either upstream (cereals) or downstream of *FT*-like genes (legumes). The *MAF/FLC*-like genes are potentially predisposed to recruitment to function in vernalization-response pathways through being temperature responsive, with evidence that this class of genes can be regulated by both cold and warm temperatures. There is also the possibility that conserved interactions between these genes led to their co-recruitment into vernalization dependent flowering; e.g., regulation of *FT*-like genes by *MAF/FLC*-like. A better understanding of global transcriptional responses of diverse plants to seasonal temperature and daylength cues, together with further functional analyses of these important classes of genes across diverse species could test these hypotheses in the future.

Variation in vernalization requirement, also described as growth habit, is an important trait in crop breeding since it adapts varieties to local seasonal conditions and management practices such as different sowing dates. Identification of genes controlling growth habit allows sequence-based approaches to be used to explore and capture genetic diversity for this trait. Molecular markers for genes controlling growth habit can then be used to facilitate parent selection in breeding crosses and also allow rapid selection of progeny. A key question arising from this study is: do any of the genes identified control safflower growth habit? The safflower spring growth habit is dominant to the winter growth-habit, such that F1 plants flower at the same time as the spring parent, and our genetic analysis suggested that S317 carries two independent genes for spring growth habit. One mechanism that could give rise to dominant genes for spring growth habit is gain-of-function in genes that activate flowering. Increased transcription is one mechanism that drives gain-of-function, so *CtFT1*, *CtFUL1*, *CtMAF1* and *CtMAF2* are possible candidates for the two genes controlling growth habit of safflower. Equally, mutations in a regulator of any of these genes, could give rise to a dominant spring growth habit.

This study generated a greatly improved genome sequence for safflower (S317 accession), and we used our assembled genome in combination with the transcriptome data to construct gene models for the candidate genes. These models will form the basis for future screening of diversity to determine the causal variation underlying the differences in responses to vernalization. Of particular interest are the first introns of *CtFUL1* and the *CtMAF1-2* genes of the MIKC-MADS box gene family. The first introns of MIKC-MADS box genes have been found to be key regions for the function genes controlling response to vernalization in other species. In Arabidopsis the first intron of *FLC* has been found to be essential for a stable repression by cold (Sheldon et al., 2002), and in barley and wheat, large deletions in the first intron of *VRN1*, also a MIKC-MADS box gene closely related to *AP1* (Yan et al., 2003), control the spring type growth thereby repressing the vernalization requirement (Fu et al., 2005).

Safflower has an estimated 1.35 Gb genome and the PacBio-based reference genome reported here is a significant improvement upon previously published resources, both in terms of completeness and length of contigs (Mayerhofer et al., 2011; Bowers et al., 2016). Nevertheless further improvements in the overall safflower genome can be made by incorporating all of the existing genome databases together generating a range of hybrid assemblies that together will improve the confidence in mapping long contigs to pseudo-chromosomes/linkage groupings and eventually building an even more complete genome.

In conclusion, this study demonstrates that a facultative requirement for vernalization is a feature of the winter growth habit of safflower. Transcriptome analyses identified a small list of safflower genes that are associated with both the memory of winter in vernalized plants and with differences in growth habit. Based on gene expression and sequence relationships with genes known to control vernalization-induced flowering and growth habit in other plants, these genes are interesting candidates for further research to explore the molecular basis of vernalization-induced flowering in safflower, which can provide insights into the evolution of vernalization as well as inform future crop improvement.

DATA AVAILABILITY STATEMENT

All sequencing data has been deposited in, and downloadable from, the CSIRO Data Access Portal (DAP):

Supplementary Dataset 1. Excel Spreadsheet for the calculations of data presented in Figure 3 and Supplementary Figure 3: https://doi.org/10.25919/611f-t870

Safflower S317 Genome Illumina Raw Reads and Assembly: https://doi.org/10.25919/xf81-3m21

Safflower S317 Genome PacBio Raw Reads: https://doi.org/10.25919/pbtp-kt44

Safflower S317 Genome PacBio Final Assembly: https://doi.org/10.25919/3jen-ht92

Safflower S317 Transcriptome Raw Reads: https://doi.org/10.25919/15sc-cn48

Safflower C311 and S317 Transcriptome Raw Reads during a vernalization time course: https://doi.org/10.25919/pqxw-f838

Safflower C311 transcriptome assembly: https://doi.org/10.25919/5jsa-p138.

AUTHOR CONTRIBUTIONS

DC, SF, BT, AE, and CW conceived and designed the experiments. DC conducted the experiments. DC and AS analyzed genomic data. DC and AS prepared data repositories for public release. DC, SF, BT, and CW analyzed the data. BT, SF, DC, AE, and CW wrote the manuscript. AE, BT, and CW wrote the funding applications. All authors contributed to the article and approved the submitted version.

FUNDING

This study was funded by the GRDC (Grains Research and Development Corporation) and CSIRO (Commonwealth Scientific and Industrial Research Organisation).

ACKNOWLEDGMENTS

The authors are grateful for the expert technical assistance from Anu Mathew and Amratha Menon regarding nuclear DNA isolations and maintenance of safflower plants. The authors thank Drs. Stuart Stephen and Jen Taylor for guidance and advice on early stages of bioinformatics and genome assemblies. DC was funded via a University of Newcastle Ph.D. scholarship and a CSIRO Ph.D. top-up stipend.

SUPPLEMENTARY MATERIAL

The Supplementary Material for this article can be found online at: https://www.frontiersin.org/articles/10.3389/fpls.2021.639014/full#supplementary-material

REFERENCES

Altschul, S. F., Madden, T. L., Schaffer, A. A., Zhang, J., Zhang, Z., Miller, W., et al. (1997). Gapped BLAST and PSI-BLAST: a new generation of protein database search programs. *Nucleic Acids Res.* 25, 3389–3402. doi: 10.1093/nar/25.17.3389

Andrews, S., Krueger, F., Krueger, C., and Wingate, S. (2012). *FastQC*. Babraham: Babraham Institute.

Baloch, D. M., Karow, R. S., Marx, E., Kling, J. G., and Witt, M. D. (2003). Vernalization studies with Pacific Northwest wheat. *Agron. J.* 95, 1201–1208. doi: 10.2134/agronj2003.1201

Baskin, J. M., and Baskin, C. C. (1989). Seed-germination ecophysiology of jeffersonia-diphylla, a perennial herb of mesic deciduous forests. *Am. J. Bot.* 76, 1073–1080. doi: 10.1002/j.1537-2197.1989.tb15088.x

Bastow, R., Mylne, J. S., Lister, C., Lippman, Z., Martienssen, R. A., and Dean, C. (2004). Vernalization requires epigenetic silencing of FLC by histone methylation. *Nature* 427, 164–167. doi: 10.1038/nature02269

Bender, M. H., Baskin, J. M., and Baskin, C. C. (2002). Flowering requirements of *Polymnia canadensis* (Asteraceae) and their influence on its life history variation. *Plant Ecol.* 160, 113–124.

Bentley, D. R., Balasubramanian, S., Swerdlow, H. P., Smith, G. P., Milton, J., Brown, C. G., et al. (2008). Accurate whole human genome sequencing using reversible terminator chemistry. *Nature* 456, 53–59.

Bowers, J. E., Pearl, S. A., and Burke, J. M. (2016). Genetic mapping of millions of SNPs in safflower (*Carthamus tinctorius* L.) via whole-genome resequencing. *G3 Genes Genomes Genet.* 6, 2203–2211. doi: 10.1534/g3.115.026690

Chouard, P. (1960). Vernalization and its relations to dormancy. *Annu. Rev. Plant Physiol. Plant Mol. Biol.* 11, 191–238. doi: 10.1146/annurev.pp.11.060160.001203

Cuesta-Marcos, A., Munoz-Amatriain, M., Filichkin, T., Karsai, I., Trevaskis, B., Yasuda, S., et al. (2015). The relationships between development and low temperature tolerance in barley near isogenic lines differing for flowering behavior. *Plant Cell Physiol.* 56, 2312–2324. doi: 10.1093/pcp/pcv147

Czechowski, T., Stitt, M., Altmann, T., Udvardi, M. K., and Scheible, W. R. (2005). Genome-wide identification and testing of superior reference genes for transcript normalization in *Arabidopsis*. *Plant Physiol.* 139, 5–17. doi: 10.1104/pp.105.063743

Dally, N., Xiao, K., Holtgrawe, D., and Jung, C. (2014). The B2 flowering time locus of beet encodes a zinc finger transcription factor. *Proc. Natl. Acad. Sci. U.S.A.* 111, 10365–10370. doi: 10.1073/pnas.1404829111

Danyluk, J., Kane, N. A., Breton, G., Limin, A. E., Fowler, D. B., and Sarhan, F. (2003). TaVRT-1, a putative transcription factor associated with vegetative to reproductive transition in cereals. *Plant Physiol.* 132, 1849–1860. doi: 10.1104/pp.103.023523

Deng, W. W., Casao, M. C., Wang, P. H., Sato, K., Hayes, P., Finnegan, J., et al. (2015). Direct links between the vernalization response and other key traits of cereal crops. *Nat. Commun.* 6:5882.

Dereeper, A., Guignon, V., Blanc, G., Audic, S., Buffet, S., Chevenet, F., et al. (2008). Phylogeny.fr: robust phylogenetic analysis for the non-specialist. *Nucleic Acids Res.* 36, W465–W469.

Dole, J. M. (2015). Photoperiod responses of ten specialty cut flowers. *Acta Hortic.* 1097, 163–168. doi: 10.17660/actahortic.2015.1097.19

Edgar, R. C. (2004). MUSCLE: multiple sequence alignment with high accuracy and high throughput. *Nucleic Acids Res.* 32, 1792–1797. doi: 10.1093/nar/gkh340

Eid, J., Fehr, A., Gray, J., Luong, K., Lyle, J., Otto, G., et al. (2009). Real-time DNA sequencing from single polymerase molecules. *Science* 323, 133–138.

El-Gebali, S., Mistry, J., Bateman, A., Eddy, S. R., Luciani, A., Potter, S. C., et al. (2019). The Pfam protein families database in 2019. *Nucleic Acids Res.* 47, D427–D432.

Elsworth, B., and Weitemier, K. (2013). *SCUBAT –Scaffolding Contigs Using BLAT and Transcripts*. Available online at: https://github.com/elswob/SCUBAT

Finnegan, E. J., and Dennis, E. S. (2007). Vernalization-induced trimethylation of histone H3 lysine 27 at FLC is not maintainedin mitotically quiescent cells. *Curr. Biol.* 17, 1978–1983. doi: 10.1016/j.cub.2007.10.026

Fu, D. L., Szucs, P., Yan, L. L., Helguera, M., Skinner, J. S., Zitzewitz, J. V., et al. (2005). Large deletions within the first intron in VRN-1 are associated with spring growth habit in barley and wheat. *Mol. Genet. Genomics* 273, 54–65. doi: 10.1007/s00438-004-1095-4

Fu, Z. X., Jiao, B. H., Nie, B., Zhang, G. J., Gao, T. G., and China Phylogeny Consortium (2016). A comprehensive generic-level phylogeny of the sunflower family: implications for the systematics of chinese asteraceae. *J. Syst. Evol.* 54, 416–437. doi: 10.1111/jse.12216

Ghanavati, N. A., and Knowles, P. F. (1977). Variation among winter-type selections of safflower. *Crop Sci.* 17, 44–46. doi: 10.2135/cropsci1977.0011183x001700010013x

Greenup, A. G., Sasani, S., Oliver, S. N., Walford, S. A., Millar, A. A., and Trevaskis, B. (2011). Transcriptome analysis of the vernalization response in barley (*Hordeum vulgare*) seedlings. *PLoS One* 6:e17900. doi: 10.1371/journal.pone.0017900

Ha, T. M., and Johnston, M. E. (2013). The effect of low temperature on flowering of rhodanthe floribunda. *Asian J. Agric. Food Sci.* 1, 205–209.

Harwood, R. R., and Markaria, D. (1968). Annual culture of globe artichoke (*Cynara Scolymus* L) .I. preliminary report. *Proc. Natl. Acad. Sci. U.S.A.* 92:400.

Helliwell, C. A., Wood, C. C., Robertson, M., Peacock, W. J., and Dennis, E. S. (2006). The Arabidopsis FLC protein interacts directly in vivo with SOC1 and FT chromatin and is part of a high-molecular-weight protein complex. *Plant J.* 46, 183–192. doi: 10.1111/j.1365-313x.2006.02686.x

Hemming, M. N., Peacock, W. J., Dennis, E. S., and Trevaskis, B. (2008). Low-temperature and daylength cues are integrated to regulate FLOWERING LOCUS T in barley. *Plant Physiol.* 147, 355–366. doi: 10.1104/pp.108.116418

Irwin, J. A., Soumpourou, E., Lister, C., Ligthart, J. D., Kennedy, S., and Dean, C. (2016). Nucleotide polymorphism affecting FLC expression underpins heading date variation in horticultural brassicas. *Plant J.* 87, 597–605. doi: 10.1111/tpj.13221

Jaudal, M., Yeoh, C. C., Zhang, L. L., Stockum, C., Mysore, K. S., Ratet, P., et al. (2013). Retroelement insertions at the Medicago FTa1 locus in spring mutants eliminate vernalisation but not long-day requirements for early flowering. *Plant J.* 76, 580–591. doi: 10.1111/tpj.12315

Jaudal, M., Zhang, L. L., Che, C., and Putterill, J. (2015). Three Medicago MtFUL genes have distinct and overlapping expression patterns during vegetative and reproductive development and 35S:MtFULb accelerates flowering and causes a terminal flower phenotype in *Arabidopsis*. *Front. Genet.* 6:50. doi: 10.3389/fgene.2015.00050

Johanson, U., West, J., Lister, C., Michaels, S., Amasino, R., and Dean, C. (2000). Molecular analysis of FRIGIDA, a major determinant of natural variation in *Arabidopsis* flowering time. *Science* 290, 344–347. doi: 10.1126/science.290.5490.344

Johnson, R. C., and Dajue, L. (2008). Safflower winter survival and selection response relates to fall growth morphology and acclimation capacity. *Crop Sci.* 48, 1872–1880. doi: 10.2135/cropsci2008.01.0047

Kim, D. H., and Sung, S. (2013). Coordination of the vernalization response through a VIN3 and FLC gene family regulatory network in *Arabidopsis*. *Plant Cell* 25, 454–469. doi: 10.1105/tpc.112.104760

Koren, S., Walenz, B. P., Berlin, K., Miller, J. R., Bergman, N. H., and Phillippy, A. M. (2017). Canu: scalable and accurate long-read assembly via adaptive k-mer weighting and repeat separation. *Genome Res.* 27, 722–736. doi: 10.1101/gr.215087.116

Laurie, R. E., Diwadkar, P., Jaudal, M., Zhang, L., Hecht, V., Wen, J., et al. (2011). The medicago FLOWERING LOCUS T Homolog, MtFTa1, is a key regulator of flowering time. *Plant Physiol.* 156, 2207–2224. doi: 10.1104/pp.111.180182

Love, M. I., Huber, W., and Anders, S. (2014). Moderated estimation of fold change and dispersion for RNA-seq data with DESeq2. *Genome Biol.* 15:550.

Madeira, F., Park, Y. M., Lee, J., Buso, N., Gur, T., Madhusoodanan, N., et al. (2019). The EMBL-EBI search and sequence analysis tools APIs in 2019. *Nucleic Acids Res.* 47, W636–W641.

Mandel, J. R., Dikow, R. B., Siniscalchi, C. M., Thapa, R., Watson, L. E., and Funk, V. A. (2019). A fully resolved backbone phylogeny reveals numerous dispersals and explosive diversifications throughout the history of Asteraceae. *Proc. Natl. Acad. Sci. U.S.A.* 116, 14083–14088. doi: 10.1073/pnas.1903871116

Mayerhofer, M., Mayerhofer, R., Topinka, D., Christianson, J., and Good, A. G. (2011). Introgression potential between safflower (*Carthamus tinctorius*) and wild relatives of the genus Carthamus. *BMC Plant Biol.* 11:47. doi: 10.1186/1471-2229-11-47

McKeown, M., Schubert, M., Marcussen, T., Fjellheim, S., and Preston, J. C. (2016). Evidence for an early origin of vernalization responsiveness in temperate pooideae grasses. *Plant Physiol.* 172, 416–426. doi: 10.1104/pp.16.01023

Michaels, S. D., and Amasino, R. M. (1999). FLOWERING LOCUS C encodes a novel MADS domain protein that acts as a repressor of flowering. *Plant Cell* 11, 949–956. doi: 10.1105/tpc.11.5.949

Michaels, S. D., Himelblau, E., Kim, S. Y., Schomburg, F. M., and Amasino, R. M. (2005). Integration of flowering signals in winter-annual *Arabidopsis*. *Plant Physiol.* 137, 149–156. doi: 10.1104/pp.104.052811

Morgat, A., Lombardot, T., Coudert, E., Axelsen, K., Neto, T. B., Gehant, S., et al. (2020). Enzyme annotation in UniProtKB using Rhea. *Bioinformatics* 36, 1896–1901.

Mundel, H. H., and Bergman, J. W. (2009). Safflower. *Oil Crops* 4, 423–447.

Naim, F., Nakasugi, K., Crowhurst, R. N., Hilario, E., Zwart, A. B., Hellens, R. P., et al. (2012). Advanced engineering of lipid metabolism in nicotiana benthamiana using a draft genome and the V2 viral silencing-suppressor protein. *PLoS One* 7:e52717. doi: 10.1371/journal.pone.0052717

Niu, G. H., Heins, R., Cameron, A., and Carlson, W. (2002). Prevernalization daily light integral and vernalization temperature influences flowering of herbaceous perennials. *Hortscience* 37, 1028–1031. doi: 10.21273/hortsci.37.7.1028

Nykiforuk, C. L., Shewmaker, C., Harry, I., Yurchenko, O. P., Zhang, M., Reed, C., et al. (2012). High level accumulation of gamma linolenic acid (C18:3 Delta 6,9,12 cis) in transgenic safflower (*Carthamus tinctorius*) seeds. *Transgenic Res.* 21, 367–381. doi: 10.1007/s11248-011-9543-5

O'Neill, C. M., Lu, X., Calderwood, A., Tudor, E. H., Robinson, P., Wells, R., et al. (2019). Vernalization and floral transition in autumn drive winter annual life history in oilseed rape. *Curr. Biol.* 29, 4300–4306. doi: 10.1016/j.cub.2019.10.051

Oliver, S. N., Finnegan, E. J., Dennis, E. S., Peacock, W. J., and Trevaskis, B. (2009). Vernalization-induced flowering in cereals is associated with changes in histone methylation at the VERNALIZATION1 gene. *Proc. Natl. Acad. Sci. U.S.A.* 106, 8386–8391. doi: 10.1073/pnas.0903566106

Parenicova, L., De Folter, S., Kieffer, M., Horner, D. S., Favalli, C., Busscher, J., et al. (2003). Molecular and phylogenetic analyses of the complete MADS-box transcription factor family in *Arabidopsis*: new openings to the MADS world. *Plant Cell* 15, 1538–1551. doi: 10.1105/tpc.011544

Perilleux, C., Pieltain, A., Jacquemin, G., Bouché, F., Detry, N., D'Aloia, M., et al. (2013). A root chicory MADS box sequence and the *Arabidopsis* flowering repressor FLC share common features that suggest conserved function in vernalization and de-vernalization responses. *Plant J.* 75, 390–402. doi: 10.1111/tpj.12208

Prins, A. H., Vrieling, K., Klinkhamer, P. G. L., and Dejong, T. J. (1990). Flowering behavior of senecio-jacobaea–effects of nutrient availability and size-dependent vernalization. *Oikos* 59, 248–252. doi: 10.2307/3545541

R Core Team (2016). *R: A Language and Environment for Statistical Computing*. Vienna: R Foundation for Statistical Computing.

Ruelens, P., De Maagd, R. A., Proost, S., Theissen, G., Geuten, K., and Kaufmann, K. (2013). FLOWERING LOCUS C in monocots and the tandem origin of angiosperm-specific MADS-box genes. *Nat. Commun.* 4:2280.

Sasani, S., Hemming, M. N., Oliver, S. N., Greenup, A., Tavakkol-Afshari, R., Mahfoozi, S., et al. (2009). The influence of vernalization and daylength on

expression of flowering-time genes in the shoot apex and leaves of barley (*Hordeum vulgare*). *J. Exp. Bot.* 60, 2169–2178. doi: 10.1093/jxb/erp098

Schubert, D., Primavesi, L., Bishopp, A., Roberts, G., Doonan, J., Jenuwein, T., et al. (2006). Silencing by plant Polycomb-group genes requires dispersed trimethylation of histone H3 at lysine 27. *EMBO J.* 25, 4638–4649. doi: 10.1038/sj.emboj.7601311

Sheldon, C. C., Burn, J. E., Perez, P. P., Metzger, J., Edwards, J. A., Peacock, W. J., et al. (1999). The FLF MADS box gene: a repressor of flowering in *Arabidopsis* regulated by vernalization and methylation. *Plant Cell* 11, 445–458. doi: 10.1105/tpc.11.3.445

Sheldon, C. C., Conn, A. B., Dennis, E. S., and Peacock, W. J. (2002). Different regulatory regions are required for the vernalization-induced repression of FLOWERING LOCUS C and for the epigenetic maintenance of repression. *Plant Cell* 14, 2527–2537. doi: 10.1105/tpc.004564

Sheldon, C. C., Hills, M. J., Lister, C., Dean, C., Dennis, E. S., and Peacock, W. J. (2008). Resetting of FLOWERING LOCUS C expression after epigenetic repression by vernalization. *Proc. Natl. Acad. Sci. U.S.A.* 105, 2214–2219. doi: 10.1073/pnas.0711453105

Sheldon, C. C., Rouse, D. T., Finnegan, E. J., Peacock, W. J., and Dennis, E. S. (2000). The molecular basis of vernalization: the central role of FLOWERING LOCUS C (FLC). *Proc. Natl. Acad. Sci. U.S.A.* 97, 3753–3758. doi: 10.1073/pnas.97.7.3753

Simao, F. A., Waterhouse, R. M., Ioannidis, P., Kriventseva, E. V., and Zdobnov, E. M. (2015). BUSCO: assessing genome assembly and annotation completeness with single-copy orthologs. *Bioinformatics* 31, 3210–3212. doi: 10.1093/bioinformatics/btv351

Tadege, M., Sheldon, C. C., Helliwell, C. A., Stoutjesdijk, P., Dennis, E. S., and Peacock, W. J. (2001). Control of flowering time by FLC orthologues in *Brassica napus*. *Plant J.* 28, 545–553. doi: 10.1046/j.1365-313x.2001.01182.x

Teper-Bamnolker, P., and Samach, A. (2005). The flowering integrator FT regulates SEPALLATA3 and FRUITFULL accumulation in *Arabidopsis* leaves. *Plant Cell* 17, 2661–2675. doi: 10.1105/tpc.105.035766

Trevaskis, B., Bagnall, D. J., Ellis, M. H., Peacock, W. J., and Dennis, E. S. (2003). MADS box genes control vernalization-induced flowering in cereals. *Proc. Natl. Acad. Sci. U.S.A.* 100, 13099–13104. doi: 10.1073/pnas.1635053100

Trevaskis, B., Hemming, M. N., Dennis, E. S., and Peacock, W. J. (2007). The molecular basis of vernalization-induced flowering in cereals. *Trends Plant Sci.* 12, 352–357. doi: 10.1016/j.tplants.2007.06.010

Tudor, E. H., Jones, D. M., He, Z. S., Bancroft, I., Trick, M., Wells, R., et al. (2020). QTL-seq identifies BnaFT.A02 and BnaFLC.A02 as candidates for variation in vernalization requirement and response in winter oilseed rape (*Brassica napus*). *Plant Biotechnol. J.* 18, 2466–2481. doi: 10.1111/pbi.13421

Wood, C. C., Okada, S., Taylor, M. C., Menon, A., Mathew, A., Cullerne, D., et al. (2018). Seed-specific RNAi in safflower generates a superhigh oleic oil with extended oxidative stability. *Plant Biotechnol. J.* 16, 1788–1796. doi: 10.1111/pbi.12915

Wood, C. C., Robertson, M., Tanner, G., Peacock, W. J., Dennis, E. S., and Helliwell, C. A. (2006). The *Arabidopsis thaliana* vernalization response requires a polycomb-like protein complex that also includes VERNALIZATION INSENSITIVE 3. *Proc. Natl. Acad. Sci. U.S.A.* 103, 14631–14636. doi: 10.1073/pnas.0606385103

Yan, L., Fu, D., Li, C., Blechl, A., Tranquilli, G., Bonafede, M., et al. (2006). The wheat and barley vernalization gene VRN3 is an orthologue of FT. *Proc. Natl. Acad. Sci. U.S.A.* 103, 19581–19586. doi: 10.1073/pnas.0607142103

Yan, L., Loukoianov, A., Tranquilli, G., Helguera, M., Fahima, T., and Dubcovsky, J. (2003). Positional cloning of the wheat vernalization gene VRN1. *Proc. Natl. Acad. Sci. U.S.A.* 100, 6263–6268. doi: 10.1073/pnas.0937399100

Yan, L. L., Loukoianov, A., Blechl, A., Tranquilli, G., Ramakrishna, W., SanMiguel, P., et al. (2004). The wheat VRN2 gene is a flowering repressor down-regulated by vernalization. *Science* 303, 1640–1644. doi: 10.1126/science.1094305

Yazdisamadi, B., and Zali, A. A. (1979). Comparison of winter-type and spring-type safflower. *Crop Sci.* 19, 783–785. doi: 10.2135/cropsci1979.0011183x001900060009x

Yeoh, C. C., Balcerowicz, M., Zhang, L. L., Jaudal, M., Brocard, L., Ratet, P., et al. (2013). Fine mapping links the FTa1 flowering time regulator to the dominant spring1 locus in medicago. *PLoS One* 8:e53467. doi: 10.1371/journal.pone.0053467

Yin, S., Wan, M., Guo, C. C., Wang, B., Li, H., Li, G., et al. (2020). Transposon insertions within alleles of BnaFLC.A10 and BnaFLC.A2 are associated with seasonal crop type in rapeseed. *J. Exp. Bot.* 71, 4729–4741. doi: 10.1093/jxb/eraa237

Zohary, D., Hopf, M., and Weiss, E. (2012). *Domestication of Plants in the Old World The origin and Spread of Domesticated Plants in South-West Asia, Europe, and the Mediterranean Basin Fourth Edition Preface to the Fourth Edition*, 4th Edn. Oxford: Oxford University Press.

Conflict of Interest: The authors declare that the research was conducted in the absence of any commercial or financial relationships that could be construed as a potential conflict of interest.

Copyright © 2021 Cullerne, Fjellheim, Spriggs, Eamens, Trevaskis and Wood. This is an open-access article distributed under the terms of the Creative Commons Attribution License (CC BY). The use, distribution or reproduction in other forums is permitted, provided the original author(s) and the copyright owner(s) are credited and that the original publication in this journal is cited, in accordance with accepted academic practice. No use, distribution or reproduction is permitted which does not comply with these terms.

frontiers in Plant Science

ORIGINAL RESEARCH
published: 13 April 2021
doi: 10.3389/fpls.2021.640163

A 598-bp InDel Variation in the Promoter Region of *Bna.SOC1.A05* Is Predominantly Present in Winter Type Rapeseeds

*Sarah Matar and Siegbert Melzer**

Plant Breeding Institute, Christian-Albrechts-University of Kiel, Kiel, Germany

During rapeseed domestication and breeding, genetic diversity allowed to adapt it to different eco-geographical regions and to shape its useful traits. Structural variations (SVs), including presence/absence variations (PAVs), are thought to play a major role in the genetic diversity and phenotypic plasticity of rapeseed. In this study, we detected a 598-bp PAV within the promoter region of an *Arabidopsis* ortholog of a major flowering time gene and a downstream target of *FLC*, *SOC1*, which is one of the first genes that are upregulated in rapeseed during vernalization. Further analysis showed that the insertion is present predominantly in winter types while absent in spring types. The 589-bp sequence is present only in the A sub-genome indicating that it originated from *Brassica rapa*. Since the genomic region around *Bna.SOC1.A05* showed a strong reduction in nucleotide diversity, the insertion might represent a larger selected sweep for rapeseed adaptation. Cis-element analysis showed that the insertion contains an ACGTG box, which is the strongest binding motif for the HY5 transcription factor in *Arabidopsis*. In addition, expression analyses showed that mRNA levels of *Bna.SOC1.A05* were lower in accessions carrying the insertion compared to the ones that had no insertion.

Keywords: *Brassica napus*, *Bna.SOC1*, flowering, structural variation, presence/absence variation

OPEN ACCESS

Edited by:
Caroline Dean,
John Innes Centre, United Kingdom

Reviewed by:
Jo Hepworth,
John Innes Centre, United Kingdom
Min Chul Kim,
Gyeongsang National University, South Korea

***Correspondence:**
Siegbert Melzer
s.melzer@plantbreeding.uni-kiel.de

Specialty section:
This article was submitted to Plant Development and EvoDevo, a section of the journal Frontiers in Plant Science

Received: *10 December 2020*
Accepted: *11 March 2021*
Published: *13 April 2021*

Citation:
Matar S and Melzer S (2021) A 598-bp InDel Variation in the Promoter Region of Bna.SOC1.A05 Is Predominantly Present in Winter Type Rapeseeds. Front. Plant Sci. 12:640163. doi: 10.3389/fpls.2021.640163

INTRODUCTION

Rapeseed (*Brassica napus*) is an allotetraploid crop formed by spontaneous interspecific hybridization of two diploid species; *Brassica rapa* and *Brassica oleracea* around 7,500 years ago (Chalhoub et al., 2014). In the last decades, rapeseed evolved rapidly to become one of the most important oil crops grown worldwide. Its dynamic allopolyploid genome plays a prime role in its diversification and adaptation to different natural environments. According to vernalization requirement, *B. napus* can be divided into three different growth types; winter, semi-winter, and spring rapeseed (Zou et al., 2019). Winter types are grown mainly in Europe; they have an obligate vernalization requirement, and are suggested to be the original type of rapeseed (Lu et al., 2019). Spring types are grown in Australia and North America and flower without any vernalization requirement. Semi-winter types were formed gradually after the introduction of winter types into China in the 20th century, where they were adapted to flower after a short period of vernalization (Qian et al., 2006). The divergence in growth types

of rapeseed accessions has been associated mainly to allelic variation, represented by short (SNPs or InDels) or large-scale structural variations (SVs), within or upstream of flowering time genes, especially in vernalization responsive genes such as *Bna.FRI (FRIGIDA) Bna.FLC (FLOWERING LOCUS C)* and downstream targets like *Bna.FT* genes (*FLOWERING LOCUS T*; Wang et al., 2011; Wu et al., 2019).

Whole genome sequencing of *B. napus* revealed a highly complex and redundant genome, with high frequency of homologous exchanges between the two subgenomes (Chalhoub et al., 2014). Homologous exchanges can be translocations, duplications, and deletions, which lead to extensive presence/absence variations (PAVs) and segmental deletions, therefore representing an additional source of genetic diversity (Schiessl et al., 2017; Hurgobin et al., 2018). Several studies have revealed the association of PAVs with important agronomic traits such as disease resistance and oil content in rapeseed (Liu et al., 2012; Qian et al., 2016; Stein et al., 2017; Gabur et al., 2018). For instance, deletion of the orthologous *Arabidopsis* gene *NON-YELLOWING 1* (*NYE1*; *Bna.NYE.A01*) was associated with increased chlorophyll content, which simultaneously affected oil-content and adaptation to cooler environments (Qian et al., 2016). It is known that transposable elements are another important driving force for genomic diversity. They can affect gene functions through insertions into coding regions, or influence gene expression through insertion into regulatory elements or by affecting local chromatin structure (Lisch, 2013; Chuong et al., 2017; Anderson et al., 2019). For instance, the insertion of tourist-like miniature inverted-repeat transposable elements (MITE), upstream of the *Bna.FLC.A10* gene was found to be associated with vernalization requirement (Hou et al., 2012). Moreover, an 810-bp MITE insertion in exon 7 of *Bna.FLC.A02* silenced the gene and was found to be associated with a spring habit of rapeseed plants lacking the MITE insertion in *Bna.FLC.A10* (Yin et al., 2020). Recently, a study revealed that up to 10% of genes in the rapeseed genome are affected by SVs, for which half of these variations are between 100 to 1,000 bp long (Chawla et al., 2020). The study also reported a SV upstream of *Bna.FT.A02* that was associated with the eco-geographical distribution of different rapeseed cultivars. Therefore, studying SVs in flowering time genes might be a useful approach to further understand the history of evolution and adaptation of rapeseed and it might also facilitate the development of molecular markers to differentiate between different growth types.

Assuming that genomic variation in other flowering time genes might have also played a role in the evolution and divergence of rapeseed, we analyzed SVs within and upstream of orthologs of key downstream targets of *Bna.FLC* genes. We used the comprehensive resource of genomic sequences of a worldwide collection of 991 rapeseed germplasms (Wu et al., 2019) from which we selected 80 accessions with relatively high sequencing depth. As we compared the upstream regions of certain flowering time genes between spring and winter accessions, we uncovered a previously unidentified sequence insertion upstream of *Bna.SOC1.A05*, which is associated with winter types. We also confirmed this variation in the ASSYST *B. napus* diversity set (Bus et al., 2011). Further analysis suggested that the sequence was inserted in the promoter region of *Bna.SOC1.A05* after the merge of the two ancestral genomes. Evidence of a selective sweep was reflected by the dramatic reduction of nucleotide diversity in the region harboring this insertion compared to its surrounding region. The strong co-segregation of this SV with the crop type indicated an additionally and potentially crucial role of this genomic re-arrangement for the eco-geographical adaptation of rapeseed.

MATERIALS AND METHODS

Plant Materials and Growth Conditions

For expression analysis, the two spring rapeseed accessions that carry the insertion, Bingo and Adamo, and the winter inbred line Express617, from ERANET-ASSYST panel (Bus et al., 2011), in addition to the spring accession Haydn that lacks the insertion, were used. Seeds were sown on soil in 9 cm pots and grown under greenhouse conditions in 16 h-light/8 h-dark cycles at 20°C. Flowering time was measured in days from sowing to opening of the first flower.

RNA Extraction and Expression Analysis

For RT-qPCR, leaves and shoot apices were sampled at 2, 4, and 6 weeks after sowing. Apical buds were dissected under a binocular microscope using scalpel and forceps and immediately frozen in liquid nitrogen. Around 8–10 apical buds were pooled for one biological replicate. RNA isolation and DNase treatment were carried out according to the instruction manual provided with the PeqGold Total RNA Kit (PeqLab, Germany).

RT-qPCR was performed for three biological replicates each with three technical repeats for each time point. RT-qPCR was carried out using Platinum™ SYBR™ Green qPCR SuperMix (ThermoFischer Scientific). Expression levels were calculated with the comparative $\Delta\Delta$Ct method (Livak and Schmittgen, 2001). Primers used for gene expression analysis are listed in (**Supplementary Table S1**). *Bna.ACTIN2* was used to normalize gene expression levels.

Transcriptome Analysis

For RNA-Seq analyses, the raw RNA-Seq reads of 72 rapeseed accessions including 31 winter and 41 spring types from a previous transcriptomics study (Harper et al., 2012; Havlickova et al., 2018) were downloaded from SRA NCBI[1] using parallel-fastq-dump. The reads were mapped to the Express617 genome (Matar et al., 2021) using STAR (Dobin et al., 2013; v.2.5.4). For transcriptome assembly, the RNA-Seq read alignments were used as an input file to run Cufflinks (v2.2.1; Trapnell et al., 2012). The Cufflinks module Cuffnorm was used to generate normalized transcript expression levels [normalized fragments per kilobase per million mapped reads (FPKM)] from all rapeseed accessions studied. Expression levels of six *Bna.SOC1* genes were plotted in RStudio (Boston, Massachusetts), using the data visualization package ggplot2 (Wickham, 2011).

[1]https://www.ncbi.nlm.nih.gov/search/all/?term=PRJNA309367

Sequence Analysis and Detection of Presence/Absence Variation

Whole genome sequencing data of 80 rapeseed accessions were downloaded from SRA NCBI (https://www.ncbi.nlm.nih.gov/sra/SRP155312; Wu et al., 2019) using parallel-fastq-dump. Reads of each accession were mapped to the Darmor-*bzh*-based genome assembly of winter rapeseed Express617 (Matar et al., 2021) using Burrows-Wheeler Aligner mem (BWA-MEM v.0.7.17) software package (Li and Durbin, 2009). Visual detection of read alignments was performed using the Integrative Genome Viewer (IGV). Per base depth of coverage was calculated for each accession at the genomic region of six *Bna.SOC1* orthologs in the Express617 genome, including 3,000 bp upstream, using Samtools (Li et al., 2009). PCR using genomic DNA from the ASSYST *B. napus* diversity set of different spring and winter rapeseed accessions (Bus et al., 2011), followed by Sanger sequencing was used to further confirm the PAV. Sequence alignment was visualized on the multiple sequence alignment visualization and editing program Jalview (Waterhouse et al., 2009).

NSITE-PL (Solovyev et al., 2010) was used to analyze the putative promoter region and the composition of functional motifs upstream of *Bna.SOC1.A05*, of other *Bna.SOC1* orthologs in addition to *At.SOC1*.

Phylogenetic Analysis

For evolutionary analyses, SNPs within 10.5 kb genomic fragments including the insertion and 5,000 bp flanking sequence were extracted from whole genome SNP files of 80 rapeseed accessions (Wu et al., 2019). The neighbor-joining tree cladogram was constructed using Tassel software package (v5.2.59), and visualized using iTOL. To study whether the upstream region of *Bna.SOC1.A05* was under selection, nucleotide diversity (π) was calculated for chromosome A05 using VCFtools (v0.1.13) in a 1,000 bp sliding window with 100 bp steps.

Screening of Homologous Sequences in *Brassica napus* and *Brassica rapa* Genomes

To identify homologous sequences, the inserted sequence was queried against the Express617 and *B. rapa* (Chiifu-401-42) reference genomes using BLAST+ package from NCBI. Circos software package (Krzywinski et al., 2009) was used to visualize the position of the insertion sequence in *B. napus* and *B. rapa* genomes. RepeatMasker Web Server[2] and MITE-Tracker (Crescente et al., 2018) were used to search for putative repetitive and transposable elements. Multiple sequence alignments and phylogenetic analyses of homologous sequences from *B. napus* and *B. rapa* were performed using the multiple sequence alignment program Clustal Omega (McWilliam et al., 2013).

RESULTS

A 598-bp PAV Upstream of *Bna.SOC1.A05* Co-segregates With Crop Type in Rapeseed

Previously, we identified certain flowering time genes that were upregulated in the shoot apical meristem in winter rapeseed upon the downregulation of *Bna.FLC* during vernalization. These genes included orthologs of the flowering time integrator and downstream target of *FLC*, *SOC1*, in addition to certain members of the *SPL* gene family (Matar et al., 2021). To study SVs between spring and winter rapeseed cultivars, within or upstream of the identified genes, we used the whole genome sequencing reads of 40 winter and 40 spring accessions, with an average sequencing depth ranging from 5 to 23. The reads were aligned to our Darmor-bzh reference-based genome assembly of the winter rapeseed cultivar Express617 (Matar et al., 2021), using Bwa-mem (v.0.7.17). We first carried out a visual detection of read alignments using IGV with a mapping quality threshold of 5. We observed that certain accessions had no reads that mapped upstream to a distinct region of *Bna.SOC1.A05* (**Supplementary Figure S1**) indicating the presence of a SV upstream of the gene. A closer examination showed that most of the spring accessions had no reads mapping to this region, while in most of the winter accessions reads were mapping. To further ascertain the boundaries of this SV, we used Samtools to calculate the depth of coverage in the genomic regions including the gene sequence and 3,000-bp upstream of *Bna.SOC1.A05*. At 1.8-kb upstream of *Bna.SOC1.A05* (**Figure 1A**), the sequencing coverage in spring accessions gradually dropped to zero, while in winter accessions it remained at the same level (**Figure 1B**). Average sequence coverage was higher in winter types compared to spring types because certain spring types had low sequencing depth (**Figure 1B**). The sequence-depth analysis further confirmed the segregation of the SV between winter and spring types, where more than 87% of the spring accessions showed absence of the genomic sequence at the analyzed region, while 85% of the winter accessions showed the presence of the insertion (**Figure 1C**; **Supplementary Table S2**). Therefore, we concluded that this SV upstream of *Bna.SOC1.A05* segregates with the growth types of *B. napus*.

None of the other analyzed *Bna.SOC1* paralogs or the *Bna.SPL* genes showed a SV similar to that observed for *Bna.SOC1.A05*. Based on SNP data of a 10.5-kb region flanking the insertion, we performed a phylogenetic analysis and found that the 80 rapeseed accessions were clustered into two groups that corresponded largely to winter and spring crop types, which suggested that the genomic variation in the region containing the insertion and *Bna.SOC1.A05* might have contributed to growth-type diversification (**Supplementary Figure S3**).

The 598-bp Insertion in the Upstream Region of *Bna.SOC1.A05* Originated From *Brassica rapa*

Low sequencing depth is not always reliable to detect SVs; therefore, we further validated the PAV upstream of *Bna.SOC1.A05 via* PCR with flanking primers and using genomic DNA from spring and winter accessions of the ASSYST-PANEL (Bus et al., 2011). The variation could be clearly distinguished by PCR, and showed that an insertion is present in 25 out of 30 of the winter types but absent in 27 out of 30 of the

[2]http://www.repeatmasker.org

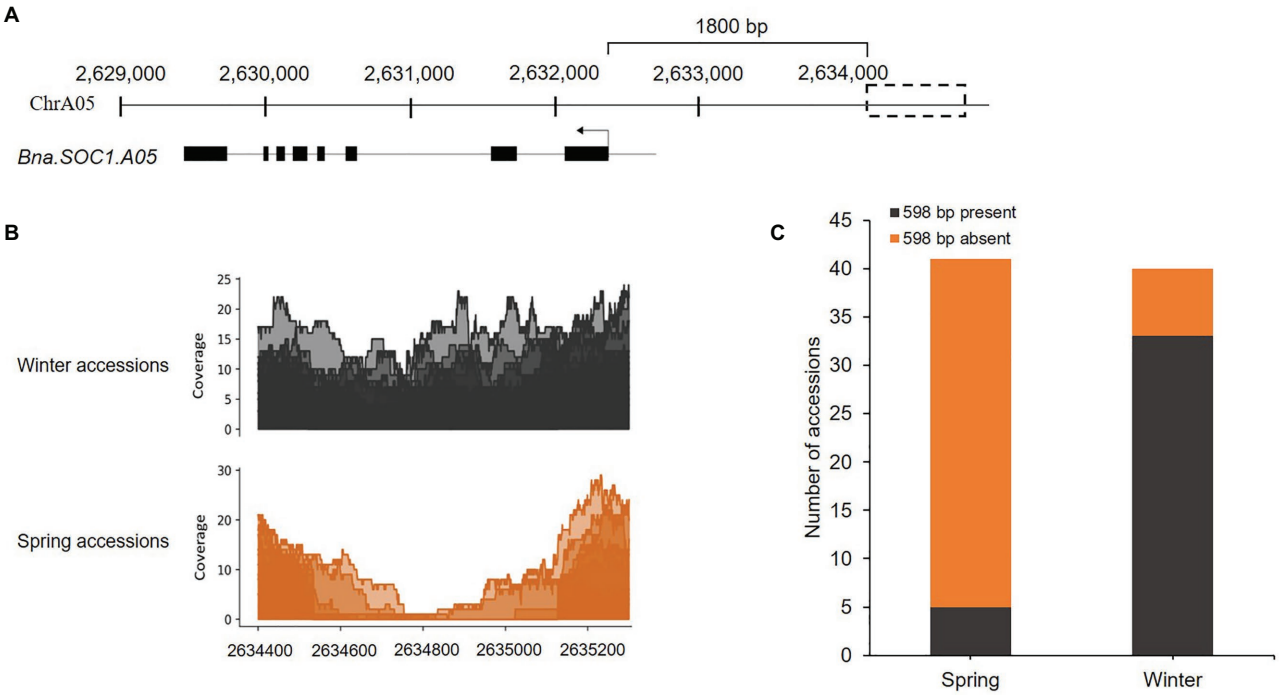

FIGURE 1 | Presence/absence variation (PAV) upstream of *Bna.SOC1.A05* is associated with growth type. **(A)** Genomic region harboring *Bna.SOC1.A05* and the PAV in Express617 genome (dotted box). **(B)** Per base depth of coverage in the region 2,634,400 to 2,635,200, showing drop in coverage in the spring accessions. **(C)** Stack plot showing the presence of the insertion in 85% of the winter accession and deletion in 87% of the spring accessions studied.

spring types (**Supplementary Table S3**). Out of the 60 tested accessions from the ASSYST panel, 22 accessions were common with accessions from the whole genome sequencing data. The PCR results of the 22 rapeseed accessions were in accordance with the whole genome sequencing data.

The PCR products from different rapeseed genotypes were Sanger sequenced and aligned. The insertion upstream of *Bna.SOC1.A05* and the region flanking the insertion site showed a high sequence identity in all accessions tested (98–100%), indicating that this intergenic region is conserved among different rapeseed genotypes (**Supplementary Figure S2**). The insertion sequence had no sequence similarity to repetitive and transposable elements on the RepeatMasker web server. In addition, the MITE annotating software, MITE Tracker (Crescente et al., 2018) did not annotate the insertion sequence as a putative MITE. Further sequence analysis showed that the first 151 nucleotides are only present in these sequences, however, the following 313 nucleotides, showed a high sequence identity (*e*-value < 7*e*-29) with the gene *SIMILAR TO RCD ONE 2* (*SRO2*) from *Arabidopsis*. SRO2 proteins have a poly (ADP-ribose) polymerase (PARP) domain, which is a signature domain known to modify a variety of proteins by attaching the ADP-ribose-moiety from NAD+ to the target molecule (Kraus and Lis, 2003). PARPs are best studied in mammals and they have a broad range of functions, including DNA repair, genome integrity, and epigenetic regulation (Citarelli et al., 2010). Analysis of cis-regulatory elements in the inserted fragment uncovered an ACGTG box, which has been shown to be the strongest element for binding the ELONGATED HYPOCOTYL 5 (HY5) transcription factor in *Arabidopsis* (Burko et al., 2020; **Figure 2A**). It is worth mentioning that four functional homologs of the *SRO2* gene are present with two copies in each subgenome of rapeseed.

To trace the origin of the 598-bp DNA fragment, we performed a local blast search and identified three homologous sequences of the insertion sequence (*e*-value = 0.0) that were present only in the A subgenome (**Figure 2B**; **Supplementary Table S4**), indicating that the sequence might have originated from *B. rapa*. A local blast search of the insertion sequence identified four homologous sequences (*e*-value < 9.41*e*-75) in the *B. rapa* genome (Chiifu-401-42; **Supplementary Table S5**). However, none of the homologous sequences that were identified in *B. rapa*, were located on chromosome A05 (**Figure 2B**), and the upstream region of *Br.SOC1.A05* was almost 100% identical to the upstream sequence of *Bna.SOC1.A05* in the spring rapeseed accessions. Chromosome A06 in *B. rapa* carries two copies of the insertion, while the other copies are present on chromosomes A10 and A09 (**Figure 2B**). We also analyzed sequences of other *B. rapa* accessions, including winter turnip that was suggested to be the ancestor of *B. napus* (Lu et al., 2019), but no insertion was found on chromosome A05. This indicates that, although the sequence was present in the *B. rapa* genome, it was inserted upstream of *Bna.SOC1.A05* only after the hybridization of the two ancestral genomes.

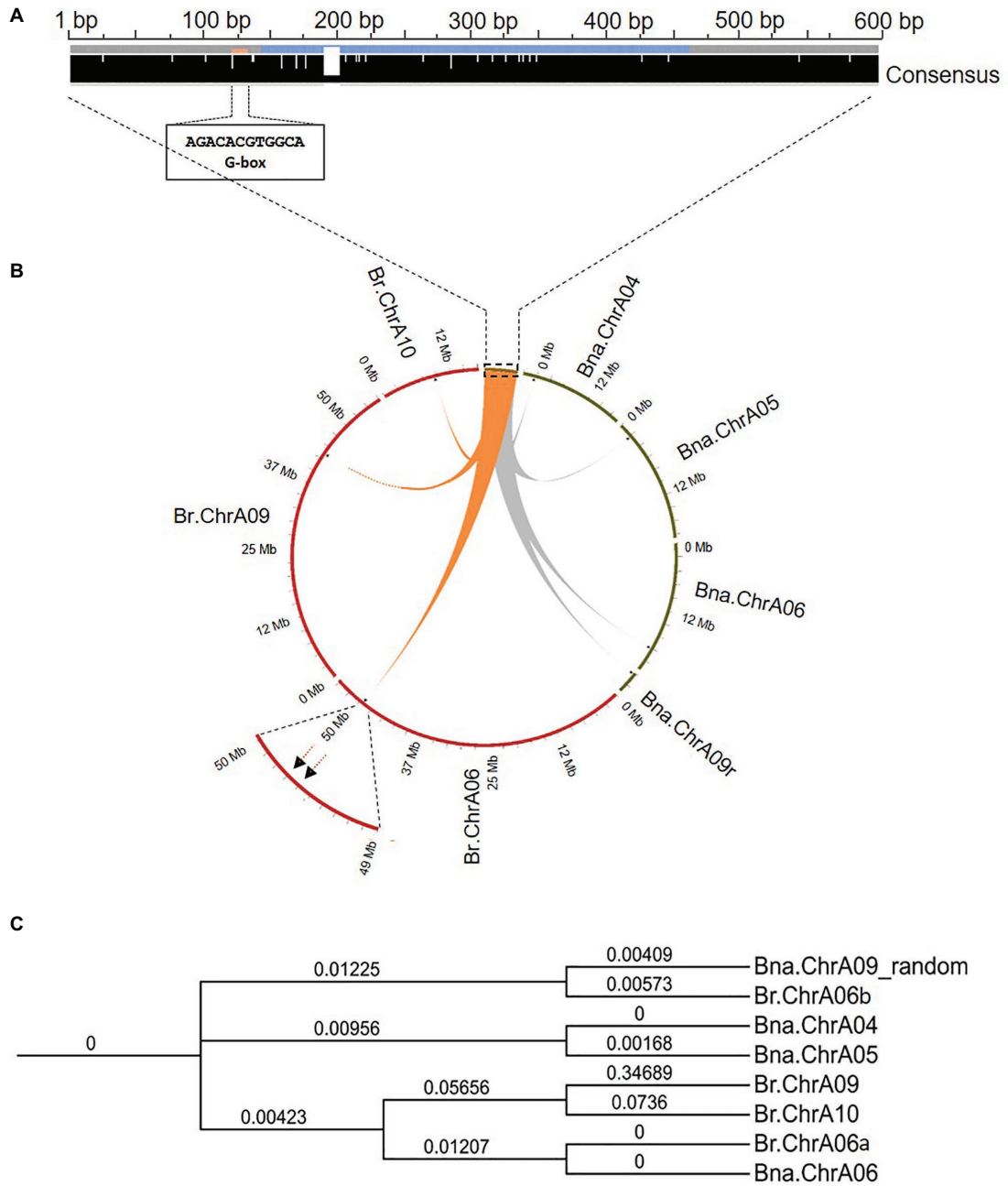

FIGURE 2 | Sequence analysis and genomic positions of the insertion-homologous sequences in *Brassica napus* and *Brassica rapa*. **(A)** Multiple sequence alignment of the four homologous sequences from *B. napus*, showing consensus (black bar) with a high modal residue per column, and the postion of the G-box HY5 binding motif. Blue color in the middle of the insertion sequence corresponds to the region matching to *SRO2*. **(B)** Circos plot showing genomic positions of the insertion-homologous sequences on chromosomes of *B. rapa* (red) and *B. napus* (green). **(C)** Phylogenetic tree showing the evolutionary relationship between the eight identified sequences in the genomes of *Bna. napus* and *B. rapa*.

To estimate the evolutionary relationship between the identified homologous sequences from *B. napus* and *B. rapa* genomes, we conducted a phylogenetic analysis using multiple sequence alignment of the eight identified sequences. Phylogenetic analysis of the homologous sequences was constructed using Clustal Omega and resulted in four distinct pairs (**Figure 2C**), where the sequence on chromosome A06 in *B. rapa* (Br. ChrA06a) and its surrounding sequences showed 100% identity to that on Bna.ChrA06, indicating that the sequence on Bna. ChrA06 is the same as that on Br.ChrA06. The other sequence on the *B. rapa* chromosome A06 (Br.ChrA06b) showed a high sequence identity to the insertion sequence on Bna.

ChrA09-random (**Figure 2C**). Insertions on chromosomes A04 and A05 in *B. napus* formed a separate clade, and showed less sequence identity to sequences on Br.ChrA10 and Br. ChrA09 compared to that on Br.ChrA06 (**Figure 2C**; **Supplementary Table S5**), suggesting that the sequences on Bna.ChrA04 and Bna.ChrA05 are distinct from the sequences on Br.ChA10 and Br.Chr.A09, and that they might have arisen in the *B. napus* genome and were not present the *Br. rapa* genome.

Reduced Nucleotide Diversity in the Genomic Region Surrounding *Bna.SOC1.A05*

To determine whether the genomic region harboring the insertion was potentially affected by selection, we used whole genome SNP information, of the 80 rapeseed accessions studied, to analyze nucleotide diversity in the region around *Bna.SOC1.A05* (*BnaA05g05010D*), compared to the nucleotide diversity of 40-kb surrounding that region (**Figure 3A**). The rapeseed accessions exhibited dramatically reduced nucleotide diversity in a genomic region of 15 kb (**Figures 3B,C**). In addition to *Bna.SOC1.A05*, a homolog of the MADS-box gene *AGAMOUS-LIKE 6* (*AGL6*; *BnaA05g05000D*) is also present in this region (**Figure 3A**). The low level of diversity in the genomic region suggests that the region has evolved under functional constraints.

Bna.SOC1.A05 Is Highly Expressed in Spring Types Lacking the Insertion

To get an idea whether the PAV is associated with transcriptional activity of the *Bna.SOC1.A05* gene, we compared the expression of three spring accessions and one winter rapeseed accession. Two spring accessions that carried the insertion upstream of *Bna.SOC1.A05* were from the ERRANET-ASSYST panel, and the third spring accession was Haydn that has no insertion. The winter accession was Express617 that carries the insertion. We analyzed expression levels in apices of 2, 4, and 8 week-old plants and found that the expression of *Bna.SOC1.A05* was consistently lower in Bingo and Adamo compared to Haydn (**Figure 4A**). In fact, the expression levels of *Bna.SOC1.A05* were more comparable to that of the winter accessions Express617 (**Figure 4A**). In addition, Haydn flowered around 55 days after sowing, while Adamo and Bingo flowered 5 and 10 days later (**Figure 4B**). However, the expression of *Bna.SOC1.A05* did not explain the difference in flowering time between Bingo and Adamo, as Adamo was earlier flowering, but exhibited lower expression levels of *Bna.SOC1.A05*.

To further study the expression level of *Bna.SOC1.A05* in comparison to other *Bna.SOC1* genes, we analyzed the leaf transcriptome of 72 rapeseed accessions, including 31 winter and 41 spring accessions. The whole transcriptome reads

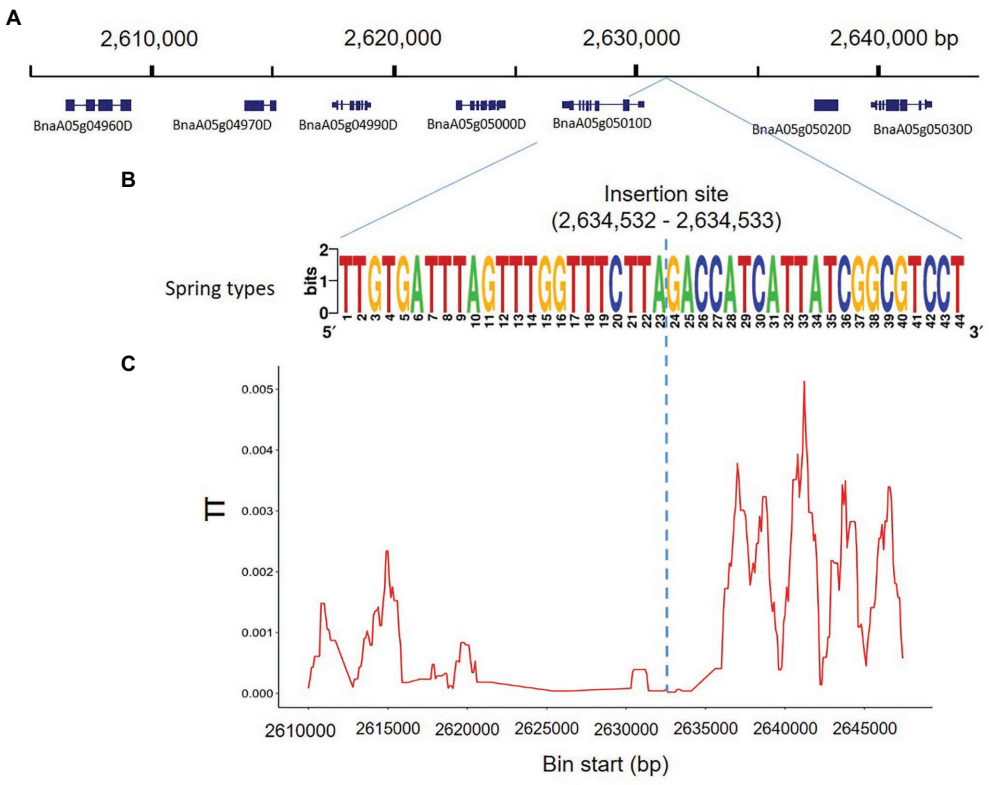

FIGURE 3 | Nucleotide diversity accross the insertion site on chromosome 5. **(A)** 0.4-Mb genomic region surrounding the insertion sequence, and the genes annotated in this region according to Darmor-*bzh* reference genome. **(B)** The consenus sequence covering the breakpoint of the PAV in 18 rapeseed accessions. The breakpoint of the PAV is located between 2,634,532 and 2,634,533 in Darmor-*bzh* reference genome. **(C)** Nucleotide diversity (π) calculated based on SNP data of the 80 studied rapeseed accessions showing reduced nucleotide diversity in the region 2,620,000–2,635,000 surrounding the PAV.

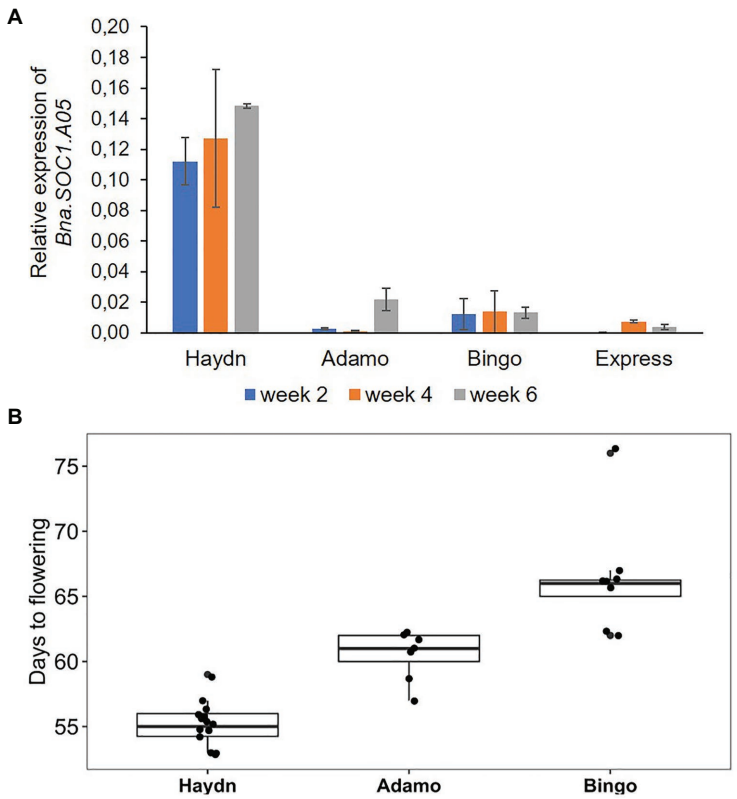

FIGURE 4 | Expression and flowering time variation in different rapeseed accessions. **(A)** Expression levels of *Bna.SOC1.A05* in the apices four different rapeseed accessions, 2, 4, and 6 weeks after sowing. Expression was normalized to *Bna.Actin2*. Error bars represent SEM of three biological replicates. **(B)** Days to flowering determined by scoring the opening of the first flower in three different spring accessions.

(Havlickova et al., 2018) were downloaded from SRA NCBI and mapped to the Express617 genome assembly. The 60 ASSYST panel accessions that were genotyped for the PAV were also included in the RNA-seq analysis.

The expression levels of all *Bna.SOC1* genes in winter accessions were significantly lower than the expression of *Bna.SOC1* in spring accessions, except for *Bna.SOC1.C04* (**Figure 5**). This is expected considering that flowering in winter types is vernalization dependent, and that winter types are expected to have higher levels of *Bna.FLC* (Schiessl et al., 2019). In spring types, *Bna.SOC1.A03-random* and *Bna.SOC1.A04* showed the highest expression levels compared to other *Bna.SOC1* genes (**Figure 5**). Interestingly, in winter types, *Bna.SOC1.A05* was the only gene that was not detected before vernalization (**Figure 5**). In a transcriptome analysis of the winter accession during the course of vernalization, *Bna.SOC1.A05* was the first gene to be induced during floral transition (Matar et al., 2021). This tight vernalization-controlled expression of *Bna.SOC1.A05* further reinforces a pivotal role of this gene for the vernalization-driven floral transition in winter rapeseed. Further analysis of *Bna.SOC1* expression showed that the expressions levels *Bna.A03-random* and *Bna.SOC1.A04* were higher in Adamo compared to Bingo (**Figure 5**), which might explain the earlier flowering of Adamo.

DISCUSSION

In addition to SNPs and InDels, SVs, represented mainly by PAVs are prevalent in the *B. napus* genome, and are believed to be a driving force for its diversification and adaptation to different environments. Several studies have investigated the genetic variation of flowering-time divergence among the three rapeseed crop types. Most of the studies focused on the orthologs of *FLC*, as major genes contributing to the vernalization requirement, thus to the divergence between spring and winter types. PAVs upstream of certain *Bna.FLC* genes have been shown to be associated with flowering-time divergence in rapeseed (Hou et al., 2012; Yin et al., 2020).

Since downstream targets of *Bna.FLC* genes, might have also played a role in the evolution and diversification of flowering-time in rapeseed, we analyzed SVs within and upstream of orthologs of key downstream targets of *Bna.FLC*. Utilizing the comprehensive resource of genomic sequences of a worldwide collection of 991 rapeseed accessions (Wu et al., 2019), we looked for SVs within or upstream of orthologs of *Bna.SOC1* genes. Detection of SVs requires a high sequencing depth; therefore, we started to analyze only accessions that had a sequencing depth of 10X or more. However, out of 991 accessions, 188 were spring types, from which only few had sequencing depths

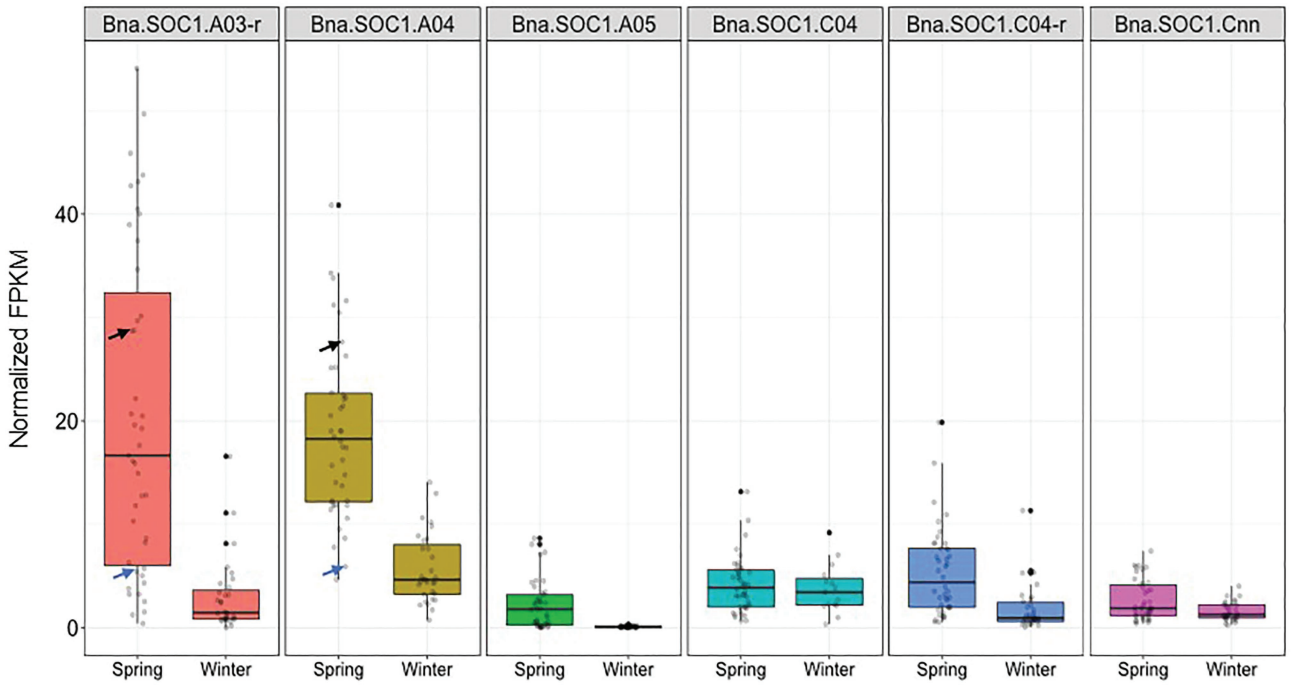

FIGURE 5 | Expression levels of *Bna.SOC1* genes in spring and winter rapeseed accessions. Boxplot of normalized fragments per kilobase per million mapped reads (FPKM) values of the six *Bna.SOC1* paralogs in leaf transcriptome of 31 winter and 41 spring rapeseed accessions. Black arrow corresponds to the normalized FPKM values of Adamo, while blue arrows correspond to the normalized FPKM values of Bingo.

of more than 10X (Wu et al., 2019). Therefore, our set of spring types included accessions with sequencing depth of 5 and 6X.

SOC1 is a main floral integrator and a downstream target of *FLC* in *Arabidopsis* (Searle et al., 2006; Lee and Lee, 2010). In a previous study, we showed that two *Bna.SOC1* paralogs, *Bna.SOC1.A05* and *Bna.SOC1.C04-random*, are significantly induced during vernalization (Matar et al., 2021), suggesting a significant role of these two genes in floral transition. Analysis of the upstream regions of the *Bna.SOC1* genes, uncovered a 598-bp PAV upstream of *Bna.SOC1.A05*. The PAV is located 1.8-kb upstream of the transcription start site, suggesting that it is part of the promoter region of *Bna.SOC1.A05*. We used genomic DNA of accessions from the ERANET-ASSYST panel to further confirm the PAV by PCR. More than 90% of the tested spring accessions lacked the insertion, while around 84% of the winter accessions had the insertion (**Supplementary Table S3**), indicating that this PAV is associated with crop type in rapeseed.

Although it is in an intergenic region, sequencing of the insertion from different rapeseed accessions showed that the sequence is highly conserved, which suggested that the insertion is of functional importance and might contain certain motifs that are relevant to the activity of the downstream gene. Motif analysis revealed a CACGTG box, which is known to be a binding site for the transcription factors HY5 (Burko et al., 2020). In *Arabidopsis*, *SOC1* mediates the crosstalk between cold response and flowering through regulating cold-responsive (COR) genes (Seo et al., 2009). *SOC1* is known to be a downstream target of HY5, but through the binding motif CACGTA (Lee et al., 2007), which was also present in the promoter region of *Bna.SOC.A05*. Using SNP data from Wu et al. (2019), we observed that the sequence conservation is not only in the inserted sequence but also is extended to the surrounding genomic region. This extremely low nucleotide diversity was probably caused by a selective sweep including the presence of the insertion in winter types while its absence in spring types.

Presence/absence variations in the promoter regions can affect the expression level or pattern of the corresponding downstream gene. Changes in expression might be due to new cis-regulatory elements that are introduced to the region, or due to the elimination of certain motifs that were present at the breakpoint of the insertion. Changes in expression could also be a result of DNA methylation levels in the inserted sequence. In a study that aimed to understand the evolution of *SOC1* sequences, expression and regulation in *Brassica* species, Sri et al. (2020) showed that divergence in regulatory sequences was correlated with the expression divergence of different *SOC1* orthologs in *Brassica juncea*. The study also showed that *Brassica SOC1* promoters comprised most of *A. thaliana* transcription factor binding sites (TFBSs), with homolog specific loss or conservation of certain binding sites. The effect of loss of certain TFBS was tested *via* analysis of reporter gene expression pattern. For instance, one of the *SOC1* homologs (*BjuSOC1AAMF1*) had lost its function due to loss of critical TFBS in its promoter region. In addition, Sri et al. (2020) analyzed sequence length and distribution of

TFBS in promoters of six *SOC1* homologs in *B. napus* which also showed diversification in length and TFBS content. In our analysis, the expression level of *Bna.SOC1.A05* in the two accessions that contained the insertion was significantly lower than in the spring accessions that lacked the insertion. Since the expression levels of *Bna.SOC1.A05* did not correlate with flowering time, we analyzed the expression levels of other *Bna.SOC1* paralogs using leaf transcriptome data from Havlickova et al. (2018). Interestingly, *Bna.SOC1.A05* was the only gene that was not expressed in 2-week-old winter type plants, indicating that it might be involved in the vernalization driven flowering response in winter rapeseed. In spring types, *Bna.SOC1.A03* showed the highest expression levels, with a higher level in Adamo compared to Bingo, which is in line with the observed flowering time in these two varieties. However, these transcriptome data were from 2-week-old plants and might not reflect the activity of the genes directly before and during the transition to flowering.

Further analyses revealed that the inserted sequence has three homologous sequences in the *B. napus* A genome, indicating that the sequences originated from the *B. rapa* ancestor. Surprisingly, analyses of homologous sequences in *B. rapa* showed that the sequences are not located on the same chromosomes as in *B. napus* A genome, except for one sequence that is present on chromosome A06, indicating that these sequences might be mobile by a hitherto unknown mechanism. As the upstream region of *Br.SOC1.A05* was similar to that in spring types, it is evident that this 598-bp sequence was introduced to the upstream region of *Bna.SOC1.A05* after the hybridization event. The known PAVs upstream of certain *Bna.FLC* genes are MITE-like transposable elements that were activated after the generation of *B. napus* and got introduced to the upstream regions of *Bna.FLC* also after hybridization (Hou et al., 2012). However, as our analyses showed that the 598-bp DNA sequence upstream of *Bna.SOC1.A05* is not a transposable element, we were further intrigued to determine how the new insertion appeared on different chromosomes in the *B. napus* genome. The phylogenetic analysis showed that the sequences on chromosomes Bna.ChrA04 and Bna.ChrA05 are distinct from the ones that were found on chromosomes A09 and A10 of *B. rapa* suggesting that they originated in the *B. napus* genome. Although the insertion sequence seems to include a fragment of a PARP gene, the fact that it contains two other unique sequences that are surrounding the PARP fragment and are conserved in all the insertion sequences found in *B. napus*, it is conceivable that the origin of these new sequences is more likely to be from a homologous sequence which was already present in the genome such as that on chromosome A06 and not from any of the SRO2 genes present in the genome. The mechanism by which the exact size of the sequence got translocated or multiplied in the genome is not understandable by current known transposition mechanisms. However, the strong association of this PAV with growth types and the association with *Bna.SOC1.A05* expression might either indicate that this PAV is of functional relevance or was transmitted to all current winter types through breeding history.

DATA AVAILABILITY STATEMENT

The original contributions presented in the study are included in the article/**Supplementary Material**, further inquiries can be directed to the corresponding author.

AUTHOR CONTRIBUTIONS

SMa designed and performed the experiments, conducted the data analysis, and wrote the manuscript. SMe designed the experiments and wrote the manuscript. All authors contributed to the article and approved the submitted version.

FUNDING

This work was financially supported by the German Research Foundation (DFG; ME4457/2-1) and the Federal Ministry of Education and Research (BMBF; FKZ 031B0204B).

ACKNOWLEDGMENTS

We thank Prof. Lixi Jiang for kindly providing the SNP data for 991 rapeseed accessions. We also thank Dr. Smit Shah for kindly providing genomic DNA of the accessions from the ERANET_ASSYST panel. We acknowledge financial support by Land Schleswig-Holstein within the funding programme Open Access Publikationsfonds.

SUPPLEMENTARY MATERIAL

The Supplementary Material for this article can be found online at: https://www.frontiersin.org/articles/10.3389/fpls.2021.640163/full#supplementary-material

REFERENCES

Anderson, S. N., Stitzer, M. C., Brohammer, A. B., Zhou, P., Noshay, J. M., O'Connor, C. H., et al. (2019). Transposable elements contribute to dynamic genome content in maize. *Plant J.* 100, 1052–1065. doi: 10.1111/tpj.14489

Burko, Y., Seluzicki, A., Zander, M., Pedmale, U. V., Ecker, J. R., and Chory, J. (2020). Chimeric activators and repressors define HY5 activity and reveal a light-regulated feedback mechanism. *Plant Cell* 32, 967–983. doi: 10.1105/tpc.19.00772

Bus, A., Körber, N., Snowdon, R. J., and Stich, B. (2011). Patterns of molecular variation in a species-wide germplasm set of *Brassica napus*. *Theor. Appl. Genet.* 123, 1413–1423. doi: 10.1007/s00122-011-1676-7

Chalhoub, B., Denoeud, F., Liu, S., Parkin, I. A. P., Tang, H., Wang, X., et al. (2014). Early allopolyploid evolution in the post-Neolithic *Brassica napus* oilseed genome. *Science* 345, 950–953. doi: 10.1126/science.1253435

Chawla, H. S., Lee, H., Gabur, I., Vollrath, P., Tamilselvan-Nattar-Amutha, S., Obermeier, C., et al. (2020). Long-read sequencing reveals widespread intragenic structural variants in a recent allopolyploid crop plant. *Plant Biotechnol. J.* 19, 240–250. doi: 10.1111/pbi.13456

Chuong, E. B., Elde, N. C., and Feschotte, C. (2017). Regulatory activities of transposable elements: from conflicts to benefits. *Nat. Rev. Genet.* 18, 71–86. doi: 10.1038/nrg.2016.139

Citarelli, M., Teotia, S., and Lamb, R. S. (2010). Evolutionary history of the poly(ADP-ribose) polymerase gene family in eukaryotes. *BMC Evol. Biol.* 10:308. doi: 10.1186/1471-2148-10-308

Crescente, J. M., Zavallo, D., Helguera, M., and Vanzetti, L. S. (2018). MITE tracker: an accurate approach to identify miniature inverted-repeat transposable elements in large genomes. *BMC Bioinform.* 19:348. doi: 10.1186/s12859-018-2376-y

Dobin, A., Davis, C. A., Schlesinger, F., Drenkow, J., Zaleski, C., Jha, S., et al. (2013). STAR: ultrafast universal RNA-seq aligner. *Bioinformatics* 29, 15–21. doi: 10.1093/bioinformatics/bts635

Gabur, I., Chawla, H. S., Liu, X., Kumar, V., Faure, S., von Tiedemann, A., et al. (2018). Finding invisible quantitative trait loci with missing data. *Plant Biotechnol. J.* 16, 2102–2112. doi: 10.1111/pbi.12942

Harper, A. L., Trick, M., Higgins, J., Fraser, F., Clissold, L., Wells, R., et al. (2012). Associative transcriptomics of traits in the polyploid crop species Brassica napus. *Nat. Biotechnol.* 30, 798–802. doi: 10.1038/nbt.2302

Havlickova, L., He, Z., Wang, L., Langer, S., Harper, A. L., Kaur, H., et al. (2018). Validation of an updated associative transcriptomics platform for the polyploid crop species *Brassica napus* by dissection of the genetic architecture of erucic acid and tocopherol isoform variation in seeds. *Plant J.* 93, 181–192. doi: 10.1111/tpj.13767

Hou, J., Long, Y., Raman, H., Zou, X., Wang, J., Dai, S., et al. (2012). A tourist-like MITE insertion in the upstream region of the *BnFLC.A10* gene is associated with vernalization requirement in rapeseed (*Brassica napus L.*). *BMC Plant Biol.* 12:238. doi: 10.1186/1471-2229-12-238

Hurgobin, B., Golicz, A. A., Bayer, P. E., Chan, C.-K. K., Tirnaz, S., Dolatabadian, A., et al. (2018). Homoeologous exchange is a major cause of gene presence/absence variation in the amphidiploid *Brassica napus*. *Plant Biotechnol. J.* 16, 1265–1274. doi: 10.1111/pbi.12867

Kraus, W. L., and Lis, J. T. (2003). PARP goes transcription. *Cell* 113, 677–683. doi: 10.1016/S0092-8674(03)00433-1

Krzywinski, M., Schein, J., Birol, I., Connors, J., Gascoyne, R., Horsman, D., et al. (2009). Circos: an information aesthetic for comparative genomics. *Genome Res.* 19, 1639–1645. doi: 10.1101/gr.092759.109

Lee, J., He, K., Stolc, V., Lee, H., Figueroa, P., Gao, Y., et al. (2007). Analysis of transcription factor HY5 genomic binding sites revealed its hierarchical role in light regulation of development. *Plant Cell* 19, 731–749. doi: 10.1105/tpc.106.047688

Lee, J., and Lee, I. (2010). Regulation and function of *SOC1*, a flowering pathway integrator. *J. Exp. Bot.* 61, 2247–2254. doi: 10.1093/jxb/erq098

Li, H., and Durbin, R. (2009). Fast and accurate short read alignment with burrows-wheeler transform. *Bioinformatics* 25, 1754–1760. doi: 10.1093/bioinformatics/btp324

Li, H., Handsaker, B., Wysoker, A., Fennell, T., Ruan, J., Homer, N., et al. (2009). The sequence alignment/map format and SAMtools. *Bioinformatics* 25, 2078–2079. doi: 10.1093/bioinformatics/btp352

Lisch, D. (2013). How important are transposons for plant evolution? *Nat. Rev. Genet.* 14, 49–61. doi: 10.1038/nrg3374

Liu, J., Hua, W., Yang, H. L., Zhan, G. M., Li, R. J., Deng, L. B., et al. (2012). The *BnGRF2* gene (*GRF2-like* gene from *Brassica napus*) enhances seed oil production through regulating cell number and plant photosynthesis. *J. Exp. Bot.* 63, 3727–3740. doi: 10.1093/jxb/ers066

Livak, K. J., and Schmittgen, T. D. (2001). Analysis of relative gene expression data using real-time quantitative PCR and the 2-ΔΔCT method. *Methods* 25, 402–408. doi: 10.1006/meth.2001.1262

Lu, K., Wei, L., Li, X., Wang, Y., Wu, J., Liu, M., et al. (2019). Whole-genome resequencing reveals *Brassica napus* origin and genetic loci involved in its improvement. *Nat. Commun.* 10:1154. doi: 10.1038/s41467-019-09134-9

Matar, S., Kumar, A., Holtgräwe, D., Weisshaar, B., and Melzer, S. (2021). The transition to flowering in winter rapeseed during vernalization. *Plant Cell Environ.* 44, 506–518. doi: 10.1111/pce.13946

McWilliam, H., Li, W., Uludag, M., Squizzato, S., Park, Y. M., Buso, N., et al. (2013). Analysis tool web services from the EMBL-EBI. *Nucleic Acids Res.* 41, W597–W600. doi: 10.1093/nar/gkt376

Qian, W., Meng, J., Li, M., Frauen, M., Sass, O., Noack, J., et al. (2006). Introgression of genomic components from Chinese *Brassica rapa* contributes to widening the genetic diversity in rapeseed (*B. napus L.*), with emphasis on the evolution of Chinese rapeseed. *Theor. Appl. Genet.* 113, 49–54. doi: 10.1007/s00122-006-0269-3

Qian, W., Samans, B., Obermeier, C., and Snowdon, R. J. (2016). Deletion of a stay-green gene associates with adaptive selection in *Brassica napus*. *Mol. Plant* 9, 1559–1569. doi: 10.1016/j.molp.2016.10.017

Schiessl, S., Huettel, B., Kuehn, D., Reinhardt, R., and Snowdon, R. J. (2017). Targeted deep sequencing of flowering regulators in *Brassica napus* reveals extensive copy number variation. *Sci. Data* 4:170013. doi: 10.1038/sdata.2017.13

Schiessl, S., Quezada-Martinez, D., Tebartz, E., Snowdon, R. J., and Qian, L. (2019). The vernalisation regulator *FLOWERING LOCUS C* is differentially expressed in biennial and annual *Brassica napus*. *Sci. Rep.* 9:14911. doi: 10.1038/s41598-019-51212-x

Searle, I., He, Y., Turck, F., Vincent, C., Fornara, F., Kröber, S., et al. (2006). The transcription factor *FLC* confers a flowering response to vernalization by repressing meristem competence and systemic signaling in *Arabidopsis*. *Genes Dev.* 20, 898–912. doi: 10.1101/gad.373506

Seo, E., Lee, H., Jeon, J., Park, H., Kim, J., Noh, Y.-S., et al. (2009). Crosstalk between cold response and flowering in *Arabidopsis* is mediated through the flowering-time gene SOC1 and its upstream negative regulator FLC. *Plant Cell* 21, 3185–3197. doi: 10.1105/tpc.108.063883

Solovyev, V. V., Shahmuradov, I. A., and Salamov, A. A. (2010). "Identification of promoter regions and regulatory sites" in *Computational biology of transcription factor binding*. ed. I. Ladunga (Totowa, NJ: Humana Press), 57–83.

Sri, T., Gupta, B., Tyagi, S., and Singh, A. (2020). Homologs of Brassica SOC1, a central regulator of flowering time, are differentially regulated due to partitioning of evolutionarily conserved transcription factor binding sites in promoters. *Mol. Phylogenet. Evol.* 147:106777. doi: 10.1016/j.ympev.2020.106777

Stein, A., Coriton, O., Rousseau-Gueutin, M., Samans, B., Schiessl, S. V., Obermeier, C., et al. (2017). Mapping of homoeologous chromosome exchanges influencing quantitative trait variation in *Brassica napus*. *Plant Biotechnol. J.* 15, 1478–1489. doi: 10.1111/pbi.12732

Trapnell, C., Roberts, A., Goff, L., Pertea, G., Kim, D., Kelley, D. R., et al. (2012). Differential gene and transcript expression analysis of RNA-seq experiments with TopHat and Cufflinks. *Nat. Protoc.* 7, 562–578. doi: 10.1038/nprot.2012.016

Wang, N., Qian, W., Suppanz, I., Wei, L., Mao, B., Long, Y., et al. (2011). Flowering time variation in oilseed rape (*Brassica napus L.*) is associated with allelic variation in the *FRIGIDA* homologue *BnaA.FRI.a*. *J. Exp. Bot.* 62, 5641–5658. doi: 10.1093/jxb/err249

Waterhouse, A. M., Procter, J. B., Martin, D. M. A., Clamp, M., and Barton, G. J. (2009). Jalview version 2—a multiple sequence alignment editor and analysis workbench. *Bioinformatics* 25, 1189–1191. doi: 10.1093/bioinformatics/btp033

Wickham, H. (2011). ggplot2. *WIREs Comp. Stats.* 3, 180–185. doi: 10.1002/wics.147

Wu, D., Liang, Z., Yan, T., Xu, Y., Xuan, L., Tang, J., et al. (2019). Whole-genome resequencing of a worldwide collection of rapeseed accessions reveals the genetic basis of ecotype divergence. *Mol. Plant* 12, 30–43. doi: 10.1016/j.molp.2018.11.007

Yin, S., Ming, W., Chaocheng, G., Bo, W., Haitao, L., Ge, L., et al. (2020). Transposon insertions within alleles of *BnaFLC.A10* and *BnaFLC.A2* are associated with rapeseed (*Brassica napus L.*) seasonal crop-type. *J. Exp. Bot.* 71, 4729–4741. doi: 10.1093/jxb/eraa237

Zou, J., Mao, L., Qiu, J., Wang, M., Jia, L., Wu, D., et al. (2019). Genome-wide selection footprints and deleterious variations in young Asian allotetraploid rapeseed. *Plant Biotechnol. J.* 17, 1998–2010. doi: 10.1111/pbi.13115

Conflict of Interest: The authors declare that the research was conducted in the absence of any commercial or financial relationships that could be construed as a potential conflict of interest.

Copyright © 2021 Matar and Melzer. This is an open-access article distributed under the terms of the Creative Commons Attribution License (CC BY). The use, distribution or reproduction in other forums is permitted, provided the original author(s) and the copyright owner(s) are credited and that the original publication in this journal is cited, in accordance with accepted academic practice. No use, distribution or reproduction is permitted which does not comply with these terms.

frontiers in Plant Science

ORIGINAL RESEARCH
published: 12 July 2021
doi: 10.3389/fpls.2021.693285

SNP Alleles Associated With Low Bolting Tendency in Sugar Beet

Samathmika Ravi[1], *Giovanni Campagna*[2], *Maria Cristina Della Lucia*[1], *Chiara Broccanello*[1], *Giovanni Bertoldo*[1], *Claudia Chiodi*[1], *Laura Maretto*[1], *Matteo Moro*[1], *Azam Sadat Eslami*[1], *Subhashini Srinivasan*[3], *Andrea Squartini*[1], *Giuseppe Concheri*[1] *and Piergiorgio Stevanato*[1]*

[1] Department of Agronomy, Food, Natural Resources, Animals and Environment, University of Padova, Legnaro, Italy, [2] Cooperativa Produttori Agricoli Società Cooperativa Agricola (COPROB), Minerbio, Italy, [3] Institute of Bioinformatics and Applied Biotechnology, Bengaluru, India

The identification of efficient molecular markers related to low bolting tendency is a priority in sugar beet (*Beta vulgaris* L.) breeding. This study aimed to identify SNP markers associated with low bolting tendency by establishing a genome-wide association study. An elaborate 3-year field trial comprising 13 sugar beet lines identified L14 as the one exhibiting the lowest bolting tendency along with an increased survival rate after autumnal sowing. For SNP discovery following phenotyping, contrasting phenotypes of 24 non-bolting and 15 bolting plants of the L14 line were sequenced by restriction site-associated DNA sequencing (RAD-seq). An association model was established with a set of 10,924 RAD-based single nucleotide polymorphism (SNP) markers. The allelic status of the most significantly associated SNPs ranked based on their differential allelic status between contrasting phenotypes ($p < 0.01$) was confirmed on three different validation datasets comprising diverse sugar beet lines and varieties adopting a range of SNP detection technologies. This study has led to the identification of SNP_36780842 and SNP_48607347 linked to low bolting tendency and can be used for marker-assisted breeding and selection in sugar beet.

Keywords: sugar beet, autumnal sowing, vernalization, bolting tolerance, SNP detection technologies, SNP association, marker-assisted breeding

OPEN ACCESS

Edited by:
Christian Jung,
University of Kiel, Germany

Reviewed by:
J. Mitchell McGrath,
Retired, East Lansing, MI, United States
Diana Mihaela Buzas,
University of Tsukuba, Japan

***Correspondence:**
Piergiorgio Stevanato
stevanato@unipd.it

Specialty section:
This article was submitted to Plant Development and EvoDevo, a section of the journal Frontiers in Plant Science

Received: *10 April 2021*
Accepted: *07 June 2021*
Published: *12 July 2021*

Citation:
Ravi S, Campagna G, Della Lucia MC, Broccanello C, Bertoldo G, Chiodi C, Maretto L, Moro M, Eslami AS, Srinivasan S, Squartini A, Concheri G and Stevanato P (2021) SNP Alleles Associated With Low Bolting Tendency in Sugar Beet. Front. Plant Sci. 12:693285. doi: 10.3389/fpls.2021.693285

INTRODUCTION

Sugar beet is an important crop in the temperate areas providing about 30% of total sugar (OECD-FAO, 2020). In the global change scenario, an emerging priority for sugar beet breeding is to increase the yield in the face of recurrent and adverse environmental conditions, such as cold, thermal, water, and nutritional stresses (Hoffmann and Kenter, 2018; Abou-Elwafa et al., 2020).

One of the ways to increase sugar beet yield is by taking advantage of different cultivation patterns. Biennial beets, grown for their sugar, are conventionally sown in the spring in temperate climates and harvested in summer–autumn. To avoid drought and thermal stresses late in the season, the practice of early sowing and/or autumnal sowing of sugar beet is weighed fundamental for increasing sugar yield (Hoffmann and Kluge-Severin, 2011; Schnepel and Hoffmann, 2016; Hoffmann and Kenter, 2018; Höft et al., 2018a,b). While widening the cultivation period has several advantages, the problem of premature bolting becomes more pertinent in the early sowing and winter breeding of beets.

Bolting or elongation of the stem followed by flowering under certain environmental conditions (e.g., variation in day length, changes in temperature, water stress, and/or hormone imbalance)

affects different plant species, such as sugar beet (Dally et al., 2018; Höft et al., 2018a). During this vegetative to reproductive transition, most resources of plants are diverted away from the vegetative parts, rendering them not only inedible by affecting the sugar content but also affecting the harvest (Nelson and Deming, 1952; Scott et al., 1973; Lasa, 1977). In addition to this, the fertile seeds produced have high disseminating potential. Due to the above-mentioned undesirable consequences, the control of bolting is crucial (Mutasa-Göttgens et al., 2010; Kuroda et al., 2019). Several mechanical, electrical, and chemical methods for bolting control have been proposed and experimented with, but studies report them as cost-prohibitive in large breeding programs (Diprose et al., 1985; Ferrandino et al., 2008).

The genetic basis and improvement of bolting control in sugar beet have been well-studied (Dally et al., 2014). The annual habit in *B. vulgaris* was shown to be controlled by a major dominant gene, commonly referred to as the bolting gene *B*, which promotes the initiation of bolting under long days without prior vernalization (Abou-Elwafa et al., 2012). Although annual beets that are heterozygous at the *B* locus (*Bb*) bolt readily without vernalization, heterozygotes derived from crosses between annual and biennial beets exhibit a delay in bolting compared with annual (*BB*) beets (Mutasa-Göttgens et al., 2010; Abou-Elwafa et al., 2012). In a study with three F_3 mapping populations, it was demonstrated that the vernalization requirement co-segregated with the bolting locus *B* on chromosome 2, and seasonal bolting was controlled by two major quantitative trait loci (QTLs) located in chromosomes 4 and 9 of sugar beet. In the same study, it was shown that late seasonal bolting alleles, SBT_4 and SBT-9 (BR1) in combination with biennial alleles at B might provide beet genotypes with bolting resistance (Tränkner et al., 2017). The haplotype sequences of important flowering genes, such as *BTC1*, *BvBBX19*, *BvFT1*, and *BvFT2* in sugar beet have also been exploited to understand their adaptation and cultivation of biennial beets in the context of bolting resistance (Höft et al., 2018a,b). Literature also shows that few major loci enrich the variation of bolting time in beet and that the identification of further alleles will support the development of beet genotypes with purpose-oriented bolting time (Broccanello et al., 2015; Stevanato and Biscarini, 2016; Tränkner et al., 2016; Pfeiffer et al., 2017). The genetic analysis of bolting phenotypes has used a variety of DNA markers for the detection of QTLs controlling bolting (Hébrard et al., 2016; Tränkner et al., 2016; Pfeiffer et al., 2017; Kuroda et al., 2019). These have been primarily performed on mortal mapping populations, i.e., either F_2 or F_3, and the identified bolting linked markers may segregate as a consequence of crossing over between markers and QTLs in subsequent generations. These methods are often laborious and limited by the density of markers. Single nucleotide polymorphisms or SNPs are attractive because of their large presence in the genome and ease of detection, allowing high throughput use in marker-assisted breeding and selection in various crops (Agarwal et al., 2008; McCouch et al., 2010; Choi et al., 2020).

However, the identification of novel SNP markers to efficiently control bolting is still a key challenge.

In this study, SNP markers associated with bolting tolerance post-winter and vernalization were identified by (a) phenotyping 13 sugar beet lines for bolting tolerance after autumnal sowing from a 3-year field trial, (b) RAD-sequencing of the line L14 combining highest survival and the lowest bolting percentage, (c) establishing a Genome-wide association study (GWAS) to identify favorable alleles related to low bolting tendency, and (d) validating the identified SNP markers using a range of SNP genotyping methods on diverse sugar beet lines and varieties. The results from this study precede controlled bolting of sugar beet breeding through marker-assisted selection and provides insights into candidate genes involved in the complex process of flowering and cold tolerance in sugar beet.

RESULTS

Bolting and Survival Rates of 13 Assessed Sugar Beet Lines

The meteorology data revealed that the experimental site experienced 50 days of temperatures $< 0°C$ from November 2016 to March 2017 (**Figure 1A**, 1st-year field trial), 35 days of temperatures $< 0°C$ from November 2017 to March 2018 (**Figure 1B**, 2nd-year field trial), and 33 days of temperatures $< 0°C$ from November 2018 to March 2019 (**Figure 1C**, 3rd-year field trial). The contrast in the bolter count and survival rates among the sugar beet genotypes are shown in **Table 1**. It was observed that individuals of the L14, L8, and L3 lines presented a lower percentage of bolters along with higher survival rates post-winter. Although the lines L5 and L13 showed a lower bolter percentage, they had a very low survival rate post-winter of <10% of the initial plants. The remaining lines L12, L6, L1, L4, L7, L11, L9, and L2 combined phenotypes of high bolting percentage along with lower survival rates post-winter. Subsequently, the field trial resulted in the identification of a line, L14, combining characteristics of least bolting tendency and highest survival rate after autumnal sowing. Additionally, we genotyped the material with the SNP marker, *SNP183*, linked to bolting tolerance generated in an earlier effort by our lab (Broccanello et al., 2015). The genotyping results from *SNP183* are presented in **Supplementary Table 1** and are suggestive of L14 having 95% frequency of the low bolting allele. L14 was, thus, considered as an ideal plant material for further sequencing and understanding the basis of bolting tolerance post vernalization.

Analysis of the Genetic Structure of L14 Line

The sequencing of 15 bolting and 24 non-bolting individuals of the L14 line, identified as the best material from phenotyping, generated a total 10,924 SNPs based on the EL10 reference genome (NCBI PRJNA413079). The SNP markers had a high call rate of 97% across all the samples and were 100% reproducible *in-silico*. A crude usage of the different alleles of the 10,924 SNP markers to understand the genetic structure resulted in the separation of bolters and non-bolters of L14 (**Figure 2**). The first two axes of the PCA contributed to 28% of the overall variance. This allowed us to proceed with further analysis to

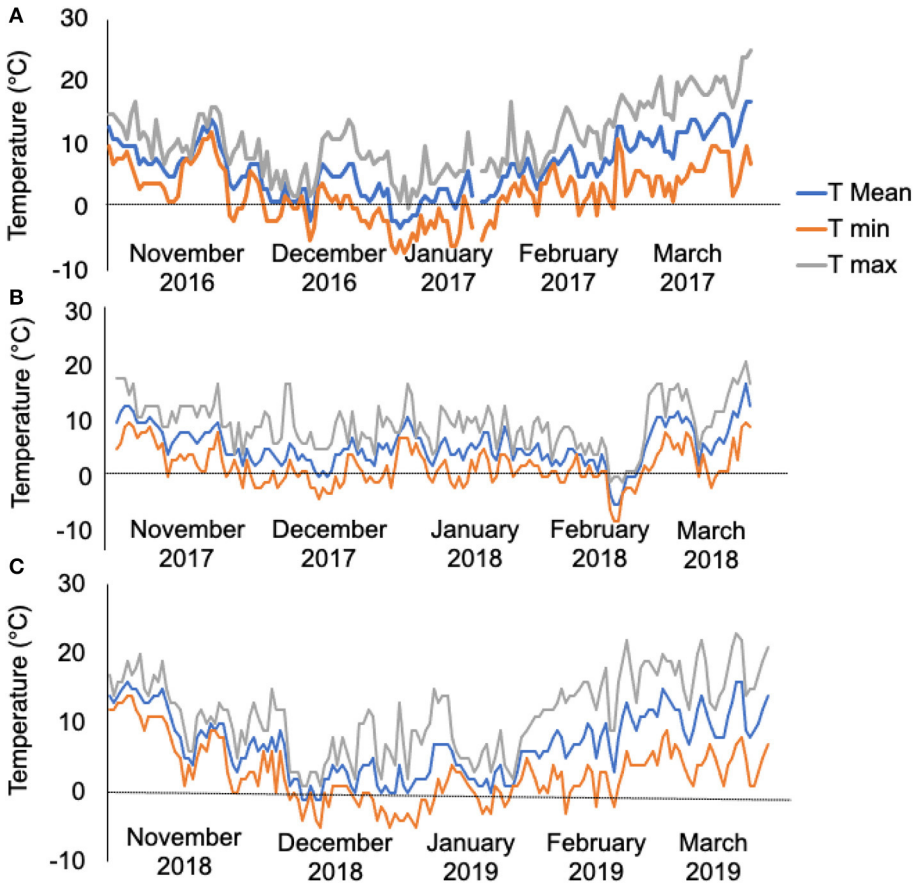

FIGURE 1 | (A) Temperature profiles as recorded from the field during 2016–2017, 50 days of temperatures < 0°C. **(B)** Temperature profiles as recorded from the field during 2017–2018, 35 days of temperatures < 0°C. **(C)** Temperature profiles as recorded from the field during 2018–2019, 33 days of temperature < 0°C. The trend line in gray, orange, and blue represents maximum temperature (T max), minimum temperature (T min), and mean temperature (T mean) per day of the month, respectively.

determine the strength of association of SNPs with the trait of lower bolting tendency.

GWAS for the Identification of SNPs Linked to Post-winter Bolting Tolerance

The genotypes of all the identified SNPs were used to build an association analysis resulting in the identification of key SNPs discriminating the bolting from the non-bolting individuals of the L14 line. The assumption was that the most significant SNPs, located in key causal genes, should ideally show a discrete separation of genotype calls or patterns of association. The model also considered rare alleles (MAF < 0.05). These variants were mined using two likelihood ratio tests: (i) Fisher exact test and (ii) nbinom test (**Supplementary Figure 1**). The results from the association analyses indicated that the SNP density was found to be the highest at the beginning of chromosomes 1 and 4, and the most significant SNP associations based on differential allele frequencies were found in chromosomes 2, 4, 6, and 7 (**Figure 3**, cyan dots). This was consistent with the identification of markers associated with flowering time and bolting phenotype reported by other authors (Abou-Elwafa et al., 2012; Pfeiffer et al., 2014; Tränkner et al., 2017). Further, the annotations of the genes harboring the SNP markers based on the EL10 genome resulted in the implication of flowering-related genes and loci. More specifically, seven genes were involved in vernalization responsiveness, six genes were related to flower development, and 13 other genes were found involved in flowering time. These observations have been summarized in **Supplementary Table 2**. For downstream validation based on molecular methods, common SNPs resulting from the two statistical methods were considered and further filtered based on their degree of association using the *p*-value (**Supplementary Figure 1**).

Molecular Validation of Identified Single Nucleotide Polymorphisms Using Different Single Nucleotide Polymorphism-Based Technologies

The molecular validation strategy involved three technologies: (1) high-resolution melting analysis (HRM), (2) Sanger sequencing, and (3) SNP genotyping using rhAmp based assays.

TABLE 1 | Mean values (and standard error) from the phenotyping of 13 sugar beet lines assessed for the number of bolting plants and the number of survived plants post-winter.

Name	Number of individuals before winter	Number of plants that survived post winter	Number of bolters
L14	750	296 ± 6	12 ± 2
L8	750	221 ± 9	26 ± 4
L3	750	219 ± 4	51 ± 3
L5	750	73 ± 12	6 ± 2
L13	750	67 ± 9	11 ± 3
L12	750	76 ± 11	42 ± 2
L6	750	64 ± 12	64 ± 2
L1	750	75 ± 5	75 ± 6
L4	750	77 ± 4	77 ± 2
L7	750	72 ± 3	72 ± 3
L11	750	70 ± 4	70 ± 5
L9	750	71 ± 8	71 ± 3
L2	750	67 ± 6	67 ± 4

L14 was identified as the line combining the highest survival percentage with the lowest bolting percentage post-winter.

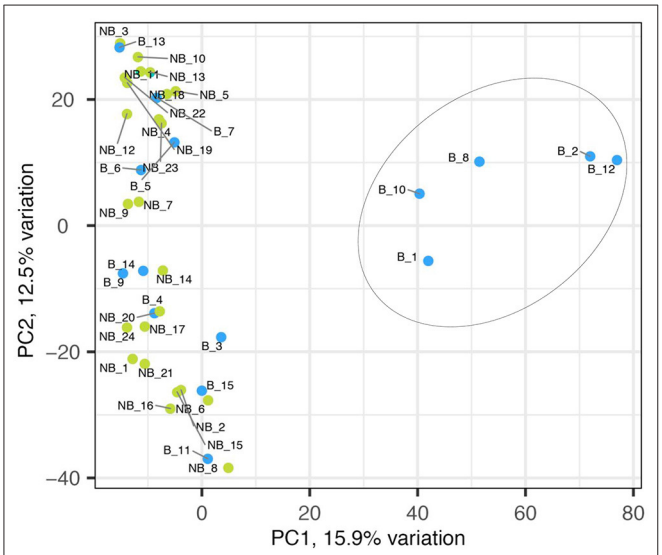

FIGURE 2 | Principal component analyses of 10,924 SNP markers on bolter and non-bolter phenotypes of L14 plants. Each dot represents a sample, and the blue color represents bolters (B) while the green color represents non-bolters (NB). The first two axes of the PCA explain 28% of the overall variance and separated the bolter and non-bolter phenotypes.

We adopted a rapid and reliable approach to screening SNP markers identified from the bioinformatic association analyses using, as the first step, 384-well plate based high-resolution melting (HRM) assays. Thirty SNP targets were evaluated on nine individuals of bolters and non-bolters of the L14 line in triplicates. The difference in the melt curve profiles of the bolter and non-bolter phenotypes of L14 as a result of their sequence composition can be seen in **Figure 4** for some of the best discriminating SNPs. The largest differences in

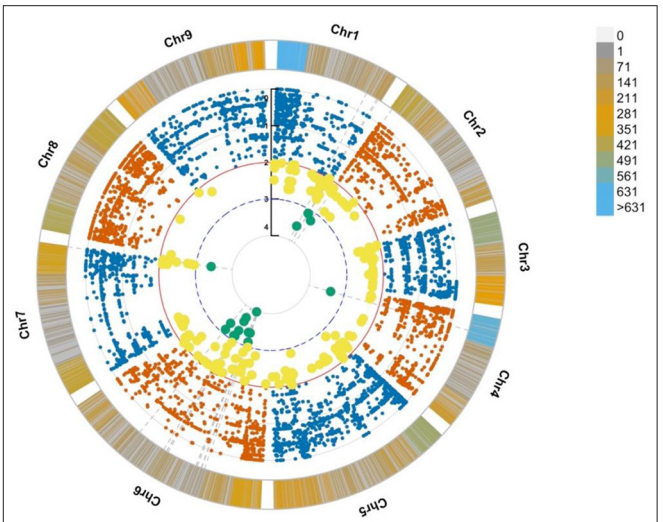

FIGURE 3 | Circular Manhattan plot from association analyses showing SNP density per chromosome along with significant SNP associations. The bars along the chromosomes present the SNP density in a window size of 10 M base pairs. The most significantly associated SNPs are highlighted in yellow ($p \leq 0.01$) and cyan ($p \leq 0.001$).

the melting temperatures between the bolters and the non-bolters were weighed using by non-parametric test (*T*-test; **Supplementary Figure 2**) for the discriminating SNPs to proceed with Sanger sequencing-based validation.

Sanger sequencing-based validation was carried out for 10 promising SNP targets from HRM based validation (**Figure 4**). **Figure 5** shows the multiple sequence alignments and representative chromatograms of two SNPs, SNP_36780842 (top) and SNP_48607347 (bottom), which were best substantiated between the bolters and the non-bolters of L14. For SNP_36780842, the non-bolters of the L14 line showed the G allele, while the bolters showed the C allele (**Figure 5A**), which is also confirmed in the chromatogram (**Figure 5B**). Concerning SNP_48607347, most of the non-bolters presented the C allele, while all the bolters showed the A allele (**Figure 5C**), a representative chromatogram is also shown (**Figure 5D**).

To further understand the association of these two SNPs with bolting tolerance, we developed genotyping assays corresponding to the SNPs validated by Sanger sequencing. The validation was performed on three sets of plant material to understand their ability to discriminate (1) annual vs. biennial habits, (2) bolters- vs. non-bolters of biennial habits, and (3) spring-sown and autumn-sown hybrid varieties. The results of the association test with chi-square and p-value are reported in **Table 2**. Both the SNPs described in this study, SNP_36780842 and SNP_48607347, were found to be significantly associated with the three validation datasets tested for bolting tendency. The allele frequencies observed were highly statistically significant between annual and biennial beet individuals, bolter and non-bolter beet individuals, and for spring-sown and autumn-sown varieties ($p < 0.0001$) as shown by the contingency table (**Table 2**).

The chi-square test of independence was used to analyze the contingency table formed by the evaluated alleles and phenotypes

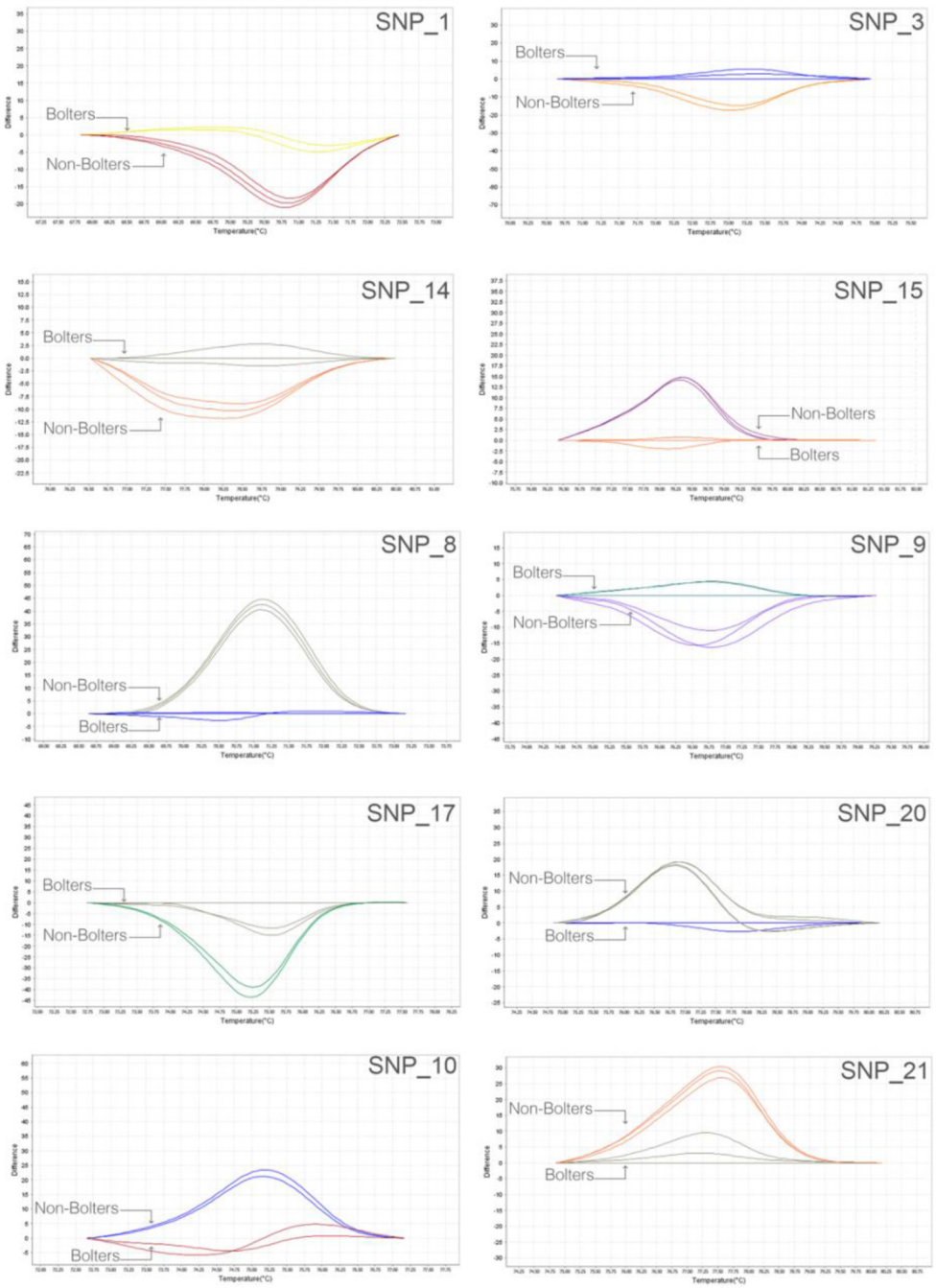

FIGURE 4 | Robust and quick SNP screening by high-resolution melting (HRM) of selected SNP targets: representative melt curve profiles discriminating three biological replicates of bolters and non-bolters from the L14 line are presented here as an example. The two different melt curve colors for each SNP target correspond to samples of bolters and non-bolters labeled respectively.

as categorical variables. Particularly, this test evaluated whether there is a significant association between the categories. As the output of this test, the mosaic plot in **Figure 6** shows the combination of positive and negative associations between phenotypes, alleles C and G of SNP_36780842, and alleles C and A of SNP_48607347. It is interesting to observe the strength of positive association of the low bolting allele G of SNP_36780842 in biennial, biennial non-bolter, and autumn-sown categories. The exact opposite of a strong negative association is seen between C of SNP_36780842 and spring-sown varieties, biennial bolters, and annual beets. With respect to SNP_48607347, the contribution of the C allele to the biennial, biennial non-bolter and autumn-sown hybrid categories can be well-appreciated differing from the negative correlation from the A allele observed in annual beets, biennial bolters, and spring-sown varieties (**Figure 6**). A qualitative separation of the alleles for the bolter

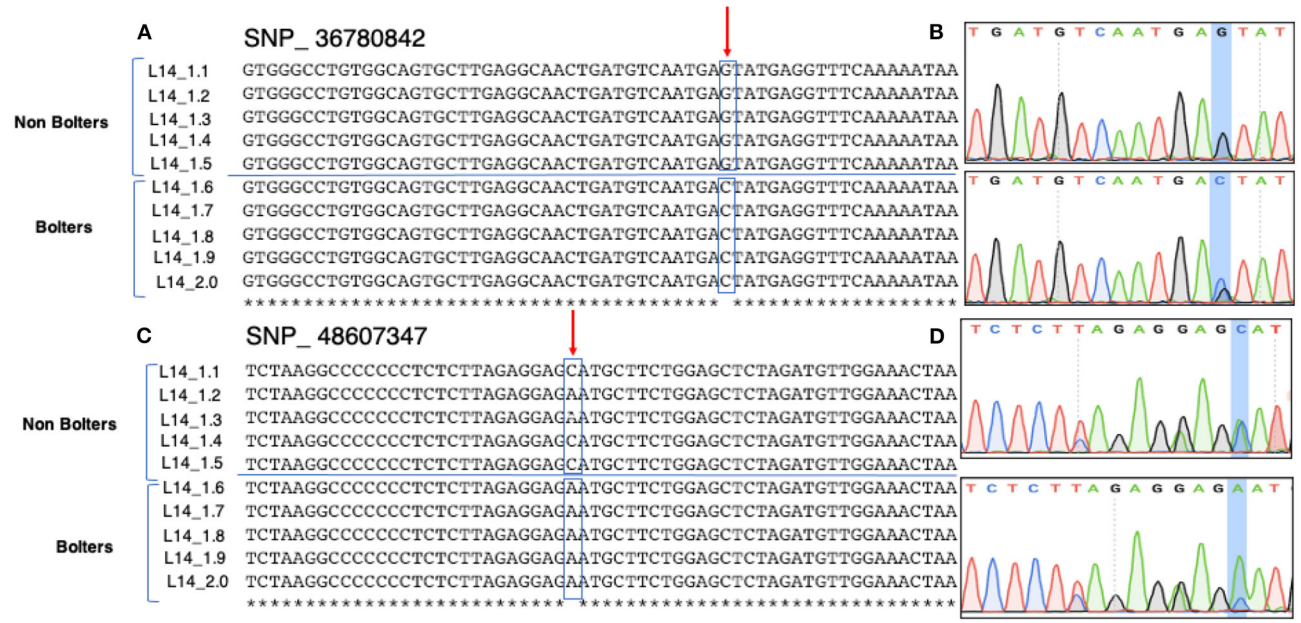

FIGURE 5 | Sanger sequencing-based validation of SNP_36780842 (Chr1, position 36780842) and SNP_ 48607347 (Chr2, 48607347) on five biological replicates of bolters and non-bolters of the L14 line. Top: **(A)** multiple sequence alignments and **(B)** the corresponding chromatogram of SNP_36780842 show non-bolters of the L14 line with the G allele. Bottom: **(C)** multiple sequence alignments and **(D)** corresponding chromatogram of SNP_48607347 show non-bolters of the L14 line with the C allele. Both SNPs were found to be segregating within the L14 line.

and non-bolter checks is also shown in **Supplementary Figure 4**. These associations further confirmed observations from Sanger sequencing (**Figure 5**). Bolting tolerance in biennial beets can, thus, be linked to a higher frequency of the G allele at SNP_36780842 and a higher frequency of the C allele for SNP_48607347.

The strong association of the two SNPs markers compelled the authors to also investigate the molecular effect of the SNP and understand its chromosomal context. SNP_36780842, located within a gene coding for a hypothetical protein in chromosome 1, was found to be a 3'UTR variant (**Figure 7**). To annotate the gene, an ortholog search in *Arabidopsis* was done and pointed to AT1G47410, which was still uncharacterized in terms of function and protein domains. In fact, orthologs in many species remained uncharacterized but provided a 75% overlap between the protein in question and Chaperone J-domain superfamily proteins. Further, PSI-BLAST resulted in its annotation as "DNAJ heat shock N-terminal domain-containing protein" in *Prunus dulcis*. The protein similarity and overlaps along with the ortholog tree specifically looking at orthologs of *B. vulgaris*, *Arabidopsis*, and *Prunus* can be observed in **Supplementary Figure 3**. The second validated SNP, SNP_48607347, located in chromosome 2 of sugar beet was found to be a non-synonymous variant in exon 3 of the gene encoding xylose isomerase changing the amino acid arginine to histidine (**Figure 7**). Non-synonymous variants more often end up having functional consequences ranging from protein structure to enzyme activity because of amino acid substitution. The gene xylose isomerase is located ∼10 Mb from other important flowering-related genes in sugar beet (**Figure 7**), such as *BvBTC*, *BvFT1*, and *BvFT2* (Pin et al., 2012; Dally et al., 2018; Höft et al., 2018b).

DISCUSSION

In *B. vulgaris* L., there is a trade-off between sugar yield and bolting, which is the first visible sign of reproductive transition (Mutasa-Göttgens et al., 2010). Specifically, the cultivation of sugar beet as a winter crop is considered far-fetched, primarily because of bolting. Further, large variations have been found in the natural beet populations consisting of a mixture of semel- and iteroparous plants with different reproductive behaviors (Hautekèete et al., 2002; Van Dijk, 2009; Dijk and Hautekèete, 2014). These culminate in the complex genetic and epigenetic control of bolting, vernalization and flowering time in sugar beet. While the candidate genes for these processes are well-mapped in the model species *Arabidopsis thaliana*, it is still being investigated in an important crop like sugar beet (Pfeiffer et al., 2014; Höft et al., 2018a).

The goal of this study was to identify candidate genes and validate SNP alleles linked to low bolting tendency after autumnal sowing and vernalization. The lack of prior information on bolting-tolerant sugar beets post-winter urged the authors to compare available sugar beet materials for their survival rate and bolting percentage post-winter. Thus, a 3-year field trial was organized and resulted in the identification of a suitable plant material, L14, to further understand the molecular basis of tolerance to bolting post vernalization.

The use of contrasting phenotypes of the L14 line and high-throughput sequencing resulted in the identification of a large number of SNPs (10,924). Mining the most useful SNPs discriminating the phenotypes involved the use of both (a) Fisher exact test and (b) nbinom test from DESeq2 to identify SNP signatures strongly linked to bolting tolerance post-winter

TABLE 2 | Contingency table based on rhAmp genotyping of SNP_36780842 and SNP_48607347 at three levels—annual vs. biennial beets, bolters and non-bolters of the biennial beets, and autumn-sown and spring-sown varieties.

SNP_ 36780842		**C**	**G**	***Chi-square***	***p-value***
Validation dataset 1	Annual	**83**	**9**	***43.34***	***<0.0001***
	(*n* = 46)	**90.20%**	**9.80%**		
	Biennial	**40**	**52**		
	(*n* = 46)	**43.50%**	**56.50%**		
Validation dataset 2	Bolters	**196**	**30**	***80.95***	***<0.0001***
	(*n* = 113)	**86.73%**	**13.27%**		
	Non-bolters	**84**	**102**		
	(*n* = 93)	**45.16%**	**54.84%**		
Validation dataset 3	Autumn-sown	**268**	**116**	***126.34***	***<0.0001***
	(*n* = 191)	**70.15%**	**30.00%**		
	Spring-sown	**379**	**3**		
	(*n* = 192)	**98.69%**	**0.78%**		
SNP_ 48607347		**C**	**A**	***Chi-square***	***p-value***
Validation dataset 1	Annual	**12**	**78**	***94.74***	***<0.0001***
	(*n* = 46)	**13%**	**85%**		
	Biennial	**80**	**14**		
	(*n* = 46)	**87%**	**15%**		
Validation dataset 2	Bolters	**81**	**107**	***25.25***	***<0.0001***
	(*n* = 94)	**43%**	**57%**		
	Non-bolters	**148**	**70**		
	(*n* = 108)	**69%**	**32%**		
Validation dataset 3	Autumn-sown	**234**	**144**	***29.66***	***<0.0001***
	(*n* = 189)	**61.90%**	**38.09%**		
	Spring-sown	**162**	**222**		
	(*n* = 192)	**42.18%**	**57.81%**		

The bold values represent the count of individuals obtained in each category along with a percentage calculated based on the total number of individuals test. The chi-square value provides a measure of the correlation between the categorial variables (the phenotype and the allele of the SNP in each case), and the p-value indicates if the statistical test resulted significant ($p < 0.05$).

(**Supplementary Figure 1**). Several other studies using similar test statistics resulted in the identification of good causal markers (Liang et al., 2016; Yang et al., 2016; Lee et al., 2018).

While we confirmed the strong association of two markers in this study on three validation datasets containing contrasting bolting phenotypes, we were also able to identify and map candidate genes related to vernalization responsiveness, flowering time, and floral development through bioinformatics analyses (**Supplementary Table 2**). SNP_36780842 was found to be located within the 3' UTR of a gene coding for a hypothetical protein in chromosome 1 (**Figure 7**). The importance of the 3' end of genes in transcription control and protein targeting is well-understood in model organisms. Particularly, the different modes of 3' RNA processing and flowering time control were reviewed with respect to the FLC in *Arabidopsis* (Rataj and Simpson, 2014). Post-transcriptional coordination in the control of flowering time through 3' UTR-mediated decay of flowering time control protein *SOC1* was shown in another study (Kim et al., 2013). However, since the gene under study was uncharacterized for its function and domains by most preliminary search tools and bioinformatics prediction of orthologs for the same resulted in 75% overlap with proteins constituting the chaperone-J-domain superfamily (**Supplementary Figure 3**). The role of J-domain-containing proteins and their relevance in flowering have been shown in many studies (Yang et al., 2010; Shen et al., 2011; Pulido and Leister, 2018).

It was equally interesting to understand the involvement of SNP_48607347 in flowering (**Figure 7**), located within the coding region, exon 3 of xylose-isomerase gene in chromosome 2 of sugar beet. This enzyme is important for the utilization of sugar substrates as shown in *Arabidopsis thaliana* (Cho et al., 2018). We identified a non-synonymous mutation in the xylose isomerase gene possibly affecting the protein structure because of the substitution of arginine with histidine (**Figures 5**, **7**). It has also been previously shown that mutations in certain starch metabolic genes may result in late flowering (Yu et al., 2000). To further understand its biological relevance, we looked at literature related to the effects of point mutations in xylose-isomerases. In a patent application (US20160040151A1), point mutations resulting in the substitution of asparagine to histidine were shown to increase xylose utilization in yeast. More evidence supporting a tight link between sugar metabolism and late-flowering has been reported in a recent study (Seo et al., 2011). In this study, it was shown that sufficiently high levels of sugar resulted in flowering in

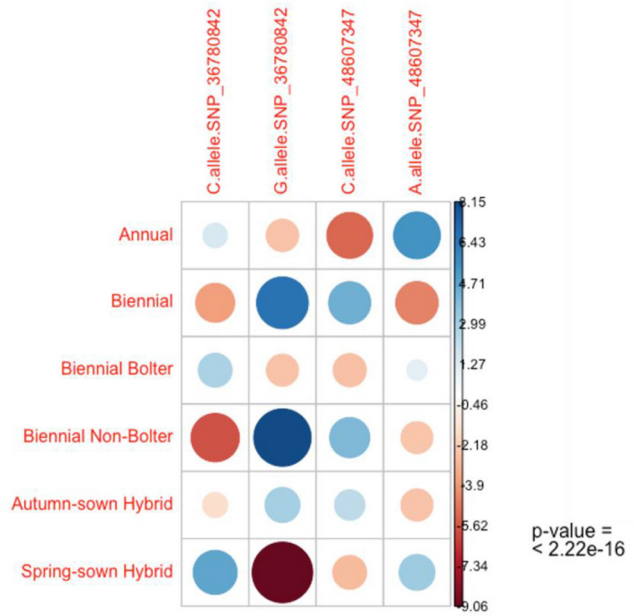

FIGURE 6 | The chi-square test of independence reveals the nature of dependence of the alleles with the phenotypic categories of sugar beets. A strong positive association of the G allele of SNP_36780842 is seen in the biennial, biennial-non-bolter, and autumn-sown categories contrary to the strong negative association seen in the spring-sown varieties and moderate negative association observed in biennial bolters and annual beets. Similarly, a moderate positive association of the C allele of SNP_48607347 is seen in the biennial, biennial-non-bolter, and autumn-sown categories inverse to the negative association seen in the spring-sown variety, biennial bolter and annual individuals. The *p*-value of the standardized residuals is significant ($p < 0.001$).

Arabidopsis, and a drop in sugar levels beyond a threshold resulted in prolonged vegetative growth. Taken together, it could be reasoned that non-bolters presenting the amino acid histidine might be better utilizers of sugar resulting in prolonged vegetative growth. Since xylose is the second most abundant sugar source in plants, we hypothesize the involvement of xylose-isomerases in utilizing available sugars, such as arabinose and xylose, to modulate endogenous sugar levels and metabolism important in the complex signaling for floral transition.

In addition to understanding the molecular effect of the validated SNPs, we have provided the flanking sequences of all significantly associated SNPs for use as a panel associated with low bolting tendency in **Supplementary Text 1**. The availability of SNPs from this study linked to bolting resistance provides further insights into bolting tolerance, vernalization responsiveness, and flowering in sugar beet. They can have a compelling impact on the breeding process, considering that the selection of high yielding sugar beet varieties against bolting is highly needed. This becomes even more necessary when many genotypes are to be tested or in the case of genetic purity assessments in seed companies.

To the knowledge of the authors, this study led to the identification of (1) sugar beet lines with high survival rate and bolting tolerance post-winter, (2) SNP alleles associated with low bolting tendency post-winter, and (3) description of candidate genes involved in bolting resistance in sugar beet.

MATERIALS AND METHODS

Plant Materials and Experimental Field

The plant material used in the phenotyping for bolting tolerance after autumnal sowing from a three-year field trial consists of 13 sugar beet lines provided by the Department of Agronomy, Food, Natural Resources, Animals and Environment, University of Padova, Italy and is summarized in **Supplementary Table 1**. All lines were pollinators, diploid, and endowed with resistance to rhizomania. There are pollinators carrying the allele for biennial habit at the *BTC1* locus in the homozygous state (Stevanato and Biscarini, 2016). One line selected from phenotyping was then involved in the RAD-sequencing and association analysis aimed to identify SNPs associated. For validating the identified SNP markers, the plant material comprised seven annual sea beets and 14 biennial sugar beet varieties further consisting of both bolting and non-bolting individuals. The seven annual *B. vulgaris* subsp. *maritima* populations were sampled along the Adriatic Sea coastline of Italy and Croatia. The sampling of populations was performed according to Bartsch et al. (1999). These populations, separated by at least 15 km or by physical barriers, were considered distinct. The seeds were collected from randomly selected plants more than 5 m apart for each population. The seeds were cleaned and stored at 7°C and 30% relative humidity. These populations are carrying the allele for annual habit at the *BTC1* locus in the homozygous state (Stevanato and Biscarini, 2016). The annual and biennial material used for validation is presented in **Supplementary Table 5**.

The experimental site for the 3-year field trial was located in Minerbio, Bologna, Italy (N44.629902, E11.552059). The seeds of each genotype were sown on November 19–20, 2016 for the 1st year, November 20, 2017 for the 2nd year, and November 22, 2018 for the consecutive year. Sugar beet plants were thinned after germination in the field to obtain 250 individuals per line distributed in three randomized plots. The plots were managed following local recommendations until the bolters and survival count date. The final count was carried out in the middle of June across the 3 years. Plants displaying stem elongation were scored as bolting individuals, while plants that did not show stem elongation were labeled as non-bolting individuals (**Table 1**).

Genotyping by Sequencing of L14 Bolters and Non-bolters

Genomic DNA was obtained from 15 bolting and 24 non-bolting individuals of the L14 line using a modified CTAB DNA extraction method (Doyle and Doyle, 1990). The quality of the extracted DNA was checked on a 0.8% agarose gel, and quantification of the same was done using a Qubit 4.0 fluorimeter (Thermo Fisher Scientific, Waltham, MA, Unites States). The DNA samples were subjected to a Restriction site-associated DNA technology (RAD-seq) with a HiSeq 2000 sequencing system using 150-bp paired-end sequencing (Illumina Inc., San Diego, CA, United States). Briefly, the extracted genomic DNA was digested using PstI (New England Biolabs, Ipswich, MA,

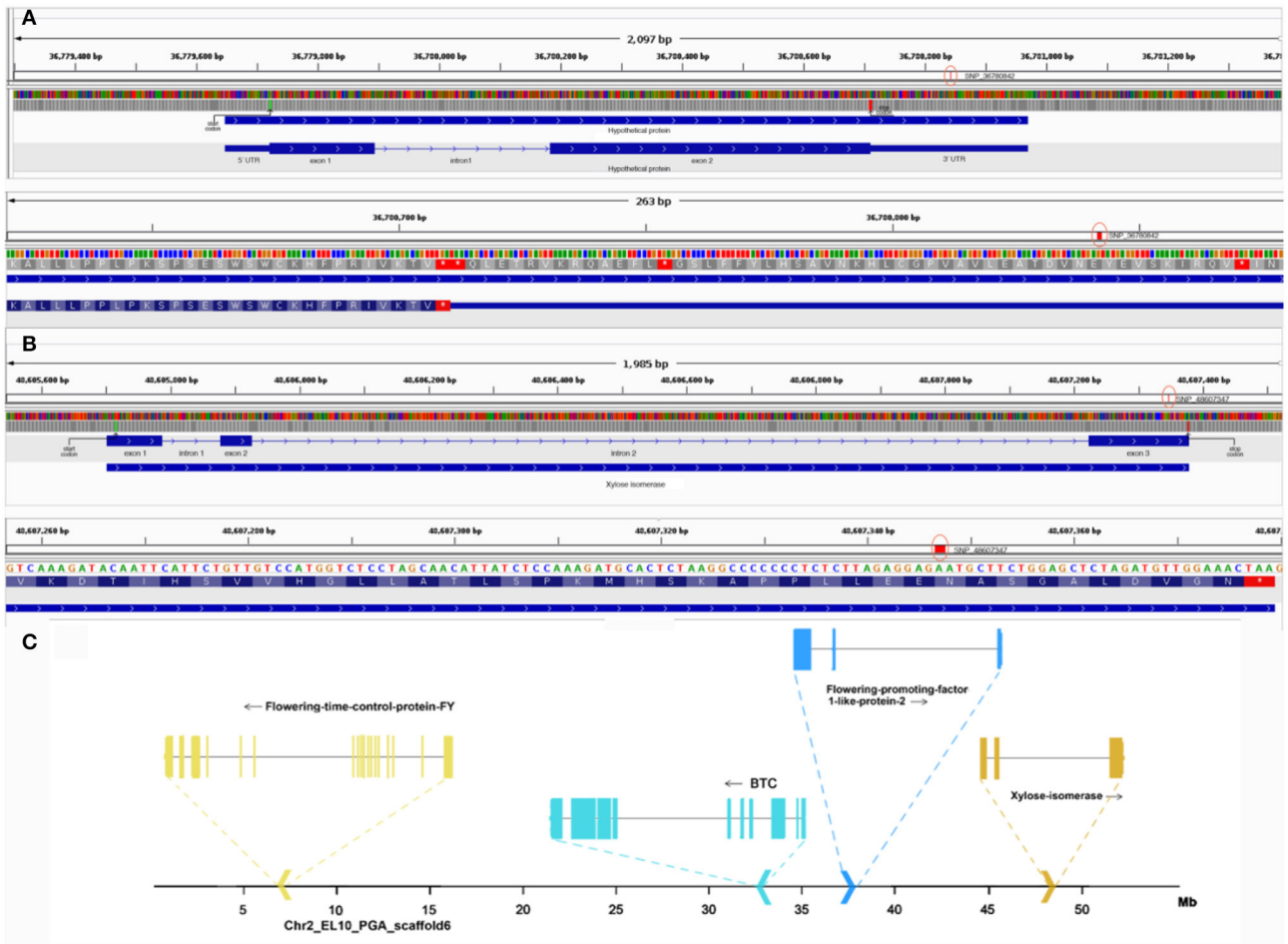

FIGURE 7 | (A) Top: gene structure of hypothetical protein in Chr1 containing SNP_36780842. Here, the green line represents the start codon, red line represents the stop codon and red circle highlights the SNP. Bottom: closer view of SNP_36780842 in context of the 3' UTR. **(B)** Top: gene structure of xylose isomerase in Chr2 containing SNP_48607347. Here, the green line represents the start codon, the red line represents the stop codon, and the red circle highlights the SNP. Bottom: closer view of SNP_48607347 in exon 3 of the gene. **(C)** Chromosomal context of other flowering-related genes in chromosome 2 near the locus of xylose isomerase containing SNP_48607347 is highlighted.

United States) and ligated with Illumina RE-site compatible P1 adapters (Illumina Inc., San Diego, CA, United States). The size selection of 300–500 bp was performed using solid-phase reversible immobilization (SPRI) beads (AgencourtAMPure XP Beads) from Beckman Coulter (Indianapolis, IN, United States). The resulting fragments were end-repaired, 3′-adenylated, and ligated with universal P2 adapters. The libraries were diluted and pooled with an equimolar concentration of each library and sequenced on an Illumina HiSeq 2500 platform (Illumina, San Diego, CA, United States) following the recommendations of the manufacturer.

Bioinformatics Data Analyses

Variant calling was performed using an in-house pipeline, which uses fastqc (version 0.11.5), bowtie2 (version 2.3.5.1), samtools (version 1.9), picard-tools (version 2.18.12), samtools (version 1.9) mpileup, and bcftools (version 1.9) to extract variants. The resulting vcf files were filtered using bcftools (version 1.9). The reference genome used was the EL10 Sugar Beet reference genome (NCBI PRJNA413079). The base file for all the bioinformatics analyses described was the merged vcf file containing genotypes of the 10,924 markers across 15 bolters and 24 non-bolters. The genotype matrix was analyzed using the SNPRelate package in R to build PCA plots and understand the genetic structure (**Figure 2**). For the genome-wide association analyses, the genotypes for each of the SNP markers were reduced to allele frequencies using the genetics package in R. Statistical Fisher test of independence using custom R scripts (attached as **Supplementary Text 2**) was then conducted to test the difference of partial association of genotypes in two strata of contingency tables, corresponding to two groups of bolters and non-bolters (Liang et al., 2016; Yang et al., 2016; Lee et al., 2018). Manhattan plots to visualize the data were generated using the qqman package in R (**Figure 3**). Then, to come up with the best SNP signatures discriminating against the two phenotypes, the results from the SNP-trait association analyses were also processed with

the DESeq package using the pairwise nbinom function. A subset of highly associated SNPs ($p < 0.01$) was selected as candidates for downstream molecular validation (**Supplementary Text 1**).

The commonly resulting signatures from the association study and DESeq approach (**Supplementary Figure 1**) were also used in SNP effect prediction and gene annotation to catalog genes related to flowering in sugar beet (**Supplementary Table 2**). With respect to the annotation of orthologs of genes identified here, OrthoDB (v9), TAIR-BLAST (2.9.0 +), and PSI-BLAST (hosted at NCBI) were used to compile the details presented in **Supplementary Table 2**. For SNP effect prediction, the snpEff tool (version 5.0) was used, and effects were predicted using the custom-built EL10 reference genome and gff file. Flanking sequences of significantly associated SNPs are shared in **Supplementary Text 1**. Visualization of the gene structures and SNPs was done using IGV (version 2.9).

MOLECULAR VALIDATION

High-Resolution Melting Analysis

Flanking sequences of 150 bp around the target SNP were extracted using the bedtools getfasta tool (version 2.28.0). The list of sequences was given as input to the stand-alone version of the Primer3 software (version 4.0) to design primers with suitable amplicon lengths. The HRM primer sequences are available in **Supplementary Table 3**. Nine biological replicates of biennial bolters and non-bolters of the L14 line were tested in triplicates. The HRM analyses were carried out in 384 well plates on the QuantStudio 12K Flex (Life Technologies, Carlsbad, CA, United States). Reactions were carried out using a 5 μL reaction volume comprising 2.5 μL of MeltDoctor™ HRM Master Mix (Thermo Fisher Scientific, Waltham, MA, United States), 0.45 μL of 10 μM forward and reverse primer, and 1.6 μL of sample DNA of concentration 5 ng/μL. The thermocycler program consisted of 10 min of pre-incubation at 95°C, followed by 40 cycles of 15 s at 95°C, and 1 min at 60°C. This was followed by the melt curve of 10 s at 95°C, 1 min at 60°C, 15 s at 95 °C, and 15 s at 60°C. The melt curve profiles were analyzed using the HRM software. The primers showing a significant difference in Tm between bolters and non-bolters, established by a non-parametric statistical test (*T*-test; **Supplementary Figure 2**), were taken downstream for validation based on Sanger sequencing, and their sequences are available in **Supplementary Table 4**.

Sanger Sequencing

Flanking sequences of 250 bp around the target SNP were extracted using the bedtools getfasta tool (version 2.28.0). The list of sequences was given as input to the stand-alone version of the Primer3 software (version 4.0) to design primers with suitable amplicon lengths. Five biological replicates of bolters and non-bolters of the L14 biennial line were tested. The reaction setup used comprised of 10 μL of 5X Reaction Buffer (PCR Biosystems Ltd., London, UK), 2 μL each of 10 μM forward and reverse primers, 2 μL of 2u/μl of HiFi Polymerase (PCR Biosystems), 5 μL of 50 ng/μL sample DNA made up to a 50 μL using nuclease-free water. The thermocycler program consisted of 1 min of initial denaturation at 95°C, followed by 30 cycles of 15 s at 95°C, 30 s at 60°C, and 30 s at 72°C. The amplicons were run on a 1.5% agarose gel to verify the amplification. PCR products were purified using NucleoSpin Gel and PCR Clean-up (Macherey-Nagel, Bethlehem, PA, United States) and were sent for sequencing. The resulting sequences were analyzed using ClustalW2 (http://www.ebi.ac.uk/Tools/msa/clustalw2/) and SnapGene 5.1.7 (Chicago, IL, United States) to generate multiple sequence alignments and chromatograms (**Figure 5**).

Genotyping

Validated SNPs from Sanger sequencing were used to design rhAmp assays (Integrated DNA Technologies, United States). Their sequences are available upon request. Three hundred biological samples were subjected to rhAmp genotyping, which was performed in 5 μL using 384-well plates, and low Rox was used as a passive reference dye. 5 ng of DNA was mixed with 2.65 μL of rhAmp Genotyping Master Mix, 0.25 μL of rhAmp SNP assay mix, and 1 μL of nuclease-free water. The thermal cycle parameters were adopted from Broccanello et al. (2018). The association between the two SNPs and phenotypes of bolting was also evaluated and confirmed by chi-square statistics using the chi.square() function in R. Chi-square residual analyses and visualizations were performed using the library corrplot and gplots.

DATA AVAILABILITY STATEMENT

The datasets presented in this study can be found in online repositories. The names of the repository/repositories and accession number(s) can be found at: https://www.ebi.ac.uk/ena/browser/view/PRJEB42403.

AUTHOR CONTRIBUTIONS

SR, GCa, and PS made the experimental design. SR, GCa, MD, GB, and PS carried out the sampling. SR, CB, CC, LM, AE, and MM performed molecular analyses. SR conducted the statistical and bioinformatics analyses and wrote the study. AS, GCo, SS, and PS contributed to the critical writing and review of the manuscript. All the authors reviewed the manuscript and gave final approval for publication.

FUNDING

This project was funded by Veneto Region in the framework of the PSR 2014–2020 (Project: Implementation and validation of innovative plant protection methods to increase the environmental sustainability of organic and sugar beet production).

SUPPLEMENTARY MATERIAL

The Supplementary Material for this article can be found online at: https://www.frontiersin.org/articles/10.3389/fpls.2021.693285/full#supplementary-material

REFERENCES

Abou-Elwafa, S. F., Amin, A. E.-E. A., and Eujayl, I. (2020). Genetic diversity of sugar beet under heat stress and deficit irrigation. *Agron. J.* 112, 3579–3590. doi: 10.1002/agj2.20356

Abou-Elwafa, S. F., Büttner, B., Kopisch-Obuch, F. J., Jung, C., and Müller, A. E. (2012). Genetic identification of a novel bolting locus in *Beta vulgaris* which promotes annuality independently of the bolting gene B. *Mol. Breeding* 29, 989–998. doi: 10.1007/s11032-011-9671-x

Agarwal, M., Shrivastava, N., and Padh, H. (2008). Advances in molecular marker techniques and their applications in plant sciences. *Plant Cell Rep.* 27, 617–631. doi: 10.1007/s00299-008-0507-z

Bartsch, D., Lehnen, M., Clegg, J., Pohl-Orf, M., Schuphan, I., and Ellstrand, N. C. (1999). Impact of gene flow from cultivated beet on genetic diversity of wild sea beet populations. *Mol. Ecol.* 8, 1733–1741. doi: 10.1046/j.1365-294x.1999.00769.x

Broccanello, C., Chiodi, C., Funk, A., McGrath, J. M., Panella, L., and Stevanato, P. (2018). Comparison of three PCR-based assays for SNP genotyping in plants. *Plant Methods* 14:28. doi: 10.1186/s13007-018-0295-6

Broccanello, C., Stevanato, P., Biscarini, F., Cantu, D., and Saccomani, M. (2015). A new polymorphism on chromosome 6 associated with bolting tendency in sugar beet. *BMC Genet.* 16:2. doi: 10.1186/s12863-015-0300-2

Cho, L.-H., Pasriga, R., Yoon, J., Jeon, J.-S., and An, G. (2018). Roles of sugars in controlling flowering time. *J. Plant Biol.* 61, 121–130. doi: 10.1007/s12374-018-0081-z

Choi, S. R., Oh, S. H., Dhandapani, V., Jang, C. S., Ahn, C.-H., Rameneni, J. J., et al. (2020). Development of SNP markers for marker-assisted breeding in Chinese cabbage using Fluidigm genotyping assays. *Hortic. Environ. Biotechnol.* 61, 327–338. doi: 10.1007/s13580-019-00211-y

Dally, N., Eckel, M., Batschauer, A., Höft, N., and Jung, C. (2018). Two CONSTANS-LIKE genes jointly control flowering time in beet. *Sci. Rep.* 8:4. doi: 10.1038/s41598-018-34328-4

Dally, N., Xiao, K., Holtgräwe, D., and Jung, C. (2014). The B2 flowering time locus of beet encodes a zinc finger transcription factor. *Proc. Natl. Acad. Sci. U. S. A.* 111, 10365–10370. doi: 10.1073/pnas.1404829111

Dijk, H. V., and Hautekèete, N.-C. (2014). Evidence of genetic change in the flowering phenology of sea beets along a latitudinal cline within two decades. *J. Evol. Biol.* 27, 1572–1581. doi: 10.1111/jeb.12410

Diprose, M. F., Fletcher, R., Longden, P. C., and Champion, M. J. (1985). Use of electricity to control bolters in sugar beet (*Beta vulgaris* L.): a comparison of the electrothermal with chemical and mechanical cutting methods. *Weed Res.* 25, 53–60. doi: 10.1111/j.1365-3180.1985.tb00617.x

Doyle, J. J., and Doyle, J. L. (1990). Isolation of plant DNA from fresh tissue. *Focus* 12, 13–15.

Ferrandino, P., Zavenella, M., and Zuffrano, M. (2008). "Bolting in sugar beet autumal sowing in South Italy," in *71st IIRB Congress*. Ferrara.

Hautekèete, N.-C., Piquot, Y., and Dijk, H. V. (2002). Life span in *Beta vulgaris* ssp. maritima: the effects of age at first reproduction and disturbance. *J. Ecol.* 90, 508–516. doi: 10.1046/j.1365-2745.2002.00688.x

Hébrard, C., Peterson, D. G., Willems, G., Delaunay, A., Jesson, B., Lefèbvre, M., et al. (2016). Epigenomics and bolting tolerance in sugar beet genotypes. *J. Exp. Bot.* 67, 207–225. doi: 10.1093/jxb/erv449

Hoffmann, C. M., and Kenter, C. (2018). Yield potential of sugar beet – have we hit the ceiling? *Front. Plant Sci.* 9:289. doi: 10.3389/fpls.2018.00289

Hoffmann, C. M., and Kluge-Severin, S. (2011). Growth analysis of autumn and spring sown sugar beet. *Eur. J. Agron.* 34, 1–9. doi: 10.1016/j.eja.2010.09.001

Höft, N., Dally, N., Hasler, M., and Jung, C. (2018a). Haplotype variation of flowering time genes of sugar beet and its wild relatives and the impact on life cycle regimes. *Front. Plant Sci.* 8:2211. doi: 10.3389/fpls.2017.02211

Höft, N., Dally, N., and Jung, C. (2018b). Sequence variation in the bolting time regulator BTC1 changes the life cycle regime in sugar beet. *Plant Breeding* 137, 412–422. doi: 10.1111/pbr.12579

Kim, H.-S., Abbasi, N., and Choi, S.-B. (2013). Bruno-like proteins modulate flowering time *via* 3′ UTR-dependent decay of SOC1 mRNA. *New Phytol.* 198, 747–756. doi: 10.1111/nph.12181

Kuroda, Y., Takahashi, H., Okazaki, K., and Taguchi, K. (2019). Molecular variation at BvBTC1 is associated with bolting tolerance in Japanese sugar beet. *Euphytica* 215:43. doi: 10.1007/s10681-019-2366-9

Lasa, J. M. (1977). Sugar beet bolting in the root crop. *J. Agric Sci.* 89, 223–228. doi: 10.1017/S0021859600027404

Lee, J., Lee, S., Jang, J.-Y., and Park, T. (2018). Exact association test for small size sequencing data. *BMC Med. Genom.* 11:30. doi: 10.1186/s12920-018-0344-z

Liang, X., Wang, Z., Sha, Q., and Zhang, S. (2016). An adaptive fisher's combination method for joint analysis of multiple phenotypes in association studies. *Sci. Rep.* 6:34323. doi: 10.1038/srep34323

McCouch, S. R., Zhao, K., Wright, M., Tung, C.-W., Ebana, K., Thomson, M., et al. (2010). Development of genome-wide SNP assays for rice. *Breeding Sci.* 60, 524–535. doi: 10.1270/jsbbs.60.524

Mutasa-Göttgens, E. S., Qi, A., Zhang, W., Schulze-Buxloh, G., Jennings, A., Hohmann, U., et al. (2010). Bolting and flowering control in sugar beet: relationships and effects of gibberellin, the bolting gene B and vernalization. *AoB Plants* 2010:plq012. doi: 10.1093/aobpla/plq012

Nelson, R., and Deming, G. W. (1952). Effect of bolters on yield and sucrose content of sugar beet. *Proc. Am. Soc. Sugar Beet Technol.* 6, 441–444.

OECD-FAO (2020). *OECD Agriculture Statistics*. Available at: https://www.oecd-ilibrary.org/agriculture-and-food/data/oecd-agriculture-statistics_agr-data-en (accessed June 27, 2021).

Pfeiffer, N., Müller, A. E., Jung, C., and Kopisch-Obuch, F. J. (2017). QTL for delayed bolting after winter detected in leaf beet (*Beta vulgaris* L.). *Plant Breeding* 136, 237–244. doi: 10.1111/pbr.12452

Pfeiffer, N., Tränkner, C., Lemnian, I., Grosse, I., Müller, A. E., Jung, C., et al. (2014). Genetic analysis of bolting after winter in sugar beet (*Beta vulgaris* L.). *Theor. Appl. Genet.* 127, 2479–2489. doi: 10.1007/s00122-014-2392-x

Pin, P. A., Zhang, W., Vogt, S. H., Dally, N., Büttner, B., Schulze-Buxloh, G., et al. (2012). The role of a pseudo-response regulator gene in life cycle adaptation and domestication of beet. *Curr. Biol.* 22, 1095–1101. doi: 10.1016/j.cub.2012.04.007

Pulido, P., and Leister, D. (2018). Novel DNAJ-related proteins in *Arabidopsis thaliana*. *New Phytol.* 217, 480–490. doi: 10.1111/nph.14827

Rataj, K., and Simpson, G. G. (2014). Message ends: RNA 3' processing and flowering time control. *J. Exp. Bot.* 65, 353–363. doi: 10.1093/jxb/ert439

Schnepel, K., and Hoffmann, C. M. (2016). Effect of extending the growing period on yield formation of sugar beet. *J. Agron. Crop Sci.* 202, 530–541. doi: 10.1111/jac.12153

Scott, R. K., English, S. D., Wood, D. W., and Unsworth, M. H. (1973). The yield of sugar beet in relation to weather and length of growing season. *J. Agri. Sci.* 81:2.

Seo, P. J., Ryu, J., Kang, S. K., and Park, C.-M. (2011). Modulation of sugar metabolism by an INDETERMINATE DOMAIN transcription factor contributes to photoperiodic flowering in Arabidopsis. *Plant J.* 65, 418–429. doi: 10.1111/j.1365-313X.2010.04432.x

Shen, L., Kang, Y. G. G., Liu, L., and Yu, H. (2011). The J-domain protein J3 mediates the integration of flowering signals in Arabidopsis[W]. *Plant Cell* 23, 499–514. doi: 10.1105/tpc.111.083048

Stevanato, P., and Biscarini, F. (2016). Digital PCR as new approach to SNP genotyping in sugar beet. *Sugar Tech* 18, 429–432. doi: 10.1007/s12355-015-0408-8

Tränkner, C., Lemnian, I. M., Emrani, N., Pfeiffer, N., Tiwari, S. P., Kopisch-Obuch, F. J., et al. (2016). A detailed analysis of the BR1 locus suggests a new mechanism for bolting after winter in sugar beet (*Beta vulgaris* L.). *Front. Plant Sci.* 7:1662. doi: 10.3389/fpls.2016.01662

Tränkner, C., Pfeiffer, N., Kirchhoff, M., Kopisch-Obuch, F. J., van Dijk, H., Schilhabel, M., et al. (2017). Deciphering the complex nature of bolting time regulation in *Beta vulgaris*. *Theor. Appl. Genet.* 130, 1649–1667. doi: 10.1007/s00122-017-2916-2

Van Dijk, H. (2009). Evolutionary change in flowering phenology in the iteroparous herb *Beta vulgaris* ssp. maritima: a search for the underlying mechanisms. *J. Exp. Bot.* 60, 3143–3155. doi: 10.1093/jxb/erp142

Yang, J. J., Li, J., Williams, L. K., and Buu, A. (2016). An efficient genome-wide association test for multivariate phenotypes based on the Fisher combination function. *BMC Bioinformat.* 17:19. doi: 10.1186/s12859-015-0868-6

Yang, Y., Qin, Y., Xie, C., Zhao, F., Zhao, J., Liu, D., et al. (2010). The Arabidopsis chaperone J3 regulates the plasma membrane H+-ATPase through interaction with the PKS5 kinase. *Plant Cell* 22, 1313–1332. doi: 10.1105/tpc.109.069609

Yu, T.-S., Lue, W.-L., Wang, S.-M., and Chen, J. (2000). Mutation of arabidopsis plastid phosphoglucose isomerase affects leaf starch synthesis and floral initiation. *Plant Physiol.* 123, 319–326. doi: 10.1104/pp.123.1.319

Conflict of Interest: The authors declare that the research was conducted in the absence of any commercial or financial relationships that could be construed as a potential conflict of interest.

Copyright © 2021 Ravi, Campagna, Della Lucia, Broccanello, Bertoldo, Chiodi, Maretto, Moro, Eslami, Srinivasan, Squartini, Concheri and Stevanato. This is an open-access article distributed under the terms of the Creative Commons Attribution License (CC BY). The use, distribution or reproduction in other forums is permitted, provided the original author(s) and the copyright owner(s) are credited and that the original publication in this journal is cited, in accordance with accepted academic practice. No use, distribution or reproduction is permitted which does not comply with these terms.

Advantages of publishing in Frontiers

OPEN ACCESS
Articles are free to read for greatest visibility and readership

FAST PUBLICATION
Around 90 days from submission to decision

HIGH QUALITY PEER-REVIEW
Rigorous, collaborative, and constructive peer-review

TRANSPARENT PEER-REVIEW
Editors and reviewers acknowledged by name on published articles

Frontiers
Avenue du Tribunal-Fédéral 34
1005 Lausanne | Switzerland

Visit us: www.frontiersin.org
Contact us: frontiersin.org/about/contact

REPRODUCIBILITY OF RESEARCH
Support open data and methods to enhance research reproducibility

DIGITAL PUBLISHING
Articles designed for optimal readership across devices

FOLLOW US
@frontiersin

IMPACT METRICS
Advanced article metrics track visibility across digital media

EXTENSIVE PROMOTION
Marketing and promotion of impactful research

LOOP RESEARCH NETWORK
Our network increases your article's readership